

New data on bioacoustics and courtship behaviour in grasshoppers (Orthoptera, Acrididae, Gomphocerinae) from Russia and adjacent countries

Varvara Vedenina¹, Nikita Sevastianov¹, Evgenia Kovalyova¹

¹ Institute for Information Transmission Problems, Russian Academy of Sciences, Bolshoy Karetny per. 19, Moscow 127051, Russia
Corresponding author: Varvara Vedenina (vvedenina@googlemail.com)

Abstract

The songs of seven grasshopper species of subfamily Gomphocerinae from Russia, Ukraine, Georgia, and Kazakhstan were studied. We analysed not only the sound, but also the stridulatory movements of the hind legs to more entirely describe the songs. In *Mesasippus kozhevnikovi*, *Chorthippus macrocerus*, and *C. hammarstroemi*, the legs are moved in a relatively simple pattern; four other species, *Myrmeleotettix palpalis*, *Stenobothrus newskii*, *C. pullus*, and *Megaulacobothrus aethalinus* demonstrate more complex leg movements. In six of the seven species studied, the courtship songs contain more sound elements than the calling songs. The highest number of courtship sound elements was found in *M. palpalis* and *M. aethalinus*. The different parts of a remarkably long stridulatory file in *M. aethalinus* are thought to participate in the production of different sound elements. The songs in *S. newskii* are shown for the first time. This species produces sound not only by common stridulation but also by wing beats. A relationship of *S. newskii* to some other species of the genus *Stenobothrus*, which are able to crepitate, is discussed. We also analyse the frequency spectra of the songs. A maximum energy of the song power spectra in six species studied lies in ultrasound range (higher than 20 kHz). In only *M. aethalinus*, the main peaks in the song power spectra lie lower than 20 kHz. The courtship behaviour in *M. palpalis*, *C. macrocerus*, and *C. hammarstroemi* was shown to include conspicuous visual display (movements of antennae, palps and the whole body).

Key words: Calling song, courtship song, frequency spectrum, stridulatory leg movements, visual display



Academic editor: Jun-Jie Gu
Received: 8 January 2024
Accepted: 31 March 2024
Published: 2 May 2024

ZooBank: <https://zoobank.org/4F62E5E1-95BA-4F1C-99E2-765E6340EFA9>

Citation: Vedenina V, Sevastianov N, Kovalyova E (2024) New data on bioacoustics and courtship behaviour in grasshoppers (Orthoptera, Acrididae, Gomphocerinae) from Russia and adjacent countries. ZooKeys 1200: 1–26. <https://doi.org/10.3897/zookeys.1200.118422>

Copyright: © Varvara Vedenina et al.
This is an open access article distributed under terms of the Creative Commons Attribution License (Attribution 4.0 International – CC BY 4.0).

Introduction

In many species of Orthoptera, the song is an important component of reproductive isolation. This is the reason why acoustic signals are often used in taxonomy, when sibling species are similar in morphology, but have quite different songs. Among the Acrididae subfamilies, acoustic communication in Gomphocerinae is most developed in terms of structure of acoustic apparatus, temporal pattern of the song, and mating strategies (e.g., Otte 1970; von Helversen and von Helversen 1994; Ragge and Reynolds 1998). The song is produced by

stroking a stridulatory file on each hind femur across a raised vein on the fore wing. Using both hind legs, the grasshoppers have two separate sound-producing devices that must be coordinated with one another. The stridulatory movements of the two legs often differ in amplitude and form, and the legs can exchange roles from time to time, leading to increased song complexity (Elsner 1974; von Helversen and Elsner 1977; Elsner 1994). Various species demonstrate different degrees of song complexity. The song in Gomphocerinae also varies according to the behavioural situation. A solitary male produces a calling song, listening for the response song of a female that is ready to mate. Several males sitting in a close vicinity can produce rival songs. When a male finds a female, in many species the male begins a special courtship song, which may reach a high complexity and may be accompanied by conspicuous movements of different parts of the body such as the abdomen, head, antennae, or palps (Faber 1953; Otte 1970; von Helversen and von Helversen 1994).

To make a comprehensive analysis of songs between the species, it is necessary to compare not only the sound but also the stridulatory leg movements. Sometimes, a similar sound pattern can be produced by completely different leg movements (Vedenina and Mogue 2011). The leg movement analysis may help in the sound analysis when the gaps between sound elements are not distinct because of the phase shift between the two legs. A comparison of the leg movements in different species rather than the sound analysis may indicate a relationship between the species (Sevastianov et al. 2023). During the courtship behaviour, a male may also demonstrate species-specific leg movements without producing the sound.

It was previously argued that the specificity of the Gomphocerinae songs lies not in their frequency band but almost without exception in the pattern of amplitude over time. However, several studies showed that despite a relatively broad spectra of the grasshopper songs, there are pronounced interspecific differences in maxima or peaks (Meyer and Elsner 1996, 1997). It was also shown that male calling and female response songs may differ in the frequency spectra, and these differences can be used during species recognition (von Helversen and von Helversen 1997). It was also shown that various parts of elaborate courtship songs may significantly differ in the carrier frequency (Vedenina et al. 2007; Ostrowski et al. 2009; Vedenina et al. 2020). The differences in the frequency spectra between the various song elements may influence the amplitude ratio on the oscillogram. If the song is recorded by portable recorders with a frequency range not exceeding 12.5–15 kHz, the amplitude ratio of different elements may be distorted (Vedenina and Shestakov 2014).

In the current paper, we describe the calling and courtship songs in seven species of Gomphocerinae from Russia, Ukraine, Kazakhstan, and Georgia. To gain a better description of the songs, we analyse not only the sound, but also the underlying stridulatory movements of the hind legs. We also consider the whole visual display accompanying the courtship song in some species. And finally, we analyse the frequency spectra of the songs and different song elements.

Materials and methods

The calling song was recorded from a solitary male; the courtship song was recorded when a male was sitting near a female. All song recordings were made in the laboratory. Both the sound and the movements of the hind legs

were recorded with a custom-built opto-electronic device (von Helversen and Elsner 1977; Hedwig 2000). A piece of reflecting foil was glued to the distal part of each hind leg femur of the male and two opto-electronic cameras were focused on the illuminated reflecting dots. Each camera was equipped with a position-sensitive photodiode that converted the upward and downward movements of the hind legs into voltage signals. These signals, together with the recordings of the sounds (a microphone type 4191, ½ inch; a conditioning amplifier type 2690; Brüel & Kjaer, Nærum, Denmark), were A/D-converted with a custom-built PC card. The sampling rate was 1325 Hz for recording the stridulatory movements and 100 kHz for sound recordings. The ambient temperature near the singing male was 30–32 °C. The temporal parameters and power spectra of the songs were analysed with COOLETIT (Syntrillium, Seattle, WA) and TURBOLAB 4.0 (Bressner Technology, Gröbenzell, Germany). Courtship behaviour was also recorded with a Sony HDR-CX 260E digital video camera; the video signals were analysed with the VIRTUAL DUB program.

Localities where the song recordings were made are shown in Fig. 1. The numbers of localities in the text (paragraphs Material in description of each species) correspond to the numbers on the map. Data on species distribution were obtained from Bey-Bienko and Mistshenko (1951) and Ragge and Reynolds (1998).

For the song description we used the following terms: **pulse** – the sound produced by one stroke of a hind leg and representing the shortest measurable unit; **syllable** – the sound produced by one complete up and down movement of the hind legs, starting when the legs leave their initial position and ending when the legs return to their original position; **element** – the sound produced by the same leg movements and usually including a series of equal syllables; **echeme** – series of consistent syllables separated by pauses (Fig. 2).

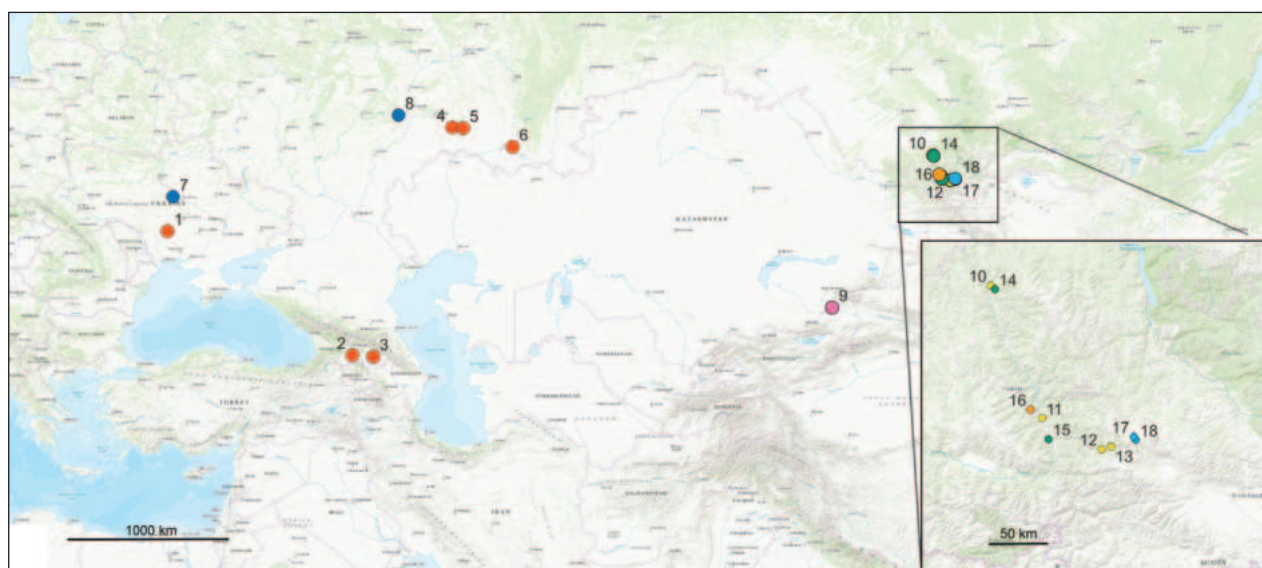


Figure 1. Map of localities where the specimens were collected for the song recordings. 1–6: *Chorthippus macrocerus*; 7, 8: *Chorthippus pullus*; 9: *Mesasippus kozhevnikovi*; 10–13: *Megaulacobothrus aethalinus*; 14, 15 *C. hammarstroemi*; 16: *Myrmeleotettix palpalis*; 17, 18: *Stenobothrus newskii*. The localities of the same species are indicated by the same colour.

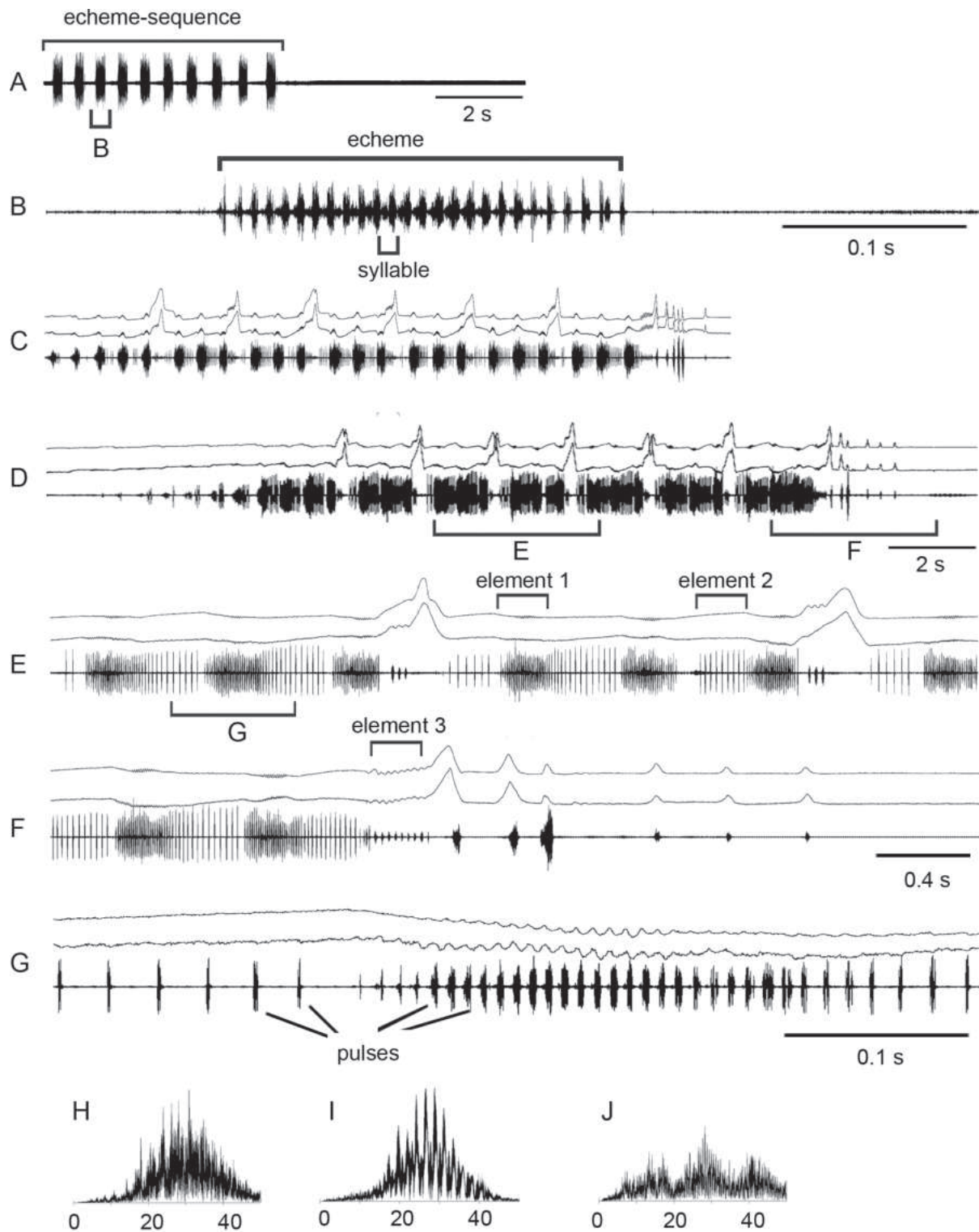


Figure 2. Oscillograms of the calling song **A, B**, courtship songs **C–G** and frequency spectra **H–J** in *Myrmeleotettix palpalis*. Courtship songs of two males are shown in **C** and **D**. Song recordings are presented at three different speeds. In oscillograms **C–G** the two upper lines are recordings of hind leg movements and the lower line is the sound recording. Different elements of the courtship song are shown in **E, F**. Frequency spectra are shown in kHz for the courtship elements 1 **H**, 2 **I** and 3 **J**.

Results and discussion

Myrmeleotettix palpalis (Zubowsky, 1900)

Distribution. Southern Siberia from Altai to Transbaikalia, south-west of Amur region to Mongolia. Abundant in dry steppes and semi-deserts.

Material (Fig. 1). 16. RUSSIA: Altai Republic, ~ 26 km SE of Ongudai, environs of Kupchehen', 50°37.3'N, 86°26.2'E, 922 m a.s.l., 05.08.2023, song recordings in 3 ♂.

References to song. Tishechkin and Bukhvalova 2009: recordings of calling song from Buryatia and Chita region.

Song. The calling song is an echeme-sequence lasting for ~ 7 s and consisting of ~ 14 echemes (Fig. 2A–B). The echemes usually lasts ~ 0.2–0.25 s and the intervals between them are ~ 0.3–0.4 s. Each echeme consists of ~ 25 pulses repeated at the rate of 120–125 /s. Oscillograph analysis shows that the low-amplitude pulses are sometimes produced in gaps between the main pulses.

In the courtship song, one can distinguish three sound elements (Fig. 2C–J; see Suppl. material 1). The element 1 is similar to the calling echeme, although with clear gaps between pulses. The pulses are produced by synchronous leg movements repeated at the rate of ~ 115–120 /s. Each pulse is generated by only downstroke. The element 1 gradually transforms to element 2: the rate of pulses decreases to ~ 40–50 /s and they become ~ 2 × as long. It is remarkable that they are produced by very weak up-movement of one leg. After three alternations of elements 1 and 2, a male produces a high-amplitude stroke with both legs, despite two legs produce different patterns. One leg is moved up in a stepwise manner, which results to generation of 3–7 low-amplitude pulses (element 3), whereas another leg is moved up straighter without low-amplitude vibrations. Then elements 1 and 2 alternate again 3×, followed by the high-amplitude stroke of the legs, which change the roles. After repeating ~ 6–7 cycles with high-amplitude strokes, the two legs are moved synchronously producing element 3, followed by precopulatory leg movements. The frequency spectra of elements 1 and 2 are similar, occupying a broad range from 15 to 40 kHz with maximum energy between 25 and 35 kHz (Fig. 2H, I). The spectrum of element 3 has three maxima at ~ 15, 30, and 40 kHz (Fig. 2J).

When producing alternation of elements 1 and 2, a male slightly moves his body from side to side, generates low-amplitude movements with antennae keeping them turned to the sides, and conspicuously moves with black and white palps up and down (Fig. 3).

Comparative remarks. The recordings of calling song in *M. palpalis* from Altai are similar to the recordings from Buryatia and Chita region (Tishechkin and Bukhvalova 2009). The courtship song of *M. palpalis* is shown for the first time. The calling song and the courtship element 1 are produced during the leg movements repeated at the rate of ~ 115–120 /s. According to Vedenina and Mogue (2011) and to Sevastianov et al. (2023), this pattern can be considered as relatively complex and advanced pattern: the leg-movement rate could originate from the double rates of the wing beat. The complex structure of the courtship song with several sound elements found in *M. palpalis* are concordant with the overall complexity of the courtship songs in the genus *Myrmeleotettix*. (Ragge and Reynolds 1998; Berger and Gottsberger 2010; Vedenina and Mogue 2011; Vedenina et al. 2020).

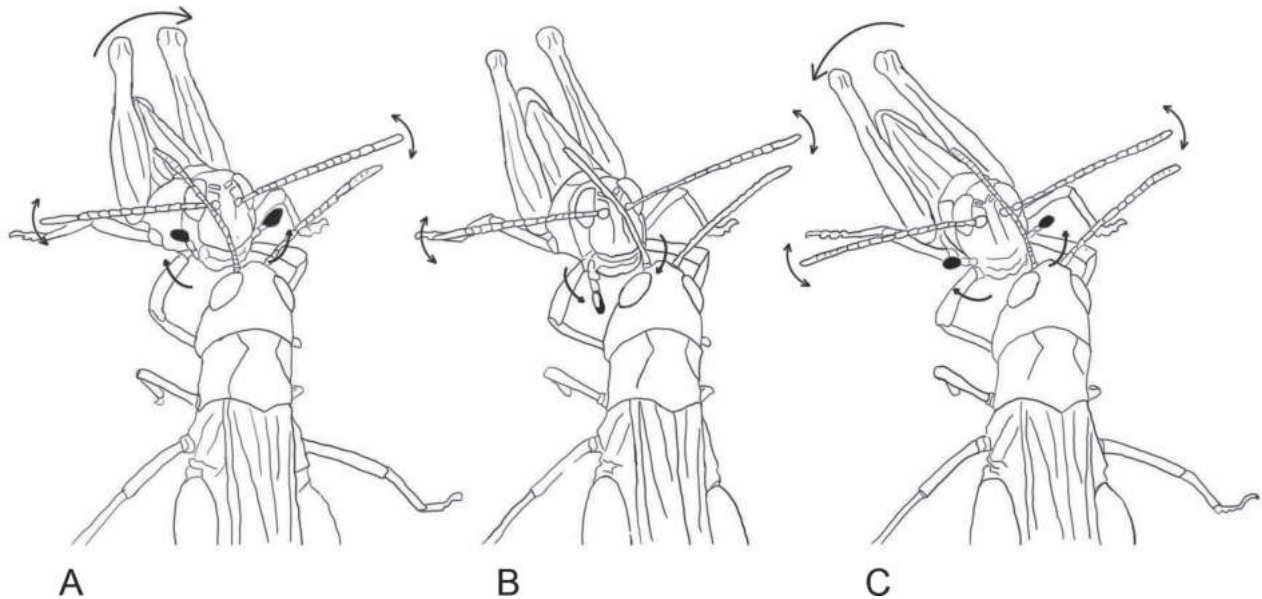


Figure 3. Movements of antennae, black and white palps and the whole body in *Myrmeleotettix palpalis* during courtship. The palps are raised up **A** lowered down **B** and raised up again **C**.

We suggest the movements with palps to be a remarkable visual display that distinguishes *M. palpalis* from most gomphocerine species. In one more species of this genus, *M. antennatus*, the palp movements were also described during courtship (Berger and Gottsberger 2010). *M. antennatus*, however, moves palps much more rapidly than *M. palpalis*, and the most conspicuous visual display in *M. antennatus* comprises a large swing of antennae with well-developed clubs. In contrast to *M. palpalis*, pulps in *M. antennatus* are not coloured in black and white. Within the genus *Myrmeleotettix*, antennae in *M. palpalis* are least thickened at the ends, which is probably correlated with very weak antennal movements during courtship. Other two species of this genus, *M. maculatus* (Ragge and Reynolds 1998; Vedenina and Shestakov 2014) and *M. pallidus* (Vedenina et al. 2020) move conspicuously with antennae but not with palps. Thus, the visual display in various *Myrmeleotettix* species seems to evolve independently. The palp movements are also known in *Aeropus sibiricus* and *Gomphocerippus rufus* (e.g., Elsner 1974; Ragge and Reynolds 1998). However, these species that are distantly related to the species of *Myrmeleotettix*, demonstrate very different patterns of the palp movements. It is evident that the pulp movements in *Myrmeleotettix*, *A. sibiricus*, and *G. rufus* evolved convergently.

***Stenobothrus newskii* Zubowsky, 1900**

Distribution. Altai Mountains, Tuva, NW Mongolia. Usually associated with alpine meadows.

Material (Fig. 1). RUSSIA: 17. Altai Republic, Ulagan district, 3.5 km N of Lake Cheybek-Kohl, 50°25.854'N, 87°34.561'E, 1907 m a.s.l., 06.08.2023, song recordings in 3 ♂; 18. Altai Republic, Ulagan district, ab. 10 km N of Aktash, near Lake Cheybek-Kohl, 50°24.5'N, 87°35.8'E, 1821 m a.s.l., 14.08.2021, song recordings in 5 ♂, 06.08.2023, song recordings in 3 ♂.

References to song. Unknown.

Song. The calling song is an echeme-sequence that may last for tens of seconds, up to a minute (Fig. 4A–C). The echemes usually lasts ~ 0.25 s and the intervals between them are ~ 0.6 s. Each echeme begins quietly, reaching maximum intensity at the second half of its duration. Each echeme is generated by the low-amplitude, antidromic up and down leg movements at the rate of ~ 120 /s. During both up and down movements, the legs produce distinct pulses so, that the pulse rate is 2 \times as high as the leg-movement rate.

During courtship, the males generate a sequence of echemes almost identical to the calling echeme-sequence. However, sometimes a courting male shortly crepitates by wings (Fig. 4D–G; see Suppl. material 2) or / and starts a noisy flight. After such a flight, the male is trying to copulate. The frequency spectrum of crepitation has a rather narrow maximum around 20 kHz; by contrast, the spectrum of echeme is more usual for Gomphocerinae, ranging from 10 to 40 kHz with numerous maxima between 18 and 30 kHz.

Comparative remarks. The acoustic behaviour in *S. newskii* is described for the first time. It is remarkable that this species crepitates in flight and is also able to generate short sequences of wing beats sitting on the ground. Such crepitation on the ground is also known in some other species of the genus *Stenobothrus*, namely, *S. rubicundulus* (Elsner and Wasser 1995), *S. cotticus* (Berger et al. 2010), and *S. hyalosuperficies* (Tarasova et al. 2021).

The song and mating behaviour of *S. newskii* is almost identical to those in *S. cotticus* (Ragge and Reynolds 1998; Berger 2008; Berger et al. 2010). It is surprising considering the large distance between the localities of the two species. *Stenobothrus cotticus* was originally assumed to be endemic to the southwestern Alps, and it was later found in the Rila mountains in Bulgaria (Berger et al. 2010). The authors suggested that *S. cotticus* had a wider distribution during colder periods, when its range was expanded to lower altitudes. It is remarkable that *S. newskii* is similar to *S. cotticus* not only in song but also in morphology (Zubowsky 1900; Kruseman and Jeekel 1967) and ecological preferences: both species occur in alpine meadows at altitudes higher than 1700 m a.s.l. Taking into account that the leg-movement patterns of both species are relatively complex and may be considered as evolutionary advanced (Vedenina and Mogue 2011; Sevastianov et al. 2023), we suppose that the two species may represent one taxon. However, this conclusion requires more confirmation.

***Mesasippus kozhevnikovi* Tarbinski, 1925**

Distribution. Eastern and southern Kazakhstan, Uzbekistan.

Material (Fig. 1). 9. KAZAKHSTAN: Almaty region, national park Altyn-Emel', environs of Basshi, along stream, 44°10.1'N, 78°45.1'E, 05.07.2016, song recordings in 2 ♂, 22.06.2023, song recordings in 3 ♂.

References to song. Bukhvalova and Vedenina 1998: recordings of calling song from Kazakhstan.

Song. The calling song is an echeme lasting for 3–4 s (Fig. 5). It begins quietly and reaches maximum intensity $\sim 2/3$ of its duration (Fig. 5A–B). The two legs are moved synchronously at the rate of 21–25 /s, generating homogenic syllables. During the upstroke, the legs generate a soft sound, whereas during the downstroke, the sound intensity gradually increases (Fig. 5C).

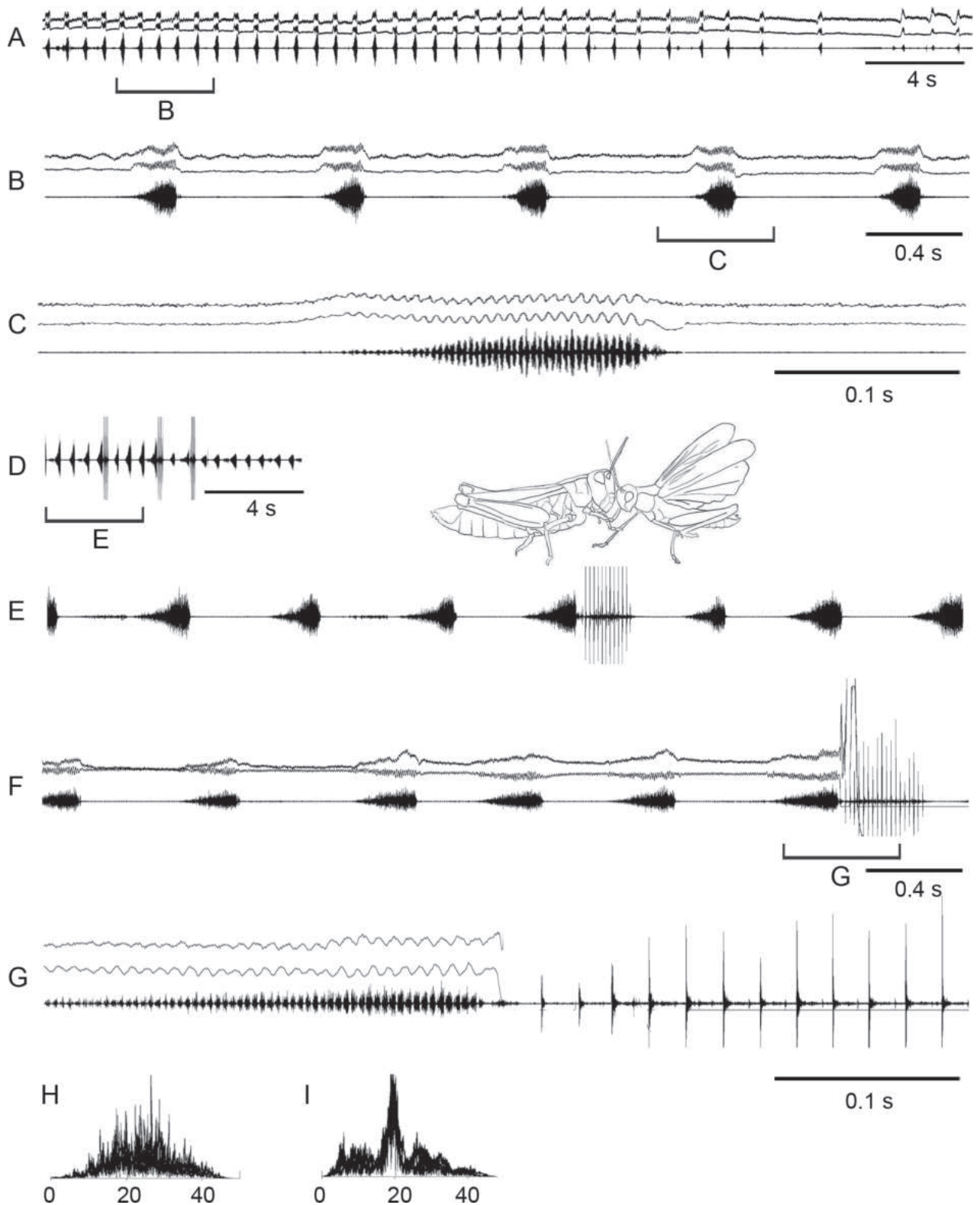


Figure 4. Oscillograms of the calling song **A–C** courtship song **D–G** and frequency spectra **H, I** in *Stenobothrus newskii*. Courtship songs of two males are shown in **E** and **F**. Song recordings are presented at three different speeds. In oscillograms **A–C, F–G** the two upper lines are recordings of hind leg movements and the lower line is the sound recording. The drawing shows the wing clapping, which generates the high-amplitude pulses shown in **D–G**. Frequency spectra are shown in kHz for the main echeme **H** and wing beats **I**.

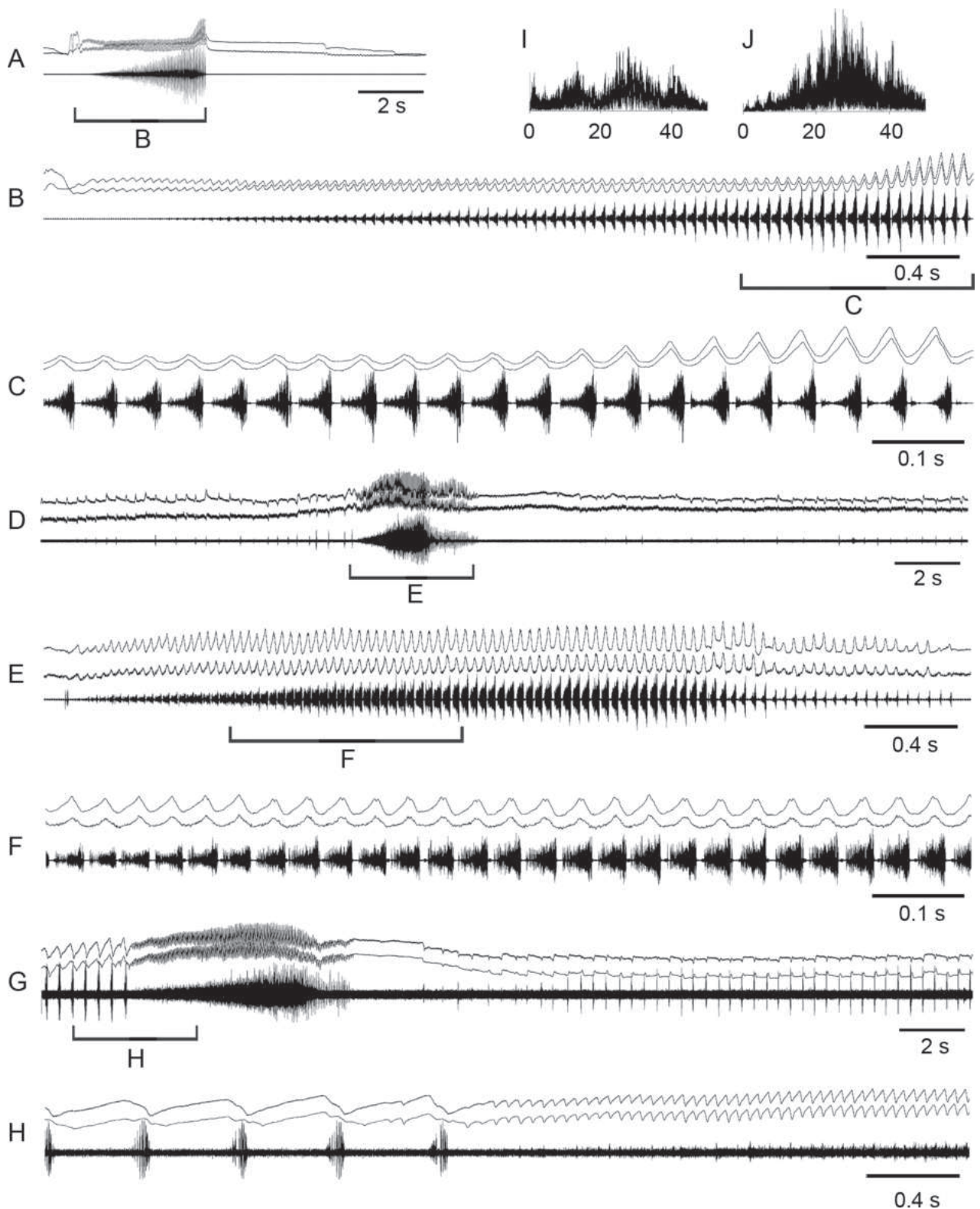


Figure 5. Oscillograms of the calling song **A**, **B** courtship song **C–H** and frequency spectra **I**, **J** in *Mesaspipus kozhevnikovi*. Courtship songs of two males are shown in **D** and **G**. Song recordings are presented at three different speeds. In all oscillograms the two upper lines are recordings of hind leg movements and the lower line is the sound recording. Frequency spectra are shown in kHz for the short syllables **I** and the main echeme **J** of courtship.

The courtship song starts with producing soft and short syllables, repeated at the rate of $\sim 2\text{--}3$ /s (Fig. 5G); however, sometimes these syllables are repeated very irregularly (Fig. 5D). When producing element 1, the legs are moved with a very small amplitude. In ~ 30 s–1 min a male starts an element 2 that is similar to the calling song. However, the echeme duration is longer, up to $\sim 7\text{--}8$ s. The echeme also begins quietly, reaching maximum intensity in $\sim 2\text{--}4$ s. The amplitude of the leg movements gradually increases but abruptly decreases close to the end; as a result, the syllables of smaller amplitude are generated at the end of each echeme. Then, the long element 1 is again produced, followed by element 2. The frequency spectrum of element 1 shows three maxima in a wide range (Fig. 5I), whereas the spectrum of element 2 is characterised by many peaks between 18 and 35 kHz (Fig. 5J).

Comparative remarks. The current recordings of calling song are similar to the recordings published by Bukhvalova and Vedenina (1998), despite usage of the different recording equipment. The courtship song of *M. kozhevnikovi* is shown for the first time. According to Bey-Bienko and Mistshenko (1951), the localities where our material and that collected by Bukhvalova and Vedenina (1998) are situated within the range of subspecies *M. kozhevnikovi iliensis* Mistsh. In the genus *Mesasippus*, there are nine species occurring in Kazakhstan, Uzbekistan, western China, and north-western Mongolia. Currently, we have information on bioacoustics in only one species of the genus.

***Chorthippus pullus* (Philippi, 1830)**

Distribution. Europe from France to the east of European Russia, reaching as far north as Leningrad region and as far south as the northern Caucasus. This species occurs very locally, either in mountains or in dry pine forests (sandy heathlands and forest clearings).

Material (Fig. 1). 7. UKRAINE: Cherkassy region, ~ 17 km S of Kanev, glades in pine forest, $49^{\circ}35.58'N$, $31^{\circ}29.51'E$, 22.06.2010, song recordings in 3 ♂; 8. RUSSIA: Ul'yanovsk region, Novospassky district, Monastyrsky Sungur, $53^{\circ}14.483'N$, $47^{\circ}39.839'E$, 05.07.2022, song recordings in 2 ♂.

References to song. Ragge and Reynolds 1998: recordings of calling song from Germany. Bukhvalova and Vedenina 1998: recordings of calling song from Ukraine, Zakarpat'je.

Song. During courtship, a male generates several echemes each lasting $\sim 2\text{--}4$ s and repeated at $\sim 3\text{--}4$ s intervals (Fig. 6A). Each echeme has either one or two elements. The first element is a whizzing sound produced by the low-amplitude leg movements at the rate of ~ 34 /s. It begins quietly showing a gradual crescendo for approximately the first half of its duration. The two legs are moved with the notable phase shift (Fig. 6F). During the short up movement, each leg generates one soft pulse, whereas during stepwise down movement, each leg produces four pulses of increasing sound intensity. Thus, each syllable contains five pulses repeated at the rate of ~ 170 /s. Sometimes, immediately after the first echeme element, the legs are moved asynchronously with the high amplitude, which produces almost no sound (Fig. 6A, D; see Suppl. material 3). Before the copulation attempts, a male moves the legs synchronously with high amplitude generating several noisy syllables repeated at

the rate of ~ 3.5 /s (Fig. 6A, C, E). The frequency spectrum of the main echeme is broad with maximum energy between 13 and 30 kHz (Fig. 6H); the spectrum of precopulatory sound has several maxima between 5 and 20 kHz (Fig. 6I).

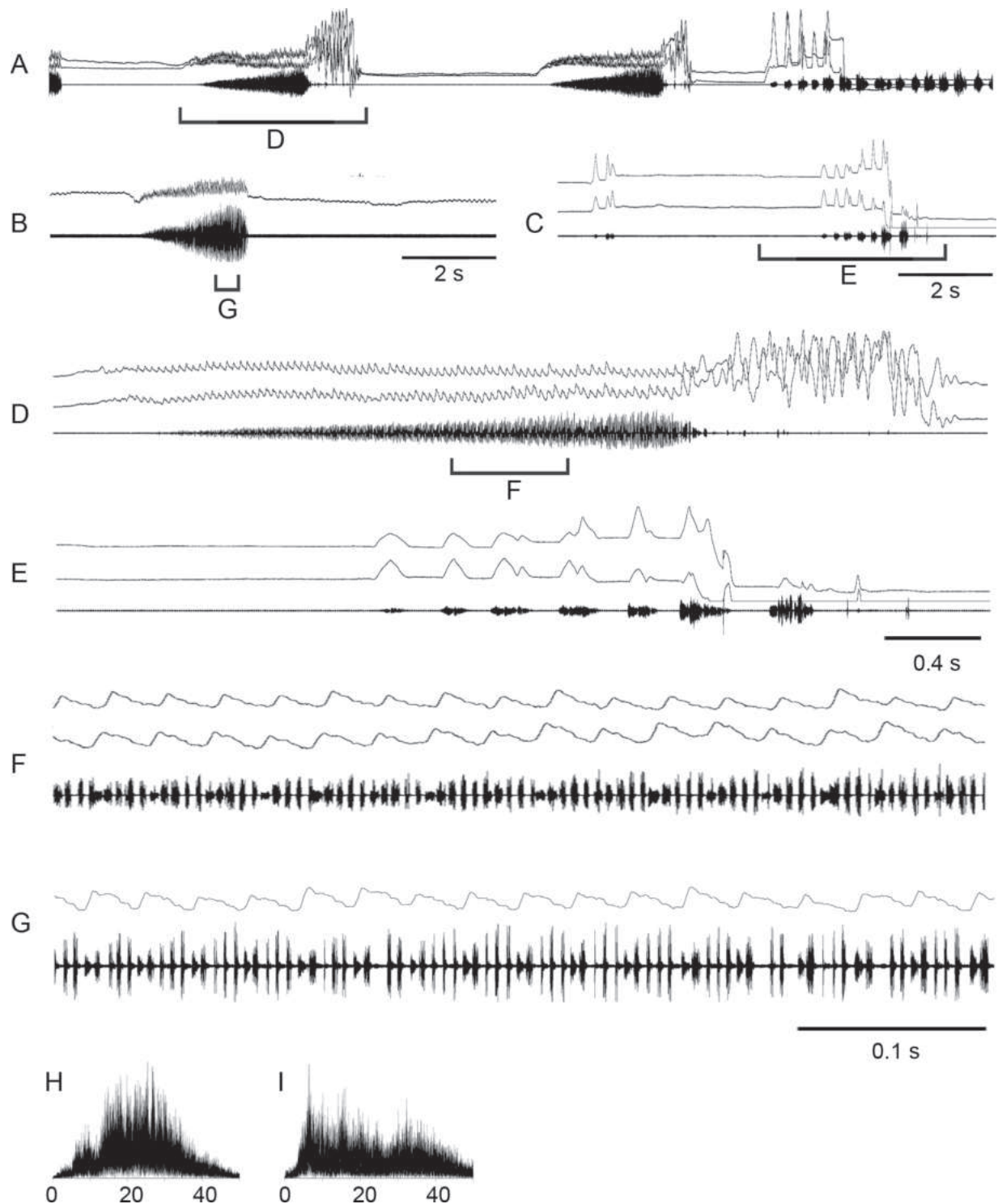


Figure 6. Oscillograms of the courtship song **A–G** and frequency spectra **H, I** in *Chorthippus pullus*. Courtship songs are shown in males from Ukraine **A, D, F** and Russia **B, C, E, G**. Song recordings are presented at three different speeds. In all oscillograms except **B, G** the two upper lines are recordings of hind leg movements and the lower line is the sound recording. Courtship song of one-legged male is shown in **B, G**. Frequency spectra are shown in kHz for the main echeme **H** and precopulatory sound **I**.

Comparative remarks. Ragge and Reynolds (1998) suggested sometimes two elements in the calling song of *C. pullus*, the first one being produced by the fast, low-amplitude leg vibrations and the second one by the slower, high-amplitude leg movements. We suggest that the second element mainly serves as a visual display during courtship, especially given the absence of the sound during the high-amplitude leg movements. Ragge and Reynolds (1998) also supposed that the leg movements producing the whizzing noise could be complex and asynchronous. We support their assumption by analysing the leg-movement pattern. The main rhythm of the leg movements (34 /s) could originate from the half rates of the wing beat (Vedenina and Mugue 2011). However, rapid vibratory movements during each downstroke (170 /s) are higher than the double rates of the wing beat. We consider the leg-movement pattern of *C. pullus* to be rare, if not unique, within Gomphocerinae.

The uniqueness of the leg-movement pattern of *C. pullus* within Gomphocerinae is in a concordance with its controversial taxonomic status. Despite this species is attributed to the genus *Chorthippus*, different phylogenetic reconstructions based on various molecular markers (Sevastianov et al. 2023; Schmidt et al. 2024) indicate that *C. pullus* forms an outgroup not only to the genus *Chorthippus*, but even to the tribes Stenobothrini and Gomphocerini. At the same time, morphologically this species could be easily attributed to *Chorthippus*, although being a rather brachypterous species.

***Chorthippus macrocerus* (Fischer-Waldheim, 1846)**

Distribution. *Chorthippus macrocerus macrocerus*: Transcaucasia, Asia Minor, Iraq, northern Iran. *Chorthippus macrocerus purpuratus* (Vorontsovski, 1928): from Ukraine to northern and western Kazakhstan, reaching as far south the northern Caucasus.

Material (Fig. 1). 1. UKRAINE: Nikolaev region, Pervomaisk district, Ostapovka, 47°58.2'N, 31°05.8'E, 05.07.2005, song recordings in 1 ♂; GEORGIA: 2. Algeti national park, 41°40.55'N, 44°21.55'E, 1252 m a.s.l., 27.08.2023, song recordings in 5 ♂; 3. environs of Sighnaghi, 41°35.91'N, 45°51.18'E, 770 m a.s.l., song recordings in 1 ♂; RUSSIA: 4. Samara region, Alekseevka district, Gerasimovka, 52°42.636'N, 51°30.584'E, 12.07.2012, song recordings in 2 ♂; 5. Orenburg region, environs of Buzuluk, 52°40.7'N, 52°17.8'E, 30.06.2020, song recording in 1 ♂; 6. Orenburg region, Saraktash district, Studentzy, 51°51.639'N, 55°51.312'E, 14.07.2012, song recordings in 1 ♂.

References to song. Vedenina and Zhantiev 1990; Bukhvalova and Zhantiev 1994; Vedenina and Bukhvalova 2001: recordings of calling song from Moldova, Ukraine, south-eastern part of European Russia and northern Caucasus.

Song. The calling song is an echeme lasting 14–18 s in nominative subspecies, and shorter, ~ 4–10 s, in *C. macrocerus purpuratus* (Fig. 7). The legs are moved with a small phase shift at the rate of ~ 3.5–4.5 /s in nominative subspecies, and faster, at the rate of ~ 5–7 /s, in another subspecies. At the beginning of the echeme, each upstroke of the legs produces almost no sound, whereas each downstroke generates syllables of distinct pulses (Fig. 7C). Close to the echeme end, the legs produce a louder, but still relatively soft sound during each upstroke. Very often, the legs are moved faster close to the echeme end than at the begin-

ning; as a result, distinct pulses disappear in the last syllables (Fig. 7D). This, however, occur only in *C. macrocerus purpuratus*. The nominative subspecies usually does not increase the rate of the leg movements close to the echeme end.

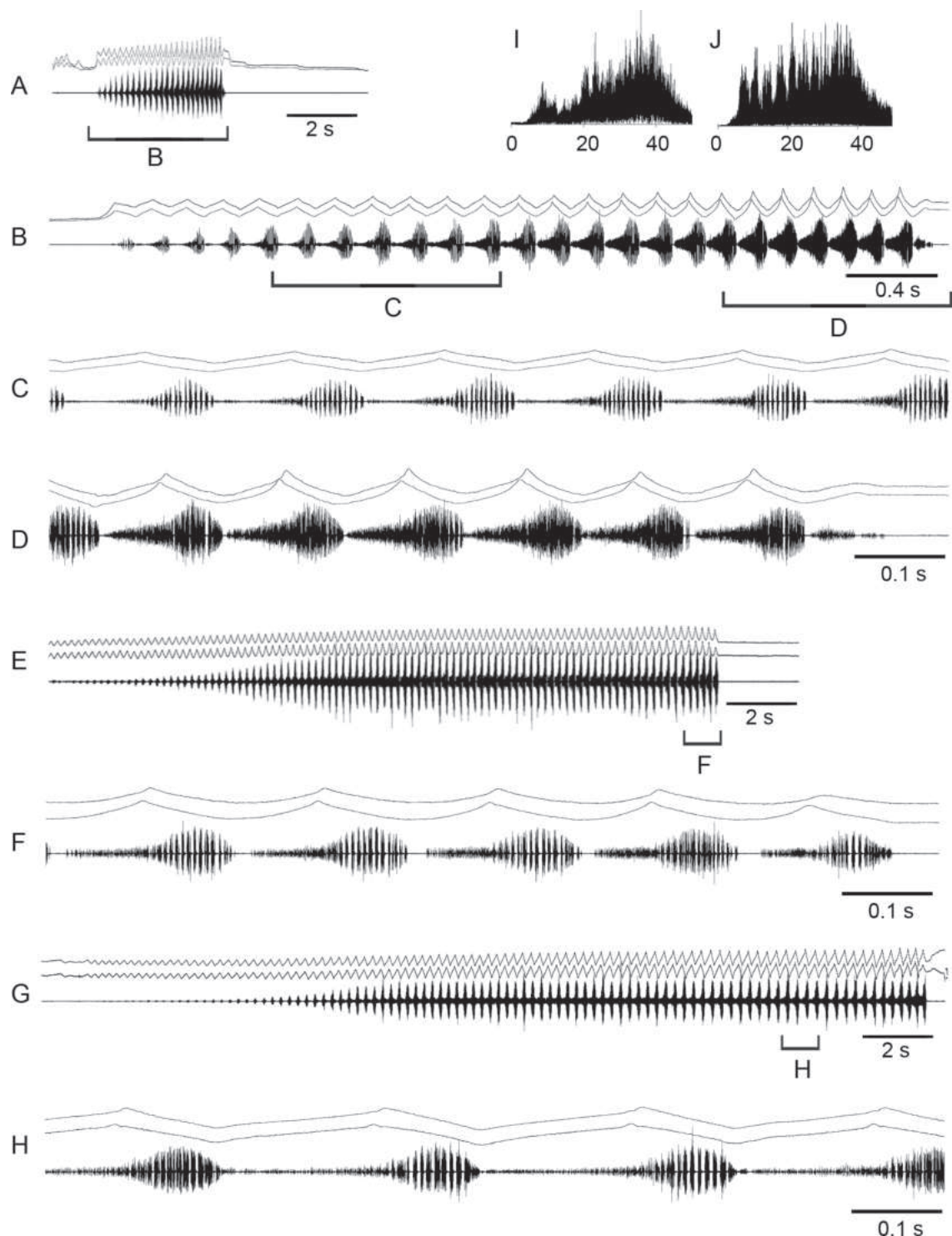


Figure 7. Oscillograms of the calling song **A–D**, courtship songs **E–H** and frequency spectra **I, J** in *Chorthippus macrocerus*. Courtship songs are shown in males from Orenburg region **E–F** and from Georgia **G–H**. Song recordings are presented at three different speeds. In all oscillograms the two upper lines are recordings of hind leg movements and the lower line is the sound recording. Frequency spectra are shown in kHz for the courtship songs from Orenburg region **I** and from Georgia **J**.

The courtship song is similar to the calling song but lasts longer. For example, in nominative subspecies the echeme duration varies in the range of 18–30 s (Fig. 7G). The frequency spectra are also similar in the calling and courtship songs. We, however, found some differences between the spectra of two subspecies. The spectrum of the *C. macrocerus purpuratus* song has the main maximum around 35 kHz but also a small peak around 10 kHz (Fig. 7I). The spectrum of the song in nominative subspecies has many periodical peaks in the broad range of 5–40 kHz (Fig. 7J).

After finishing the long courtship echeme, a male produces a very conspicuous display with his long antennae (the ratio of antennae length to head and pronotum length averages 1.89 ± 0.07 in *C. macrocerus* in contrast to 1.64 ± 0.1 in *C. apricarius* or 1.70 ± 0.17 in *C. fallax*). First, antennae are moved in longitudinal plane backwards, and the two antennae are moved asymmetrically (Fig. 8A). Then, antennae are moved in horizontal plane, from side to side (Fig. 8B) and finally, antennae are moved in a circular manner (Fig. 8C). Immediately after the antennal movements (see Suppl. material 4), a male is trying to mate. We documented the antennal movements in the only males from Georgia (nominative subspecies). Concerning the males from other localities (*C. macrocerus purpuratus*), we cannot say whether they show such visual display or not, since we did not pay attention to the antennal movements.

Comparative remarks. The current recordings of calling song in *C. macrocerus purpuratus* are similar to the previous recordings. Vedenina and Bukhvalova (2001) showed that in two subspecies, *C. macrocerus purpuratus* and *C. macrocerus ponticus*, the echeme duration varies greatly (in the range of ~ 3.5–15 s); however, it varies in different specimens referred to the same subspecies. On the basis of this similarity and similarity in morphology between *C. macrocerus purpuratus* and *C. macrocerus ponticus*, the authors doubt whether these subspecies should be distinguished. By contrast, nominative subspecies differs from *C. macrocerus purpuratus* by some morphological characters (the body and wing lengths are larger in nominative subspecies) and some song parameters (the echeme duration is higher and the syllable rate is less in nominative subspecies).

The leg-movement and song patterns in *C. macrocerus* are relatively simple and may be considered as plesiomorphic (Vedenina and Mugue 2011; Sevas-

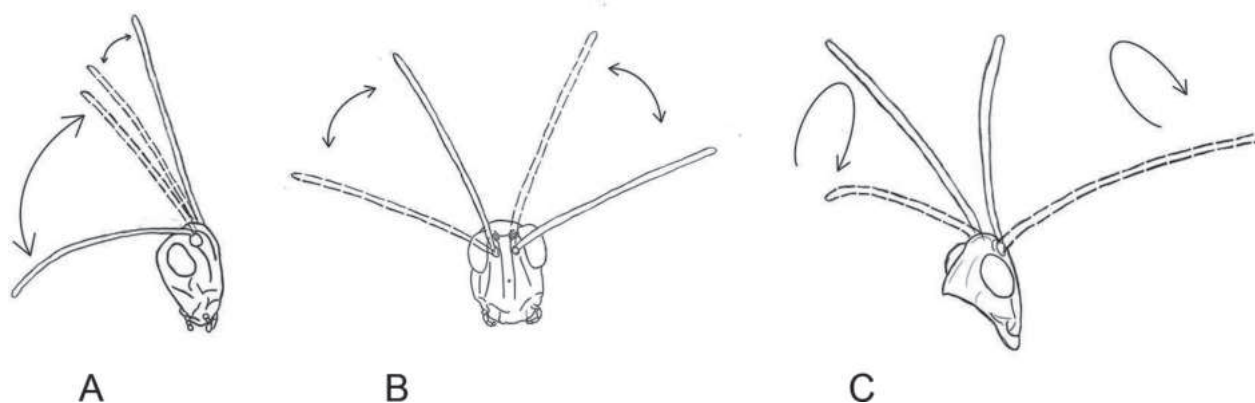


Figure 8. Movements of antennae during courtship in *Chorthippus macrocerus*. Successive stages of the antennae position are shown in **A–C**.

tianov et al. 2023). Moreover, it was suggested that the calling and courtship songs are similar in this species. Therefore, our discover of specific movements with antennae during courtship in *C. macrocerus* is remarkable. In future, it would be important to study if the males in *C. macrocerus purpuratus* demonstrate similar movements with antennae as it was found in nominative subspecies. Considering the very long antennae typical for this species, we expect similar visual display in different subspecies.

***Chorthippus hammarstroemi* (Miram, 1907)**

Distribution. Southern Siberia from Altai to Transbaikalia, southern part of the Russian Far East, Mongolia, China.

Material (Fig. 1). RUSSIA: 14. Altai Republic, Chermal district, Elekmonar, 51°27.372'N, 86°02.524'E, 459 m a.s.l., 03.08.2023, song recordings in 2 ♂; 15. Altai Republic, Ongudai district, ab. 3.5 km S of Inya, 50°24.840'N, 86°38.120'E, 769 m a.s.l., 05.08.2023, song recordings in 6 ♂.

References to song. Benediktov 2005: recordings of calling song from Tuva; Tishechkin and Bukhvalova 2009: recordings of calling and courtship songs from Buryatia, Chita region and Maritime Province.

Song. The calling song is an echeme of variable duration ranging from ~ 6 to 20 s. Sometimes a male can produce several echemes with intervals of ~ 4–6 s (Fig. 9A). The legs being moved with a small phase shift at the rate of ~ 4–4.5 /s generate syllables where one can distinguish soft and loud parts (Fig. 9B, C). During each upstroke, almost no (in the beginning of echeme) or relatively soft (in the end of echeme) sound is produced; during downstroke, a loud sound is generated. The oscillograph analysis shows that the legs slightly vibrate during downstroke, which result to producing distinct pulses, especially at the beginning of echeme.

The rivalry song is a sequence of short echemes (Fig. 9D), which number can greatly vary. Each echeme consists of two or three syllables. The legs are moved almost synchronously at the rate of ~ 7.5 /s. The first syllable usually contains distinct pulses that are similar to those in the calling song. In the noisy second and third syllables the pulses are not distinguishable (Fig. 9E).

A courted male generates an echeme or several echemes that are similar to the calling song. The legs are moved at the slightly higher rate than during calling (of ~ 5–6 /s). After this, a male can produce noisy syllables by the high-amplitude synchronous leg movements at the rate of ~ 2–3 /s (Fig. 9F, G). Before copulation attempt, males move with the long antennae (the ratio of antennae length to head and pronotum length averages 2.07 ± 0.14). The movement pattern is simpler than in *C. macrocerus*: antennae in *C. hammarstroemi* are only moved in a circular manner as in Fig. 8C. Sometimes, the courting male produces the song similar to rivalry song, and the short echemes containing two types of syllables (as in Fig. 9E) can alternate with the noisy courtship element (as in Fig. 9G).

The power spectra of the calling and rivalry songs are similar and have maximum energy between 20 and 35 kHz (Fig. 9H, I). The power spectrum of specific courtship element has two broad peaks, between 5 and 15 kHz and between 20 and 30 kHz (Fig. 9J).

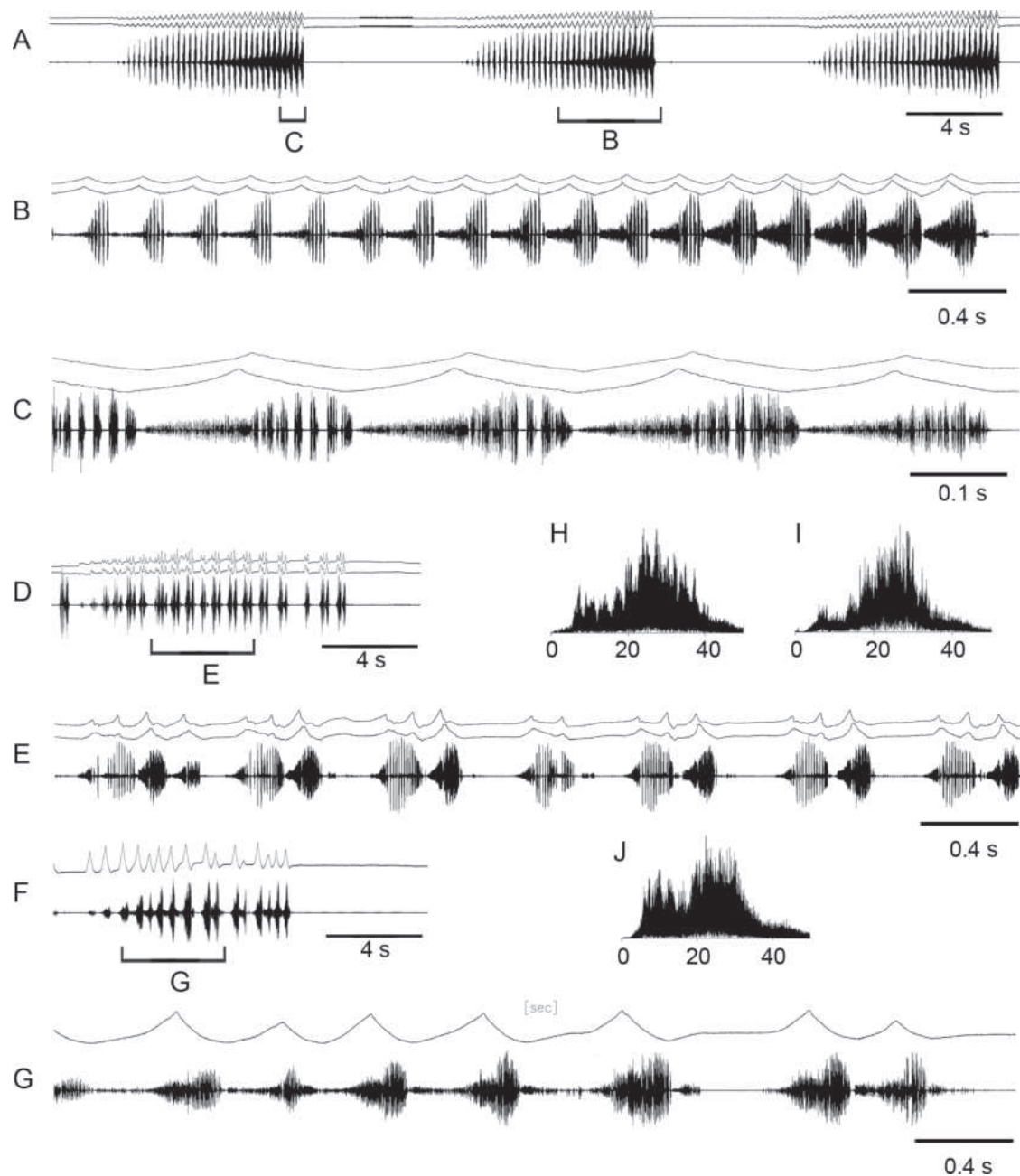


Figure 9. Oscillograms of the calling song **A–C** rivalry song **D–E** courtship song **F–G** and frequency spectra **H–J** in *Chorthippus hammarstroemi*. Song recordings are presented at three different speeds. In all oscillograms except **F**, **G** the two upper lines are recordings of hind leg movements and the lower line is the sound recording. In **F**, **G** the movements of only one leg are shown. Frequency spectra are shown in kHz for the calling song **H** rivalry song **I** and courtship song **J**.

Comparative remarks. The current recordings from Altai are similar to the previous recordings from the more eastern localities of this species (Benediktov 2005; Tishechkin and Bukhvalova 2009). We, however, found slight differences in courtship songs between specimens from Altai and those from Buryatia, Chita region, and Maritime Province (Tishechkin and Bukhvalova 2009). At the same time, considering variable courtship behaviour and different technique of sound recordings, we suggest no principal differences between the recordings.

By contrast, the antennal movements in *C. hammarstroemi* during courtship are documented for the first time. This species is similar to *C. macrocerus* by the remarkably long antennae. The two species are also similar in plesiomorphic pattern of the leg movements during calling behaviour. Tishechkin and Vedenina (2016) suggested that these two allopatric species are characterised by similar song type and acoustic strategy. The usage of long antennae in courtship behaviour in both species even confirms such similarity. On the other hand, both morphological (Bey-Bienko and Mistshenko 1951) and molecular studies (Sevastianov et al. 2023) suggest that *C. macrocerus* and *C. hammarstroemi* are not closely related species. We suggest one of the reasons of their allopatric distribution to be a similarity of acoustic niches, which prevents them from effectively finding members of their own species at the same biotope (Bukhvalova and Zhantiev 1994; Tishechkin and Vedenina 2016).

***Megaulacobothrus aethalinus* (Zubowsky, 1899)**

Distribution. Southern Siberia, the southern part of Russian Far East, the north-eastern China, Korea.

Material (Fig. 1). RUSSIA: 10. Altai Republic, ab. 6 km of Chemal, environs of Elekmonar, 51°29.0'N, 85°59.9'E, 417 m a.s.l., 06.08.2017, song recordings in 2 ♂, 12.08.2021, song recordings in 4 ♂; 11. Altai Republic, Ongudai district, ab. 7 km N of Malyi Yaloman, 50°33.602'N, 86°33.783'E, 740 m a.s.l., 09.08.2023, song recordings in 1 ♂; 12. Altai Republic, Ongudai district, near Shirlak waterfall, 50°20.6'N, 87°13.3'E, 1064 m a.s.l., 14.08.2021, song recordings in 3 ♂; 13. Altai Republic, Ongudai district, ab. 15 km NWW of Chibit, 50°21.637'N, 87°19.480'E, 1056 m a.s.l., 09.08.2023, song recordings in 1 ♂.

References to song. Bukhvalova and Vedenina 1998; Vedenina and Bukhvalova 2001; Benediktov 2005: recordings of calling song from Altai and Maritime Province.

Song. The calling song is a sequence of several echemes lasting ~ 1.5–3 s and separated by intervals of ~ 2–6 s (Fig. 10A). In each echeme, one can distinguish two parts (see Suppl. material 5). In the first part, the legs are moved synchronously at the rate of 7.5–10 /s, which result to generation of simple regular syllables (element 1, Fig. 10B). The sound is generated mainly during downstroke. In the second part, the legs are moved asynchronously, which results to generation of the louder element 2 containing pulses of varying amplitude. The duration of element 2 is usually 2× as short as duration of element 1.

The courtship song starts similarly to the first part of the calling song: the legs are moved synchronously and generate the soft sound during upstroke and the louder sound during downstroke (Fig. 10C, D). In ~ 2–10 s, however, the temporal structure of syllables is gradually changing. The intervals between syllables become fuzzy and the very syllables become louder. Sometimes, the intervals between syllables become completely indistinguishable (Fig. 10H). This main echeme (element 1 of courtship) usually lasts for ~ 15–30 s, but can continue for more than 1 min. Oscillographic analysis of the leg movements shows that amplitude of the two neighbouring strokes slightly differs, however, this is more expressed in one leg (Fig. 10D, E). After the prolonged element 1, a much shorter (lasting ~ 6–9 s) element 2 follows. The legs are moved syn-

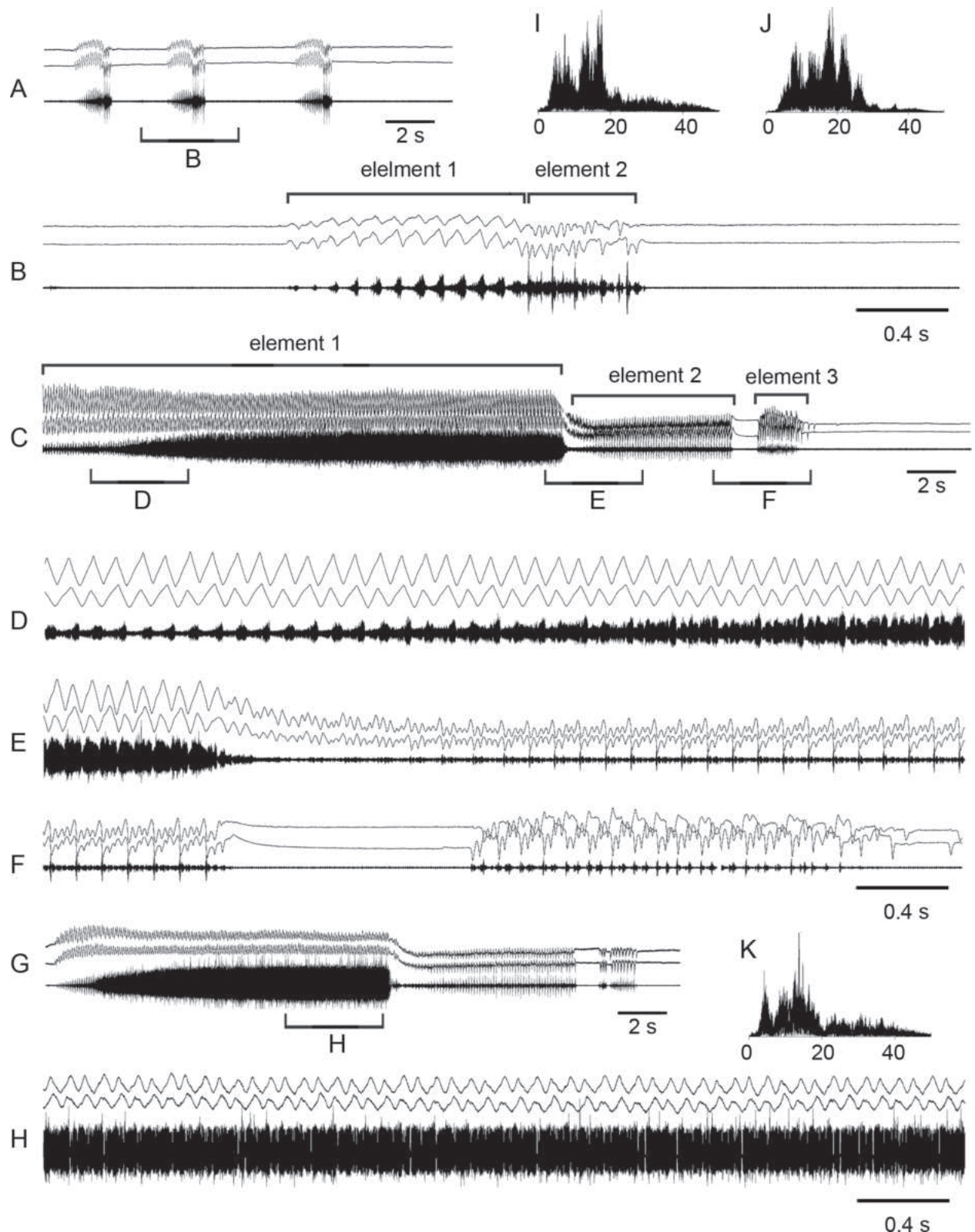


Figure 10. Oscillograms of the calling song **A**, **B** courtship songs **C–H** and frequency spectra **I–K** in *Megaulacobothrus aethalinus*. Courtship songs of two males are shown in **C** and **G**. Song recordings are presented at two different speeds. In all oscillograms the two upper lines are recordings of hind leg movements and the lower line is the sound recording. Different elements of the calling song are shown in **B** of the courtship song – in **C**. Frequency spectra are shown in kHz for the calling song **I** for the courtship element 1 **J** and courtship element 2 **K**.

chronously but at the lower position, and the leg movements have the more complex pattern than during element 1, which implies alternation of several low-amplitude strokes with one higher-amplitude stroke. The legs generate syllables repeated at the rate of 8–10 /s (Fig. 10E); each syllable contains one high-amplitude pulse and several soft pulses. In ~ 1 s after the end of element 2, the shortest (lasting ~ 1–2 s) element 3 follows (Fig. 10C, F, G; see Suppl. material 6). The leg movements have the more irregular pattern than during element 2, moreover, the two legs are moved alternately. As a result, one can distinguish sound pulses repeated at the rate of ~ 15–20 /s.

The frequency spectra of both types of the song are remarkable because they occupy the band lower than 25 kHz. The spectrum of the calling song has two peaks around 7 and 18 kHz (Fig. 10I), the spectrum of the courtship element 1 has several peaks in the range from 5 to 25 kHz (Fig. 10J), and the spectrum of the courtship element 2 has two peaks at approximately 5 and 15 kHz (Fig. 10K).

The elements 1 and 2 of the calling song and the elements 1–3 of the courtship song are produced at the different leg positions. During generation of the calling element 1 and the courtship elements 2 and 3, the legs are moved at the low position. Presumably the distal stridulatory pegs of the hind femora are used in generation of these elements. We compared the lengths of the stridulatory files between *M. aethalinus* and *C. macrocerus*, the species with the simpler song. The file length appeared to be almost 2× longer in *M. aethalinus* than that in *C. macrocerus*. In *M. aethalinus*, the most distal stridulatory pegs are at about the level of the first tibial spine if tibia is pressed to femur (Fig. 11A). In *C. macrocerus*, the most distal stridulatory pegs are at the level between 5th and 6th tibial spines (Fig. 11B).

Comparative remarks. Our recordings of both types of the song are generally similar to those previously described by different authors (Vedenina and Bukhvalova 2001; Benediktov 2005). However, previous authors argued about

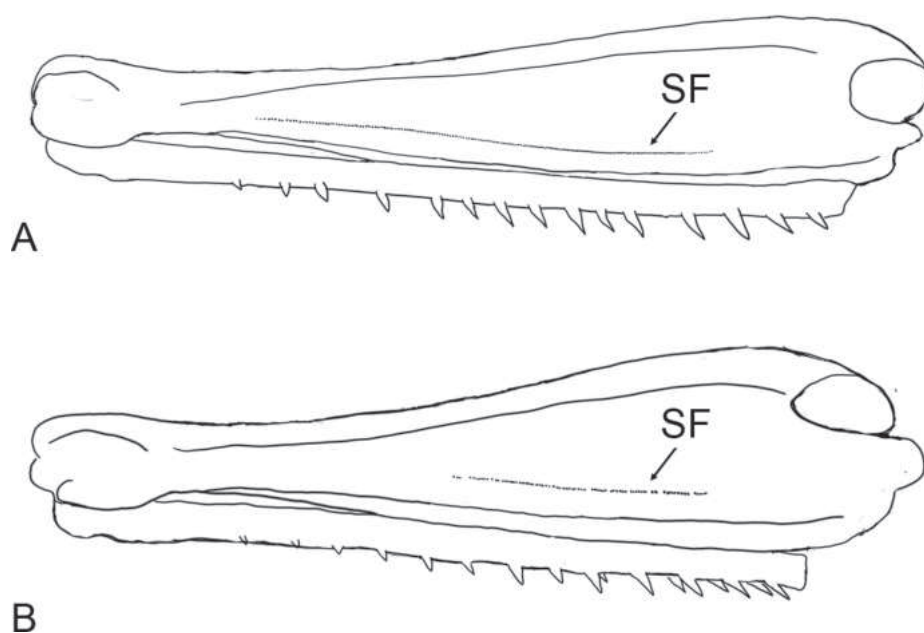


Figure 11. Stridulatory files SF on the hind femora in *Megaulacobothrus aethalinus* **A** and *Chorthippus macrocerus* **B**.

the functions of the two song types in *M. aethalinus*. According to Vedenina and Bukhvalova (2001), different song types are produced by a male sitting alone, therefore they can be considered as the calling song variants. Benediktov (2005) suggested the first song type to be the calling song and the second song type to be the courtship song. Our current data are more concordant with the data of Benediktov (2005). However, our observations of behaviour in this species show that the males sitting without females in laboratory for several days start to produce both song types almost equally often. In nature, by contrast, solitary males usually sing the first song type, whereas the males sitting near by the females typically produce the second song type. Therefore, we also assign the different functions to the different song types.

Analysis of the elaborate leg movements during stridulation in *M. aethalinus* allowed us to suggest unusually long stridulatory file. Up to now, only several species of *C. biguttulus* group with the long stridulatory files were known (Benediktov 1999; Willemse et al. 2009; Tarasova et al. 2021). One of these species, *C. biguttulus ehedicki*, also uses its distal part of the stridulatory file in generation of a relatively soft 'aftersong'. *M. aethalinus*, however, produces a relatively loud sound with the distal part of the stridulatory file.

Conclusions

1. In seven species of subfamily Gomphocerinae, the stridulatory leg movements were recorded and analysed for the first time. In *Mesaspippus kozhevnikovi*, *Chorthippus macrocerus* and *C. hammarstroemi*, the legs are moved in a relatively simple pattern that is considered to be plesiomorphic (Vedenina and Mugue 2011; Sevastianov et al. 2023). Other four species, *Myrmeleotettix palpalis*, *Stenobothrus newskii*, *C. pullus*, and *Megaulacothrus aethalinus* demonstrate more complex leg movements, which are considered to be the more evolutionary advanced patterns.
2. The number of sound elements in the calling and courtship songs is the same in *C. macrocerus*. The courtship song contains one additional sound element in *S. newskii*, *M. kozhevnikovi*, *C. pullus*, and *C. hammarstroemi*. The highest number of courtship sound elements is found in *M. palpalis* and *M. aethalinus*.
3. The songs in *S. newskii* are shown for the first time. This species is remarkable by crepitation in flight and generation of short wing beats, which brings this species closer to other three species of *Stenobothrus* (*S. rubicundulus*, *S. coticus*, and *S. hyalosuperficies*). Moreover, we found a high similarity between *S. newskii* and *S. coticus* in acoustic behaviour, morphology and ecological preferences, which may indicate that these species belong to the same taxon. However, a large distance between habitats of these species do not allow us to make final conclusions.
4. The courtship songs in two species, *M. palpalis* and *M. aethalinus*, contain several sound elements. The complexity of the courtship song in *M. palpalis* is in a concordance with the complexity of courtship behaviour in other species of the genus *Myrmeleotettix*. The song complexity in *M. aethalinus* stands apart because it is not typical for the tribe Gomphocerini. The different courtship song elements in *M. aethalinus* are produced by vibrat-

ing hind femora at the different positions. Analysis of the leg movements revealed the participation of different parts of the long stridulatory file in sound production.

5. A maximum energy of the song power spectra in 6 species studied lies in ultrasound range (higher than 20 kHz). In only *M. aethalinus*, the main peaks in the song power spectra lie lower than 20 kHz. This should be considered during analysis of the recordings made by portable recorders with a frequency range not exceeding 12.5–15 kHz.
6. The courtship behaviour in *M. palpalis*, *C. macrocerus*, and *C. hammarstroemi* includes a different visual display. For the first time we documented conspicuous movements with long antennae in *C. macrocerus* and *C. hammarstroemi*, which are demonstrated just before a copulation attempt. We suggest a correlation between the antenna length and the antennal movements during courtship. *M. palpalis* shows slight movements with antennae and the whole body, and very conspicuous movements with palps during courtship, which are very different from those in other species of the genus *Myrmeleotettix*.

Acknowledgments

We are grateful to Tatiana Tarasova and Lev Schestakov (Institute for Information Transmission Problems, Moscow) for their help with the field trips and song recordings. We also thank the reviewers, Charlie Woodrow (University of Lincoln, UK) and Zhu-Qing He (East China Normal University, China), who substantially improved our manuscript.

Additional information

Conflict of interest

The authors have declared that no competing interests exist.

Ethical statement

No ethical statement was reported.

Funding

The current study was supported by the Russian Scientific Foundation (grant 23-24-00533).

Author contributions

All authors have contributed equally.

Author ORCIDs

Varvara Vedenina  <https://orcid.org/0000-0002-2694-4152>

Nikita Sevastianov  <https://orcid.org/0000-0002-1563-5194>

Data availability

All of the data that support the findings of this study are available in the main text or Supplementary Information.

References

- Benediktov AA (1999) Little-known taxa of grasshoppers of the *Chorthippus biguttulus* group (Orthoptera, Acrididae, Gomphocerinae). *Moscow University Biological Sciences Bulletin* 54(1): 41–45.
- Benediktov AA (2005) Fauna and acoustic signals of the genus *Chorthippus* Fieb. (Orthoptera, Acrididae) from southern Siberia. *Proceedings of the Russian Entomological Society* 76: 118–130. [in Russian with English summary]
- Berger D (2008) The evolution of complex courtship songs in the genus *Stenobothrus* Fischer 1853 (Orthoptera, Caelifera, Gomphocerinae). PhD Thesis, Friedrich-Alexander-Universität Erlangen-Nürnberg, Erlangen. <https://open.fau.de/items/499555d2-9c85-438b-aa1a-332f43fc3eec>
- Berger D, Gottsberger B (2010) Analysis of the courtship of *Myrmeleotettix antennatus* (Fieber, 1853) – with general remarks on multimodal courtship behavior in gomphocerine grasshoppers. *Articulata* 25: 1–21. https://dgfo-articulata.de/downloads/articulata/articulata_XXV_2010/berger_gottsberger_2010.pdf
- Berger D, Chobanov D, Mayer F (2010) Interglacial refugia and range shifts of the alpine grasshopper *Stenobothrus coticus* (Orthoptera: Acrididae: Gomphocerinae). *Organisms Diversity & Evolution* 10: 123–133. <https://doi.org/10.1007/s13127-010-0004-4>
- Bey-Bienko GJa, Mistshenko LL (1951) Locusts and grasshoppers of the USSR and adjacent countries. Part II. Academy of Sciences of USSR Publisher, Moscow-Leningrad, 287 pp. [pp. 381–667, in Russian, English translation of Russian original: Bey-Bienko GJa, Mistshenko LL (1964) Locusts and Grasshoppers of the U.S.S.R and Adjacent Countries. Part II. Jerusalem, Israel Program for Scientific Translations, 291 pp.]
- Bukhvalova MA, Vedenina VY (1998) Contributions to the study of acoustic signals of grasshoppers (Orthoptera: Acrididae: Gomphocerinae) from Russia and adjacent countries. I. New recordings of the calling songs. *Russian Entomological Journal* 7: 109–125. <https://www.cabidigitallibrary.org/doi/full/10.5555/20001105695>
- Bukhvalova MA, Zhantiev RD (1994) Acoustic signals in the grasshopper communities (Orthoptera: Acrididae: Gomphocerinae). *Entomological Review* 73: 121–136.
- Elsner N (1974) Neuroethology of sound in gomphocerine grasshoppers. I. Song patterns and stridulatory movements. *Journal of Comparative Physiology* 88: 72–102. <https://doi.org/10.1007/BF00695923>
- Elsner N (1994) The search for the neural centres of cricket and grasshopper song. In: Schildberger K, Elsner N (Eds) *Neural basis of behavioral adaptation* (Vol. 39). *Fortschritte der Zoologie*, 167–193.
- Elsner N, Wasser G (1995) Leg and wing stridulation in various populations of the gomphocerine grasshopper *Stenobothrus rubicundus* (Germar 1817). I. Sound patterns and singing movements. *Zoology* 98: 179–190. <https://www.cabidigitallibrary.org/doi/full/10.5555/19961101668>
- Faber A (1953) Laut- und Gebärdensprache bei Insekten. Orthoptera (Geradflügler). I. Vergleichende Darstellung von Ausdrucksformen als Zeitgestalten und ihren Funktionen. Stuttgart, 198 pp.
- Hedwig B (2000) A highly sensitive opto-electronic system for the measurement of movements. *Journal of Neuroscience Methods* 100(1–2): 165–171. [https://doi.org/10.1016/S0165-0270\(00\)00255-7](https://doi.org/10.1016/S0165-0270(00)00255-7)
- Kruseman C, Jeekel CAW (1967) *Stenobothrus* (*Stenobothrodes*) *coticus* nov. spec., a new grasshopper from the French Alps (Orthoptera, Acrididae). *Entomologische Berichten* 27(1): 1–7.

- Mayer J, Elsner N (1996) How well are frequency sensitivities of grasshopper ears tuned to species-specific song spectra? *The Journal of Experimental Biology* 199(7): 1631–1642. <https://doi.org/10.1242/jeb.199.7.1631>
- Meyer J, Elsner N (1997) Can spectral cues contribute to species separation in closely related grasshoppers? *Journal of Comparative Physiology A* 180: 171–180. <https://link.springer.com/article/10.1007/s003590050038>
- Ostrowski TD, Sradnick J, Stumpner A, Elsner N (2009) The elaborate courtship behavior of *Stenobothrus clavatus* Willemse, 1979 (Acrididae: Gomphocerinae). *Journal of Orthoptera Research* 18: 171–182. <https://doi.org/10.1665/034.018.0206>
- Otte D (1970) A comparative study of communicative behavior in grasshoppers. Ann Arbor, Museum of Zoology, University of Michigan, Michigan, 167 pp.
- Ragge D, Reynolds WJ (1998) The songs of the grasshoppers and crickets of western Europe. Harley Books, Colchester. 591 pp. <https://doi.org/10.1163/9789004632189>
- Sevastianov N, Neretina T, Vedenina V (2023) Evolution of calling songs in the grasshopper subfamily Gomphocerinae (Orthoptera, Acrididae). *Zoologica Scripta* 52(2): 154–175. <https://doi.org/10.1111/zsc.12579>
- Schmidt R, Dufresnes C, Krištín A, Künzel S, Vences M, Hawlitschek O (2024) Phylogenetic insights into Central European *Chorthippus* and *Pseudochorthippus* (Orthoptera: Acrididae) species using ddRADseq data. *Molecular Phylogenetics and Evolution* 193: 108012. <https://doi.org/10.1016/j.ympev.2024.108012>
- Tarasova TA, Sevastianov NS, Vedenina VYu (2021) Songs and morphology in grasshoppers of the *Stenobothrus eurasius* group (Orthoptera: Acrididae: Gomphocerinae) from Russia and adjacent countries: clarifying of taxonomic status. *Zootaxa* 4965(2): 244–260. doi.org/10.11646/zootaxa.4965.2.2
- Tarasova T, Tishechkin D, Vedenina V (2021) Songs and morphology in three species of the *Chorthippus biguttulus* group (Orthoptera, Acrididae, Gomphocerinae) in Russia and adjacent countries. *ZooKeys* 1073: 21–53. <https://doi.org/10.3897/zookeys.1073.75539>
- Tishechkin DYu, Bukhvalova MA (2009) New data on calling signals of Gomphocerinae grasshoppers (Orthoptera: Acrididae) from South Siberia and the Russian Far East. *Russian Entomological Journal* 18: 25–46.
- Tishechkin DY, Vedenina VY (2016) Acoustic signals in insects: A reproductive barrier and a taxonomic character. *Entomological Review* 96(9): 1127–1164. <https://doi.org/10.1134/S0013873816090013>
- Vedenina VY, Bukhvalova MA (2001) Contributions to the study of acoustic signals of grasshoppers (Orthoptera, Acrididae, Gomphocerinae) from Russia and adjacent countries. 2. Calling songs of widespread species recorded in different localities. *Russian Entomological Journal* 10: 93–123.
- Vedenina V, Mague N (2011) Speciation in gomphocerine grasshoppers: Molecular phylogeny versus bioacoustics and courtship behavior. *Journal of Orthoptera Research* 20(1): 109–125. <https://doi.org/10.1665/034.020.0111>
- Vedenina VY, Shestakov LS (2014) Stable and variable parameters in courtship songs of grasshoppers of the subfamily Gomphocerinae (Orthoptera, Acrididae). *Entomological Review* 94(1): 1–20. <https://doi.org/10.1134/S0013873814010011>
- Vedenina VYu, Zhantiev RD (1990) Recognition of acoustic signals in sympatric species of grasshoppers. *Zoologicheskii Zhurnal* 69: 36–45. [in Russian with English summary]
- Vedenina VY, Panyutin AK, von Helversen O (2007) The unusual inheritance pattern of the courtship songs in closely related grasshopper species of the *Chorthippus al-*

- bomarginatus*-group (Orthoptera: Gomphocerinae). *Journal of Evolutionary Biology* 20(1): 260–277. <https://doi.org/10.1111/j.1420-9101.2006.01204.x>
- Vedenina V, Sevastianov N, Tarasova T (2020) Contributions to the study of the grasshopper (Orthoptera: Acrididae: Gomphocerinae) courtship songs from Kazakhstan and adjacent territories. *Zootaxa* 4895(4): 505–527. <https://doi.org/10.11646/zootaxa.4895.4.3>
- von Helversen O, Elsner N (1977) The stridulatory movements of acridid grasshoppers recorded with an opto-electronic device. *Journal of Comparative Physiology. A, Neuroethology, Sensory, Neural, and Behavioral Physiology* 122(1): 53–64. <https://doi.org/10.1007/BF00611248>
- von Helversen O, von Helversen D (1994) Forces driving coevolution of song and song recognition in grasshoppers. *Fortschritte der Zoologie* 39: 253–284.
- von Helversen D, von Helversen O (1997) Recognition of sex in the acoustic communication of the grasshopper *Chorthippus biguttulus* (Orthoptera, Acrididae). *Journal of Comparative Physiology. A, Neuroethology, Sensory, Neural, and Behavioral Physiology* 180(4): 373–386. <https://doi.org/10.1007/s003590050056>
- Willemse F, von Helversen O, Odé B (2009) A review of *Chorthippus* species with angled pronotal lateral keels from Greece with special reference to transitional populations between some Peloponnesean taxa (Orthoptera, Acrididae). *Zoologische Mededeelingen* 83(2): 319–507. <https://repository.naturalis.nl/pub/314191>
- Zubowsky N (1900) Beitrag zur Kenntnis der sibirischen Acridiideen. *Horae Societatis Entomologicae Rossicae* 34: 1–23.

Supplementary material 1

Courtship in *Myrmeleotettix palpalis*

Authors: Varvara Vedenina, Nikita Sevastianov, Evgenia Kovalyova

Data type: mpg

Explanation note: The male produces high-amplitude strokes with hind legs, moves his body from side to side, generates low-amplitude movements with antennae, and conspicuously moves with palps up and down. In this movie and some others, the pieces of reflecting foil glued to the distal part of each hind femur remained from the leg-movement recordings.

Copyright notice: This dataset is made available under the Open Database License (<http://opendatacommons.org/licenses/odbl/1.0/>). The Open Database License (ODbL) is a license agreement intended to allow users to freely share, modify, and use this Dataset while maintaining this same freedom for others, provided that the original source and author(s) are credited.

Link: <https://doi.org/10.3897/zookeys.1200.118422.suppl1>

Supplementary material 2

Courtship in *Stenobothrus newskii*

Authors: Varvara Vedenina, Nikita Sevastianov, Evgenia Kovalyova

Data type: mpg

Explanation note: The male generates sound by both femoral-tegmina stridulation and wing clapping. The female responds by stridulation. The male attempts to copulate.

Copyright notice: This dataset is made available under the Open Database License (<http://opendatacommons.org/licenses/odbl/1.0/>). The Open Database License (ODbL) is a license agreement intended to allow users to freely share, modify, and use this Dataset while maintaining this same freedom for others, provided that the original source and author(s) are credited.

Link: <https://doi.org/10.3897/zookeys.1200.118422.suppl2>

Supplementary material 3

Courtship in *Chorthippus pullus*

Authors: Varvara Vedenina, Nikita Sevastianov, Evgenia Kovalyova

Data type: mpg

Explanation note: The first whizzing element is produced by the low-amplitude leg movements, after which the legs are moved asynchronously with the high amplitude, which produces almost no sound.

Copyright notice: This dataset is made available under the Open Database License (<http://opendatacommons.org/licenses/odbl/1.0/>). The Open Database License (ODbL) is a license agreement intended to allow users to freely share, modify, and use this Dataset while maintaining this same freedom for others, provided that the original source and author(s) are credited.

Link: <https://doi.org/10.3897/zookeys.1200.118422.suppl3>

Supplementary material 4

Courtship in *Chorthippus macrocerus*

Authors: Varvara Vedenina, Nikita Sevastianov, Evgenia Kovalyova

Data type: mpg

Explanation note: Immediately after the song generation, the male conspicuously moves with antennae and attempts to copulate.

Copyright notice: This dataset is made available under the Open Database License (<http://opendatacommons.org/licenses/odbl/1.0/>). The Open Database License (ODbL) is a license agreement intended to allow users to freely share, modify, and use this Dataset while maintaining this same freedom for others, provided that the original source and author(s) are credited.

Link: <https://doi.org/10.3897/zookeys.1200.118422.suppl4>

Supplementary material 5

Calling in *Megaulacobothrus aethalinus*

Authors: Varvara Vedenina, Nikita Sevastianov, Evgenia Kovalyova

Data type: mpg

Explanation note: The male produces two elements, one element when the legs are maintained at the higher position, the second element when the legs are kept at the lower position.

Copyright notice: This dataset is made available under the Open Database License (<http://opendatacommons.org/licenses/odbl/1.0/>). The Open Database License (ODbL) is a license agreement intended to allow users to freely share, modify, and use this Dataset while maintaining this same freedom for others, provided that the original source and author(s) are credited.

Link: <https://doi.org/10.3897/zookeys.1200.118422.suppl5>

Supplementary material 6

Courtship in *Megaulacobothrus aethalinus*

Authors: Varvara Vedenina, Nikita Sevastianov, Evgenia Kovalyova

Data type: mpg

Explanation note: Three elements of the courtship song are produced: element 1 is produced by synchronous leg movements kept at the higher position, element 2 is produced by also synchronous leg movements but kept at the lower position, the short element 3 is produced by asynchronous leg movements.

Copyright notice: This dataset is made available under the Open Database License (<http://opendatacommons.org/licenses/odbl/1.0/>). The Open Database License (ODbL) is a license agreement intended to allow users to freely share, modify, and use this Dataset while maintaining this same freedom for others, provided that the original source and author(s) are credited.

Link: <https://doi.org/10.3897/zookeys.1200.118422.suppl6>

Type specimens, taxonomic history, and genetic analysis of the Japanese dancing mouse or waltzer, *Mus wagneri* variety *rotans* Droogleever Fortuyn, 1912 (Mammalia, Muridae)

Mónica Cruz¹, Wim Bergmans^{1†}, Toyoyuki Takada², Toshihiko Shiroishi², Atsushi Yoshiki²

¹ Naturalis Biodiversity Center, Darwinweg 2, 2333 CR Leiden, Netherlands

² RIKEN BioResource Research Center, Tsukuba Ibaraki 305-0074, Japan

Corresponding author: Mónica Cruz (monica.guimaraescruz@naturalis.nl)

Abstract

In the present paper, the existence and location of the type series of the Japanese dancing mouse or waltzer, *Mus wagneri* variety *rotans* Droogleever Fortuyn, 1912, are established, and a lectotype is designated. Available type specimens are measured, and some morphological parameters, sex, and general condition of the specimens are recorded. A literature survey was conducted, and an attempt is made to clarify the position of *M. wagneri* variety *rotans* in the taxonomy of *Mus*. A genetic analysis suggests that the type series of the Japanese dancing mouse represent a crossbred, or derivation of a crossbred, between the original Japanese dancing mouse of *Mus musculus molossinus* Temminck 1844 origin and European fancy or laboratory mice of *Mus musculus domesticus* Schwarz & Schwarz, 1943 origin. Much of their genome was replaced and occupied by *Mus musculus domesticus* type genome, probably through extensive breeding with European mice.

Key words: Crossbred, genetic analysis, genome, Japanese dancing mouse, lectotype, taxonomic position



Academic editor: Nedko Nedyalkov

Received: 15 January 2024

Accepted: 21 March 2024

Published: 2 May 2024

ZooBank: <https://zoobank.org/F55D421E-AD11-4191-8919-CB845CA8A04C>

Citation: Cruz M, Bergmans W, Takada T, Shiroishi T, Yoshiki A (2024) Type specimens, taxonomic history, and genetic analysis of the Japanese dancing mouse or waltzer, *Mus wagneri* variety *rotans* Droogleever Fortuyn, 1912 (Mammalia, Muridae). ZooKeys 1200: 27–39. <https://doi.org/10.3897/zookeys.1200.118823>

Copyright: © Mónica Cruz et al.
This is an open access article distributed under terms of the Creative Commons Attribution License (Attribution 4.0 International – CC BY 4.0).

Introduction

In 1912 Æ.B. Droogleever Fortuyn, a Dutch scientist who worked mainly on the anatomy and the heredity of traits in the common house mouse, *Mus musculus* Linnaeus, 1758, and related taxa, described *Mus wagneri* variety *rotans*, the Japanese dancing mouse, a form owing its name to its peculiar rotatory movements. In the fancy mice literature, it is often referred to as waltzing mice, or waltzers. He based his description on 11 specimens, 10 of which were imported from Vienna, Austria, by Dr. C. Kerbert, the director of the Royal Zoological Society Natura Artis Magistra in Amsterdam. The remaining specimen was bred in a laboratory in Utrecht by prof. Dr Zwaardemaker and made available to Droogleever Fortuyn by Dr C.U.A. Kappers (Droogleever Fortuyn 1912). In his description, Droogleever Fortuyn did not designate a holotype. He also did not state where the type specimens were deposited.

† Deceased.

During routine curating activities by the second author in the Mammal Department of the former Zoological Museum of the University of Amsterdam (ZMA; now incorporated in Naturalis Biodiversity Center in Leiden, the Netherlands), a glass jar with piebald mice was found labelled (slashes added): “G / Typen / *Mus wagneri* varietas *rotans* Droogl. Fort. / Japansche Dansmuis”. The jar contained 10 specimens of Japanese dancing mice preserved in 70% ethanol. Given the fact that the specimens are labelled “typen” (= types) there can be no doubt that they-together with the specimen from Utrecht, which has not been located-constituted the basis for Droogleever Fortuyn’s description and that they are the type specimens of *M. wagneri* variety *rotans* Droogleever Fortuyn, 1912. The “G” on the label indicates that at the time of their description the type specimens formed part of the zoological collection of Amsterdam’s municipality (Dutch: gemeente). Droogleever Fortuyn based his description on several measurements of these specimens. In addition, he found that, in comparison with *M. musculus*, the specimens had fewer tail rings (Droogleever Fortuyn 1912). Apart from the fact that they are type material, the specimens are highly valuable to elucidate the origin of common laboratory mouse strains.

When Droogleever Fortuyn described the Japanese dancing mouse in 1912, *Mus wagneri* Eversmann, 1848 was considered a full species. Its low tail ring number constituted one of the characters used to distinguish it from the otherwise closely related *M. musculus*. Due to this, and to the fact that *M. wagneri* was the only Asian wild mouse species known to Droogleever Fortuyn (Schwarz 1942), he was convinced that the Japanese dancing mouse was a form of *M. wagneri* characterized by abnormal spinning or rotatory movements.

The Japanese have long nurtured the tradition of keeping and breeding mice as pets. The varieties of mice kept and bred by Japanese collectors (or “fanciers”) have been known through the centuries as “fancy mice” and include agouti, albino, and piebald fur colours, pink-eyed dilution, and dwarf-built (Koide et al. 1998), as well as Japanese dancing mice, which in the fancy mice literature are often referred to as waltzing mice, or waltzers. The coat colour pattern of the present specimens is typical non-agouti and piebald, highly resembling that of the Japanese Fancy Mouse 1 (JF1) inbred strain (Koide et al. 1998). The JF1 strain has been established from a pair of mice with non-agouti and piebald coat colour kept as Japanese Mice at a market in Denmark. Similar fancy mice with non-agouti piebald coat colour were described in the Japanese literature at the end of the 1700s, suggesting ancestors of JF1 mice were transferred overseas. Moreover, the Japanese dancing mice or Japanese waltzers are known to have contributed in the early stage of establishment of laboratory mouse strains widely used in biomedical studies (Keeler 1931; Morse 1978). Later, it was proven by whole genome sequencing of JF1 mice and genome comparison with a classical inbred laboratory strain C57BL/6J (Takada et al. 2013). Fig. 1 shows a Japanese dancing mouse, and video showing both fur colour and rotatory movements thought to resemble those of the Japanese dancing mouse can be found on the Internet (<http://www.youtube.com/watch?v=hmMfAvxyBh4>).

The aims of the present study are to trace the history of the Japanese dancing mouse, *Mus wagneri* variety *rotans* Droogleever Fortuyn, 1912, in taxonomy, to establish the existence and location of the types and to designate a lectotype, to give descriptive notes, and to present a genetic analysis of the type material to define their genetic status in comparison with JF1 mice.



Figure 1. The JF1 mouse strain has been developed at the National Institute of Genetics in Mishima, Japan, and is available for distribution to biomedical researchers from the RIKEN BioResource Center in Tsukuba, Japan.

Materials and methods

Materials

Lectotype, 1 male, ZMA.MAM.27233, in 70% ethanol; a laboratory animal preserved in 1912 by Æ.B. Droogleever Fortuyn in Amsterdam, no further data.

Paralectotypes, 5 males, 3 females, 1 cf. female, ZMA.MAM.27234-27242, same data. All specimens are now incorporated in the collections of the Naturalis Biodiversity Center in Leiden (NBC). They were individually labelled by Droogleever Fortuyn with Greek letters. Prior to their inclusion in the ZMA collections, the specimens formed part of the natural history collection of Amsterdam's municipality.

Methods

All specimens were measured, and some morphological parameters, sex, and general condition were recorded. In addition, a lectotype was designated. A literature survey was conducted, and an attempt was made to clarify the taxonomic position of *Mus wagneri* variety *rotans* in *Mus*. Three specimens, registered as ZMA.MAM.27233, 27239, and 27241, were used for a genetic analysis. A 5 × 5 mm-square skin fragment of each of these specimens was dissected and processed using the DNA extraction kit (QIAGEN) to obtain genomic DNA for genotyping analyses. Genotyping was performed with a panel of 95 simple sequence length polymorphism markers, which can distinguish C57BL/6J and JF1 mouse strains (Kikkawa et al. 2001; Takada et al. 2008). Single nucleotide polymorphism (SNP) genotyping was carried out for 977 SNP marker loci which had been found to be polymorphic between MSM, belonging to the same substrain as JF1 and C57BL/6J in a previous study (Takada et al. 2013) using the MassARRAY iPLEX system (Sequenom Inc., San Diego, USA). The SNP information is also available at MoG+ (Mouse Genome variation database) (Takada et al. 2021), <https://molossinus.brc.riken.jp/mogplus/#JF1>). The data were recorded and interpreted using MassARRAY software (Sequenom Inc.). Analyses were repeated twice and only reproduced results were counted.

Genomic DNA extracted by a standard method from JF1 and MSM as controls of *Mus musculus molossinus*-origin subspecies, and that of C57BL/6J mice as controls of *M. musculus domesticus*-origin subspecies, were used to compare the genotype with the ZMA series.

Definitions and abbreviations

BT	broken tail
CB	condylobasal length: distance between anterior face of incisor or anterior tip of nasal bones (depending on which is more anterior) and posterior face of occipital condyle
E	ear length
HB	head and body length: distance between tip of snout and anus
HF	hind foot length: distance between tip of longest digit excluding claw and posterior tip of heel
ID	individual identification on original label
JF1	Japanese fancy mouse 1
MR	molar row length: distance between anterior rim of M ¹ alveolus and posterior rim of M ³ alveolus
MSM	an inbred strain established from Japanese wild mice, <i>M. m. molossinus</i> , collected in 1978 in Mishima, Shizuoka-ken
NIG	National Institute of Genetics, Mishima, Japan
S	sex
SC	skull crushed: skull severely damaged; no skull measurements can be taken
SD	skull damaged: not all measurements can be taken
Sd	standard deviation
SI	skull intact
SO	skin opening on head
T	tail length: distance between anus and tip of tail, excluding terminal hair tip
TL	total length: distance between tip of snout and tip of tail, excluding terminal hair tip
ZB	zygomatic breadth: distance across most distal points of zygomata
ZMA	Zoological Museum of the University of Amsterdam
ZMAcd	code number in former ZMA database (now incorporated in the database of Naturalis Biodiversity Center; all numbers now have a new prefix: ZMA.MAM.)

Results

Origin and taxonomic history of the Japanese dancing mouse

Japanese fancy mice are mentioned in the literature before 1800. In the Edo era (1603–1868) fancy mice were very popular in Japan and were bred as a hobby (Yoshiki and Moriwaki 2006). Artists such as Hokusai Katsushika and Kyōsai Kawanabe used fancy mice as subjects in their drawings (Yoshiki and Moriwaki 2006). The booklet “Chingan Sodategusa”, translated as “How to breed fancy mice”, was published by Chobe Zeniya in Kyoto in 1787 (Yoshiki and Moriwaki

2006). The earliest scientific record pertaining to the origin of the dancing mouse was found in the work of Yerkes (1907), who was unable to find mention of the animal in the scientific literature before 1890. After consulting several Japanese and European sources he concluded that these mice originated in China and were imported to Japan where they were bred as pets. From there they were brought to Europe and America and bred as pets and as laboratory animals for studies of physiology, anatomy, and heredity. According to Yerkes (1907: 15), “historical research indicates that a structural variation or mutation which occasionally appears in *Mus musculus*, and causes those peculiarities of movement which are known as dancing, has been preserved and accentuated through selective breeding by the Chinese and the Japanese, until finally a distinct race of mice which breeds true to the dance character has been established. The age of the race is not definitely known, but it is supposed to have existed for several centuries.”

In 1912 the Japanese dancing mouse was described, as *Mus wagneri* var. *rotans*, by Æmilius Bernardus Droogleever Fortuyn (1886–1970), a Dutch scientist who worked mainly on the anatomy and the heredity of traits in the common house mouse and related species (e.g. Droogleever Fortuyn 1928, 1929, 1931, 1934, 1935, 1939) and Droogleever Fortuyn and Meng (1937); he also focused on brain histology of rodents (Droogleever Fortuyn 1911, 1927). Droogleever Fortuyn (1912) noticed that the average number of tail rings in the Japanese dancing mouse is lower than that in *M. musculus* and similar to that in *M. wagneri*, which at the time was considered a full species. He considered the number of tail rings to be of paramount importance to distinguish the Japanese dancing mouse from *M. musculus* since the former has on average 136 tail rings versus 180 in the latter. Droogleever Fortuyn (1912) believed that this character was unrelated to the relative length of the tail (which is shorter in *M. wagneri rotans*) because he had found that young *Mus musculus* had shorter tails than adults while showing the same number of tail rings. For this reason, he assigned the Japanese dancing mouse to *M. wagneri*, the only Asian wild *Mus* species he knew, and given the fact that the Japanese dancing mouse exhibits a spinning behaviour not seen in typical *M. wagneri*, he chose to name the Japanese dancing mouse *Mus wagneri* variety *rotans*. Gates (1925: 651–652) corroborated these findings: “... in all probability, the Japanese mouse, of both the waltzing and the non-waltzing form, is a derivative of *Mus wagneri* and not *M. musculus*, the common house mouse. ... In all body measurements, such as length of body, tail, fore foot, hind foot, skull, number of vertebrae, number of scale rings of the tail, position of posterior nares and incisor alveoli, the Japanese waltzer resembles Wagner’s mouse quite closely. ... A characteristic pigmentation of the eye is apparently common to both the Japanese and Wagner’s mouse, but is not found in the house mouse. ... The protein specificities, as determined by precipitin tests of both the Japanese and Wagner’s mouse, differs from that of the common fancy varieties. This indicates that the Japanese mouse is not a derivative of the ordinary races nor intimately related to them.”

Allen (1927) placed *M. wagneri* in the synonymy of *M. bactrianus* Blyth, 1846 and assigned *M. wagneri rotans* to *M. bactrianus gansuensis* Satunin, 1902 on the basis of the T/TL ratio. According to Allen (1927: 10), this form is derived from *M. bactrianus tantillus*: “It seems altogether likely that some form of this Chinese mouse represents the original stock from which the tame black-and-white mouse of Japan is derived. ... Droogleever Fortuyn (1912) has proposed the name *Mus wagneri rotans* for the tame animal, a name which on account of

the shortness of the tail-to-total-length ratio may be included in the synonymy of the race *gansuensis*." Droogleever Fortuyn (1931, 1939) continued to use the name *M. wagneri* for the Chinese house mouse at least up to 1939.

The Japanese dancing (or waltzing) mouse was later allocated to *Mus molossinus* Temminck, 1844, a name used by Tokuda (Makino 1941: 308) to classify the Japanese wild mouse: "... this form (*Mus molossinus*) represents the sole species of the house mouse widely distributed through Hokkaido, Honsyu and Kyusyu. ... There has been long known in Japan a remarkable variety of this species under domestication, including the white or spotted forms, being famous as the so-called Japanese waltzing mice. Although they have occasionally been described as a variety of *Mus bactrianus* (or often designated as *Mus wagneri* var. *rotans*), the recent status of taxonomical conception shows, according to Dr Tokuda, that they are derivatives of *Mus molossinus*." In a study of the comparative morphology of chromosomes of three species of mouse and their varieties, Makino (1941) found no difference between the chromosomes of the Japanese dancing mouse and of the wild form of *M. molossinus*. Furthermore, all crossings between *M. musculus* and *M. molossinus* produce fertile offspring with a normal sex ratio (Makino 1941). Schwarz (1942: 46) believed "the Japanese waltzer agrees in size and tail length with the Japanese commensal *Mus musculus molossinus*", and according to him "There is no need to suppose that it has been taken to Japan from elsewhere". Schwarz and Schwarz (1943) lumped the Japanese wild mouse with *M. musculus* and classified it as a subspecies: *M. musculus molossinus*.

Minezawa et al. (1981) supported the view that the Japanese wild mouse belongs to *M. musculus molossinus*, on the basis of genetic distance and comparison of allelic composition between Japanese and Western Hemisphere populations. These findings agreed with previous morphological studies, especially on the shape of the anterior border of the zygomatic plate (Makino 1941; Marshall 1977).

Yonekawa et al. (1981) found that mice collected in the central and southern parts of Japan all had the same monomorphic type of mtDNA that was unique to *M. musculus molossinus*, but later they realized that this mtDNA was closely related to that of *M. musculus musculus* from Bulgaria (Yonekawa et al. 1982) and proposed that Japanese mice are not an independent subspecies but rather a "local race" of *M. musculus*.

Marshall (1998), in his turn, pleaded for the adoption of *M. musculus manchu* Thomas, 1909 as the name for the Japanese house mouse instead of *M. molossinus*, a name he believes describes a hybrid between *M. musculus manchu* and *M. castaneus castaneus* Waterhouse, 1842 and, therefore, should be excluded from zoological nomenclature.

Mus musculus manchu was recognized by Marshall (1998) as a subspecies after examination of all the skins and skulls of the *Mus musculus* group in the Smithsonian Institution collection, and comparison with their original descriptions. Marshall (1998) considers *rotans* to be a pet-store mutant of *M. musculus manchu*.

Based on Yonekawa et al.'s (1994) mtDNA analysis, Carleton and Musser (2005) recognized four subspecies of the house mouse: *M. musculus castaneus*, *M. m. domesticus*, *M. m. musculus*, and *M. m. bactrianus*. A fifth group, *gentilulus*, is recognized as a possible species. Because the type specimen of *M. molossinus* is a hybrid of two species, Carleton and Musser (2005) left it unassigned. Furthermore, Carleton and Musser (2005) placed *manchu*, *wagneri*, and *rotans* in the synonymy of *M. musculus musculus*.

Summarizing the taxonomic ideas on *Mus wagneri rotans*

- *Mus wagneri rotans* Droogleever Fortuyn, 1912 is described.
- Allen (1927) includes *rotans* in the synonymy of *M. bactrianus gansuensis* Satunin, 1902, based on the T/TL ratio.
- Tokuda (Makino 1941) includes *rotans* in the synonymy of *M. molossinus* Temminck, 1844.
- Makino (1941) finds no difference in chromosome morphology of the Japanese dancing mouse and *M. molossinus*.
- Schwarz (1942) includes the Japanese dancing mouse in the synonymy of *M. musculus molossinus* based on size and TL.
- Marshall (1998) considered *rotans* to be a pet-store mutant of *M. musculus manchu* Thomas, 1909, a name he believes should designate the Japanese house mouse.
- Carleton and Musser (2005) placed *rotans* in the synonymy of *M. musculus musculus*, based on an mtDNA analysis by Yonekawa et al. (1994).

Type series of *Mus wagneri rotans*: measurements, morphological parameters, sex, and condition

The body measurements, morphological parameters, sex, and condition of all 10 type specimens and the cranial measurements of the lectotype are summarized in Table 1. HB ranges from 52.0 to 63.8 mm; T from 46.5 to 56.1 mm; HF from 10.8 to 12.7 mm, and E from 7.7 to 9.6 mm. All specimens have a black-and-white fur colour pattern (Fig. 2). The specimen labelled with the Greek letter μ (mu) was chosen as lectotype because of its generally good condition. All other type specimens are paralectotypes.

The HB variation of the specimens studied in the present work is compared with that of other *Mus* taxa in Table 2.

Genetic analysis

Specimen ZMA.MAM.27233 was homozygous of C57BL/6-type allele in 50 out of 51 loci tested, except for one heterozygous locus on chromosome X

Table 1. Selected measurements (in mm), morphological parameters, sex, and condition of lectotype (μ ; ZMA.MAM.27233) and paralectotypes (all others) of *Mus wagneri rotans* Droogleever Fortuyn, 1912.

Id	ZMAcd	S	HB	T	T/HB (%)	HF	E	CB	ZB	MR	Condition
α	27234	m	58.20	46.50	79.90	11.60	8.60				SC
β	27235	m	58.30	47.20	80.96	12.55	8.70				SC
γ	27236	m	53.70			12.00	7.70				BT, SI, SO
δ	27237	f	53.90	47.30	87.76	12.65	8.40	17.20	8.00	1.20	SD, SO
ϵ	27238	m	59.70	54.65	91.54	12.50	9.60				SC
ζ	27239	m	56.90	51.35	90.25	12.05	8.90				SI, SO
η	27240	f	53.05	48.00	90.48	10.80	9.20				SI, SO
λ	27241	f	52.00	47.75	91.83	11.00	8.80				SC
μ	27233	m	56.10	56.10	100.00	12.70	8.90	17.50	8.00	1.40	SI
ν	27242	f (cf.)	63.80	50.50	79.15	12.45	9.50				SI
mean			56.57	49.93	87.98	12.03	8.83	17.35	8.00	1.30	
SD			3.60	3.49	6.85	0.69	0.55	0.21	0.00	0.14	



Figure 2. The type series of *Mus wagneri rotans* Droogleever Fortuyn, 1912. From top to bottom and from left to right: Droogleever Fortuyn’s specimens α, β, γ, δ, ε, ζ, η, λ, μ, and ν (ZMA.MAM.27233–27242). Specimen μ (ZMA.MAM.27233) in the middle at the bottom is the lectotype.

Table 2. Comparison of the HB variation (mean ± SD in mm) of the subjects of the present study (*rotans*) with the “optimum HB” of other taxa of *Mus* as given by Schwarz and Schwarz (1943).

	<i>M. rotans</i>	<i>M. molossinus</i>	<i>M. bactrianus</i>	<i>M. wagneri</i>	<i>M. manchu</i>	<i>M. musculus</i>
female	50–61	65–70	75–80	80–85	85–90	85–90
male	55–59	65–70	65–70	75–80	75–80	85–90

(Table 3). This result clearly indicates that the major genomic component of the specimen was of *Mus musculus domesticus* origin. SNP-based genotyping using the MassArray system also detected that most of the alleles of the three specimens of *M. wagneri rotans* were also of C57BL/6-type, and only 7.6, 23.2 and 37.0% of the alleles were JF1-type in ZMA.MAM.27233, 27239, and 27241, respectively.

Table 3. Results of genotyping of Japanese Waltzing mice. 1. B and J indicate C57BL/6J and JF1-type alleles, respectively. 2. J-type allele ratio (%) was calculated as follows: No. of loci in B/J + 2 × No. loci in J/J / 2 × Total no. of loci successfully genotyped × 100. 3. SSLP: 95 simple sequence length polymorphism (SSLP) markers which can distinguish C57BL/6J and JF1 were used. 4. SNP: MassArray SNP analysis was conducted for 977 SNP marker loci which was known as polymorphic between C57BL/6J and JF1.

Genotyping method	Sample name	Number of loci in each genotype ¹					
		B/B	B/J	J/J	Total	Not detected	J-type allele ratio ² (%)
SSLP ³	ZMA.MAM.27233	50	1	0	51	44	0.98
SNP ⁴	ZMA.MAM.27233	840	64	40	944	33	7.6
SNP ⁴	ZMA.MAM.27239	77	35	11	123	854	23.2
SNP ⁴	ZMA.MAM.27241	74	17	40	131	846	37.0

Discussion

The place of *Mus wagneri rotans* in the taxonomy of *Mus*

When comparing HB variation (mean \pm SD) in *Mus wagneri rotans* with the “optimum HB” of related taxa given by Schwarz and Schwarz in 1943, the most obvious observation is that *rotans* is considerably smaller than all the others (Table 2). Also noteworthy is the fact that the HB optimum of *molossinus* is “closest to *rotans*”.

Moriwaki found pairs of original fancy mice at a market in Denmark in 1987 and introduced them into the animal facility of the National Institute of Genetics (NIG) in Mishima, Japan (1998). By the 20th generation resulting from sister-brother matings, a new inbred strain of Japanese fancy mouse called JF1 was established in 1993 (Koide et al. 1998). The JF1 strain carries a “spotting phenotype on the coat resembling an old mutation piebald” and is phenotypically similar to the Japanese dancing mice described by Gates (1926) and by other authors in the early 1900s (Koide et al. 1998). The phenotypical similarity of the *M. w. rotans* types as described in the present paper with the mice belonging to the JF1 strain (Fig. 1) is striking.

Morphological and genetic analysis carried out by Koide et al. (1998) indicated that the JF1 strain originated from the Japanese wild mouse, *M. musculus molossinus*. Yoshiki and Moriwaki (2006) reported that the morphological and genetic characters of the JF1 strain are those of the *musculus* subspecies group.

The data of SNP-based genotyping suggest that the Japanese dancing mice from the ZMA described as *M. w. rotans* represent a crossbred, or derivatives thereof, between original Japanese waltzer of *M. musculus molossinus* origin and European fancy or laboratory mice of *M. musculus domesticus* origin. Most of their genome was replaced and occupied by *M. musculus domesticus* type genome, probably through extensive breeding with European mice. The ZMA specimens have significant value to further elucidate the genetic status of the Japanese waltzer mice described in the old literature, and the origin of laboratory mice if their genome and morphology will be analysed in more detail, since it was reported that the JF1 ancestor is the origin of the *molossinus* genome in the classical inbred laboratory strains, contributing to the genetic diversity among the strains (Takada et al. 2013).

The house mouse has long been used in the laboratory and constitutes the “universal mammalian model” (Bonhomme 1986). However, the genealogy of laboratory strains and their relationships to one another and to wild forms is not yet completely clear. Nevertheless, it is critical to interpreting experimental results in laboratories and phylogenetic comparison between inbred strains and wild populations of *M. musculus* and other species (Carleton and Musser 2005).

Conclusion

The knowledge of the whereabouts of the type specimens of the Japanese dancing mouse is of great importance not only in a historical perspective but also for the development of further studies to clarify the genetic background of laboratory mice.

The results of the present study indicate that the Japanese dancing mouse was derived from the Japanese house mouse before 1800 as a mutation with

a characteristic black-and-white coat coloration and spinning behaviour. This mutation was maintained by inbreeding, first by mouse fanciers in Japan and in Europe and later in laboratories all over the world. The Japanese house mouse has been classified as *M. musculus molossinus* and as *M. musculus manchou*, but, in the latest classification (Carleton and Musser 2005), house mouse populations in Japan are considered to belong to either *M. musculus musculus* or *M. musculus castaneus*, or to a hybrid between these two subspecies.

The remarkable similarity between the coat colour of the type specimens of *M. wagneri rotans* and the specimens that constitute the JF1 strain, a laboratory mouse strain bred in the NIG, Japan, and thought to be derived from the Japanese house mouse based on genetic analysis, cannot be ignored. The variation of HB of the subjects also shows more similarity with the specimens described as *molossinus* by Schwarz and Schwarz (1943), than with other *Mus musculus* subspecies. Given the complexity of *Mus musculus*' taxonomy and in particular the uncertainty of the origin of the Japanese house mouse (Nunome et al. 2010) caution should be taken when stating that the Japanese dancing mouse is derived from both *M. musculus musculus* and *M. musculus castaneus*.

Acknowledgements

We express our sincere appreciation to Dr Kazuo Moriwaki for establishing Japanese wild mice-derived inbred strains and Japanese fancy mice-derived JF1/Ms strain. We thank Dr Hatsumi Nakata, Ayumi Murakami, Hiroyuki Yasuda, and Tomomi Hashimoto for their excellent technical assistance. We gratefully acknowledge Dr Guy G. Musser in Charleston, USA, for his interest in this paper and for providing us with a copy of the rare 1998 publication by Dr Joe Marshall. We much appreciate Ms Reina de Raat of the University Museum of the University of Utrecht, the Netherlands, who researched Dr Hendrik Zwaardemaker, the physiologist who provided Dr Droogleever Fortuyn with one specimen of the type series of *Mus wagneri rotans*. We are indebted to Mr Martin Braak of the Nederlandse Knaagdierenfokkers Vereniging (Dutch Society for Rodent Breeding), who informed us about the present situation of the Japanese dancing mouse in the Netherlands, where it is no longer kept, and of dancing in some other rodent species as well.

Additional information

Conflict of interest

The authors have declared that no competing interests exist.

Ethical statement

No ethical statement was reported.

Funding

No funding was reported.

Author contributions

Writing - original draft: MC, AY, TT, TS, WB. Writing - review and editing: MC.

Author ORCIDs

Toyoyuki Takada  <https://orcid.org/0000-0001-6796-2085>

Toshihiko Shiroishi  <https://orcid.org/0000-0003-0535-2016>

Atsushi Yoshiki  <https://orcid.org/0000-0002-9450-5151>

Data availability

All of the data that support the findings of this study are available in the main text

References

- Allen GM (1927) Murid rodents from the Asiatic expeditions. *American Museum Novitates* 270: 1–12.
- Bonhomme F (1986) Evolutionary relationships in the genus *Mus*. In: Potter M, Nadeau JH, Cancro MP (Eds) *The Wild Mouse in Immunology. Current Topics in Microbiology and Immunology*, vol. 127. Springer, Berlin & Heidelberg, 19–34. https://doi.org/10.1007/978-3-642-71304-0_3
- Carleton M, Musser G (2005) Order Rodentia. In: Wilson DE, Reeder DM (Eds) *Mammal Species of the World: a Taxonomic and Geographic Reference*. The Johns Hopkins University Press, Baltimore, 745–752.
- Droogleever Fortuyn AB (1911) *De cyto-architectonie der Groote Hersenschors van eenige knaagdieren*. Scheltema en Hokema's Boekhandel, Amsterdam, 179 pp.
- Droogleever Fortuyn AB (1912) Über den systematischen Wert der japanischen Tanzmaus (*Mus wagneri* varietas *rotans* nov. var.). *Zoologischer Anzeiger* 39: 177–190.
- Droogleever Fortuyn AB (1927) Histological experiments with the brain of some rodents. *The Journal of Comparative Neurology* 42(3): 349–391. <https://doi.org/10.1002/cne.900420302>
- Droogleever Fortuyn AB (1928) Selection of the number of tailrings in the albino *Mus musculus*. *Experimental Biology and Medicine* (Maywood, N.J.) 25(7): 543–544. <https://doi.org/10.3181/00379727-25-3944>
- Droogleever Fortuyn AB (1929) The Chinese house-mouse and its tame varieties: A comparative study with *Mus musculus*. *Bulletin of the Peking Society of Natural History* 3: 59–64.
- Droogleever Fortuyn AB (1931) A cross between mice with different numbers of tailrings. *Genetics* 16(6): 591–594. <https://doi.org/10.1093/genetics/16.6.591>
- Droogleever Fortuyn AB (1934) A remarkable cross in *Mus musculus*. *Genetica* 16(3–4): 321–359. <https://doi.org/10.1007/BF02071501>
- Droogleever Fortuyn AB (1935) The influence of the sex chromosome on the number of tailrings in *Mus musculus*. *Genetica* 17(3–4): 291–298. <https://doi.org/10.1007/BF01985015>
- Droogleever Fortuyn AB (1939) A polydactylous strain of mice. *Genetica* 21(1–2): 97–108. <https://doi.org/10.1007/BF01508571>
- Droogleever Fortuyn AB, Meng T (1937) Abnormalities in the shaker mouse. *Peking Natural History Bulletin* 12: 9–12.
- Gates WH (1925) The Japanese waltzing mouse, its origin and genetics. *Proceedings of the National Academy of Sciences of the United States of America* 11(10): 651–653. <https://doi.org/10.1073/pnas.11.10.651>
- Gates WH (1926) The Japanese waltzing mouse: its origin, heredity and relation to the genetic characters of other varieties of mice. In: Castle WE (Ed.) *Contributions to a Knowledge of Inheritance in Mammals*. Carnegie Institute, Washington, DC, 83–138.

- Keeler CE (1931) The laboratory mouse: Its origin, heredity and culture. *Nature* 128(3228): 431. <https://doi.org/10.1038/128431b0>
- Kikkawa Y, Miura I, Takahama S, Wakana S, Yamazaki Y, Moriwaki K, Shiroishi T, Yonekawa H (2001) Microsatellite database for MSM/Ms and JF1/Ms, *molossinus*-derived inbred strains. *Mammalian Genome* 12(9): 750–752. <https://doi.org/10.1007/s003350030008>
- Koide T, Moriwaki K, Uchida K, Mita A, Sagai T, Yonekawa H, Katoh H, Miyashita N, Tsuchiya K, Nielsen TJ, Shiroishi T (1998) A new inbred strain JF1 established from Japanese fancy mouse carrying the classic piebald allele. *Mammalian Genome* 9(1): 15–19. <https://doi.org/10.1007/s003359900672>
- Makino S (1941) Studies on the murine chromosomes. I. Cytological investigations of mice, included in the genus *Mus*. *Journal of the Faculty of Science of the Hokkaido Imperial University Series VI Zoology* 7: 305–380.
- Marshall JT (1977) A synopsis of Asian species of *Mus* (Rodentia, Muridae). *Bulletin of the American Museum of Natural History* 158: 216–220.
- Marshall JT (1998) Identification and Scientific Names of Eurasian House Mice and their European allies, Subgenus *Mus* (Rodentia: Muridae). National Museum of Natural History, Springfield, 80 pp.
- Minezawa M, Moriwaki K, Kondo K (1981) Geographical survey of protein variations in wild populations of Japanese house mouse, *Mus musculus molossinus*. *Japanese Journal of Genetics* 56(1): 27–39. <https://doi.org/10.1266/jjg.56.27>
- Morse HCI (1978) Origins of Inbred Mice: Proceedings of a Workshop, Bethesda, Maryland, February 14–16, 1978, Sponsored by Cancer Research Institute, Inc. and National Institute of Allergy and Infectious Diseases. Academic Press, New York, 719 pp.
- Nunome M, Ishimori C, Aplin KP, Tsuchiya K, Yonekawa H, Moriwaki K, Suzuki H (2010) Detection of recombinant haplotypes in wild mice (*Mus musculus*) provides new insights into the origin of Japanese mice. *Molecular Ecology* 19: 2474–2489. <https://doi.org/10.1111/j.1365-294X.2010.04651.x>
- Schwarz E (1942) Origin of the Japanese Waltzing Mouse. *Science* 95(2454): 46. <https://doi.org/10.1126/science.95.2454.46>
- Schwarz E, Schwarz HK (1943) The Wild and Commensal Stocks of the House Mouse, *Mus musculus* Linnaeus. *Journal of Mammalogy* 24(1): 59. <https://doi.org/10.2307/1374781>
- Takada T, Mita A, Maeno A, Sakai T, Shitara H, Kikkawa Y, Moriwaki K, Yonekawa H, Shiroishi T (2008) Mouse inter-subspecific consomic strains for genetic dissection of quantitative complex traits. *Genome Research* 18(3): 500–508. <https://doi.org/10.1101/gr.7175308>
- Takada T, Ebata T, Noguchi H, Keane TM, Adams DJ, Narita T, Shin-I T, Fujisawa H, Toyoda A, Abe K, Obata Y, Sakaki Y, Moriwaki K, Fujiyama A, Kohara Y, Shiroishi T (2013) The ancestor of extant Japanese fancy mice contributed to the mosaic genomes of classical inbred strains. *Genome Research* 23(8): 1329–1338. <https://doi.org/10.1101/gr.156497.113>
- Takada T, Fukuta K, Usuda D, Kushida T, Kondo S, Kawamoto S, Yoshiki A, Obata Y, Fujiyama A, Toyoda A, Noguchi H, Shiroishi T, Masuya H (2021) MoG+: A database of genomic variations across three mouse subspecies for biomedical research. *Mammalian Genome* 33(1): 31–43. <https://doi.org/10.1007/s00335-021-09933-w>
- Yerkes RM (1907) *The Dancing Mouse: a Study in Animal Behavior*. Vol. 1. The Macmillan Company, New York, 290 pp. <https://doi.org/10.1037/10935-001>
- Yonekawa H, Moriwaki K, Gotoh O, Hayashi JI, Watanabe J, Miyashita N, Petras ML, Tagashira Y (1981) Evolutionary relationships among five subspecies of *Mus musculus*

- based on restriction enzyme cleavage patterns of mitochondrial DNA. *Genetics* 98(4): 801–816. <https://doi.org/10.1093/genetics/98.4.801>
- Yonekawa H, Moriwaki K, Gotoh O, Miyashita N, Migita S, Bonhomme F, Hjorth JP, Petras ML, Tagashira Y (1982) Origins of laboratory mice deduced from restriction patterns of mitochondrial DNA. *Differentiation. Research in Biological Diversity* 22: 222–226. <https://doi.org/10.1111/j.1432-0436.1982.tb01255.x>
- Yonekawa H, Takahama S, Gotoh O, Miyashita N, Moriwaki K (1994) Genetic diversity and geographic distribution of *Mus musculus* subspecies based on the polymorphism of mitochondrial DNA. In: Kazuo M, Toshihiko S, Hiromichi Y (Eds) *Genetics in Wild Mice: 1st Application to Biomedical Research*. S. Karger AG, Basel, 25–40. <https://doi.org/10.1159/000424145>
- Yoshiki A, Moriwaki K (2006) Mouse phenome research: Implications of genetic background. *ILAR Journal* 47(2): 94–102. <https://doi.org/10.1093/ilar.47.2.94>

New species and records of *Hybos* Meigen (Diptera, Empidoidea) from Huaping National Nature Reserve, China

Meilin Li¹, Jingyu Wang², Ding Yang¹

¹ Department of Entomology, College of Plant Protection, China Agricultural University, Beijing 100193, China

² Comprehensive Technology Service Center of Rizhao Customs, Rizhao 276826, China

Corresponding author: Ding Yang (dyangcau@126.com)

Abstract

In this study, 21 species of *Hybos* Meigen, 1803 are reviewed in Huaping National Nature Reserve, China. Among these, three species, i.e., *Hybos denticulatus* **sp. nov.**, *Hybos forcipata* **sp. nov.** and *H. paraterminalis* **sp. nov.**, are described as new to science. In addition, nine known species of this genus are reported for the first time in Guangxi. All the known species were enumerated, and an identification key to the species of *Hybos* from Huaping National Nature Reserve based on morphological characteristics is provided.

Key words: Checklist, hybotid flies, key, new species, newly recorded species, South China region, taxonomy,



Academic editor: Marija Ivković

Received: 5 February 2024

Accepted: 2 April 2024

Published: 2 May 2024

ZooBank: <https://zoobank.org/4346D5B4-D587-4DFC-BF91-367C12698B5C>

Citation: Li M, Wang J, Yang D (2024) New species and records of *Hybos* Meigen (Diptera, Empidoidea) from Huaping National Nature Reserve, China. ZooKeys 1200: 41–63. <https://doi.org/10.3897/zookeys.1200.120258>

Copyright: © Meilin Li et al.
This is an open access article distributed under terms of the Creative Commons Attribution License (Attribution 4.0 International – CC BY 4.0).

Introduction

Hybos Meigen, 1803 is a species-rich genus of Empidoidea occurring worldwide. To date, 242 species of *Hybos* have been recorded worldwide, of which 28 species are distributed in the Palaearctic Realm and 191 species are distributed in the Oriental Realm (Yang and Yang 2004; Yang et al. 2007; Plant 2013; Shamshev et al. 2013; Shamshev et al. 2015; Li et al. 2017; Cao et al. 2018; Kanavalová et al. 2021; Li et al. 2022; Li and Yang 2023).

Huaping National Nature Reserve, the oldest national-level nature reserve established in Guangxi, has rich and diverse animal and plant resources and is an important gene bank of biological species in China. The climate here is humid, with relative humidity ranging from 85% to 90% during the rainy season from April to August, and a forest coverage rate of 98.2%, providing a relatively suitable environment for the survival of *Hybos*. During the collection investigation of Huaping National Nature Reserve in June 1982, five new *Hybos* species were discovered and reported (*H. ensatus* Yang & Yang, 1986, *H. flaviscutellum* Yang & Yang, 1986, *H. longshengensis* Yang & Yang, 1986, *H. orientalis* Yang & Yang, 1986, *H. truncatus* Yang & Yang, 1986), showcasing its rich biodiversity (Yang and Yang, 2004).

We surveyed the insect diversity in the national nature reserve twice in 2023 to update the faunal information of the South China region. In this study, three new species, *H. denticulatus* **sp. nov.**, *H. forcipata* **sp. nov.** and *H. paraterminalis* **sp. nov.**, are reported and described. While, nine species, *H. bawanglingensis*

Yang, 2008, *H. fujianensis* Li & Yang, 2023, *H. guizhouensis* Yang & Yang, 1988, *H. jianyangensis* Yang & Yang, 2004, *H. leucopogus* Li & Yang, 2023, *H. obtusatus* Yang & Grootaert, 2005, *H. particularis* Yang, Yang & Hu, 2002, *H. pingbianensis* Yang & Yang, 2004 and *H. xiaohuangshanensis* Yang, Gaimari & Grootaert, 2005 are newly recorded in Guangxi.

Diagnosis and figures are provided for all 21 species, including related known ones (*H. anae* Yang & Yang, 2004, *H. chinensis* Yang & Yang, 2004, *H. ensatus* Yang & Yang, 1986, *H. flaviscutellum* Yang & Yang, 1986, *H. longshengensis* Yang & Yang, 1986, *H. orientalis* Yang & Yang, 1986 and *H. truncatus* Yang & Yang, 1986). Further, the male genitalia of *H. bawanglingensis* and *H. nasutus* Yang & Yang, 1986 are re-illustrated, and 13 known species are photographed (*H. bawanglingensis*, *H. ensatus*, *H. fujianensis*, *H. guizhouensis*, *H. jianyangensis*, *H. longshengensis*, *H. nasutus*, *H. obtusatus*, *H. orientalis*, *H. particularis*, *H. pingbianensis*, *H. truncatus* and *H. xiaohuangshanensis*). A checklist and key of *Hybos* from Huaping National Nature Reserve are also provided.

Material and methods

Material for this study were collected by sweeping in Huaping National Nature Reserve, Guangxi in May and August 2023. All the studied specimens are preserved in 80% ethanol and deposited in the Entomological Museum of China Agricultural University (CAU), Beijing.

Specimens were examined using a ZEISS Stemi 2000c. Images were made by connecting the microscope with a Canon EOS 5D Mark IV camera. Image plates were post-processed with Adobe Photoshop CS6 Extended. Representative specimens were dissected. Male external genitalia were drawn after macerating the apical portion of the abdomen with cold 20% hydroxide (NaOH) for 4–8 h. Species of *Hybos* from China have been thoroughly reviewed and keyed (Yang and Yang 2004), providing us with a useful tool to identify the species in this study.

Abbreviations and morphological terms used in the text: **acr**–acrostichal bristle(s), **ad**–anterodorsal bristle(s), **av**–anteroventral bristle(s), **dc**–dorsocentral bristle(s), **ppn**–postpronotal humeral bristle(s), **npl**–notopleural bristle(s), **oc**–ocellar bristle(s), **pd**–posterodorsal bristle(s), **prsc**–prescutellar bristle(s), **psa**–postalar bristle(s), **pv**–posteroventral bristle(s), **sc**–scutellar bristle(s).

Taxonomy

Family Hybotidae Meigen, 1820

Hybotinae Meigen, 1820: x. Type genus *Hybos* Meigen, 1803.
Hybotidae Macquart, 1827: 136.

Genus *Hybos* Meigen, 1803.

Hybos Meigen, 1803: 269. Type species: *Hybos funebris* Meigen, 1804.
Neozia Meigen, 1800: 27. Type species: *Musca grossipes* Linnaeus, 1767.
Pseudosyneches Frey, 1953: 66. Type species: *Hybos (Pseudosyneches) palawanus* Frey, 1953.

Diagnosis. *Hybos* is distinguished from all other Empidoidea genera by the following combination of characters: (1) vein Rs short arising distal to the middle of cell bm; (2) cell cup usually distinctly longer than bm; (3) eyes narrowly but distinctly separated on face, not virtually contiguous; (4) proboscis narrow, long spine-like, as long as head or longer, lacking pseudotracheae; (5) hind femur usually strongly thickened with strong ventral bristles; and (6) hind tibia linear (apart from basal geniculation) or slightly thickened apically.

Key to species of *Hybos* from Huaping National Nature Reserve

This key is used for identifying *Hybos* in Huaping National Nature Reserve. Users are urged to confirm all decisions by referring to detailed descriptions. There are likely to be other undiscovered new species in Huaping National Nature Reserve. Therefore, it needs to be used with caution.

- 1 All legs uniformly dark brown to black excluding hind knee 2
 - Legs at least partly yellow to yellow-brown excluding hind knee..... 9
- 2 All legs uniformly black-brown to black including hind knee..... 3
 - Legs dark brown to blackish, but only hind knee dark yellow
..... *H. fujianensis* Li & Yang, 2023
- 3 Hind tibia apically without one pd and one av 4
 - Hind tibia apically with one pd and one av *H. paraterminalis* sp. nov.
- 4 Hind tibia without distinct bristles 5
 - Hind tibia with one dorsal bristle near apex 7
- 5 Mid tibia with one or two dorsal bristles..... 6
 - Mid tibia with four dorsal bristles..... *H. jianyangensis* Yang & Yang, 2004
- 6 R_{4+5} and M_1 nearly parallel apically; mid tibia with two long dorsal bristles on basal $\frac{1}{2}$ *H. anae* Yang & Yang, 2004
 - R_{4+5} and M_1 weakly convergent apically; mid tibia with one very long dorsal bristle at middle..... *H. leucopogus* Li & Yang, 2023
- 7 Mid femur with ad and pv 8
 - Mid femur only with pv..... *H. obtusatus* Yang & Grootaert, 2005
- 8 Hypandrium with row of long bristles near apical margin.....
..... *H. denticulatus* sp. nov.
 - Hypandrium without long bristles near apical margin
..... *H. forcipata* sp. nov.
- 9 Fore and mid femora brownish to black 10
 - Fore and mid femora uniformly or mostly yellow..... 15
- 10 Mid tibia black-brown to black..... 11
 - Mid tibia yellow to brownish 12
- 11 Hind knee black-brown and fore tibia only with one dorsal bristle at middle..... *H. ensatus* Yang & Yang, 1986
 - Hind knee yellow and fore tibia with four to five dorsal bristles
..... *H. xiaohuangshanensis* Yang, Gaimari & Grootaert, 2005
- 12 Legs uniformly brownish *H. truncatus* Yang & Yang, 1986
 - Legs partly brownish..... 13
- 13 Fore tarsomeres 1–2 yellow *H. guizhouensis* Yang & Yang, 1988
 - Fore tarsomeres 1–2 black-brown to black..... 14

14	Left surstylus with two processes	16
 <i>H. longshengensis</i> Yang & Yang, 1986	
–	Left surstylus with three processes	
 <i>H. particularis</i> Yang, Yang & Hu, 2002	
15	Fore and mid femora uniformly yellow including dorsally	16
–	Fore and mid femora mostly yellow except dark yellow-brown dorsally	
 <i>H. serratus</i> Yang & Yang, 1992	
16	Hind femur black-brown to black	17
–	Hind femur mostly yellow	18
17	Fore coxa black-brown	<i>H. chinensis</i> Yang & Yang, 2004
–	Fore coxa yellow	<i>H. pingbianensis</i> Yang & Yang, 2004
18	Hind tibia with one dorsal bristle at middle	19
–	Hind tibia without dorsal bristles at middle	
 <i>H. flaviscutellum</i> Yang & Yang, 1986	
19	Arista with short pubescence	20
–	Arista bare	<i>H. nasutus</i> Yang & Yang, 1986
20	Right surstylus furcated, with three processes	
 <i>H. bawanglingensis</i> Yang, 2008	
–	Right surstylus triangular, without processes	
 <i>H. orientalis</i> Yang & Yang, 1986	

Checklist of *Hybos* in Huaping National Nature Reserve of China

New records in Guangxi in bold

- Hybos anae* Yang & Yang, 2004 (Fujian, Guangxi)
Hybos bawanglingensis Yang, 2008 (**Guangxi**, Hainan)
Hybos chinensis Yang & Yang, 2004 (Fujian, Guangxi, Guizhou, Zhejiang)
Hybos denticulatus sp. nov. (Guangxi)
Hybos ensatus Yang & Yang, 1986 (Guangxi, Guizhou, Henan, Sichuan)
Hybos flaviscutellum Yang & Yang, 1986 (Guangxi, Zhejiang)
Hybos forcipata sp. nov. (Guangxi)
Hybos fujianensis Li & Yang, 2023 (Fujian, **Guangxi**)
Hybos guizhouensis Yang & Yang, 1988 (**Guangxi**, Guizhou)
Hybos jianyangensis Yang & Yang, 2004 (Fujian, **Guangxi**, Guizhou, Zhejiang)
Hybos leucopogus Li & Yang, 2023 (Fujian, **Guangxi**)
Hybos longshengensis Yang & Yang, 1986 (Fujian, Guangxi)
Hybos nasutus Yang & Yang, 1986 (Guangxi)
Hybos obtusatus Yang & Grootaert, 2005 (Guangdong, **Guangxi**, Guizhou)
Hybos orientalis Yang & Yang, 1986 (Fujian, Guangxi, Henan)
Hybos paraterminalis sp. nov. (Guangxi)
Hybos particularis Yang, Yang & Hu, 2002 (**Guangxi**, Hainan)
Hybos pingbianensis Yang & Yang, 2004 (**Guangxi**, Yunnan)
Hybos serratus Yang & Yang, 1992 (Fujian, Guangxi, Guizhou, Henan, Sichuan, Yunnan, Zhejiang; Thailand)
Hybos truncatus Yang & Yang, 1986 (Guangxi)
Hybos xiaohuangshanensis Yang, Gaimari & Grootaert, 2005 (Fujian, Guangdong, **Guangxi**)

***Hybos anae* Yang & Yang, 2004**

Fig. 1

Hybos anae Yang & Yang, 2004: 124.

Type locality. CHINA: Guangxi, Longsheng.

Diagnosis. Legs entirely black-brown. R_{4+5} and M_1 nearly parallel apically. Hypandrium shallowly incised apically, with one long thick finger-like right process, bifurcated apically, and small subtriangular left process.

Distribution. China (Fujian, Guangxi).

***Hybos bawanglingensis* Yang, 2008**

Fig. 2

Hybos bawanglingensis Yang, 2008: 618.

Type locality. China: Hainan, Bawangling.

Material examined. CHINA • 2♂ 1♀, Guangxi, Guilin, Huaping, Tianpingshan; 770 m, 1 June 2023; Wei Zeng; CAU. China • 1♂ 3♀, Guangxi, Laibin, Dayaoshan, Shengtangshan; 1434 m, 14 August 2023; Wenqiang Cao; CAU.

Diagnosis. Legs yellow except hind knee dark brown, tarsomeres 3–5 black. Hind tibia with one ad at middle. Hypandrium with a narrow cleft apically.

Distribution. China (Guangxi, Hainan).

***Hybos chinensis* Yang & Yang, 2004**

Fig. 3

Hybos chinensis Frey, 1953: 64; Yang and Yang 2004: 143.

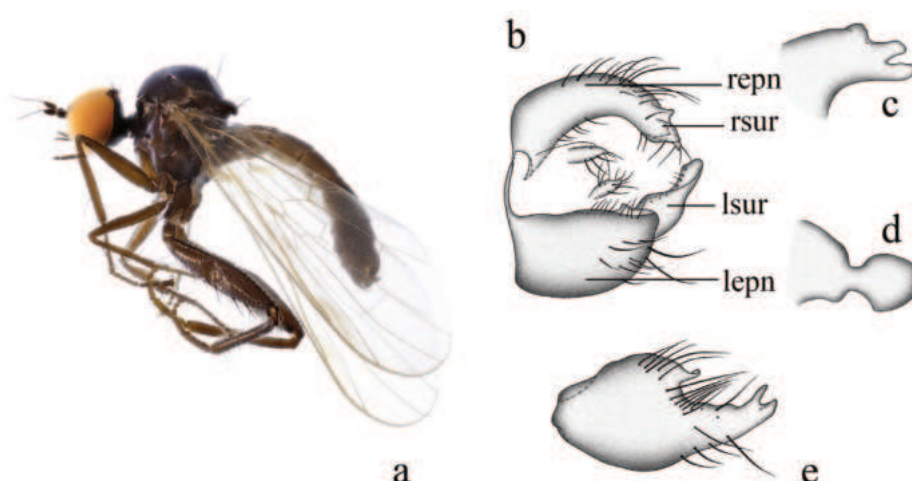


Figure 1. *Hybos anae* a male habitus, lateral view b genitalia, dorsal view c right surstylus d left surstylus e hypandrium, ventral view (after Li and Yang 2023). Abbreviations: lepn = left epandrial lamella; lsur = left surstylus; repn = right epandrial lamella; rsur = right surstylus.

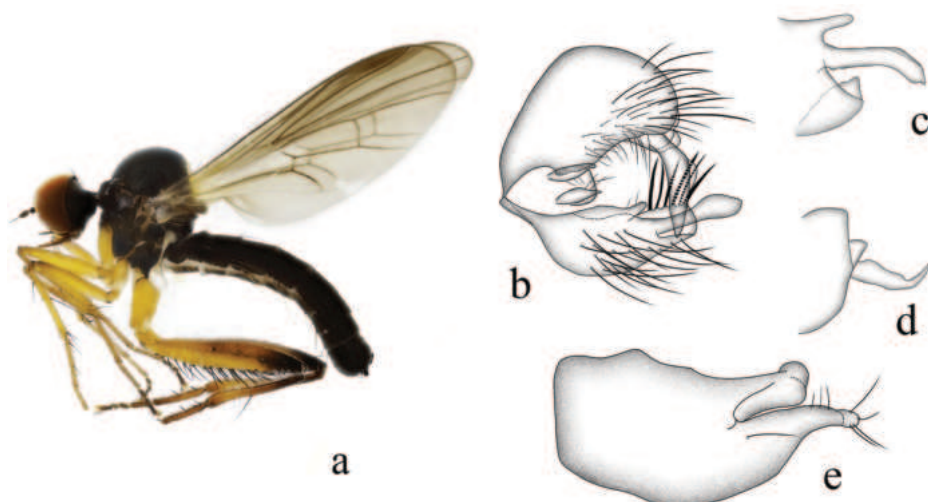


Figure 2. *Hybos bawanglingensis* a male habitus, lateral view b genitalia, dorsal view c right surstylus d left surstylus e hypandrium, ventral view

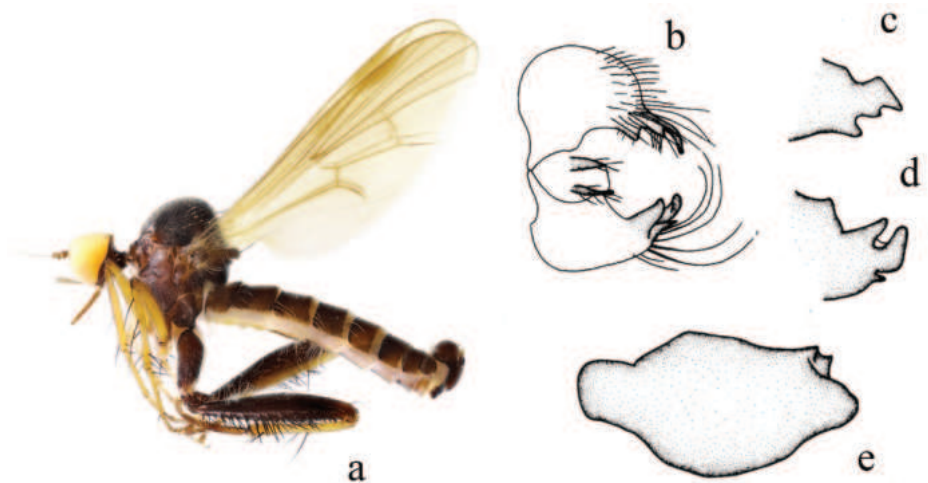


Figure 3. *Hybos chinensis* a male habitus, lateral view b genitalia, dorsal view c right surstylus d left surstylus e hypandrium, ventral view (after Yang and Yang 2004)

Type locality. China: Fujian.

Material examined. CHINA • 6♂, Guangxi, Guilin, Huaping, Anjiangping; 1340 m, 26 May 2023; Wei Zeng; CAU.

Diagnosis. Legs black-brown, except fore and mid knees, femora, tarsomeres 1–2 and all tibiae yellow; fore and mid tarsomeres 3–5 yellow-brown, hind tarsus yellow-brown. Hypandrium with small process on left corner.

Distribution. China (Fujian, Guangxi, Guizhou, Zhejiang).

***Hybos denticulatus* sp. nov.**

<https://zoobank.org/416CDB05-FFAF-415A-BA07-45606E7C65F1>

Fig. 4

Type material examined. Holotype: CHINA • ♂; Guangxi, Guilin, Huaping, Anjiangping; (25°33'44.2"N, 109°56'42.4"E, 1340 m), 28 May 2023, Wei Zeng; CAU.

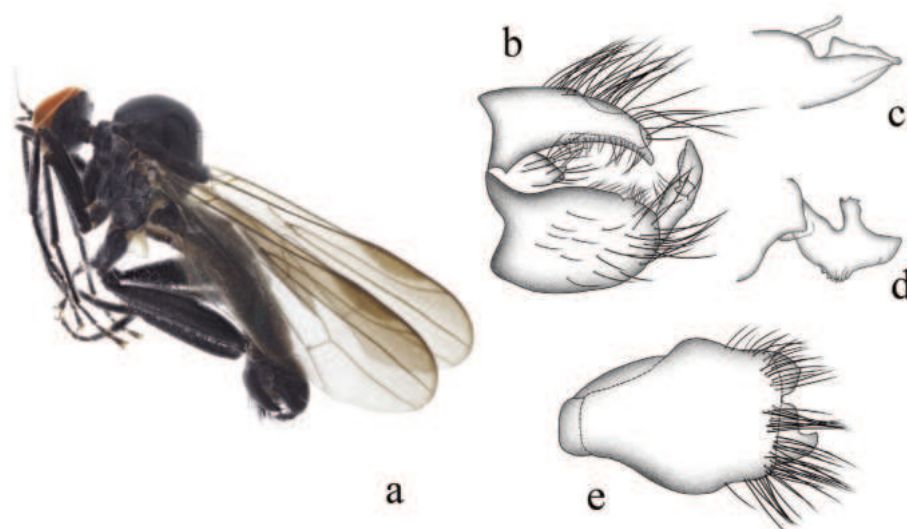


Figure 4. *Hybos denticulatus* sp. nov. **a** male habitus, lateral view **b** genitalia, dorsal view **c** right surstylus **d** left surstylus **e** hypandrium, ventral view

Diagnosis. Legs entirely black. Hind tibia with one ad near apex. R_{2+3} curved, R_{4+5} and M_1 slightly convergent apically. Hypandrium with row of long bristles near apical margin.

Description. Male. Body length 4.7 mm. Wing length 4.3 mm.

Head black with gray pollen. Eyes contiguous on frons, black-brown with slightly enlarged dorsal facets yellow-brown. Hairs and bristles on head black except posteroventral surface with partly dark brown hairs; ocellar tubercle distinct with two long oc and two short posterior hairs. Antenna black; scape without hairs, pedicel with circlet of blackish subapical hairs; first flagellomere blackish, not elongated, nearly as long as scape and pedicel combined, without dorsal hairs; arista blackish, short pubescent except apical $\frac{1}{4}$ or so thin and bare. Proboscis shorter than head, black. Palpus blackish, with one blackish apical hair.

Thorax black with gray pollen. Hairs on thorax blackish, bristles black; hairs on mesonotum slightly long, ppn absent, two npl (anterior npl rather short), uniserial hair-like dc nearly as long as irregularly quadriserial acr, two prsc, one psa; scutellum with eight marginal hairs and two sc. Legs entirely black. Hairs on legs mostly dark brown to blackish, bristles black-brown to black, but those on coxae partly brownish. Fore femur 1.3 \times and hind femur 1.9 \times as wide as mid femur. Fore femur with row of pv distinctly longer than femur thickness. Mid femur with 3–4 ad on basal $\frac{1}{3}$ and row of pv distinctly longer than femur thickness; apically with one weak ad. Hind femur with row of ad on apical $\frac{2}{3}$, ~ three rows of spine-like ventral bristles on tubercles and some dorsal hairs on basal $\frac{1}{5}$. Fore tibia with row of short or slightly long ad and some long thin pv hairs; apically with 4 bristles including one thick ad. Mid tibia with row of thin or slightly thick ad; apically with one long av. Hind tibia with one ad near apex. Fore tarsomere 1 with some long ad and pv hairs. Mid tarsomere 1 with one ad near middle; apically with one slightly long ad. Hind tarsomere 1 with short dense spine-like ventral bristles. Wing hyaline, stigma dark brown; veins brown to black-brown, R_{2+3} curved, R_{4+5} and M_1 slightly convergent apically. Squama dark yellow with dark yellow hairs. Halter dark yellow with dark brown stem and pale-yellow knob.

Abdomen short thick, black with pale gray pollen, hypopygium slightly thicker than pregenital segments. Hairs and bristles on abdomen yellow-brown to brown except those on hypopygium black.

Male genitalia. Left epandrial lamella distinctly wider than right epandrial lamella (Fig. 4b); left surstylus with wide finger-like process, right lateral margin with one process, left lateral margin with some middle denticles (Fig. 4d). Right epandrial lamella with concave inner margin; right surstylus with long wide subtriangular process, lateral margin with one thin finger-like process apically (Fig. 4c). Hypandrium ~ 1.5× longer than wide, narrow basally and wide apically, apical margin with two wide processes, with row of long bristles near apical margin (Fig. 4e).

Female. Unknown.

Etymology. This specific name refers to the left surstylus with some middle denticles on the lateral margin.

Distribution. China (Guangxi).

Remarks. The new species is similar to *H. brevis* Yang & Yang from Zhejiang, 1995, but may be separated by the arista and the left surstylus. In the new species, the arista is short pubescent, and the left surstylus has some middle denticles on the lateral margin. In *H. brevis*, the arista is bare, and the left surstylus lacks denticles (Yang and Yang 2004).

Hybos ensatus Yang & Yang, 1986

Fig. 5

Hybos ensatus Yang & Yang, 1986: 83; Yang and Yang 2004: 155.

Type locality: CHINA: Guangxi, Longsheng.

Diagnosis. Legs black-brown, except mid tarsi yellow-brown. Mid tibia with 2 long bristles on basal half. Male genitalia: left epandrial lobe with process at inner margin near middle; right surstylus sword-shaped.

Distribution. China (Guangxi, Guizhou, Henan, Sichuan).

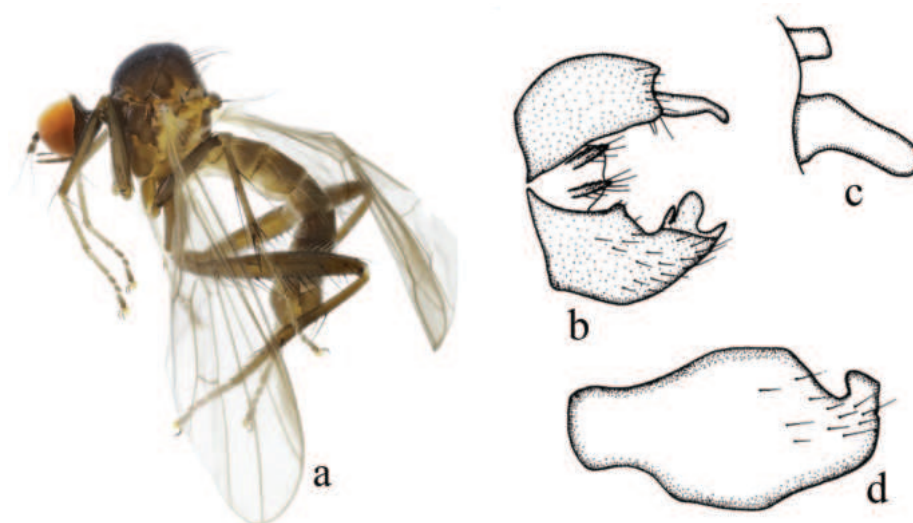


Figure 5. *Hybos ensatus* **a** male habitus, lateral view **b** genitalia, dorsal view **c** right surstylus **d** hypandrium, ventral view. (b–d: after Yang and Yang 2004)

***Hybos flaviscutellum* Yang & Yang, 1986**

Fig. 6

Hybos flaviscutellum Yang & Yang, 1986: 81; Yang and Yang 2004: 158.

Type locality. CHINA: Guangxi, Longsheng.

Diagnosis. Scutellum yellow. Legs yellow to yellow-brown, except tarsomeres 3–5 dark yellow. Male genitalia: left epandrial lobe rather wide; left surstylus knife-shaped.

Distribution. China (Guangxi, Zhejiang).

***Hybos forcipata* sp. nov.**

<https://zoobank.org/4CC29607-1E47-49BA-8153-8C19966E2407>

Fig. 7

Type material examined. Holotype: CHINA ♂; Guangxi, Guilin, Huaping, Anjiangping; (25°33'42.0"N, 109°56'37.2"E, 1413 m), 7 August 2023, Wenqiang Cao; CAU.

Diagnosis. Legs entirely black. Mid tarsomere 1 with one ad near apex and some short or long hairs. R_{4+5} and M_1 slightly convergent apically. Left surstylus claw-shaped in lateral view.

Description. Male. Body length 3.3 mm. Wing length 2.8 mm.

Head black with gray pollen. Eyes contiguous on frons, black-brown with slightly enlarged dorsal facets yellow-brown. Hairs and bristles on head black except posteroventral surface with partly dark brown hairs; ocellar tubercle distinct with two very short hairs. Antenna blackish; scape without hairs, pedicel with circlet of black-brown subapical hairs; first flagellomere black-brown, slightly elongated, longer than scape and pedicel combined, without dorsal hairs; arista black-brown, short pubescent. Proboscis distinctly shorter than head, black-brown. Palpus blackish, with one black-brown apical hair.

Thorax black with gray pollen. Hairs on thorax blackish, bristles black; hairs on mesonotum short, ppn absent, two npl (anterior npl rather short), uniserial hair-like dc nearly as long as irregularly quadriserial acr, two prsc, one psa;

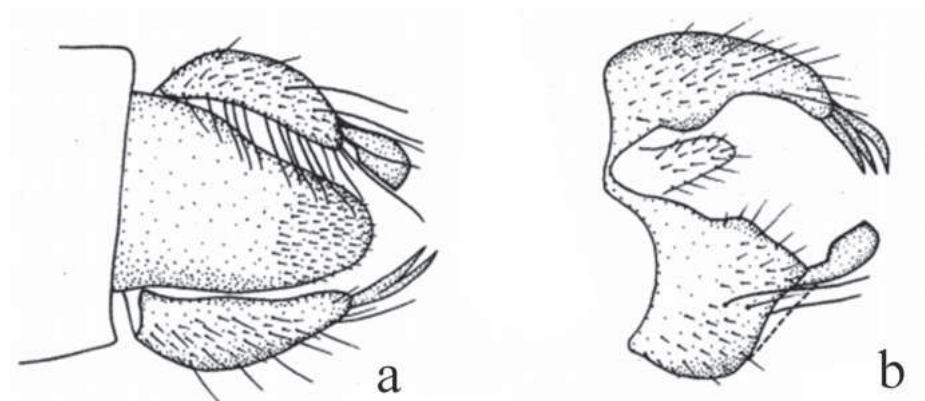


Figure 6. *Hybos flaviscutellum* **a** hypandrium, ventral view **b** genitalia, dorsal view (after Yang and Yang 2004)



Figure 7. *Hybos forcipata* sp. nov. **a** male habitus, lateral view **b** genitalia, dorsal view **c** right surstylus **d** left surstylus **e** hypandrium, ventral view

scutellum with eight marginal hairs and two sc. Legs entirely black. Hairs on legs mostly black-brown to black, bristles blackish to black, but those on coxae partly brown. Fore femur 1.5× and hind femur 2.4× as wide as mid femur. Fore femur with row of pv distinctly longer than femur thickness. Mid femur with row of ad on apical $\frac{1}{3}$ and row of long thin pv distinctly longer than femur thickness. Hind femur with two ad on apical $\frac{1}{2}$ and ~ three rows of long spine-like ventral bristles on tubercles. Fore tibia with some short or long ad and pv hairs. Mid tibia with two ad on basal $\frac{1}{2}$ and some long hairs; apically with one very long av. Hind tibia with one ad near apex. Fore tarsomere 1 with some short or long ad and pv hairs. Mid tarsomere 1 with one ad near apex and some short or long hairs. Hind tarsomere 1 with row of short dense spine-like ventral bristles. Wing hyaline, stigma brownish; veins brownish to dark brown, R_{4+5} and M_1 slightly convergent apically. Squama dark yellow with dark yellow hairs. Halter dark yellow with brown stem and pale-yellow knob.

Abdomen black with pale gray pollen. Hairs and bristles on abdomen brown except those on hypopygium blackish. Hypopygium distinctly thicker than pre-genital segments.

Male genitalia. Left epandrial lamella slightly narrower than right epandrial lamella, with inner margin obliquely subtruncate (Fig. 7b); left surstylus claw-shaped in lateral view; with one curved apical lateral process and one long process, furcated apically (Fig. 7d). Right epandrial lamella with weakly convex inner margin near middle; right surstylus furcated into one small triangular process and one finger-like process (Fig. 7c). Hypandrium ~ 2.2× longer than wide, narrow apically, right lateral margin with one trapezoid process and one triangle-like process (Fig. 7e).

Female. Unknown.

Etymology. This specific name refers to the claw-shaped left surstylus, in lateral view.

Distribution. China (Guangxi).

Remarks. The new species is similar to *H. curvatus* Yang & Grootaert, 2005 from Guangdong, but may be separated by the form of the fore tibia and hypan-

drium. In the new species, the fore tibia bears some ad and pv hairs, and the hypandrium has two processes at lateral margin. In *H. curvatus*, the fore tibia has one av and one pv apically, and the hypandrium lacks processes on the lateral margin (Yang and Grootaert 2005).

***Hybos fujianensis* Li & Yang, 2023**

Fig. 8

Hybos fujianensis Li & Yang, 2023: 313–351

Type locality. CHINA: Fujian, Wuyishan.

Material examined. CHINA • 1♂, Guangxi, Guilin, Huaping, Anjiangping; 1413 m, 7 August 2023; Wenqiang Cao; CAU.

Diagnosis. First flagellomere with two blackish dorsal hairs; arista bare. Legs mostly dark brown to black-brown. Hind tibia apically with long thin pd.

Distribution. China (Fujian, Guangxi).

***Hybos guizhouensis* Yang & Yang, 1988**

Fig. 9

Hybos guizhouensis Yang & Yang, 1988: 136; Yang and Yang 2004: 168.

Type locality. CHINA: Guizhou, Fanjingshan.

Material examined. CHINA • 1♂, Guangxi, Guilin, Huaping, Hongtan; 849 m, 30 May 2023; Wei Zeng; CAU.

Diagnosis. Legs brownish, except base of mid and hind tibia, fore and mid tarsomeres 1–2 yellow. Hypandrium with irregular process on apical margin.

Distribution. China (Guangxi, Guizhou).

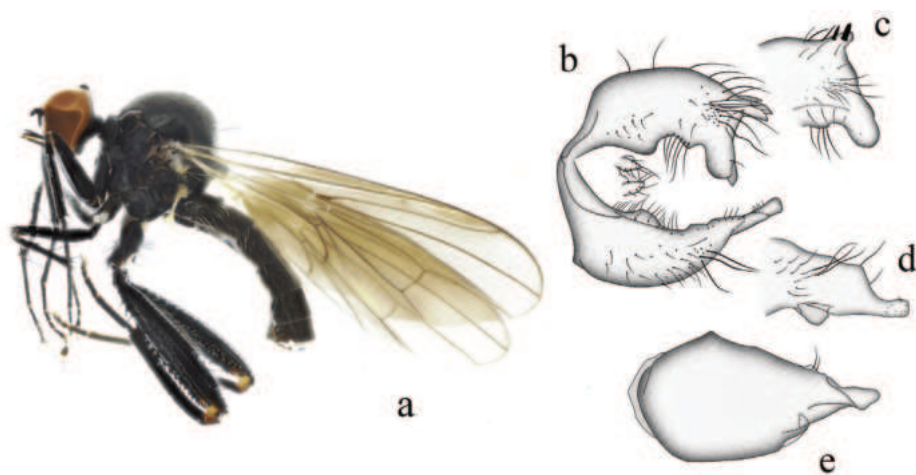


Figure 8. *Hybos fujianensis* a male habitus, lateral view b genitalia, dorsal view c right surstylus d left surstylus e hypandrium, ventral view (b–e: after Li and Yang 2023)

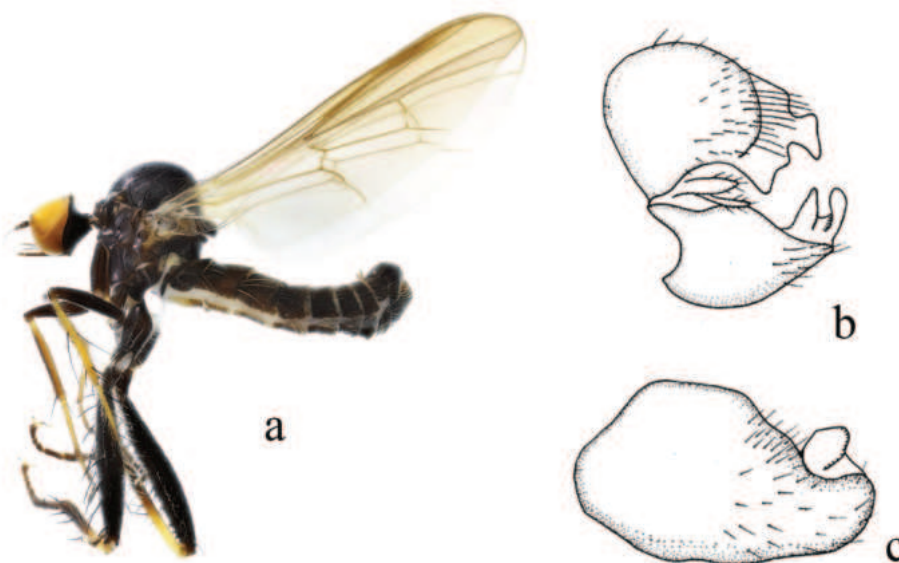


Figure 9. *Hybos guizhouensis* a male habitus, lateral view b genitalia, dorsal view c hypandrium, ventral view (b, c: after Yang and Yang 2004)

***Hybos jianyangensis* Yang & Yang, 2004**

Fig. 10

Hybos jianyangensis Yang & Yang, 2004: 178.

Type locality. CHINA: Fujian, Jianyang.

Material examined. CHINA • 2♂, Guangxi, Guilin, Huaping, Hongtan; 849 m, 30 May 2023; Wei Zeng; CAU.

Diagnosis. Legs entirely black. Mid tibia with 4 dorsal bristles and 2 ventral bristles. Male genitalia: left surstylus rather wide with short finger-like inner lateral process.

Distribution. China (Fujian, Guangxi, Guizhou, Zhejiang).

***Hybos leucopogus* Li & Yang, 2023**

Fig. 11

Hybos fujianensis Li & Yang, 2023: 313–351

Type locality. China: Fujian, Wuyishan.

Material examined. CHINA • 1♂ 1♀, Guangxi, Laibin, Dayaoshan, Yinshangongyuan; 1150 m, 15 August 2023; Wenqiang Cao; CAU.

Diagnosis. Legs entirely black. Hind femur distinctly thickened. Hind tibia with one row of ad hairs and four pd hairs on basal ½. R_{2+3} weakly curved, R_{4+5} and M_1 weakly convergent apically. Hypandrium narrow basally, bifurcated apically.

Distribution. China (Fujian, Guangxi).

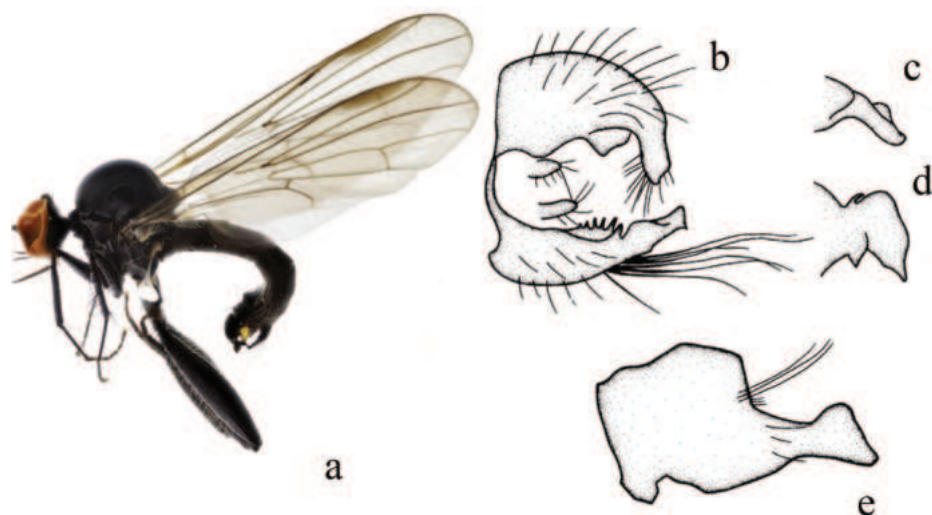


Figure 10. *Hybos jianyangensis* **a** male habitus, lateral view **b** genitalia, dorsal view **c** right surstylus **d** left surstylus **e** hypandrium, ventral view (**b–e**: after Yang and Yang 2004)

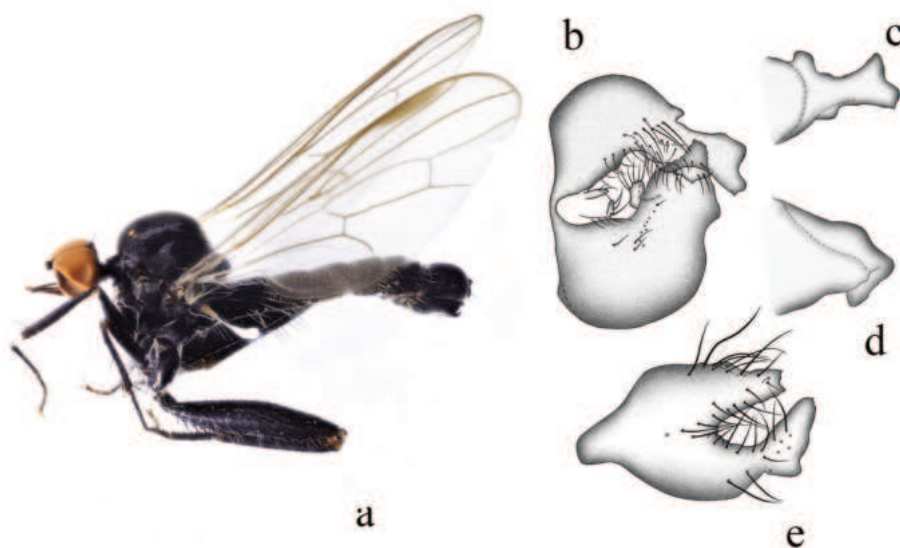


Figure 11. *Hybos leucopogus* **a** male habitus, lateral view **b** genitalia, dorsal view **c** right surstylus **d** left surstylus **e** hypandrium, ventral view (after Li and Yang 2023)

***Hybos longshengensis* Yang & Yang, 1986**

Fig. 12

Hybos longshengensis Yang & Yang, 1986: 78; Yang and Yang 2004: 187.

Type locality. CHINA: Guangxi, Longsheng.

Diagnosis. Arista bare. Legs black-brown, except mid tibia and tarsomeres 1–2 yellow, tips of hind femur, base and tips of tibia and all tarsi yellow. Hypandrium with right apical corner elongated outwards into one process.

Distribution. China (Fujian, Guangxi).

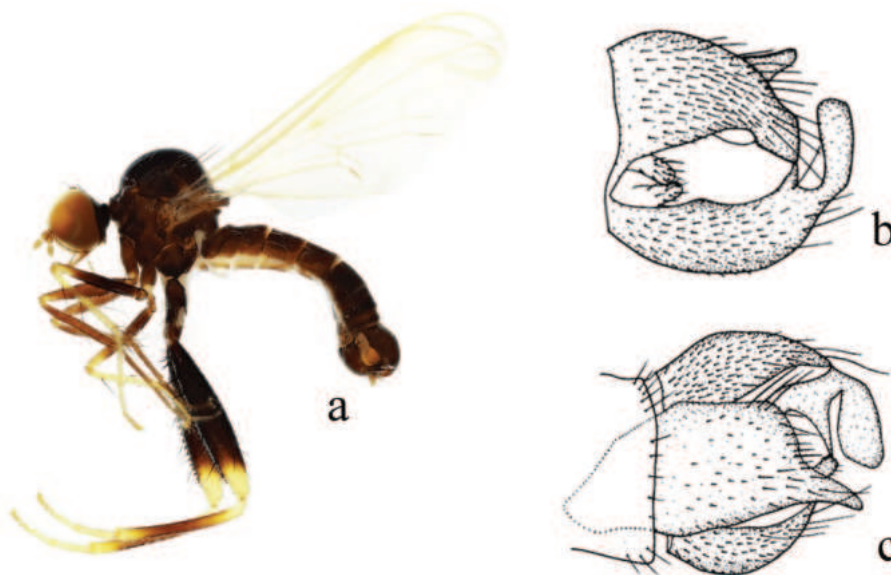


Figure 12. *Hybos longshengensis* a male habitus, lateral view b genitalia, dorsal view c hypandrium, ventral view (b, c: after Yang and Yang 2004)

***Hybos nasutus* Yang & Yang, 1986**

Fig. 13

Hybos nasutus Yang & Yang, 1986: 79; Yang and Yang 2004: 197.

Type locality. CHINA: Guangxi, Jinxiu.

Material examined. China • 4♂, Guangxi, Guilin, Huaping, Anjiangping; 1413 m, 7 August 2023; Wenqiang Cao; CAU. China • 3♂, Guangxi, Guilin, Huaping, Anjiangping; 1413 m, 7 August 2023, Wenqiang Cao; CAU.

Diagnosis. Arista bare. Legs yellow, except tarsomeres 3–5 dark yellow. Hind tibia with one dorsal bristle at middle; apically with one dorsal bristle and one ventral bristle.

Distribution. China (Guangxi).

***Hybos obtusatus* Yang & Grootaert, 2005**

Fig. 14

Hybos obtusatus Yang & Grootaert, 2005: 410.

Type locality. CHINA: Guangdong.

Material examined. China • 1♂, Guangxi, Guilin, Huaping, Anjiangping; 1340 m, 26 May 2023; Wei Zeng; CAU.

Diagnosis. Palpus blackish with two long bristles at tip. Legs entirely black. R_{4+5} and M_1 parallel apically.

Distribution. China (Guangdong, Guangxi, Guizhou).

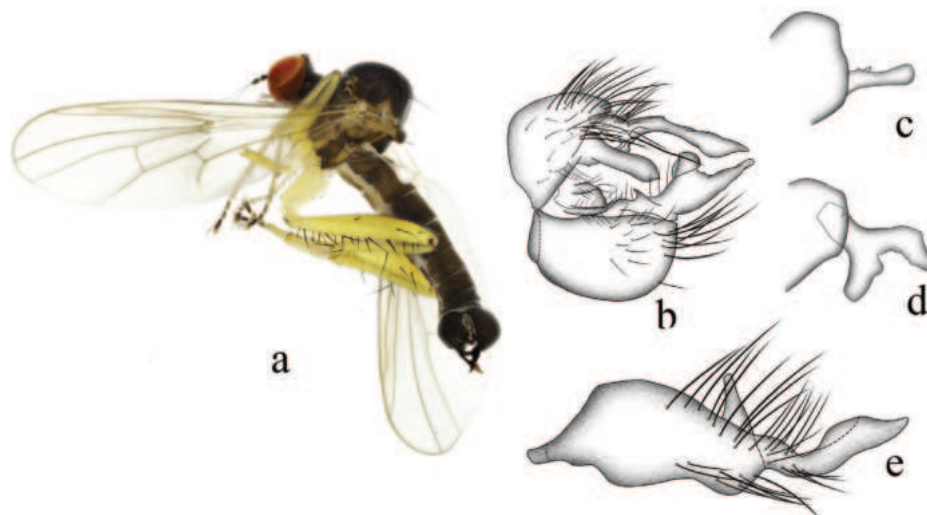


Figure 13. *Hybos longshengensis* a male habitus, lateral view b genitalia, dorsal view c right surstylus d left surstylus e hypandrium, ventral view

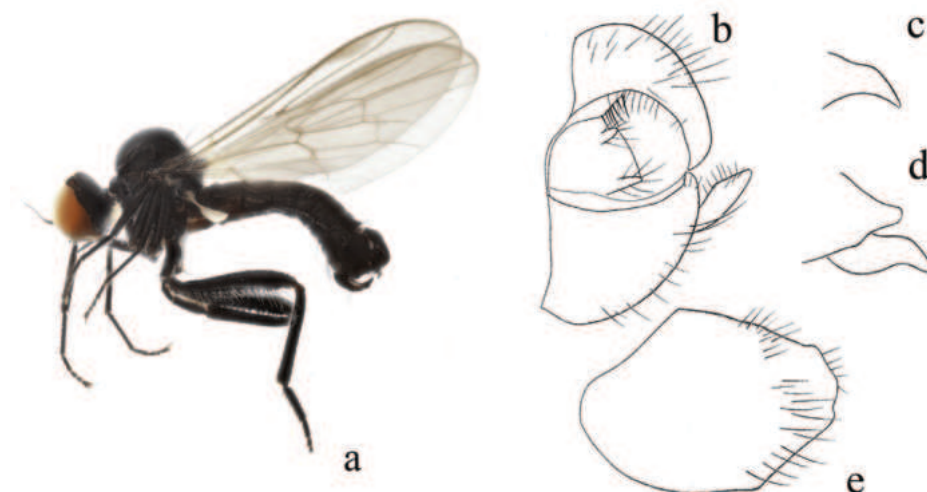


Figure 14. *Hybos obtusatus* a male habitus, lateral view b genitalia, dorsal view c right surstylus d left surstylus e hypandrium, ventral view (b–e: after Yang and Grootaert 2005)

Hybos orientalis Yang & Yang, 1986

Fig. 15

Hybos orientalis Yang & Yang, 1986: 82; Yang and Yang 2004: 201.

Type locality. CHINA: Guangxi, Longsheng; Fujian, Jianyang.

Material examined. CHINA • 5♂5♀, Guangxi, Guilin, Huaping, Anjiangping; 1494 m, 7 August 2023; Wenqiang Cao; CAU. China • 5♂15♀, Guangxi, Guilin, Huaping, Anjiangping; 1514 m, 7 August 2023; Wenqiang Cao; CAU.

Diagnosis. Legs yellow, except tarsomeres 3–5 dark yellow and extreme tip of hind femur black. Hypandrium wide basally and small and obtuse apically.

Distribution. China (Fujian, Guangxi, Henan).

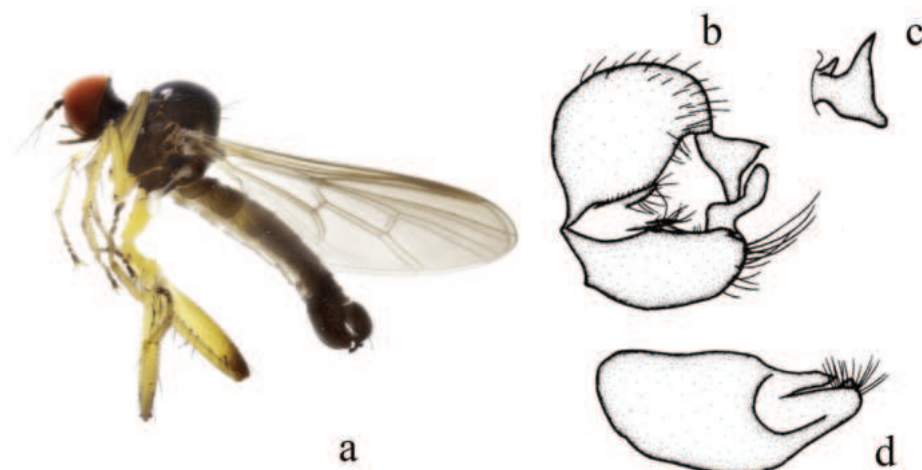


Figure 15. *Hybos orientalis* **a** male habitus, lateral view **b** genitalia, dorsal view **c** right surstylus **d** hypandrium, ventral view (**b–d**: after Yang and Yang 2004)

***Hybos paraterminalis* sp. nov.**

<https://zoobank.org/2AB98B64-7EC8-4962-94E3-2F4DCFEAE076>

Fig. 16

Type material examined. Holotype: CHINA ♂; Guangxi, Guilin, Huaping, Anji-angping; (25°33'39.8"N, 109°56'41.9"E, 1340 m), 26 May 2023, Wei Zeng; CAU.

Diagnosis. Legs mostly black-brown to black except extreme base of hind femur and all tarsi brown to dark brown. Mid tarsomere 1 with two pv on basal $\frac{1}{2}$. R_{4+5} and M_1 divergent apically.

Description. Male. Body length 4.2 mm. Wing length 4.3 mm.

Head black with gray pollen. Eyes contiguous on frons, black-brown with distinctly enlarged dorsal facets yellow-brown. Hairs and bristles on head black except posteroventral surface with partly dark yellow hairs; ocellar tubercle indistinct. Antenna dark brown; scape without hairs, pedicel with circlet of brown subapical hairs; first flagellomere and arista absent. Proboscis slightly shorter than head, dark brown. Palpus dark brown, with one brown apical hair.

Thorax black with gray pollen. Hairs on thorax blackish, bristles black; hairs on mesonotum short, ppn absent, two npl (anterior npl rather short), uniserial hair-like dc nearly as long as irregularly quadriserial acr, two long prsc, one psa; scutellum with 6 marginal hairs and two very long sc. Legs mostly black-brown to black except extreme base of hind femur and all tarsi brown to dark brown. Hairs on legs mostly brownish to dark brown, bristles black-brown to black, but those on coxae partly dark yellow, fore and mid femora with brownish bristles and hind femur with partly dark yellow hairs and bristles. Fore femur 1.2× and hind femur 1.6× as wide as mid femur. Fore femur with row of weak pv shorter than femur thickness. Mid femur with row of weak pv; apically with one ad. Hind femur with 4 ad on apical $\frac{1}{2}$, ~ two rows of long spine-like ventral bristles on tubercles and row of long thin outer pv on apical $\frac{1}{2}$. Fore tibia with one short ad near middle; apically with one ad. Mid tibia with one very long ad at apical $\frac{1}{3}$, one very long av near middle; apically with 5 bristles including one rather long av. Hind tibia with two ad near middle; apically with one pd and one short av. Fore tarsomere 1 with one pv at extreme base. Mid tarsomere 1 with two pv on basal $\frac{1}{2}$; apically with circle of bristles including one pv. Hind tarsomere 1 with

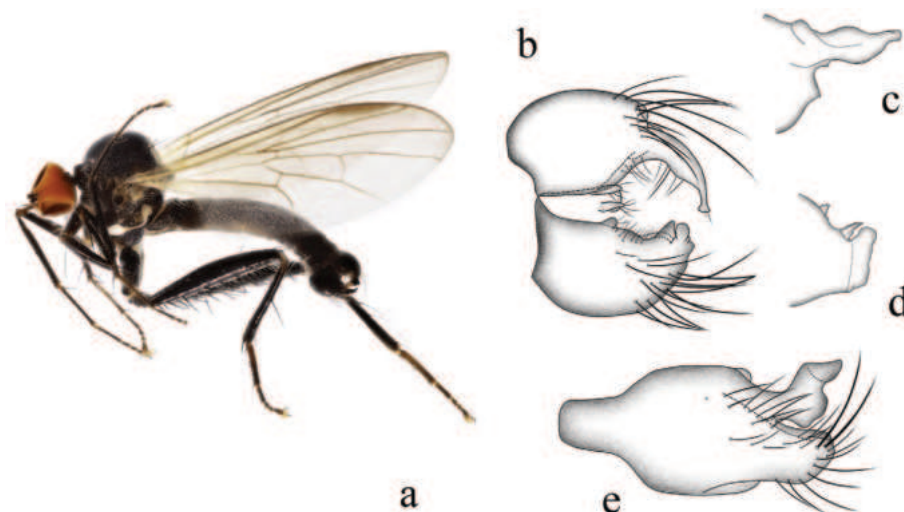


Figure 16. *Hybos paraterminalis* sp. nov. **a** male habitus, lateral view **b** genitalia, dorsal view **c** right surstylus **d** left surstylus **e** hypandrium, ventral view.

row of short spine-like ventral bristles. Wing hyaline, stigma dark brown; veins brown to black-brown, R_{4+5} and M_1 divergent apically. Squama dark yellow with dark yellow hairs. Halter dark yellow with brownish stem and pale-yellow knob.

Abdomen black with pale gray pollen. Hairs and bristles on abdomen dark yellow to brownish except those on hypopygium blackish. Hypopygium distinctly thicker than pregenital segments.

Male genitalia. Left epandrial lamella as wide as right epandrial lamella, with inner margin slightly convex medially (Fig. 16b); left surstylus with apical margin very wide, truncate, apico-lateral portion with one small subtriangular process (Fig. 16d). Right epandrial lamella with concave inner margin near apex; right surstylus slightly wider at middle, long narrow apical portion (Fig. 16c). Hypandrium $\sim 2.0\times$ longer than wide, bilobate apically (left process wide and irregular in shape; right process wide finger-like, straight) (Fig. 16e).

Female. Unknown.

Etymology. This specific name refers to the left surstylus with the very wide and truncate apical margin.

Distribution. China (Guangxi).

Remarks. The new species is similar to *H. guizhouensis* Yang & Yang, 1988 from Guizhou, but may be separated by having all tarsi brown to dark brown and the right surstylus slightly wider in the middle and a long narrow tip. In *H. guizhouensis*, the fore and mid tarsomeres 1–2 are yellow; and the right surstylus is narrow in the middle and slightly wider at the tip (Yang and Yang 2004).

***Hybos particularis* Yang, Yang & Hu, 2002**

Fig. 17

Hybos particularis Yang, Yang & Hu, 2002: 734; Yang and Yang 2004: 205.

Type locality. CHINA: Hainan, Jianfengling.

Material examined. CHINA • 1♂, Guangxi, Guilin, Huaping, Tianpingshan; 542 m, 4 August 2023; Wenqiang Cao; CAU.

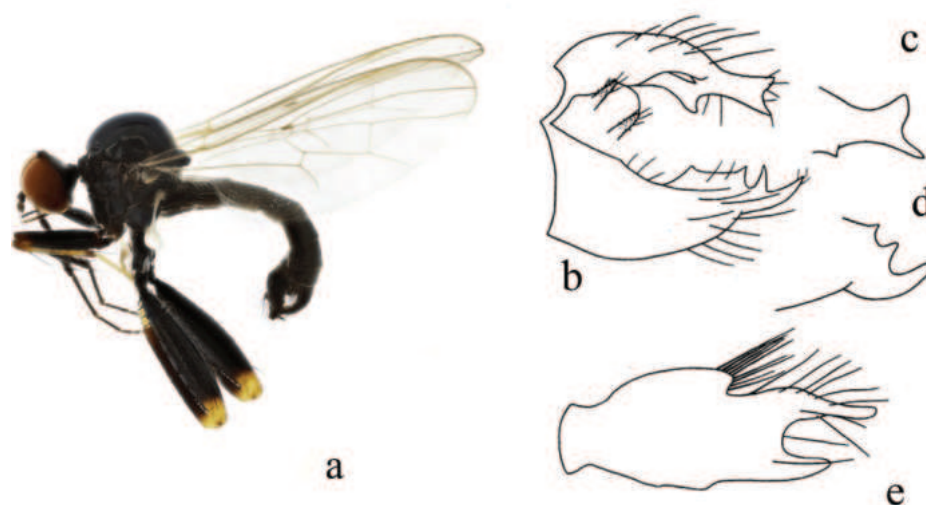


Figure 17. *Hybos particularis* a male habitus, lateral view b genitalia, dorsal view c right surstylus d left surstylus e hypandrium, ventral view (b–e: after Yang and Yang 2004)

Diagnosis. Legs black, except tips of mid femur brownish, mid tibia and tarsomeres 1–2 yellow. Hypandrium long narrow, apically with deep incision.

Distribution. China (Guangxi, Hainan); Thailand.

Hybos pingbianensis Yang & Yang, 2004

Fig. 18

Hybos pingbianensis Yang & Yang, 2004: 207

Type locality: China: Yunnan, Pingbian, Daweishan.

Material examined. CHINA • 1♂, Guangxi, Guilin, Huaping, Anjiangping; 1413 m, 7 August 2023; Wenqiang Cao; CAU.

Diagnosis. Legs yellow; hind coxae black; hind trochanter and femur black, hind tibia (except basal portion) blackish; tarsi dark brown, except fore and mid tarsomeres 1–2 and hind tarsomere 1 yellow. Right and left surstyli with three processes.

Distribution. China (Guangxi, Yunnan).

Hybos serratus Yang & Yang, 1992

Fig. 19

Hybos serratus Yang & Yang, 1992: 1089; Yang and Yang 2004: 210.

Type locality. CHINA: Sichuan, Xichang.

Material examined. China • 2♂, Guangxi, Guilin, Huaping, Anjiangping; 1413 m, 7 August 2023; Wenqiang Cao; CAU.

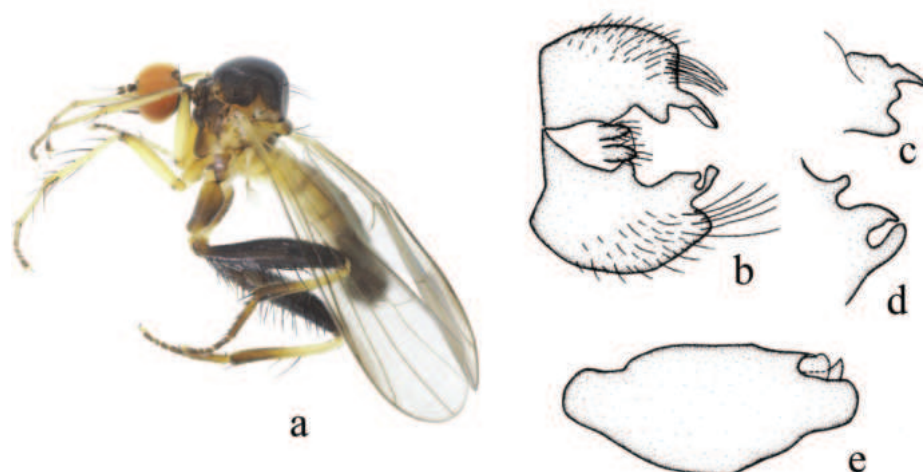


Figure 18. *Hybos pingbianensis* **a** male habitus, lateral view **b** genitalia, dorsal view **c** right surstylus **d** left surstylus **e** hypandrium, ventral view (**b–e**: after Yang and Yang 2004)

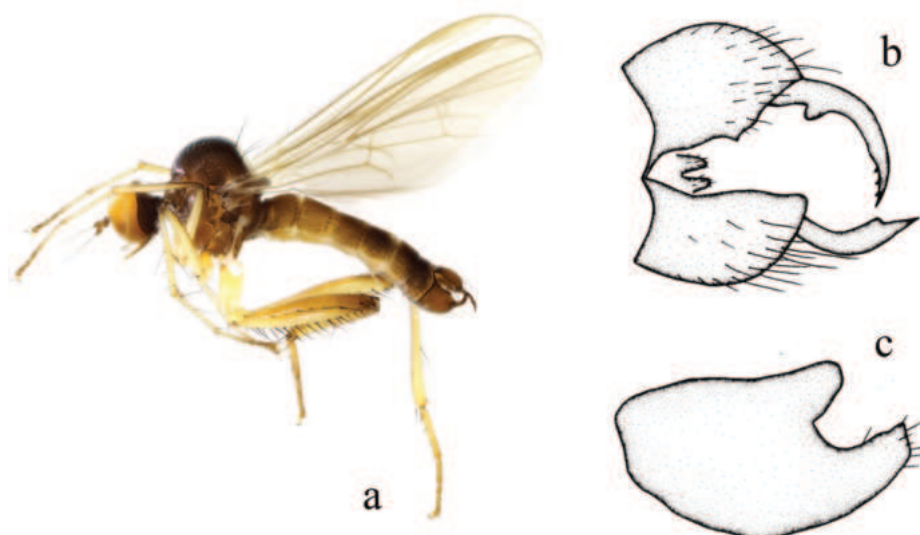


Figure 19. *Hybos serratus* **a** male habitus, lateral view **b** genitalia, dorsal view **c** hypandrium, ventral view (**b, c**: after Yang and Yang 2004)

Diagnosis. Legs yellow, except coxae yellow-brown, femora dark yellow, tarsomeres 2–5 dark yellow. Hypandrium large and wide with apical margin weakly incised medially

Distribution. China (Fujian, Guangxi, Gzuihou, Henan, Sichuan, Yunnan, Zhejiang); Thailand

***Hybos truncatus* Yang & Yang, 1986**

Fig. 20

Hybos truncatus Yang & Yang, 1986: 80; Yang and Yang 2004: 220.

Type locality. CHINA: Guangxi, Longsheng.

Diagnosis. Legs brownish. Mid tibia with one dorsal bristle at base, two long thin dorsal bristles at middle; apically with one long thin ventral bristle. Hypandrium large and wide, apical margin obliquely subtruncate with row of long bristles.

Distribution. China (Guangxi).

***Hybos xiaohuangshanensis* Yang, Gaimari & Grootaert, 2005**

Fig. 21

Hybos xiaohuangshanensis Yang, Gaimari & Grootaert, 2005: 5.

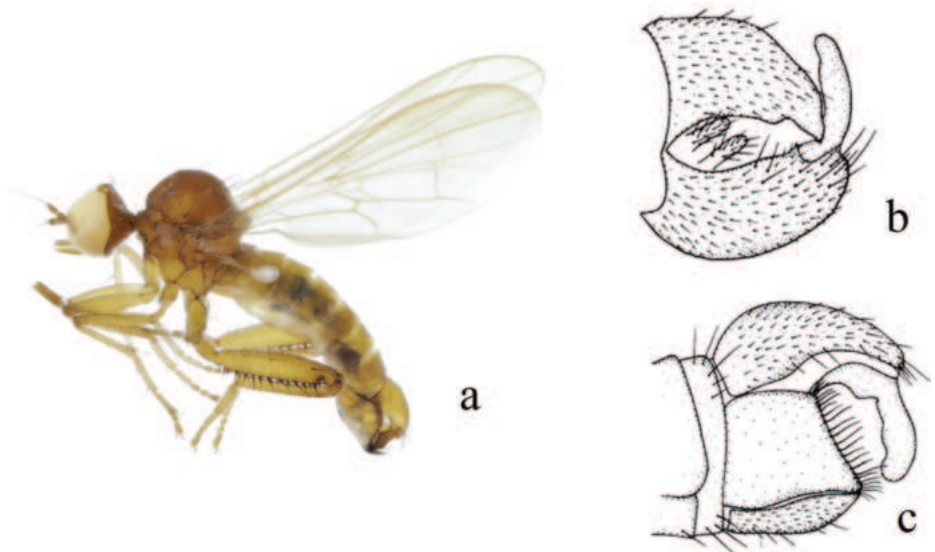


Figure 20. *Hybos truncatus* **a** male habitus, lateral view **b** genitalia, dorsal view **c** hypandrium, ventral view (**b, c**: after Yang and Yang 2004)

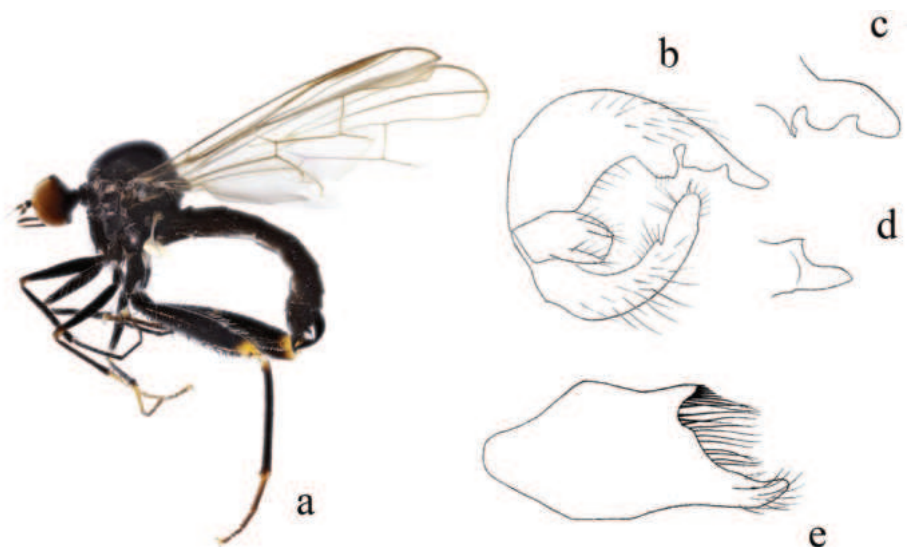


Figure 21. *Hybos xiaohuangshanensis* **a** male habitus, lateral view **b** genitalia, dorsal view; **c** right surstylus **d** left surstylus **e** hypandrium, ventral view (**b–e**: after Yang, Gaimari and Grootaert 2005)

Type locality. CHINA: Guangdong, Nanling.

Material examined. CHINA • 3♂2♀, Guangxi, Guilin, Huaping, Anjiangping; 1340 m, 28 May 2023; Wei Zeng; CAU. China • 1♂, Guangxi, Guilin, Huaping, Hongtan; 849 m, 30 May 2023; Wei Zeng; CAU.

Diagnosis. Arista bare. Legs black except hind knee (distal femur and proximal tibia) and mid and hind tarsi yellow-brown. Hypandrium obliquely incised apically, with long marginal bristles.

Distribution. China (Fujian, Guangdong, Guangxi).

Discussion

The main interspecific diagnostic characteristics in this genus include the short pubescent or bare arista, the color of the legs, the position of bristles on the legs, the relationship between R_{4+5} and M_1 apically, and the shape of the hypandrium. Sexual dimorphism frequently occurs in *Hybos*, particularly in groups with yellow legs. The diverse female genitalia have also been identified as important specific characteristics (Plant 2013; Li and Yang 2023). Unfortunately, the females of the new species mentioned in the article have not been collected yet. They will be collected more extensively in the future for further study and supplementation.

Huaping National Nature Reserve is part of the Nanling Mountain range. Nanling Mountain Area is the largest mountain system and an important geographical boundary in southern China. It is also the largest oasis around 25 degrees north latitude and has a high diversity of flora and fauna. Two studies on local species richness in the family Argentiidae (Hymenoptera) and butterflies (Lepidoptera) revealed that the insect fauna was predominantly composed of Oriental elements (You 2009; Zhou et al. 2016). This is consistent with the research findings of the article, where all nine new record species are from the Oriental region.

Huaping National Nature Reserve is a typical subtropical monsoon climate, with vegetation belonging to the category of evergreen broad-leaved forests. During the period we investigated from May to August, it was the rainy season, and the weather was mostly very humid. In the collected specimens, *Hybos particularis* is widely distributed in Thailand but is often found in seasonal dry forest biotopes. This provides an interesting example for further exploration of the habitat of *Hybos*. This genus is species-rich and widely distributed in various ecoregions in China. Further research on *Hybos* biology, phenology, distribution patterns, and endemism would be valuable and meaningful.

Acknowledgements

We are very grateful to Ms Wei Zeng and Mr Wenqiang Cao (Beijing) for collecting specimens. We thank Dr Scott Williams and Dr Yan Yan (Boston) for checking this manuscript.

Additional information

Conflict of interest

The authors have declared that no competing interests exist.

Ethical statement

No ethical statement was reported.

Funding

This research was supported by the National Natural Science Foundation of China (No. 31970444)

Author contributions

All authors have contributed equally.

Author ORCIDs

Meilin Li  <https://orcid.org/0000-0003-2473-110X>

Jingyu Wang  <https://orcid.org/0009-0009-0396-8547>

Ding Yang  <https://orcid.org/0000-0002-7685-3478>

Data availability

All of the data that support the findings of this study are available in the main text.

References

- Cao YK, Yu H, Wang N, Yang D (2018) *Hybos* Meigen (Diptera: Empididae) from Wangdongyang Nature Reserve, Zhejiang with descriptions of three new species. *Transactions of the American Entomological Society* 144(1): 197–218. <https://doi.org/10.3157/061.144.0110>
- Frey R (1953) Studien über ostasiatische Dipteren. II. Hybotinae, Ocydromiinae, *Hormopeza* Zett. *Notulae Entomologicae* 33: 57–71.
- Kanavalová L, Grootaert P, Kubík S, Barták M (2021) Four new West Palaearctic species and new distributional records of Hybotidae (Diptera). *ZooKeys* 1019: 141–162. <https://doi.org/10.3897/zookeys.1019.61496>
- Li ML, Yang D (2023) New species and records of the genus *Hybos* Meigen (Diptera, Empidoidea, Hybotinae) from Wuyishan National Park, China. *ZooKeys* 1172: 313–351. <https://doi.org/10.3897/zookeys.1172.105952>
- Li XL, Wang N, Yang D (2017) *Hybos* Meigen (Diptera: Empididae) from Wanglang National Nature Reserve, Sichuan. *Transactions of the American Entomological Society* 143(2): 435–452. <https://doi.org/10.3157/061.143.0212>
- Li ML, Fatima N, Lin C, Yang D (2022) Four new species of *Hybos* (Diptera: Empididae) from Gaoligongshan, China. *Entomotaxonomia* 44(02): 134–143.
- Macquart J (1827) *Insectes diptères du nord de la France. Platypézines, dolichopodes, empides, hybotides*. Lille, 159 pp. <https://doi.org/10.5962/bhl.title.148911>
- Meigen JW (1800) *Nouvelle classification des mouches à deux ailes (Dipter L.) d'après un plan tout nouveau*. Paris, 40 pp. <https://doi.org/10.5962/bhl.title.119764>
- Meigen JW (1803) *Versuch einer neuen Gattungseintheilung der europäischen zweiflügeligen Insekten*. *Magazin für Insektenkunde* 2: 259–281.
- Meigen JW (1820) *Systematische Beschreibung der bekannten Europäischen zweiflügeligen Insekten. Zweiter Theil*. Forstmann, Aachen, 363 pp.
- Plant AR (2013) The genus *Hybos* Meigen (Diptera: Empidoidea: Hybotidae) in Thailand. *Zootaxa* 3690(1): 1–98. <https://doi.org/10.11646/zootaxa.3690.1.1>

- Shamshev IV, Grootaert P, Yang D (2013) New data on the genus *Hybos* (Diptera: Hybotidae) from the Russian Far East, with description of a new species. *Russian Entomological Journal* 22(2): 141–144.
- Shamshev IV, Grootaert P, Kustov S (2015) New data on the genus *Hybos* Meigen (Diptera: Hybotidae) from the Palaearctic Region. *Zootaxa* 3936(4): 451–484. <https://doi.org/10.11646/zootaxa.3936.4.1>
- Yang D, Grootaert P (2005) Two new species of *Hybos* from Guangdong (Diptera: Empidoidea: Hybotinae). *Annales Zoologici* 55(3): 409–411.
- Yang D, Yang CK (2004) Diptera, Empididae, Hemerodromiinae and Hybotinae. *Fauna Sinica Insecta* Vol. 34. Science Press, Beijing, 329 pp.
- Yang D, Gaimari SD, Grootaert P (2005) New species of *Hybos* Meigen from Guangdong Province, South China (Diptera: Empididae). *Zootaxa* 912(1): 1–7. <https://doi.org/10.11646/zootaxa.912.1.1>
- Yang D, Zhang KY, Yao G, Zhang JH (2007) *World Catalog of Empididae* (Insecta: Diptera). China Agricultural Press, Beijing, 599 pp.
- You Q (2009) Species and fauna of Argidae (Hymenoptera) in Nanling Mountains, China. *Caoye Xuebao* 18: 130–135.
- Zhou GY, Gu MB, Gong YN, Wang SK, Wu ZM, Xie GG (2016) Diversity and fauna of butterflies in Nanling National Nature Reserve. *Environmental Entomology* 38: 971–978.

Rediscovery of *Lycodon gammiei* (Blanford, 1878) (Serpentes, Colubridae) in Xizang, China, with comments on its systematic position

Fu Shu^{1*}, Bing Lyu^{2*}, Keji Guo¹, Tong Zhang¹, Xiaoqi Mi³, Li Li², Yayong Wu², Peng Guo²

1 Central South Academy of Inventory and Planning of National Forestry and Grassland Administration, Changsha 410014, China

2 Faculty of Agriculture, Forestry and Food Engineering, Yibin University, Yibin 644005, China

3 College of Agriculture and Forestry Engineering and Planning, Guizhou Provincial Key Laboratory of Biodiversity Conservation and Utilization in the Fanjing Mountain Region, Tongren University, Tongren 554300, Guizhou, China

Corresponding author: Peng Guo (ybguo@163.com)

Abstract

Lycodon gammiei (Blanford, 1878), a rarely encountered species of Asian snake, is characterized by ambiguous systematics and biology. Based on a sole specimen of *L. gammiei* rediscovered in southeastern Xizang, China, we conduct a detailed morphological examination and description, and investigate the systematic position of this species. Morphologically, the newly collected specimen is closely aligned with specimens previously described. Mitochondrial DNA-based phylogenetic analyses reveal that *L. gammiei* constitutes an independent evolutionary lineage, forming a clade with *L. fasciatus* (Anderson, 1879), *L. gongshan* Vogel & Luo, 2011, *L. butleri* Boulenger, 1900, and *L. cavernicolus* Grismer, Quah, Anuar, Muin, Wood & Nor, 2014. The closest genetic distance between *L. gammiei* and its congeners was 10.2%. The discovery of *L. gammiei* in Medog County, China, signifies an eastward expansion of its known geographical distribution.

Key words: Himalayas, phylogeny, Qinghai-Xizang Plateau, snake



Academic editor: Robert Jadin

Received: 16 December 2023

Accepted: 13 March 2024

Published: 7 May 2024

ZooBank: <https://zoobank.org/B1D16759-3896-43B9-86C0-64691CD2C466>

Citation: Shu F, Lyu B, Guo K, Zhang T, Mi X, Li L, Wu Y, Guo P (2024) Rediscovery of *Lycodon gammiei* (Blanford, 1878) (Serpentes, Colubridae) in Xizang, China, with comments on its systematic position. ZooKeys 1200: 65–74. <https://doi.org/10.3897/zookeys.1200.117260>

Copyright: © Fu Shu et al.
This is an open access article distributed under terms of the Creative Commons Attribution License (Attribution 4.0 International – CC BY 4.0).

Introduction

Exploring the boundaries of geographic distribution and systematic position of species is crucial for understanding their evolutionary origins and diversification and for devising appropriate conservation strategies. Despite considerable progress in recent years, many species remain poorly known and explored. This is particularly evident for some snake species due to their rarity and cryptic habitats.

Lycodon gammiei (Blanford, 1878), a rare non-venomous snake species within the family Colubridae, was initially described as *Ophites gammiei* based on a single specimen collected from Darjeeling, West Bengal, India (Blanford 1878). Subsequently, it was reclassified into the genus *Lycodon* (Boulenger 1890) or *Dinodon* (Wall 1923; Smith 1943), identifying it as *Lycodon gammiei*. Wall (1911) compared *L. gammiei* and *L. fasciatus* (Anderson, 1879), and he synonymized *L. fasciatus* with *L. gammiei*. However, Wall (1923) later revised this view,

* These authors contributed equally to this work.

recognizing its distinctiveness and validity of *L. fasciatus*. Mahendra (1984) proposed that *L. gammiei* was a color variety of *L. septentrionalis* (Gunther, 1875), while this synonymy was not accepted by all authors. Since its initial description, *L. gammiei* has been found in southeastern Xizang, China (Agarwal et al. 2010) and in Bhutan (Wangyal 2013). To date, however, few specimens of the species have been collected, and no genetic data have been reported.

In 2023, we collected a living specimen of *L. gammiei* in Medog County, southeastern Xizang, China. The rediscovery of this species in Xizang not only extends this species' geographic distribution but also allows the exploration of its systematic position through molecular data.

Materials and methods

Morphological examination

The specimen deposited at Yibin University (YBU 230088) was collected in Beibeng Town, Medog County, southeastern Xizang, China (29°14'02"N, 95°10'38"E) (Fig. 1) on 14 August 2023 at an elevation of 1,431 m by Xiaoqi Mi. The snake was found on a tree near a road at 23:30 hours. Characters relating to scalation, color pattern, and body proportions were recorded from the preserved specimen in laboratory. Snout–vent length (SVL) and tail length (TL) were measured using a meter ruler to the nearest 0.5 centimeter, while all remaining measurements were taken using digital calipers to the nearest millimeter. Symmetric mensural head characters were taken on the right side unless unavailable (e.g. damaged), while meristic characters were recorded on both sides and reported in left/right order.

Comparative data of other specimens of this species were taken from the literature (Blanford 1878; Mistry et al. 2007; Chettri and Bhupathy 2009; Wangyal 2013).

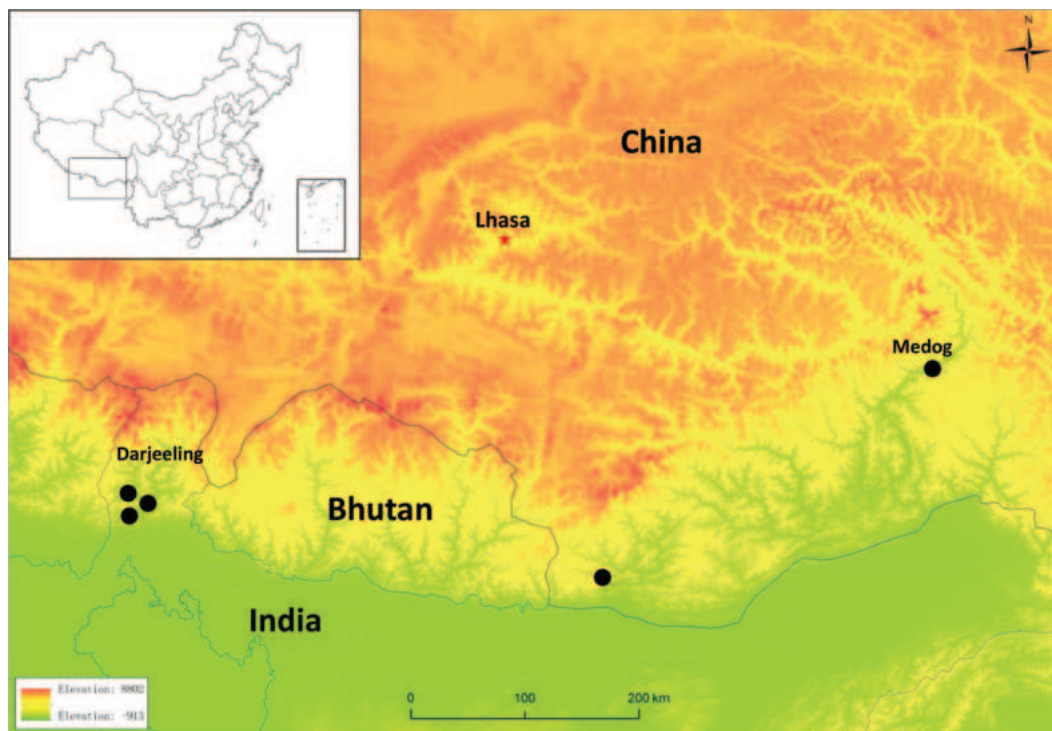


Figure 1. Map showing currently known localities of *Lycodon gammiei*.

Molecular phylogeny

Genomic DNA was extracted from the liver tissue of the newly collected specimen using an Animal Genomic DNA Purification Kit (TIANGEN Bio-tech Co., Ltd, Beijing, China). Subsequently, a fragment of the mitochondrial gene cytochrome b (cyt b) was amplified using primers H14919 (5'-AACCACCGTTGT-TATTCAACT-3') and L16064 (5'-CTTTGGTTTACAAGAACAATGCTTTA-3') (Burbink et al. 2000). The polymerase chain reaction (PCR) products were purified and sequenced in both directions by Sangon Biotech Co., Ltd (Chengdu, China). The obtained sequences were manually edited using SeqMan in Lasergene v. 7.1 (DNASTAR, USA), and aligned using the ClustalW algorithm with default parameters in MEGA v. 7.0 (Kumar et al. 2016), followed by a visual inspection for minor manual adjustments. The DNA sequences were translated into amino acid sequences using MEGA v. 7.0 to verify sequence quality and detect any unexpected stop codons (Kumar et al. 2016). Furthermore, 80 additional sequences were downloaded from GenBank (Table 1).

Both Bayesian-inference (BI) and maximum-likelihood (ML) analyses were executed for the final dataset. Prior to analyses, the best-fit model of nucleotide substitution was selected for each partition (codon position) using Akaike In-

Table 1. Detail information for the samples used in this study.

No.	Species	Voucher Number	Locality	GenBank No.
1	<i>Lycodon albobfuscus</i>	LSUHC 3867	–	KX660500
2	<i>Lycodon albobfuscus</i>	LSUHC 4588	–	KX660501
3	<i>Lycodon alcalai</i>	KU 327847	Barangay San Antonio, Batanes Province, Philippines	KC010344
4	<i>Lycodon alcalai</i>	KU 327848	Municipality of Sabtang, Batanes, Philippines	KC010345
5	<i>Lycodon anakradaya</i>	SIEZC 20247	Song Giang River, Khanh Hoa Province, Vietnam	OM674283
6	<i>Lycodon anakradaya</i>	SIEZC 20248	Song Giang River, Khanh Hoa Province, Vietnam	OM674284
7	<i>Lycodon aulicus</i>	KU 315378	Tablas Island, Romblon Province, Philippines	KC010350
8	<i>Lycodon aulicus</i>	PNM 7705	Leyte Island, Leyte province, Philippines	KC010349
9	<i>Lycodon banksi</i>	VNUF R2015.20	Khammouane, Laos	MH669272
10	<i>Lycodon bibonius</i>	KU 304589	Cagayan, Philippines	KC010351
11	<i>Lycodon butleri</i>	LSUHC 8365	Perak, Malaysia	KJ607892
12	<i>Lycodon butleri</i>	LSUHC 9137	Perak, Malaysia	KJ607891
13	<i>Lycodon capucinus</i>	–	–	MK844525
14	<i>Lycodon capucinus</i>	MVZ 291703	Timor	MK844522
15	<i>Lycodon capucinus</i>	MVZ 291704	Timor	MK844523
16	<i>Lycodon cathaya</i>	SYS r001542	Longsheng County, Guangxi, China	MT602075
17	<i>Lycodon cathaya</i>	SYS r001630	Longsheng County, Guangxi, China	MT602076
18	<i>Lycodon cavernicolus</i>	LSUHC 10500	Perlis, Malaysia	KJ607890
19	<i>Lycodon cavernicolus</i>	LSUHC 9985	Perlis, Malaysia	KJ607889
20	<i>Lycodon cf. flavozonatus</i>	KIZ 032400	Zayu, Xizang, China	MW199792
21	<i>Lycodon chapaensis</i>	KIZ 27593	Tengchong, Yunnan, China	MW353741
22	<i>Lycodon chapaensis</i>	KIZ 35013	Lushui, Yunnan, China	MW353742
23	<i>Lycodon chrysoprateros</i>	KU 307720	Cagayan, Philippines	KC010360
24	<i>Lycodon deccanensis</i>	–	Tumkur District, Karnataka, India	MW006487
25	<i>Lycodon deccanensis</i>	NCBS NRC AA0010	Karnataka, India	MW006486
26	<i>Lycodon dumerilii</i>	KU 305168	Dinagat Island, Philippines	KC010362
27	<i>Lycodon dumerilii</i>	KU 319989	Mindanao Island, Agusan del Sur Province, Philippines	KC010361
28	<i>Lycodon dumerilii</i>	PNM 7751	Leyte Island, Leyte Province, Philippines	KC010363

No.	Species	Voucher Number	Locality	GenBank No.
29	<i>Lycodon effraenis</i>	KU 328526	Karome, Nakhon Si Thammarat, Thailand	KC010364
30	<i>Lycodon effraenis</i>	LSUHC 9670	Kedah, West Malaysia	KC010376
31	<i>Lycodon fasciatus</i>	CHS 837	Yunnan, China	MK201559
32	<i>Lycodon fasciatus</i>	KIZ 46120	Himalayan region in China	MW111468
33	<i>Lycodon flavicollis</i>	–	Devarayanadurga, Karnataka, India	MW006488
34	<i>Lycodon flavicollis</i>	AIWC 081	India	MZ029434
35	<i>Lycodon flavozonatus</i>	KIZ 023279	Xizang, China	MW199789
36	<i>Lycodon flavozonatus</i>	KIZ 07067	Xizang, China	MW199790
37	<i>Lycodon futsingensis</i>	CHS 670	Nankunshan, Guangdong, China	MK201463
38	<i>Lycodon futsingensis</i>	CHS 751	Guangdong, China	MK201504
39	<i>Lycodon gammiei</i>	YBU 230088	Medog, Xizang, China	OR842906
40	<i>Lycodon gongshan</i>	GP 3547	Lingcang, Yunnan, China	KP901025
41	<i>Lycodon gongshan</i>	GP 3548	Lingcang, Yunnan, China	KP901026
42	<i>Lycodon jara</i>	CAS 235387	Putao, Kachin, Myanmar	KC010367
43	<i>Lycodon laoensis</i>	FMNH 258659	Salavan, Laos	KC010368
44	<i>Lycodon laoensis</i>	LSUHC 8481	O'Lakmeas, Pursat Province, Cambodia	KC010370
45	<i>Lycodon liuchengchaoi</i>	CHS 158	Sanjiazhai, Yunnan, China	MK201303
46	<i>Lycodon liuchengchaoi</i>	CHS 843	Ningshan, Shaanxi, China	MK201563
47	<i>Lycodon liuchengchaoi</i>	CHS 873	Shennongjia, Hubei, China	MK201580
48	<i>Lycodon mackinnoni</i>	ADR 197	Dhobighat, BWLS, Mussoorie, Uttarakhand	MW862977
49	<i>Lycodon meridionalis</i>	CHS 870	Hechi, Guangxi, China	MK201578
50	<i>Lycodon meridionalis</i>	VNUF R2012.4	Bac Kan, Vietnam	MH669271
51	<i>Lycodon meridionalis</i>	VNUF R2017.123	Thanh Hoa Province, Vietnam	MH669270
52	<i>Lycodon muelleri</i>	DLSUD 031	Luzon Island, Cavite Province, Philippines	KC010373
53	<i>Lycodon muelleri</i>	KU 313891	Luzon Island, Camarines Norte Province, Philippines	KC010375
54	<i>Lycodon muelleri</i>	KU 323384	Luzon Island, Aurora Province, Philippines	KC010374
55	<i>Lycodon namdongensis</i>	VNUF R2017.23	ThanhHoa, Vietnam	MK585007
56	<i>Lycodon obvelatus</i>	KIZ 040146	Panzhuhua, Sichuan, China	MW353745
57	<i>Lycodon pictus</i>	CIB 115609	Longzhou, Guangxi, China	MT845095
58	<i>Lycodon pictus</i>	VNMN 011227	Ha Lang, Cao Bang, Vietnam,	MT845094
59	<i>Lycodon rosozonatus</i>	CHS 794	Jianfengling, Hainan, China	MK201531
60	<i>Lycodon rufozonatus</i>	CHS 601	Huangshan, Anhui, China	MK201427
61	<i>Lycodon rufozonatus</i>	CHS 710	Yingpanxu, Hunan, China	MK201482
62	<i>Lycodon ruhstrati</i>	CHS 776	Guangxi, China	MK201521
63	<i>Lycodon ruhstrati</i>	CHS 803	Huaping, Guangxi, China	MK201538
64	<i>Lycodon semicarinatus</i>	KUZJPN 28044	–	LC640371
65	<i>Lycodon septentrionalis</i>	CHS 162	Yunnan, China	MK201305
66	<i>Lycodon septentrionalis</i>	KIZ 46117	Xizang, China	MW199801
67	<i>Lycodon serratus</i>	KIZ 038335	Deqin, Yunnan, China	MW353746
68	<i>Lycodon stormi</i>	JAM 7487	Air Terjun Moramo, Sulawesi, Indonesia	KC010380
69	<i>Lycodon striatus</i>	–	Savandurga, Karnataka, India	MW006489
70	<i>Lycodon striatus</i>	CUHC 10368	Pakistan	OQ282988
71	<i>Lycodon striatus</i>	CUHC 11257	–	OQ282989
72	<i>Lycodon striatus</i>	CUHC 9457	–	OQ282987
73	<i>Lycodon subcinctus</i>	CHS 734	Guangdong, China	MK201493
74	<i>Lycodon subcinctus</i>	CHS 797	Diaoluoshan Mountain, Hainan, China	MK201534
75	<i>Lycodon synaptor</i>	GP 3515	Lingcang, Yunnan, China	KP901021
76	<i>Lycodon synaptor</i>	KIZ 046953	Xizang, China	MW199805
77	<i>Lycodon truongi</i>	SIEZC 20249	Song Giang River, Khanh Hoa Province, Vietnam	OM674282
78	<i>Lycodon zawi</i>	CAS 210323	Thabakesay, Saging, Myanmar	AF471040
79	<i>Lycodon zawi</i>	CAS 239944	Kyaukpyu, RakhineState, Myanmar	KC010386
80	<i>Lycodon zayuensis</i>	GP 7327	Zayu, Xizang, China	OP434398
81	<i>Lycodon zayuensis</i>	GP 7329	Zayu, Xizang, China	OP434399

formation Criterion (AIC) implemented in PartitionFinder (Lanfear et al. 2012). The BI analyses were conducted using MrBayes v. 3.2.2 (Ronquist et al. 2012). Searches consisted of three independent runs, each involving four Markov chains (three heated chains and one cold chain), with 10 million generations, sampling every 2,000 generations and with 25% of initial samples discarded as burn-in. Convergence was determined via effective sample size (ESS > 200) and likelihood plots against time using Tracer v. 1.7 (Rambaut et al. 2018). The resulting trees were combined to determine the posterior probabilities (PP) for each node based on a 50% majority-rule consensus tree. The ML trees were constructed in IQ-tree (Lam-Tung et al. 2015) using the GTRCAT model and the same partitioning scheme. In total, 1,000 Ultrafast bootstraps (UFB) topological replicates were performed for branch support assessment. *Boiga cynodon* (Boie, 1827) was selected as the outgroup following previous research (Guo et al. 2013).

Uncorrected genetic distance (p -distance) was calculated in MEGA v. 7.0 (Kumar et al. 2016).

Results

Morphological description

Female, SVL 698 mm and TL 223 mm. Body elongated; head rather flattened; snout blunt. Rostral large, trapezoid; internasals much broader than long; prefrontals 3.0 mm in length, distinctly wider than long, extending beyond both sides and touching preocular and loreal; frontal peltate, 4.6 mm in length and 4.1 mm in width; parietals subrectangular, 7.9 mm in length and 4.2 mm in width. Nasals large, nostril located anteriorly and opening backward; loreal scale 1, long, nearly rectangular, failing to touch eye; preocular 1, postoculars 2; temporals 2+2+3. Supralabials 8, 1st small, 3rd, 4th, and 5th entering orbit, 6th highest, 7th largest; infralabials 10, first pair in contact, 1st to 5th in contact with anterior chin shields. Chin shield pairs 2, elongate, anterior pair slightly larger than latter pair. Dorsal scales 17-17-15 rows, scales weakly keeled, except for outermost several rows; scales reduced from 17 to 15 at 143rd ventral position. Ventrals 228 (+ 1 preventral); cloacal plate entire; subcaudals 106, paired, dorsal scales of the tail reduced from 6 to 4 at 16th subcaudal position.

Head black, with yellow spots or short lines on some shields. Large, yellow spots on each side of posterior part of head. Conspicuous yellow collar on neck. Supralabials and anterior infralabials light yellow with dusky margins. Body surrounded by alternating dusky and light-yellow rings with very irregular, crooked margins. Yellow rings on body totaling 43, first pale ring clear above, anterior dark patch not continuous across throat, remaining rings encircling body. Lower part of head and neck light yellow. On belly, across anterior part of body, dark rings only about half as broad as light-yellow rings, less difference above, dark rings near head much broader above than white rings. Yellow rings on tail totaling 21 (Fig. 2). Preserved specimen somewhat faded, with no yellow visible (Fig. 3).

Molecular phylogeny

In total, 1,047 bp of sequence data from 84 samples were aligned, with the generated novel sequence deposited in GenBank (Table 1). No deletions, insertions, or stop codons were detected, indicating that unintentional amplification of



Figure 2. General view of the studied specimen (YBU 230088) in life and its microhabitat a big tree trunk (by XQ Mi).

pseudogenes was unlikely (Zhang and Hewitt 1996). The best-fit evolutionary models of the data were: GTR+I+G for the first codon position, HKY+I+G for the second codon position, and GTR+G for the third codon position.

The mtDNA-based BI and ML analyses depicted relatively consistent topologies, with slight disagreement in several shallow nodes (Fig. 4). Both analyses indicated that all putative species of *Lycodon* formed a highly supported lineage (100 PP and 84% UFB). The newly collected specimen formed a clade with *L. fasciatus*, *L. gongshan* Vogel & Luo, 2011, *L. butleri* Boulenger, 1900, and *L. cavernicolus* Grismer, Quah, Anuar, Muin, Wood & Nor, 2014 with high support (100 PP and 97% UFB). Nevertheless, it occupied a basal position in relation to this clade and did not exhibit monophyly with any individual member. Uncorrected *p*-distances among the species within this clade ranged from 7.2% (*L. gongshan* and *L. fasciatus*) to 12.9% (*L. gammiei* and *L. cavernicolus*), while genetic distances between *L. gammiei* and its congeners within this clade ranged from 10.2% to 12.9% (data not shown).

Discussion

Lycodon gammiei is an exceedingly rare species, with a global record of only approximately 10 specimens. The majority of these are from Sikkim and West Bengal, India (Mistry et al. 2007; Chettri and Bhupathy 2009), with only two specimens reported in Cona County, Xizang, China (originally recorded in Eagle-nest Wildlife Sanctuary, India) (Mistry et al. 2007) and Bhutan (Wangyal 2013), respectively. Based on the record by Mistry et al. (2007), Luo et al. (2010) recognized the existence of this species in China, although this recognition has been overlooked in subsequent publications (Wallach et al. 2014; Wang et al. 2020; Uetz et al. 2024). The discovery of this species in Medog County, Xizang, China,



Figure 3. Views of the studied specimen (YBU 230088) in preservation. General dorsal (A) and ventral (B) views of specimen, dorsal (C), ventral (D) and lateral (E) views of head (by P Guo).

not only confirms its presence in China but also indicates a further eastward extension of its distribution.

Morphologically, the newly collected specimen shares most characters with the other conspecific specimens (Blanford 1878; Mistry et al. 2007; Chettri and Bhupathy 2009), including eight supralabials (3rd to 5th touching eye, 6th largest), single loreal, 2+3 temporals, one preocular, two postoculars, two genial pairs, cloacal plate entire, and dorsal scales in 17-17-15 rows. However, the new specimen has a greater number of ventral scales (228+1) than all previously reported specimens (205–220) (Mistry et al. 2007; Chettri and Bhupathy 2009).

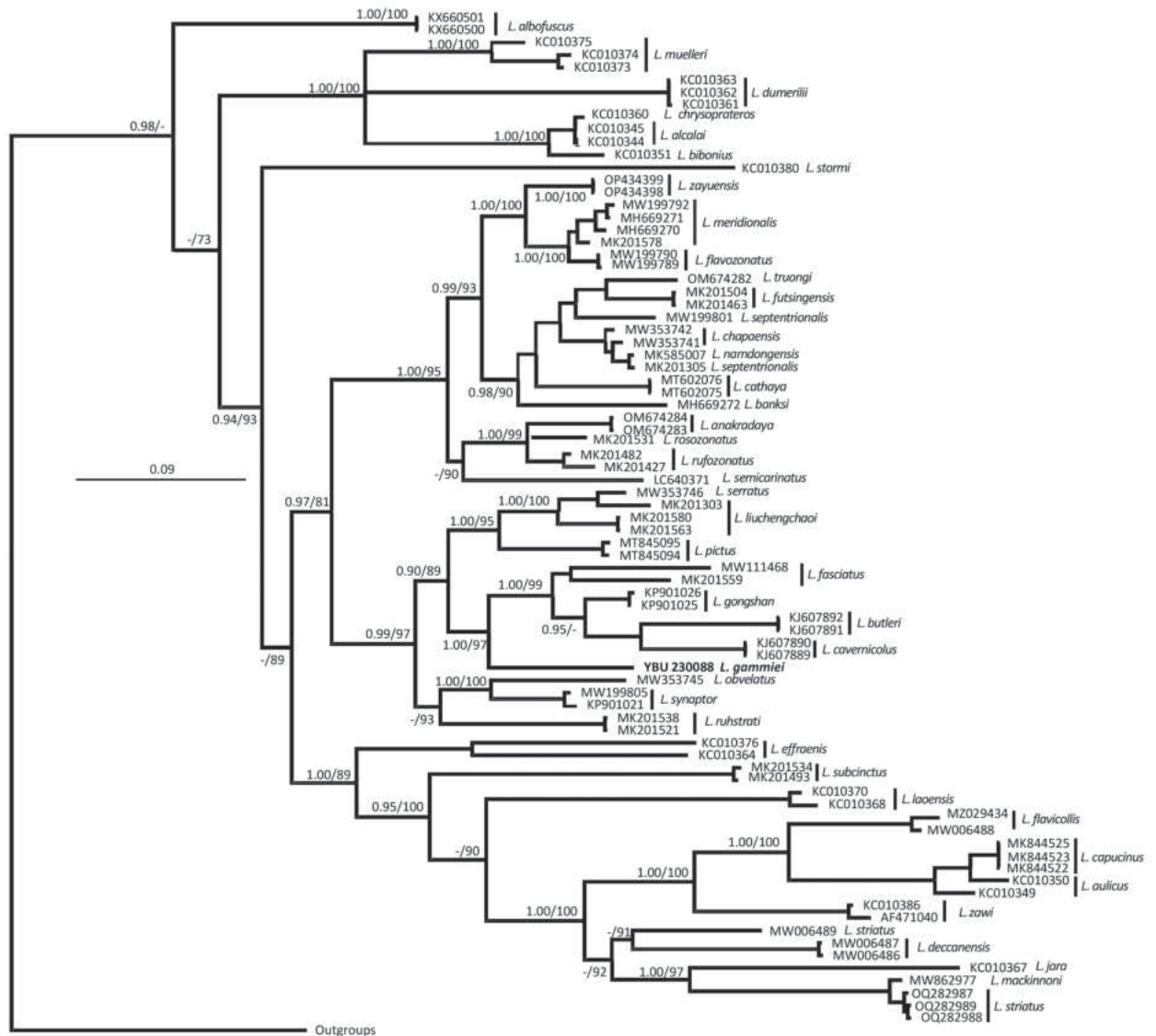


Figure 4. Bayesian 50% majority-rule consensus tree of *Lycodon* inferred from cyt b sequences analyzed using models detailed in the text. Posterior probabilities from BI analysis (>0.50) and Ultrafast bootstraps from ML analysis (>50%) are given adjacent to respective nodes for major nodes. Branch support indices are not given for most nodes to preserve clarity.

The taxonomic status of *L. gammiei* has a controversial history. Although previously misidentified as both *L. fasciatus* (Wall 1911) and *L. septentrionalis* (Mahendra 1984), Mistry et al. (2007) later clarified its distinct status and validity based on morphological comparisons. In the current study, we present the first genetic data pertaining to this species. Notably, mtDNA-based phylogenetic analyses indicated that *L. gammiei* formed a highly supported monophyly with a clade containing *L. fasciatus* but was not the closest congener to *L. fasciatus* within this assemblage (Fig. 4). *Lycodon gammiei* shows a greater genetic distance from *L. septentrionalis* than from *L. fasciatus*, further affirming its validity and unique taxonomic position. The closer genetic affinity of *L. gammiei* with the clade encompassing *L. fasciatus* aligns with their geographical closeness along the southern slopes of the Himalayas.

Lycodon zayuensis Jiang, Wang, Jin & Che, 2020 coexists with *L. gammiei* in southeastern Xizang, China (Che et al. 2020; Lyu et al. 2022). Both species exhibit similarities in external morphology, including dorsal scales in 17-17-15

rows, eight supralabials, one preocular, and two postoculars. However, the two species are genetically divergent (Fig. 2), and *L. gammiei* can be easily distinguished from *L. zayuensis* by its broader and fewer yellow body cross-bands (30–43 vs 88–93) (Blanford 1878; Lyu et al. 2022).

Additional information

Conflict of interest

The authors have declared that no competing interests exist.

Ethical statement

No ethical statement was reported.

Funding

This study was supported by the Second Tibetan Plateau Scientific Expedition and Research (STEP) Program (2019QZKK05010105), National Natural Science Foundation of China (32000308 and 32370486), and Yarlung Zangbo Grand Canyon National Nature Reserve Research and Monitor Program (Linzhi Forestry and Grassland Bureau)

Author contributions

Conceptualization: XM. Formal analysis: BL. Methodology: TZ. Resources: KG. Software: YW. Supervision: PG. Validation: LL. Writing – original draft: FS.

Author ORCIDs

Fu Shu  <https://orcid.org/0000-0002-6082-8112>

Bing Lyu  <https://orcid.org/0000-0001-5594-1543>

Keji Guo  <https://orcid.org/0000-0001-7508-1173>

Tong Zhang  <https://orcid.org/0009-0009-1492-585X>

Xiaoqi Mi  <https://orcid.org/0000-0003-1744-3855>

Li Li  <https://orcid.org/0009-0007-4149-6662>

Yayong Wu  <https://orcid.org/0000-0003-2752-4085>

Peng Guo  <https://orcid.org/0000-0001-5585-292X>

Data availability

All of the data that support the findings of this study are available in the main text.

References

- Agarwal I, Mistry VK, Athreya R (2010) A preliminary checklist of the reptiles of Eaglenest Wildlife Sanctuary, West Kameng district, Arunachal Pradesh, India. *Russian Journal of Herpetology* 17(2): 81–93.
- Blanford WT (1878) Notes on some Reptilia from the Himalayas and Burma. Part II. *Journal of the Asiatic Society of Bengal (Natural History)* 47(3): 125–131.
- Burbrink FT, Lawson R, Slowinski JB (2000) Mitochondrial DNA phylogeography of the polytypic north American rat snake (*Elaphe obsoleta*): A critique of the subspecies concept. *Evolution* 54(6): 2107–2118. <https://doi.org/10.1111/j.0014-3820.2000.tb01253.x>
- Che J, Jiang K, Yan F, Zhang YP (2020) *Amphibians and Reptiles in Tibet – Diversity and Evolution*. Science Press, Beijing, 691 pp.

- Chettri B, Bhupathy S (2009) Occurrence of *Dinodon gammiei* (Blanford, 1878) in Sikkim, Eastern Himalaya, India. *Journal of Threatened Taxa* 1(1): 60–61. <https://doi.org/10.11609/JoTT.o1960.60-1>
- Guo P, Zhang L, Liu Q, Li C, Pyron RA, Jiang K, Burbrink FT (2013) *Lycodon* and *Dinodon*: One genus or two? Evidence from molecular phylogenetics and morphological comparisons. *Molecular Phylogenetics and Evolution* 68(1): 144–149. <https://doi.org/10.1016/j.ympev.2013.03.008>
- Kumar S, Stecher G, Tamura K (2016) MEGA7: Molecular evolutionary genetics analysis version 7.0 for bigger datasets. *Molecular Biology and Evolution* 33(7): 1870–1874. <https://doi.org/10.1093/molbev/msw054>
- Lam-Tung N, Schmidt HA, Arndt VH, Quang MB (2015) IQ-tree: A fast and effective stochastic algorithm for estimating maximum-likelihood phylogenies. *Molecular Biology and Evolution* (1): 268–274. <https://doi.org/10.1093/molbev/msu300>
- Lanfear R, Calcott B, Ho SYW, Guindon S (2012) PartitionFinder: Combined selection of partitioning schemes and substitution models for phylogenetic analyses. *Molecular Biology and Evolution* 29(6): 1695–1701. <https://doi.org/10.1093/molbev/mss020>
- Luo J, Ryabov SA, Luo Y, Gao HY, Luo ZR, Hu XC (2010) Classification and distribution of the genus *Dinodon*. *Sichuan Journal of Zoology* 29(4): 579–582.
- Lyu B, Li QL, Li K, Li L, Shu F, Wu YY, Guo P (2022) Expanded morphological description of the recently described *Lycodon zayuensis* (Serpentes: Colubridae). *Zootaxa* 5213(2): 159–168. <https://doi.org/10.11646/zootaxa.5213.2.4>
- Mahendra BC (1984) Handbook of the snakes of India, Ceylon, Burma, Bangladesh, and Pakistan. *Annals of Zoology*, 22B, 412 pp.
- Mistry V, Vogel G, Tillack F (2007) Rediscovery of *Dinodon gammiei* (Blanford 1878) (Serpentes, Colubridae), with description of its validity. *Hamadryad* 31(2): 265–273.
- Rambaut A, Drummond AJ, Xie D, Baele G, Suchard MA (2018) Posterior summarization in Bayesian phylogenetics using Tracer 1.7. *Systematic Biology* 67(5): 901–904. <https://doi.org/10.1093/sysbio/syy032>
- Ronquist F, Teslenko M, Mark PVD, Ayres D, Darling A, Hohna S, Larget B, Liu L, Suchard MA, Huelsenbeck JP (2012) MrBayes 3.2: Efficient Bayesian phylogenetic inference and model choice across a large model space. *Systematic Biology* 61(3): 539–542. <https://doi.org/10.1093/sysbio/sys029>
- Smith MA (1943) The Fauna of British India, Ceylon and Burma, Including the Whole of the Indo-Chinese Sub-region. Reptilia and Amphibia. 3 (Serpentes). Taylor and Francis, London, 583 pp.
- Uetz P, Freed P, Aguilar R, Reyes F, Kudera J, Hošek J (2024) The Reptile Database. <http://www.reptile-database.org> [Accessed on Jan. 2024]
- Wall F (1923) A hand-list of snakes of the Indian empire. Part II. *The Journal of the Bombay Natural History Society* 29(3): 598–632.
- Wallach V, Williams KL, Boundy J (2014) Snakes of the World: A Catalogue of Living and Extinct Species. Taylor and Francis, CRC Press, 1237 pp. <https://doi.org/10.1201/b16901>
- Wang K, Ren JL, Chen HM, Lyu ZT, Guo XG, Jiang K, Chen JM, Li JT, Guo P, Wang YY, Che J (2020) The updated checklists of amphibians and reptiles of China. *Biodiversity Science* 28(2): 189–218. <https://doi.org/10.17520/biods.2019238>
- Wangyal JT (2013) New records of reptiles and amphibians from Bhutan. *Journal of Threatened Taxa* 5(13): 4774–4783. <https://doi.org/10.11609/JoTT.o3539.4774-83>
- Zhang DX, Hewitt GM (1996) Nuclear integrations: Challenges for mitochondrial DNA markers. *Trends in Ecology & Evolution* 11: 247–251. [https://doi.org/10.1016/0169-5347\(96\)10031-8](https://doi.org/10.1016/0169-5347(96)10031-8)

Matrix-based key to the click beetle genera of Canada and USA with a summary of habitat use (Coleoptera, Elateridae)

Hume B. Douglas¹, Frank E. Etzler², Paul J. Johnson³, H.E. James Hammond⁴

¹ Agriculture and Agri-Food Canada, Canadian National Collection of Insects, Arachnids and Nematodes, 960 Carling Avenue, Ottawa, Ontario, K1A 0C6, Canada

² Montana Department of Agriculture, 302 N. Roberts St., Helena, MT, 59601, USA

³ Insect Biodiversity Lab, Box 2100A, 1030 N. Campus Drive, South Dakota State University, Brookings, South Dakota 57007, USA

⁴ Natural Resources Canada, Canadian Forest Service, Northern Forestry Centre, 5320 – 122 Street NW, Edmonton, Alberta, T6H 3S5 Canada

Corresponding author: Hume B. Douglas (hume.douglas@agr.gc.ca)

Abstract

The Elateridae, or click beetles are abundant and diverse in most terrestrial ecosystems in North America, acting as plant pests and filling many other ecological roles. The 112 genera of Elateridae Leach, 1815, or click beetles, known from Canada and USA are included in a first comprehensive digital interactive key to adults. A link to an online peer-reviewed LUCID key to elaterid genera and downloadable LUCID files are provided. Diagnostic morphological summaries using information from the 61 characters and 158 character states of the matrix key are presented for all genera. A table summarizes current understanding of habitat use by all elaterid genera in Canada and USA from literature, collections, citizen science, and our own observations. Diversity of elaterid genera was high throughout warm and cool temperate regions, especially in mountainous areas and mesic woodlands. Larvae of most genera were associated with soil, litter and decaying wood.

Key words: Click beetle, crop pests, digital identification tools, interactive key, invasive alien species, key, LUCID, matrix key, wireworms



Academic editor: Vinicius S. Ferreira

Received: 22 January 2024

Accepted: 25 March 2024

Published: 7 May 2024

ZooBank: <https://zoobank.org/EC676896-635D-4AB3-9D84-EF5A2E2932C9>

Citation: Douglas HB, Etzler FE, Johnson PJ, Hammond HEJ (2024) Matrix-based key to the click beetle genera of Canada and USA with a summary of habitat use (Coleoptera, Elateridae). ZooKeys 1200: 75–144. <https://doi.org/10.3897/zookeys.1200.119315>

Copyright: This is an open access article distributed under terms of the CC0 Public Domain Dedication.

Introduction

Click beetles (Coleoptera: Elateridae) are common as adults and larvae in terrestrial ecosystems throughout the world. Adults are recognizable by the presence of a thoracic clicking mechanism combined with non-clubbed antennae and a labrum that is separated from the head capsule by a suture. The dorsoventrally compressed to nearly cylindrical larvae of Elateridae are present in soils and dead wood, with larvae of plant-damaging species known as wireworms. There are more than 400 valid elaterid genera worldwide, with 112 of these known from USA and Canada (Table 1), comprising nearly 1000 species (Johnson 2002). Phylogenetic analyses have prompted transfers of several genera from other beetle families into Elateridae (Kundrata and Bocak 2011; Kusy et al. 2018), and also demonstrate widespread homoplasy in morphological characters (Kundrata et al. 2018) making some elaterid genera (e.g., *Megapenthes* Kiesenwetter, 1858, see Douglas et al. 2021) difficult to define morphologically.

Elateridae are hard-bodied (although the abdomen is soft in some), mostly elongate beetles with a pro-mesothoracic clicking mechanism. The peg-like prosternal process fits into the mesothoracic intercoxal cavity but is not fixed there. Additionally, the labrum is exposed, antennae are not clubbed, and each leg has five tarsomeres. Elateridae can mostly be recognized and identified to genera by adult external morphology, although some generic concepts need further analysis. Elaterid genera are distinguished primarily by characters of the head, thorax, and legs. Identification usually begins by examining the frons, pronotum, mesosternum, mesothoracic cavities, elytra, and tarsi to form an overall impression of a specimen's morphology. Northern North America is one of few world regions which are covered by recent comprehensive keys to elaterid genera as adults (Arnett 1968; Johnson 2002). Larvae are also treated by partial keys to genera (Becker and Dogger 1991; Johnson 1993). Prior keys to adults are dichotomous and require readers to interpret difficult characters early in the specimen identification process. Digital matrix keys have improved ease of identification in other beetle groups (e.g., Hulcr and Smith 2010; Staines 2012), and we hope this approach will also work for Elateridae.

Digital matrix keys can facilitate taxonomic identifications by allowing flexible identification pathways, allowing users to select the characters that they can observe and interpret most easily. This can reduce the number of difficult character interpretations and allow for identification using fewer characters. We used a wide selection of mainly external morphological characters to generate a key to genera in the LUCID platform (Identix Ltd. 2020) to facilitate identification of adult Elateridae.

Materials and methods

Specimens used to generate the key were examined from the Canadian National Collection of Insects, Arachnids and Nematodes (CNC, Ottawa, Canada), and the South Dakota State University Insect Collection. These specimens were previously identified to species by E.C. Becker, W.J. Brown, M.C. Lane and the authors using a wide variety of literature and often comparison to type specimens. Specimen characters were photographed using a Leica M205c stereoscope and multifocus images assembled using Leica LAS 4.8 software. Habitus photos were taken using a Leica M80 dissecting scope with Leica EC3 camera attachment. Subsequent images were then rendered using CombineZ stacking software and GIMP v. 2.10.34 photo editor. The key and informal taxon descriptions were built using LUCID 3.6 software.

Most diagnostic characters were modified from keys by Stibick (1976; 1978; 1990), and Johnson (2002). Some, including presence of microserration of edges of the pronotum, abdominal ventrites and paramere setal counts, were adapted from Douglas (2011). Others were diagnostic characters for genera described from Douglas (2017), Etzler (2019), Etzler and Johnson (2018), Fuller (1994), and Johnson (2021). We also developed several new characters here for pronotal setal vestiture direction, and microserration of the edges of the mesosternal cavity. The key includes some aedeagal characters because these are useful and readily observable in standard dissection of males and in specimens with extended aedeagi. Other genitalic characters including those

from pregenital segments and internal genitalia were not included. Character definitions were edited for objectivity and tested by multiple users to improve diagnostic effectiveness.

Measurements: body length was measured from the anterior edge of the head capsule to the apex of the closed elytra; antennomeres were measured along their dorsal edges as the entire distance between the two adjacent antennomeres; pronotum length was measured at the midline, and width at the widest part. Informal descriptions and diagnostic summaries were generated in LUCID from morphological data used to encode genera and groups of species, together with LUCID's natural language description template tool.

We encoded specimens from more than 400 species directly into LUCID. One to 38 species were encoded per genus representing most or all species in most genera. Taxon sampling and testing were most extensive for diagnostically problematic or morphologically divergent genera. The morphologically diverse genus *Athous* Eschscholtz, 1829 was divided into species groups defined by Becker (1979). A further 14 genera were subdivided in the key matrix to accommodate morphological divergence in diagnostic characters and improve the genus-level diagnostic efficacy.

Distributional and habitat associations of Elateridae were compiled (Table 1) for the areas where they have been observed at scales including general bioregion, habitat, and larval substrate. Sources include published literature (including larval ecology inferences for the same genus from other world regions); museum specimen labels; records from research grade iNaturalist (2023) observations reviewed by HD; and our own field notes and observations. Data entered in each cell was designed for maximum specificity, so that cell contents within a column may require reader interpretation prior to comparison. Meadow includes all non-wetland herbaceous habitats such as cropland, abandoned cropland, native meadow, and grassland. This summary includes both tested knowledge and preliminary hypotheses in need of further study.

Result and discussion

Key to adults

The interactive LUCID key and accompanying diagnostic summaries include multiple routes to identification of one or both sexes of many species at the following internet URL: https://keys.lucidcentral.org/keys/v4/nearctic_elateridae/.

In more than 95% of cases, specimens could be accurately identified to genus via the key using morphology alone. Our testing did not lead to any incorrect identifications. However, some specimens of 11 genera were resolved only as belonging to one of two or three genera based on morphology. Here some *Margaiostus* Stibick, 1978 specimens were not separated from *Hypnoidus* Dillwyn, 1829; *Paractenicera fulvipes* (Bland, 1863) and *Proludius silvaticus* (Van Dyke, 1932) were not separated from *Acteniceromorphus* Kishii; *Selatosomus nigricans* (Fall, 1910) was not separated from *Hypoganus* Kiesenwetter, 1858; *Setasomus aratus* (LeConte, 1853) was not separated from *Selatosomus* Stephens, 1830 or *Tesolasomus* Johnson, 2021; *Setasomus nitidulus* (LeConte, 1853) and *S. rufopleuralis* (Fall, 1933) were not separated from *Billbrownia* Johnson, 2023; some *Blauta* LeConte specimens were not separated

from *Dipropus* Germar, 1839. In some cases, these could be discriminated by entering specimen collection locality data. We believe incompletely resolved identifications result from incomplete generic concepts needing further revisions in the Hypnoidinae, and parts of the Dendrometrinae, and Elaterinae. Diagnostic data from the key are also available as an LIF3 file (Suppl. material 1), and as a comma separated values file (Suppl. material 2).

Elaterid genera in the study area have mostly been diagnosed and defined in the taxonomic literature based on morphological similarity but the monophyly of most has not been tested phylogenetically. Some generic concepts do not match those applied to other parts of the world fauna, nor do they include useful larval characters. For example, North American *Athous*, *Ctenicera* Latreille, 1829, and *Megapenthes* include species matching multiple Palearctic genera. Our goal was to provide a diagnostic tool to match all species to their current taxonomic placement. Further future changes are expected.

Using the key

Instructions for using this key mostly match instructions from other recent LUCID keys (e.g., Brust et al. 2020; Klimov et al. 2016). We generally recommend using the LUCID wand tool to select characters for identification, plus the geographic characters at the bottom. Experienced elaterid identifiers may instead wish to focus efforts on observed distinctive characteristics of the specimen. The key is only reliable for identification of Elateridae from Canada and USA because the morphologies of species of these genera occurring elsewhere were not considered.

Table 1. Genera of Elateridae of Canada and USA with distribution and larval microhabitat.

Genus	Ecosystem/region	Habitat	Larval substrate	Source
<i>Acteniceromorpha</i> Kishii, 1955	Cool mesic, montane	Woodland, ecotones (edge habitats)	Soil, litter	18, 22, 27, 31, 32, 33
<i>Actenicerus</i> Kiesenwetter, 1858	Cool wetland, mesic prairie	Riparian meadow, woodland, wetland ecotones	Soil: organic	12, 16, 22, 33
<i>Aeolus</i> Eschscholtz, 1829	Warm temperate, not dry	Xeric to riparian meadow; suburban, agricultural	Soil, ant and termite nests	0, 3, 6, 9, 21, 29, 30, 33, 35
<i>Agriotes</i> Eschscholtz, 1829	Widespread, mesic	Meadow, woodland, desert, ecotones	Soil	0, 19, 21, 27, 28, 29, 30, 31, 36
<i>Agrypnus</i> Eschscholtz, 1829	Warm temperate	Xeric to mesic meadow, dunes, woodland, suburban	Soil, wood: subcortical	0, 20, 22, 24, 33
<i>Alaus</i> Eschscholtz, 1829	Temperate to warm temperate	Woodland, suburban	Wood	0, 5, 20, 22
<i>Ampedus</i> Dejean, 1833	Mesic temperate, montane	Woodland, savannah	Wood, litter	0, 12, 18, 19, 27, 29, 32, 33
<i>Anchastus</i> LeConte, 1853	Temperate	Woodland, desert steppe, suburban	Soil; wood: subcortical	1, 20, 22, 24, 33
<i>Anostirus</i> Thomson, 1859	Cool temperate	Woodland, embankments, savannah	Soil	12, 20, 22
<i>Anthracalaus</i> Fairmaire, 1888	Arizona	Desert riparian woodland, scrub	Unknown	22
<i>Anthracopteryx</i> Horn, 1891	Colorado and Wyoming	Mountain foothills; short grassland	Soil	9
<i>Aphricus</i> LeConte, 1853	Warm desert	Desert, chaparral	Unknown	22
<i>Aplastus</i> LeConte, 1859	Warm, dry	Scrub, savannah	Unknown	22, 33
<i>Aptopus</i> Eschscholtz, 1829	Warm desert	Scrubland, woodland	Soil	20, 22
<i>Ascoliocerus</i> Mequignon, 1930	Cool temperate	Subalpine meadow, tundra, riparian	Soil	9
<i>Athoplastus</i> Johnson & Etzler, 2018	Cool western, humid	Woodland, savannah	Litter	15
<i>Athous</i> Eschscholtz, 1829	Widespread	Woodland, savannah, meadow	Wood: subcortical, soil, litter,	12, 16, 18, 27, 38

Genus	Ecosystem/region	Habitat	Larval substrate	Source
<i>Barrelater</i> Johnson, 2014	Great Basin	Shrub-steppe, dunes	Sandy soils	23
<i>Beckerus</i> Johnson, 2008	Boreal/montane	Woodland, springs, bogs	Moss mats, litter	9, 16, 33
<i>Berninelsonius</i> Leseigneur, 1970	Boreal/montane	Meadow, riparian	Soil	22
<i>Billbrownia</i> Johnson, 2023	Cool to warm temperate	Woodland, savannah	Wood: subcortical	22, 33
<i>Bladus</i> LeConte, 1861	Warm temperate	Riparian woodland	Unknown	22
<i>Blauta</i> LeConte, 1853	Mesic warm temperate	Woodland, scrub, suburban	Unknown	22
<i>Campylomorphus</i> Jacquelin du Val, 1860	Western mountains	Woodland ecotone	Wood, litter	12, 22
<i>Cardiophorus</i> Eschscholtz, 1829	Temperate/tropical	Meadow, dune, woodland, alpine	Sandy soil, decayed wood	0, 14, 22
<i>Chalcolepidius</i> Eschscholtz, 1829	Warm temperate	Woodland, desert scrub	Wood	20, 22
<i>Corymbitodes</i> Buysson, 1904	Cool temperate	Woodland, mesic meadow	Soil	20, 22, 28, 33
<i>Ctenicera</i> Latreille, 1829	Boreal	Woodland, savannah	Soil	12, 16, 22, 32
<i>Dalopius</i> Eschscholtz, 1829	Temperate, mesic	Mesic woodland, meadow	Soil	0, 1, 12, 27, 29, 31, 35
<i>Danosoma</i> Thomson, 1859	Cool temperate	Woodland, savannah	Wood, subcortical	19, 20, 22
<i>Deilelater</i> Costa, 1975	Subtropical	Woodland, desert shrub	Soil, wood	22, 33
<i>Denticollis</i> Piller and Mitterpacher, 1783	Boreal	Woodland	Wood, litter	16, 18, 19, 22
<i>Deronocus</i> Johnson, 1997	California	Dry woodland, savannah, chaparral	Probably soil	22, 33
<i>Desolakerrus</i> Stibick, 1978	Montane	Desert, riparian (intermittent)	Soil	9
<i>Diacanthous</i> Reitter, 1905	Boreal	Woodland	Wood	9, 16, 18
<i>Dicrepidius</i> Eschscholtz, 1829	Temperate/tropical	Woodland, savannah, scrub, suburban	Wood	0, 3, 4, 7, 20, 22
<i>Diplostethus</i> Schwarz, 1907	Warm	Woodland, scrub, desert	Soil, wood	0, 20, 22, 24
<i>Dipropus</i> Germar, 1839	Temperate/tropical	Woodland, scrub, suburban	Wood, soil	0, 3, 4, 7, 20, 22
<i>Dixicollis</i> Johnson, 2021	Southeastern USA	Woodland	Soil	16, 22
<i>Dolerosomus</i> Motschulsky, 1859	Temperate	Montane woodland, hilltop meadow?	Unknown	20, 22, 33
<i>Drapetes</i> Dejean, 1821	Warm Temperate	Woodland, savannah	Wood, subcortical	2, 20, 22, 33
<i>Eanus</i> LeConte, 1861	Boreal and cool montane	Woodland, peatland, subalpine	Litter, mosses, soil	1, 9, 16, 18, 19, 26, 33
<i>Elater</i> Linnaeus, 1758	Warm Temperate	Woodland, savannah, suburban	Tree cavities	0, 20, 22, 28, 34
<i>Elathous</i> Reitter, 1890	Widespread	Woodland, savannah	Soil, wood,	12, 16, 20, 22, 33, 37, 38
<i>Esthesopus</i> Eschscholtz, 1829	Warm Temperate/tropical	Desert, dune, woodland, savannah	Soil	20, 22, 24, 33
<i>Euplastius</i> Schwarz, 1903	Warm temperate	Woodland, meadow	Soil	22
<i>Euthysanius</i> LeConte, 1853	California	Scrub, savannah	Unknown	22
<i>Fleutiauxellus</i> Mequignon, 1930	Subarctic/boreal, eastern and western montane	Coastal meadow, montane meadow, riparian	Soil	9
<i>Floridelater</i> Douglas, 2017	Subtropical	Coastal dune	Soil	20, 22
<i>Gambrinus</i> LeConte, 1853	Widespread	Woodland, savannah, mesic meadow	Soil, litter, wood	12, 16, 22, 27, 31, 33
<i>Glyphonyx</i> Candèze, 1863	Mesic warm temperate	Woodland, meadow, suburban	Soil	0, 8, 10, 22
<i>Hadromorphus</i> Motschulsky, 1859	Cool temperate; lower montane	Woodland, mesic meadow, shrub steppe	Soil	16, 22, 29, 33, 35
<i>Hemicrepidius</i> Germar, 1839	Widespread	Woodland, savannah, meadow, coastal beach, montane, agricultural	Soil, litter, wood,	5, 16, 21, 26, 28, 29, 30, 33
<i>Heteroderes</i> Latreille, 1834	Warm	Dry meadow, woodland, desert, suburban	Soil	11, 22, 30, 33
<i>Horistonotus</i> Candèze, 1860	Temperate/tropical	Desert, woodland, meadow	Soil	0, 20, 22, 24
<i>Hypnoidus</i> Dillwyn, 1829	Cool temperate-boreal, alpine	Meadow, riparian, woodland, agricultural	Soil	12, 16, 18, 21, 22, 28, 29, 32
<i>Hypoganus</i> Kiesenwetter, 1858	Temperate, humid	Woodland, savannah	Wood: subcortical	8, 9, 10, 11, 36, 37
<i>Hypolithus</i> Eschscholtz, 1829	Cool temperate to subarctic	Marine shoreline	Soil	9, 12
<i>Idolus</i> Desbrochers des Loges, 1875	Cool temperate	Montane and hilltop meadow, woodland (<i>I. debilis</i>)	Soil, wood, litter/moss	0, 18, 20, 22, 33
<i>Ignelater</i> Costa, 1975	Subtropical	Woodland, scrub, suburban	Wood, litter, soil	20, 22, 33

Genus	Ecosystem/region	Habitat	Larval substrate	Source
<i>Lacon</i> Laporte, 1838	Widespread	Woodland, savannah	Wood: subcortical	0, 20, 22
<i>Laneganus</i> Johnson, 2021	Temperate, humid	Woodland, savannah	Wood	16, 20, 22,
<i>Lanelater</i> Arnett, 1952	Warm	Desert steppe, woodland, marine beach	Soil	13, 20, 22, 33
<i>Leptoschema</i> Horn, 1884	California	Woodland, savannah	Unknown	22
<i>Ligmargus</i> Stibick, 1976	Boreal/Montane	Riparian, alpine meadow	Soil	9
<i>Limonius</i> Eschscholtz, 1829	Widespread	Meadow, woodland, subalpine, marine dune	Soil, moss, litter	16, 21, 28, 29, 30, 31, 35
<i>Liotrichus</i> Kiesenwetter, 1858	Cool temperate, moist	Woodland	Soil, litter	12, 22
<i>Margaiostus</i> Stibick, 1978	Boreal/montane	Subalpine meadow, woodland	Soil	9, 27, 28
<i>Megapenthes</i> Kiesenwetter, 1858	Widespread	Woodland, desert	Soil, wood	0, 18, 19, 20, 22
<i>Melanactes</i> LeConte, 1853	Warm temperate	Woodland, savannah	Wood: subcortical	16, 22, 33
<i>Melanotus</i> Eschscholtz, 1829	widespread, tropical to cool temperate	Woodland, meadow, suburban, agricultural	Soil, wood	0, 27, 28, 29, 30, 31, 35
<i>Meristhus</i> Candèze, 1857	Warm temperate	Riparian	Sandy soil	20, 22, 33
<i>Metanomus</i> Buysson, 1887	Boreal	Woodland	Wood, litter	18, 20, 22, 31, 33
<i>Microhyphnus</i> Kishii, 1976	Cool temperate to boreal	Riparian (lake and stream shores)	Soil	22
<i>Migiwa</i> Kishii, 1966	Temperate, dry	Meadow slopes, riparian	Soil	1, 9
<i>Monocrepidius</i> Eschscholtz, 1829	Tropical to warm temperate	Meadow, woodland, desert, suburban, agricultural	Soil	0, 10, 21, 22, 30
<i>Negastris</i> Thomson, 1859	Cool temperate	Riparian, wetland, marine shoreline	Sand, gravel	0, 12, 20, 22
<i>Neohypdonus</i> Stibick, 1971	Cool temperate	Riparian, tundra, woodland	Soil	20, 22, 27, 31
<i>Neopristilophus</i> Buysson, 1894	Temperate, humid	Woodland	Wood	20, 22, 33
<i>Nitidolimonius</i> Johnson, 2008	Boreal/montane	Woodland, savannah, meadow	Litter, wood, mosses/soil	16, 18, 19, 27, 31, 33
<i>Octinodes</i> Candèze, 1863	Warm, dry	Savannah, scrub	Unknown	22, 33
<i>Oedostethus</i> LeConte, 1853	Cool temperate	Riparian, woodland, mesic meadow	Soil	1, 20, 22
<i>Oestodes</i> LeConte, 1853	Cool	Riparian, sandy meadow, saline mesic meadow	Soil	1, 20, 22
<i>Oistus</i> Candèze, 1857	Temperate west, mesic	Woodland, savannah	Wood	22, 26
<i>Orthostethus</i> Lacordaire, 1857	Warm	Woodland, dunes	Wood, soil	0, 20, 22
<i>Oxygonus</i> LeConte, 1863	Temperate, humid	Woodland, savannah, riparian	Soil	20, 22, 27, 33
<i>Paracardiophorus</i> Schwarz, 1895	Cool temperate, subalpine	Riparian, coastal and inland dunes, eroding banks	Soil: sandy	14, 22, 25
<i>Paractenicera</i> Johnson, 2008	Temperate, humid	Woodland	Unknown	22, 27
<i>Paradonus</i> Stibick, 1971	Cool temperate	Riparian, stream and lake shores	Soil	20, 22
<i>Parallellostethus</i> Schwarz, 1907	Warm, mesic	Woodland, savannah, suburban	Wood, Tree cavities	0, 22, 33
<i>Perissarthron</i> Hyslop, 1917	South Central U.S.A.	Riparian woodland, savannah	Unknown	22, 33
<i>Pheletes</i> Kiesenwetter, 1858	Cool temperate west	Woodland, savannah	Soil, wood	12
<i>Pherhimius</i> Fleutiaux, 1942	Warm humid	Woodland, savannah	Wood, soil	0, 20, 22
<i>Physorhinus</i> Germar, 1840	Subtropical/tropical, desert riparian woodland	Woodland, scrub	Wood	20, 22, 33
<i>Pityobius</i> LeConte, 1853	Warm temperate, east and west	Woodland, savannah	Wood, subcortical	0, 9, 33
<i>Procludius</i> Lane, 1971	Temperate, humid	Woodland, montane meadow	Soil	16, 20, 22
<i>Prosternon</i> Latreille, 1834	Cool temperate	Woodland, montane meadow	Soil, litter	12, 16, 22, 27, 28
<i>Pseudanostirus</i> Dolin, 1964	Temperate-boreal	Woodland, savannah	Soil, wood, litter	16, 18, 27, 28, 31, 33
<i>Pyrophorus</i> Billberg, 1820	Tropical, not established	Woodland, savannah	Soil, wood, litter	20, 22, 33
<i>Rismethus</i> Fleutiaux, 1947	Warm	Riparian	Riparian gravel	20, 22
<i>Scaptolenus</i> LeConte, 1853	Warm, seasonally dry	Dry meadow, savannah, desert steppe	Soil	22, 33
<i>Selatosomus</i> Stephens, 1830	Cool temperate, subalpine	Woodland, mesic meadow	Soil, moss/litter	12, 16, 21, 27, 28, 29, 32, 31, 33, 35
<i>Selonodon</i> Latreille, 1834	Warm	Meadow, woodland, savannah	Soil	22, 33
<i>Sericus</i> Eschscholtz, 1829	Cool temperate	Woodland, peatland, mesic meadow	Soil, peat, litter, wood	0, 12, 22, 19
<i>Setasomus</i> Gurjeva, 1985	Cool temperate	Woodland, savannah	Litter, wood	16, 18, 22, 33

Genus	Ecosystem/region	Habitat	Larval substrate	Source
<i>Strophenron</i> Johnson, 2021	Temperate, humid	Woodland, savannah	Litter, wood	16, 18, 27, 31, 27, 33
<i>Sylvanelater</i> Johnson, 2008	Cool temperate	Woodland, meadow, savannah, suburban	Soil	16, 18, 27, 28, 29, 33
<i>Tesolasomus</i> Johnson, 2021	Cool temperate	Woodland, meadow, montane steppe	Soil	16, 20, 22, 33
<i>Tetralimonius</i> Etzler, 2019	Temperate east and west	Woodland	Unknown	
<i>Vesperelater</i> Costa, 1975	Riparian in desert woodland, savannah	woodland, savannah, scrub	Unknown	22
<i>Vittathous</i> Johnson, 2021	Warm temperate	Woodland, mesic meadow	Soil, litter	22, 33
<i>Zorochros</i> Thomson, 1859	Cool temperate	Riparian	Sand, gravel	12, 20, 22

Key to sources: 0, Becker and Dogger (1991); 1, Brooks (1961); 2, Burakowski (1973); 3, Casari (1996); 4, Casari (2002); 5, Casari (2003); 6, Casari (2006); 7, Casari and Biffi (2012); 8, Cheshire and Jones (1988); 9, CNC specimens; 10, Deen and Cuthbert (1955); 11, Dobrovsky (1954); 12, Dolin (1978); 13, Donlan et al. (2004); 14, Douglas (2003); 15, Etzler and Johnson (2018); 16, Glen (1950); 18, Hammond (1997); 19, Hammond et al. (2017); 20, HD experience; 21, Hoernemann et al. (2001); 22, iNaturalist (2023); 23, Johnson (2014); 24, Johnston et al. (2023); 25, Lanchester and Lane (1972); 26 Lane (1972); 27) Levesque and Levesque (1980); 28) Levesque and Levesque (1993); 29, Milosavljevic et al. (2016); 30, Morrill (1978); 31, Nol et al. (2006); 32, Papp (1978); 33, PJJ experience; 34, Svensson et al. (2004); 35 Toba and Campbell (1992); 36, Traugott et al. (2014); 37 Van Dyke (1932); 38, Webster et al. (2012). Litter here also includes decayed wood fragments.

Ecological insights

Looking at regional diversity of elaterid genera from the online key, and the summary genus distributions, habitat, and microhabitat (Table 1) use allows preliminary insights into regional elaterid ecology. We found that some northern areas like Ontario (72 of 143 genera), New York (75 genera), or British Columbia (76 genera) have similar or higher numbers of genera than some southern areas like Florida (43 genera), Texas (44 genera), or even mountainous Arizona and New Mexico (51) genera. This shows that generic level diversity is not necessarily higher in unglaciated warm temperate areas than in once glaciated cool temperate areas. However, California (88 genera) did have the highest diversity, perhaps because of its diverse habitat types. Surprisingly, even this most diverse state was home to only ~ 60% of genera. The most northern regions like Alaska (37 genera) and Northwest Territories (32) genera had the lowest diversity, with a number of specialized northern genera. Overall, latitude was not a primary driver of elaterid genus-level diversity, except in subarctic and arctic areas.

By habitat type, most genera (89 of 143) were found, at least in part, in woodland. Some 36–38 genera were known from grassland. Many species were not restricted to either, with 30–32 genera inhabiting both woodland and grassland, and a further 31 genera known from intermediate habitats including scrub and savannah. At least three genera were known from peatlands. We expect genera with wood-dwelling larvae (and litter-dwelling larvae) to inhabit woody habitats, while those with soil dwelling larvae could inhabit both woody and herbaceous habitats. This hypothesis is consistent with the finding that only four genera were restricted to grassland (i.e., herbaceous) habitats.

By larval substrate type, most genera (80 of 143) were associated with soil and litter (including sand and gravel) and 40 with wood (partially decayed). Of these, 52 were associated with soil and litter but not wood, and 19 were associated with wood but not soil or litter. Plant pest genera include those known only from soil and genera with species known from both soil and wood. A further 21–23 genera had larvae known from both wood and soil or litter. These came from a combination of genera with species with different habitat specializations and from individual species with larva in both in decayed wood and soil or litter.

Informal descriptions and diagnostic summaries

Condensed informal descriptions and diagnostic summaries are provided for each genus or partial genus below. Summaries are condensed sets of characters meant to diagnose each from all other genera in this text. The informal descriptions give a wider morphological summary of a genus or partial genus, but do not repeat common characteristics of the subfamily or tribe (Table 2) to which it belongs. Where a character state is attributed to most members of a higher-level taxon, only alternate character states are reported for genera within that group. Expanded informal descriptions are provided in Suppl. material 3, and in the online key. Supporting figures can be found in the online lucid key. Informal descriptions and summaries are also provided for local members of subfamilies and tribes including two or more genera in the study area.

In some cases, these treatments may be more useful than established diagnoses and descriptions because they include standardized information for a broader set of diagnostic characters. However, their direct utility is mostly limited to Canada and USA because only species from there were used to characterize the genera. This means some generic concepts differ from those applied elsewhere in the world (e.g., *Athous*, *Ctenicera*, *Megapenthes*), and that some morphological variability within widely distributed genera were not included (e.g., the larger-bodied Neotropical species of *Monocrepidius* Eschscholtz, 1829 with spinose elytral apices, Marinho et al. 2023).

Table 2. Summary of the classification used for genera of Elateridae found in Canada and USA.

Subfamily	Tribe	Genus
Lissominae		<i>Drapetes</i> Dejean, 1821
Oestodinae		<i>Bladus</i> LeConte, 1861
Oestodinae		<i>Oestodes</i> LeConte, 1853
Elaterinae	Melanotini	<i>Melanotus</i> Eschscholtz, 1829
Elaterinae	Dicrepidiini	<i>Blauta</i> LeConte, 1853
Elaterinae	Dicrepidiini	<i>Dicrepidius</i> Eschscholtz, 1829
Elaterinae	Dicrepidiini	<i>Dipropus</i> Germar, 1839
Elaterinae	Ampedini	<i>Ampedus</i> Dejean, 1833
Elaterinae	Physorhinini	<i>Anchastus</i> LeConte, 1853
Elaterinae	Physorhinini	<i>Physorhinus</i> Germar, 1840
Elaterinae	Megapenthini	<i>Megapenthes</i> Kiesenwetter, 1858
Elaterinae	Aplastini	<i>Aplastus</i> LeConte, 1859
Elaterinae	Aplastini	<i>Euthysanius</i> LeConte, 1853
Elaterinae	Aplastini	<i>Octinodes</i> Candèze, 1863
Elaterinae	Cebrionini	<i>Scaptolenus</i> LeConte, 1853
Elaterinae	Cebrionini	<i>Selonodon</i> Latreille, 1834
Elaterinae	Elaterini	<i>Campylomorphus</i> Jacquelin du Val, 1860
Elaterinae	Elaterini	<i>Diplostethus</i> Schwarz, 1907
Elaterinae	Elaterini	<i>Dolerosomus</i> Motschulsky, 1859
Elaterinae	Elaterini	<i>Elater</i> Linnaeus, 1758
Elaterinae	Elaterini	<i>Orthostethus</i> Lacordaire, 1857
Elaterinae	Elaterini	<i>Parallelostethus</i> Schwarz, 1907
Elaterinae	Elaterini	<i>Sericus</i> Eschscholtz, 1829
Elaterinae	Pomachiliini	<i>Idolus</i> Desbrochers, 1875
Elaterinae	Pomachiliini	<i>Leptoschema</i> Horn, 1885
Elaterinae	Agriotini	<i>Agriotes</i> Eschscholtz, 1829
Elaterinae	Agriotini	<i>Dalopius</i> Eschscholtz, 1829

Subfamily	Tribe	Genus
Elaterinae	Synaptini	<i>Glyphonyx</i> Candèze, 1863
Pityobiinae		<i>Pityobius</i> LeConte, 1853
Agrypninae	Pseudomelanactini	<i>Anthracalaus</i> Fairmaire, 1888
Agrypninae	Pseudomelanactini	<i>Lanelater</i> Arnett, 1952
Agrypninae	Agrypnini	<i>Agrypnus</i> Eschscholtz, 1829
Agrypninae	Agrypnini	<i>Danosoma</i> Thompson, 1859
Agrypninae	Agrypnini	<i>Lacon</i> Laporte, 1838
Agrypninae	Agrypnini	<i>Meristhus</i> Candèze, 1857
Agrypninae	Agrypnini	<i>Rismethus</i> Fleutiaux, 1947
Agrypninae	Hemirhipini	<i>Alaus</i> Eschscholtz, 1829
Agrypninae	Hemirhipini	<i>Chalcolepidius</i> Eschscholtz, 1829
Agrypninae	Hemirhipini	<i>Pherhimius</i> Fleutiaux, 1942
Agrypninae	Pyrophorini	<i>Deilelater</i> Costa, 1975
Agrypninae	Pyrophorini	<i>Ignelater</i> Costa, 1975
Agrypninae	Pyrophorini	<i>Pyrophorus</i> Billberg, 1820
Agrypninae	Pyrophorini	<i>Vesperelater</i> Costa, 1975
Agrypninae	Oophorini	<i>Aeolus</i> Eschscholtz, 1829
Agrypninae	Oophorini	<i>Deronocus</i> Johnson, 1995
Agrypninae	Oophorini	<i>Heteroderes</i> Latreille, 1834
Agrypninae	Oophorini	<i>Monocrepidius</i> Eschscholtz, 1829
Hypnoidinae		<i>Ascoliocerus</i> Méquignon, 1930
Hypnoidinae		<i>Berninelsonius</i> Leseigneur, 1970
Hypnoidinae		<i>Desolakerrus</i> Stibick, 1978
Hypnoidinae		<i>Hypnoidus</i> Dillwyn, 1829
Hypnoidinae		<i>Hypolithus</i> Eschscholtz, 1829
Hypnoidinae		<i>Ligmargus</i> Stibick, 1976
Hypnoidinae		<i>Margaiostus</i> Stibick, 1978
Negastrinae		<i>Fleutiauxellus</i> Méquignon, 1930
Negastrinae		<i>Microhypnus</i> Kishii, 1976
Negastrinae		<i>Migiwa</i> Kishii, 1966
Negastrinae		<i>Negastrius</i> Thomson, 1859
Negastrinae		<i>Neohypdonus</i> Stibick, 1971
Negastrinae		<i>Oedostethus</i> LeConte, 1853
Negastrinae		<i>Paradonus</i> Stibick, 1971
Negastrinae		<i>Zorochros</i> Thomson, 1859
Cardiophorinae		<i>Aphricus</i> LeConte, 1853
Cardiophorinae		<i>Aptopus</i> Eschscholtz, 1829
Cardiophorinae		<i>Cardiophorus</i> Eschscholtz, 1829
Cardiophorinae		<i>Esthesopus</i> Eschscholtz, 1829
Cardiophorinae		<i>Floridelater</i> Douglas, 2017
Cardiophorinae		<i>Horistonotus</i> Candèze, 1860
Cardiophorinae		<i>Paracardiophorus</i> Schwarz, 1895
Dendrometrinae	Oxynopterini	<i>Melanactes</i> LeConte, 1853
Dendrometrinae	Oxynopterini	<i>Oistus</i> Candèze, 1857
Dendrometrinae	Oxynopterini	<i>Perissarthron</i> Hyslop, 1917
Dendrometrinae	Prosternini	<i>Acteniceromorphus</i> Kishii, 1955
Dendrometrinae	Prosternini	<i>Actenicerus</i> Kiesenwetter, 1858
Dendrometrinae	Prosternini	<i>Anostirus</i> C.G. Thomson, 1859
Dendrometrinae	Prosternini	<i>Anthracoptyx</i> Horn, 1891
Dendrometrinae	Prosternini	<i>Athoplastus</i> Johnson & Etzler, 2018
Dendrometrinae	Prosternini	<i>Beckerus</i> Johnson, 2008
Dendrometrinae	Prosternini	<i>Billbrownia</i> Johnson, 2023
Dendrometrinae	Prosternini	<i>Corymbitodes</i> Buysson, 1904
Dendrometrinae	Prosternini	<i>Ctenicera</i> Latreille, 1829
Dendrometrinae	Prosternini	<i>Dixicollis</i> Johnson, 2021
Dendrometrinae	Prosternini	<i>Eanus</i> LeConte, 1861
Dendrometrinae	Prosternini	<i>Hadromorphus</i> Motschulsky, 1859
Dendrometrinae	Prosternini	<i>Hypoganus</i> Kiesenwetter, 1858
Dendrometrinae	Prosternini	<i>Laneganus</i> Johnson, 2001

Subfamily	Tribe	Genus
Dendrometrinae	Prosternini	<i>Liotrichus</i> Kiesenwetter, 1858
Dendrometrinae	Prosternini	<i>Metanomus</i> Buysson, 1887
Dendrometrinae	Prosternini	<i>Neopristilophus</i> Buysson, 1894
Dendrometrinae	Prosternini	<i>Nitidolimonius</i> Johnson, 2008
Dendrometrinae	Prosternini	<i>Oxygonus</i> LeConte, 1863
Dendrometrinae	Prosternini	<i>Paractenicera</i> Johnson, 2008
Dendrometrinae	Prosternini	<i>Proludius</i> Lane, 1971
Dendrometrinae	Prosternini	<i>Prosternon</i> Latreille, 1834
Dendrometrinae	Prosternini	<i>Pseudanostirus</i> Dolin, 1964
Dendrometrinae	Prosternini	<i>Selatosomus</i> Stephens, 1830
Dendrometrinae	Prosternini	<i>Setasomus</i> Gurjeva, 1985
Dendrometrinae	Prosternini	<i>Stropenron</i> Johnson, 2021
Dendrometrinae	Prosternini	<i>Sylvanelater</i> Johnson, 2008
Dendrometrinae	Prosternini	<i>Tesolasomus</i> Johnson, 2021
Dendrometrinae	Dendrometrini	<i>Athous</i> Eschscholtz, 1829
Dendrometrinae	Dendrometrini	<i>Barrelater</i> Johnson, 2014
Dendrometrinae	Dendrometrini	<i>Denticollis</i> Piller & Mitterpacher, 1783
Dendrometrinae	Dendrometrini	<i>Diacanthous</i> Reitter, 1852
Dendrometrinae	Dendrometrini	<i>Elathous</i> Reitter, 1890
Dendrometrinae	Dendrometrini	<i>Euplastius</i> Reitter, 1890
Dendrometrinae	Dendrometrini	<i>Gambrinus</i> LeConte, 1853
Dendrometrinae	Dendrometrini	<i>Hemicrepidius</i> Germar, 1839
Dendrometrinae	Dendrometrini	<i>Limonius</i> Eschscholtz, 1829
Dendrometrinae	Dendrometrini	<i>Pheletes</i> Kiesenwetter, 1858
Dendrometrinae	Dendrometrini	<i>Tetralimonius</i> Etzler, 2019
Dendrometrinae	Dendrometrini	<i>Vittathous</i> Johnson, 2021

Subfamily Lissominae

Genus *Drapetes* Dejean, 1821

Habitus. Body length 2–6 mm. Scale-like setae absent. **Head.** Supra-antennal carinae variable; hypognathous; frons without triangular depression. Antennae with 11 antennomeres, not pectinate, sensory elements beginning on antennomere IV. **Prothorax.** Pronotum with dorsal punctures uniform sized, simple, without tubercles between punctures; pronotal lateral carinae complete, meeting anterior edge of prothorax at ~ 90° in lateral view, not serrate; bioluminescent spots absent; hind angle carinae present (single); posterior edge of pronotum without sublateral notches, crenellations absent; pronotosternal sutures excavate (able to contain antennae). Prosternum with sides straight at midlength; prosternal process not curved upward $\geq 40^\circ$ in lateral view. **Mesothorax.** Mesocoxal cavities open to mesepimeron only; mesoventral cavity without serration along sides. Scutellar shield (scutellum hereafter) with anterior edge not concave, posterior edge pointed (acuminate). Elytra. Anterior edge straight to arcuate near humeri in dorsal view, integument marked with spots or bands in most; some with pattern from differences in setal color; setal vestiture sparse on disk in most, apex not spinose. **Legs.** Metacoxal plate reaching side; tarsal pads or membranous lobes present on multiple tarsomeres, (I, II, III, and IV or II, III, and IV); claws without setae, appendiculate, or bifid. **Ventriles.** Sides not microserrate. **Aedeagus.** Parameres with articulation at base, apical lateral expansions absent.

Summary. Pronotosternal sutures excavate, multiple tarsomeres lobed. Small, distinctive Elateridae, but sometimes mistaken for other beetle families.

Subfamily Oestodinae

Habitus. Body length 4–9 mm. Scale-like setae absent. **Head.** Supra-antennal carinae fading on frons or absent; hypognathous; frons without triangular depression. Antennae with 11 antennomeres, not pectinate. **Prothorax.** Pronotum punctures uniform sized; without tubercles between punctures; lateral carinae complete, meeting anterior edge of prothorax at $\sim 90^\circ$ in lateral view, not serrate; bioluminescent spots absent; posterior edge with crenellations absent. Prosternum with sides straight or concave at midlength; prosternal process curved upward $> 40^\circ$ in lateral view. **Mesothorax.** Mesocoxal cavities open; mesoventral cavity without serration along sides. Scutellum with anterior edge not concave. Elytra. Anterior edge straight to arcuate near humeri in dorsal view, integument unmarked with spots or transverse bands, elytral apex not spinose. **Legs.** Metacoxal plate reaching side, plate without elongation in mesal half; tarsal pads absent; claws without setae, apex simple. **Ventrites.** Sides not microserrate. **Aedeagus.** Parameres articulated at base.

Genus *Bladus* LeConte, 1861

Habitus. Body length 4–6 mm. **Head.** Supra-antennal carinae fading on frons or absent; frons without triangular depression. Antennae with sensory elements beginning on antennomere IV. **Prothorax.** Pronotum with some punctures umbilicate; hind angle carinae absent; posterior edge of pronotum without sublateral notches; pronotosternal sutures closed, hypomeral bead present; hypomeron with posterior edge near hind angle without concavity. Prosternum with sides straight at midlength. **Mesothorax.** Scutellum with posterior edge rounded (arcuate). Elytra. Striae present; setal vestiture even and mainly parallel. **Aedeagus.** Parameres without apical lateral expansions.

Summary. Hypognathous, supra-antennal carinae absent or fading on frons, sensory elements beginning on antennomere IV (apical sensorium with short erect setae), prosternal sides straight, prosternal process ascendent, posterior edge of scutellum rounded.

Genus *Oestodes* LeConte, 1853

Habitus. Body length 4–9 mm. **Head.** Supra-antennal carinae fading on frons (not reaching another structure). Antennae with sensory elements beginning on antennomere III. **Prothorax.** Pronotum with dorsal punctures all simple; hind angle carinae present (single); posterior edge of pronotum with sublateral notches present; pronotosternal sutures open or closed; hypomera with arcuate concavity on posterior edge near hind angle. Prosternum with sides concave at midlength. **Mesothorax.** Scutellum rounded posterad or pointed (acuminate). Elytra. Setal vestiture sparse on disk or, if present, even and mainly parallel. **Aedeagus.** Parameres apical lateral expansions present, without setae or each paramere with three or more setae.

Summary. Hypognathous, supra-antennal carinae fading on frons, pronotum with sublateral notches, prosternal sides concave at midlength, prosternal process ascendant.

Subfamily Elaterinae

Habitus. Body length 3–35 mm. Scale-like setae absent. **Prothorax.** Pronotum without tubercles between punctures, lateral carinae not serrate; crenellations absent, bioluminescent spots absent. Prosternum with sides concave at mid-length in most. **Mesothorax.** Mesocoxal cavities not closed. Elytra. Setal vestiture even and mainly parallel, apex not spinose. **Legs.** Tarsal pads or membranous lobes absent, present on tarsomere III only, or present tarsomeres II and III; claws without setae, apex simple or with 3 or more points. **Ventrites.** Sides not microserrate. **Aedeagus.** Parameres with articulation at base, apical lateral expansions present or absent.

This group is defined based on evidence from larvae and DNA. It is difficult to define based on adult morphology.

Tribe Melanotini

Genus *Melanotus* Eschscholtz, 1829

Habitus. Body length 3–30 mm. **Head.** Supra-antennal carinae joining medially (forming shelf); nasale (head capsule below edge of frontal carina) with outline concave in lateral view; frons without triangular depression; gena not broadened anteriorly below eye, not extending spine-like anterior to basal tubercle of mandible (ventral condyle). Antennae not pectinate, sensory elements beginning on antennomere IV. **Prothorax.** Pronotum with some punctures umbilicate; pronotal lateral carinae complete, meeting anterior edge of prothorax at ~ 90° in lateral view; hind angle carinae present (one or two carinae); posterior edge of pronotum with sublateral notches present; pronotosternal sutures open, hypomerical bead present; hypomera with arcuate or angulate concavity on posterior edge near hind angle. Prosternum with sides concave at midlength; prosternal process not curved upward $\geq 40^\circ$ in lateral view. **Mesothorax.** Mesocoxal cavities not closed; mesoventral cavity without serration along sides. Scutellum with anterior edge not concave, posterior edge rounded (arcuate) or bilobed (concave at midline). Elytra. Striae present; anterior edge straight to arcuate or sinuate (recurved) near humeri in dorsal view, integument unmarked; without pattern from differences in setal color; setal vestiture even and mainly parallel. **Legs.** Metacoxal plate without elongation in mesal half; tarsal pads absent, tarsal claws with three or more points. **Aedeagus.** Each paramere with three or more setae.

Summary. Tarsal claws each with six or more points per side, pronotal lateral carina reaching anterior edge of pronotum.

Tribe Dicrepidiini

Habitus. Body length 4–18 mm. **Head.** Supra-antennal carinae joining medially (forming shelf); hypognathous; frons without triangular depression; gena not broadened anteriorly below eye, not extending spine-like anterior to basal tubercle of mandible (ventral condyle). **Prothorax.** Pronotum with dorsal punctures uniform sized, some or all punctures umbilicate, lateral carinae hidden anteriorly

in dorsal view, meeting anterior edge of prothorax at $\sim 90^\circ$ in lateral view; hind angle carinae present (single); pronotosternal sutures open; hypomera with arcuate concavity on posterior edge near hind angle. Prosternum with sides concave at midlength. **Mesothorax.** Mesocoxal cavities open; mesoventral cavity without serration along sides. Scutellum with anterior edge not concave. Elytra. Striae present; anterior edge straight to arcuate near humeri in dorsal view, integument unmarked; without pattern from differences in setal color; setal vestiture even and mainly parallel. **Legs.** Tarsal pads or membranous lobes present on multiple tarsomeres, (II and III), tarsal claws simple. **Aedeagus.** Parameres with apical lateral expansions present; each paramere with three or more setae.

Genus *Blauta* LeConte, 1853

Habitus. Body length 4–18 mm. **Head.** Nasale (head capsule below edge of frontal carina) with outline concave in lateral view; hypognathous. Antennae not pectinate, sensory elements beginning on antennomere III or IV. **Prothorax.** Pronotal lateral carinae complete or incomplete anteriorly; posterior edge of pronotum with sublateral notches in some; prosternal process not curved upward $\geq 40^\circ$ in lateral view. **Mesothorax.** Mesocoxal cavities open, scutellum with posterior edge rounded (arcuate). **Legs.** Metacoxal plate without elongation in mesal half.

Summary. Nasale without dorsally convergent carinae, hypognathous, pronotal sculpture rugose, pronotosternal sutures open, tarsomeres II and III lobed. Incompletely separated from *Dipropus* here.

Genus *Dicrepidius* Eschscholtz, 1829

Habitus. Body length 10–15 mm. **Head.** Nasale (head capsule below edge of frontal carina) with outline not concave in lateral view, nasale with two dorsally convergent carinae. Antennae pectinate or not, sensory elements beginning on antennomere III. **Prothorax.** Pronotal lateral carinae complete; posterior edge of pronotum with sublateral notches present, hypomeral bead present; prosternal process not curved upward $\geq 40^\circ$ in lateral view. **Mesothorax.** Mesocoxal cavities open, scutellum rounded posterad. **Legs.** Metacoxal plate without elongation in mesal half.

Summary. With dorsally convergent carinae above labrum.

Genus *Dipropus* Germar, 1839

Habitus. Body length 6–18 mm. **Head.** Nasale (head capsule below edge of frontal carina) with outline concave in lateral view; hypognathous. Antennae not pectinate, sensory elements beginning on antennomere III. **Prothorax.** Pronotal lateral carinae complete; posterior edge of pronotum with sublateral notches present, hypomeral bead present. **Mesothorax.** Mesocoxal cavities open, scutellum rounded posterad or pointed (acuminate).

Summary. Nasale without dorsally convergent carinae, hypognathous, pronotal sculpture fine to moderately rugose, pronotosternal sutures open, tarsomeres II and III lobed. Incompletely separated from *Blauta* here.

Tribe Ampedini

Genus *Ampedus* Dejean, 1833

Habitus. Body length 3–18 mm. **Head.** Supra-antennal carinae complete across frons in most, but narrowly separated from labrum; hypognathous in most; frons without triangular depression; gena not broadened anteriorly below eye, not extending spine-like anterior to basal tubercle of mandible (ventral condyle). Antennae not pectinate, sensory elements beginning on antennomere IV. **Prothorax.** Pronotum with dorsal punctures uniform sized; pronotal lateral carinae complete, meeting anterior edge of prothorax at ~ 90° in lateral view; hind angle carinae present (one or two carinae); posterior edge of pronotum without sublateral notches; pronotosternal sutures open, hypomerical bead present; hypomera with arcuate concavity on posterior edge near hind angle. Prosternum with sides straight or concave at midlength. **Mesothorax.** Mesocoxal cavities open; mesoventral cavity without serration along sides. Scutellum with anterior edge not concave, posterior edge pointed (acuminate). Elytra. Striae present; anterior edge straight to arcuate near humeri in dorsal view, integument marked with spots or transverse bands, or unmarked; without pattern from differences in setal color; setal vestiture even and mainly parallel. **Legs.** Metacoxal plate elongate in mesal half, plate reaching side; tarsal pads absent, claws simple. **Aedeagus.** Parameres with apical lateral expansions present; each paramere with three or more setae.

Summary. Supra-antennal carina complete, antennae not pectinate, pronotosternal sutures open, mesoventral cavity non-serrate, mesocoxal cavities open, metacoxal plates elongate, tarsi simple.

Tribe Physorhinini

Habitus. Body length 3–15 mm. **Head.** Supra-antennal carinae joining medially (forming shelf); nasale (head capsule below edge of frontal carina) with outline concave in lateral view; hypognathous; frons without triangular depression. Antennae not pectinate, sensory elements beginning on antennomere IV. **Prothorax.** Pronotum with dorsal punctures uniform sized; pronotal lateral carinae complete, meeting anterior edge of prothorax at ~ 90° in lateral view; hind angle carinae present (one or two carinae); hypomerical bead present; hypomera with arcuate concavity on posterior edge near hind angle. Prosternum with sides concave at midlength. **Mesothorax.** Mesoventral cavity without serration along sides. Scutellum with anterior edge not concave. Elytra. Striae present; anterior edge straight to arcuate near humeri in dorsal view; without pattern from differences in setal color; setal vestiture even and mainly parallel. **Legs.** Metacoxal plate elongate in mesal half; tarsal pads or membranous lobes present on tarsomere III only, tarsal claws simple. **Aedeagus.** Each paramere with three or more setae.

Genus *Anchastus* LeConte, 1853

Habitus. Body length 3–15 mm. **Head.** Hypognathous. Antennae with sensory elements beginning on antennomere IV. **Prothorax.** Pronotum with lateral carinae hidden anteriorly in dorsal view; hind angle carinae present (one or

two carinae). **Mesothorax.** Mesocoxal cavities open, scutellum with posterior edge rounded (arcuate) or pointed (acuminate). Elytra. Integument marked with spots or bands in some. **Aedeagus.** Parameres with apical lateral expansions present.

Summary. Legs with only tarsomere 3 lobed and head with frons not contrasting orange.

Genus *Physorhinus* Germar, 1840

Habitus. Body length 6–12 mm. **Head.** Hypognathous; gena not broadened anteriorly below eye, not extending spine-like anterior to basal tubercle of mandible (ventral condyle). Antennae with sensory elements beginning on antennomere IV. **Prothorax.** Pronotum with hind angle carinae present (single); posterior edge of pronotum without sublateral notches; pronotosternal sutures open; prosternal process not curved upward $\geq 40^\circ$ in lateral view. **Mesothorax.** Mesocoxal cavities not closed; scutellum rounded posterad. Elytra. Integument marked with spots or bands in some. **Legs.** Metacoxal plate reaching side. **Aedeagus.** Parameres without apical lateral expansions.

Summary. Legs with only tarsomere 3 lobed and head with frons orange and pronotum dark brown.

Tribe Megapenthini

Genus *Megapenthes* Kiesenwetter, 1858

Habitus. Body length 4–20 mm. **Head.** Supra-antennal carinae joining medially (forming shelf) or reaching anterior edge of head capsule; hypognathous in most; frons without triangular depression; gena not broadened anteriorly below eye in most, not extending spine-like anterior to basal tubercle of mandible (ventral condyle) in most. Antennae not pectinate, sensory elements beginning on antennomere III or IV. **Prothorax.** Pronotum with lateral carinae complete, hidden anteriorly in dorsal view, meeting anterior edge of prothorax at $\sim 90^\circ$ in lateral view; hind angle carinae present (single); pronotosternal sutures closed, hypomerical bead present; hypomera with arcuate or angulate concavity on posterior edge near hind angle. Prosternum with sides concave at midlength; prosternal process not curved upward $\geq 40^\circ$ in lateral view. **Mesothorax.** Mesocoxal cavities open; mesoventral cavity without serration along sides. Scutellum with anterior edge not concave. Elytra. Striae present; anterior edge straight to arcuate near humeri in dorsal view, integument marked with spots or bands in some; some with pattern from differences in setal color; setal vestiture even and mainly parallel. **Legs.** Metacoxal plate elongate in mesal half; tarsal pads absent, claws simple. **Aedeagus.** Each paramere with three or more setae.

Summary. Supra-antennal carina complete across frons or reaching anterior edge of head capsule, pronotal lateral carina complete, pronotosternal sutures closed, prosternum with sides concave, prosternal process with ventral apex near dorsal apex (not stair step-like), mesocoxal cavities open, elytra striate, metacoxal plates elongate and claws and tarsi simple. Polyphyletic.

Tribe Aplastini

Habitus. Body length 6–30 mm. **Head.** Supra-antennal carinae fading on frons or absent; labrum notched, gena not broadened anteriorly below eye, not extending spine-like anterior to basal tubercle of mandible (ventral condyle). Antennae pectinate or not. **Prothorax.** Pronotum with dorsal punctures uniform sized; lateral carinae meeting anterior edge of prothorax at $\sim 90^\circ$ in lateral view; posterior edge of pronotum without sublateral notches, concavity on posterior edge of hypomeron arcuate. Prosternum with sides concave at midlength; prosternal process curved upward $> 40^\circ$ in lateral view. **Mesothorax.** Mesocoxal cavities open; mesoventral cavity without serration along sides. Scutellum with anterior edge not concave. Elytra. Integument unmarked; without pattern from differences in setal color; setal vestiture even and mainly parallel. **Legs.** Tarsal pads absent, claws simple. **Aedeagus.** Parameres without apical lateral expansions, without setae, each paramere with three or more setae.

Genus *Aplastus* LeConte, 1859

Habitus. Body length 10–30 mm. **Head.** Supra-antennal carinae fading on frons or absent; prognathous in most; frons without triangular depression. Antennae not pectinate, sensory elements beginning on antennomere IV; antennomere III closer in length to II than IV. **Prothorax.** Pronotum with punctures simple; pronotal lateral carinae complete or incomplete anteriorly, visible throughout length in dorsal view; hind angle carinae present (single); pronotosternal sutures open or closed; hypomera with concavity on posterior edge near hind angle. **Mesothorax.** Scutellum with posterior edge not bilobed. Elytra. Anterior edge straight to arcuate near humeri in dorsal view. **Legs.** Metacoxal plate without elongation in mesal half.

Summary. Male antennae not pectinate (strongly serrate) with sensory elements beginning on antennomere IV (widespread rough texture and short erect setae), pronotum with setae oriented posterad throughout, lateral carinae visible throughout length in dorsal view, prosternum with sides concave near midlength, scutellum not bilobed posterad. Females unknown.

Genus *Euthysanius* LeConte, 1853

Habitus. Body length 12–30 mm. **Head.** Supra-antennal carinae absent; prognathous. Antennae with 12 antennomeres and pectinate in males, sensory elements beginning on antennomere IV. **Prothorax.** Pronotum with hypomeral bead present. **Mesothorax.** Scutellum with posterior edge bilobed (concave at midline) or straight (truncate). Elytra. Striae present; anterior edge straight to arcuate near humeri in dorsal view. **Legs.** Metacoxal plate without elongation in mesal half, plate not reaching side.

Summary. Supra-antennal carinae absent, male antennae pectinate with 12 antennomeres. Females with short elytra and 11 or 12 antennomeres.

Genus *Octinodes* Candèze, 1863

Habitus. Body length 6–20 mm. **Head.** Supra-antennal carinae absent; prognathous; frons without triangular depression. Antennae pectinate in males,

sensory elements beginning on antennomere IV. **Prothorax.** Pronotum with punctures simple; pronotal lateral carinae complete, visible throughout length in dorsal view; hind angle carinae present (single) or absent; pronotosternal sutures open or closed, hypomerical bead present. **Mesothorax.** Scutellum with posterior edge bilobed (concave at midline). Elytra. Striae present; anterior edge straight to arcuate near humeri in dorsal view. **Legs.** Metacoxal plate without elongation in mesal half, plate not reaching side.

Summary. Lack of supra-antennal carina, antennae pectinate with 11 antennomeres, scale-like setae absent. Females unknown.

Tribe Cebrionini

Habitus. Body length 6–30 mm. **Head.** Supra-antennal carinae absent; gena not broadened anteriorly below eye, not extending spine-like anterior to basal tubercle of mandible (ventral condyle). Antennae not pectinate. **Prothorax.** Pronotum with dorsal punctures uniform sized; lateral carinae incomplete anteriorly, also hidden anterad in dorsal view; posterior edge of pronotum without sublateral notches, concavity on posterior edge of hypomeron arcuate; pronotosternal sutures closed. Prosternum with sides concave at midlength. **Mesothorax.** Mesocoxal cavities open; mesoventral cavity without serration along sides. Scutellum with anterior edge not concave. Elytra. Integument unmarked; without pattern from differences in setal color; setal vestiture even and mainly parallel. **Legs.** Metacoxal plate not reaching side; tarsal pads absent, claws simple. **Aedeagus.** Parameres without apical lateral expansions.

Genus *Scaptolenus* LeConte, 1853

Habitus. Body length 12–30 mm. **Head.** Supra-antennal carinae absent; prognathous; frons without triangular depression. Antennae with sensory elements beginning on antennomere IV (evidence: erect hairs). **Prothorax.** Pronotum with punctures simple; hind angle carinae absent; hypomerical bead absent; hypomera with concavity on posterior edge near hind angle. **Mesothorax.** Scutellum with posterior edge pointed (acuminate). Elytra. Striae absent, anterior edge straight to arcuate near humeri in dorsal view. **Aedeagus.** Each paramere with two setae.

Summary. Supra-antennal carina absent, protibia with obtuse dorsal digging spine (or widening) near midlength. Also, prothorax with longest setae as long as antennomere I.

Genus *Selonodon* Latreille, 1834

Habitus. Body length 7–30 mm. **Head.** Supra-antennal carinae absent; frons without triangular depression. Antennae with sensory elements beginning on antennomere IV. **Prothorax.** Pronotum with punctures umbilicate in some; hind angle carinae present (single) or absent. **Mesothorax.** Scutellum with posterior edge rounded (arcuate), pointed (acuminate) or straight (truncate). **Aedeagus.** Parameres without setae or each paramere with three or more setae.

Summary. Supra-antennal carina absent, prosternum anterad of procoxae > 2× as wide as long, protibia without obtuse dorsal digging spine (or widening) near midlength. Also, prothorax with longest setae shorter than antennomere I.

Tribe Elaterini

Habitus. Body length 4–40 mm. **Head.** Hypognathous or weakly prognathous. Supra-antennal carinae fading on frons or vaguely reaching anterior edge of head capsule; frons without triangular depression; gena broadened anteriorly below eye and extending spine-like anterior to basal tubercle of mandible (ventral condyle) in most. Antennae not pectinate in most, sensory elements beginning on antennomere IV in most. **Prothorax.** Pronotum with dorsal punctures uniform sized, simple (not umbilicate) in most; lateral carinae, if complete, meeting anterior edge of prothorax at $\sim 90^\circ$ in lateral view; hind angle carinae present (single); posterior edge of pronotum without sublateral notches in most; hypomera with arcuate concavity on posterior edge near hind angle in most; pronotosternal sutures closed in most. Prosternum with sides concave at midlength. **Mesothorax.** Mesoventral cavity without serration along sides. Scutellum with anterior edge not concave. Mesocoxal cavities not closed. Elytra with anterior edge straight to arcuate near humeri in dorsal view, integument unmarked; without pattern from differences in setal color; setal vestiture even and mainly parallel. **Legs.** Metacoxal plate reaching side; tarsal pads absent, claws simple. **Aedeagus.** Each paramere with three or more setae.

Genus *Campylomorphus* Jacquelin du Val, 1860

Habitus. Body length 5–10 mm. **Head.** Gena not broadened anteriorly below eye, not extending spine-like anterior to basal tubercle of mandible (ventral condyle). Antennae with sensory elements beginning on antennomere III. **Prothorax.** Pronotal lateral carinae complete, visible throughout length in dorsal view; hypomeral bead present; prosternal process curved upward $> 40^\circ$ in lateral view. **Mesothorax.** Scutellum with posterior edge rounded (arcuate) or pointed (acuminate). Elytra. Striae present. **Legs.** Metacoxal plate without elongation in mesal half. **Aedeagus.** Parameres with apical lateral expansions present.

Summary. Antennal sensory elements beginning on III (widespread rough texture), pronotum with setae directed posterad on anterior half, lateral carinae complete, sublateral notches absent, prosternal sides concave, prosternal process ascending, tarsomeres simple. Previously placed in Dendrometrinae: Prosternini.

Genus *Diplostethus* Schwarz, 1907

Habitus. Body length 12–35 mm. **Prothorax.** Pronotum with punctures umbilicate in some; pronotal lateral carinae complete, visible throughout length in dorsal view; hypomeral bead absent; prosternal process not curved upward $\geq 40^\circ$ in lateral view. **Mesothorax.** Scutellum rounded posterad or pointed (acuminate). Elytra. Striae present or absent. **Legs.** Metacoxal plate elongate in mesal half. **Aedeagus.** Parameres without apical lateral expansions.

Summary. Supra antennal carinae fading on frons or reaching anterior of head capsule, antennomere III closer in length to II than to IV, gena produced spine-like beyond base of mandible, pronotal lateral carina complete anterad and visible throughout length in dorsal view, sublateral notches absent, pronotosternal sutures closed, sides of prosternum concave, mesosternal fossa

with sides not ledge-like in lateral view (not projecting below anterior part of mesocoxae) and prosternal process stair-step like in side view.

Genus *Dolerosomus* Motschulsky, 1859

Habitus. Body length 5–10 mm. **Head.** Gena not broadened anteriorly below eye, not extending spine-like anterior to basal tubercle of mandible (ventral condyle) or broadened anteriorly below eye, and extending spine-like anterior to basal tubercle of mandible. **Prothorax.** Pronotum with some punctures umbilicate; pronotal lateral carinae complete, hidden anteriorly in dorsal view; posterior edge of pronotum with sublateral notches in some; hypomera without concavity on posterior edge near hind angle in some; prosternal process not curved upward in lateral view. **Mesothorax.** Scutellum with posterior edge pointed (acuminate). Elytra. Striae present. **Legs.** Metacoxal plate without elongation in mesal half.

Summary. Supra-antennal carina reaching anterior edge of head capsule or fading on frons, gena produced beyond base of mandible, pronotosternal sutures closed, prosternal sides concave, scutellum pointed posterad, metacoxal plate not elongate.

Genus *Elater* Linnaeus, 1758

Habitus. Body length 12–18 mm. **Head.** Supra-antennal carinae reaching anterior edge of head capsule. **Prothorax.** Pronotal lateral carinae complete or incomplete anteriorly, hidden anteriorly in dorsal view; hypomerall bead present; prosternal process not curved upward $\geq 40^\circ$ in lateral view. **Mesothorax.** Scutellum with posterior edge pointed (acuminate). Elytra. Striae absent. **Aedeagus.** Parameres with apical lateral expansions in some.

Summary. Body length less than 20 mm, supra-antennal carina reaching anterior of head capsule, pronotum with lateral carina complete but, hidden from above in dorsal view, sides of prosternum concave, elytral striae absent (suggested by linear depressions in some).

Genus *Orthostethus* Lacordaire, 1857

Habitus. Body length 20–40 mm. **Head.** Supra-antennal carinae reaching anterior edge of head capsule. Antennae pectinate or not. **Prothorax.** Pronotal lateral carinae complete; hypomerall bead present; prosternal process not curved upward $\geq 40^\circ$ in lateral view. **Mesothorax.** Elytra. Striae absent. **Legs.** Metacoxal plate without elongation in mesal half. **Aedeagus.** Parameres without apical lateral expansions.

Summary. Body length > 20 mm, supra-antennal carina reaching anterior of head capsule, pronotum with lateral carina complete, sides of prosternum concave, mesosternal fossa with sides ledge-like in lateral view (projecting below anterior part of mesocoxae), elytra without striae.

Genus *Parallelostethus* Schwarz, 1907

Habitus. Body length 12–30 mm. **Prothorax.** Pronotal lateral carinae incomplete anteriorly; hypomerall bead present; prosternal process not curved upward $\geq 40^\circ$ in lateral view. **Mesothorax.** Scutellum rounded posterad or bilobed

(concave at midline). Elytra. Striae absent. **Legs.** Metacoxal plate elongate in mesal half. **Aedeagus.** Parameres without apical lateral expansions.

Summary. Supra antennal carinae fading on frons or reaching anterior edge of head capsule, pronotal lateral carinae incomplete anterad, mesoventral cavity with sides parallel along entire length, scutellum bilobed posterad, elytral striae absent.

Genus *Sericus* Eschscholtz, 1829

Habitus. Body length 6–17 mm. **Prothorax.** Pronotum with punctures umbilicate in some; pronotal lateral carinae complete, visible throughout length in dorsal view or hidden anterad; pronotosternal sutures open, hypomeral bead present; hypomera in some without concavity on posterior edge near hind angle; prosternal process not curved upward $\geq 40^\circ$ in lateral view. **Mesothorax.** Scutellum narrowly rounded posterad. Elytra. Striae present. **Legs.** Metacoxal plate without elongation in mesal half. **Aedeagus.** Parameres without apical lateral expansions.

Summary. Hypognathous, supra-antennal carina not complete across frons, gena produced spine-like beyond base of mandible, lateral carinae meeting anterior edge of pronotum at right angle, pronotum with most setae on anterior half directed posterad, prosternal sides concave, elytra striate, mesoventral cavity not serrate, metacoxal plate not elongate (slight rounded elongation in some), width at side greater than half width near midline.

Tribes Pomachiliini, Agriotini, and Synaptini

Habitus. Body length 3–18 mm. **Head.** Supra-antennal carinae variable; gena broadened anteriorly below eye, extending spine-like anterior to basal tubercle of mandible (ventral condyle). Antennae not pectinate, sensory elements beginning on antennomere IV. **Prothorax.** Pronotum with dorsal punctures uniform sized, setae on anterior half directed posterad; pronotal lateral carinae complete in most; pronotosternal sutures open in most; hind angle carinae present (single); posterior edge of pronotum without sublateral notches in most; hypomeral bead present in most; prosternal process not curved upward $\geq 40^\circ$ in lateral view. **Mesothorax.** Mesoventral cavity with serration along sides in most. Elytra. Striae present; anterior edge straight to arcuate near humeri in dorsal view; without pattern from differences in setal color; setal vestiture even and mainly parallel in most. **Legs.** Metacoxal plate reaching side in most; tarsal pads absent in most, claws simple in most.

These three similar and closely related tribes are treated collectively here.

Genus *Idolus* Desbrochers, 1875

Habitus. Body length 3–8 mm. **Head.** Supra-antennal carinae joining medially (forming shelf), becoming vague in some; nasale (head capsule below edge of frontal carina) with outline not concave in lateral view; hypognathous. **Prothorax.** Pronotum with some punctures umbilicate; pronotal lateral carinae hidden anteriorly in dorsal view, meeting mesal edge of hypomeron at $\sim 30^\circ$ in lateral view; hypomera with arcuate concavity on posterior edge near hind angle.

Prosternum with sides concave at midlength. **Mesothorax.** Mesocoxal cavities not closed; mesoventral cavity with serration along sides. Scutellum with anterior edge not concave, posterior edge rounded (arcuate) or pointed (acuminate). Elytra. Integument marked with spots or bands in most. **Legs.** Metacoxal plate elongate in mesal half. **Aedeagus.** Parameres with apical lateral expansions present; each paramere with two setae.

Summary. Supra-antennal carinae complete across frons touching anterior edge of head capsule only at midline in some, lateral carinae meeting anterior edge of pronotum at an acute angle, microserrate mesosternal cavity, and simple claws.

***I. debilis* (LeConte)**

Habitus. Body length 3–5 mm. **Head.** Supra-antennal carinae joining medially (forming shelf); nasale (head capsule below edge of frontal carina) with outline concave in lateral view. **Prothorax.** Pronotum with punctures simple; pronotal lateral carinae meeting anterior edge of prothorax at ~ 90° in lateral view; pronotosternal sutures closed; hypomera with arcuate or angulate concavity on posterior edge near hind angle. Prosternum with sides straight at midlength. **Mesothorax.** Mesocoxal cavities open; mesoventral cavity without serration along sides. Scutellum with anterior edge not concave, posterior edge rounded (arcuate). Elytra. Integument marked with spots or transverse bands, or unmarked. **Legs.** Metacoxal plate elongate in mesal half. **Aedeagus.** Parameres without apical lateral expansions, without setae.

Summary. Supra-antennal carinae complete across frons, pronotum with all setae oriented posterad near midlength, pronotosternal sutures straight, mesocoxal cavities open, metacoxal plates elongate, and tarsomeres simple. Like some Megapenthini.

Genus *Leptoschema* Horn, 1885

Habitus. Body length 12–18 mm. **Head.** Supra-antennal carinae joining medially (forming shelf); prognathous. **Prothorax.** Pronotum with some punctures umbilicate; pronotal lateral carinae hidden anteriorly in dorsal view, meeting anterior edge of prothorax at ~ 90° in lateral view hypomera with arcuate concavity on posterior edge near hind angle in most specimens. Prosternum with sides concave at midlength. **Mesothorax.** Mesocoxal cavities open; mesoventral cavity with serration along sides in most. Scutellum with posterior edge bilobed (concave at midline). Elytra. Integument unmarked. **Legs.** Metacoxal plate without elongation in mesal half. **Aedeagus.** Parameres with apical lateral expansions present; each with three or more setae.

Summary. Supra-antennal carinae complete across frons, lateral carinae meeting anterior edge of pronotum at a right angle, concave prosternal sides, open mesocoxal cavities, short metacoxal plates, and simple tarsi.

Genus *Agriotus* Eschscholtz, 1829

Habitus. Body length 3–12 mm. **Head.** Supra-antennal carinae fading on frons or reaching anterior edge of head capsule; hypognathous. **Prothorax.** Pronotum with lateral carinae complete or incomplete anteriorly, hidden

anteriorly in dorsal view, approaching mesal edge of hypomeron at ~ 30° in lateral view; posterior edge of pronotum with sublateral notches in some; hypomera with arcuate concavity on posterior edge near hind angle. **Mesothorax.** Mesocoxal cavities open; mesoventral cavity with serration along sides in most. Scutellum with anterior edge not concave, posterior edge rounded (arcuate) or pointed (acuminate). Elytra. Integument unmarked, setal vestiture direction and evenness variable. **Legs.** Metacoxal plate reaching side or not. **Aedeagus.** Parameres with apical lateral expansions present; apices setose.

Summary. Supra-antennal carinae reaching anterior edge of head capsule or fading in a few, lateral pronotal carina approaching anterior edge of pronotum at ~ 30°, open mesocoxal cavity, striate elytra, and simple claws.

Genus *Dalopius* Eschscholtz, 1829

Habitus. Body length 3–8 mm. **Head.** Supra-antennal carinae fading on frons (not reaching another structure); hypognathous in most. **Prothorax.** Pronotum with some punctures umbilicate; pronotal lateral carinae visible throughout length in dorsal view, meeting anterior edge of prothorax at ~ 90° in lateral view; hypomera with arcuate or angulate concavity on posterior edge near hind angle. Prosternum with sides concave at midlength. **Mesothorax.** Mesocoxal cavities open; mesoventral cavity with serration along sides. Elytra with integument unmarked. **Legs.** Metacoxal plate elongate in mesal half in some. **Aedeagus.** Parameres with apical lateral expansions present; apices setose.

Summary. Lateral carinae meeting anterior edge of pronotum at a right angle, carina visible in dorsal view anterad, edges of mesosternal fossa microserrate.

D. inordinatus Brown

Habitus. Body length 3–5 mm. **Head.** Supra-antennal carinae fading on frons; hypognathous. **Prothorax.** Pronotum with some punctures umbilicate; pronotal lateral carinae meeting anterior edge of prothorax at ~ 90° in lateral view; hypomera with arcuate concavity on posterior edge near hind angle. Prosternum with sides concave at midlength. **Mesothorax.** Mesocoxal cavities open; mesoventral cavity without serration along sides. Scutellum with anterior edge concave, posterior edge rounded (arcuate) or pointed (acuminate). Elytra. Integument unmarked. **Legs.** Metacoxal plate slightly elongate in mesal half. **Aedeagus.** Parameres with apical lateral expansions present; each paramere with two or more setae.

Summary. Supra-antennal carinae fading on frons, gena produced spine-like beyond base of mandible, lateral carinae of meeting anterior edge of pronotum at right angle, pronotum with most setae on anterior half directed posterad, posterior edge without sublateral notches, prosternal sides concave, mesoventral cavity not serrate, metacoxal plate slightly elongate. Like *Sericus* spp.

Genus *Glyphonyx* Candèze, 1863

Habitus. Body length 3–8 mm. **Head.** Supra-antennal carinae joining medially (forming shelf) or reaching anterior edge of head capsule; nasale (head capsule

below edge of frontal carina) with outline not concave in lateral view; hypognathous. **Prothorax.** Pronotum with punctures simple; pronotal lateral carinae hidden anteriorly in dorsal view, meeting mesal edge of hypomeron at $\sim 30^\circ$ in lateral view; posterior edge of pronotum with sublateral notches present; hypomera with arcuate concavity on posterior edge near hind angle. Prosternum with sides straight or concave at midlength. **Mesothorax.** Mesocoxal cavities not closed; mesoventral cavity with serration along sides. Elytra with integument unmarked with spots or transverse bands. **Legs.** Metacoxal plate without elongation in mesal half; tarsal pads present on tarsomere IV only, tarsal claws with 3 or more points. **Aedeagus.** Parameres without apical lateral expansions; each paramere with one or two setae.

Summary. Lateral pronotal carina meeting anterior edge of pronotum at $\sim 30^\circ$, sides of mesoventral cavity serrate, and claws with 3–4 points per side.

Subfamily Pityobiinae

Genus *Pityobius* LeConte, 1853

Habitus. Body length 20–40 mm. Scale-like setae absent. **Head.** Supra-antennal carinae joining medially (forming shelf); nasale (head capsule below edge of frontal carina) with outline concave in lateral view; prognathous; frons with triangular depression. Antennae with 11 or 12 antennomeres, bipectinate or not, sensory elements beginning on antennomere IV. **Prothorax.** Pronotum with dorsal punctures uniform sized, simple, without tubercles between punctures; pronotal lateral carinae complete, meeting anterior edge of prothorax at $\sim 90^\circ$ in lateral view, not serrate; bioluminescent spots absent; hind angle carinae present (single); posterior edge of pronotum without sublateral notches, crenellations absent; pronotosternal sutures closed, hypomeral bead present; hypomera with arcuate concavity on posterior edge near hind angle. Prosternum with sides straight or concave at midlength. **Mesothorax.** Mesocoxal cavities open; mesoventral cavity without serration along sides. Scutellum with anterior edge not concave, posterior edge rounded (arcuate). Elytra. Striae present; anterior edge straight to arcuate near humeri in dorsal view, integument unmarked; without pattern from differences in setal color; setal vestiture even and mainly parallel. **Legs.** Metacoxal plate without elongation in mesal half, plate reaching side; membranous lobes present on multiple tarsomeres, (I–IV); claws without setae, apex simple. **Ventrites.** Sides not microserrate. **Aedeagus.** Parameres with articulation at base, apical lateral expansions present, without setae.

Summary. Body length > 20 mm, antennomere III closer in length to II than IV (antennae bipectinate in males), pronotum longer than wide, tarsomeres I–IV with short lobes.

Subfamily Agrypninae

Habitus. Body length 3–30 mm. **Prothorax.** Pronotum crenellations absent. **Mesothorax.** Mesoventral cavity without serration along sides. **Legs.** Tarsal claws with setae in most, claws simple. **Ventrites.** Sides not microserrate. **Aedeagus.** Parameres with articulation at base; each paramere with three or more setae.

Tribe Pseudomelanactini

Habitus. Body length 20–40 mm. Scale-like setae absent. **Head.** Prognathous; frons without triangular depression. Antennae with 11 antennomeres, not pectinate, sensory elements beginning on antennomere IV. **Prothorax.** Pronotum with dorsal punctures uniform sized, simple, without tubercles between punctures; pronotal lateral carinae complete, visible throughout length in dorsal view, meeting anterior edge of prothorax at $\sim 90^\circ$ in lateral view, not serrate; bioluminescent spots absent; hind angle carinae present (single); posterior edge of pronotum without sublateral notches, hypomerical bead present; prosternal process not curved upward $\geq 40^\circ$ in lateral view. **Mesothorax.** Mesocoxal cavities open. Elytra. Striae present; anterior edge straight to arcuate near humeri in dorsal view, integument unmarked; without pattern from differences in setal color, apex not spinose. **Legs.** Metacoxal plate without elongation in mesal half; tarsal pads absent; claws with setae. **Aedeagus.** Parameres with apical lateral expansions present.

Genus *Anthracalaus* Fairmaire, 1888

Habitus. Body length 20–40 mm. **Head.** Supra-antennal carinae fading on frons or reaching anterior edge of head capsule. **Prothorax.** Pronotosternal sutures open; hypomera with arcuate or angulate concavity on posterior edge near hind angle. Prosternum with sides straight at midlength. **Mesothorax.** Scutellum with posterior edge rounded (arcuate). **Legs.** Metacoxal plate reaching side.

Summary. Body length > 20 mm, scale-like setae absent, bioluminescent spots absent, pronotosternal sutures open but not excavate, tarsal claws with setae.

Genus *Lanelater* Arnett, 1952

Habitus. Body length 12–30 mm. **Head.** Supra-antennal carinae variable; nasale (head capsule below edge of frontal carina) with outline concave or not in lateral view. **Prothorax.** Pronotum pronotosternal sutures excavate (able to contain antennae); hypomeron with posterior edge near hind angle without concavity. Prosternum with sides straight at midlength. **Mesothorax.** Elytra with setal vestiture even and mainly parallel.

Summary. Body length > 20 mm, scale-like setae absent, pronotosternal sutures excavate.

Tribe Agrypnini

Habitus. Body length 3–28 mm. Scale-like setae present. **Head.** Supra-antennal carinae fading on frons or reaching anterior edge of head capsule. Antennae with 11 antennomeres, not pectinate. **Prothorax.** Pronotum with punctures simple; bioluminescent spots absent; posterior edge of pronotum without sublateral notches; pronotosternal sutures excavate (able to contain antennae), hypomerical bead absent. **Mesothorax.** Elytra. Integument unmarked; setal vestiture even and mainly parallel, apex not spinose. **Legs.** Metacoxal plate reaching side; claws with or without setae.

Summary. Combination of scale-like setae and excavate pronotosternal sutures is distinctive.

Genus *Agrypnus* Eschscholtz, 1829

Habitus. Body length 6–12 mm. **Head.** Supra-antennal carinae fading on frons (not reaching another structure); hypognathous. **Prothorax.** Pronotum with dorsal punctures uniform sized, without tubercles between punctures; pronotal lateral carinae complete, visible throughout length in dorsal view, not serrate; hind angle carinae absent, hypomera with posterior concavities angulate. Prosternum with sides straight at midlength. **Mesothorax.** Mesocoxal cavities closed. Scutellum with anterior edge not concave. Elytra. Striae present; anterior edge sinuate (recurved) near humeri in dorsal view; without pattern from differences in setal color. **Legs.** Metacoxal plate without elongation in mesal half; tarsal pads absent; claws with setae. **Aedeagus.** Parameres without apical lateral expansions.

Summary. Scale-like setae present, supra-antennal carinae fading on frons, pronotosternal sutures excavate, mesocoxal cavities closed.

Genus *Danosoma* Thompson, 1859

Habitus. Body length 12–18 mm. **Head.** Supra-antennal carinae fading on frons or reaching anterior edge of head capsule. Antennal sensory elements beginning on antennomere III or IV. **Prothorax.** Pronotum with dorsal punctures uniform sized, without tubercles between punctures; pronotal lateral carinae complete, visible throughout length in dorsal view, not serrate; hind angle carinae absent, hypomera with posterior concavities angulate. Prosternum with sides convex at midlength; prosternal process not curved upward $\geq 40^\circ$ in lateral view. **Mesothorax.** Mesocoxal cavities not closed. Scutellum rounded posterad. Elytra. Striae absent, anterior edge straight to arcuate near humeri in dorsal view; with pattern from differences in setal color. **Legs.** Tarsal pads absent; claws without setae.

Summary. Body length > 10 mm, scale-like setae present, tarsal claws without setae.

Genus *Lacon* Laporte, 1838

Habitus. Body length 7–28 mm. **Head.** Supra-antennal carinae fading on frons or reaching anterior edge of head capsule. Antennal sensory elements beginning on antennomere III. **Prothorax.** Pronotum with dorsal punctures uniform sized, without tubercles between punctures; pronotal lateral carinae complete, not serrate; hind angle carinae present (single) or absent, concavity arcuate. Prosternum with sides straight or convex at midlength; prosternal process not curved upward $\geq 40^\circ$ in lateral view. **Mesothorax.** Mesocoxal cavities not closed. Scutellum with anterior edge concave or not. Elytra. Anterior edge straight to arcuate near humeri in dorsal view; some with pattern from differences in setal color. **Legs.** Metacoxal plate without elongation in mesal half; tarsal pads present on tarsomere IV only or absent; claws with setae. **Aedeagus.** Parameres with apical lateral expansions present.

Summary. Scale-like setae present, pronotosternal sutures excavate, mesepimeron reaching mesocoxal cavities, claws with basal setae.

Genus *Meristhus* Candèze, 1857

Habitus. Body length 3–5 mm. **Head.** Supra-antennal carinae reaching anterior edge of head capsule; hypognathous. Antennal sensory elements beginning on antennomere IV. **Prothorax.** Pronotum with dorsal punctures uniform-sized, with tubercles between punctures; pronotal lateral carinae incomplete anteriorly, visible throughout length in dorsal view; hind angle carinae absent, hypomera with posterior concavities angulate. Prosternum with prosternal process not curved upward $\geq 40^\circ$ in lateral view. **Mesothorax.** Mesocoxal cavities closed. Scutellum with anterior edge not concave, posterior edge rounded (arcuate). Elytra without pattern from differences in setal color. **Legs.** Tarsal pads absent; claws with setae. **Aedeagus.** Parameres with apical lateral expansions present.

Summary. Scale-like setae present, scutellum with carina along midline, prothorax with hemispherical tubercles between punctures.

Genus *Rismethus* Fleutiaux, 1947

Habitus. Body length 3–5 mm. **Head.** Supra-antennal carinae reaching anterior edge of head capsule. Antennal sensory elements beginning on antennomere IV. **Prothorax.** Pronotum with dorsal punctures of two distinct intermixed sizes (heterogeneous), without tubercles between punctures; pronotal lateral carinae incomplete anteriorly in most, carina visible throughout length in dorsal view, not serrate; hind angle carinae absent, hypomera with posterior concavities angulate. Prosternal process not curved upward $\geq 40^\circ$ in lateral view. **Mesothorax.** Mesocoxal cavities closed. Scutellum with anterior edge not concave, posterior edge rounded (arcuate). Elytra. Striae present; anterior edge sinuate (recurved) or with rectangular projections (crenellate) near humeri in dorsal view; without pattern from differences in setal color. **Legs.** Tarsal pads absent. **Aedeagus.** Parameres with apical lateral expansions present.

Summary. Scale-like setae present, scutellum with carina along midline, prothorax without tubercles between punctures (but some with projecting scales).

Tribe Hemirhipini

Habitus. Body length 13–35 mm. **Prothorax.** Pronotum with dorsal punctures uniform sized, without tubercles between punctures; pronotal lateral carinae complete, visible throughout length in dorsal view, not serrate; bioluminescent spots absent; posterior edge of pronotum without sublateral notches; pronotosternal sutures open or closed but not excavate; hypomera with concavity on posterior edge near hind angle; prosternal process not curved upward $\geq 40^\circ$ in lateral view. **Mesothorax.** Mesocoxal cavities open. Scutellum with anterior edge not concave. Elytra. Striae present, apex not spinose. **Legs.** Metacoxal plate reaching side; tarsal pads absent; claws with setae.

Summary. Large size, lack of bioluminescent spots, non-excavate, pronotosternal sutures, elytra with either scales or integument color pattern (or both), and presence of setae on tarsal claws are distinctive.

Genus *Alaus* Eschscholtz, 1829

Habitus. Body length 17–35 mm. Scale-like setae present, not metallic. **Head.** Supra-antennal carinae variable; prognathous. Antennae with 11 antennomeres, not pectinate. **Prothorax.** Pronotum with punctures simple; pronotosternal sutures closed. **Mesothorax.** Scutellum rounded posterad. Elytra. Integument unmarked; with pattern from differences in setal color; vestiture with bare patches in some. **Legs.** Metacoxal plate without elongation in mesal half. **Aedeagus.** Parameres with apical lateral expansions present.

Summary. Body length > 15 mm, pronotosternal sutures closed, posterior edge of scutellum rounded, elytra with non-metallic scales. Most or all with two eye-like dark patches of scales on pronotum.

Genus *Chalcolepidius* Eschscholtz, 1829

Habitus. Body length 17–35 mm. Scale-like setae present, metallic in some. **Head.** Supra-antennal carinae absent; prognathous. Antennae with 11 antennomeres, pectinate or not, sensory elements beginning on antennomere IV. **Prothorax.** Pronotum with punctures simple; hind angle carinae absent; hypomeral bead absent, concavity angulate. Prosternum with sides convex at midlength. **Mesothorax.** Scutellum with posterior edge bilobed (concave at midline) or straight (truncate). Elytra. Anterior edge sinuate (recurved) near humeri in dorsal view, integument unmarked; some with pattern from differences in setal color; setal vestiture even and mainly parallel. **Legs.** Metacoxal plate without elongation in mesal half.

Summary. Body length > 15 mm, posterior edge of scutellum bilobed or truncate, and elytra with scales are distinctive. Scales metallic in some.

Genus *Pherhimius* Fleutiaux, 1942

Habitus. Body length 15–20 mm. Scale-like setae absent. **Head.** Supra-antennal carinae joining medially (forming shelf); hypognathous. Antennae with 11 or 12 antennomeres, pectinate, sensory elements beginning on antennomere IV. **Prothorax.** Pronotum with some punctures umbilicate; hind angle carinae present (two carinae); pronotosternal sutures open, hypomeral bead present; hypomera with posterior concavities arcuate. **Mesothorax.** Elytra with anterior edge straight to arcuate near humeri in dorsal view, integument marked longitudinal and transverse bands, also with pattern from differences in setal color; setal vestiture even and mainly parallel. **Aedeagus.** Parameres with apical lateral expansions present.

Summary. Body length > 15 mm, antennae pectinate, vestiture not scale-like and elytra with color pattern.

Tribe Pyrophorini

Habitus. Body length 10–40 mm. Scale-like setae absent. **Head.** Supra-antennal carinae joining medially (forming shelf) or reaching anterior edge of head capsule. Antennae with 11 antennomeres, not pectinate, sensory elements be-

ginning on antennomere IV. **Prothorax.** Pronotum with dorsal punctures uniform sized, without tubercles between punctures; pronotal lateral carinae complete, visible throughout length in dorsal view, not serrate; bioluminescent spots present; posterior edge of pronotum without sublateral notches; pronotosternal sutures not excavate; hypomera with arcuate concavity on posterior edge near hind angle. Prosternum with sides straight at midlength; prosternal process not curved upward $\geq 40^\circ$ in lateral view. **Mesothorax.** Mesocoxal cavities open. Elytra. Anterior edge straight to arcuate near humeri in dorsal view, integument unmarked; without pattern from differences in setal color; setal vestiture even and mainly parallel. **Legs.** Metacoxal plate without elongation in mesal half, plate reaching side; profemur without carina across anterior face; tarsal pads absent; claws with setae.

Summary. Bioluminescent organs on pronotum are distinctive.

Genus *Deilelater* Costa, 1975

Habitus. Body length 12–18 mm. **Head.** Supra-antennal carinae joining medially (forming shelf); nasale (head capsule below edge of frontal carina) with outline not concave in lateral view; prognathous. **Prothorax.** Pronotum with punctures simple; hind angle carinae present (single) or absent, hypomeral bead present. **Mesothorax.** Scutellum with anterior edge not concave, posterior edge rounded (arcuate). Elytra. Striae present, apex not spinose. **Aedeagus.** Parameres with apical lateral expansions present.

Summary. Antennae reaching beyond midlength of pronotum, pronotum with bioluminescent spots, and punctures simple, elytral apices not spinose.

Genus *Ignelater* Costa, 1975

Habitus. Body length 17–35 mm. **Head.** Supra-antennal carinae joining medially (forming shelf); nasale (head capsule below edge of frontal carina) with outline not concave in lateral view; prognathous; frons without triangular depression. **Prothorax.** Pronotum with punctures simple; hind angle carinae present (single). **Mesothorax.** Scutellum rounded posterad or pointed (acuminate). Elytra. Striae present, apex spinose. **Aedeagus.** Parameres with apical lateral expansions present.

Summary. Pronotum with bioluminescent spots, antennae reaching beyond midlength of pronotum, elytral apices spinose.

Genus *Pyrophorus* Billberg, 1820

Habitus. Body length 20–40 mm. **Head.** Supra-antennal carinae joining medially (forming shelf); prognathous; frons without triangular depression. **Prothorax.** Pronotum with punctures simple; hind angle carinae present (single); pronotosternal sutures open. **Mesothorax.** Scutellum with anterior edge not concave, posterior edge rounded (arcuate). Elytra. Elytral apex spinose. **Aedeagus.** Parameres without apical lateral expansions.

Summary. Pronotum with bioluminescent spots, antennae not reaching beyond midlength of pronotum. Not established in USA or Canada.

Genus *Vesperelater* Costa, 1975

Habitus. Body length 20–40 mm. **Head.** Supra-antennal carinae joining medially (forming shelf); nasale (head capsule below edge of frontal carina) with outline not concave in lateral view; prognathous. **Prothorax.** Pronotum with some punctures umbilicate; hind angle carinae present (single); hypomeral bead present. **Mesothorax.** Scutellum with anterior edge not concave, posterior edge rounded (arcuate). Elytra. Striae present, apex not spinose. **Aedeagus.** Parameres with apical lateral expansions present.

Summary. Antennae reaching beyond midlength of pronotum, pronotum with bioluminescent spots, and punctures umbilicate, elytral apices not spinose.

Tribe Oophorini

Habitus. Body length 3–12 mm. Scale-like setae absent. **Head.** Supra-antennal carinae joining medially (forming shelf) in most; frons without triangular depression. Antennae with 11 antennomeres, not pectinate, sensory elements beginning on antennomere IV. **Prothorax.** Pronotum with punctures simple, without tubercles between punctures; pronotal lateral carinae complete, not serrate; bioluminescent spots absent; pronotosternal sutures not excavate. **Mesothorax.** Scutellum with anterior edge not concave. Elytra. Striae present, elytra with anterior edge straight to arcuate near humeri in dorsal view, integument marked with spots or bands in many; setal vestiture even and mainly parallel. **Legs.** Metacoxal plate reaching side in most; tarsal pads present on tarsomere IV in most (not on any others); claws with setae in most.

Small to moderate size, lack of scale-like setae and bioluminescent spots, non-excavate pronotosternal sutures and presence of setae on tarsal claws are distinctive. Setae on claws are difficult to observe on small specimens (not to be confused with setae projecting between the claw bases). Most or all with striae not merging before elytral apex.

Genus *Aeolus* Eschscholtz, 1829

Habitus. Body length 3–10 mm. **Head.** Nasale (head capsule below edge of frontal carina) with outline concave in lateral view. **Prothorax.** Pronotum with dorsal punctures uniform sized; hind angle carinae present (single); posterior edge of pronotum without sublateral notches; pronotosternal sutures closed, hypomeral bead present; hypomera with concavity on posterior edge near hind angle. Prosternum with sides straight at midlength; prosternal process not curved upward $\geq 40^\circ$ in lateral view. **Mesothorax.** Mesocoxal cavities not closed; scutellum rounded posterad. Elytra. Integument marked with spots or bands in many; without pattern from differences in setal color. **Legs.** Metacoxal plate elongate in mesal half; profemur with carina across anterior face (basidorsal to apicoventral); claws with or without setae. **Aedeagus.** Parameres without apical lateral expansions.

Summary. Profemur with carina across anterior face is distinctive. Most with body orange with darker markings.

Genus *Deronocus* Johnson, 1995

Habitus. Body length 6–12 mm. **Head.** Supra-antennal carinae fading on frons or reaching anterior edge of head capsule; prognathous. **Prothorax.** Pronotum with dorsal punctures uniform sized, lateral carinae hidden anteriorly in dorsal view; hind angle carinae present (single); posterior edge of pronotum with sublateral notches present; pronotosternal sutures open, hypomeral bead present; hypomera with arcuate or angulate concavity on posterior edge near hind angle. Prosternum with sides straight at midlength; prosternal process not curved upward $\geq 40^\circ$ in lateral view. **Mesothorax.** Mesocoxal cavities open, scutellum rounded posterad. Elytra. Integument unmarked; without pattern from differences in setal color. **Legs.** Metacoxal plate without elongation in mesal half, plate reaching side; profemur without carina across anterior face; tarsal pads absent. **Aedeagus.** Parameres with apical lateral expansions present.

Summary. Size moderate (6–12 mm), scale-like setae and bioluminescent spots absent, pronotal lateral carina hidden anterad in dorsal view, pronotosternal sutures open (but not excavate), simple tarsomeres, tarsal claws with setae.

Genus *Heteroderes* Latreille, 1834

Habitus. Body length 5–10 mm. **Head.** Prognathous. **Prothorax.** Pronotum with dorsal punctures of two distinct intermixed sizes (heterogeneous), carina visible throughout length in dorsal view or hidden anterad; hind angle carinae present (one or two carinae); posterior edge of pronotum with sublateral notches in some; pronotosternal sutures open, hypomeral bead absent; hypomera with arcuate or angulate concavity on posterior edge near hind angle. Prosternum with sides straight or concave at midlength. **Mesothorax.** Mesocoxal cavities open, scutellum rounded posterad or pointed (acuminate). Elytra. Integument marked with spots or bands in some; without pattern from differences in setal color. **Legs.** Profemur without carina across anterior face. **Aedeagus.** Parameres with apical lateral expansions present.

Summary. Scale-like setae absent; hypomeral bead present, legs with profemur non-carinate, tarsomere IV lobed, tarsal claws setose.

Genus *Monocrepidius* Eschscholtz, 1829

Habitus. Body length 3–12 mm. **Head.** Nasale (head capsule below edge of frontal carina) with outline concave in lateral view. **Prothorax.** Pronotum with dorsal punctures uniform sized, lateral carinae visible throughout length in dorsal view or hidden anterad; hind angle carinae present (one or two carinae) or absent; hypomeral bead present; hypomera with posterior concavities present. Prosternal process not curved upward $\geq 40^\circ$ in lateral view. **Mesothorax.** Mesocoxal cavities not closed. Elytra. Integument marked with spots or bands in some, some with pattern from differences in setal color. **Legs.** Profemur without carina across anterior face.

Summary. Scale-like setae absent; hypomeral bead present, legs with profemur non-carinate, tarsomere IV lobed, tarsal claws setose. Genus *Conoderus* Eschscholtz, 1829 is treated as a synonym here.

Subfamily Hypnoidinae

Habitus. Body length 3–12 mm. **Head.** Prognathous. Antennae with 11 antennomeres, not pectinate. **Prothorax.** Pronotum with punctures simple, without tubercles between punctures; pronotal lateral carinae complete, visible throughout length in dorsal view, meeting anterior edge of prothorax at $\sim 90^\circ$ in lateral view, not serrate; bioluminescent spots absent; hind angle carinae present (single), crenellations absent; pronotosternal sutures closed; hypomera with arcuate concavity on posterior edge near hind angle; prosternal process not curved upward $\geq 40^\circ$ in lateral view. **Mesothorax.** Mesocoxal cavities not closed; mesoventral cavity without serration along sides. Scutellum with anterior edge not concave. Elytra. Striae present; anterior edge straight to arcuate near humeri in dorsal view, integument unmarked or marked with spot or band in apical half only; without pattern from differences in setal color; setal vestiture even and mainly parallel, apex not spinose. **Legs.** Tarsal pads absent; claws without setae, apex simple. **Ventrites.** Sides not microserrate. **Aedeagus.** Parameres with articulation at base.

Summary. Pronotosternal sutures closed, tarsi and claws simple (not distinctive). All, except arctic genus *Hypolithus*, have mesocoxal cavities open to mesepimeron only. All, except some *Ligmargus* and *Margaiostus* have the supra-antennal carinae joining medially. Most 10 mm long or less and with sublateral plicae and notches present. Identification of this group can be difficult at all levels.

Genus *Ascoliocerus* Méquignon, 1930

Habitus. Body length 3–10 mm. Setae not thickened at midlength. **Head.** Supra-antennal carinae joining medially (forming shelf); nasale (head capsule below edge of frontal carina) with outline concave in lateral view. Antennal sensory elements beginning on antennomere IV. **Prothorax.** Pronotum with dorsal punctures uniform sized; posterior edge of pronotum with sublateral notches present, hypomeral bead absent. **Mesothorax.** Mesocoxal cavities open to mesepimeron only; scutellum rounded posterad. Elytra. Integument unmarked. **Legs.** Metacoxal plate elongate in mesal half, plate not reaching side. **Aedeagus.** Parameres with articulation at base, apical lateral expansions absent; each paramere with three or more setae.

Summary. Supra-antennal carinae joining medially, antennae with sensory elements beginning on antennomere IV (dense sculpture and short erect setae), pronotum with most setae on anterior half directed posterad or mesad, hypomeral bead absent, mesocoxal cavities partly open, tarsi simple, male parameres with three or more setae. Also, pronotal hind angles and posterior part near midline with short pale setae in addition to longer setae.

Genus *Berninelsonius* Leseigneur, 1970

Habitus. Body length 5–10 mm. Setae not thickened at midlength. **Head.** Supra-antennal carinae joining medially (forming shelf); nasale (head capsule below edge of frontal carina) with outline not concave in lateral view. Antennal sensory elements beginning on antennomere IV. **Prothorax.** Pronotum with dorsal

punctures uniform sized; posterior edge of pronotum with sublateral notches present, hypomeral bead absent. Prosternum with sides convex at midlength. **Mesothorax.** Mesocoxal cavities open to mesepimeron only; scutellum with posterior edge rounded (arcuate). Elytra. Integument unmarked. **Aedeagus.** Parameres with articulation at base, apical lateral expansions absent, without setae.

Summary. Supra-antennal carinae joining medially, antennae with sensory elements beginning on antennomere IV (apical sensorium), pronotum with most setae on anterior half directed posterad, hypomeral bead absent, tarsi simple, parameres without setae.

Genus *Desolakerrus* Stibick, 1978

Habitus. Body length 5–10 mm. Setae not thickened at midlength. **Head.** Supra-antennal carinae joining medially (forming shelf). Antennal sensory elements beginning on antennomere IV. **Prothorax.** Pronotum with dorsal punctures of two distinct intermixed sizes (heterogeneous); posterior edge of pronotum without sublateral notches, hypomeral bead present. **Mesothorax.** Mesocoxal cavities open to mesepimeron only; scutellum rounded posterad. Elytra. Integument unmarked. **Legs.** Metacoxal plate elongate in mesal half, plate not reaching side. **Aedeagus.** Parameres with articulation at base, apical lateral expansions absent; each paramere with three or more setae.

Summary. Elongate bodied, pronotum with setae directed anterad, mesocoxal cavities open to mesepimeron only, hypomeron metacoxal plates elongate medially. Also, hypomeron with larger punctures elongate.

Genus *Hypnoidus* Dillwyn, 1829

Habitus. Body length 3–10 mm. Setae thickened at midlength on scutellum in some. **Head.** Supra-antennal carinae joining medially (forming shelf). Antennal sensory elements beginning on antennomere IV or V. **Prothorax.** Pronotum with dorsal punctures uniform sized, with or without tubercles between punctures; posterior edge of pronotum with sublateral notches present, hypomeral bead absent. **Mesothorax.** Mesocoxal cavities open to mesepimeron only; scutellum rounded posterad. Elytra. Integument unmarked or marked with spot or band in apical half only. **Legs.** Metacoxal plate elongate in mesal half, plate not reaching side. **Aedeagus.** Parameres with articulation at base; each paramere with one seta.

Summary. Supra-antennal carinae joining medially, antennae with sensory elements beginning on antennomere IV or V (apical sensorium), hypomeral bead absent, tarsi simple, each paramere with one seta. We could not write a diagnosis that distinguished all specimens from *Margaiostus*.

Genus *Hypolithus* Eschscholtz, 1829

Habitus. Body length 6–12 mm. Setae not thickened at midlength. **Head.** Supra-antennal carinae joining medially (forming shelf); nasale (head capsule below edge of frontal carina) with outline not concave in lateral view. Antennal sensory elements beginning on antennomere IV. **Prothorax.** Pronotum with dorsal punctures uniform sized, without tubercles between punctures; posterior edge of pronotum without sublateral notches, hypomeral bead absent. Prosternum with sides straight at

midlength. **Mesothorax.** Mesocoxal cavities open, scutellum rounded posterad. Elytra. Integument unmarked. **Legs.** Metacoxal plate without elongation in mesal half, plate not reaching side. **Aedeagus.** Parameres with articulation at base, apical lateral expansions present; each paramere with three or more setae.

Summary. Supra-antennal carinae joining medially, pronotum dark with pale sides, pronotal sublateral notches absent, hypomeral bead absent, mesocoxal cavities open, metacoxal plate not reaching side of metacoxa. Also, hindwings short.

Genus *Ligmargus* Stibick, 1976

Habitus. Body length 6–12 mm. Setae not thickened at midlength. **Head.** Supra-antennal carinae joining medially (forming shelf) or reaching anterior edge of head capsule; nasale (head capsule below edge of frontal carina) with outline not concave in lateral view. Antennal sensory elements beginning on antennomere III or IV. **Prothorax.** Pronotum with dorsal punctures of two distinct intermixed sizes (heterogeneous), with or without tubercles between punctures; posterior edge of pronotum with sublateral notches present, hypomeral bead absent. **Mesothorax.** Mesocoxal cavities open to mesepimeron only. Elytra. Integument unmarked. **Legs.** Metacoxal plate not reaching side. **Aedeagus.** Parameres with articulation at base or at midlength, without setae or each paramere with three or more setae.

Summary. Supra-antennal carinae joining medially, pronotum with two size classes of intermixed punctures, posterior slope of pronotum with setae directed posterad, pronotosternal sutures closed, mesocoxal cavities open to mesepimeron only. Also, pronotum with dense longitudinal sculpture around punctures.

Genus *Margaiostus* Stibick, 1978

Habitus. Body length 6–12 mm. Setae not thickened at midlength. **Head.** Supra-antennal carinae joining medially (forming shelf) or reaching anterior edge of head capsule; nasale (head capsule below edge of frontal carina) with outline not concave in lateral view. Antennal sensory elements beginning on antennomere IV or V. **Prothorax.** Pronotum with dorsal punctures uniform sized; posterior edge of pronotum with sublateral notches present, hypomeral bead absent. **Mesothorax.** Mesocoxal cavities open to mesepimeron only; scutellum rounded posterad. Elytra. Integument unmarked. **Legs.** Metacoxal plate elongate in mesal half, plate not reaching side. **Aedeagus.** Parameres with articulation at base, apical lateral expansions present; each paramere with one or two setae.

Summary. Body length 6–12 mm. Supra-antennal carinae joining medially, antennae with sensory elements beginning on antennomere IV or V (apical sensorium), tarsi simple, aedeagus with one seta. We could not write a diagnosis that distinguished all specimens from *Hypnoidus*.

Subfamily Negastrinae

Habitus. Body length 3–6 mm. Setae not thickened at midlength. **Head.** Frons without triangular depression. Antennae with 11 antennomeres, not pectinate. **Prothorax.** Pronotal lateral carinae complete, meeting anterior edge of prothorax at ~ 90° in lateral view, not serrate; bioluminescent spots absent; hind angle

carinae present (single); posterior edge of pronotum without sublateral notches, crenellations absent; hypomera with concavity on posterior edge near hind angle; pronotosternal sutures closed. Prosternum with sides convex at midlength; prosternal process not curved upward $\geq 40^\circ$ in lateral view. **Mesothorax.** Mesocoxal cavities closed; mesoventral cavity without serration along sides. Elytra. Striae present; integument marked with spots or bands in some; without pattern from differences in setal color; setal vestiture even and mainly parallel, apex not spinose. **Legs.** Tarsal pads absent; claws without setae, apex simple, appendiculate, or bifid. **Ventriles.** Sides not microserrate. **Aedeagus.** Parameres with articulation at midlength, fused at base, apical lateral expansions absent.

Summary. Small beetles. Wide prosternum and closed mesocoxal cavities are diagnostic in combination with simple setae. Most like Cardiophorinae, Hypnoidinae, and some Agrypnini.

Genus *Fleutiauxellus* Méquignon, 1930

Habitus. Body length 2–6 mm. **Head.** Prognathous. Antennal sensory elements beginning on antennomere III. **Prothorax.** Pronotum with dorsal punctures uniform sized, simple, antero-medial portion with or without tubercles between punctures; pronotal lateral carinae visible throughout length in dorsal view, hypomeral bead present; hypomera with posterior concavities arcuate. **Mesothorax.** Elytra. Striae present; anterior edge straight to arcuate near humeri in dorsal view, integument unmarked. **Legs.** Tarsal claws simple. **Aedeagus.** Each paramere with three or more setae.

Summary. Small size, pronotum not strigose or tuberculate between punctures, prosternum with sides convex, mesocoxal cavities closed (barely in some), claws simple, parameres each with three or more setae (two in *Neohypdonus*).

Genus *Microhypnus* Kishii, 1976

Habitus. Body length 3–5 mm. **Head.** Supra-antennal carinae joining medially (forming shelf); prognathous. Antennal sensory elements beginning on antennomere IV. **Prothorax.** Pronotum with dorsal punctures uniform sized, simple, with elongate tubercles between punctures; pronotal lateral carinae visible throughout length in dorsal view, hypomeral bead present. **Mesothorax.** Scutellum with anterior edge not concave. Elytra. Striae present; anterior edge straight to arcuate near humeri in dorsal view, integument unmarked. **Legs.** Metacoxal plate elongate in mesal half, plate reaching side, tarsal claws simple. **Aedeagus.** Each paramere with two setae.

Summary. Small size, elytron without contrasting spots or bands, pronotum with elongate tubercles between punctures, prosternum with sides convex, mesocoxal cavities closed, claws simple. Incompletely distinguished from *Negastrius*.

Genus *Migiwa* Kishii, 1966

Habitus. Body length 3–5 mm. **Head.** Supra-antennal carinae joining medially (forming shelf); hypognathous. Antennal sensory elements beginning on antennomere IV. **Prothorax.** Pronotum with dorsal punctures uniform sized,

some or all punctures umbilicate, without tubercles between punctures; pronotal lateral carinae hidden anteriorly in dorsal view, hypomeral bead present; hypomera with posterior concavities arcuate. **Mesothorax.** Scutellum with anterior edge concave, posterior edge rounded (arcuate). Elytra. Striae present; integument unmarked with spots or transverse bands. **Legs.** Metacoxal plate elongate in mesal half, plate reaching side, tarsal claws simple. **Aedeagus.** Each paramere with three or more setae.

Summary. Prothorax with umbilicate punctures (requires 80X magnification), prosternum with sides convex, mesocoxal cavities closed, metacoxal plate reaching side.

Genus *Negastrius* Thomson, 1859

Habitus. Body length 3–5 mm. **Head.** Supra-antennal carinae joining medially (forming shelf); prognathous. Antennal sensory elements beginning on antennomere IV. **Prothorax.** Pronotum with dorsal punctures uniform sized, simple, with longitudinal carinae between punctures; pronotal lateral carinae complete or incomplete anteriorly, visible throughout length in dorsal view, hypomeral bead present; hypomera with posterior concavities arcuate. **Mesothorax.** Elytra. Striae present integument marked with spots or bands in many. **Legs.** Metacoxal plate elongate in mesal half, plate reaching side, tarsal claws simple. **Aedeagus.** Each paramere with two setae.

Summary. Small size, pronotum strigose between punctures, prosternum with sides convex, mesocoxal cavities closed. Most with elytra bicolored, and evenly convex in lateral view.

Genus *Neohypdonus* Stibick, 1971

Habitus. Body length 2–5 mm. **Head.** Supra-antennal carinae variable. Antennal sensory elements beginning on antennomere III or IV. **Prothorax.** Pronotum with dorsal punctures all simple, without tubercles between punctures. **Mesothorax.** Elytra. Integument marked with spots or bands in some. **Legs.** Metacoxal plate elongate in mesal half, tarsal claws simple. **Aedeagus.** Each paramere with two setae.

Summary. Small size, pronotum not strigose or tuberculate between punctures (ambiguous in *N. musculus* (Erichson)), prosternum with sides convex, mesocoxal cavities closed, claws simple, parameres each with two setae (three or more in *Fleutiauxellus*). Elytral striae weak near apex.

Genus *Oedostethus* LeConte, 1853

Habitus. Body length 3–5 mm. **Head.** Supra-antennal carinae joining medially (forming shelf); prognathous. Antennal sensory elements beginning on antennomere IV. **Prothorax.** Pronotum with dorsal punctures uniform sized, simple, without tubercles between punctures; hypomeral concavity arcuate. **Mesothorax.** Scutellum with anterior edge concave. Elytra. Striae present; anterior edge sinuate (recurved), with projection near humeri in dorsal view, integument unmarked with spots or transverse bands. **Legs.** Metacoxal plate reaching side, tarsal claws appendiculate. **Aedeagus.** Each paramere with two setae.

Summary. Small size, sides of prothorax convex, and claws appendiculate or at least thickened at base.

Genus *Paradonus* Stibick, 1971

Habitus. Body length 1–4 mm. **Head.** Supra-antennal carinae joining medially (forming shelf). Antennal sensory elements beginning on antennomere IV. **Prothorax.** Pronotum with dorsal punctures uniform sized, simple, without tubercles between punctures; pronotosternal sutures open, hypomeral bead present; hypomera with posterior concavities arcuate. **Mesothorax.** Scutellum with anterior edge concave, posterior edge pointed (acuminate). Elytra. Striae absent, anterior edge sinuate (recurved) with projection near humeri in dorsal view, integument marked with spots or transverse bands, or unmarked. **Legs.** Tarsal claws simple. **Aedeagus.** Each paramere with one seta.

Summary. Small size, sides of prothorax convex and elytral striae absent.

Genus *Zorochros* Thomson, 1859

Habitus. Body length 2–5 mm. **Head.** Supra-antennal carinae joining medially (forming shelf). Antennal sensory elements beginning on antennomere IV. **Prothorax.** Pronotum with antero-medial portion with or without tubercles between punctures; hypomeral bead present. **Mesothorax.** Scutellum with anterior edge concave. Elytra. Striae present; integument marked with spots or transverse bands, or unmarked. **Legs.** Metacoxal plate elongate in mesal half, plate not reaching side, tarsal claws simple. **Aedeagus.** Each paramere with three or more setae.

Summary. Small size, sensory elements beginning on antennomere IV (antennomere III cylindrical), sides of prosternum convex, mesocoxal cavities closed, elytra with striae present, metacoxal plate not reaching side (most). Most with tubercles on anterior half of pronotum near midline.

Subfamily Cardiophorinae

Habitus. Body length 3–12 mm. Scale-like setae absent. **Head.** Supra-antennal carinae joining medially (forming shelf); nasale (head capsule below edge of frontal carina) with outline concave in lateral view. Antennae with 11 antennomeres, not pectinate. **Prothorax.** Pronotum with sides not serrate; posterior crenellations absent; bioluminescent spots absent; without tubercles or ridges between punctures (but punctures on tubercles in *Floridelater*) hypomera with concavity on posterior edge near hind angle. Prosternum with sides straight or concave at midlength. **Mesothorax.** Mesocoxal cavities closed; mesoventral cavity without serration along sides. Scutellum with anterior edge concave in most (notched in many), posterior edge pointed (acuminate) in most or bilobed (concave at midline). Elytra. Striae present; integument marked with spots or bands in some; setal vestiture even and mainly parallel, apex not spinose. **Legs.** Tarsal claws without setae. **Aedeagus.** Parameres with articulation at midlength, fused at base.

Mid-sized beetles. Non-convex sides of prosternum, closed mesocoxal cavities and absence of scale-like setae are distinctive.

Genus *Aphricus* LeConte, 1853

Habitus. Body length 5–10 mm. **Head.** Hypognathous. Antennal sensory elements beginning on antennomere III. **Prothorax.** Pronotum with dorsal punctures uniform sized, simple; pronotal lateral carinae incomplete anteriorly; posterior edge of pronotum without sublateral notches; pronotosternal sutures open, hypomeral bead absent. Prosternal process curved upward $> 40^\circ$ in lateral view. **Mesothorax.** Scutellum with anterior edge concave, posterior edge pointed (acuminate). Elytra. Anterior edge straight to arcuate near humeri in dorsal view, integument unmarked; without pattern from differences in setal color. **Legs.** Metacoxal plate without elongation in mesal half; tarsal pads absent, claws simple. **Ventrites.** Sides not microserrate. **Aedeagus.** Each paramere with three or more setae.

Summary. Mesocoxal cavities closed, scutellum pointed posterad, claws simple, parameres each with three or more setae. Most or all with mandibles simple and antennae reaching beyond scutellum. Females unknown.

Genus *Aptopus* Eschscholtz, 1829

Habitus. Body length 6–12 mm. **Head.** Hypognathous. Antennal sensory elements beginning on antennomere III in most. **Prothorax.** Pronotum with dorsal punctures of two distinct intermixed sizes (heterogeneous), all simple; pronotal lateral carinae incomplete anteriorly, hidden in dorsal view; hind angle carinae present (single); posterior edge of pronotum with sublateral notches present; pronotosternal sutures closed. **Mesothorax.** Scutellum with anterior edge notched, posterior edge pointed (acuminate). Elytra. Integument unmarked; without pattern from differences in setal color. **Legs.** Metacoxal plate elongate in mesal half, plate not reaching side; tarsal pads absent, tarsal claws more than three points. **Aedeagus.** Each paramere with two setae.

Summary. Scutellum shaped like valentine heart, claws pectinate (6 or 7 apices per side).

Genus *Cardiophorus* Eschscholtz, 1829

Habitus. Body length 6–12 mm. **Head.** Antennal sensory elements beginning on antennomere III. **Prothorax.** Pronotum with dorsal punctures of two distinct intermixed sizes (heterogeneous), simple; pronotal lateral carinae incomplete anteriorly, hidden in dorsal view; hind angle carinae present (single); posterior edge of pronotum with sublateral notches present; pronotosternal sutures closed, hypomera with posterior concavity angulate. **Mesothorax.** Scutellum with anterior edge notched, posterior edge pointed (acuminate). Elytra. Anterior edge sinuate (recurved) or with rectangular projection near humeri in dorsal view, integument marked with humeral spots or bands in some; some with pattern from differences in setal color. **Legs.** Metacoxal plate not reaching side; tarsal pads absent, claws simple. **Ventrites.** Microserration at sides (e.g., 100 points per mm) present or absent. **Aedeagus.** Each paramere with one or two setae.

Summary. Scutellum shaped like valentine heart, pronotal lateral carinae incomplete (or absent), if present then visible from ventral view but not dorsal view, hypomera with posterior emargination angulate, claws simple.

Genus *Esthesopus* Eschscholtz, 1829

Habitus. Body length 3–10 mm. **Head.** Hypognathous. Antennal sensory elements beginning on antennomere III or IV. **Prothorax.** Pronotum with dorsal punctures of two distinct intermixed sizes (heterogeneous), all simple; pronotal lateral carinae incomplete anteriorly in most; hind angle carinae present (single) or absent; posterior edge of pronotum without sublateral notches; pronotosternal sutures closed. **Mesothorax.** Scutellum with posterior edge pointed (acuminate). Elytra. Integument marked with spots or bands in some; without pattern from differences in setal color. **Legs.** Metacoxal plate not reaching side; tarsal pads present on tarsomere IV, tarsal claws appendiculate. **Ventrites.** Microserration at sides (e.g., 100 points per mm) present. **Aedeagus.** Parameres without apical lateral expansions; each paramere with two setae.

Summary. Scutellum pointed posterad, mesocoxal cavities closed, tarsomere IV lobed, claws appendiculate.

Genus *Floridelater* Douglas, 2017

Habitus. Body length 3–10 mm. **Head.** Hypognathous. Antennal sensory elements beginning on antennomere III. **Prothorax.** Pronotum with dorsal punctures uniform sized, simple, with punctures situated on tubercles; pronotal lateral carinae incomplete anteriorly, hidden in dorsal view; hind angle carinae present (single); posterior edge of pronotum with sublateral notches present; pronotosternal sutures open, hypomeral bead present. Prosternal process curved upward $> 40^\circ$ in lateral view. **Mesothorax.** Scutellum with anterior edge concave, posterior edge bilobed (concave at midline). Elytra. Anterior edge straight to arcuate near humeri in dorsal view, integument unmarked; without pattern from differences in setal color. **Legs.** Metacoxal plate without elongation in mesal half; tarsal pads absent, claws simple. **Ventrites.** Sides not microscrate. **Aedeagus.** Each paramere with two setae.

Summary. Pronotum with punctures situated on tubercles. Also, flight wings short (rudimentary), elytron short ($\sim 2.3\times$ longer than pronotum in dorsal view) and evenly arched in lateral view.

Genus *Horistonotus* Candèze, 1860

Habitus. Body length 3–10 mm. **Head.** Hypognathous. Antennal sensory elements beginning on antennomere III or IV. **Prothorax.** Pronotum with dorsal punctures of two distinct intermixed sizes (heterogeneous); pronotal lateral carinae incomplete anteriorly; hind angle carinae not distinct from lateral carinae; pronotosternal sutures closed, hypomera with posterior concavity angulate. Prosternal process not curved upward $\geq 40^\circ$ in lateral view. **Mesothorax.** Scutellum with anterior edge concave or not, posterior edge pointed (acuminate). Elytra. Anterior edge sinuate (recurved) or with rectangular projection near humeri in dorsal view, integument marked with spots or bands in some; without pattern from differences in setal color. **Legs.** Metacoxal plate not reaching side; tarsal pads absent, tarsal claw apices appendiculate, or bifid in most, simple in a few. **Ventrites.** Microserration at sides (e.g., 100 points per mm) present. **Aedeagus.** Parameres without apical lateral expansions; each paramere with two setae.

Summary. Pronotal lateral carinae not reaching anterior edge of pronotum, hind angle carinae absent, scutellum pointed posterad, mesocoxal cavities closed.

Genus *Paracardiophorus* Schwarz, 1895

Habitus. Body length 6–12 mm. **Head.** Antennal sensory elements beginning on antennomere III. **Prothorax.** Pronotum with dorsal punctures uniform sized or of two distinct intermixed sizes (heterogeneous), all simple; pronotal lateral carinae incomplete anteriorly, hidden in dorsal view; hind angle carinae present (single); posterior edge of pronotum with sublateral notches present; pronotosternal sutures closed, hypomeral bead present; hypomera with posterior concavities arcuate. **Mesothorax.** Scutellum with anterior edge notched, posterior edge pointed (acuminate). Elytra. Anterior edge straight to arcuate near humeri in dorsal view, integument marked with spots or bands in many; without pattern from differences in setal color. **Legs.** Metacoxal plate elongate in mesal half, plate not reaching side; tarsal pads absent, claws simple. **Ventrites.** Sides not microserrate. **Aedeagus.** Parameres without apical lateral expansions; each paramere with one or two setae.

Summary. Scutellum shaped like valentine heart, pronotal lateral carinae incomplete, visible from ventral view but not dorsal view, hypomera with posterior emarginations arcuate, claws simple.

Subfamily Dendrometrinae

Habitus. Body length 3–35 mm. **Vestiture.** Scale-like setae absent. **Prothorax.** Pronotum with lateral carinae meeting anterior edge of prothorax at ~ 90° in lateral view; bioluminescent spots absent; pronotal punctures not of two discrete size classes, and without associated tubercles or carinae in most. **Mesothorax.** Mesoventral cavity without serration along sides; mesocoxal cavities not closed by juncture of mesoventrite and metaventrite laterad of cavities. Elytra. Apex not spinose. **Legs.** Metacoxal plate without elongation in mesal half; claws without setae. **Aedeagus.** Parameres with articulation at base.

This group is defined based on evidence from larvae and DNA. It is difficult to define based on adult morphology.

Tribe Oxynopterini

Habitus. Body length 17–35 mm. **Head.** Prognathous; frons without triangular depression. Antennae not pectinate. **Prothorax.** Pronotum with punctures simple, without tubercles between punctures; pronotal lateral carinae complete, visible throughout length in dorsal view, not serrate; posterior edge of pronotum without sublateral notches, crenellations present or absent; hypomera with concavity on posterior edge near hind angle; pronotosternal sutures closed. Prosternum with sides straight at midlength. **Mesothorax.** Scutellum with anterior edge not concave. Elytra with anterior edge straight to arcuate near humeri in dorsal view; without pattern from differences in setal color. **Legs.** Tarsal pads absent, claws simple. **Ventrites.** Sides not microserrate.

Summary. Large, prognathous, dark-bodied beetles. Most with crenellations at posterior edge of pronotum.

Genus *Melanactes* LeConte, 1853

Habitus. Body length 20–40 mm. **Head.** Supra-antennal carinae reaching anterior edge of head capsule. Antennae with 11 antennomeres, sensory elements beginning on antennomere IV. **Prothorax.** Pronotum hind angle carinae present (single), crenellations present or absent, hypomeral bead present. Prosternal process not curved upward $\geq 40^\circ$ in lateral view. **Mesothorax.** Mesocoxal cavities open, scutellum with posterior edge rounded (arcuate). Elytra. Striae absent, integument unmarked; setal vestiture sparse on disk. **Legs.** Metacoxal plate reaching side. **Aedeagus.** Each paramere with three or more setae.

Summary. Large beetles with elytra not striate and mostly bare of setae. Also, hind edge of pronotum crenellate in most, claws without setae.

Genus *Oistus* Candèze, 1857

Habitus. Body length 17–35 mm. **Head.** Supra-antennal carinae not complete across frons. Antennae with 11 antennomeres, sensory elements beginning on antennomere IV. **Prothorax.** Pronotum hind angle carinae absent, crenellations present, hypomera with posterior concavity present. Prosternal process not curved upward $\geq 40^\circ$ in lateral view. **Mesothorax.** Mesocoxal cavities not closed. Elytra. Striae present; integument marked with spots or bands in some; setal vestiture even and mainly parallel or with bare patches. **Legs.** Metacoxal plate reaching side. **Aedeagus.** Parameres with apical lateral expansions present, without setae.

Summary. Posterior edge of pronotum crenellate (weak in some), antennal sensory elements beginning on antennomere IV (widespread rough texture), elytra setose (setae longer than width of antennomere II).

Genus *Perissarthron* Hyslop, 1917

Habitus. Body length 17–35 mm. **Head.** Supra-antennal carinae fading on frons or reaching anterior edge of head capsule. Antennae with 12 antennomeres in most, sensory elements beginning on antennomere III. **Prothorax.** Pronotum hind angle carinae present (single), crenellations present, hypomeral bead present; hypomera with posterior concavities arcuate. **Mesothorax.** Mesocoxal cavities open. Elytra. Striae present; integument unmarked; setal vestiture even and mainly parallel. **Aedeagus.** Each paramere with two setae.

Summary. Large beetles with posterior edge of pronotum crenellate, antennal sensory elements beginning on antennomere III (widespread rough texture).

Tribe Prosternini

Habitus. Body length 3–30 mm. **Head.** Supra-antennal carinae, fading on frons (not reaching another structure) in most; most prognathous. Antennae with 11 antennomeres, not pectinate in most. **Prothorax.** Pronotum without tubercles between punctures; pronotal lateral carinae complete in most, visible throughout length in most or all, not serrate; hind angle carinae single or absent, posterior edge with crenellations absent in most; pronotosternal sutures closed in most; hypomeron with posterior edge near hind angle with concavity in most;

prosternal process not curved upward $\geq 40^\circ$ in lateral view in most. **Mesothorax.** Mesocoxal cavities fully open in most, not closed; scutellum with anterior edge not concave in most or all. Elytra. Anterior edge straight to arcuate near humeri in dorsal view in most, striate in most, setal vestiture even and mainly parallel in most; most without pattern from differences in setal color. **Legs.** Metacoxal plate reaching side in most; tarsal pads absent, claws simple and long in most. **Ventrites.** Sides not microserrate in most, ventrite V apex arcuate without paired setal brushes in most.

Summary. It is difficult to define this group collectively. They include most Dendrometrinae with supra-antennal carinae not both continuous and raised across frons. Tarsomeres simple. Hind edge of pronotum defined by a right-angled ledge near hind angles in dorsal view (edge rounded in some Dendrometrini).

Genus *Acteniceromorphus* Kishii, 1955

Habitus. Body length 12–18 mm. **Head.** Antennal, sensory elements beginning on antennomere III. **Prothorax.** Pronotum with punctures simple; hind angle carinae present; posterior edge of pronotum with sublateral notches present; pronotosternal sutures closed, hypomeral bead absent. Prosternum with sides straight at midlength. **Mesothorax.** Scutellum with posterior edge rounded (arcuate) or pointed (acuminate). Elytra. Integument unmarked. **Aedeagus.** Each paramere with two or more setae.

Summary. Supra-antennal carinae fading on frons, sensory elements beginning on antennomere III (widespread rough sculpturing and appressed setae); pronotum with setae on anterior half directed anterad, without setae directed mesad near midlength, hind angles with carinae, sublateral notches present; parameres each with two or more setae. Not distinguished here from all *Paractenicera* and *Proludius* species.

A. sagitticollis (Eschscholtz)

Habitus. Body length 10–15 mm. **Head.** Antennae with sensory elements beginning on antennomere IV (widespread rough sculpturing and appressed setae). **Prothorax.** Pronotum with punctures simple, lateral carinae complete; hind angle carinae present; posterior edge of pronotum with sublateral notches present; pronotosternal sutures closed, hypomeral bead absent. Prosternum with sides straight at midlength. **Mesothorax.** Scutellum with posterior edge rounded (arcuate). Elytra. Integument unmarked. **Aedeagus.** Parameres without apical lateral expansions; each with three or more setae.

Summary. Supra-antennal carinae fading on frons, sensory elements beginning on antennomere IV, pronotal sublateral notches present, hypomeral bead absent, ventrites without microserration, parameres without preapical expansions, each with three or more setae.

Genus *Actenicerus* Kiesenwetter, 1858

Habitus. Body length 12–18 mm. **Head.** Antennae with sensory elements beginning on antennomere III. **Prothorax.** Pronotal lateral carinae complete, posterior crenellations absent; pronotosternal sutures closed, hypomeral bead

present. Prosternum with sides straight at midlength. **Mesothorax**. Scutellum with posterior edge rounded (arcuate). Elytra. Integument unmarked, but with pattern from differences in setal color. **Aedeagus**. Parameres with apical lateral expansions present, without setae.

Summary. Dark bodied with elytral pattern from patches of pale setae among darker setae, supra-antennal carinae fading on frons, pronotum with most setae near midline on anterior half directed mesad.

Genus *Anostirus* C.G. Thomson, 1859

Habitus. Body length 6–12 mm. **Head**. Antennae serrate, sensory elements beginning on antennomere III or IV. **Prothorax**. Pronotum with punctures simple; hind angle carinae absent; posterior edge of pronotum with sublateral notches present; hypomera with concavity on posterior edge near hind angle; pronotosternal sutures closed. Prosternum with sides straight at midlength. **Mesothorax**. Scutellum rounded posterad. Elytra. Integument marked with spots or transverse bands on a pale background; some with pattern from differences in setal color. **Ventrites**. Microserration at sides (e.g., 100 points per mm) present. **Aedeagus**. Each paramere with two or more setae.

Summary. Supra-antennal carinae fading on frons, pronotal hind angles carinae absent (or faint); elytra pale with paired dark markings, abdominal ventrites microserrate.

Genus *Anthracopteryx* Horn, 1891

Habitus. Body length 5–10 mm. **Head**. Antennae with sensory elements beginning on antennomere IV. **Prothorax**. Pronotum with punctures simple; hind angle carinae present; posterior edge of pronotum without sublateral notches; pronotosternal sutures closed, hypomeral bead absent; hypomera with angulate concavity on posterior edge near hind angle. Prosternum with sides concave at midlength. **Mesothorax**. Scutellum with anterior edge concave or not, posterior edge rounded (arcuate). Elytra. Integument unmarked. **Legs**. Metacoxal plate reaching side or not. **Aedeagus**. Parameres with apical lateral expansions present; each paramere with three or more setae.

Summary. All black, supra-antennal carinae fading on frons, pronotum on anterior half with setae oriented posterad or mesad, and with some setae near midlength oriented laterad, hind angles with carinae, sublateral notches absent, pronotosternal sutures closed, prosternum with sides concave, prosternal process not ascendent. Also, hind wings short.

Genus *Athoplastus* Johnson & Etzler, 2018

Habitus. Body length 12–18 mm. **Head**. Antennae with sensory elements beginning on antennomere IV. **Prothorax**. Pronotum with punctures simple; hind angle carinae present; posterior edge of pronotum with sublateral notches present; pronotosternal sutures closed. Prosternum with sides concave at midlength; prosternal process curved upward > 40° in lateral view. **Mesothorax**. Scutellum rounded posterad. Elytra. Integument unmarked. **Aedeagus**. Parameres with apical lateral expansions present; each paramere with three or more setae.

Summary. Supra-antennal carinae fading on frons, sensory elements beginning on antennomere IV (erect setae), pronotum with sublateral notches present, pronotum and elytra not contrasting, prosternum with sides concave, prosternal process ascendent, parameres with three or more setae. Not completely separated from *Metanomus*.

Genus *Beckerus* Johnson, 2008

Habitus. Body length 6–10 mm. **Head.** Antennae serrate to pectinate, sensory elements beginning on antennomere III. **Prothorax.** Pronotum with punctures simple; hind angle carinae present; posterior edge of pronotum without sublateral notches, but with crenellations present; pronotosternal sutures closed, hypomeral bead absent. Prosternum with sides concave at midlength; prosternal process curved upward > 40° in lateral view. **Mesothorax.** Scutellum rounded posterad or pointed (acuminate). Elytra. Integument marked with spots or transverse bands; setal vestiture sparse on disk or even and mainly parallel. **Aedeagus.** Parameres with apical lateral expansions present; each paramere with three or more setae.

Summary. Pronotum and elytra each with contrasting color patterns, posterior edge of pronotum crenellate, antennal sensory elements beginning on antennomere III (erect setae, widespread rough sculpturing).

Genus *Billbrownia* Johnson, 2023

Habitus. Body length 6–12 mm. **Head.** Supra-antennal carinae fading on frons or reaching anterior edge of head capsule. Antennae with sensory elements beginning on antennomere IV. **Prothorax.** Pronotum with punctures simple; hind angle carinae present; posterior edge of pronotum with sublateral notches present; pronotosternal sutures closed, hypomeral bead weak or absent. Prosternum with sides straight at midlength. **Mesothorax.** Scutellum rounded posterad. Elytra. Integument unmarked; setal vestiture sparse on disk or even and mainly parallel. **Aedeagus.** Parameres without apical lateral expansions, without setae.

Summary. Sensory elements (apical sensorium) beginning on antennomere IV, pronotum with punctures simple, setae on anterior half directed anterad or laterad, sublateral notches present, elytra bare or with vestiture even and mainly parallel, parameres without lateral expansions or setae. We could not write a diagnosis that distinguished this from some *Setasomus*.

***B. signaticollis* (Melsheimer, 1845), and similar species**

Habitus. Body length 6–12 mm. **Head.** Supra-antennal carinae fading on frons or reaching anterior edge of head capsule. Antennae with sensory elements beginning on antennomere III (apical sensorium). **Prothorax.** Pronotum with punctures simple; hind angle carinae present; posterior edge of pronotum with sublateral notches present; pronotosternal sutures closed, hypomeral bead absent. Prosternum with sides straight or convex at midlength. **Mesothorax.** Scutellum rounded posterad. Elytra. Integument unmarked with spots or transverse bands; setal vestiture sparse on disk or even and mainly parallel. **Aedeagus.** Parameres with apical lateral expansions in some, without setae.

Summary. Differ from type species by having sensory elements begin on antennomere III. Remaining characters: pronotum with punctures simple, setae on anterior half directed anterad or laterad, hind angles carinate, parameres without lateral expansions or setae.

Genus *Corymbitodes* Buysson, 1904

Habitus. Body length 6–12 mm. **Head.** Supra-antennal carinae fading on frons or reaching anterior edge of head capsule. Antennae with sensory elements beginning on antennomere III. **Prothorax.** Pronotum with some punctures umbilicate; hind angle carinae absent; posterior edge of pronotum with sublateral notches in some; pronotosternal sutures closed, hypomeral bead present. Prosternum with sides straight at midlength. **Mesothorax.** Scutellum rounded posterad or pointed (acuminate). Elytra. Integument unmarked except for humeral spots or dark sutural striae in some. **Legs.** Metacoxal plate reaching side or not. **Aedeagus.** Parameres without apical lateral expansions, without setae, each paramere with one or two setae.

Summary. Supra-antennal carina not complete across frons, sensory elements beginning on antennomere III (apical sensorium, widespread appressed setae), pronotum with umbilicate punctures at sides, some setae directed laterad near midlength (near sides), pronotal hind angles non-carinate, pronotosternal sutures with hypomeral bead (narrow).

Genus *Ctenicera* Latreille, 1829

Habitus. Body length 12–18 mm. **Head.** Antennae serrate to pectinate, sensory elements beginning on antennomere III. **Prothorax.** Pronotum with punctures simple; hind angle carinae present; posterior edge of pronotum with sublateral notches present; pronotosternal sutures closed, hypomeral bead present. Prosternum with sides straight at midlength. **Mesothorax.** Scutellum rounded posterad. Elytra. Integument marked with diagonal band in apical half only. **Aedeagus.** Parameres without apical lateral expansions; each paramere with three or more setae.

Summary. Supra-antennal carinae fading on frons, antennae serrate or pectinate, prosternum with sides straight, elytra with dark markings only in apical third.

***C. angularis* (LeConte)**

Habitus. Body length 6–12 mm. **Head.** Antennae with sensory elements beginning on antennomere IV. **Prothorax.** Pronotum with punctures simple; hind angle carinae present; hind angles pale; posterior edge of pronotum with sublateral notches present; pronotosternal sutures closed, hypomeral bead present; hypomeron with posterior edge near hind angle with slight concavity, concavity arcuate. Prosternum with sides straight at midlength. **Mesothorax.** Scutellum rounded posterad. Elytra. Integument unmarked. **Aedeagus.** Parameres with apical lateral expansions present; each paramere with one or two setae.

Summary. Dark bodied with pale pronotal hind angles. Supra-antennal carinae fading on frons, prognathous, pronotum with setae on anterior half near midline directed posterad, pronotum with sublateral notches present (small),

parameres with one or two setae. The key distinguished all specimens from *Liotrichus*, although this diagnosis does not. This species is associated with *Ctenicera* for historical reasons only.

***C. uliginosa* (Van Dyke)**

Habitus. Body length 6–12 mm. **Head.** Antennae with sensory elements beginning on antennomere IV. **Prothorax.** Pronotum with punctures simple; hind angle carinae present; posterior edge of pronotum with sublateral notches present; pronotosternal sutures closed, hypomeral bead absent. Prosternum with sides straight at midlength. **Mesothorax.** Scutellum with anterior edge concave or not, posterior edge rounded (arcuate). Elytra. Integument dark. **Aedeagus.** Parameres with apical lateral expansions present; each paramere with two or more setae.

Summary. Supra-antennal carinae fading on frons, sensory elements beginning on antennomere IV, antennomere IV not longer than each of V to VII, pronotum with setae near midline on anterior half directed mesad, sublateral notches present, hypomeral bead absent, elytra dark throughout, parameres lateral expansions present and with two or more setae. This species is associated with *Ctenicera* for historical reasons only.

Genus *Dixicollis* Johnson, 2021

Habitus. Body length 6–12 mm. **Head.** Antennae with sensory elements beginning on antennomere III. **Prothorax.** Pronotum with punctures simple; hind angle carinae present; posterior edge of pronotum without sublateral notches; pronotosternal sutures open, hypomeral bead present; hypomera with arcuate or angulate concavity on posterior edge near hind angle. Prosternum with sides straight at midlength; prosternal process curved upward > 40° in lateral view. **Mesothorax.** Scutellum rounded posterad. Elytra. Integument unmarked. **Aedeagus.** Parameres with apical lateral expansions present, without setae.

Summary. Supra-antennal carinae fading on frons, sensory elements beginning on antennomere III (not dense), pronotum without sublateral notches, pronotosternal sutures narrowly open.

Genus *Eanus* LeConte, 1861

Habitus. Body length 3–10 mm. **Head.** Antennae with sensory elements beginning on antennomere III or IV. **Prothorax.** Pronotum with punctures simple; pronotal lateral carinae complete or not; hind angle carinae absent; posterior edge of pronotum without sublateral notches; pronotosternal sutures closed, hypomeral bead present. Prosternum with sides concave at midlength; prosternal process curved upward > 40° in lateral view. **Mesothorax.** Scutellum with posterior edge pointed (acuminate). Elytra. Integument in some marked with spots or transverse bands. **Aedeagus.** Each paramere with one or two setae.

Summary. Supra-antennal carinae fading on frons, antennomere III closer in length to antennomere IV than to II, pronotum with setae near midline on anterior half directed anterad, with some setae directed laterad near midlength, prosternal sides concave, prosternal process ascendant, parameres with one or two setae each.

***E. striatipennis* Brown**

Habitus. Body length 5–10 mm. **Head.** Antennae with sensory elements beginning on antennomere IV. **Prothorax.** Pronotum with punctures simple; hind angle carinae absent; posterior edge of pronotum without sublateral notches; pronotosternal sutures closed, hypomeral bead absent. Prosternum with sides straight or concave at midlength; prosternal process curved upward > 40° in lateral view. **Mesothorax.** Scutellum rounded posterad or pointed (acuminate). Elytra. Striae present or absent, integument with metallic reflections. **Aedeagus.** Parameres with apical lateral expansions present; each paramere with three or more setae.

Summary. Supra-antennal carinae fading on frons, antennomere III closer in length to antennomere II than to IV, prosternal sides concave, prosternal process ascendant, elytra with metallic reflections. Treated as distinctive to improve overall effectiveness of the key.

Genus *Hadromorphus* Motschulsky, 1859

Habitus. Body length 6–12 mm, setal vestiture dense but not hiding integument. **Head.** Antennae with sensory elements beginning on antennomere IV. **Prothorax.** Pronotum with some punctures umbilicate; hind angle carinae absent in most; posterior edge of pronotum with sublateral notches in some; pronotosternal sutures open, hypomeral bead present in most. Prosternum with sides straight at midlength. **Mesothorax.** Mesocoxal cavities not closed. Scutellum rounded posterad. Elytra. Integument unmarked. **Legs.** Metacoxal plate reaching side or not. **Ventrites.** Microserration at sides (e.g., 100 points per mm) present or absent. **Aedeagus.** Parameres with apical lateral expansions present; each paramere with three or more setae.

Summary. Supra-antennal carinae fading on frons, sensory elements beginning on antennomere IV, pronotum with setae directed both mesad and laterad near midlength (converging or swirled), pronotosternal sutures open, and straight at midlength.

Genus *Hypoganus* Kiesenwetter, 1858

Habitus. Body length 6–12 mm. **Head.** Antennae with sensory elements beginning on antennomere IV. **Prothorax.** Pronotum with punctures simple; hind angle carinae present; posterior edge of pronotum without sublateral notches; pronotosternal sutures closed, hypomeral bead present. Prosternum with sides straight or convex at midlength. **Mesothorax.** Scutellum rounded posterad. Elytra. Integument unmarked. **Aedeagus.** Parameres with apical lateral expansions present, without setae.

Summary. Brown or black bodied, some with red on pronotum, hypognathous, supra-antennal carinae fading on frons, sensory elements beginning on antennomere IV, pronotum wider than long with setae fine and mainly directed laterad, sublateral notches absent, parameres with sublateral expansions present and setae absent. Not separated here from *Selatossomus nigricans*.

Genus *Laneganus* Johnson, 2001

Habitus. Body length 6–18 mm. **Head.** Supra-antennal carinae fading on frons, or complete but without concavity below in lateral view. Antennae with sensory elements beginning on antennomere IV. **Prothorax.** Pronotum with punctures simple; hind angle carinae present; posterior edge of pronotum without sublateral notches; pronotosternal sutures closed, hypomeral bead present. Prosternum with sides straight or convex at midlength. **Mesothorax.** Mesocoxal cavities not closed. Scutellum rounded posterad. Elytra. Integument unmarked or marked with spot or band in apical half only. **Legs.** Metacoxal plates reaching side or not. **Aedeagus.** Parameres with apical lateral expansions present, without setae or each paramere with three or more setae.

Summary. Supra-antennal carinae fading on frons or complete across frons but not concave below, sensory elements beginning on antennomere IV, pronotum longer than wide with setae fine and mainly directed posterad or laterad on anterior half, sublateral notches absent, long pronotal hind angles reaching to midlength of scutellum when body straightened, pronotosternal sutures closed and straight, hypomeral bead present, tarsal claws without basal setae.

Genus *Liotrichus* Kiesenwetter, 1858

Habitus. Body length 6–12 mm. **Head.** Antennae with sensory elements beginning on antennomere IV. **Prothorax.** Pronotum with punctures simple; hind angle carinae present or absent; posterior edge of pronotum with sublateral notches in some; pronotosternal sutures closed, hypomeral bead present; hypomera with posterior concavities arcuate or angulate. Prosternum with sides straight or concave at midlength. **Mesothorax.** Scutellum rounded posterad. Elytra. Integument marked with bands in some. **Aedeagus.** Parameres with apical lateral expansions present.

Summary. Pronotum darker than elytra, supra-antennal carinae fading on frons, prognathous, antennae not pectinate or serrate, antennomere III closer in length to IV than to II, pronotum with setae on anterior half near midline directed posterad, some directed laterad near midlength, and directed anterad on posterior part near midline, pronotosternal sutures closed, hypomeral bead present, mesocoxal cavities open, claws simple. The key distinguished all specimens from *Setasomus*, although this diagnosis does not.

Genus *Metanomus* Buysson, 1887

Habitus. Body length 6–12 mm. **Head.** Antennae with sensory elements beginning on antennomere IV. **Prothorax.** Pronotum with punctures simple; hind angle carinae present; posterior edge of pronotum with sublateral notches present; pronotosternal sutures closed. Prosternum with sides straight to concave at midlength. **Mesothorax.** Scutellum rounded posterad. Elytra. Integument unmarked. **Aedeagus.** Parameres with apical lateral expansions present; each paramere with three or more setae.

Summary. Supra-antennal carinae fading on frons, sensory elements beginning on antennomere IV, antennomere III closer in length to II than to IV,

pronotum on anterior part with most setae directed posterad, some directed laterad near midlength, and anterad on posterior slope, prosternum with sides straight or concave, claws simple, parameres with three or more setae. Not completely separated from *Athoplastus* here.

Genus *Neopristilophus* Buysson, 1894

Habitus. Body length 12–25 mm. **Head.** Supra-antennal carinae fading on frons or reaching anterior edge of head capsule. Antennae with sensory elements beginning on antennomere III or IV. **Prothorax.** Pronotum with some punctures umbilicate; hind angle carinae present; posterior edge of pronotum with sublateral notches present in most; pronotosternal sutures closed, hypomerall bead absent. Prosternum with sides straight at midlength. **Mesothorax.** Scutellum rounded posterad. Elytra. Integument unmarked. **Aedeagus.** Parameres without apical lateral expansions, without setae.

Summary. Large, dark-bodied beetles. Supra-antennal carinae fading on frons or directed anterad, pronotum with some punctures umbilicate, pronotum with hind angles carinate, pronotosternal sutures closed, parameres with both preapical expansions and setae absent.

Genus *Nitidolimonius* Johnson, 2008

Habitus. Body length 6–12 mm. **Head.** Supra-antennal carinae variable. Antennae with sensory elements beginning on antennomere IV. **Prothorax.** Pronotum with punctures umbilicate in some; hind angle carinae present; posterior edge of pronotum with sublateral notches present; pronotosternal sutures open, hypomerall bead present. Prosternum with sides straight at midlength. **Mesothorax.** Scutellum rounded posterad. Elytra. Integument with metallic reflections in most; setal vestiture sparse on disk or even and mainly parallel. **Aedeagus.** Parameres with apical lateral expansions present, without setae or each paramere with three or more setae.

Summary. Pronotum with metallic reflections, pronotosternal sutures open, prosternum with sides straight, ventrites without microserration at sides.

Genus *Oxygonus* LeConte, 1863

Habitus. Body length 3–12 mm. **Head.** Supra-antennal carinae fading on frons or reaching anterior edge of head capsule. Antennae with sensory elements beginning on antennomere IV. **Prothorax.** Pronotum with punctures umbilicate in some; hind angle carinae present or absent; posterior edge of pronotum with sublateral notches in some; pronotosternal sutures closed, hypomerall bead present. Prosternum with sides straight at midlength. **Mesothorax.** Scutellum rounded posterad. Elytra. Integument unmarked; setal vestiture even and mainly parallel or partially transverse in patches. **Legs.** Tarsal claws appendiculate. **Aedeagus.** Parameres with apical lateral expansions present, without setae or each paramere with three or more setae.

Summary. Pronotosternal sutures straight, tarsi simple, tarsal claws appendiculate.

Genus *Paractenicera* Johnson, 2008

Habitus. Body length 12–18 mm. **Head.** Antennae with sensory elements beginning on antennomere III. **Prothorax.** Pronotum with some punctures umbilicate; hind angle carinae present; posterior edge of pronotum with sublateral notches present; pronotosternal sutures closed, hypomeral bead absent. Prosternum with sides straight at midlength. **Mesothorax.** Scutellum with posterior edge pointed (acuminate). Elytra. Integument unmarked. **Aedeagus.** Parameres without apical lateral expansions; each paramere with two setae.

Summary. Supra-antennal carinae fading on frons, pronotum with setae on anterior half directed anterad, some setae directed laterad near midlength, hind angles with carinae, sublateral notches present, scutellum obtusely pointed posterad, parameres with two setae. *Paractenicera fulvipipes* is not distinguished from *Acteniceromorphus* here.

Genus *Proludius* Lane, 1971

Habitus. Body length 12–18 mm. **Head.** Supra-antennal not complete across frons or complete, but without concavity below in lateral view. Antennae with sensory elements beginning on antennomere III. **Prothorax.** Pronotum with punctures umbilicate in some; hind angle carinae present; posterior edge of pronotum with sublateral notches in some; pronotosternal sutures closed; hypomera with arcuate or angulate concavity on posterior edge near hind angle. Prosternum with sides straight at midlength. **Mesothorax.** Scutellum with anterior edge concave or not, posterior edge rounded (arcuate). Elytra. Integument unmarked. **Aedeagus.** Parameres with apical lateral expansions present; each paramere with two or more setae.

Summary. Supra-antennal carina not complete across frons or complete, but without concavity below in lateral view, sensory elements beginning on antennomere III, pronotum not contrasting with elytra in color, with setae on anterior half directed anterad or mesad, some setae directed laterad or mesad near midlength, hind angles with carinae (faint in some), prosternal process not ascendant, scutellum rounded posterad, mesocoxal cavities open, elytral setal color pattern absent, tarsal pads absent. *Proludius* is not distinguished from some *Acteniceromorphus* or *Sylvanelater* here.

P. angusticollis (Mannerheim), and similar species

Habitus. Body length 12–18 mm. **Head.** Antennae with sensory elements beginning on antennomere IV. **Prothorax.** Pronotum with punctures umbilicate in some; hind angle carinae present; posterior edge of pronotum with sublateral notches present; pronotosternal sutures closed. Prosternum with sides straight at midlength. **Mesothorax.** Scutellum rounded posterad. Elytra. Integument unmarked. **Aedeagus.** Parameres with apical lateral expansions present, without setae.

Summary. Antennomere III closer in length to II than IV, anterior half of pronotum with most setae directed mesad, posterior slope of pronotum without setae directed anterad, parameres without setae. Captures species with sensory elements beginning on antennomere IV and parameres without setae.

***P. sylvaticus* (Van Dyke)**

Habitus. Body length 12–18 mm. **Head.** Antennae with sensory elements beginning on antennomere III. **Prothorax.** Pronotum with some punctures umbilicate; hind angle carinae present; posterior edge of pronotum with sublateral notches present; pronotosternal sutures closed, hypomerical bead absent. Prosternum with sides straight at midlength. **Mesothorax.** Scutellum rounded posterad. Elytra. Integument unmarked. **Aedeagus.** Parameres with apical lateral expansions present, without setae.

Summary. Sensory elements beginning on antennomere III, antennomere IV longer than each of V to VII, pronotum with most setae near midline on anterior half directed anterad, some directed laterad near midlength, parameres with rounded preapical expansions and without setae. Captures species with sensory elements beginning on antennomere III and parameres without setae.

Genus *Prosternon* Latreille, 1834

Habitus. Body length 6–12 mm. **Head.** Antennae with sensory elements beginning on antennomere IV. **Prothorax.** Pronotum with punctures umbilicate in some; hind angle carinae present; posterior edge of pronotum with sublateral notches present in most; pronotosternal sutures closed, hypomerical bead present; hypomeron with posterior edge near hind angle without concavity. Prosternum with sides straight at midlength. **Mesothorax.** Scutellum rounded posterad. Elytra. Integument unmarked; setal vestiture partially transverse in patches. **Ventrites.** Microserration at sides (e.g., 100 points per mm) present. **Aedeagus.** Parameres with apical lateral expansions present, each paramere without or with two or more setae.

Summary. Prognathous, elytra with setae swirled and pale, claws simple.

Genus *Pseudanostirus* Dolin, 1964

***P. ochreipennis* (LeConte), and similar species**

Habitus. Body length 6–12 mm. **Head.** Supra-antennal carinae fading on frons. Antennae with sensory elements beginning on antennomere IV. **Prothorax.** Pronotum with punctures simple; hind angle carinae present or absent; posterior edge of pronotum with sublateral notches present; pronotosternal sutures closed. Prosternum with sides straight at midlength. **Mesothorax.** Scutellum rounded posterad. Elytra. Integument unmarked with spots or transverse bands, vestiture not swirled. **Ventrites.** Microserration at sides (e.g., 100 points per mm) present. **Aedeagus.** Parameres without apical lateral expansions; each paramere with two or more setae.

Summary. Supra-antennal carinae fading on frons, pronotosternal sutures closed, elytra without transverse bands or apical markings, vestiture not swirled, ventrites microserrate. Species without swirled elytral vestiture, with ventrites microserrate, and without paramere expansions treated as distinctive sub-group here to improve diagnostic effectiveness.

***P. laricis* (Brown)**

Habitus. Body length 5–10 mm. **Head.** Antennae with sensory elements beginning on antennomere IV. **Prothorax.** Pronotum with punctures simple; hind angle carinae present or absent; posterior edge of pronotum with sublateral notches present; pronotosternal sutures closed, hypomerical bead absent. Prosternum with sides straight at midlength. **Mesothorax.** Scutellum rounded posterad. Elytra. Integument unmarked, vestiture not swirled. **Aedeagus.** Parameres with apical lateral expansions present; each paramere with three or more setae.

Summary. Pronotum not darker than elytra, supra-antennal carinae fading on frons, sensory elements beginning on antennomere IV, antennomere III closer in length to IV than II, pronotal punctures simple, setae on anterior half of pronotum directed posterad, sublateral notches present, hypomerical bead absent, parameres with three or more setae. Treated as distinctive subgroup to improve diagnostic effectiveness.

***P. triundulatus* (Randall), and similar species**

Habitus. Body length 6–12 mm. **Head.** Antennal sensory elements beginning on antennomere IV. **Prothorax.** Pronotum with punctures simple; hind angle carinae absent; posterior edge of pronotum without sublateral notches; pronotosternal sutures closed, hypomerical bead present; hypomeron with posterior edge near hind angle without concavity. Prosternum with sides straight at midlength. **Mesothorax.** Scutellum rounded posterad. Elytra. Integument unmarked with spots or transverse bands; but with pattern from differences in setal color, vestiture not swirled. **Aedeagus.** Parameres without apical lateral expansions, without setae or each paramere with one seta.

Summary. Pronotum darker than elytra, elytra with transverse bands of dark and pale setae, supra-antennal carinae fading on frons, sublateral notches absent, pronotosternal sutures closed. Species with pronotal sublateral notches, concavity on posterior edge of hypomeron, and bands of dark setae on elytra treated included as distinctive sub-group here to improve diagnostic effectiveness.

Genus *Selatosomus* Stephens, 1830

Habitus. Body length 7–18 mm. **Head.** Antennae with sensory elements beginning on antennomere IV. **Prothorax.** Pronotum with punctures umbilicate in some; hind angle carinae present; posterior edge of pronotum with sublateral notches present; pronotosternal sutures closed. Prosternum with sides straight or concave at midlength. **Mesothorax.** Scutellum rounded posterad. Elytra. Integument marked with spots or transverse bands, with metallic reflections in some; setal vestiture sparse on disk. **Legs.** Metacoxal plate reaching side or not. **Aedeagus.** Parameres with apical lateral expansions present, each paramere without or with two or more setae.

Summary. Sensory elements (apical sensorium) beginning on antennomere IV, pronotum with sublateral notches, pronotosternal sutures closed, elytral

disk mostly without setal vestiture (if present then appressed and only 1/4 as long as interstrial width), ventrite V with apex arcuate, parameres with lateral expansions. We could not write a diagnosis that distinguished some species of *Billbrownia* from this, although the key accurately diagnosed all specimens.

***S. nigricans* (Fall)**

Habitus. Body length 6–12 mm. **Head.** Antennae with sensory elements beginning on antennomere IV. **Prothorax.** Pronotum with punctures simple; hind angle carinae present; posterior edge of pronotum without sublateral notches; pronotosternal sutures closed, hypomeral bead present. Prosternum with sides straight or convex at midlength. **Mesothorax.** Scutellum rounded posterad. Elytra. Integument unmarked; setal vestiture sparse on disk or even and mainly parallel. **Aedeagus.** Parameres with apical lateral expansions present, without setae.

Summary. Brown or black bodied, some with red on pronotum, sensory elements beginning on antennomere IV, pronotum wider than long with setae fine and mainly directed laterad, sublateral notches absent, hypomeral bead impunctate. We could not write a diagnosis that distinguished this from *Hypogonus*. Treated as distinctive subgroup to improve diagnostic effectiveness because of lack of pronotal sublateral notches.

***S. pruininus* (Horn)**

Habitus. Body length 6–12 mm. **Head.** Antennae with sensory elements beginning on antennomere IV. **Prothorax.** Pronotum with punctures umbilicate in some; hind angle carinae present; posterior edge of pronotum with sublateral notches present; pronotosternal sutures closed, hypomeral bead present. Prosternum with sides concave at midlength. **Mesothorax.** Scutellum rounded posterad. Elytra. Integument unmarked. **Aedeagus.** Parameres with apical lateral expansions present; each paramere with three or more setae.

Summary. Supra-antennal carinae fading on frons, sensory elements beginning on antennomere IV (apical sensorium), pronotum setae on anterior half directed posterolaterad, and posterior slope without setae directed anterad, with sublateral notches present, pronotosternal sutures closed, hypomeral bead present at midlength (partly punctate), elytra with setae evenly distributed and mainly parallel, ventrite V not sinuate apicad and without setal brushes. Treated as distinctive subgroup to improve diagnostic effectiveness because of setose elytra. Not morphologically distinguished here from *Setasomus*.

Genus *Setasomus* Gurjeva, 1985

Habitus. Body length 6–12 mm. **Head.** Supra-antennal carinae joining medially (forming shelf) or fading on frons; nasale (head capsule below edge of frontal carina) with outline not concave in lateral view. Antennae with sensory elements beginning on antennomere IV. **Prothorax.** Pronotum with punctures simple; hind angle carinae present; posterior edge of pronotum with sublateral notches present; pronotosternal sutures closed, hypomeral bead present. Prosternum with sides straight at midlength. **Mesothorax.** Mesocoxal cavities not closed. Scutellum rounded posterad. Elytra. Integument marked with spots

or bands in some. **Aedeagus.** Parameres with apical lateral expansions present or absent, without setae or each paramere with three or more setae.

Summary. Supra-antennal carinae fading on frons, or joining medially (not concave below in lateral view), sensory elements beginning on antennomere IV, antennomere III closer in length to IV than to II, pronotum with sublateral notches present, pronotosternal sutures closed, hypomeral bead present at midlength (punctate in some), prosternal sides straight, elytra with setae evenly distributed and mainly parallel, tarsi and claws simple, ventrites not microserrate at sides and without setal brushes apically, parameres with zero or more than three setae. We could not write a diagnosis that distinguished this from some *Liotrichus* or *Sylvanelater*.

Genus *Strophenron* Johnson, 2021

Habitus. Body length 6–12 mm. **Head.** Supra-antennal carinae fading on frons. Antennae with sensory elements beginning on antennomere IV. **Prothorax.** Pronotum with punctures simple; hind angle carinae present; posterior edge of pronotum with sublateral notches present; pronotosternal sutures closed. Prosternum with sides straight at midlength. **Mesothorax.** Scutellum rounded posterad. Elytra. Integument marked with spots or transverse bands or marked in apical half only. **Ventrites.** Microserration at sides (e.g., 100 points per mm) present. **Aedeagus.** Parameres setose.

Summary. Supra-antennal carinae fading on frons, pronotum with hind angle carina present in most, elytra pale with angulate paired dark markings at least on apical half, abdominal ventrites microserrate. Incompletely separated from *Anostirus* in key.

Genus *Sylvanelater* Johnson, 2008

Habitus. Body length 6–18 mm. **Head.** Antennae with sensory elements beginning on antennomere III. **Prothorax.** Pronotum with punctures simple; hind angle carinae present; posterior edge of pronotum with sublateral notches present; pronotosternal sutures closed; hypomera with arcuate or angulate concavity on posterior edge near hind angle. Prosternum with sides straight at midlength; prosternal process curved upward > 40° in lateral view in some. **Mesothorax.** Scutellum rounded posterad. Elytra. Integument unmarked. **Aedeagus.** Parameres with apical lateral expansions present, without setae or each paramere with three or more setae.

Summary. Supra-antennal carinae fading on frons, sensory elements beginning on antennomere III, pronotum with setae on anterior half directed anterad or mesad, some setae directed mesad near midlength, sublateral notches present, pronotosternal sutures closed, elytral setal and integument color patterns absent. Not distinguished from some *Proludius* here.

***S. atropurpureus* (Melsheimer)**

Habitus. Body length 6–12 mm. **Head.** Supra-antennal carinae joining medially (forming shelf) or reaching anterior edge of head capsule; nasale (head capsule below edge of frontal carina) with outline not concave in lateral view.

Antennae with sensory elements beginning on antennomere III. **Prothorax.** Pronotum with punctures simple; hind angle carinae present or absent; posterior edge of pronotum with sublateral notches present; pronotosternal sutures open, hypomeral bead present. **Mesothorax.** Scutellum rounded posterad or pointed (acuminate). Elytra. Anterior edge variable in shape, integument with metallic reflections or unmarked. **Aedeagus.** Parameres with apical lateral expansions present, without setae.

Summary. Sensory elements beginning on antennomere III, pronotum with setae on anterior half directed anterad or mesad, pronotosternal sutures open.

***S. mendax* (LeConte), and similar species**

Habitus. Body length 6–12 mm. **Head.** Supra-antennal carinae fading on frons, or complete across frons but not concave below in lateral view. Antennae with sensory elements beginning on antennomere IV. **Prothorax.** Pronotum with punctures simple; hind angle carinae present or absent; posterior edge of pronotum with sublateral notches present; pronotosternal sutures open, hypomeral bead present. Prosternum with sides straight or concave at midlength. **Mesothorax.** Scutellum rounded posterad. Elytra. Integument with metallic reflections or unmarked. **Aedeagus.** Parameres with apical lateral expansions present, without setae.

Summary. Sensory elements beginning on antennomere IV, pronotum non-metallic, with setae on anterior half not directed posterad, some setae directed mesad near midlength, sublateral notches present, pronotosternal sutures open.

Genus *Tesolasomus* Johnson, 2021

Habitus. Body length 6–18 mm. **Head.** Antennae with sensory elements beginning on antennomere IV. **Prothorax.** Pronotum with punctures simple; hind angle carinae present; posterior edge of pronotum with sublateral notches present; pronotosternal sutures closed, hypomeral bead absent. Prosternum with sides straight or concave at midlength. **Mesothorax.** Scutellum rounded posterad. Elytra. Integument marked with spots or bands in some. **Aedeagus.** Parameres with apical lateral expansions present, without setae.

Summary. Sensory elements beginning on antennomere IV, pronotum with setae on anterior half directed posterad, hind angles with sublateral notches present, hypomeral bead absent (not raised, punctate), mesocoxal cavities open, parameres without setae.

***T. morulus* (LeConte) and *T. deceptor* (Brown)**

Habitus. Body length 6–12 mm. **Head.** Antennae with sensory elements beginning on antennomere IV. **Prothorax.** Pronotum with punctures simple; hind angle carinae present; posterior edge of pronotum with sublateral notches present; pronotosternal sutures closed, hypomeral bead present; hypomera with concavity on posterior edge near hind angle. Prosternum with sides straight

or concave at midlength. **Mesothorax.** Scutellum rounded posterad. Elytra. Integument unmarked; setal vestiture sparse on disk or even and mainly parallel. **Ventrites.** Ventrite V apex bisinuate with paired setal brushes (larger in males). **Aedeagus.** Parameres with apical lateral expansions present; each paramere with three or more setae.

Summary. Supra-antennal carinae fading on frons, sensory elements beginning on antennomere IV, hind angles with sublateral notches present, ventrite V apex bisinuate in ventral view with paired setal brushes. Species with hypomer- al bead present and modified ventrite V treated as distinctive here.

Tribe Dendrometrini

Habitus. Body length 3–30 mm. **Head.** Prognathous in most; most with supra-antennal carinae joining medially forming a shelf across the frons with a concavity below in lateral view, frons with triangular depression in some. Antennae with 11 antennomeres, not pectinate. **Prothorax.** Pronotum without tubercles between punctures in most, pronotal lateral carinae complete, visible throughout length in dorsal view in most, microserrate near hind angles in some; posterior crenellations absent, posterior edge of hind angles not defined by a dorsal carina in some; most with setae directed anterad throughout; pronotosternal sutures straight in most. **Mesothorax.** Scutellum with posterior edge rounded in most. Elytra. Striae present in most, setal vestiture even and mainly parallel, elytral integument unmarked with spots or transverse bands in most, setae not forming color pattern in most. **Legs.** Tarsal pads or membranous lobes present in many. Tarsal claws simple. **Ventrites.** Microserration at sides (e.g., 100 points per mm) present in some. Ventrite V arcuate apicad, without setal brushes. **Aedeagus.** Parameres with more than three setae each in most.

Notes. It is difficult to define this group collectively based on adult morphology. Most with supra-antennal carinae continuous and raised across frons and some with tarsal pads lobed. Some with hind angles of prothorax depressed or not defined mesally by a right-angled edge (carina) in dorsal view.

Genus *Athous* Eschscholtz, 1829

Habitus. Body length 3–30 mm. **Head.** Supra-antennal carinae joining medially (forming shelf), nasale (head capsule below edge of frontal carina) with outline concave in lateral view; frons with triangular depression in most. **Prothorax.** Pronotum with lateral carina microserrate in some; pronotosternal sutures closed, hypomer- on with posterior edge near hind angle without concavity in most. Prosternum with sides straight at midlength in most. **Mesothorax.** Scutellum with posterior edge rounded in most; mesocoxal cavities fully open in most. Elytra. Striae present; integument unmarked in most; without pattern from differences in setal color. **Legs.** Tarsal pads or membranous lobes present on multiple tarsomeres in most (II and III). **Aedeagus.** Parameres with apical lateral expansions present in most; each paramere with three or more setae in most.

Diagnostic summaries are provided separately here for Becker's (1979) species groups and European subgenera present in North America.

***A. brightwelli* (Kirby) group**

Habitus. Body length 6–18 mm. **Head.** Antennal sensory elements beginning on antennomere III. **Prothorax.** Pronotum with punctures simple, lateral carina microserrate at hind angles only (posterior 10%, in concavity); hind angle carinae absent; posterior edge of pronotum with sublateral notches in some; hypomeral bead present. Prosternal process not curved upward $\geq 40^\circ$ in lateral view. **Mesothorax.** Scutellum with anterior edge concave. Elytra. Anterior edge straight to arcuate or sinuate (recurved) or with rectangular projection near humeri in dorsal view. **Legs.** Metacoxal plate reaching side. **Ventrites.** Sides not microserrate.

Summary. Supra-antennal carina complete and elevated, frons with broad semi-triangular impression across much of dorsal surface, sensory elements beginning on antennomere III (widespread rough texture and/or apical sensorium), pronotum without dorsal hind angle carinae, tarsomeres II and III with lobes, ventrites not microserrate at sides.

***A. campyloides* Newman group**

Habitus. Body length 6–18 mm. **Head.** Antennal sensory elements beginning on antennomere IV. **Prothorax.** Pronotum with punctures umbilicate in some, lateral carina microserrate along entire side (e.g., ~ 70 points per mm) or at hind angles only (posterior 10%, in concavity); hind angle carinae absent; posterior edge of pronotum with sublateral notches present; hypomeral bead present. Prosternal process not curved upward $\geq 40^\circ$ in lateral view. **Mesothorax.** Scutellum with anterior edge not concave. Elytra. Anterior edge sinuate (recurved) in dorsal view. **Legs.** Metacoxal plate reaching side or not. **Ventrites.** Sides not microserrate.

Summary. Supra-antennal carina complete and elevated, frons with broad semi-triangular impression across much of dorsal surface, sensory elements beginning on antennomere IV (apical sensorium), pronotum without dorsal hind angle carinae, tarsomeres II and III with lobes, ventrites not microserrate at sides.

***A. cucullatus* (Say) group**

Habitus. Body length 6–12 mm. **Head.** Antennal sensory elements beginning on antennomere III. **Prothorax.** Pronotum with some punctures umbilicate, lateral carina microserrate along entire side (e.g., ~ 70 points per mm); hind angle carinae present or absent; posterior edge of pronotum with sublateral notches in some; hypomeral bead absent. Prosternum with sides straight or convex at midlength; prosternal process not curved upward $\geq 40^\circ$ in lateral view. **Mesothorax.** Scutellum with anterior edge concave or not, posterior edge rounded (arcuate) or pointed (acuminate). Elytra. Anterior edge straight to arcuate or sinuate (recurved) in dorsal view. **Legs.** Metacoxal plate reaching side or not. **Ventrites.** Microserration at sides (e.g., 100 points per mm) present or absent. **Aedeagus.** Parameres without apical lateral expansions.

Summary. Supra-antennal carina complete and elevated, frons with broad semi-triangular impression across much of dorsal surface, lateral carina

microserrate for much of length (best observed from below, not necessary to see), pronotal hind angles with dorsal carina (weak in some), multiple tarsomeres with lobes, parameres without preapical expansions.

A. *imitans* Fall group

Habitus. Body length 3–12 mm. **Head.** Frons without triangular depression. Antennal sensory elements beginning on antennomere IV. **Prothorax.** Pronotum with punctures simple, lateral carina microserrate at hind angles only (posterior 10%, in concavity) or not serrate; hind angle carinae absent; posterior edge of pronotum without sublateral notches; pronotosternal sutures closed. Prosternal process not curved upward $\geq 40^\circ$ in lateral view. **Mesothorax.** Mesocoxal cavities open to mesepimeron only. Scutellum with anterior edge concave. Elytra. Anterior edge straight to arcuate near humeri in dorsal view, integument marked with spots or bands in some. **Legs.** Metacoxal plate not reaching side. **Ventrites.** Sides not microserrate.

Summary. Supra-antennal carina complete and elevated, frons without triangular impression, pronotal hind angles without dorsal carina, posterior edge depressed and without basal notches, prosternal process not ascendant, multiple tarsomeres with lobes.

A. *productus* (Randall) group

Habitus. Body length 12–18 mm. **Head.** Antennal sensory elements beginning on antennomere III. **Prothorax.** Pronotum with some punctures umbilicate, lateral carinae not serrate; hind angle carinae absent; posterior edge of pronotum without sublateral notches; hypomeral bead present; hypomera with arcuate concavity on posterior edge near hind angle. Prosternum with sides straight or concave at midlength; prosternal process not curved upward $\geq 40^\circ$ in lateral view. **Mesothorax.** Scutellum with anterior edge not concave, posterior edge rounded (arcuate) or straight (truncate). Elytra. Anterior edge straight to arcuate near humeri in dorsal view. **Legs.** Metacoxal plate reaching side. **Ventrites.** Sides not microserrate.

Summary. Supra-antennal carina complete and elevated, frons with broad triangular impression across much of dorsal surface, pronotum without hind angle carinae, lateral carinae not microserrate (even at hind angles), multiple tarsomeres with lobes.

A. *rufifrons* (Randall) group

Habitus. Body length 12–18 mm. **Head.** Antennal sensory elements beginning on antennomere III. **Prothorax.** Pronotum with some punctures umbilicate, lateral carina microserrate at hind angles only (posterior 10%, in concavity); hind angle carinae absent; posterior edge of pronotum with sublateral notches present; hypomeral bead present. Prosternal process not curved upward $\geq 40^\circ$ in lateral view. **Mesothorax.** Scutellum with anterior edge concave. Elytra. Anterior edge sinuate (recurved) in dorsal view. **Legs.** Metacoxal plate not reaching side; tarsal pads absent. **Ventrites.** Microserration at sides (e.g., 100 points per mm) present.

Summary. Supra-antennal carina complete and elevated, frons with broad triangular impression across much of dorsal surface, pronotum without hind angle carinae, tarsi without ventral lobes, claws without basal setae, ventrites microserrate (especially apex of ventrite V).

***A. scapularis* (Say) group**

Habitus. Body length 6–18 mm. **Head.** Antennal sensory elements beginning on antennomere III or IV. **Prothorax.** Pronotum with some punctures umbilicate, lateral carina microserrate along entire side (e.g., ~ 70 points per mm) or at hind angles only (posterior 10%, in concavity); hind angle carinae present (single); posterior edge of pronotum without sublateral notches; hypomerall bead absent. Prosternal process not curved upward $\geq 40^\circ$ in lateral view. **Mesothorax.** Scutellum with anterior edge concave, posterior edge rounded (arcuate) or pointed (acuminate). Elytra. Anterior edge straight to arcuate near humeri in dorsal view. **Legs.** Metacoxal plate reaching side. **Ventrites.** Sides not microserrate.

Summary. Supra-antennal carinae complete and elevated, lateral carinae microserrate at least near hind angle, pronotal hind angles with dorsal carina, multiple tarsomeres with lobes, parameres with preapical expansions.

***A. scissus* LeConte group**

Habitus. Body length 12–30 mm. **Head.** Antennal sensory elements beginning on antennomere III or IV. **Prothorax.** Pronotum with some punctures umbilicate, lateral carina microserrate at hind angles only (posterior 10%, in concavity); hind angle carinae absent; posterior edge of pronotum with sublateral notches present; pronotosternal sutures closed. **Mesothorax.** Scutellum with anterior edge not concave, posterior edge rounded (arcuate) or pointed (acuminate). Elytra. Anterior edge straight to arcuate or sinuate (recurved) in dorsal view. **Legs.** Metacoxal plate reaching side or not. **Ventrites.** Microserration at sides (e.g., 100 points per mm) present.

Summary. Supra-antennal carina complete and elevated, frons with broad semi-triangular impression across much of dorsal surface, sensory elements beginning on antennomere III in most or all (apical sensorium), pronotum without dorsal hind angle carinae, lateral carina briefly microserrate near hind angle, multiple tarsomeres with lobes, ventrites not microserrate at sides.

Athous*, subgenus *Athous

Habitus. Body length 10–15 mm. **Head.** Frons without triangular depression. Antennal sensory elements beginning on antennomere IV. **Prothorax.** Pronotum with punctures umbilicate in some, lateral carina microserrate along entire side (e.g., ~ 70 points per mm); hind angle carinae absent; posterior edge of pronotum with sublateral notches present; pronotosternal sutures closed. Prosternal process not curved upward $\geq 40^\circ$ in lateral view. **Mesothorax.** Scutellum with anterior edge concave. Elytra. Anterior edge straight to arcuate near humeri in dorsal view. **Legs.** Metacoxal plate reaching side or not. **Ventrites.**

Microserration at sides (e.g., 100 points per mm) present. **Aedeagus.** Parameres without setae or each paramere with three or more setae.

Summary. Supra-antennal carina complete and elevated (slightly), frons without triangular impression (weak transverse anterior impression only), pronotum with lateral carina microserrate throughout (best seen in lateroventral view), multiple tarsomeres lobed. For *A. haemorrhoidalis* (Fabricius).

Genus *Barrelater* Johnson, 2014

Habitus. Body length 12–18 mm. **Head.** Supra-antennal carinae joining medially (forming shelf), nasale (head capsule below edge of frontal carina) with outline concave in lateral view; frons without triangular depression. Antennal sensory elements beginning on antennomere III. **Prothorax.** Pronotum with some punctures umbilicate, lateral carina microserrate at hind angles only (posterior 10%, in concavity); hind angle carinae absent; posterior edge of pronotum with sublateral notches present; pronotosternal sutures closed, hypomeral bead absent; hypomeron with posterior edge near hind angle without concavity. Prosternum with sides straight at midlength; prosternal process curved upward > 40° in lateral view. **Mesothorax.** Mesocoxal cavities open. Scutellum with anterior edge concave. Elytra. Striae present; anterior edge straight to arcuate near humeri in dorsal view. **Legs.** Metacoxal plate reaching side; tarsal pads or membranous lobes present on multiple tarsomeres (or appearing absent), (I, II, III, and IV or II, III, and IV). **Ventrites.** Sides not microserrate. **Aedeagus.** Parameres with apical lateral expansions present; each paramere with three or more setae.

Summary. Supra-antennal carina complete and elevated, frons without triangular impression, pronotum with umbilicate punctures, dorsal hind angles without carinae, lateral carinae briefly microserrate near hind angle. Incompletely separated from *Hemicrepidius* here.

Genus *Denticollis* Piller & Mitterpacher, 1783

Habitus. Body length 7–13 mm. **Head.** Supra-antennal carinae joining medially (forming shelf), nasale (head capsule below edge of frontal carina) with outline concave in lateral view; nasale (head capsule below edge of frontal carina) with outline concave in lateral view; frons with triangular depression. Antennal sensory elements beginning on antennomere III. **Prothorax.** Pronotum with punctures umbilicate in some, lateral carinae not serrate; hind angle carinae absent; posterior edge of pronotum without sublateral notches; pronotosternal sutures closed, hypomeral bead present; hypomeron with posterior edge near hind angle without concavity. **Mesothorax.** Mesocoxal cavities open. Scutellum with anterior edge concave or not. Elytra. Anterior edge straight to arcuate or sinuate (recurved) in dorsal view. **Legs.** Metacoxal plate reaching side or not; tarsal pads or membranous lobes absent (or present on tarsomere IV only). **Ventrites.** Sides not microserrate. **Aedeagus.** Parameres with apical lateral expansions present.

Summary. Supra-antennal carina complete and elevated (concave below in lateral view), frons with triangular impression, pronotum without dorsal hind angle carinae, tarsomeres not lobed (or tarsomere IV weakly lobed in some), ventrites not microserrate at sides.

Genus *Diacanthous* Reitter, 1852

Habitus. Body length 10–15 mm. **Head.** Supra-antennal carinae joining medially (forming shelf), nasale (head capsule below edge of frontal carina) with outline concave in lateral view; nasale (head capsule below edge of frontal carina) with outline concave in lateral view; frons with triangular depression. Antennal sensory elements beginning on antennomere III. **Prothorax.** Pronotum with some punctures umbilicate, lateral carina micro serrate along entire side (e.g., ~ 70 points per mm); hind angle carinae absent; posterior edge of pronotum without sublateral notches; pronotosternal sutures closed, hypomerical bead absent; hypomera with arcuate concavity on posterior edge near hind angle. Prosternum with sides straight or concave at midlength. **Mesothorax.** Mesocoxal cavities open. Scutellum with anterior edge not concave. Elytra. Striae present; anterior edge straight to arcuate near humeri in dorsal view; with pattern from differences in setal color. **Legs.** Metacoxal plate reaching side; tarsal pads or membranous lobes present on multiple tarsomeres, (I, II, III, and IV or II, III, and IV). **Ventrites.** Sides not micro serrate. **Aedeagus.** Parameres without apical lateral expansions.

Summary. Supra-antennal carina complete and elevated (concave below in lateral view), frons with triangular impression, elytra with diagonal bands due to differences in setal color, setae simple (not scale-like).

Genus *Elathous* Reitter, 1890

Habitus. Body length 6–12 mm. **Head.** Supra-antennal carinae joining medially (forming shelf), nasale (head capsule below edge of frontal carina) with outline concave in lateral view; nasale (head capsule below edge of frontal carina) with outline concave in lateral view; prognathous, rarely hypognathous; frons with triangular depression. Antennal sensory elements beginning on antennomere IV. **Prothorax.** Pronotum with some punctures umbilicate, lateral carinae not serrate; hind angle carinae present (single); posterior edge of pronotum with sublateral notches in some; pronotosternal sutures open, hypomerical bead present; hypomeron with posterior edge near hind angle without concavity. **Mesothorax.** Mesocoxal cavities not closed. Scutellum with anterior edge not concave. Elytra. Striae present; anterior edge straight to arcuate near humeri in dorsal view. **Legs.** Metacoxal plate reaching side; tarsal pads absent. **Ventrites.** Microserration at sides (e.g., 100 points per mm) present or absent. **Aedeagus.** Parameres with apical lateral expansions present.

Summary. Supra-antennal carina complete and elevated (concave below in lateral view), frons with broad impression, sensory elements beginning on antennomere IV (dorsal and ventral sensoria), hypomeron without concavity on posterior edge, tarsi not lobed.

Genus *Euplastius* Schwarz, 1903

Habitus. Body length 6–12 mm. **Head.** Supra-antennal carinae fading on frons; frons without triangular depression. Antennal sensory elements beginning on antennomere III. **Prothorax.** Pronotum with punctures umbilicate in some; lateral carinae hidden anteriorly in dorsal view in some, not serrate; hind angle carinae present (single) or absent; posterior edge of pronotum without sublateral

notches; pronotosternal sutures closed, hypomera with posterior concavity long and arcuate. Prosternum with sides straight or convex at midlength; prosternal process not curved upward $\geq 40^\circ$ in lateral view. **Mesothorax.** Mesocoxal cavities open. Scutellum with anterior edge not concave. Elytra. Striae present; anterior edge straight to arcuate or sinuate (recurved) or with rectangular projection near humeri in dorsal view. **Legs.** Metacoxal plate reaching side; tarsal pads absent. **Ventrites.** Sides not microserrate. **Aedeagus.** Parameres with apical lateral expansions present, without setae.

Summary. Supra-antennal carinae fading on frons, sensory elements beginning on antennomere III (widespread with short erect pubescence), pronotum punctures umbilicate, setae near midline on anterior half directed mesad, sublateral notches absent, posterior edge of pronotum not defined by a transverse carina near hind angles.

Genus *Gambrinus* LeConte, 1853

Habitus. Body length 6–18 mm. **Head.** Nasale (head capsule below edge of frontal carina) with outline concave in lateral view; frons without triangular depression. Antennal sensory elements beginning on antennomere IV. **Prothorax.** Pronotum with punctures umbilicate in some; lateral carinae hidden anteriorly in dorsal view in some, not microserrate; hind angle carinae present (single); posterior edge of pronotum without sublateral notches; pronotosternal sutures open or closed, hypomerical bead present; hypomera with arcuate or angulate concavity on posterior edge near hind angle. Prosternum with sides straight or concave at midlength. **Mesothorax.** Mesocoxal cavities not closed. Scutellum with anterior edge not concave, posterior edge rounded (arcuate) or pointed (acuminate). Elytra. Striae present; anterior edge straight to arcuate near humeri in dorsal view, integument marked with spots or transverse bands in some. **Legs.** Metacoxal plate reaching side; tarsal pads absent. **Ventrites.** Microserration at sides (e.g., 100 points per mm) present. **Aedeagus.** Parameres with apical lateral expansions present or absent.

Summary. Supra-antennal carina complete and elevated (concave below in lateral view), frons without triangular impression, pronotum with lateral carina complete, sublateral notches absent, hypomeron with concavity on posterior edge, tarsi not lobed, ventrites microserrate at sides.

G. bicolor Van Dyke

Habitus. Body length 5–10 mm. **Head.** Nasale (head capsule below edge of frontal carina) with outline concave in lateral view; frons with triangular depression. Antennal sensory elements beginning on antennomere IV. **Prothorax.** Pronotum with some punctures umbilicate; lateral carinae hidden anteriorly in dorsal view in some, not serrate; hind angle carinae present (single); posterior edge of pronotum without sublateral notches; pronotosternal sutures open, hypomerical bead present; hypomera with arcuate concavity on posterior edge near hind angle. Prosternum with sides straight at midlength; prosternal process not curved upward $\geq 40^\circ$ in lateral view. **Mesothorax.** Mesocoxal cavities open. Scutellum with anterior edge not concave, posterior edge rounded (arcuate) or pointed (acuminate). Elytra. Striae present; anterior edge straight

to arcuate near humeri in dorsal view. **Legs.** Metacoxal plate reaching side; tarsal pads absent. **Ventrites.** Microserration at sides (e.g., 100 points per mm) present. **Aedeagus.** Parameres with apical lateral expansions present.

Summary. Supra-antennal carina complete and elevated (concave below in lateral view), frons with triangular impression, pronotum without sublateral notches, hypomer on with concavity on posterior edge, ventrites microserrate at sides. Treated as distinctive here to improve diagnostic effectiveness, because of triangular depression on frons.

Genus *Hemicrepidius* Germar, 1839

Habitus. Body length 12–30 mm. **Head.** Supra-antennal carinae joining medially (forming shelf) or reaching anterior edge of head capsule; frons without triangular depression. Antennal sensory elements beginning on antennomere III or IV. **Prothorax.** Pronotum with punctures simple, lateral carina microserrate at hind angles only (posterior 10%, in concavity) or not serrate; hind angle carinae present (single); posterior edge of pronotum with sublateral notches in some; pronotosternal sutures closed; hypomer on with posterior edge near hind angle with concavity in most. **Mesothorax.** Mesocoxal cavities open. Scutellum with anterior edge concave or not, posterior edge rounded (arcuate) or pointed (acuminate). Elytra. Striae present; anterior edge straight to arcuate or sinuate (recurved) in dorsal view, integument unmarked. **Legs.** Metacoxal plate reaching side or not; tarsal pads or membranous lobes present on multiple tarsomeres, (I, II, III, and IV or II, III, and IV). **Ventrites.** Microserration at sides (e.g., 100 points per mm) present or absent. **Aedeagus.** Parameres with apical lateral expansions present.

Summary. Supra-antennal carina complete or joining anterior edge of head capsule, frons without triangular impression, pronotum wider than long, hind angle not microserrate or microserrate only in concavity at hind angle, pronotosternal sutures closed, multiple tarsomeres lobed. Pronotal hind angle carinae present (inconspicuous in some), hypomer on notched near hind angle in most. Incompletely distinguished from *Barrelater* here.

Genus *Limonius* Eschscholtz, 1829

Habitus. Body length 3–12 mm. **Head.** Supra-antennal carinae joining medially (forming shelf); frons without triangular depression. Antennal sensory elements beginning on antennomere IV. **Prothorax.** Pronotum with punctures umbilicate in some; lateral carinae hidden anteriorly in dorsal view in some, not serrate; hind angle carinae present (single) or absent; posterior edge of pronotum without sublateral notches; pronotosternal sutures open or closed, hypomer on bead present; hypomer on with posterior edge near hind angle without concavity. **Mesothorax.** Mesocoxal cavities not closed. Scutellum with anterior edge not concave. Elytra. Striae present; anterior edge straight to arcuate near humeri in dorsal view, integument marked with spots or bands in some. **Legs.** Metacoxal plate reaching side or not; tarsal pads absent. **Ventrites.** Microserration at sides (e.g., 100 points per mm) present. **Aedeagus.** Each paramere with three or more setae.

Summary. Supra-antennal carina complete and elevated, frons without triangular impression, hypomerion without concavity on posterior edge, scutellum rounded posterad, tarsi not lobed, ventrites microserrate at sides.

***L. brevis* Van Dyke**

Habitus. Body length 5–8 mm. **Head.** Nasale (head capsule below edge of frontal carina) with outline concave in lateral view; frons without triangular depression. Antennal sensory elements beginning on antennomere IV. **Prothorax.** Pronotum with punctures simple, with or without tubercles between punctures; lateral carinae hidden anteriorly in dorsal view in some, not serrate; hind angle carinae present (single) or absent; posterior edge of pronotum without sublateral notches; pronotosternal sutures open, hypomerion bead present; hypomerion with posterior edge near hind angle without concavity. Prosternum with sides straight or concave at midlength; prosternal process curved upward > 40° in lateral view. **Mesothorax.** Mesocoxal cavities open to mesepimeron only. Scutellum with anterior edge not concave. Elytra. Striae present; anterior edge straight to arcuate near humeri in dorsal view. **Legs.** Metacoxal plate reaching side; small tarsal pads or membranous lobes present on multiple tarsomeres (II and III). **Ventrites.** Microserration at sides (e.g., 100 points per mm) present. **Aedeagus.** Parameres with apical lateral expansions present.

Summary. Supra-antennal carina complete and elevated (concave below in lateral view), pronotosternal sutures open anterad, hypomerion without concavity posterad, tarsi lobed on tarsomeres II and III (short apicoventral lobes). Included as distinct sub-group here to improve diagnostic effectiveness because of lobed tarsomeres.

Genus *Pheletes* Kiesenwetter, 1858

Habitus. Body length 5–7 mm. **Head.** Supra-antennal carinae joining medially (forming shelf); frons without triangular depression. Antennal sensory elements beginning on antennomere IV. **Prothorax.** Pronotum with punctures simple, lateral carinae not serrate; hind angle carinae present (single); posterior edge of pronotum without sublateral notches; pronotosternal sutures closed, hypomerion bead present; hypomerion with posterior edge near hind angle without concavity. **Mesothorax.** Mesocoxal cavities not closed. Scutellum with anterior edge not concave, posterior edge pointed (acuminate). Elytra. Striae present. **Legs.** Metacoxal plate reaching side; tarsal pads absent. **Ventrites.** Microserration at sides (e.g., 100 points per mm) present. **Aedeagus.** Parameres with apical lateral expansions present.

Summary. Supra-antennal carina complete and elevated (concave below in lateral view), hypomerion without concavity near hind angle, scutellum pointed posterad, tarsomeres simple, parameres with preapical lateral expansions.

Genus *Tetralimonius* Etzler, 2019

Habitus. Body length 3–6 mm. **Head.** Nasale (head capsule below edge of frontal carina) with outline concave in lateral view; frons without triangular

depression. Antennal sensory elements beginning on antennomere IV. **Prothorax.** Pronotum with punctures umbilicate in some, lateral carinae not serrate; hind angle carinae present (single) or absent; posterior edge of pronotum without sublateral notches; pronotosternal sutures open, hypomeral bead present; hypomeron with posterior edge near hind angle without concavity. **Mesothorax.** Mesocoxal cavities not closed. Scutellum with anterior edge not concave, posterior edge pointed (acuminate). Elytra. Striae present; anterior edge straight to arcuate near humeri in dorsal view, integument marked with spots or bands in many. **Legs.** Metacoxal plate reaching side; tarsal pads absent. **Ventrites.** Microserration at sides (e.g., 100 points per mm) present. **Aedeagus.** Parameres without apical lateral expansions; each paramere with one or two setae.

Summary. Supra-antennal carina complete and elevated (concave below in lateral view), hypomeron without concavity near hind angle, scutellum pointed posterad, tarsomeres simple, parameres without preapical lateral expansions.

Genus *Vittathous* Johnson, 2021

Habitus. Body length 12–18 mm. **Head.** Supra-antennal carinae fading on frons or reaching anterior edge of head capsule; frons without triangular depression. Antennal sensory elements beginning on antennomere III. **Prothorax.** Pronotum with punctures large but simple, lateral carinae not serrate; hind angle carinae present (single); posterior edge of pronotum without sublateral notches; pronotosternal sutures closed, hypomeral bead absent; hypomeron with posterior edge near hind angle without concavity. Prosternal process not curved upward $\geq 40^\circ$ in lateral view. **Mesothorax.** Mesocoxal cavities open. Scutellum with anterior edge concave or not. Elytra. Striae present; anterior edge straight to arcuate near humeri in dorsal view, integument with longitudinal bands. **Legs.** Metacoxal plate reaching side; tarsal pads absent. **Ventrites.** Sides not microserrate. **Aedeagus.** Parameres with apical lateral expansions present; each paramere with two setae.

Summary. Sensory elements beginning on antennomere III, pronotum with setae near midline on anterior half directed mesad, sublateral notches absent (posterior edge of pronotum not defined by a transverse carina), parameres with two setae.

Conclusions

A first interactive key is provided for genera of Elateridae from Canada and the USA. This publication also summarizes species habitat requirements at multiple scales, and includes the most comprehensive descriptive information for genera of Elateridae from Canada and USA. Diversity of elaterid genera was high throughout warm and cool temperate regions, especially in mountainous areas and mesic woodlands. Larvae of most genera were associated with soil, litter, and decaying wood. We invite colleagues to borrow this descriptive format for their own generic descriptions and diagnoses for Elateridae. We ask researchers to cite this work in the methods section of manuscripts where it was used for generic identifications as outlined by Packer et al. (2018).

Acknowledgements

Thanks to K. Savard, M. Gamman, and J. Hsiung (all AAFC) for character detail photos. We thank the following people for testing the key: A. Fraser, McGill University; E. Fuller (Tweed, ON); S. Gilmore (Nanaimo, BC); M. Gimmel (Santa Barbara Museum of Natural History), detailed review; E. Yerger (Indiana University of Pennsylvania); and W. Van Herk (AAFC, Agassiz). Thanks to B. Mathison (Utah) for extensive curation of iNaturalist records used to develop Table 1. We thank E. Martinez-Luque (Santiago de Querétaro, Mexico) for offering collaboration to extend the range of the key to also include Mexico. Thanks to A. Prosvirov and S. Policena Rosa for helpful comments on the manuscript and key. Thanks to M. Taylor, Identic Ltd., Australia for help with sharing the key online.

Additional information

Conflict of interest

The authors have declared that no competing interests exist.

Ethical statement

No ethical statement was reported.

Funding

This study was supported by the Agriculture and Agri-Food Canada.

Author contributions

Conceptualization: HBD, HJH. Data curation: HBD. Formal analysis: HBD. Funding acquisition: HBD. Investigation: FEE, HBD. Methodology: HBD, HJH, FEE. Resources: PJJ. Validation: HBD. Visualization: HJH. Writing - original draft: HBD. Writing - review and editing: FEE, PJJ, HJH, HBD.

Author ORCIDs

Hume B. Douglas  <https://orcid.org/0000-0003-1722-7554>

Data availability

All of the data that support the findings of this study are available in the main text or Supplementary Information.

References

- Arnett RH (1968) The beetles of the United States (A Manual for Identification). American Entomological Institute, Ann Arbor, 1112 pp.
- Becker EC (1979) Review of the western Nearctic species of *Athous* (Coleoptera: Elateridae), with a key to the species north of Panama. Canadian Entomologist 111(5): 569–614. <https://doi.org/10.4039/Ent111569-5>
- Becker EC, Dogger JR (1991) Elateridae (Elateroidea)(Including Dicronychidae, Lissomidae). In: Stehr FW (Ed.) Immature Insects. Volume 2. Kendall/Hunt, Dubuque, Iowa, 410–418.
- Brooks AR (1961) Adult Elateridae of southern Alberta, Saskatchewan and Manitoba (Coleoptera). Canadian Entomologist 92: 1–63. <https://doi.org/10.4039/entm9320fv>

- Brust M, Thurman J, Reuter C, Black L, Quartarone R, Redford AJ (2020) Grasshoppers of the Western U.S., Edition 4.1. USDA APHIS Identification Technology Program (ITP). Fort Collins, CO. <https://idtools.org/id/grasshoppers/> [accessed on 27 Sept 2023]
- Burakowski B (1973) Immature stages and biology of *Drapetes biguttatus* (Filler) (Coleoptera, Lissomidae). *Annales Zoologici Warsaw* 30: 335–347.
- Casari SA (1996) Systematics and phylogenetic analysis of *Alaus* Eschscholtz, 1829 (Coleoptera, Elateridae). *Revista Brasileira de Entomologia* 40: 249–298.
- Casari SA (2002) Review of the genus *Chalcolepidius* Eschscholtz, 1829 (Coleoptera, Elateridae, Agrypninae). *Revista Brasileira de Entomologia* 46(3): 263–428. <https://doi.org/10.1590/S0085-56262002000300007>
- Casari SA (2003) New species of *Alaus* Eschscholtz, 1829 (Coleoptera: Elateridae, Agrypninae, Hemirhipini). *Annales de la Société Entomologique de France* 39(4): 315–333. <https://doi.org/10.1080/00379271.2003.10697390>
- Casari SA (2006) Larva, pupa and adult of *Aeolus cinctus* Candèze (Coleoptera, Elateridae, Agrypninae). *Revista Brasileira de Entomologia* 50(3): 347–351. <https://doi.org/10.1590/S0085-56262006000300004>
- Casari SA, Biffi G (2012) Immatures of *Dicrepidius* Eschscholtz, 1829 and *Dipropus* Germar, 1839 (Elateridae, Elaterinae, Ampedini: Dicrepidini). *Zootaxa* 3587(1): 65–77. <https://doi.org/10.11646/zootaxa.3587.1.3>
- Cheshire Jr JM, Jones DC (1988) Identification of the larva of *Glyphonyx bimarginatus* Schaeffer (Coleoptera: Elateridae). *Journal of Entomological Science* 23(3): 293–296. <https://doi.org/10.18474/0749-8004-23.3.293>
- Deen OT, Cuthbert Jr FPJ (1955) The distribution and relative abundance of wireworms in potato-growing areas of the southeastern states. *Journal of Economic Entomology* 48(2): 191–193. <https://doi.org/10.1093/jee/48.2.191>
- Dobrovsky TM (1954) Laboratory observations on *Conoderus vagus* Candèze (Coleoptera, Elateridae). *The Florida Entomologist* 37(3): 123–131. <https://doi.org/10.2307/3493085>
- Dolin VG (1978) Key to Elateridae larvae of the fauna of USSR. Urozhai, Kiev, 125 pp.
- Donlan EM, Townsend JH, Golden EA (2004) Predation of *Caretta caretta* (Testudines: Cheloniidae) eggs by larvae of *Lanelater sallei* (Coleoptera: Elateridae) on Key Biscayne, Florida. *Caribbean Journal of Science* 40: 415–420.
- Douglas H (2003) Revision of *Cardiophorus* (Coleoptera: Elateridae) species of eastern Canada and United States of America. *Canadian Entomologist* 135(4): 493–548. <https://doi.org/10.4039/n02-003>
- Douglas H (2011) Phylogenetic relationships of Elateridae inferred from adult morphology, with special reference to the position of Cardiophorinae. *Zootaxa* 2900(1): 1–45. <https://doi.org/10.11646/zootaxa.2900.1.1>
- Douglas HB (2017) World reclassification of the Cardiophorinae (Coleoptera, Elateridae), based on phylogenetic analyses of morphological characters. *ZooKeys* 655: 1–130. <https://doi.org/10.3897/zookeys.655.11894>
- Douglas HB, Kundrata R, Brunke AJ, Escalona HE, Chapados JT, Eyres J, Richter R, Svard K, Ślipiński A, McKenna D, Dettman JR (2021) Anchored Phylogenomics, Evolution and Systematics of Elateridae: Are All Bioluminescent Elateroidea Derived Click Beetles? *Biology (Basel)* 10(6): 451. <https://doi.org/10.3390/biology10060451>
- Etzler FE (2019) Generic Reclassification of *Limoni* Eschscholtz, 1829 (Elateridae: Dendrometrinae) sensu Candèze 1860 of the World. *Zootaxa* 4683(3): 301–335. <https://doi.org/10.11646/zootaxa.4683.3.1>

- Etzler FE, Johnson PJ (2018) *Athoplastus* Johnson and Etzler (Coleoptera: Elateridae: Dendrometrinae), a new genus of click beetle from the northwestern continental USA. *Coleopterists Bulletin* 72(3): 503–521. <https://doi.org/10.1649/0010-065X-72.3.503>
- Fuller ER (1994) A reclassification of the genera of the click beetle tribe Elaterini based on the reconstructed phylogeny (Coleoptera: Elateridae). University of Alberta Edmonton, 181 pp.
- Glen E (1950) Larvae of the elaterid beetles of the tribe Lepturoidini (Coleoptera: Elateridae). *Smithsonian Miscellaneous Collections* 111: 246 pp.
- Hammond HEJ (1997) Arthropod biodiversity from *Populus* coarse woody material in north-central Alberta: A review of taxa and collection methods. *Canadian Entomologist* 129(6): 1009–1033. <https://doi.org/10.4039/Ent1291009-6>
- Hammond HEJ, Langor DW, Spence JR (2017) Changes in saproxylic beetle (Insecta: Coleoptera) assemblages following wildfire and harvest in boreal *Populus* forests. *Forest Ecology and Management* 401: 319–329. <https://doi.org/10.1016/j.foreco.2017.07.013>
- Hoernemann CK, Johnson PJ, Higgins KF (2001) Effects of grazing and haying on arthropod diversity in North Dakota conservation reserve program grasslands. *Proceedings of the South Dakota Academy of Science* 80: 283–308.
- Hulcr J, Smith S (2010) Xyleborini ambrosia beetles: an identification tool to the world genera. LUCID, Australia. <https://idtools.org/id/xyleborini/index.htm>
- Identical Ltd (2020) Lucid v4 Builder. <https://www.lucidcentral.org> [accessed on 26 Sept 2023]
- iNaturalist contributors, iNaturalist (2023) iNaturalist Research-grade Observations. iNaturalist.org. Occurrence data for Elateridae. <https://www.inaturalist.org> [accessed on 28 Sept 2023]
- Johnson PJ (1993) Immature insects. Vol. 2. Notes and errata to Elateridae and Throscidae. *Mola* 2: 5–6.
- Johnson PJ (2002) Elateridae. In: Arnett RH, Thomas MC, Skelley PE, Frank JH (Eds) *American Beetles*. CRC Press, Boca Raton, 160–173.
- Johnson PJ (2014) *Barrelater audreyae*, new genus and species, from the United States Intermountain West (Coleoptera: Elateridae). *Giornale Italiano di Entomologia* 13: 407–411.
- Johnson PJ in Mathison BA (2021) Click Beetles (Coleoptera: Elateridae) of the Southeastern United States. *Occasional Papers of the Florida State Collection of Arthropods* 13: 1–414.
- Johnston MA, Waite ES, Wright ER, Reily BH, De Leon GJ, Esquivel AI, Kerwin J, Salazar M, Sarmiento E, Thiatmaja T, Lee S, Yule K, Franz N (2023) Insect collecting bias in Arizona with a preliminary checklist of the beetles from the Sand Tank Mountains. *Biodiversity Data Journal* 11: e101960. <https://doi.org/10.3897/BDJ.11.e101960>
- Klimov PB, Oconnor B, Ochoa R, Bauchan GR, Redford AJ, Scher J (2016) Bee Mite ID: Bee-Associated Mite Genera of the World. USDA APHIS Identification Technology Program (ITP), Fort Collins, CO. https://idtools.org/bee_mite/index.cfm [accessed on 26 Sept 2023]
- Kundrata R, Bocak L (2011) The phylogeny and limits of Elateridae (Insecta, Coleoptera): Is there a common tendency of click beetles to soft-bodiedness and neoteny? *Zoologica Scripta* 40(4): 364–378. <https://doi.org/10.1111/j.1463-6409.2011.00476.x>
- Kundrata R, Gunter NL, Janosikova D, Bocak L (2018) Molecular evidence for the subfamilial status of Tetralobinae (Coleoptera: Elateridae), with comments on parallel

- evolution of some phenotypic characters. *Arthropod Systematics & Phylogeny* 76(1): 137–145. <https://doi.org/10.3897/asp.76.e31946>
- Kusy D, Motyka M, Bocek M, Vogler AP, Bocak L (2018) Genome sequences identify three families of Coleoptera as morphologically derived click beetles (Elateridae). *Scientific Reports* 8(1): 17084. <https://doi.org/10.1038/s41598-018-35328-0>
- Lanchester HP, Lane MC (1972) Family Elateridae (Cardiophorinae). In: Hatch MH (Ed) *The beetles of the Pacific Northwest Part V*. University of Washington Press, Seattle, 35–48.
- Lane MC (1972) Family Elateridae (except Cardiophorinae). In: Hatch MH (Ed) *The beetles of the Pacific Northwest. Part V*. University of Washington Press, Seattle, 6–34.
- Levesque C, Levesque GY (1980) *Activité des taupins (Coleoptera: Elateridae) de biotopes forestiers décidus des Laurentides (Québec)*. *Naturaliste Canadien (Quebec)* 107: 95–99.
- Levesque C, Levesque G-Y (1993) Abundance and seasonal activity of Elateroidea (Coleoptera) in a raspberry plantation and adjacent sites in southern Quebec, Canada. *Coleopterists Bulletin* 47: 269–277.
- Marinho TAS, Casari SA, Prosvirov AS, Rosa SP (2023) Description of immature stages and redescription of adults of *Monocrepidius fuscofasciatus* (Eschscholtz, 1829) (Elateridae, Agrypninae, Oophorini). *Zootaxa* 5271(2): 329–344. <https://doi.org/10.11646/zootaxa.5271.2.7>
- Milosavljevic I, Esser AD, Crowder DW (2016) Effects of environmental and agronomic factors on soil-dwelling pest communities in cereal crops. *Agriculture, Ecosystems & Environment* 225: 192–198. <https://doi.org/10.1016/j.agee.2016.04.006>
- Morrill WL (1978) Emergence of click beetles (Coleoptera: Elateridae) from some Georgia grasslands. *Environmental Entomology* 7(6): 895–896. <https://doi.org/10.1093/ee/7.6.895>
- Nol E, Douglas H, Crins WJ (2006) Responses of syrphids, elaterids and bees to single-tree selection harvesting in Algonquin Provincial Park, Ontario. *Canadian Field Naturalist* 120(1): 15–21. <https://doi.org/10.22621/cfn.v120i1.239>
- Packer L, Monckton SK, Onuferko TM, Ferrari RR (2018) Validating taxonomic identifications in entomological research. *Insect Conservation and Diversity* 11(1): 1–12. <https://doi.org/10.1111/icad.12284>
- Papp RP (1978) Ecology and habitat preferences of high altitude Coleoptera from the Sierra Nevada. *The Pan-Pacific Entomologist* 54: 161–172.
- Staines CL (2012) *Hispines of the World*. USDA/APHIS/PPQ Science and Technology and US National Natural History Museum.
- Stibick JNL (1976) A revision of the Hypnoidinae of the world (Col. Elateridae). Part 1 Introduction, phylogeny, biogeography. *The Hypnoidinae of North and South America. The genera Berninelsonius and Ligmargus*. *Eos Madrid* 51: 143–223.
- Stibick JNL (1978) A revision of the Hypnoidinae of the world (Col. Elateridae). Part 2. *The Hypnoidinae of North and South America. The genera Ascoliocerus, Desolakerrus, Margaiostus, Hypolithus and Hypnoidus*. *Eos-Revista Espanola de Entomologia* 52: 309–386.
- Stibick JNL (1990) North American Negastrinae (Coleoptera, Elateridae): The Negastrinae of the eastern United States and adjacent Canada. *Insecta Mundi* 4: 99–131.
- Svensson GP, Larsson MC, Hedin J (2004) Attraction of the larval predator *Elater ferrugineus* to the sex pheromone of its prey, *Osmoderma eremita*, and its implication for conservation biology. *Journal of Chemical Ecology* 30(2): 353–363. <https://doi.org/10.1023/B:JOEC.0000017982.51642.8c>

- Toba HH, Campbell JD (1992) Wireworm (Coleoptera: Elateridae) survey in wheat-growing areas of northcentral and northeastern Oregon. *Journal of the Entomological Society of British Columbia* 89: 25–30.
- Traugott M, Benefer CM, Blackshaw RP, van Herk WG, Vernon RS (2014) Biology, ecology, and control of elaterid beetles in agricultural land. *Annual Review of Entomology* 60(1): 313–334. <https://doi.org/10.1146/annurev-ento-010814-021035>
- Van Dyke EC (1932) Miscellaneous studies in the Elateridae and related families of Coleoptera. *Proceedings of the California Academy of Science (4th Series)* 20: 291-405.
- Webster R, Sweeney J, DeMerchant I (2012) New Coleoptera records from New Brunswick, Canada: Elateridae. *ZooKeys* 179: 93–113. <https://doi.org/10.3897/zookeys.179.2603>

Supplementary material 1

Key to the genera of Nearctic Elateridae v. 1.0, LIF3 file

Authors: Hume B. Douglas, Frank E. Etzler, Paul J. Johnson, H.E. James Hammond

Data type: php

Explanation note: This XML-based format allows exchange of the key with other key developers. This format can be imported directly LUCID and used as a non-illustrated interactive key.

Copyright notice: This dataset is made available under the Open Database License (<http://opendatacommons.org/licenses/odbl/1.0/>). The Open Database License (ODbL) is a license agreement intended to allow users to freely share, modify, and use this Dataset while maintaining this same freedom for others, provided that the original source and author(s) are credited.

Link: <https://doi.org/10.3897/zookeys.1200.119315.suppl1>

Supplementary material 2

Key to the genera of Nearctic Elateridae v.- 1.0, CSV file

Authors: Hume B. Douglas, Frank E. Etzler, Paul J. Johnson, H.E. James Hammond

Data type: php

Explanation note: This comma-separated values file may be used to exchange the Lucid key with other CSV-compliant applications.

Copyright notice: This dataset is made available under the Open Database License (<http://opendatacommons.org/licenses/odbl/1.0/>). The Open Database License (ODbL) is a license agreement intended to allow users to freely share, modify, and use this Dataset while maintaining this same freedom for others, provided that the original source and author(s) are credited.

Link: <https://doi.org/10.3897/zookeys.1200.119315.suppl2>

Supplementary material 3

Informal descriptions for Nearctic Elateridae v. 1.0, .PDF file

Authors: Hume B. Douglas, Frank E. Etzler, Paul J. Johnson, H.E. James Hammond

Data type: pdf

Explanation note: This PDF file includes expanded diagnostic information for all Nearctic elaterid genera or distinctive subsets of species, including all information used in the online key. These often differ from formal diagnoses used to globally define these groups. However, in some cases these are more informative than original diagnoses.

Copyright notice: This dataset is made available under the Open Database License (<http://opendatacommons.org/licenses/odbl/1.0/>). The Open Database License (ODbL) is a license agreement intended to allow users to freely share, modify, and use this Dataset while maintaining this same freedom for others, provided that the original source and author(s) are credited.

Link: <https://doi.org/10.3897/zookeys.1200.119315.suppl3>

Two new species of the genus *Cheiracanthium* C. L. Koch, 1839 (Araneae, Cheiracanthiidae) from China

Zhaoyi Li¹ , Feng Zhang^{1,2} 

¹ Key Laboratory of Zoological Systematics and Application of Hebei Province, College of Life Sciences, Hebei University, Baoding, Hebei 071002, China

² Hebei Basic Science Center for Biotic Interaction, Hebei University, Baoding, Hebei 071002, China

Corresponding author: Feng Zhang (dudu06042001@163.com)

Abstract

Two species of the long-legged sac spider genus *Cheiracanthium* C. L. Koch, 1839 collected from China are diagnosed and described as new to science: *Cheiracanthium bannaensis* sp. nov. (♂♀) from Yunnan Province and *C. bifurcatum* sp. nov. (♂♀) from Xinjiang Uyger Autonomous Region. Photos of the habitus and copulatory organs are given. In addition, DNA barcode information of the two new species is provided.

Key words: COI, description, DNA barcode, long-legged sac spider, taxonomy

Introduction

The genus *Cheiracanthium* C. L. Koch, 1839 is widely known and mainly distributed in the Old World (World Spider Catalogue; WSC 2024). Compared to other genera in Cheiracanthiidae Wagner, 1887, *Cheiracanthium* is the largest, accounting for 60% of the species diversity (220 out of 369 species described in the family) (WSC 2024). Members of *Cheiracanthium* are known as long-legged sac spiders, as they have long and slender legs, and build sac-like silk nests on plant leaves (Lotz 2007a).

Although several studies on *Cheiracanthium* have been published in the last few years (Deeleman-Reinhold 2001; Lotz 2007a, 2007b, 2011, 2014, 2015; Chen and Huang 2012; Bayer 2014; Zhang et al. 2018, 2020; Li and Zhang 2019, 2020, 2023, 2024; Esyunin and Zamani 2020; Dippenaar-Schoeman et al. 2021), the global diversity of this genus is still insufficiently known, and there are likely many other, as yet undiscovered species. Currently, 47 species of *Cheiracanthium* have been recorded from China, of which 12 species are known based on a single female (8) or male (4) (WSC 2024). Therefore, the identification of species and correct sex matching in *Cheiracanthium* are often challenging.

In the present paper, two new species of *Cheiracanthium* from China are recognized and described here: *Cheiracanthium bannaensis* sp. nov. and *C. bifurcatum* sp. nov. In addition, the DNA barcode gene, cytochrome c oxidase subunit I (COI) of new species is given, as DNA information is useful for the identification of species and for correctly matching sexes (Lo et al. 2021; Li and Zhang 2023).



Academic editor: Alireza Zamani

Received: 16 March 2024

Accepted: 14 April 2024

Published: 7 May 2024

ZooBank: <https://zoobank.org/906B71DC-4D81-4E50-8CB5-829A9EA11963>

Citation: Li Z, Zhang F (2024) Two new species of the genus *Cheiracanthium* C. L. Koch, 1839 (Araneae, Cheiracanthiidae) from China. ZooKeys 1200: 145–157. <https://doi.org/10.3897/zookeys.1200.123214>

Copyright: © Zhaoyi Li & Feng Zhang. This is an open access article distributed under terms of the Creative Commons Attribution License (Attribution 4.0 International – CC BY 4.0).

Material and methods

All specimens were preserved in 75% ethanol and examined and measured under a Leica M205A stereomicroscope. Photographs were taken using an Olympus BX51 microscope equipped with a Kuy Nice CCD camera and were imported into Helicon Focus v.7 for stacking. Final figures were retouched using Adobe Photoshop 2020. All measurements are given in millimeters. Leg measurements are shown as: total length (femur, patella, tibia, metatarsus, tarsus). Epigynes were removed and cleared in a pancreatin solution. All specimens studied are deposited in the Museum of Hebei University (MHBUS), Baoding, China.

Morphological terminology follows Zhang et al. (2020) and Li and Zhang (2023). The following abbreviations are used: A, atrium; AER, anterior eye row; ALE, anterior lateral eyes; AME, anterior median eyes; AME–ALE, distance between AME and ALE; AME–AME, distance between AMEs; C, conductor; CD, copulatory duct; CF, cymbial fold; CO, copulatory opening; CS, cymbial spur; DTA, dorsal tibial apophysis; E, embolus; FD, fertilisation duct; MA, median apophysis; MOA, median ocular area; PER, posterior eye row; PLE, posterior lateral eyes; PME, posterior median eyes; PME–PLE, distance between PME and PLE; PME–PME, distance between PMEs; RTA, retrolateral tibial apophysis; S, spermatheca.

A DNA barcode was also obtained for species delimitation and matching of different sexes. A partial fragment of the mitochondrial cytochrome oxidase subunit I (CO1) gene was amplified and sequenced using the primers LC01490/HCO2198 (Folmer et al. 1994). For additional information on extraction and amplification see Li and Zhang (2023). All PCR products were purified and sequenced at Sangon Biotech (Shanghai, China) Co., Ltd.

Sequence alignments were carried out using Mafft v.7.313 (Katoh and Standley 2013) with the L-INS-I strategy and checked for the presence of stop codons of COI by translating them into amino acid sequence using Geneious Prime (Kearse et al. 2012). Ambiguously aligned positions were culled using trimAl v.1.2 (Capella-Gutierrez et al. 2009) with default parameters. The pairwise genetic distances (Kimura two-parameter [K2P]) were calculated using MEGA v.11 (Tamura et al. 2021) to assess the genetic differences.

Results

DNA barcodes

All sequences were deposited in GenBank. The accession numbers of the generated DNA barcodes are provided in Table 1. The K2P genetic distance of intra-specific and interspecific nucleotide divergences of *C. bannaensis* sp. nov. and *C. bifurcatum* sp. nov. are shown in Table 2.

The intraspecific genetic distance ranged from 0 to 1.85%, and the interspecific genetic distance ranged from 13.82% to 14.78%. The maximum intraspecific distances were much lower than the minimum interspecific distances. The results of Kimura two-parameter genetic distances confirm the correct matching of male and female of two new species.

Table 1. Voucher specimen information.

Species	Voucher code	Sex	GenBank accession number	Collection localities
<i>C. bannaensis</i> sp. nov.	ZYL599	♂	PP493004	China, Yunnan
	ZYL600	♀	PP493005	China, Yunnan
	ZYL601	♀	PP493006	China, Yunnan
	ZYL602	♀	PP493007	China, Yunnan
	ZYL603	♀	PP493008	China, Yunnan
<i>C. bifurcatum</i> sp. nov.	ZYL604	♂	PP493009	China, Xinjiang
	ZYL605	♀	PP493010	China, Xinjiang

Table 2. Intraspecific and interspecific nucleotide divergences for *C. bannaensis* sp. nov. and *C. bifurcatum* sp. nov. using the Kimura two-parameter model.

Species	ZYL599	ZYL600	ZYL601	ZYL602	ZYL603	ZYL604	ZYL605
<i>C. bannaensis</i> _ZYL599							
<i>C. bannaensis</i> _ZYL600	0.0061						
<i>C. bannaensis</i> _ZYL601	0.0030	0.0061					
<i>C. bannaensis</i> _ZYL602	0.0183	0.0183	0.0185				
<i>C. bannaensis</i> _ZYL603	0.0183	0.0152	0.0153	0.0184			
<i>C. bifurcatum</i> _ZYL604	0.1440	0.1401	0.1452	0.1478	0.1382		
<i>C. bifurcatum</i> _ZYL605	0.1440	0.1401	0.1452	0.1478	0.1382	0.0000	

Taxonomy

Family Cheiracanthiidae Wagner, 1887

Genus *Cheiracanthium* C. L. Koch, 1839

Type species. *Aranea punctoria* Villers, 1789, by subsequent designation.

Cheiracanthium bannaensis sp. nov.

<https://zoobank.org/BB44B67A-A827-45C5-B55B-9BC143B9165A>

Figs 1–3

Chinese name: 版纳红螯蛛

Type material. *Holotype* ♂ (ZYL599), CHINA: Yunnan Province, Xishuangbanna Dai Autonomous Prefecture, Menghai County, Alu Xinzhai, 21.869847°N, 100.460790°E, 1581 m elev., 11.VI.2022, leg. Zhaoyi Li. *Paratype*: 4♀ (ZYL600–ZYL603), same data as holotype.

Etymology. The species name is a toponym in apposition referring to the type locality.

Diagnosis. This new species (Figs 1C–F, 2C–E) resembles *C. murinum* (Thorell, 1895) (Gravely 1931: 263, fig. 17A, B; Majumder and Tikader 1991: 72, figs 147, 148) and *C. duanbi* Yu & Li, 2020 (Zhang et al. 2020: 180, figs 3, 4A–D) in the general shape of palp and vulva, but can be distinguished from *C. murinum* by: 1) the shorter DTA; 2) copulatory ducts coiled around the spermathecae

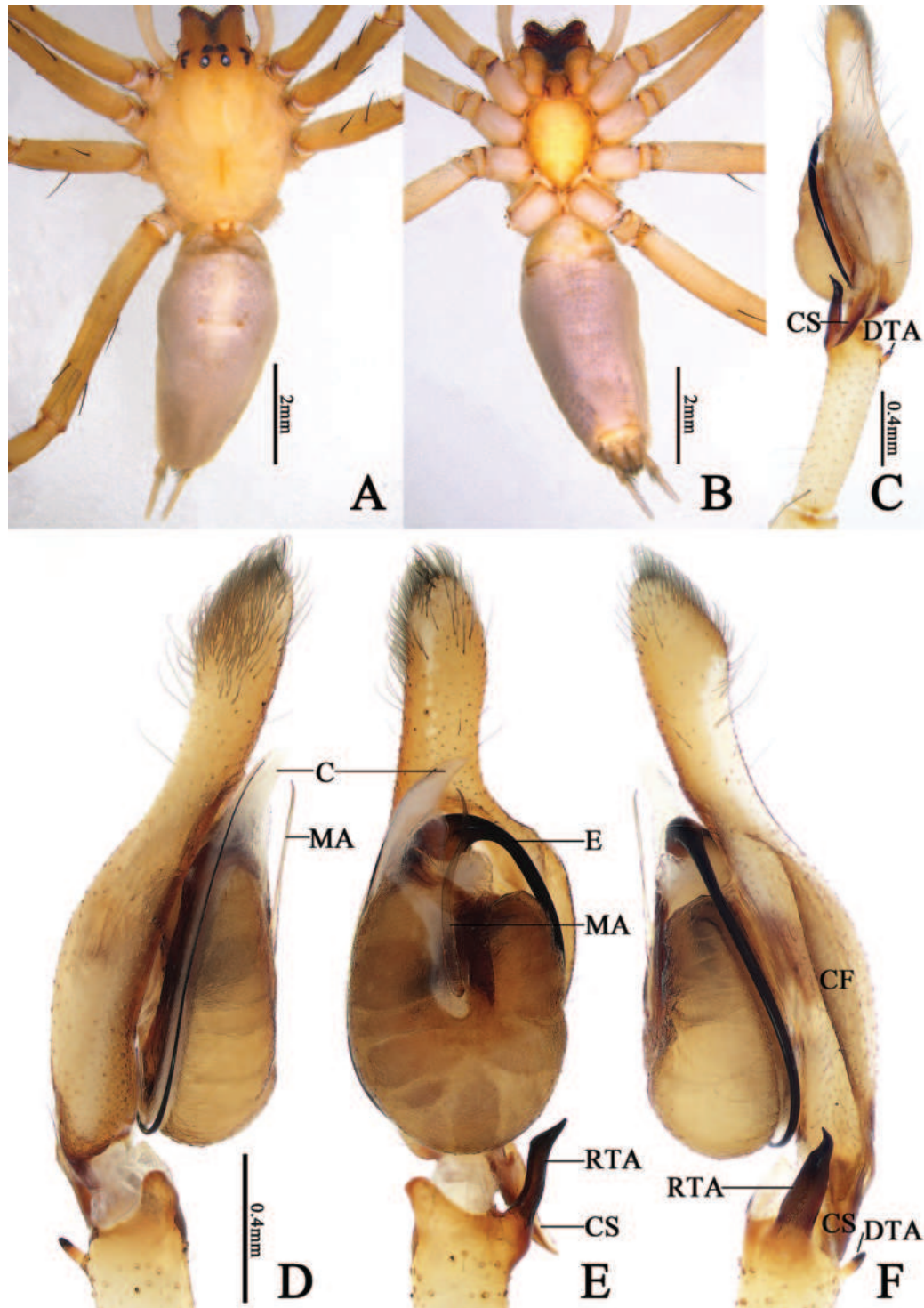


Figure 1. *Cheiracanthium bannaensis* sp. nov., male holotype (ZYL599). **A** habitus, dorsal view **B** same, ventral view **C, F** left palp, retrolateral view **D** same, prolateral view **E** same, ventral view. Abbreviations: C = conductor, CF = cymbial fold, CS = cymbial spur, DTA = dorsal tibial apophysis, E = embolus, MA = median apophysis, RTA = retrolateral tibial apophysis.

(vs. not encircling the spermathecae in *C. murinum*); and 3) lateral margin of the atrium close to the spermathecae (vs. away from the spermathecae in *C. murinum*), and from *C. duanbi* by: 1) the longer median apophysis and shorter cymbial spur; 2) DTA present (vs. absent in *C. duanbi*); 3) the wider copulatory ducts; and 4) atrial anterior margin absent (vs. arch-shaped in *C. duanbi*).

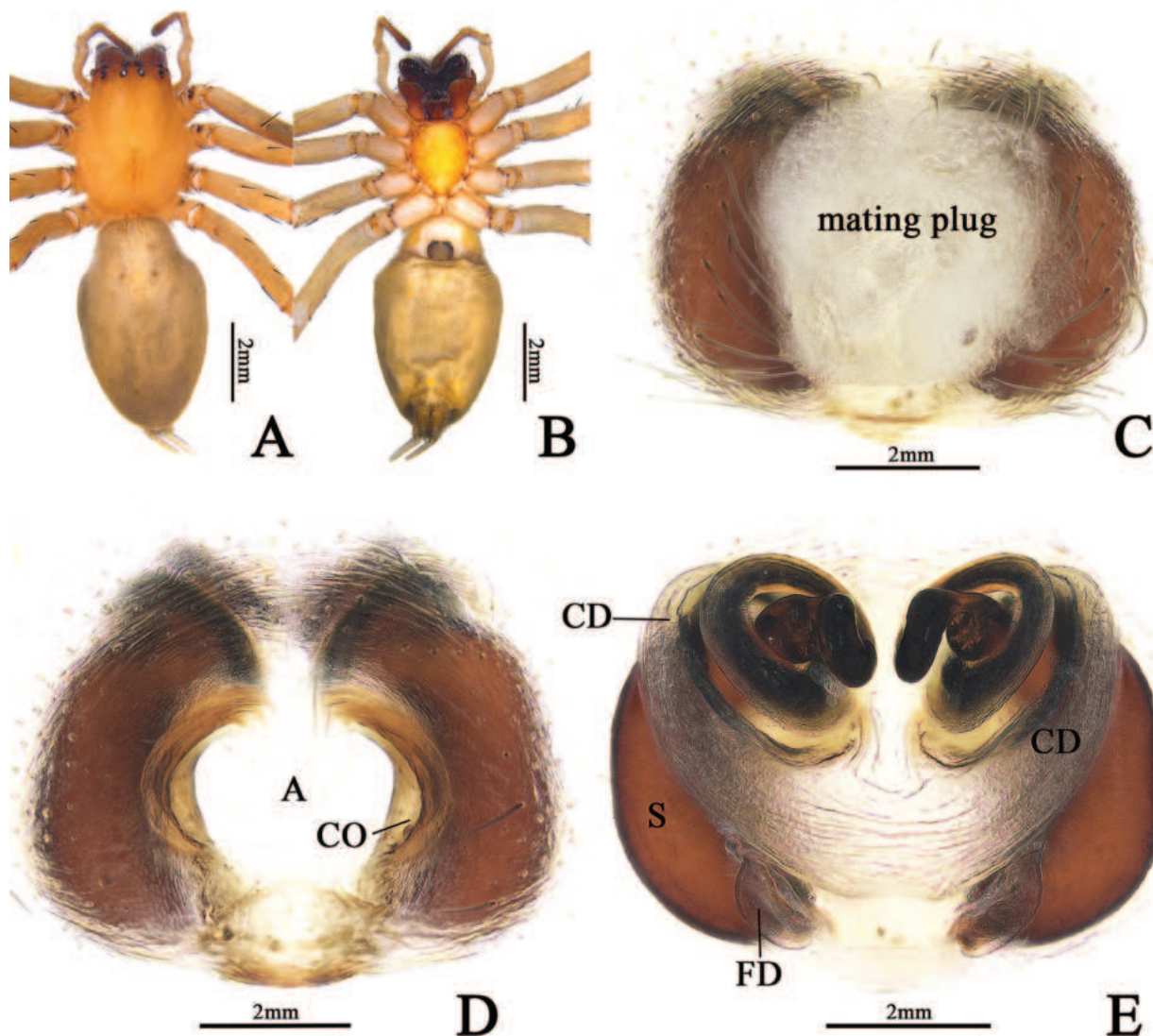


Figure 2. *Cheiracanthium bannaensis* sp. nov., female holotype (ZYL600). **A** habitus, dorsal view **B** same, ventral view **C** epigyne, intact, ventral view **D** epigyne, cleared, ventral view **E** vulva, dorsal view. Abbreviations: A = atrium, CD = copulatory duct, CO = copulatory opening, FD = fertilisation duct, S = spermatheca.

Description. Male (holotype) (Figs 1A, B, 3A): Total length 9.38. Carapace 3.98 long, 2.88 wide; abdomen 5.40 long, 2.50 wide. Carapace pale yellow, with indistinct cervical grooves and radial grooves, cephalic region inconspicuously raised. All eyes with black rings, eye area colour slightly darker than carapace. AER slightly recurved, PER slightly wider than AER, slightly procurved in dorsal view. Eye sizes and interdistances: AME 0.17, ALE 0.18, PME 0.19, PLE 0.18; AME–AME 0.17, AME–ALE 0.27, PME–PME 0.27, PME–PLE 0.34. MOA 0.51 long, front width 0.53, back width 0.63. Chelicerae reddish brown, with four pro-marginal and three retromarginal teeth, with dense scopula in both margins. Clypeus height 0.08. Sternum orange, 1.84 long, 1.49 wide. Labium coloured as chelicerae, anterior edge clearly scopula, longer than wide. Endites yellowish brown. Legs yellowish, without distinct colour markings. Leg measurements: I 24.36 (4.80, 1.79, 8.08, 6.81, 2.88), II 14.95 (4.13, 1.13, 5.54, 2.97, 1.18), III 12.16 (3.63, 0.95, 3.47, 2.86, 1.25), IV 20.99 (5.72, 1.45, 5.15, 6.70, 1.97). Abdomen elongate-oval, dorsum with two pairs of muscular impressions and numerous

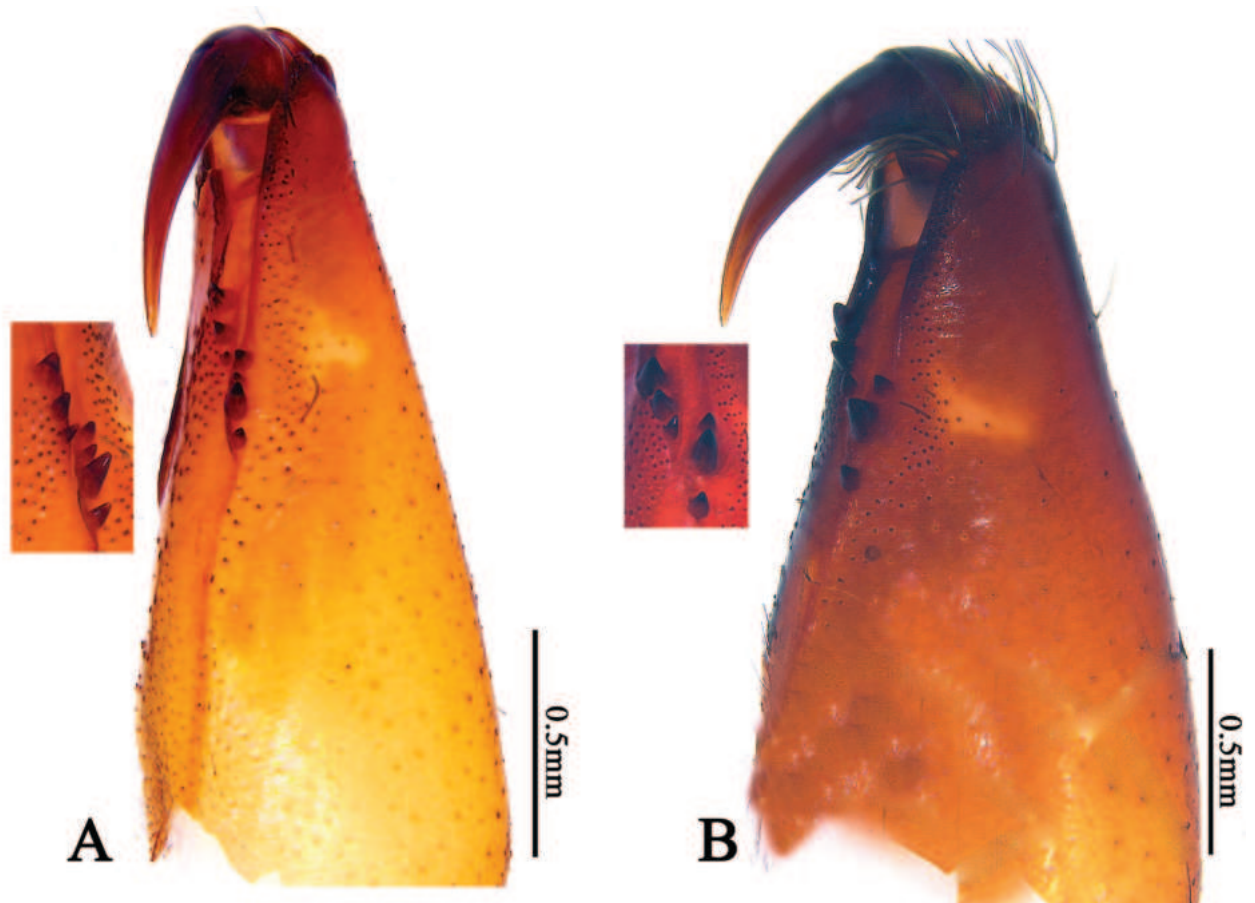


Figure 3. Right chelicerae of *Cheiracanthium bannaensis* sp. nov. **A** male, retrolateral view **B** female, retrolateral view.

grey patches, a pale narrow longitudinal band in middle, enclosed by grey freckles; venter with numerous dark grey spots. Spinnerets coniform, ALS larger and closer to each other; PMS smallest; PLS longest, with two segments, length of basal segment shorter than distal segment.

Palp (Fig. 1C–F). Tibia long, c. $\frac{3}{4}$ of cymbium length. RTA short and sclerotized, shorter than $\frac{1}{2}$ tibia length, with wide base and narrow apex, twisted around the axis from ventral view; DTA short and thin, stalk-shaped. Tip of cymbium long, c. $\frac{3}{4}$ of cymbium length. Cymbial fold well-developed and clearly visible in retrolateral view, c. $\frac{1}{2}$ of cymbium length; cymbial spur beak-like, about same length as RTA. Tegulum oval, c. two times longer than wide, surface wrinkled. Median apophysis long, more than $\frac{1}{2}$ of tegulum's length, twisted around the axis. Embolus located on distal side of tegulum, at about 12 o'clock position, extending clockwise along tegular margin, curving to distal conductor. Conductor large, membranous, gradually tapering toward apex.

Female (paratype) (Figs 2A, B, 3B): Total length 9.68. Carapace 4.04 long, 2.96 wide; abdomen 5.64 long, 3.35 wide. Carapace reddish brown, with indistinct cervical grooves. Eye area colour slightly darker than carapace, both anterior and posterior eye rows recurved, PER slightly wider than AER. Eye sizes and interdistances: AME 0.17, ALE 0.16, PME 0.18, PLE 0.18; AME–AME 0.18, AME–ALE 0.38, PME–PME 0.34, PME–PLE 0.43. MOA 0.43 long, front width 0.55, back width 0.66. Chelicerae dark reddish brown, both margins with

three teeth. Clypeus height 0.11. Sternum orange, 1.96 long, 1.57 wide. Labium coloured as chelicerae, almost equal in length and width. Leg measurements: I 19.29 (5.02, 1.45, 5.74, 4.76, 2.32), II 13.77 (3.91, 1.43, 3.79, 3.36, 1.28), III 10.56 (2.71, 1.31, 2.20, 3.08, 1.26), IV 14.41 (3.64, 1.44, 3.79, 4.04, 1.50). Abdomen oval, dorsum yellowish brown, with indistinct muscular impressions and narrow longitudinal band.

Epigyne (Fig. 2C–E). Atrium large, located at middle portion of epigynal plate, filled with mating plug; arched atrial lateral margins are easily visible after removing the plug. Copulatory openings located at lateral margins of atrium. Copulatory duct visible through tegument of epigynal plate in ventral view. Spermathecae large, banana-shaped, c. two times longer than wide. Copulatory ducts coiled, forming about three ascending turns and then descending into the spermathecae. Fertilization ducts lamellar, broad, originate from posterior parts of spermathecae.

Distribution. China (Yunnan).

***Cheiracanthium bifurcatum* sp. nov.**

<https://zoobank.org/49DECA8D-DCB1-4E8B-8E3F-2EAC6BE63B30>

Figs 4–6

Chinese name: 双叉红螯蛛

Type material. **Holotype** ♂ (ZYL604), CHINA: Xinjiang Uygur Autonomous Region, Aksu City, Wushi County, Yamansu Kirgiz Town, 41.070672°N, 78.840871°E, 1657 m elev., 26.V.2023, leg. Bo Liu. **Paratype:** 1♀ (ZYL605), same data as holotype.

Etymology. The specific epithet is an adjective from the Latin ‘bifurcate’, referring to the distally bifurcated retrolateral tibial apophysis in ventral view.

Diagnosis. The male of this new species (Fig. 6C–E) is most similar to *C. japonicum* Bösenberg & Strand, 1906 (Vertyanin and Zaitsev 2022: 95, figs 9, 10), *C. brevispinum* Song, Feng & Shang, 1982 (Zhang et al. 2022: 180, fig. 132E–G) and *C. xinjiangense* Li & Zhang, 2023 (Li and Zhang 2023: 99, fig. 10C–E) by having bifurcated RTA, hook-shaped median apophysis and a triangular tip of cymbium, but can be distinguished from *C. brevispinum* by the longer cymbial spur (c. 0.8 times the length of tibia vs. 0.5 times in *C. brevispinum*), and from *C. japonicum* and *C. xinjiangense* by the nearly equal length of RTA's two-pointed apex (vs. the prolateral apex longer than the retrolateral one in *C. japonicum* and shorter than the retrolateral one in *C. xinjiangense*). The female (Fig. 6A, B) is similar to *C. japonicum* Bösenberg & Strand, 1906 (Paik 1990: 5, figs 6–9), *C. exquestitum* Zhang & Zhu, 1993 (Li and Zhang 2024: 176, figs 4a, b, 5c, d) and *C. falcatum* Chen, Huang, Chen & Wang, 2006 (Chen et al. 2006: 12, fig. 2A, B) in having spiraling copulatory ducts and similarly shaped spermathecae, but can be distinguished by the 1:1 ratio of length to width of atrium (vs. 1:2 in other three species). Furthermore, it can be distinguished from *C. falcatum* by having four loops of copulatory ducts (vs. three loops in *C. falcatum*), from *C. exquestitum* by the fertilization ducts originating from the posterior parts of spermathecae (vs. median in *C. exquestitum*), and from *C. japonicum* by thinner transparent parts of copulatory ducts.

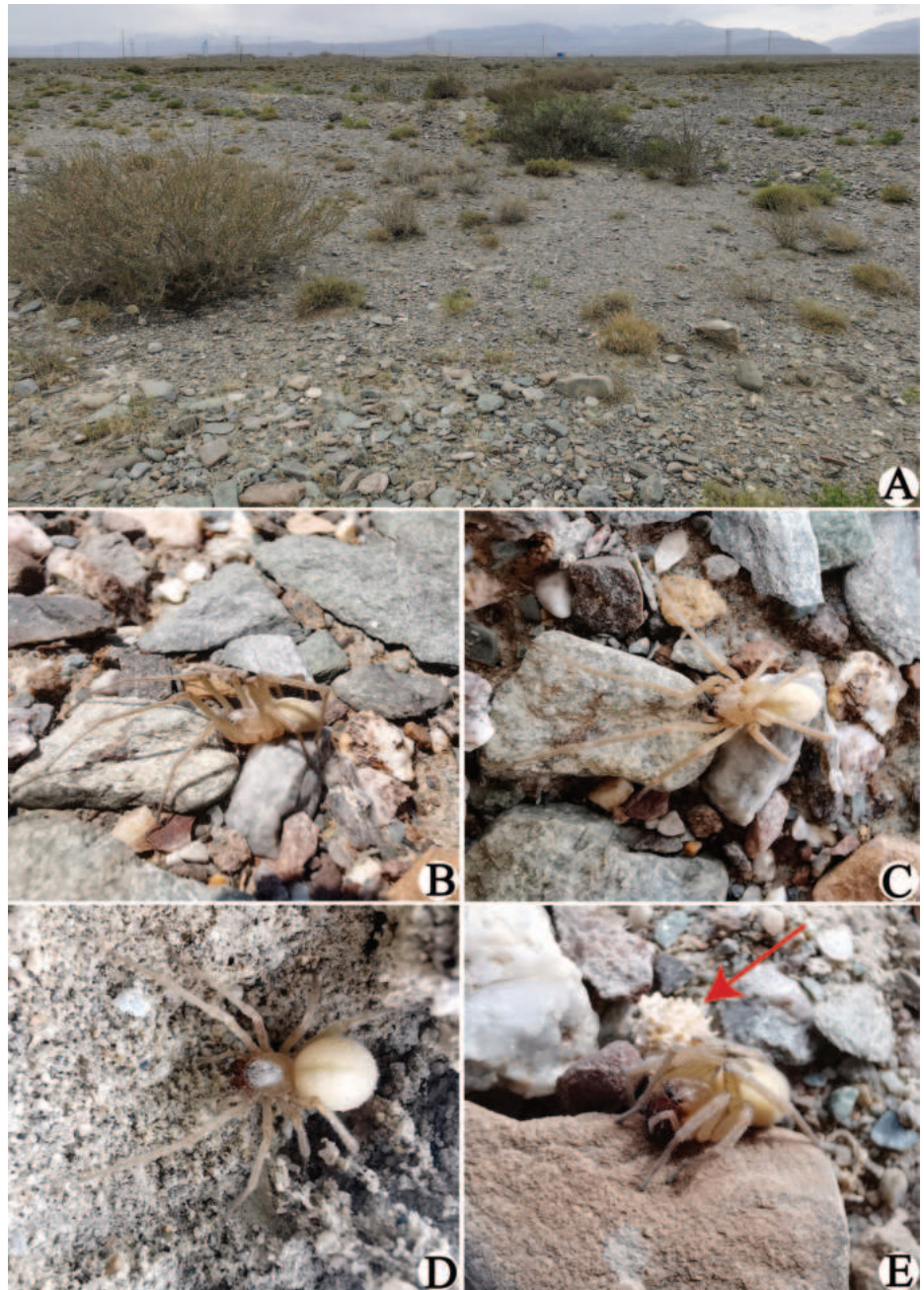


Figure 4. Habitat (A) and living specimens (B–E) of *Cheiracanthium bifurcatum* sp. nov. A camelthorn steppe in Aksu B, C male holotype D, E female paratype, with arrow pointing to egg sac.

Description. Male (holotype) (Figs 4B, C, 5A, B): Total length 7.58. Carapace 3.49 long, 2.82 wide; abdomen 4.09 long, 2.92 wide. Carapace pale yellow, with indistinct cervical grooves and radial grooves. All eyes with black rings, eye area colour slightly darker than carapace. AER slightly recurved, PER wider than AER, slightly procurved in dorsal view. Eye sizes and interdistances: AME 0.19, ALE 0.16, PME 0.15, PLE 0.17; AME–AME 0.15, AME–ALE 0.17, PME–PME 0.30, PME–PLE 0.32. MOA 0.56 long, front width 0.54, back width 0.59. Chelicerae reddish brown, with three promarginal and two retro-marginal teeth, with dense scopula in both margins. Clypeus height 0.09.

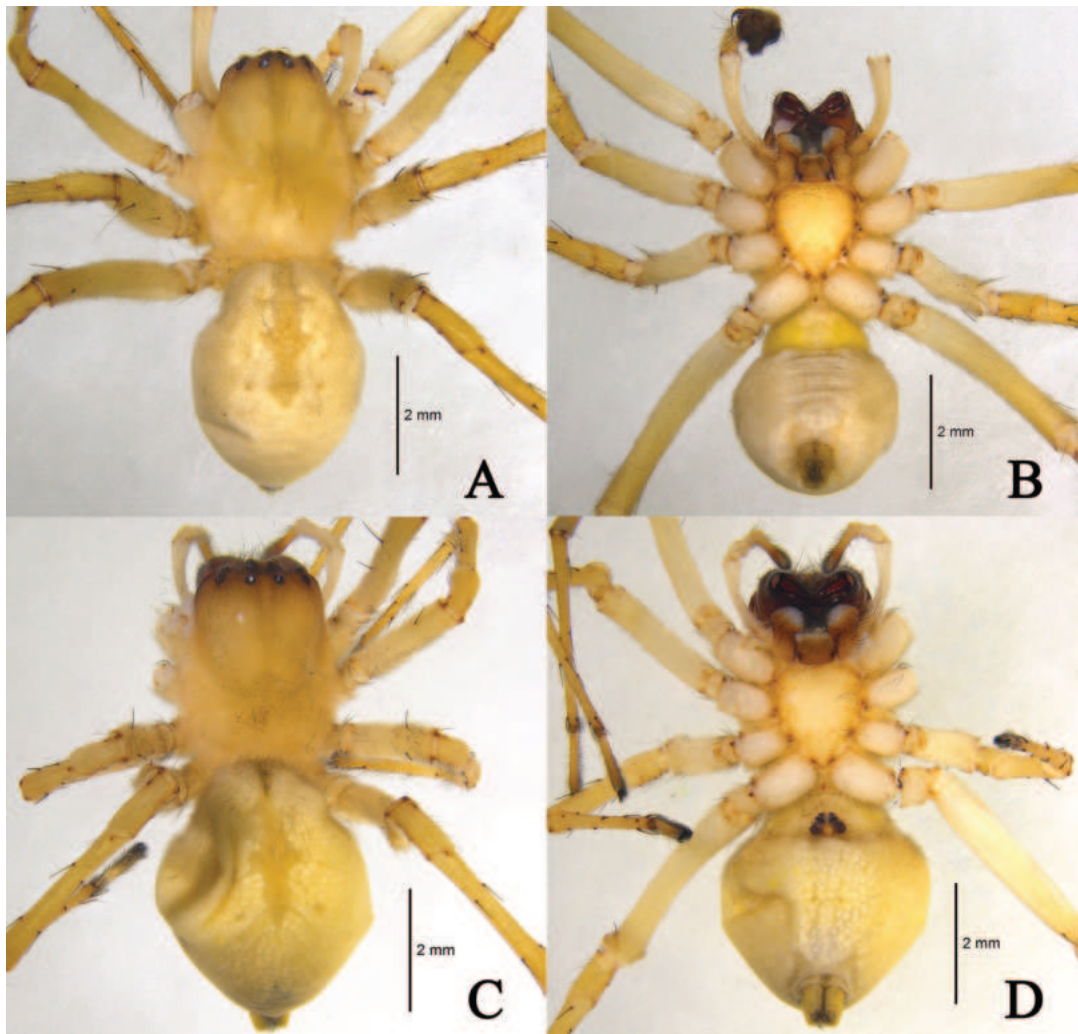


Figure 5. *Cheiracanthium bifurcatum* sp. nov. **A** male holotype (ZYL604), dorsal view **B** same, ventral view **C** female paratype (ZYL605), dorsal view **D** same, ventral view.

Sternum orange, 1.70 long, 1.55 wide. Labium and endites coloured as chelicerae, anterior edge clearly scopula. Legs yellowish. Leg measurements: I 19.91 (5.41, 1.49, 5.12, 5.74, 2.15), II 13.08 (3.10, 1.34, 3.25, 3.97, 1.42), III 10.36 (2.62, 1.21, 2.46, 3.00, 1.07), IV 16.02 (3.86, 1.45, 4.28, 4.77, 1.66). Abdomen oval, yellowish white, dorsum with indistinct muscular impressions and a dark longitudinal band; venter pale grey.

Palp (Fig. 6C–E). Tibia long, c. $\frac{2}{3}$ of cymbium length. RTA long, c. $\frac{1}{2}$ of tibia's length, finger-shaped, distally bifurcated. Cymbial furrow strongly developed and conspicuous, c. $\frac{2}{3}$ of cymbium length; cymbial spur shorter than tibia length, tapering off into a filiform. Tegulum oval, c. 1.2× as long as wide. Median apophysis long, more than $\frac{1}{2}$ of tegulum's length, with a curved tip resembling a sickle in ventral view. Embolus located on distal side of tegulum, at about 11–12 o'clock position, extending clockwise along tegular margin, curving to distal conductor. Conductor large, membranous, gradually tapering toward apex.

Female (paratype) (Figs 4D, E, 5C, D): Total length 8.04. Carapace 3.66 long, 2.67 wide; abdomen 4.38 long, 3.39 wide. Carapace yellowish brown, with indistinct cervical grooves and radial grooves, cephalic region inconspicuously raised. Eye area colour slightly darker than carapace. AER slightly recurved, PER

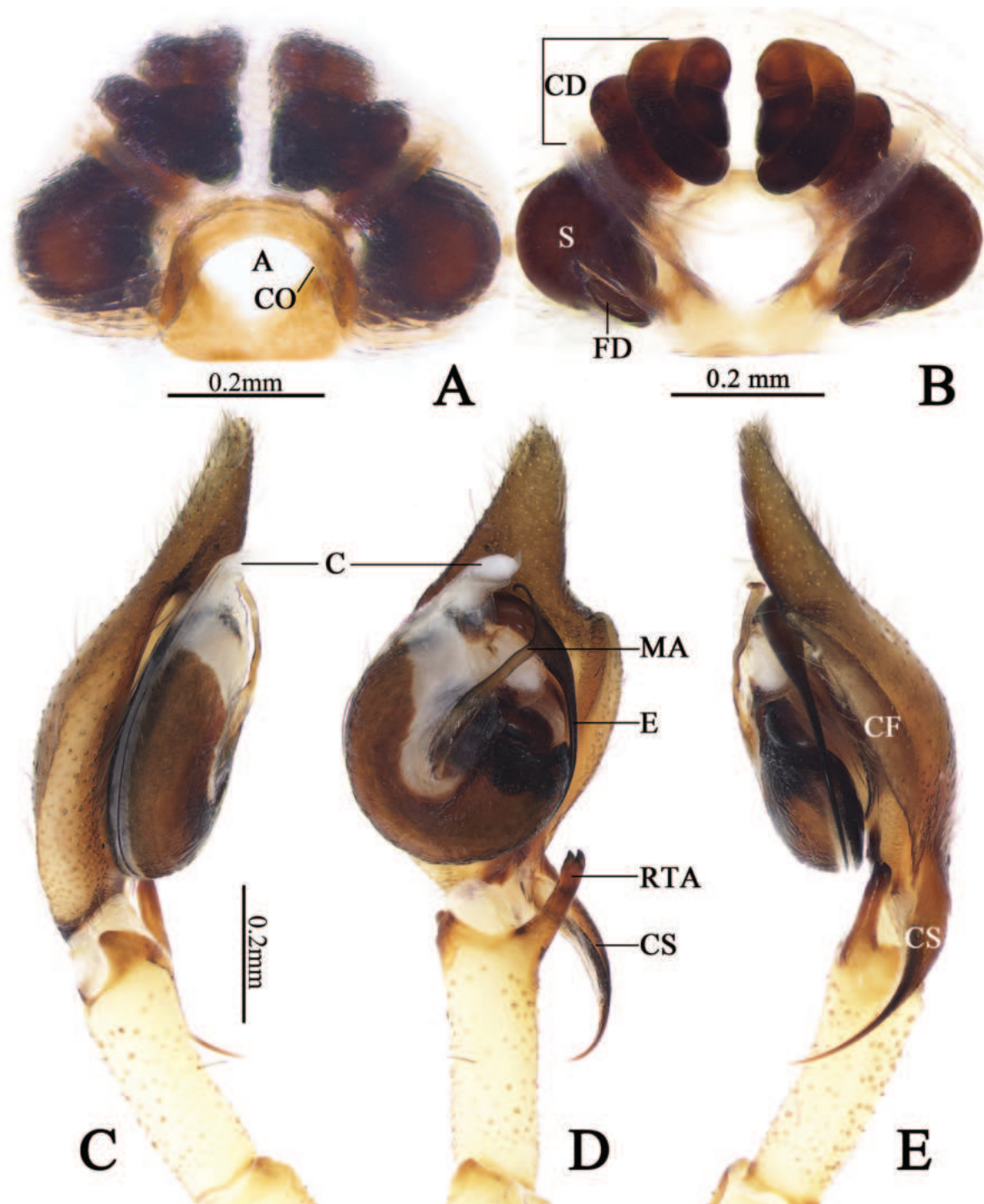


Figure 6. Copulatory organs of *Cheiracanthium bifurcatum* sp. nov. **A** epigyne, ventral view **B** same, dorsal view **C** male left palp, prolateral view **D** same, ventral view **E** same, retrolateral view. Abbreviations: A = atrium, C = conductor, CD = copulatory duct, CF = cymbial fold, CO = copulatory opening, CS = cymbial spur, DTA = dorsal tibial apophysis, E = embolus, FD = fertilisation duct, MA = median apophysis, RTA = retrolateral tibial apophysis, S = spermatheca.

wider than AER, slightly procurved in dorsal view. Eye sizes and interdistances: AME 0.19, ALE 0.16, PME 0.13, PLE 0.15; AME–AME 0.24, AME–ALE 0.24, PME–PME 0.40, PME–PLE 0.42. MOA 0.51 long, front width 0.64, back width 0.65. Chelicerae dark reddish brown, with three promarginal and two retromarginal teeth. Clypeus height 0.09. Sternum orange, 1.74 long, 1.49 wide. Labium and endites

reddish brown. Leg measurements: I 14.52 (3.81, 1.39, 3.43, 4.13, 1.76), II 9.88 (2.50, 1.16, 2.23, 3.00, 0.99), III 8.03 (1.99, 0.96, 1.81, 2.39, 0.88), IV 13.14 (3.29, 1.34, 3.28, 4.11, 1.12). Abdomen oval, dorsum with numerous yellow freckles and a dark longitudinal band; venter yellow, with numerous light spots in middle.

Epigyne (Fig. 6A, B): Atrium sclerotized, located at posterior portion of epigynal plate, with arch-shaped anterior margin. Copulatory openings located at lateral margins of atrium. Copulatory duct and spermathecae visible through tegument of epigynal plate in ventral view. Spermathecae nearly pyriform, spaced by about 1.5 diameters, connected with spiral-coiled copulatory duct (each ascending portion of copulatory duct coils forming three entwined loops and then form one descending coil and downward leading to spermatheca). Fertilization ducts lamellar, originate from posterior parts of spermathecae, extending anterolaterally.

Distribution. China (Xinjiang).

Habitat. All specimens were found under stones in a very flat area with numerous crushed stones and covered with prickly bushes, such as camelthorn and tamarisks, reaching about 30–50 cm in height (Fig. 4).

Acknowledgements

Thanks to Bo Liu (Hebei University) for collecting the specimens and providing photos of habitats and living spiders of *Cheiracanthium bifurcatum* sp. nov. We thank Zhiyong Yang (Hebei University) for assistance in photographing of copulatory organs of the new species. We also thank Dr Sergei L. Esyunin and Dr Alireza Zamani (Subject editor) for their comments and suggestions that improved our manuscript.

Additional information

Conflict of interest

The authors have declared that no competing interests exist.

Ethical statement

No ethical statement was reported.

Funding

This work was supported by the National Natural Science Foundation of China (No. 32170468), and by the Science and Technology Fundamental Resources Investigation Program (Grant No. 2022FY202100).

Author contributions

Investigation: ZL. Writing – original draft: ZL. Writing – review and editing: FZ.

Author ORCIDs

Zhaoyi Li  <https://orcid.org/0000-0001-6303-6041>

Feng Zhang  <https://orcid.org/0000-0002-3347-1031>

Data availability

All sequences were deposited in GenBank, and other data that support the findings of this study are available in the main text.

References

- Bayer S (2014) Miscellaneous notes on European and African *Cheiracanthium* species (Araneae: Miturgidae). *Arachnologische Mitteilungen* 47: 19–34. <https://doi.org/10.5431/aramit4704>
- Capella-Gutierrez S, Silla-Martinez JM, Gabaldon T (2009) TrimAl: A tool for automated alignment trimming in large-scale phylogenetic analyses. *Bioinformatics (Oxford, England)* 25(15): 1972–1973. <https://doi.org/10.1093/bioinformatics/btp348>
- Chen SH, Huang WJ (2012) Miturgidae (Arachnida: Araneae). In: Chen SH, Huang WJ (Eds) *The spider fauna of Taiwan. Araneae. Miturgidae, Anyphaenidae, Clubionidae*. National Taiwan Normal University, Taipei, 5–30, 101–102, 114–125.
- Chen SH, Huang WJ, Chen SC, Wang Y (2006) Two new species and one newly recorded species of the genus *Cheiracanthium* (Araneae: Miturgidae) from Taiwan. *Bioformosa* 41: 9–18.
- Deeleman-Reinhold CL (2001) *Forest spiders of South East Asia: with a revision of the sac and ground spiders (Araneae: Clubionidae, Corinnidae, Liocranidae, Gnaphosidae, Prodidomidae and Trochanterriidae)*. Brill, Leiden, 591 pp. <https://doi.org/10.1163/9789004475588>
- Dippenaar-Schoeman AS, Haddad CR, Foord SH, Lotz LN (2021) *The Cheiracanthiidae of South Africa. Version 1. South African national survey of Arachnida photo identification guide*. University of Venda, Thohoyandou, 62 pp.
- Esyunin SL, Zamani A (2020) ‘Conundrum of esoterica’: on the long-forgotten genus *Eutittha* Thorell, 1878, with new taxonomic considerations in *Cheiracanthium* C. L. Koch, 1839 (Araneae: Cheiracanthiidae). *Journal of Natural History* 54(19–20): 1293–1323. <https://doi.org/10.1080/00222933.2020.1781950>
- Folmer O, Black M, Hoeh W, Lutz R, Vrijenhoek R (1994) DNA primers for amplification of mitochondrial cytochrome c oxidase subunit I from diverse metazoan invertebrates. *Molecular Marine Biology and Biotechnology* 3(5): 294–299.
- Gravely FH (1931) Some Indian spiders of the families Ctenidae, Sparassidae, Selenopidae and Clubionidae. *Records of the Indian Museum* 33(3): 211–282. <https://doi.org/10.26515/rzsi/v33/i3/1931/162502>
- Katoh K, Standley DM (2013) MAFFT multiple sequence alignment software version 7: Improvements in performance and usability. *Molecular Biology and Evolution* 30(4): 772–780. <https://doi.org/10.1093/molbev/mst010>
- Kearse M, Moir R, Wilson A, Stones-Hava S, Cheung M, Sturrock S, Buxton S, Cooper A, Markowitz S, Duran C, Thiere T, Ashton B, Meintjes P, Drummond A (2012) Geneious Basic: An integrated and extendable desktop software platform for the organization and analysis of sequence data. *Bioinformatics (Oxford, England)* 28(12): 1647–1649. <https://doi.org/10.1093/bioinformatics/bts199>
- Li ZY, Zhang F (2019) Two new species of *Cheiracanthium* C. L. Koch, 1839 (Araneae, Cheiracanthiidae) from Xizang, China. *Acta Arachnologica Sinica* 28(2): 87–95. <https://doi.org/10.1007/s13131-019-1477-x>
- Li ZY, Zhang F (2020) First description of the female of *Cheiracanthium chayuense* (Araneae: Cheiracanthiidae). *Acta Arachnologica Sinica* 29(2): 107–110. <https://doi.org/10.3969/j.issn.1005-9628.2020.02.006>
- Li ZY, Zhang F (2023) Five new species of the long-legged sac spider genus *Cheiracanthium* C. L. Koch, 1839 (Araneae: Cheiracanthiidae) from China. *European Journal of Taxonomy* 900: 81–105. <https://doi.org/10.5852/ejt.2023.900.2303>

- Li ZY, Zhang F (2024) A survey of cheiracanthiid spiders (Araneae: Cheiracanthiidae) from Hainan Island, China. *Journal of Natural History* 58(1–4): 167–188. <https://doi.org/10.1080/00222933.2023.2287267>
- Lo YY, Wei C, Huang WC (2021) A newly recorded species of *Cheiracanthium* C. L. Koch, 1839 (Araneae, Cheiracanthiidae) from Taiwan. *Taiwan Journal of Biodiversity* 23(2): 136–152.
- Lotz LN (2007a) The genus *Cheiracanthium* (Araneae: Miturgidae) in the Afrotropical region. 1. Revision of known species. *Navorsing van die Nasionale Museum Bloemfontein* 23: 1–76.
- Lotz LN (2007b) The genus *Cheiracanthium* (Araneae: Miturgidae) in the Afrotropical region. 2. Description of new species. *Navorsing van die Nasionale Museum Bloemfontein* 23: 145–184.
- Lotz LN (2011) The genus *Cheiracanthium* (Araneae: Miturgidae) in the Afrotropical region. 3. Description of four new species. *Navorsing van die Nasionale Museum Bloemfontein* 27: 21–36.
- Lotz LN (2014) New species of *Cheiracanthium* (Araneae: Eutichuridae) from Madagascar and the Comoros Islands. *Zootaxa* 3857(3): 301–332. <https://doi.org/10.11646/zootaxa.3857.3.1>
- Lotz LN (2015) New species of the spider genus *Cheiracanthium* from continental Africa (Araneae: Eutichuridae). *Zootaxa* 3973(2): 321–336. <https://doi.org/10.11646/zootaxa.3973.2.7>
- Majumder SC, Tikader BK (1991) Studies on some spiders of the family Clubionidae from India. *Records of the Zoological Survey of India* 102: 1–175.
- Paik KY (1990) Korean spiders of the genus *Cheiracanthium* (Araneae: Clubionidae). *Korean Arachnology* 6: 1–30.
- Tamura K, Stecher G, Kumar S (2021) MEGA 11: Molecular evolutionary genetics analysis version 11. *Molecular Biology and Evolution* 38(7): 3022–3027. <https://doi.org/10.1093/molbev/msab120>
- Vertyankin AV, Zaitsev AV (2022) About findings on Sakhalin of previously unknown spider species (Araneae: Pisauridae, Clubionidae, Cheiracanthiidae, Gnaphosidae). *Journal of Sakhalin Museum* 41(4): 88–100.
- WSC (2024) World Spider Catalog. Version 25.0. Natural History Museum Bern. <https://doi.org/10.24436/2> [Accessed on 12 March 2024]
- Zhang JS, Zhang GR, Yu H (2018) Four species of spider genus *Cheiracanthium* C. L. Koch, 1839 (Araneae, Eutichuridae) from Jinggang Mountains, Jiangxi Province, China. *ZooKeys* 762: 33–45. <https://doi.org/10.3897/zookeys.762.23786>
- Zhang JS, Yu H, Li SQ (2020) New cheiracanthiid spiders from Xishuangbanna rainforest, southwestern China (Araneae, Cheiracanthiidae). *ZooKeys* 940: 51–77. <https://doi.org/10.3897/zookeys.940.51802>
- Zhang F, Peng JY, Zhang BS (2022) *Spiders of Mt. Xiaowutai*. Science Press, Beijing, 387 pp.

Large carrion and burying beetles evolved from Staphylinidae (Coleoptera, Staphylinidae, Silphinae): a review of the evidence

Derek S. Sikes¹, Margaret K. Thayer², Alfred F. Newton²

¹ University of Alaska Museum / Department of Biology and Wildlife, University of Alaska Fairbanks, 1962 Yukon Dr., Fairbanks, Alaska, USA

² Negaunee Integrative Research Center, Field Museum of Natural History, 1400 South DuSable Lake Shore Drive, Chicago, Illinois, USA

Corresponding author: Derek S. Sikes (dssikes@alaska.edu)

Abstract

Large carrion beetles (Silphidae) are the focus of ongoing behavioral ecology, forensic, ecological, conservation, evolutionary, systematic, and other research, and were recently reclassified as a subfamily of Staphylinidae. Twenty-three analyses in 21 publications spanning the years 1927–2023 that are relevant to the question of the evolutionary origin and taxonomic classification of Silphidae are reviewed. Most of these analyses (20) found Silphidae nested inside Staphylinidae (an average of 4.38 branches deep), two found Silphidae in an ambiguous position, and one found Silphidae outside Staphylinidae, as sister to Hydrophilidae. There is strong evidence supporting the hypothesis that large carrion beetles evolved from within Staphylinidae and good justification for their classification as the subfamily Silphinae of the megadiverse, and apparently now monophyletic, Staphylinidae. Considerable uncertainty remains regarding the interrelationships and monophyly of many staphylinid subfamilies. Nonetheless, the subfamily Tachyporinae was found to be the sister of Silphinae in more analyses (7) than any other subfamily.

Key words: Monophyly, Nicrophorini, Nicrophorus, paraphyly, rove beetles, Silphidae, Silphini



Academic editor: Jan Klimaszewski

Received: 12 March 2024

Accepted: 29 March 2024

Published: 8 May 2024

ZooBank: <https://zoobank.org/168748D9-A45C-4CE5-AE35-F87F5A7E27AE>

Citation: Sikes DS, Thayer MK, Newton AF (2024) Large carrion and burying beetles evolved from Staphylinidae (Coleoptera, Staphylinidae, Silphinae): a review of the evidence. ZooKeys 1200: 159–182. <https://doi.org/10.3897/zookeys.1200.122835>

Copyright: © Derek S. Sikes et al.
This is an open access article distributed under terms of the Creative Commons Attribution License (Attribution 4.0 International – CC BY 4.0).

“Silphidae may instead be a sister group to Staphylinidae, or an isolated basal lineage within it, and its exact relationship to Staphylinidae sensu latissimo is in our opinion the most difficult remaining issue concerning the monophyly of Staphylinidae.” – Grebennikov and Newton 2009

Introduction

Paraphyly is a common classification error often resulting from a lineage evolving into a new ecological space that differs significantly from its closest relatives. Classic examples include tetrapods from fish (Irisarri and Meyer 2016), birds from dinosaurs (Feduccia 2002), hexapods from Crustacea (von Reumont et al. 2012), termites from Blattodea (Inward et al. 2007), and parasitic lice from Psocodea (Johnson et al. 2018). At the family level, and within beetles, a well-

known and relevant example of paraphyly is that of the economically important bark beetles, formerly the family Scolytidae, now a subfamily within Curculionidae (Crowson 1955; Jordal et al. 2014). Often, the morphology of the group evolving into the new ecological space is so modified from its ancestral condition that the value of morphology for understanding the phylogenetic placement of the taxon is diminished. This led many early taxonomists to separate these groups into their own higher taxa with their sister lineages often enigmatically unknown. With advances in dataset types (e.g., larval morphology, molecules) and dataset sizes (e.g., phylogenomics), and phylogenetic methods, for the examples listed above and many more, researchers found taxonomic solutions to restore monophyly of the “parent” taxa by sinking the aberrant lineages into their parents. This yields a more phylogenetically accurate classification corresponding to the tree of life and employs best taxonomic practices (Vences et al. 2013) but can confuse people who have trouble envisioning these often-radical evolutionary transformations. To this list we propose to add the large carrion beetles having evolved from within Staphylinidae.

Large carrion beetles are a relatively well-known small monophyletic group of approximately 189 extant species worldwide. They have traditionally been treated as a family (Silphidae) with two subfamilies: *Nicrophorinae* and *Silphinae* (Sikes 2016). Their large body size (7–45 mm, usually 12–20 mm), low species richness, parental care (in the genus *Nicrophorus*), diverse ecology (primarily necrophagy), and ease of capture, identification, and culturing have made them a popular group for study in many fields of biology, e.g., behavior (Trumbo et al. 2016), ecology (Anderson 1982), conservation biology (Holloway and Schnell 1997), forensic entomology (Jakubec et al. 2019), and evolution (Ikeda et al. 2012). The group is well-known among the public and is one of the families most students who have taken a general entomology class have learned. The group is also taxonomically well-known (Anderson and Peck 1985; Peck and Anderson 1985; Sikes et al. 2002) with few new species expected, and each subfamily has received phylogenetic investigation (Dobler and Müller 2000; Ikeda et al. 2012; Sikes and Venables 2013). The family Staphylinidae, commonly known as rove beetles, is the largest family of life on earth, with 66,928 species grouped into one extinct and 34 extant (including *Silphinae*) subfamilies (Newton 2022). Most rove beetles are much smaller-bodied (< 1–35 mm, usually 2–8 mm) than large carrion beetles and primarily predatory, but also mycophagous and detritivorous with various minor exceptions (e.g., species of the genus *Aleochara* are parasitoids and *Eusphalerum* species, *inter alia*, feed on pollen).

Although there has long been consensus that Silphidae are monophyletic (Sikes 2016) and belong to the superfamily Staphylinoidea (e.g., Peck 2000), consensus was lacking regarding the relationship of Silphidae to Staphylinidae. An increasing number of phylogenetic analyses, using both morphological and molecular data, have found the lineage rooting inside Staphylinidae. Hatch (1927) was the first to formally classify the large carrion beetles as a subfamily of the Staphylinidae, but his proposed reclassification was not accepted by the scientific community. Almost a century later, Cai et al. (2022), based on their reanalysis of data from Zhang et al. (2018) and other studies that had found similar results, again formally classified the large carrion beetles as a subfamily of Staphylinidae. During the 95 years between these works, many phyloge-

netic studies on beetles have been published, some of which are relevant to the relationship of Silphidae to Staphylinidae. Herein we review chronologically, based on year of publication, works from 1927–2023 that are relevant to the question of how Silphidae are related to Staphylinidae. We aim to provide a concise summary of the evidence supporting the classification of large carrion beetles as a subfamily of Staphylinidae.

Methods

We limit our review to works that were conducted in such a way that Silphidae could root inside or outside the Staphylinidae. Thus, we excluded works that used Silphidae as an outgroup of Staphylinidae (Zhang and Zhou 2013; Liu et al. 2021), used family-only terminals (Beutel and Leschen 2005), or included no non-staphylinids (Yamamoto 2021). We also excluded works that did not bring new data to bear on the question. Thus, we excluded works that were entirely re-analyses of datasets from prior works we review (Toussaint et al. 2016; Gussarov 2018; Cai et al. 2022) and all publications that simply treated Silphidae as a family without evolutionary analysis or other justification, following the consensus classification of the time. We also excluded works investigating Coleoptera or Staphyliniform evolution prior to the 1990s, such as Jeannel and Jarige (1949), Coiffait (1972), Crowson (1981), and Naomi (1985), except for two that had novel findings regarding Silphidae (Hatch 1927; Lawrence and Newton 1982). Our goal was to focus on works that represent independent tests, using modern phylogenetic methods, of the hypothesis that Silphidae evolved from within Staphylinidae. None of these works were focused only on this question, however. Herein, we use the staphylinid subfamily name Silphinae in the new sense of Cai et al. (2022), which corresponds to the former family Silphidae (~ 189 species), not the former subfamily Silphinae (~ 119 species). We use Silphidae or Silphinae depending on context, but in all cases are referring to the same ~ 189 species. We use the current classification of Staphylinidae in our reference to the separate subfamilies Tachyporinae and Mycetoporinae (Yamamoto 2021).

For each study we provide information to help judge the robustness of the analysis and its findings relevant to the placement of Silphinae. We include the number and type of datasets used. Number of datasets was approximately equivalent to number of genes analyzed (we counted mitogenome analysis as 16 datasets because there are 15 non-tRNA genes in beetle mitochondrial genomes and we count all the tRNAs as a single gene because of their small size). Generally, phylogenetic accuracy increases with the number of genes and number of taxa used in an analysis. We indicate what type of analysis was performed (viz. non-algorithmic, parsimony, Maximum Likelihood, Bayesian). Using subfamilies as terminals, we provide a simplified figure, built using MES-QUITE v. 3.6 (Maddison and Maddison 2018), depicting each work's preferred phylogeny, limited to only Staphylinidae, for all but Korte et al. (2004). Korte et al. (2004) was the only study to find Silphinae external to Staphylinidae, so to depict their phylogeny we had to include non-staphylinid terminals. We provide a count of how many branches deep Silphinae join within Staphylinidae, based on our simplified tree figures. This count is equal to the number of branches that would need to collapse for Silphinae to be in a polytomy with basal Staphylini-

dae. We also provide a count of how many of these branches are strongly supported, using the branch support criteria of each analysis (if applicable). Based on Erixon et al. (2003) and Hoang et al. (2017) we interpreted strong branch support as Bayesian Posterior Probabilities ≥ 0.90 , bootstrap values $\geq 84\%$, and ultrafast bootstrap values $\geq 95\%$ and indicate well-supported branches on our figures. Finally, we provide counts of the total OTUs in each analysis, counts of the total Staphylinidae (including Silphinae) OTUs, and what percent of those OTUs were families of Staphyloidea. Because there is no doubt that Silphidae evolved within the superfamily Staphyloidea (Lawrence and Newton 1982), the strongest tests should have the diversity of this superfamily well represented in case Silphidae is more closely related to a non-staphylinid staphylinoid family. An analysis with many non-staphylinoid families represented but with the only staphylinoid families being Silphidae and Staphylinidae would be a weak test because these two families would be expected to join together regardless of the true relationship between them. Staphyloidea currently contains six families besides Silphidae and Staphylinidae (Cai et al. 2022; Newton 2022), so we indicate which and provide a percentage of these six families (Agyrtidae, Colonidae, Hydraenidae, Jacobsoniidae, Leiodidae, Ptiliidae) represented in each analysis. Most works had a single dataset and corresponding preferred analysis, but some had multiple datasets and corresponding analyses, so we review 23 analyses from 21 works. If the authors did not indicate a preferred analysis and used multiple methods (parsimony, Bayesian, Maximum Likelihood) we chose to present and discuss their most statistically justified analysis (Bayesian or Maximum Likelihood). We also provide brief commentary on the findings of each study. Our primary goal is to provide a concise summary of the evidence for why the family Silphidae has been sunk into the family Staphylinidae, not to provide an in-depth review of each study's strengths and weaknesses. Finally, because Hatch (1927) was the first to propose that Silphinae evolved from within Staphylinidae, for conciseness we sometimes refer to this as "Hatch's (1927) hypothesis."

Results

Hatch (1927), using evolutionary taxonomic methods (non-algorithmic) and morphological characters, explicitly classified silphids as a subfamily of Staphylinidae nine "branches" deep. He was using a now antiquated concept of Silphidae that included current Silphinae and beetles since moved to their own families (Agyrtidae and Leiodidae). We believe he was the first to formally propose that silphids should be sunk into staphylinids and thus his work is historically significant for this review. A large section of his text and corresponding key was devoted to a discussion of characters supporting this change. His key was not artificial, that is, it was intended to reflect phylogeny by arranging taxa in a natural sequence with supporting "derivative characters" (akin to synapomorphies) indicated in his key. We have mapped the hierarchically nested taxa within his key to an interpretation of his intended phylogeny (Fig. 1A). He included 31 beetle OTUs, 19 of which were Staphylinidae, and included three additional staphylinoid families: Ptiliidae, Leiodidae, and Colonidae (Table 1).

Lawrence and Newton (1982), using cladistic reasoning (but non-algorithmic) and phenotypic characters (morphology and behavior) of adults and larvae, de-

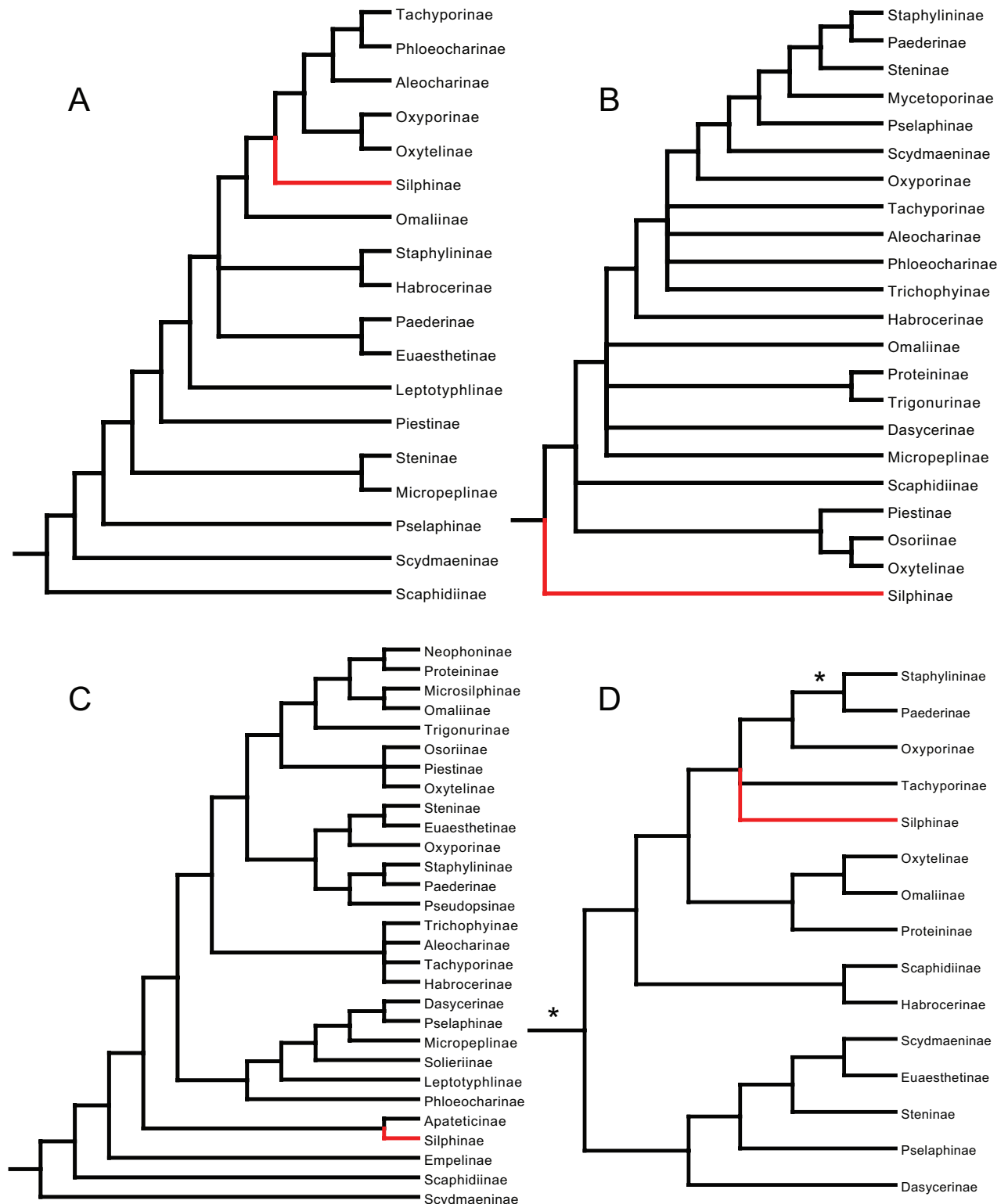


Figure 1. Simplified Staphylinidae phylogenies from **A** Hatch (1927) with non-staphylinids removed **B** Beutel and Molenda (1997: fig. 50), parsimony tree **C** Hansen (1997: fig. 5), parsimony tree, and **D** Ballard et al. (1998: fig. 3a), parsimony tree. Silphinae indicated in red, asterisks indicate well-supported branches.

limited groups of staphylinid subfamilies and commented on the family Silphidae. Their “staphylinine group” contains many mostly predatory species which share the behavior of extraoral digestion, among other characters. They added

Table 1. Analyses relevant to the evolutionary origin of the Silphinae. In/out: whether Silphinae joined inside Staphylinidae. Depth: number of branches that would need to collapse for Silphinae to fall into a polytomy with basal Staphylinidae. Depth Strength: number of such branches well supported. Methods: NA, non-algorithmic; MP, maximum parsimony; ML, Maximum Likelihood; BI, Bayesian Inference. % St-oida: Percentage of the six families of Staphyloidea represented, not counting Silphidae and Staphylinidae.

	Analysis	Year	In/out	Datasets/ genes	Data description	Method(s)	Depth	Depth Strength	OTUs	Staph OTUs	% St- oida	Sister to Silphinae
1	Hatch	1927	in	1	morphology	NA	+9	n/a	31	19	50	5 subfam. incl. Tachyporinae
2	Lawrence and Newton	1982	in	1	morphology	NA	n/a	n/a	n/a	n/a	100	n/a
3	Beutel and Molenda	1997	?	1	morphology	MP	1	n/a	29	22	50	All remaining Staphylinidae
4	Hansen	1997	in	1	morphology	MP	+5	n/a	37	22	83	Apateticinae
5	Ballard et al.	1998	in	3	rDNA (12S), mtDNA (Cyt b), morphology	MP	+4	+1	25	23	33	In polytomy with Tachyporinae
6	Korte et al.	2004	out	2	rDNA (18S, 28S)	MP, BI	n/a	n/a	35	6	33	n/a
7	Caterino et al.	2005	in	2	rDNA (18S) and morphology	MP, ML, BI	+3	+1	105	35	67	Phloeocharinae
8	Hunt et al.	2007	in	3	rDNA (18S), mt-rDNA (16S) and COI	MP, BI	+6	0	340	20	67	Tachyporinae
9	Grebennikov and Newton	2009	in	1	rDNA (18S)	MP, NJ, BI	+5	+2	93	75	67	Tachyporinae
10	Lawrence et al.	2011	in	1	morphology	MP	+4	0	359	11	100	Tachyporinae+Staphylinidae
11	Grebennikov and Newton	2012	?	1	morphology	MP	1	0	36	34	33	All remaining Staphylinidae
12	Bocak et al.	2014	in	4	rDNA (18S, 28S), mtDNA (rrnL, COI)	ML	+8	0?	8,441	349	67	Tachyporinae
13	McKenna et al.	2015	in	2	rDNA (28S), CAD	BI, ML	+3	+3	282	51	83	Tachyporinae
14	Timmermans et al.	2016	in	16	mitogenomes	ML, BI	+4	+3	245	11	33	Habrocerinae and Aleocharinae (in part)
15	Zhang et al.	2018	in	95	protDNA (Amino Acids)	ML, BI	+5	+2	373	16	83	Apateticinae, Scaphidiinae, and Osoriinae
16	Kypke (PhD diss: fig4)	2018	in	993	genomics	ML	+3	+3	33	25	50	Oxytelinae
17	Kypke (PhD diss: fig. 5)	2018	in	1,033	genomics	ML	+2	0	57	41	83	many subfamilies
18	McKenna et al.	2019	in	4,818	genomics	ML	+2	+2	146	4	50	Staphylinidae
19	McKenna et al.	2019	in	89	DNA	ML	+4	+2	521	20	83	Apateticinae, Scaphidiinae, and Osoriinae
20	Lü et al.	2019	in	6	nDNA (CAD, Wg, 28S, 18S), mtDNA (Cyt b, 16S)	ML	+6	0	664	614	83	Tachyporinae
21	Cai and Li	2021	in	13	mtDNA (protein coding genes only)	ML	+4	0	40	11	50	Staphylinidae
22	Song et al.	2021	in	16	mitogenomes	BI	+6	+3	107	95	17	Tachyporinae (in part)
23	Zhao et al.	2022	in	16	mitogenomes	ML	+7	+5	93	85	50	Tachyporinae (in part)

that the families Silphidae and Scydmaenidae share traits with this subfamily group and these families may have evolved from Staphylinidae. They did not include a phylogenetic analysis in their work, but their comprehensive review of staphylinid higher taxon relationships warrants review here. This work is historically important in being the first of the modern phylogenetic era (post-Hennig)

to suggest that Silphidae may belong inside Staphylinidae. We categorized their findings as support for Hatch's (1927) hypothesis because they included potential synapomorphies shared by Silphinae and Staphylinidae (Table 1). They considered all beetle families known at the time, including all current staphylinoid families, but did not mention Jacobsoniidae in the context of Staphylinidae because it had yet to be recognized as a member of Staphylinidae.

Beutel and Molenda (1997) investigated staphylinoid relationships using internal and external larval head morphology and parsimony methods. They, or Hansen (1997), were the first to use a modern algorithmic phylogenetic method that addressed this question. Silphidae was inferred to be the sister lineage to the remaining Staphylinidae (Fig. 1B). We categorized this finding as ambiguous because it could also be interpreted as the Silphinae being the basal lineage within Staphylinidae, depending on one's delimitation of Staphylinidae. This work therefore does not reject Hatch's (1927) hypothesis. They included 29 OTUs, 22 of which were Staphylinidae, and included three additional staphylinoid families: Hydraenidae, Leiodidae, and Agyrtidae (Table 1).

Note that the larva identified as "*Euaesthetus* sp." in Beutel and Molenda (1997) was misidentified and actually is Mycetoporinae, as can be seen by comparing their figures to those of larvae of both these groups in Kasule (1966). These groups are superficially similar in having six stemmata arranged in a circle on each side of the head and lacking a very distinct labrum but differ in several characters (listed here with reference to the figures in Kasule 1966). *Euaesthetus* larvae have a distinct antebasal neck constriction (fig. 58), the labrum completely fused to the head capsule to form a nasale bearing one or more pairs of apical teeth (fig. 57), and a maxilla with an extremely small mala that extends barely as far as the first palpomere (fig. 60). In contrast, mycetoporines lack an antebasal neck constriction (fig. 38) and have an indistinctly articulated labrum without anterior teeth (fig. 38) and a maxilla with a very large mala that extends to about the middle of the third palpomere (fig. 40). Beutel and Molenda (1997) also miscoded the labrum of this larva as completely fused (their character state 7-2) rather than partly fused (state 7-1) to the head, which probably affected the placement of the larva in their tree. In our representation of their tree here (Fig. 1B) we therefore replaced the name *Euaesthetinae* with Mycetoporinae.

Hansen (1997) conducted a phylogenetic analysis of staphyliniform beetles using morphology of adults and immatures with parsimony methods. Hansen's preferred tree has Silphinae five branches deep and sister to Apateticinae, within what modern workers would define as Staphylinidae, with Empelinae, Scaphidiinae, and Scydmaeninae joining closer to the base than Silphinae (Fig. 1C). Although Hansen (1997) did not use a statistical method such as bootstrapping to assess branch support, he did indicate the number of character state changes (apomorphies) estimated for each branch. His root branch of Staphylinidae had 17 apomorphies inferred. About this clade (Staphylinidae in the modern sense) he wrote "A very well defined and undoubtedly monophyletic group, characterized by several very weighty apomorphies, some of which are unique." He included 37 OTUs, 22 of which were Staphylinidae, and included five additional staphylinoid families: Ptiliidae, Hydraenidae, Leiodidae, Coloniidae, and Agyrtidae (Table 1).

Ballard et al. (1998) used three datasets, one of adult morphology and two molecular (12S ribosomal RNA and cytochrome b mitochondrial DNA) using parsimony methods to infer relationships among 25 staphylinoid OTUs, 23 of which were Staphylinidae, and included two additional staphylinoid families: Leiodidae and Agyrtidae. They were the first to bring molecular data to bear on this question. Their preferred tree has Silphinae four branches deep within Staphylinidae in a polytomy with Tachyporinae among other subfamilies (Fig. 1D). One of these four branches was well supported. The only silphine they included, *Oiceoptoma*, was sister to the genus *Tachinus* (Tachyporinae) and supported by a 70% bootstrap in their conditional data combination bootstrap consensus tree (not shown).

Korte et al. (2004) used two molecular datasets of nuclear ribosomal DNA (18S, 28S) to infer the relationships among 35 beetle OTUs, 6 of which were Staphylinidae. They included two additional staphylinoid families: Hydraenidae and Leiodidae, using parsimony and Bayesian methods (Table 1). Their Bayesian analysis found a polyphyletic Staphylinidae with both Silphinae (monophyletic) and Scydmaeninae joined as sister taxa to non-staphylinid lineages, viz. Hydrophilidae and Ptiliidae, respectively (Fig. 2A). Of all the works we review herein, this is the only one that found Silphinae neither inside nor as the sister group of Staphylinidae. Ribosomal DNA is notoriously hard to align properly, especially when secondary structure is not used (Buckley et al. 2000). Although these authors did due diligence in their use of a variety of phylogenetic methods that were well-justified at the time, and even explored a variety of alignments (but did not use secondary structure), some of their results were not entirely credible. They stated as much in the final sentence of their abstract “Some results, such as a placement of Silphidae as subordinate group of Hydraenidae (parsimony tree), or a sistergroup relationship between Ptiliidae and Scydmaenidae, appear unlikely from a morphological point of view.”

Caterino et al. (2005) used two datasets, one of morphological characters derived and slightly modified from Hansen (1997) and the other of nuclear ribosomal DNA (18S) to infer relationships among 105 beetle OTUs, 35 of which were Staphylinidae. They included four additional staphylinoid families: Ptiliidae, Hydraenidae, Leiodidae, and Agyrtidae, using parsimony, Maximum Likelihood, and Bayesian methods (Table 1). Their Bayesian analysis recovered a monophyletic Staphylinidae with a monophyletic Silphinae three branches deep, one of which was well supported (Fig. 2B), with Phloeocharinae sister to Silphinae.

Hunt et al. (2007) used three molecular datasets, one of nuclear ribosomal DNA (18S), one of mitochondrial ribosomal DNA (16S), and one of protein-coding mitochondrial DNA (COI) to infer relationships using parsimony and Bayesian methods among 340 beetle OTUs, 20 of which were Staphylinidae, and four additional staphylinoid families: Ptiliidae, Hydraenidae, Leiodidae, and Agyrtidae, (Table 1). Their Bayesian analysis recovered a polyphyletic Staphylinidae with Silphinae six branches deep; none of these branches were well supported (Fig. 2C). This analysis found Tachyporinae sister to Silphinae.

Grebennikov and Newton (2009) used one molecular dataset of nuclear ribosomal DNA (18S) to infer relationships among 93 beetle OTUs, 75 of which were Staphylinidae, and included four additional staphylinoid families: Ptiliidae, Hydraenidae, Leiodidae, and Agyrtidae, using parsimony, neighbor-joining, and

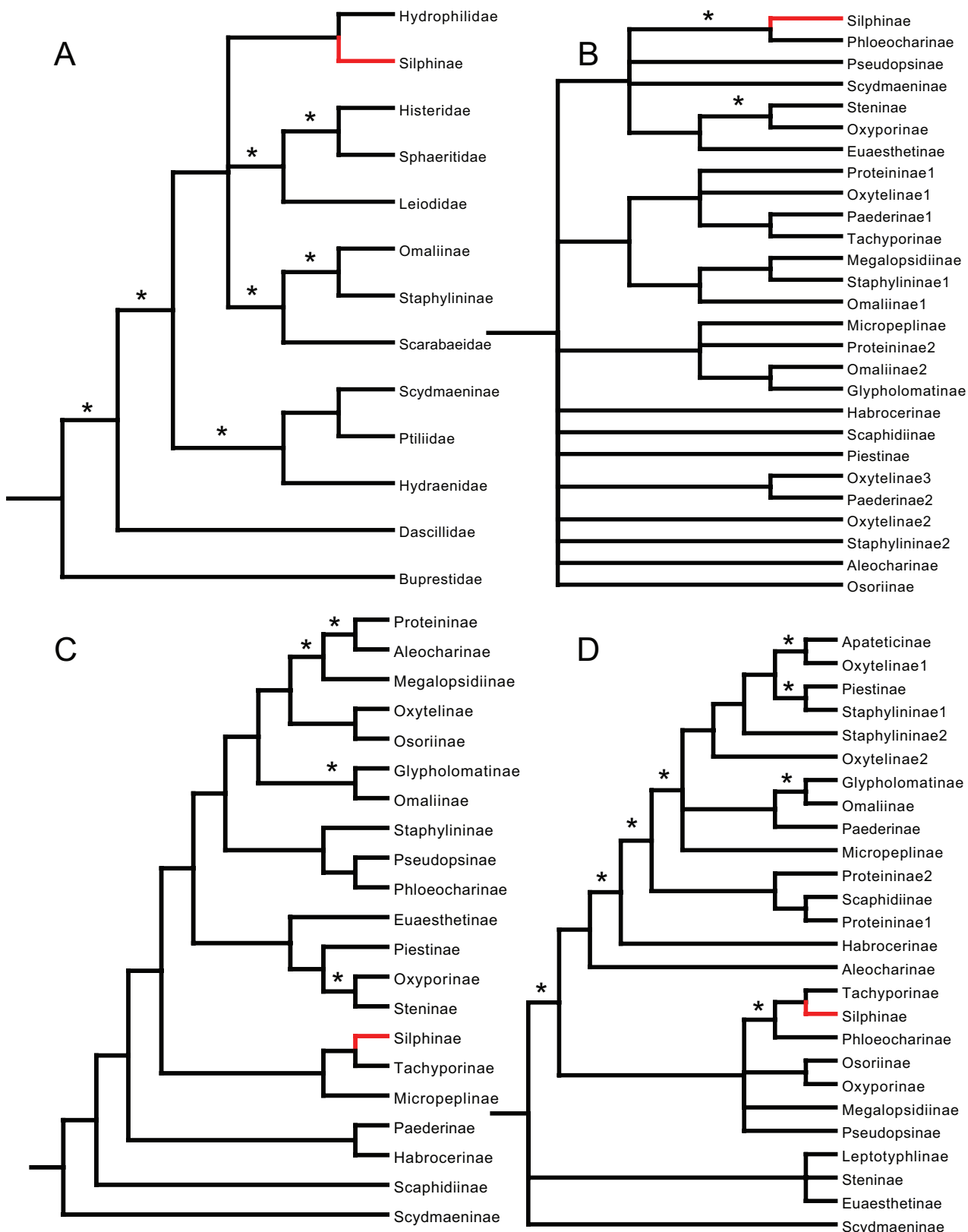


Figure 2. Simplified Staphylinidae phylogenies from **A** Korte et al. (2004: fig. 3), Bayesian tree **B** Caterino et al. (2005: fig. 5) Bayesian tree **C** Hunt et al. (2007: fig. 2) Bayesian tree, with non-staphylinids removed, and **D** Grebennikov and Newton (2009: fig. 12) Bayesian tree, with non-staphylinids removed. Because Korte et al. (2004) was the only study to find the Silphinae external to the Staphylinidae **A** is our only figure that includes non-staphylinid OTUs. Silphinae indicated in red, asterisks indicate well-supported branches.

Bayesian methods (Table 1). They also prepared and analyzed a morphological dataset, but they did not do a combined molecular-morphological analysis. Because their morphological data were improved upon and formed the basis for their later work (Grebennikov and Newton 2012) we discuss their morphological findings later. Their 18S Bayesian analysis found a monophyletic Silphinae five branches deep, two of which were well supported (Fig. 2D). This was within a Staphylinidae made paraphyletic by Ptiliidae (not shown). They, like Hunt et al. (2007), found Tachyporinae sister to Silphinae.

Lawrence et al. (2011) used a single morphological dataset and parsimony methods to infer relationships among 359 beetle OTUs, 11 of which were Staphylinidae, and included all six additional staphylinoid families: Ptiliidae, Hydraenidae, Leiodidae, Colonidae, Agyrtidae, and Jacobsoniidae (Table 1). Their analysis recovered a monophyletic Silphinae four branches deep within a monophyletic Staphylinidae, as sister to a clade of Tachyporinae and Staphylininae (Fig. 3A). None of these branches were well supported. This and Hansen (1997) were the only morphology-only studies to find the Silphinae rooting deeply inside the Staphylinidae since Hatch (1927), rather than as a sister lineage.

Grebennikov and Newton (2012), who built upon the morphological dataset they prepared for their 2009 study, used this single dataset and parsimony methods to infer relationships among 36 beetle OTUs, 34 of which were Staphylinidae, and included two additional staphylinoid families: Leiodidae and Agyrtidae. Their analysis inferred Silphinae to be the sister lineage to the remaining Staphylinidae (Fig. 3B). We categorized this finding as ambiguous because it could also be interpreted as Silphinae being the basal lineage within Staphylinidae, depending on how the family Staphylinidae was delimited. This work therefore does not reject the hypothesis of Silphinae as Staphylinidae. The synapomorphies they inferred and nicely illustrated for the branch uniting Silphinae and Staphylinidae can be used to diagnose Staphylinidae in its current sense (see discussion). Although these authors used parsimony bootstrapping to assess branch support, they did not present bootstrap values on their preferred analysis tree (their fig. 3) and none of the bootstrap values presented in their table 3 for their preferred analysis (#9) were above 83% for any of the non-terminal branches we depict in Fig. 3B.

Bocak et al. (2014) used four datasets, two nuclear (ribosomal 18S, 28S) and two mitochondrial (ribosomal rrrL and protein-coding COI) to infer relationships using Maximum Likelihood methods among 8,441 beetle OTUs, 349 of which were Staphylinidae. They included four additional staphylinoid families: Ptiliidae, Hydraenidae, Leiodidae, and Agyrtidae (Table 1). We were not able to determine if they included Colonidae. Their analysis found a monophyletic Silphinae nested eight branches deep in Staphylinidae and sister to Tachyporinae. However, we were unable to determine the branch support of these branches, or if these authors calculated branch support. We were unable to reconstruct a simplified phylogeny from this work because of the unintelligible coding system they used to label branch tips and the lack of a taxa-included list. This work represents the largest beetle taxon sampling of those we have reviewed.

McKenna et al. (2015) used two datasets, nuclear ribosomal DNA (28S), and nuclear protein-coding DNA (CAD), to infer relationships using Maximum Likelihood and Bayesian methods among 282 beetle OTUs, 51 of which were Staphylinidae, and included five additional staphylinoid families: Ptiliidae, Hy-

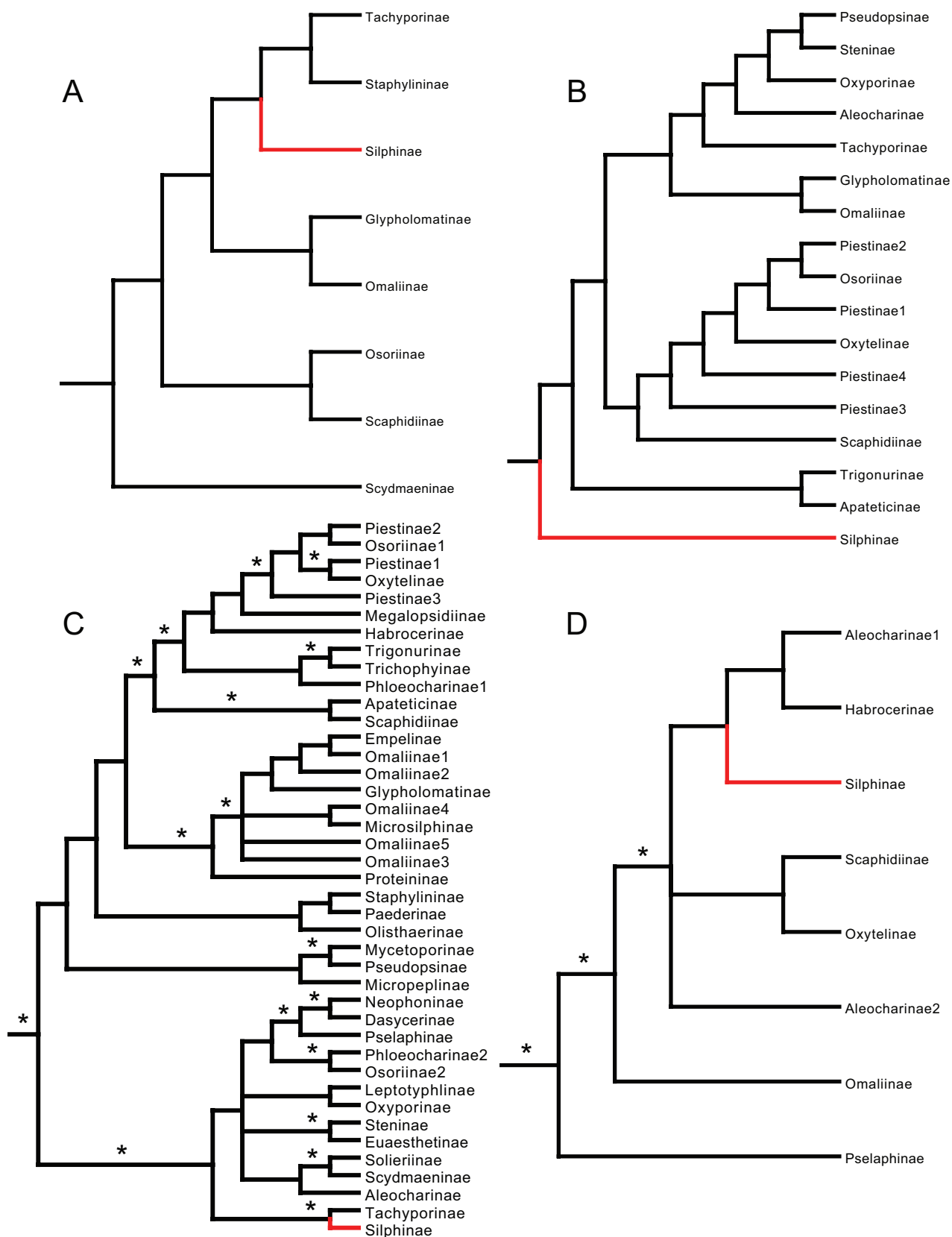


Figure 3. Simplified Staphylinidae phylogenies from **A** Lawrence et al. (2011: cladogram 2), parsimony tree **B** Grebennikov and Newton (2012: fig. 3), parsimony tree **C** McKenna et al. (2015: fig. 3), Bayesian tree, **D** Timmermans et al. (2016: fig. 1), Bayesian tree. Silphinae indicated in red, asterisks indicate well-supported branches.

draenidae, Leiodidae, Colonidae, and Agyrtidae (Table 1). They found a monophyletic Silphinae nested three branches deep in a monophyletic Staphylinidae as sister to Tachyporinae (Fig. 3C). All three branches were strongly supported in their Bayesian analysis but weakly supported in their Maximum Likelihood analysis.

Timmermans et al. (2016) used entire mitochondrial genomes, which contain 16 genes (13 protein coding and 2 ribosomal), and 22 transfer RNAs (which we treat as one gene-equivalent 'dataset' because of the small size of tRNAs) to infer the relationships using Maximum Likelihood and Bayesian methods of 245 beetle OTUs, 11 of which were Staphylinidae; they included two additional staphylinoid families: Leiodidae and Agyrtidae (Table 1). Their results had their one Silphinae (*Necrophila*) nested four branches deep in a monophyletic Staphylinidae as sister to a clade of Habrocerinae and some Aleocharinae (Fig. 3D). Three of these branches were well supported. Mitochondrial DNA in animals evolves faster than nuclear DNA, so is easier to use to infer recent splits (Avice 1986). Ancient splits are more challenging to resolve properly in mitochondrial DNA-only analyses and require careful model specification (Cameron 2014), as Timmermans et al. (2016) appear to have done.

Zhang et al. (2018) also used phylogenomic methods. They built a dataset of 95 protein coding nuclear genes and analyzed their amino acid sequences using Maximum Likelihood and Bayesian methods to infer the relationships of 373 beetle OTUs, 16 of which were Staphylinidae. They included five additional staphylinoid families: Ptiliidae, Hydraenidae, Leiodidae, Agyrtidae, and Jacobsoniidae (Table 1). Their analysis found a monophyletic Silphinae nested five branches deep within a monophyletic Staphylinidae, as sister to a clade containing Apateticinae, Scaphidiinae, and Osoriinae (Fig. 4A). Two of these five branches were well supported. Tachyporinae was the sister group to the Silphinae et al. clade, though with weak support.

Kypke (2018) conducted two analyses relevant to Hatch's (1927) hypothesis for her dissertation. She was one of the first to apply a phylogenomics approach to inference of staphylinoid relationships. One of her analyses used 993 genes and Maximum Likelihood methods to infer the relationships of 33 OTUs, 25 of which were Staphylinidae. She included three additional staphylinoid families: Hydraenidae, Leiodidae, and Agyrtidae (Table 1). This phylogeny had a monophyletic Silphinae three branches deep, sister to Oxytelinae within a monophyletic Staphylinidae (Fig. 4B). All three of these branches were well supported. Her second analysis used 1,033 genes to infer the relationships of 57 OTUs, 41 of which were Staphylinidae. In this analysis she included five additional staphylinoid families: Ptiliidae, Hydraenidae, Leiodidae, Agyrtidae, and Jacobsoniidae (Table 1). This phylogeny found a monophyletic Silphinae two branches deep but as sister to a large clade of many subfamilies (Fig. 4C). Neither of these two branches was well supported.

McKenna et al. (2019) performed two phylogenomic analyses relevant to the evolutionary origin of the Silphinae. Their first had the largest dataset size of all the studies we review, 4,818 genes, but the smallest sampling of Staphylinidae (four OTUs representing three subfamilies) among their total taxon sample of 146 beetle OTUs. They included three additional staphylinoid families: Hy-

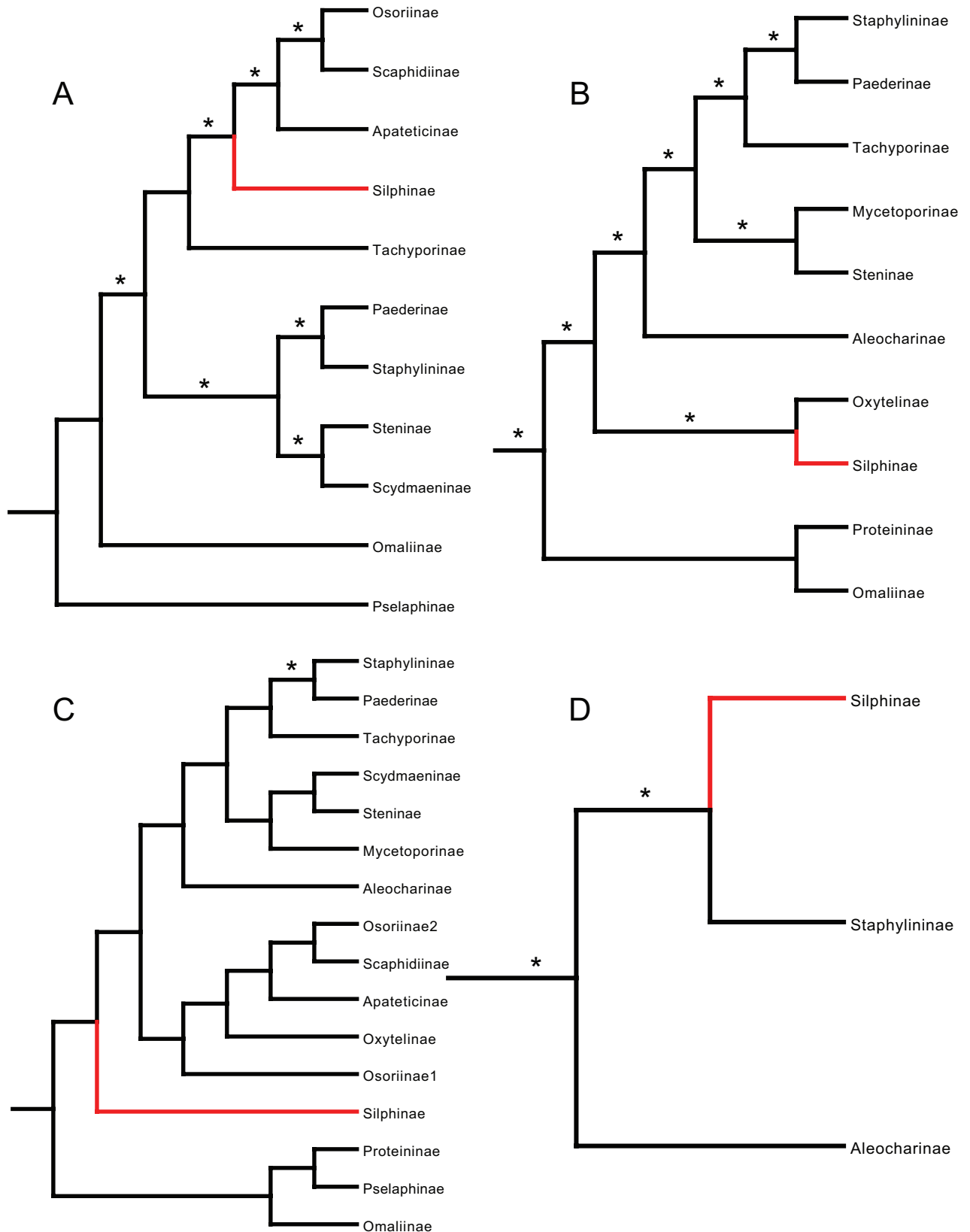


Figure 4. Simplified Staphylinidae phylogenies from **A** Zhang et al. (2018: fig. 2), ML+Bayesian tree **B** Kypke (2018: fig. 4), ML tree **C** Kypke (2018: fig. 5), ML tree **D** McKenna et al. (2019: fig. 1), ML tree. *Silphinae* indicated in red, asterisks indicate well-supported branches.

draenidae, Ptiliidae, and Jacobsoniidae. This analysis used Maximum Likelihood methods and found a monophyletic Silphinae nested two branches deep, as sister to Staphylininae, within a monophyletic Staphylinidae (Fig. 4D). Unsurprisingly, given their enormous dataset, both branches were well supported. Their second analysis, presented in the appendix of their paper, had better taxon sampling with 521 beetle OTUs, 20 of which were Staphylinidae, and included five additional staphylinoid families: Ptiliidae, Hydraenidae, Leiodidae, Agyrtidae, and Jacobsoniidae. They used 89 genes analyzed by Maximum Likelihood methods (Table 1). This analysis found a monophyletic Silphinae nested four branches deep within a monophyletic Staphylinidae, as sister to a clade containing Apateticinae, Scaphidiinae, and Osoriinae (Fig. 5A), similar to the finding of Zhang et al. (2018). Two of these four branches were well supported.

Lü et al. (2019) used six genes in total, four nuclear (CAD, Wg, 28S, 18S) and two mitochondrial (Cyt b, 16S) to infer relationships among 664 beetle OTUs, 614 of which were Staphylinidae, representing the largest staphylinid taxon sampling of any of our reviewed works (Table 1). They included five additional staphylinoid families: Ptiliidae, Hydraenidae, Leiodidae, Colonidae, and Agyrtidae. Using Maximum Likelihood methods, they found a monophyletic Silphinae nested six branches deep within a monophyletic Staphylinidae (Fig. 5B), as sister to Tachyporinae. However, none of these six branches were well supported.

Cai and Li (2021) used a dataset of all 13 protein-coding mitochondrial genes analyzed with Maximum Likelihood methods to infer the relationships of 40 beetle OTUs, 11 of which were Staphylinidae. They included three additional staphylinoid families: Ptiliidae, Hydraenidae, and Leiodidae (Table 1). Their analysis found a monophyletic Silphinae as sister to Staphylininae, nested four branches deep within Staphylinidae (Fig. 5C), but none of these branches were well supported.

Song et al. (2021), like Timmermans et al. (2016), used entire mitochondrial genomes analyzed using Bayesian methods to infer the relationships of 107 beetle OTUs, 95 of which were Staphylinidae, and included only one additional staphylinoid family, Leiodidae (Table 1). Their analysis, which had numerous genera assigned to the wrong subfamilies (corrected in our figure), found a monophyletic Silphinae as sister to part of Tachyporinae nested six branches deep in a monophyletic Staphylinidae (Fig. 5D). Three of these six branches were well supported.

Zhao et al. (2022) used entire mitochondrial genomes and Maximum Likelihood methods to infer the relationships among 93 beetle OTUs, 85 of which were Staphylinidae. They included three additional staphylinoid families: Ptiliidae, Hydraenidae, and Leiodidae (Table 1). They conducted four similar analyses and did not select a preferred tree. We selected their best-supported tree (their fig. 5a) to illustrate and discuss. All four analyses found Silphinae inside Staphylinidae, and this one found a monophyletic Silphinae as sister to part of Tachyporinae, nested seven branches deep within Staphylinidae (Fig. 6). Five of these seven branches were well supported.

Discussion

Considering all 23 analyses, it is apparent that the data type, number of genes, and analysis method do not matter: 97% failed to reject Hatch's (1927) hypothesis. The only analysis to reject it was Korte et al. (2004), in which the authors

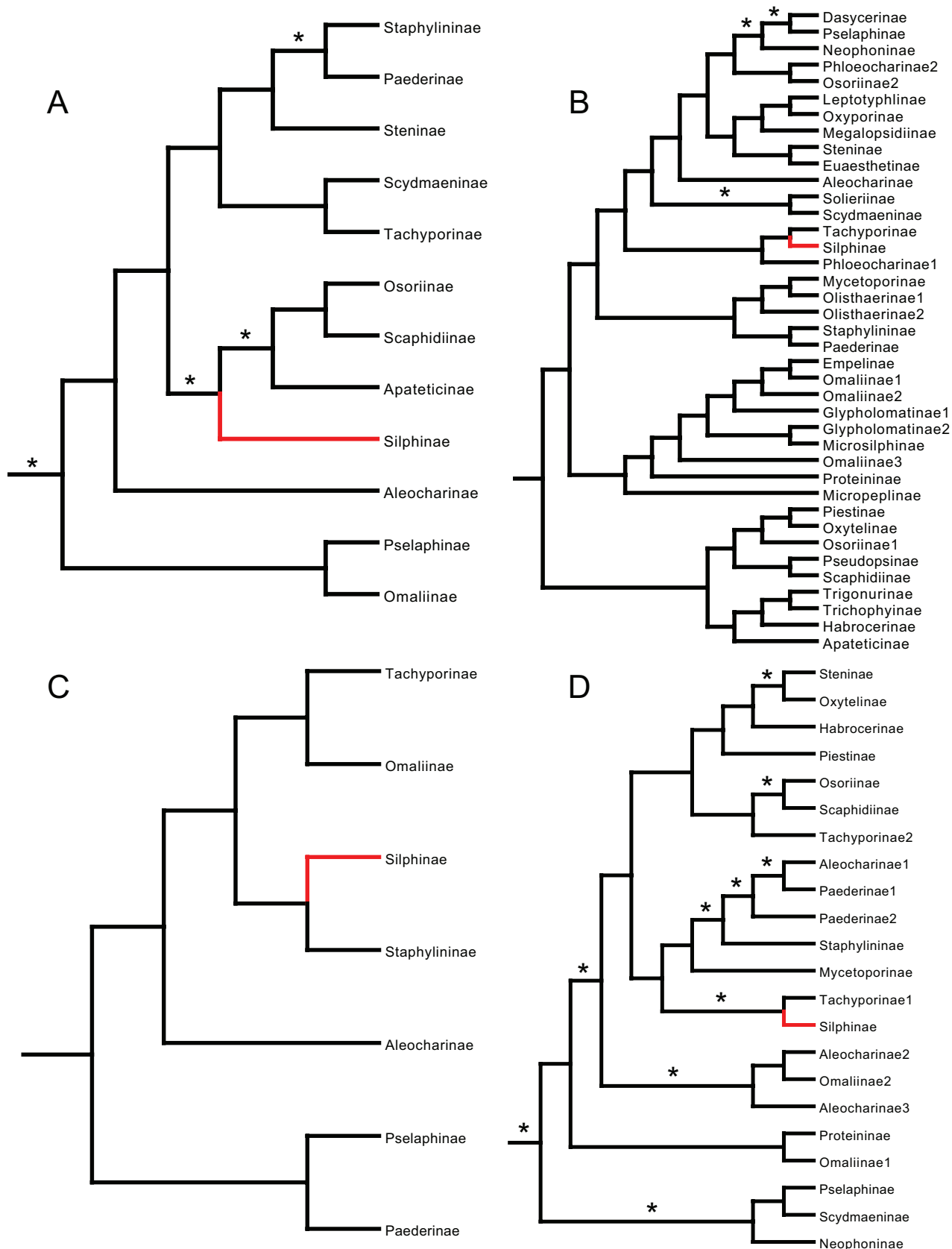


Figure 5. Simplified Staphylinidae phylogenies from **A** McKenna et al. (2019: fig. S10), ML tree **B** Lü et al. (2019: fig. S4), ML tree **C** Cai and Li (2021: fig. 1), ML tree **D** Song et al. (2021: fig. 1), Bayesian tree. Silphinae indicated in red, asterisks indicate well-supported branches.

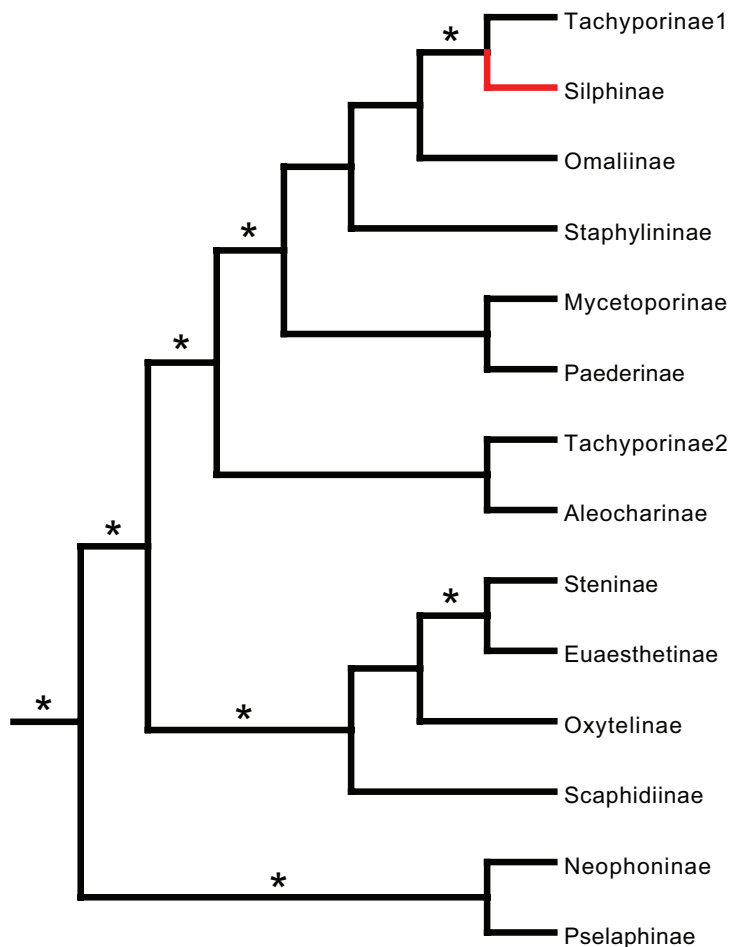


Figure 6. Simplified Staphylinidae phylogeny from Zhao et al. (2022: fig. 5a), ML tree. Silphinae indicated in red, asterisks indicate well-supported branches.

themselves expressed reservations about the reliability of their results. Two analyses found ambiguous results, both based on morphological data (Beutel and Molenda 1997; Grebennikov and Newton 2012). These two found Silphinae as sister to Staphylinidae, which could be interpreted as indicating these taxa share a staphylinid ancestor and thus do not reject Hatch's (1927) hypothesis. As mentioned in the introduction, when a lineage evolves into a new ecological space (in this case, necrophagy), the associated morphological changes can be so dramatic that phylogenetic inference with morphological data alone can be challenging because synapomorphies have evolved further into autapomorphies. It is thus not surprising that two of the four morphology-only analyses did not find Silphinae inside the Staphylinidae, as most of the molecular studies did. It is more surprising that the other two morphology-only studies (Hansen 1997; Lawrence et al. 2011) found Silphinae nested within the Staphylinidae.

With analyses ranging from a single gene to 4,818 genes and having a range of staphylinid OTUs from four to 614 with an average of 71.5, including a mega-analysis with 8,441 beetle OTUs, and most analyses including three or more of the six additional staphylinoid families, the evidence is strong for Hatch's (1927) hypothesis. There were ample independent opportunities to reject it. However, there is still room to improve. Some of these analyses had enormous dataset sizes and others enormous taxon sampling, but none had both.

Could all these independent analyses be wrong about the Silphinae rooting inside the Staphylinidae?

We do not think so. Systematic errors that are known to reduce phylogenetic accuracy, such as long branch attraction and other forms of model misspecification, do not seem to explain these results – particularly since some were based on morphological data and many used inference methods (e.g., Maximum Likelihood) known not to be predisposed to such biases. Could we have missed a significant number of publications that found contrary results? We do not think so. It is possible we have missed some analyses but doubt we have missed any large-scale, well-done, and relevant phylogenetic works that fit our criteria for inclusion and rejected Hatch's (1927) hypothesis.

Sister taxon to the Silphinae?

The reviewed analyses found a variety of different possible sister taxa of Silphinae, but Tachyporinae was found to be the sister group more often than any other subfamily (7 times in 19 analyses that included Tachyporinae). Three analyses did not include any Tachyporinae (Korte et al. 2004; Timmermans et al. 2016; McKenna et al. 2019: analysis 1) and Lawrence and Newton (1982) did not infer a tree. Although found as the sister group of Silphinae more often than any other (and three of these seven times were well supported branches), it is odd that, if Tachyporinae is the actual sister group, why this was not found in the large-dataset phylogenomic studies (e.g., Zhang et al. 2018; Kypke 2018).

Considerable uncertainty remains in our understanding of the intrafamilial relationships of the Staphylinidae. Although costly and difficult to accomplish, it would be ideal to have an analysis with hundreds of Staphylinidae representing all the subfamilies and most tribes, many outgroups including all staphylinoid families, hundreds of genes, as well as a morphological dataset, and no missing data. Given the apparent conflicting phylogenetic signal among many of the analyses we review, we suspect that even with such an ideal study design, the analysis will encounter many difficult challenges.

Monophyletic Staphylinidae?

We conclude that with the addition of Silphinae as the 34th subfamily of Staphylinidae, this megadiverse family is finally monophyletic. Grebennikov and Newton's (2012) morphological investigation included 18 synapomorphies for Staphylinidae in this modern sense that separate this clade from closely related staphylinoids like agyrtids and leiodids (character #-state#: 8-0, 10-0, 13-1, 22-2, 38-0, 44-0, 45-1, 48-0, 66-0, 138-1, 160-2, 171-1, 218-0, 219-0, 228-0, 231-1, 247-1, 250-1). Seven of the most promising are: (44-0): Larval mandible lacking a molar lobe; (160-2): Adult with truncate elytra generally exposing 3+ terga; (171-1): Adult hind wing costal hinge present proximal to radial sector; (218-0, 219-0): Adult lacking wing-folding setal patches on terga VI–VII; (231-1): Adult abdominal intersegmental membranes with minute sclerites (though lost in some subfamilies); (250-1): Aedeagus with large basal bulb, small foramen. As discussed by Lawrence and Newton (1982) and Grebennikov and Newton (2012), many of these adult characters are probably functionally correlated with shortened elytra

and the resultant exposure of multiple abdominal segments that need protection (hence the minute sclerites of the intersegmental membranes) and wings that need to be folded more compactly under the reduced elytra (hence the novel, more basal hinge). The aedeagal and larval characters, however, have no such apparent correlation with elytral length, and provide independent morphological confirmation that Staphylinidae including Silphinae is a monophyletic group, as suggested by the many molecular phylogenetic studies we review above.

Fossil record

Fossils were not formally included in any of the phylogenetic analyses discussed above, even those based at least in part on morphology. This is partly because of the lack, until recently, of fossils that are adequately preserved and clearly attributable to Silphinae until the mid–late Tertiary (ca 35 Mya or younger), when fossils resembling or placed in modern genera of Silphinae appear (e.g., Cai et al. 2014, Chatzimanolis 2018). This situation has changed with the recent discovery of well-preserved compression fossils from the mid-Jurassic and early Cretaceous of China and South Korea, and mid-Cretaceous amber fossils from Myanmar, reviewed by Grebennikov and Newton (2012), Cai et al. (2014) and Sohn and Nam (2021). These discoveries encourage us to briefly discuss whether these fossils lend support to, or help refute, the general conclusion of our review of modern phylogenetic studies above that silphines are derived from within Staphylinidae. Only one of these Mesozoic silphine fossils, *Cretosaja jinjuensis* Sohn and Nam from the early Jurassic of South Korea, is formally named (Sohn and Nam 2021), but the others are extensively described, illustrated, and discussed in the reviews of Cai et al. (2014) and Sohn and Nam (2021), on which the following comments are based. The earliest fossils, from the mid-Jurassic Daohugou Formation in China (ca. 165 Mya), closely resemble in habitus and many other characters small specimens of Nicrophorini, with strongly truncate elytra exposing at least four abdominal segments dorsally. They differ from modern Nicrophorini in being smaller (6.5–13.5 mm), with a more weakly developed antennal club (resembling modern Silphini), and notably lack any trace of stridulatory files on the abdominal terga. The early Cretaceous fossils, from the Yixian Formation of northeastern China and Jinju Formation of South Korea (both ca 125 Mya) closely resemble the Jurassic fossils in habitus and many structures, but have a more strongly developed antennal club resembling that of the modern nicrophorine genus *Ptomascopus*, and most notably have a pair of distinct stridulatory files on abdominal tergite V similar in placement and structure to those of modern Nicrophorini, suggesting that their biology, including subsocial behavior, may have resembled that of modern Nicrophorini. Finally, mid-Cretaceous amber fossils from Myanmar (ca 100 Mya) resemble the modern genus *Nicrophorus* so closely, including having the unique lamellate antennal club of this genus, that they were referred to this genus (Cai et al. 2014). In contrast to all these fossils referable to Nicrophorini, fossils referable to Silphini, including those with long or entire elytra, are still not known until the mid–late Tertiary (ca 35 Mya or younger).

Based on this current state of knowledge of silphine fossils, we can conclude that the known age of silphines is comparable to that of the earliest known fossils reliably attributable to any other group of Staphylinidae, i.e., mid-Jurassic (e.g., Cai and Huang 2010, Chatzimanolis 2018, Cai et al. 2022). Older fossils

of Triassic age (genus *Leehermania* Chatzimanolis et al.), originally attributed to Staphylinidae in Chatzimanolis (2018), were subsequently shown to belong to Hydroscaphidae (Fikáček et al. 2019). Furthermore, the earliest known silphines (i.e., all known Mesozoic fossils) have very truncate elytra and a robust habitus that at least superficially resembles many Jurassic Staphylinidae (e.g., Cai and Huang 2010) and even some modern Staphylinidae, including members of Apateticinae, Trigonurinae, some Omaliinae, and even large *Tachinus* spp. (Tachyporinae). These results are fully consistent with our conclusion from the review of modern phylogenetic analyses that Silphinae evolved from within Staphylinidae and share a suite of derived characters related to having truncate elytra as an ancestral feature. The longer elytra of many modern Silphini are thus likely to be a more recent and secondary development.

Conclusion

From the multiple lines of phylogenetic evidence presented above, supported by the ever-expanding fossil record of Staphylinidae (29, possibly 30, of the 34 subfamilies now known), it seems well justified to treat Silphinae as a subfamily of a strongly supported monophyletic Staphylinidae.

Acknowledgements

We thank Jan Klimaszewski and Jong-Seok Park for their editorial and peer review, respectively, which improved the manuscript.

Additional information

Conflict of interest

The authors have declared that no competing interests exist.

Ethical statement

No ethical statement was reported.

Funding

No funding was reported.

Author contributions

Conceptualization: DSS. Investigation: AFN, DSS, MKT. Methodology: DSS, MKT. Validation: DSS, MKT, AFN. Visualization: DSS. Writing - original draft: DSS, AFN. Writing - review and editing: DSS, MKT, AFN.

Author ORCIDs

Derek S. Sikes  <https://orcid.org/0000-0002-4336-2365>

Margaret K. Thayer  <https://orcid.org/0000-0003-0061-9981>

Alfred F. Newton  <https://orcid.org/0000-0001-9885-6306>

Data availability

All of the data that support the findings of this study are available in the main text and the respective data files of most of the analysis reviewed.

References

- Anderson RS (1982) Resource partitioning in the carrion beetle (Coleoptera: Silphidae) fauna of southern Ontario: ecological and evolutionary considerations. *Canadian Journal of Zoology* 60(6): 1314–1325. <https://doi.org/10.1139/z82-178>
- Anderson RS, Peck SB (1985) The Insects and Arachnids of Canada, Part 13. The carrion beetles of Canada and Alaska (Coleoptera: Silphidae and Agyrtidae). Publication 1778, Research Branch Agriculture Canada, Ottawa, 121 pp.
- Avise JC (1986) Mitochondrial DNA and the evolutionary genetics of higher animals. *Philosophical Transactions of the Royal Society of London. Series B, Biological Sciences* 312(1154): 325–342. <https://doi.org/10.1098/rstb.1986.0011>
- Ballard JWO, Thayer MK, Newton Jr AF, Grismer ER (1998) Data sets, partitions, and characters: Philosophies and procedures for analyzing multiple data sets. *Systematic Biology* 47(3): 367–396. <https://doi.org/10.1080/106351598260770>
- Beutel RG, Leschen RA (2005) Phylogenetic analysis of Staphyliniformia (Coleoptera) based on characters of larvae and adults. *Systematic Entomology* 30(4): 510–548. <https://doi.org/10.1111/j.1365-3113.2005.00293.x>
- Beutel RG, Molenda R (1997) Comparative morphology of selected larvae of Staphylinidea (Coleoptera, Polyphaga) with phylogenetic implications. *Zoologischer Anzeiger* 236: 37–67.
- Bocak L, Barton C, Crampton-Platt A, Chesters D, Ahrens D, Vogler AP (2014) Building the Coleoptera tree-of-life for > 8000 species: Composition of public DNA data and fit with Linnaean classification. *Systematic Entomology* 39(1): 97–110. <https://doi.org/10.1111/syen.12037>
- Buckley TR, Simon C, Flook PK, Misof B (2000) Secondary structure and conserved motifs of the frequently sequenced domains IV and V of the insect mitochondrial large subunit rRNA gene. *Insect Molecular Biology* 9(6): 565–580. <https://doi.org/10.1046/j.1365-2583.2000.00220.x>
- Cai C, Huang D (2010) Current knowledge on Jurassic staphylinids of China (Insecta, Coleoptera). *Earth Science Frontiers* 17(Special Issue): 151–153.
- Cai Y, Li X (2021) The complete mitochondrial genome of a burying beetle, *Nicrophorus nepalensis* Hope, 1831 (Coleoptera: Silphidae). *Mitochondrial DNA. Part B, Resources* 6(6): 1727–1728. <https://doi.org/10.1080/23802359.2021.1930220>
- Cai C, Thayer MK, Engel MS, Newton AF, Ortega-Blanco J, Wang B, Wang X, Huang D (2014) Early origin of parental care in Mesozoic carrion beetles. *Proceedings of the National Academy of Sciences of the United States of America* 111(39): 14170–14174. [online supporting information (9 pp.)] <https://doi.org/10.1073/pnas.1412280111>
- Cai C, Tihelka E, Giacomelli M, Lawrence JF, Ślipiński A, Kundrata R, Yamamoto S, Thayer MK, Newton AF, Leschen RA, Gimmel ML (2022) Integrated phylogenomics and fossil data illuminate the evolution of beetles. *Royal Society Open Science* 9(211771): 1–19. [Online supplement 87 pp.] <https://doi.org/10.1098/rsos.211771>
- Cameron SL (2014) Insect mitochondrial genomics: Implications for evolution and phylogeny. *Annual Review of Entomology* 59(1): 95–117. <https://doi.org/10.1146/annurev-ento-011613-162007>
- Caterino MS, Hunt T, Vogler AP (2005) On the constitution and phylogeny of Staphyliniformia (Insecta: Coleoptera). *Molecular Phylogenetics and Evolution* 34(3): 655–672. <https://doi.org/10.1016/j.ympev.2004.11.012>
- Chatzimanolis S (2018) A review of the fossil history of Staphylinidea. In: Betz O, Irmeler U, Klimaszewski J (Eds) *Biology of rove beetles (Staphylinidae): Life history,*

- evolution, ecology and distribution. Springer, Cham, Switzerland, 27–45. https://doi.org/10.1007/978-3-319-70257-5_3
- Coiffait H (1972) Coléoptères Staphylinidae de la Région Paléarctique Occidentale. Généralités, sous-familles: Xantholininae et Leptotyphlinae. Nouvelle Revue d'Entomologie, Supplement 2(2): [ix+]651. https://www.persee.fr/doc/linly_0366-1326_1974_num_43_7_14125_t2_0047_0000_3
- Crowson RA (1955) The natural classification of the families of Coleoptera. Nathaniel Lloyd and Co., London, 187 pp.
- Crowson RA (1981) The biology of the Coleoptera. Academic Press, London, [xii +] 802 pp. <https://doi.org/10.1016/C2013-0-07304-5>
- Dobler S, Müller JK (2000) Resolving phylogeny at the family level by mitochondrial cytochrome oxidase sequences: Phylogeny of carrion beetles (Coleoptera, Silphidae). Molecular Phylogenetics and Evolution 15(3): 390–402. <https://doi.org/10.1006/mpev.1999.0765>
- Erixon P, Svennblad B, Britton T, Oxelman B (2003) Reliability of Bayesian posterior probabilities and bootstrap frequencies in phylogenetics. Systematic Biology 52(5): 665–673. <https://doi.org/10.1080/10635150390235485>
- Feduccia A (2002) Birds are dinosaurs: Simple answer to a complex problem. The Auk 119(4): 1187–1201. <https://www.jstor.org/stable/4090252>
- Fikáček M, Beutel RG, Cai C, Lawrence JF, Newton AF, Solodovnikov A, Ślipiński A, Thayer MK, Yamamoto S (2019 [2020]) Reliable placement of beetle fossils via phylogenetic analyses – Triassic *Leehermania* as a case study (Staphylinidae or Myxophaga?). Systematic Entomology 45(1): 175–187. [online supplements] <https://doi.org/10.1111/syen.12386>
- Grebennikov VV, Newton AF (2009) Good-bye Scydmaenidae, or why the ant-like stone beetles should become megadiverse Staphylinidae *sensu latissimo* (Coleoptera). European Journal of Entomology 106(2): 275–301. <https://doi.org/10.14411/eje.2009.035>
- Grebennikov VV, Newton AF (2012) Detecting the basal dichotomies in the monophylum of carrion and rove beetles (Insecta: Coleoptera: Silphidae and Staphylinidae) with emphasis on the Oxytelinae group of subfamilies. Arthropod Systematics & Phylogeny 70(3): 133–165. <https://doi.org/10.3897/asp.70.e31759>
- Gusarov VI (2018). Phylogeny of the family Staphylinidae based on molecular data: A review. In: Betz O, Irmeler U, Klimaszewski J (Eds) Biology of Rove Beetles (Staphylinidae): Life History, Evolution, Ecology and Distribution. Springer, Cham, Switzerland, 7–25. https://doi.org/10.1007/978-3-319-70257-5_2
- Hansen M (1997) Phylogeny and classification of the staphyliniform beetle families (Coleoptera). Biologiske Skrifter 48: 1–339. [https://www.tandfonline.com/doi/pdf/10.1080/0165-0424\(200006\)22%3A3%3B1-1%3BFT242](https://www.tandfonline.com/doi/pdf/10.1080/0165-0424(200006)22%3A3%3B1-1%3BFT242)
- Hatch MH (1927) Studies on the carrion beetles of Minnesota, including new species. Technical Bulletin, University of Minnesota Agricultural Experiment Station 48: 1–19. https://conservancy.umn.edu/bitstream/handle/11299/203988/mn1000_agexpstn_tb_048.pdf?sequence=1&isAllowed=y
- Hoang DT, Chernomor O, von Haeseler A, Minh BQ, Vinh LS (2017) [2018]) UFBoot2: Improving the ultrafast bootstrap approximation. Molecular Biology and Evolution 35(2): 518–522. <https://doi.org/10.1093/molbev/msx281>
- Holloway AK, Schnell GD (1997) Relationship between numbers of the endangered American burying beetle *Nicrophorus americanus* Olivier (Coleoptera: Silphidae) and available food resources. Biological Conservation 81(1–2): 145–152. [https://doi.org/10.1016/S0006-3207\(96\)00158-9](https://doi.org/10.1016/S0006-3207(96)00158-9)

- Hunt T, Bergsten J, Levkanicova Z, Papadopoulou A, St. John O, Wild R, Hammond PM, Ahrens D, Balke M, Caterino MS, Gómez-Zurita J, Ribera I, Barraclough TG, Bocakova M, Bocak L, Vogler AP (2007) A comprehensive phylogeny of beetles reveals the evolutionary origins of a superradiation. *Science* 318(5858): 1913–1916. <https://doi.org/10.1126/science.1146954>
- Ikeda H, Nishikawa M, Sota T (2012) Loss of flight promotes beetle diversification. *Nature communications* 3(1): 648. <https://doi.org/10.1038/ncomms1659> [Corrigendum: <https://doi.org/10.1038/ncomms2142> (23 October 2012)]
- Inward D, Beccaloni G, Eggleton P (2007) Death of an order: A comprehensive molecular phylogenetic study confirms that termites are eusocial cockroaches. *Biology Letters* 3(3): 331–335. <https://doi.org/10.1098/rsbl.2007.0102>
- Irisarri I, Meyer A (2016) The identification of the closest living relative (s) of tetrapods: Phylogenomic lessons for resolving short ancient internodes. *Systematic Biology* 65(6): 1057–1075. <https://doi.org/10.1093/sysbio/syw057>
- Jakubec P, Novák M, Qubaiová J, Šuláková H, Růžička J (2019) Description of immature stages of *Thanatophilus sinuatus* (Coleoptera: Silphidae). *International Journal of Legal Medicine* 133(5): 1549–1565. <https://doi.org/10.1007/s00414-019-02040-1>
- Jeannel R, Jarrige J (1949) *Biospeologica* LXVIII. Coléoptères Staphylinides (Première Série). *Archives de Zoologie Expérimentale et Générale* 86: 255–392.
- Johnson KP, Dietrich CH, Friedrich F, Beutel RG, Wipfler B, Peters RS, Allen JM, Petersen M, Donath A, Walden KK, Kozlov AM, Podsiadlowski L, Mayer C, Meusemann K, Vasilikopoulos A, Waterhouse RM, Cameron SL, Weirauch C, Swanson DR, Percy DM, Hardy NB, Terry I, Liu S, Zhou X, Misof B, Robertson HM, Yoshizawa K (2018) Phylogenomics and the evolution of hemipteroid insects. *Proceedings of the National Academy of Sciences of the United States of America* 115(50): 12775–12780. <https://doi.org/10.1073/pnas.1815820115>
- Jordal BH, Smith SM, Cognato AI (2014) Classification of weevils as a data-driven science: Leaving opinion behind. *ZooKeys* 439: 1–18. <https://doi.org/10.3897/zookeys.439.8391>
- Kasule FK (1966) The subfamilies of the larvae of Staphylinidae (Coleoptera) with keys to the larvae of the British genera of Steninae and Proteininae. *Transactions of the Royal Entomological Society of London* 118(8): 261–283. <https://doi.org/10.1111/j.1365-2311.1966.tb00838.x>
- Korte A, Ribera I, Beutel RG, Bernhard D (2004) Interrelationships of Staphyliniform groups inferred from 18S and 28S rDNA sequences, with special emphasis on Hydrophiloidea (Coleoptera, Staphyliniformia). *Journal of Zoological Systematics and Evolutionary Research* 42(4): 281–288. <https://doi.org/10.1111/j.1439-0469.2004.00282.x>
- Kypke JL (2018) Phylogenetics of the world's largest beetle family (Coleoptera: Staphylinidae): A methodological exploration. PhD Thesis, University of Copenhagen, Copenhagen. vi, 106 pp. https://soeg.kb.dk/permalink/45KBDK_KGL/1pioq0f/alma99122777823905763
- Lawrence JF, Newton Jr AF (1982) Evolution and classification of beetles. *Annual Review of Ecology and Systematics* 13(1): 261–290. <https://doi.org/10.1146/annurev.es.13.110182.001401>
- Lawrence JF, Ślipiński A, Seago AE, Thayer MK, Newton AF, Marvaldi AE (2011) Phylogeny of the Coleoptera based on morphological characters of adults and larvae. *Annales Zoologici* 61(1): 1–217. <https://doi.org/10.3161/000345411X576725>
- Liu Y, Tihelka E, Thayer MK, Newton AF, Huang D, Tian L, Cai C (2021) A transitional fossil sheds light on the early evolution of the Staphylinine group of rove beetles (Coleop-

- tera: Staphylinidae). *Journal of Systematic Palaeontology* 19(4): 321–332. <https://doi.org/10.1080/14772019.2021.1917705>
- Lü L, Cai CY, Zhang X, Newton AF, Thayer MK, Zhou HZ (2019) [2020] Linking evolutionary mode to palaeoclimate change reveals rapid radiations of staphylinoid beetles in low-energy conditions. *Current Zoology* 66(4): 435–444. <https://doi.org/10.1093/cz/zoz053>
- Maddison WP, Maddison DR (2018) Mesquite: a modular system for evolutionary analysis. Version 3.6. <http://www.mesquiteproject.org>
- McKenna DD, Farrell BD, Caterino MS, Farnum CW, Hawks DC, Maddison DR, Seago AE, Short AEZ, Newton AF, Thayer MK (2015) Phylogeny and evolution of Staphyliniformia and Scarabaeiformia: Forest litter as a stepping stone for diversification of nonphytophagous beetles. *Systematic Entomology* 40(1): 35–60. <https://doi.org/10.1111/syen.12093>
- McKenna DD, Shin S, Ahrens D, Balke M, Beza-Beza C, Clarke DJ, Donath A, Escalona HE, Friedrich F, Letsch H, Liu S, Maddison D, Mayer C, Misof B, Murin PJ, Niehuis O, Peters RS, Podsiadlowski L, Pohl H, Scully ED, Yan EV, Zhou X, Ślipiński A, Beutel RG (2019) The evolution and genomic basis of beetle diversity. *Proceedings of the National Academy of Sciences of the United States of America* 116(49): 24729–24737. <https://doi.org/10.1073/pnas.1909655116>
- Naomi SI (1985) The phylogeny and higher classification of the Staphylinidae and their allied groups (Coleoptera, Staphylinodea). *Esakia* 23: 1–27. <https://doi.org/10.5109/2464>
- Newton AF (2022) StaphBase: Staphyliniformia world catalog database (version Aug 2022). In: Bánki O, Roskov Y, et al. (Eds) *Catalogue of Life Checklist (Aug 2022)*. <https://www.catalogueoflife.org/> [accessed 23 February 2024] <https://doi.org/10.48580/dfqf-3gk>
- Peck SB (2000) [2001] Silphidae Latreille, 1807. In: Arnett RH, Thomas MC (Eds) *American Beetles: Archostemata, Myxophaga, Adephaga, Polyphaga: Staphyliniformia*. Vol.1. CRC Press, Boca Raton, Florida, USA 268–271.
- Peck SB, Anderson RS (1985) Taxonomy, phylogeny and biogeography of the carrion beetles of Latin America (Coleoptera: Silphidae). *Quaestiones Entomologicae* 21(3): 247–317.
- Sikes DS (2016) Silphidae Latreille, 1807. In: Beutel RG, Leschen RAB (Eds) *Coleoptera, beetles volume I: Morphology and systematics (Archostemata, Adephaga, Myxophaga, Polyphaga partim)* 2nd edn. *Handbook of Zoology, Arthropoda: Insecta* (Beutel RG, Kristensen NP, eds). Walter de Gruyter, Berlin, Germany, 386–394.
- Sikes DS, Venables C (2013) Molecular phylogeny of the burying beetles (Coleoptera: Silphidae: Nicrophorinae). *Molecular Phylogenetics and Evolution* 69(3): 552–565. <https://doi.org/10.1016/j.ympev.2013.07.022>
- Sikes DS, Madge RB, Newton AF (2002) A catalog of the Nicrophorinae (Coleoptera: Silphidae) of the world. *Zootaxa* 65(1): 1–304. <https://doi.org/10.11646/zootaxa.65.1.1>
- Sohn JC, Nam GS (2021) New fossil genus and species of carrion beetle (Coleoptera, Silphidae) from the Lower Cretaceous Jinju Formation, South Korea. *Journal of Asia-Pacific Entomology* 24(3): 584–587. <https://doi.org/10.1016/j.aspen.2021.05.003>
- Song N, Zhai Q, Zhang Y (2021) Higher-level phylogenetic relationships of rove beetles (Coleoptera, Staphylinidae) inferred from mitochondrial genome sequences. *Mitochondrial DNA. Part A, DNA Mapping, Sequencing, and Analysis* 32(3): 98–105. <https://doi.org/10.1080/24701394.2021.1882444>
- Timmermans MJTN, Barton C, Haran J, Ahrens D, Culverwell CL, Ollikainen A, Dodsworth S, Foster PG, Bocak L, Vogler AP (2016) Family-level sampling of mitochondrial ge-

- nomes in Coleoptera: Compositional heterogeneity and phylogenetics. *Genome Biology and Evolution* 8(1): 161–175. <https://doi.org/10.1093/gbe/evv241>
- Toussaint EFA, Seidel M, Arriaga-Varela E, Hájek J, Král D, Sekerka L, Short AEZ, Fikáček M (2016) The peril of dating beetles. *Systematic Entomology* 42(1): 1–10. <https://doi.org/10.1111/syen.12198>
- Trumbo ST, Sikes DS, Philbrick PKB (2016) Parental care and competition with microbes in carrion beetles: A study of ecological adaptation. *Animal Behaviour* 118: 47–54. <https://doi.org/10.1016/j.anbehav.2016.06.001>
- Vences M, Guayasamin JC, Miralles A, De La Riva A (2013) To name or not to name: Criteria to promote economy of change in Linnaean classification schemes. *Zootaxa* 3636(2): 201–244. <https://doi.org/10.11646/zootaxa.3636.2.1>
- von Reumont BM, Jenner RA, Wills MA, Dell’Ampio E, Pass G, Ebersberger I, Meyer B, Koenemann S, Iliffe TM, Stamatakis A, Niehuis O, Meusemann K, Misof B (2012) Pancrustacean phylogeny in the light of new phylogenomic data: Support for Remipedia as the possible sister group of Hexapoda. *Molecular Biology and Evolution* 29(3): 1031–1045. <https://doi.org/10.1093/molbev/msr270>
- Yamamoto S (2021) Tachyporinae revisited: Phylogeny, evolution, and higher classification based on morphology, with recognition of a new rove beetle subfamily (Coleoptera: Staphylinidae). *Biology* 10(323): 1–156. [online supplements] <https://doi.org/10.3390/biology10040323>
- Zhang X, Zhou HZ (2013) How old are the rove beetles (Insecta: Coleoptera: Staphylinidae) and their lineages? Seeking an answer with DNA. *Zoological Science* 30(6): 490–501. <https://doi.org/10.2108/zsj.30.490>
- Zhang S-Q, Che L-H, Li Y, Liang D, Pang H, Ślipiński A, Zhang P (2018) Evolutionary history of Coleoptera revealed by extensive sampling of genes and species. *Nature Communications* 9(205): 205. <https://doi.org/10.1038/s41467-017-02644-4>
- Zhao TY, He L, Xu X, Chen ZN, Gao YY, Liang L (2022) The first mitochondrial genome of *Creophilus* Leach and *Platydracus* Thomson (Coleoptera: Staphylinidae: Staphylinini) and phylogenetic implications. *Zootaxa* 5099(2): 179–200. <https://doi.org/10.11646/zootaxa.5099.2.2>

Ant-eating spiders from Xizang, China (Araneae, Zodariidae)

Lu-Yu Wang¹, Yan-Nan Mu², Feng Lu³, Yong-Qiang Xu^{4,5}, Zhi-Sheng Zhang¹

1 Key Laboratory of Eco-environments in Three Gorges Reservoir Region (Ministry of Education), School of Life Sciences, Southwest University, Chongqing 400715, China

2 Key Laboratory of Zoological Systematics and Application, College of Life Sciences, Hebei University, Baoding, Hebei 071002, China

3 College of Life Sciences and Oceanography, Shenzhen University, Shenzhen 518000, China

4 Tibet Plateau Institute of Biology, Lhasa 850001, Xizang Autonomous Region, China

5 Medog Biodiversity Observation and Research Station of Xizang Autonomous Region, Medog, China

Corresponding author: Zhi-Sheng Zhang (zhangzs327@qq.com)

Abstract

Six species of the ant-eating spider of the family Zodariidae are described from Xizang, China, including five new species: *Asceua chayu* sp. nov. (♀), *A. dawai* sp. nov. (♂♀), *Mallinella migu* sp. nov. (♂), *M. medog* sp. nov. (♂♀), and *M. yadong* sp. nov. (♂♀). The female of *Cydrela linzhiensis* (Hu, 2001) is described here for the first time. Descriptions and photographs of all the species are provided.

Key words: Description, new species, morphology, taxonomy

Introduction

The family Zodariidae Thorell, 1881, known as ant-eating spiders, is a large spider family containing 90 genera and 1279 species worldwide, of which nine genera and 62 species have been recorded from China (WSC 2024). Among these Chinese zodariids, *Mallinella* is the largest genus, encompassing 30 known species. *Asceua* is the second largest, with 14 known species. The other genera are *Storenomorpha* with seven species, *Zodariellum* with six species, and *Cydrela*, *Euryeidon*, *Heliconilla*, *Heradion*, and *Tropizodium* with one species each.

Xizang, the second largest provincial administrative unit of China, is located in the hinterland of the Tibetan Plateau, which is known as “the roof of the world”. Xizang is also a hot spot for studying biological evolution. Knowledge of the spider diversity in Xizang is incomplete, although more than 400 species have been recorded by Hu and Li (1987a, 1987b) and Hu (2001). To date, only three zodariid species have been described from Xizang: *Cydrela linzhiensis* (Hu, 2001) (male only, near Linzhi), *Mallinella dibangensis* (B. Biswas & K. Biswas, 2006) (female only, from southern Tibet) and *Mallinella hingstoni* (Brignoli, 1982) (female only, from “Trop de Tibet, 11,000 ft”).

During our examination of zodariid specimens from Xizang, we found five new species belonging to *Asceua* and *Mallinella*, as well as the previously unknown female of *Cydrela linzhiensis* (Hu 2001). Here we describe these new species and the undescribed female.



Academic editor: Sarah Crews

Received: 8 February 2024

Accepted: 15 April 2024

Published: 8 May 2024

ZooBank: <https://zoobank.org/3ABBC9DD-3116-49C1-87FF-16E71CDD8B8E>

Citation: Wang L-Y, Mu Y-N, Lu F, Xu Y-Q, Zhang Z-S (2024) Ant-eating spiders from Xizang, China (Araneae, Zodariidae). ZooKeys 1200: 183–198. <https://doi.org/10.3897/zookeys.1200.120528>

Copyright: © Lu-Yu Wang et al.

This is an open access article distributed under terms of the Creative Commons Attribution License (Attribution 4.0 International – CC BY 4.0).

Materials and methods

All specimens are preserved in 75% ethanol and were examined, illustrated, photographed, and measured using a Leica M205A stereomicroscope equipped with a drawing tube, a Leica DFC450 Camera, and LAS software (v. 4.6). Male pedipalps and epigynes were examined and illustrated after dissection. Epigynes were cleared by immersing them in a pancreatin solution (Álvarez-Padilla and Hormiga 2007). Eye sizes were measured as the maximum dorsal diameter. Leg measurements are shown as: total length (femur, patella and tibia, metatarsus, tarsus). All measurements are in millimetres. All specimens including the holotypes examined here, are deposited in the Collection of Spiders, School of Life Sciences, Southwest University, Chongqing, China (**SWUC**).

Terminology is as follows. Abbreviations used in the text: **ALE**—anterior lateral eye; **AME**—anterior median eye; **MOA**—median ocular area; **PLE**—posterior lateral eye; **PME**—posterior median eye.

Taxonomy

Family Zodariidae Thorell, 1881 (拟平腹蛛科)

Genus *Asceua* Thorell, 1887 (阿斯蛛属)

***Asceua chayu* sp. nov.**

<https://zoobank.org/325E774B-CE2D-427F-91D0-DD872F19DDE9>

Figs 1, 3A

Chinese name: 察隅阿斯蛛

Type material. Holotype: CHINA • ♀; Xizang, Chayu County, Xiachayu Town, near Xiachayu Bridge; 28°27'24"N, 97°02'40"E; elev. 1464 m; 26 June 2018; L. Wang, Z. Wu & Y. Mu leg.; SWUCT-ZOD-01-01.

Etymology. The specific name is derived from the name of the county where the type locality is located; it is a noun in apposition.

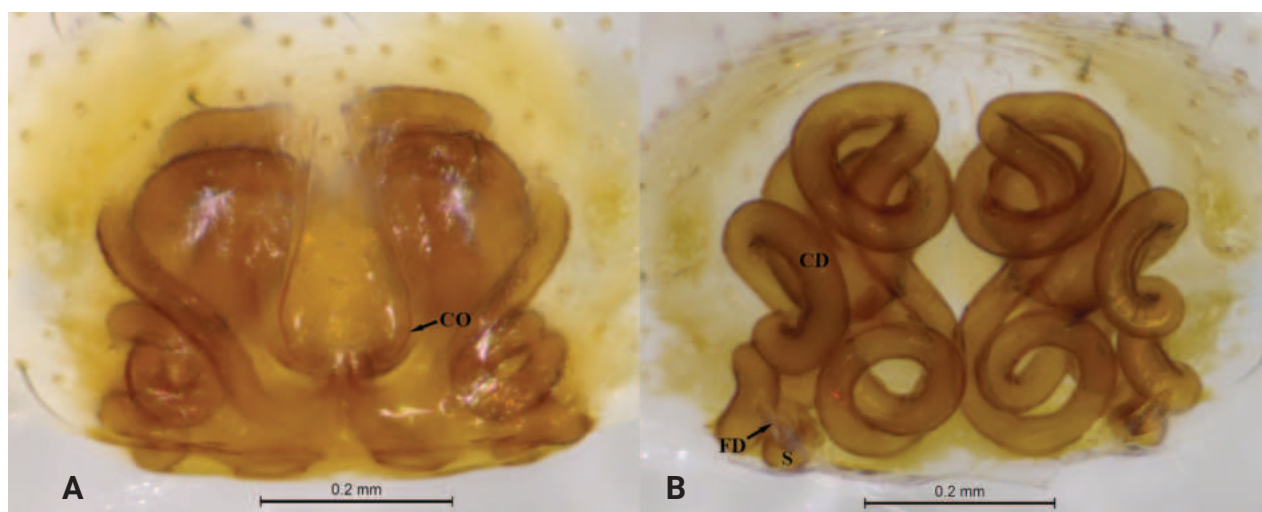


Figure 1. *Asceua chayu* sp. nov., holotype female **A** epigyne, ventral view **B** same, dorsal view. Abbreviations: CD = copulatory duct; CO = copulatory opening; FD = fertilization duct; S = spermatheca.

Diagnosis. This new species can be distinguished from all other *Asceua* species by its copulatory ducts, which are coiled more than 10 times.

Description. Female holotype (Fig. 3A) total length 5.55. Prosoma 2.40 long, 1.62 wide; opisthosoma 2.92 long, 2.09 wide. Eye sizes and interdistances: AME 0.11, ALE 0.11, PME 0.10, PLE 0.12; AME–AME 0.08, AME–ALE 0.08, PME–PME 0.14, PME–PLE 0.21, ALE–PLE 0.06. MOA 0.42 long, anterior width 0.30, posterior width 0.35. Clypeus height 0.49. Leg measurements: I 7.44 (1.97, 2.30, 1.97, 1.20); II 6.06 (1.67, 1.80, 1.62, 0.97); III 5.96 (1.67, 1.69, 1.77, 0.83); IV 7.74 (2.01, 2.41, 2.33, 0.99). Leg formula: 4123. Carapace shiny, deep brown, lateral margins darker than median, tegument smooth, median part with an indistinct, wide V-shaped black patch in front of black fovea. Radial grooves indistinct. Opisthosoma oval, black, anterior with two pairs of wing-shaped white spots, posterior with four irregular white spots. Spinnerets brown.

Epigyne (Fig. 1). Epigyne with distinct epigynal pocket, copulatory openings situated in median part of epigyne. Copulatory ducts long, visible in ventral view, coiled more than 10 times. Spermathecae small, well separated, and posteriorly situated.

Male. Unknown.

Distribution. Known only from the type locality, Xizang, China.

***Asceua dawai* sp. nov.**

<https://zoobank.org/69EA2F00-81BC-4E50-A0B4-7361B2708603>

Figs 2, 3B, C

Chinese name: 达娃阿斯蛛

Type material. Holotype: CHINA • ♂; Xizang, Medog County, Medog Town, Yarang Village; 29°17'45"N, 95°16'49"E; elev. 761 m; 19 December 2023; L. Wang, F. Lu & Y. Mu leg.; SWUCT-ZOD-02-01.

Paratypes: CHINA – Xizang, Medog County • 1 ♀; Beibeng Township; 29°14'22"N, 95°10'40"E; elev. 894 m; 28 June 2018; L. Wang, Z. Wu & Y. Mu leg.; SWUCT-ZOD-02-02 • 1 ♂; Madi Village; 29°23'42"N, 95°22'58"E; elev. 966 m; 28 June 2018; L. Wang, Z. Wu & Y. Mu leg.; SWUCT-ZOD-02-03 • 3 ♀♀; Medog Town, Yarang Village; 29°17'45"N, 95°16'49"E; elev. 761 m; 22 May 2019; L. Wang, P. Liu, T. Yuan & H. Wang leg.; SWUCT-ZOD-02-04 to SWUCT-ZOD-02-04-06 • 9 ♀♀; Medog Town, Yarang Village; 29°17'45"N, 95°16'49"E; elev. 761 m; 30 May 2022; L. Wang, B. Tan & T. Ren leg.; SWUCT-ZOD-02-07 to SWUCT-ZOD-02-15

Etymology. The specific name is a patronym in honor of Mr Dawa from the Tibet Plateau Institute of Biology in Lhasa, Xizang.

Diagnosis. This new species resembles *Asceua thrippalurensis* Sankaran, 2023 (Sankaran 2023: 389, figs 7A–J, 8A–J, 9A–F, 10A–F), but it differs from the latter by the short embolus that is not folded at its tip (vs long embolus folded at tip), bifurcate tip of retrolateral tibial apophysis (vs tip not bifurcate), epigynal plate with a pocket and two copulatory openings (vs without pocket and one copulatory opening), and copulatory ducts short (vs copulatory ducts long) (Fig. 2).

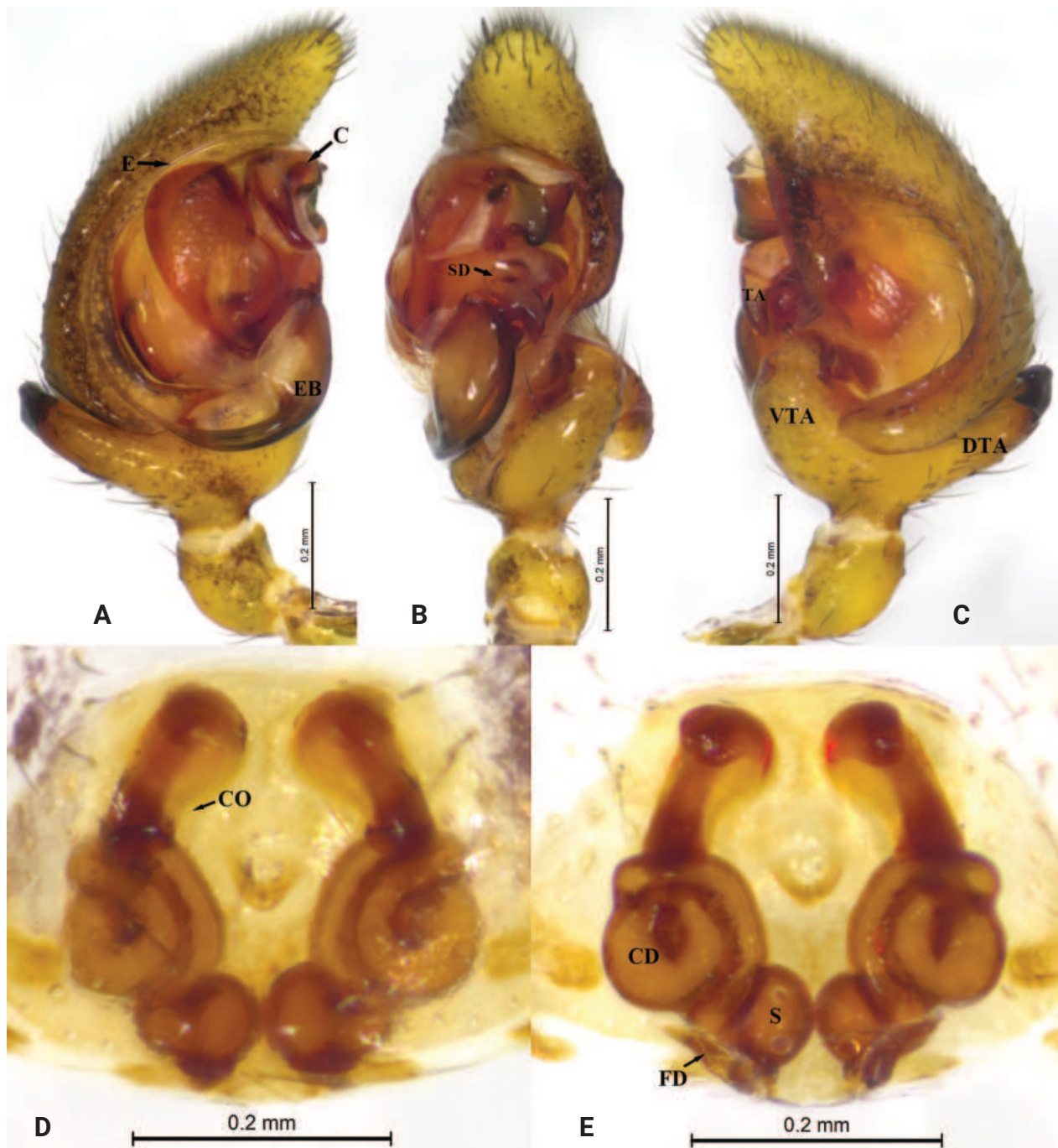


Figure 2. *Asceua dawai* sp. nov. **A–C** holotype male **D, E** paratype female **A** male left palp, prolateral view **B** same, ventral view **C** same, retrolateral view **D** epigyne, ventral view **E** same, dorsal view. Abbreviations: C = conductor; CD = copulatory duct; CO = copulatory opening; E = embolus; EB = embolic base; FD = fertilization duct; RTA = retrolateral tibial apophysis; S = spermatheca; SD = sperm duct; TA = tegular apophysis; VTA = ventral tibial apophysis.

Description. Male holotype (Fig. 3B) total length 3.23. Prosoma 1.44 long, 1.04 wide; Opisthosoma 1.56 long, 1.07 wide. Eye sizes and interdistances: AME 0.06, ALE 0.06, PME 0.07, PLE 0.10; AME–AME 0.06, AME–ALE 0.03, PME–PME 0.09, PME–PLE 0.10, ALE–PLE 0.04. MOA 0.27 long, anterior width 0.19, posterior width 0.25. Clypeus height 0.37. Chelicerae with 2 promarginal and 1 retromarginal tooth. Leg measurements: I 4.59 (1.21, 1.46, 1.20, 0.72); II 3.85 (1.04, 1.18, 1.03, 0.60); III 3.86 (1.10, 1.15, 1.03, 0.58); IV 4.71 (1.24, 1.54,

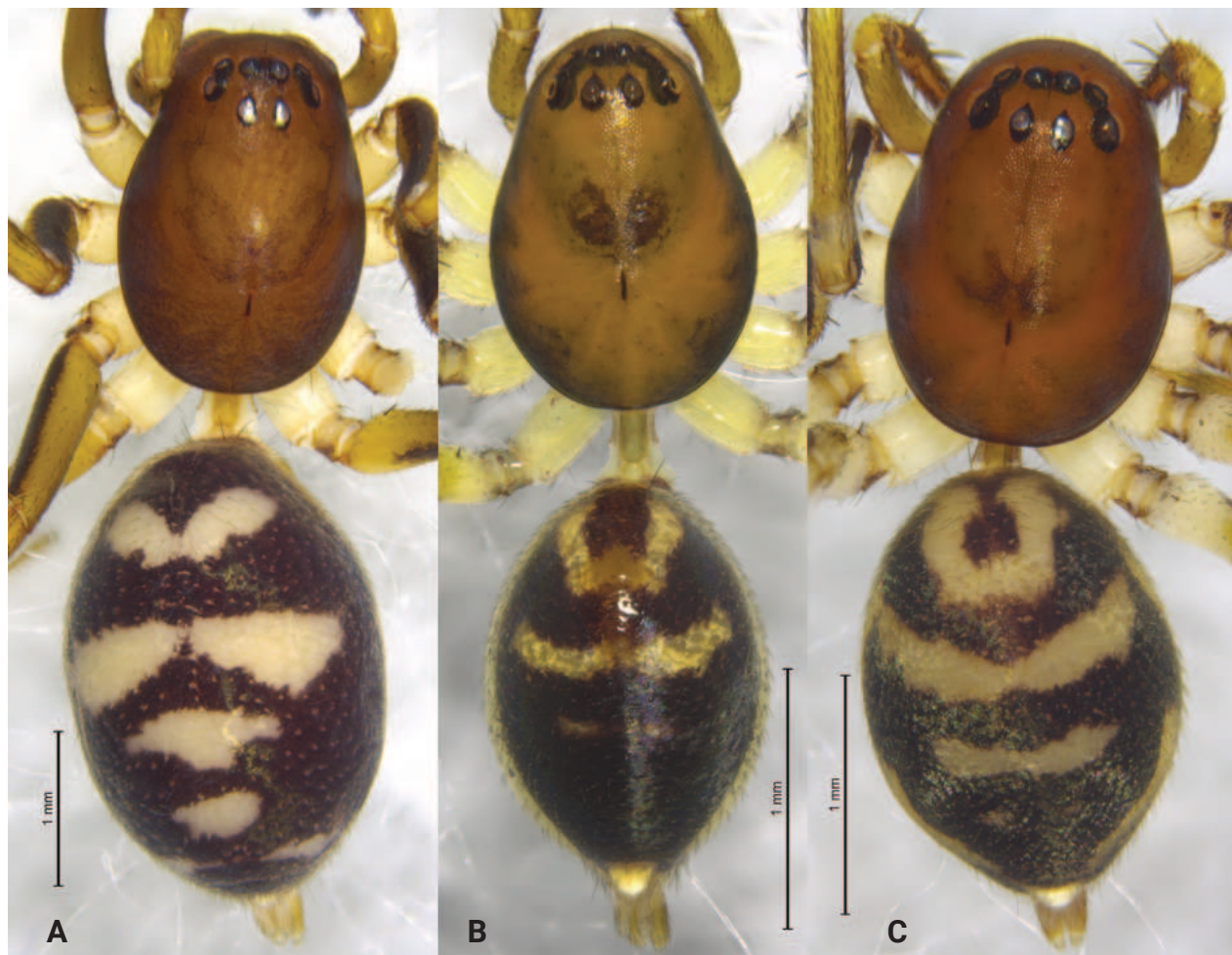


Figure 3. *Asceua* spp., habitus, dorsal view **A** *Asceua chayu* sp. nov., female holotype **B** *Asceua dawai* sp. nov., male holotype **C** *Asceua dawai* sp. nov., female paratype.

1.38, 0.55). Leg formula: 4132. Carapace shiny, brown, lateral margins dark brown, tegument smooth, median part with a wide V-shaped black patch in front of black fovea. Radial grooves indistinct. Opisthosoma oval, covered with short black hairs, with a shiny and lanceolate dorsal scutum. Dorsum of opisthosoma black, anterior with U-shaped white patches, followed by one transversal median band. Spinnerets brown, ringed with black.

Palp (Fig. 2A–C). Tibia with strong ventral and dorsal apophyses, retrolateral tibial apophysis with curved and bifurcate tip. Tegular apophysis wide and strong, retrolaterally with coracoid extension. Embolus tapering from base to tip. Cymbium with terminal spine and with pro- and retrolateral folds not reaching tip.

Female (Fig. 3C) total length 3.50. Prosoma 1.69 long, 1.21 wide; opisthosoma 1.84 long, 1.35 wide. Eye sizes and interdistances: AME 0.09, ALE 0.08, PME 0.08, PLE, 0.11; AME–AME 0.05, AME–ALE 0.05, PME–PME 0.09, PME–PLE 0.12, ALE–PLE 0.06. MOA 0.29 long, anterior width 0.23, posterior width 0.28. Clypeus height 0.50. Leg measurements: I 4.52 (1.21, 1.46, 1.17, 0.68); II 3.81 (1.06, 1.17, 0.99, 0.59); III 4.01 (1.05, 1.23, 1.13, 0.60); IV 5.19 (1.31, 1.55, 1.62, 0.71). Leg formula: 4132. Opisthosoma oval, black, anterior with white U-shaped patches, followed by two transversal median bands. Spinnerets brown. Other characters same as in male, except carapace deep brown.

Epigyne (Fig. 2D–E). Epigyne with a small epigynal pocket centrally, copulatory openings large, in anterior part of epigyne. Copulatory ducts short and thick, visible in ventral view. Spermathecae oval, close to each other, situated posteriorly.

Distribution. Known only from the type locality, Xizang, China.

Genus *Cydrela* Thorell, 1873 (斯逃蛛属)

Cydrela linzhiensis (Hu, 2001)

Fig. 4

Chinese name: 林芝斯逃蛛

Storena linzhiensis Hu, 2001: 92, figs 14.1–6 (♂).

Cydrela linzhiensis: Dankittipakul and Jocqué 2006: 100.

Material examined. CHINA – Xizang • 1 ♀; Nyingchi City, Bowo County, Tongmai Town, near Tongmai Bridge; 30°05'41"N, 95°04'13"E; elev. 2073 m; 1 July 2018; L. Wang, Z. Wu & Y. Mu leg.; SWUC-ZCL-01 • 1 ♂; near Tongmai Bridge; L. Wang, P. Liu, T. Yuan & H. Wang leg.; SWUC-ZCL-02.

Diagnosis. This species can be easily separated from other *Cydrela* species by the long retrolateral tibial apophysis of the male palp and large, globular spermathecae of the epigyne.

Description. Male (Fig. 4A) total length 4.90. Prosoma 2.74 long, 1.72 wide; Opisthosoma 2.11 long, 1.70 wide. Eye sizes and interdistances: AME 0.06, ALE 0.09, PME 0.09, PLE 0.11; AME–AME 0.05, AME–ALE 0.04, PME–PME 0.09, PME–PLE 0.18, ALE–PLE 0.24. MOA 0.29 long, anterior width 0.17, posterior width 0.26. Clypeus height 0.48. Leg measurements: I 6.40 (1.82, 2.18, 1.36, 1.04); II 5.90 (1.64, 1.92, 1.31, 1.03); III 6.04 (1.64, 1.85, 1.73, 0.82); IV 8.31 (2.14, 2.33, 2.47, 1.37). Leg formula: 4132. Carapace brown. Fovea dark red. Radial grooves indistinct. Opisthosoma oval, black, with short hairs, dorsum with five pairs of bright spots, anteriormost one largest. Spinnerets yellow brown.

Palp (Fig. 4E–G). Tibia as long as wide, protruded ventrally in lateral view, retrolateral tibial apophysis long, with wide base and triangular tip, two times longer than tibia. Cymbium with several spines on distal part. Bulb oval. Conductor membranous, posterior portion lightly sclerotized; anterior part forming a groove accommodating elongate embolus.

Female (Fig. 4B) total length 6.95. Prosoma 3.42 long, 2.08 wide; opisthosoma 3.66 long, 2.63 wide. Eye sizes and interdistances: AME 0.08, ALE 0.11, PME 0.10, PLE, 0.11; AME–AME 0.06, AME–ALE 0.05, PME–PME 0.11, PME–PLE 0.28, ALE–PLE 0.38. MOA 0.39 long, anterior width 0.21, posterior width 0.32. Clypeus height 0.47. Leg measurements: I 6.05 (1.81, 2.24, 1.14, 0.86); II 5.28 (1.61, 1.79, 1.05, 0.83); III 5.86 (1.70, 1.87, 1.34, 0.95); IV 8.04 (2.14, 2.51, 2.07, 1.32). Leg formula: 4132. Carapace deep yellow, opisthosoma gray, other characters same as male.

Epigyne (Fig. 4C, D). Epigynal plate with small hood, wider than long. Copulatory opening conspicuous, posteriorly situated. Copulatory ducts short. Spermathecae large, globular.

Distribution. China (Nyingchi, Xizang).

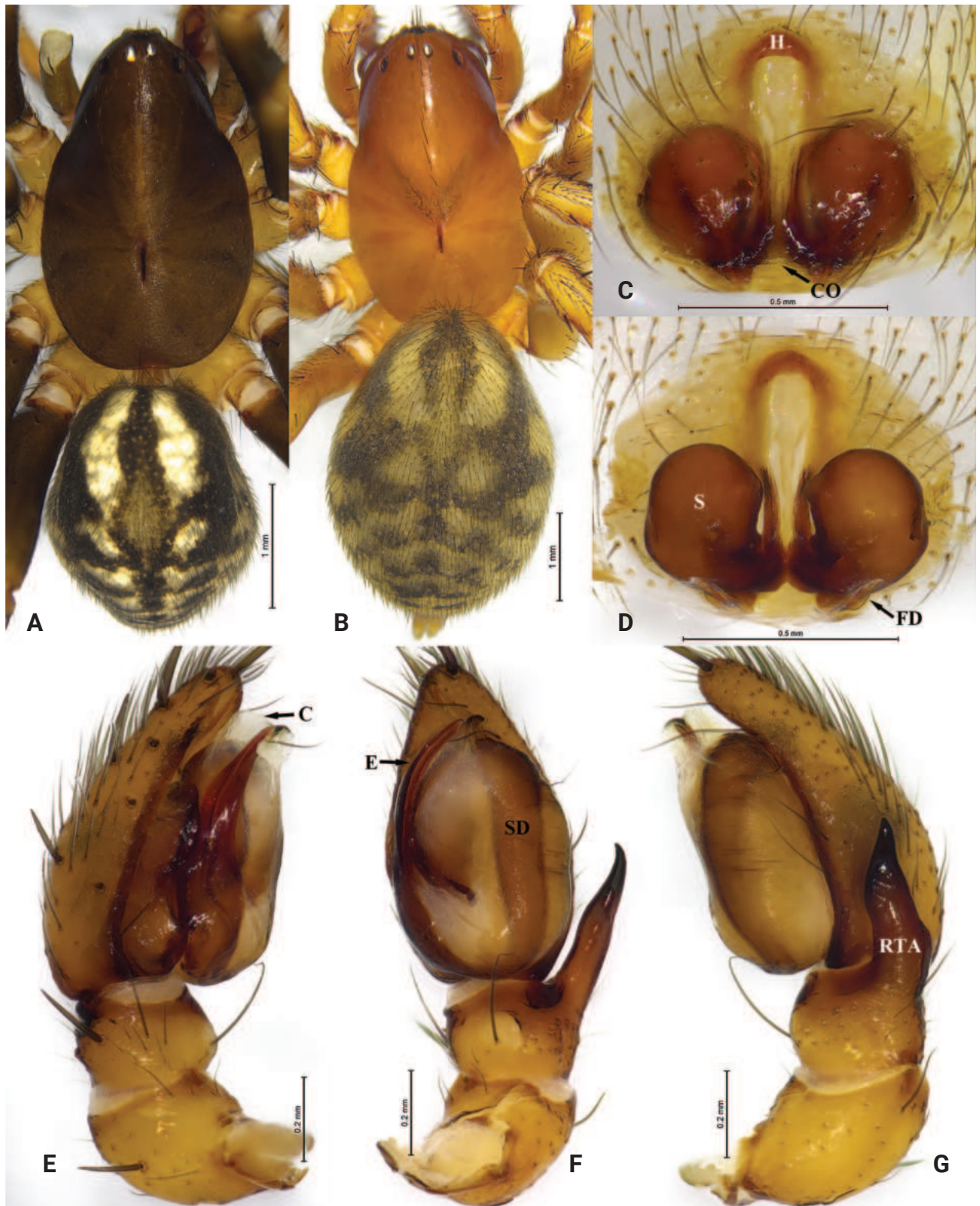


Figure 4. *Cydrela linzhiensis* (Hu, 2001) **A** male, dorsal view **B** female, dorsal view **C** epigyne, ventral view **D** same, dorsal view **E** male left palp, prolateral view **F** same, ventral view **G** same, retrolateral view. Abbreviations: C = conductor; CO = copulatory opening; E = embolus; FD = fertilization duct; H = hood; RTA = retrolateral tibial apophysis; S = spermatheca; SD = sperm duct.

Genus *Mallinella* Strand, 1906 (马利蛛属)

The *fronto*-group

***Mallinella migu* sp. nov.**

<https://zoobank.org/3A85835E-B332-46D6-AC02-3C2F84F2EAF2>

Figs 5, 10A

Chinese name: 米古马利蛛

Type material. Holotype: CHINA • ♂; Xizang, Chayu County, Shangchayu Town, Migu; 28°46'40"N, 96°43'28"E; elev. 1945 m; 27 May 2019; L. Wang, P. Liu, T. Yuan & H. Wang leg.; SWUCT-ZOD-03-01.

Etymology. The specific name is derived from the type locality; it is a noun in apposition.

Diagnosis. This new species resembles *Mallinella martensi* (Ono, 1983) (Ono 1983: 212, figs 1–4), but it differs from the latter by the stronger and wider tegular apophysis with a narrow, deep notch at external rim in retrolateral view (vs thin tegular apophysis with a wide notch), conductor with a nearly rectangular apophysis at prolateral base (vs with cambered apophysis), embolic base with a distinct, blunt protuberance (vs without protuberance) (Fig. 5).

Description. Male holotype (Fig. 10A) total length 9.57. Prosoma 4.81 long, 3.46 wide; Opisthosoma 4.35 long, 3.10 wide. Eye sizes and interdistances: AME 0.31, ALE 0.24, PME 0.25, PLE 0.26; AME–AME 0.12, AME–ALE 0.19, PME–PME 0.21, PME–PLE 0.36, ALE–PLE 0.08. MOA 0.68 long, anterior width 0.63, posterior width 0.70. Clypeus height 1.26. Leg measurements: I 14.10 (3.62, 4.24, 3.53, 2.71); II 13.00 (3.40, 3.91, 3.23, 2.46); III 12.52 (3.17, 3.71, 3.55, 2.09); IV 16.09 (3.80, 4.66, 4.92, 2.71). Leg formula: 4123. Carapace and fovea black, slightly swollen. Legs yellow. Opisthosoma oval, longer than wide, dorsum with two pairs of white spots, followed by three transverse white bands. Dorsal scutum thin, reddish brown, about half as long as opisthosoma. Spinnerets pale yellow.

Palp (Fig. 5). Tibia wider than long, with two apophyses, ventral tibial apophysis arc-shaped; retrolateral tibial apophysis digitiform, short, apically rounded, curved ventrally. Tegular apophysis wide, apico-prolateral process strongly curved, with thin, deep notch at external rim in retrolateral view. Embolus bifurcated at tip, lateral ramus shorter than mesal ramus, with blunt protuberance at base. Conductor sclerotized posteriorly; anterior part forming a groove accommodating embolus.

Female. Unknown.

Distribution. Known only from the type locality, Xizang, China.

***Mallinella medog* sp. nov.**

<https://zoobank.org/DA6D56B6-4AE4-44BC-8865-8A49415C428B>

Figs 6, 7, 10B, C

Chinese name: 墨脱马利蛛

Type material. Holotype: CHINA • ♂; Xizang, Medog County, near Dexing Bridge; 29°19'16"N, 95°17'39"E; elev. 724 m; 29 June 2018; L. Wang, Z. Wu & Y. Mu leg.; SWUCT-ZOD-04-01.

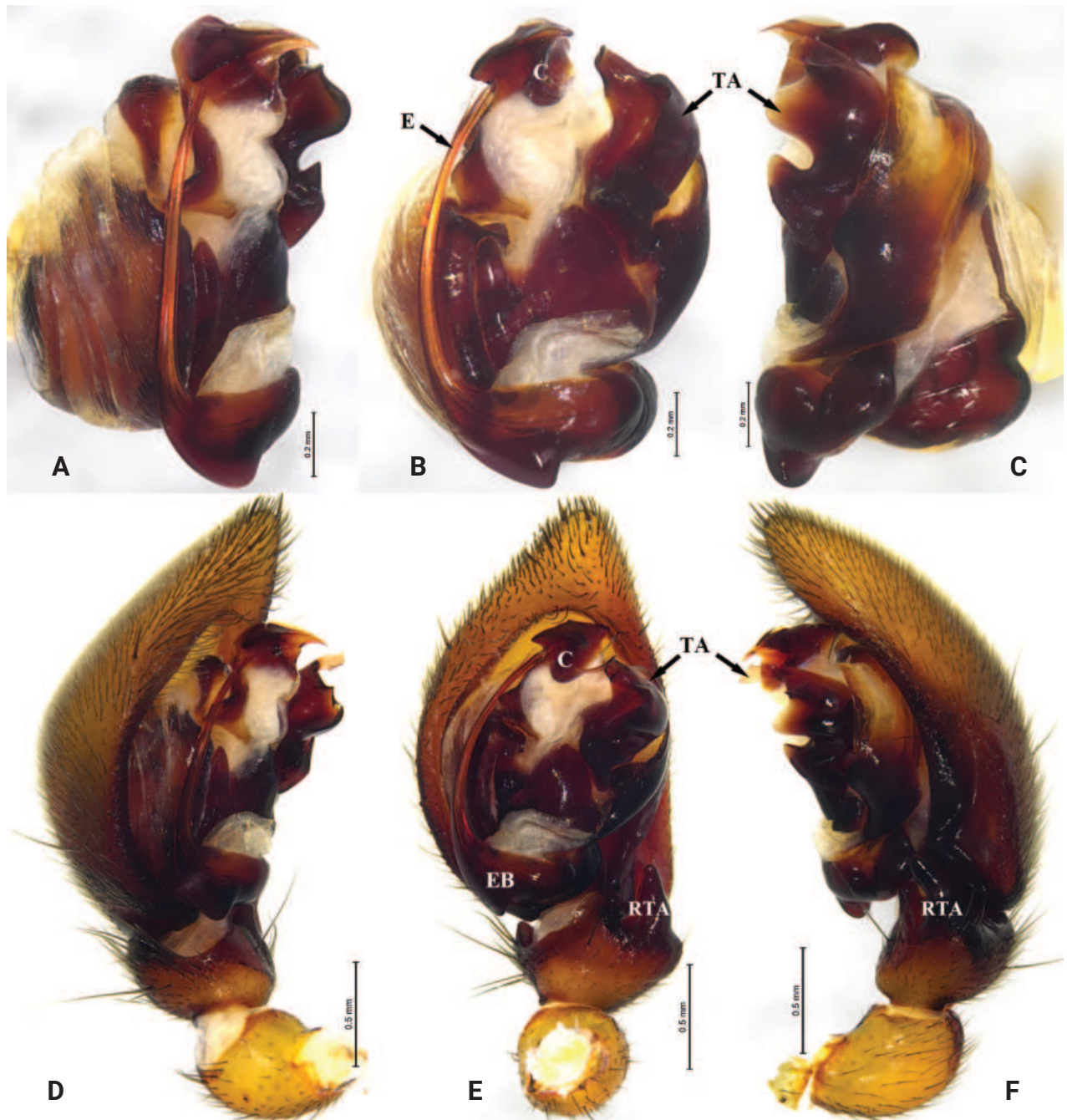


Figure 5. *Mallinella migu* sp. nov. holotype male **A** male right bulb (flipped horizontally), prolateral view **B** same, ventral view **C** same, retrolateral view **D** male left palp, prolateral view **E** same, ventral view **F** same, retrolateral view. Abbreviations: C = conductor; E = embolus; EB = embolic base; RTA = retrolateral tibial apophysis; TA = tegular apophysis.

Paratypes: CHINA – Xizang, Medog County • 1♂ 1♀; Medog County; 29°19'28"N, 95°19'37"E; elev. 1116 m; 29 June 2018; L. Wang, Z. Wu & Y. Mu leg.; SWUCT-ZOD-04-02 and SWUCT-ZOD-04-03 • 1♂ 1♀; Medog Town, Yarang Village; 29°17'45"N, 95°16'49"E; elev. 761 m; 22 May 2019; L. Wang, P. Liu, T. Yuan & H. Wang leg.; SWUCT-ZOD-04-04 and SWUCT-ZOD-04-05 • 3♂♂ 3♀♀; Medog Town, Yarang Village; 29°17'45"N, 95°16'49"E; elev. 761 m; 30 May 2022; L. Wang, B. Tan & T. Ren leg.; SWUCT-ZOD-04-06 to SWUCT-ZOD-04-11 • 3♀♀; Medog County; 29°19'37"N, 95°19'33"E; elev. 1049 m; 31 May 2022; L. Wang, B. Tan & T. Ren leg.; SWUCT-ZOD-04-12 to SWUCT-ZOD-04-14 • 2♂♂; Medog Town;

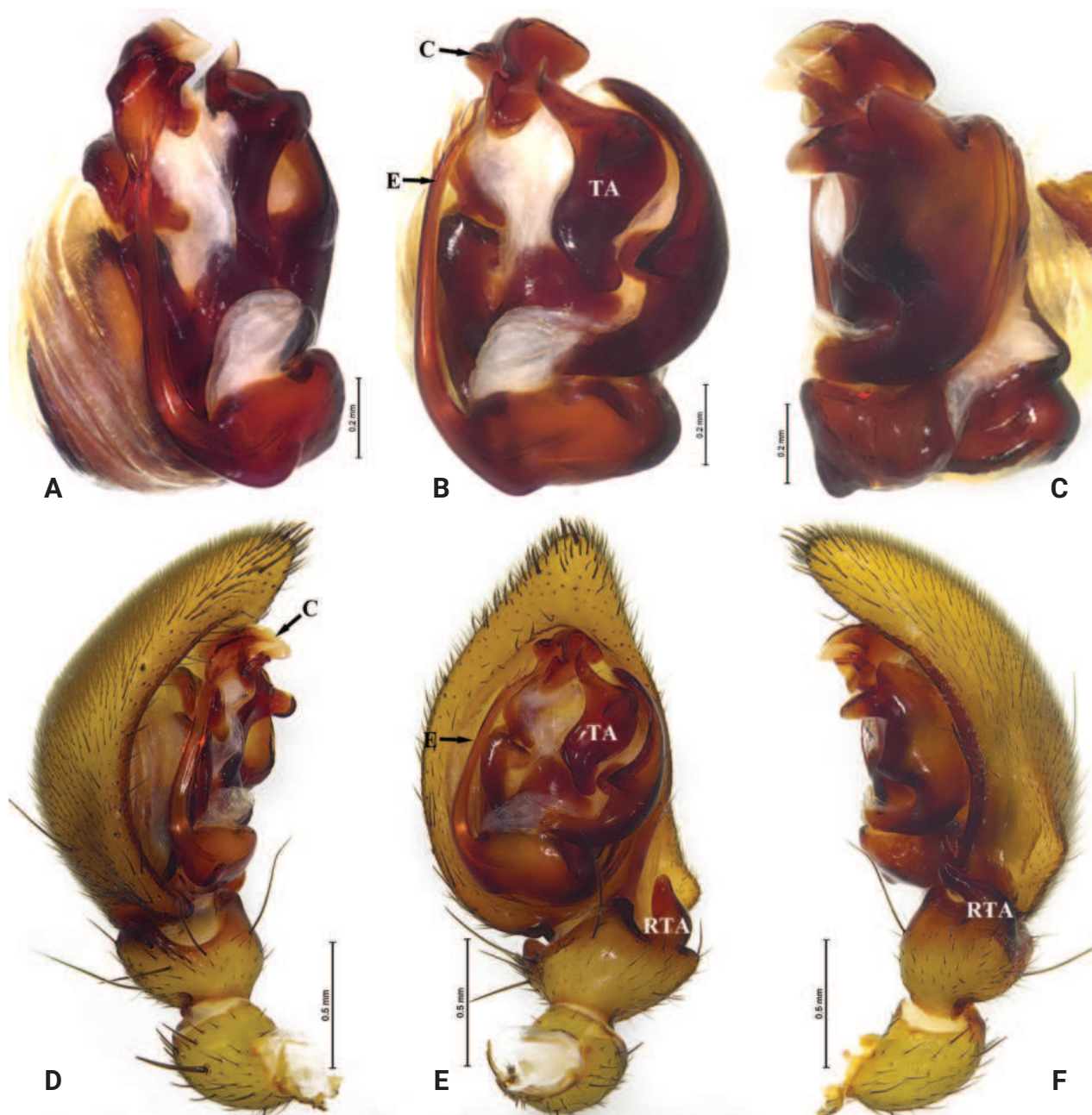


Figure 6. *Mallinella medog* sp. nov. **A–C** paratype male **D–F** holotype male **A** male left bulb, prolateral view **B** same, ventral view **C** same, retrolateral view **D** male left palp, prolateral view **E** same, ventral view **F** same, retrolateral view. Abbreviations: C = conductor; E = embolus; RTA = retrolateral tibial apophysis; TA = tegular apophysis.

29°19'36"N, 95°19'16"E; elev. 1008 m; 6 July 2023; L. Wang, F. Lu & X. Chen leg.; SWUCT-ZOD-04-15 and SWUCT-ZOD-04-16 • 10♂♂ 5♀♀; Beibeng Township, Badeng Village; 29°16'28"N, 95°10'7"E; elev. 851 m; 7 July 2023; L. Wang, F. Lu & X. Chen leg.; SWUCT-ZOD-04-17 to SWUCT-ZOD-04-31 • 1♂; Guoguo Tang; 29°19'10"N, 95°16'54"E; elev. 855 m; 8 July 2023; Z. Zhang, L. Wang, F. Lu & X. Chen leg.; SWUCT-ZOD-04-32 • 6♂♂ 2♀♀; Haishishenlou observation deck; 29°20'36"N, 95°20'43"E; elev. 1297 m; 8 July 2023; Z. Zhang, L. Wang, F. Lu & X. Chen leg.; SWUCT-ZOD-04-33 to SWUCT-ZOD-04-40.

Etymology. The specific name is derived from the type locality; it is a noun in apposition.

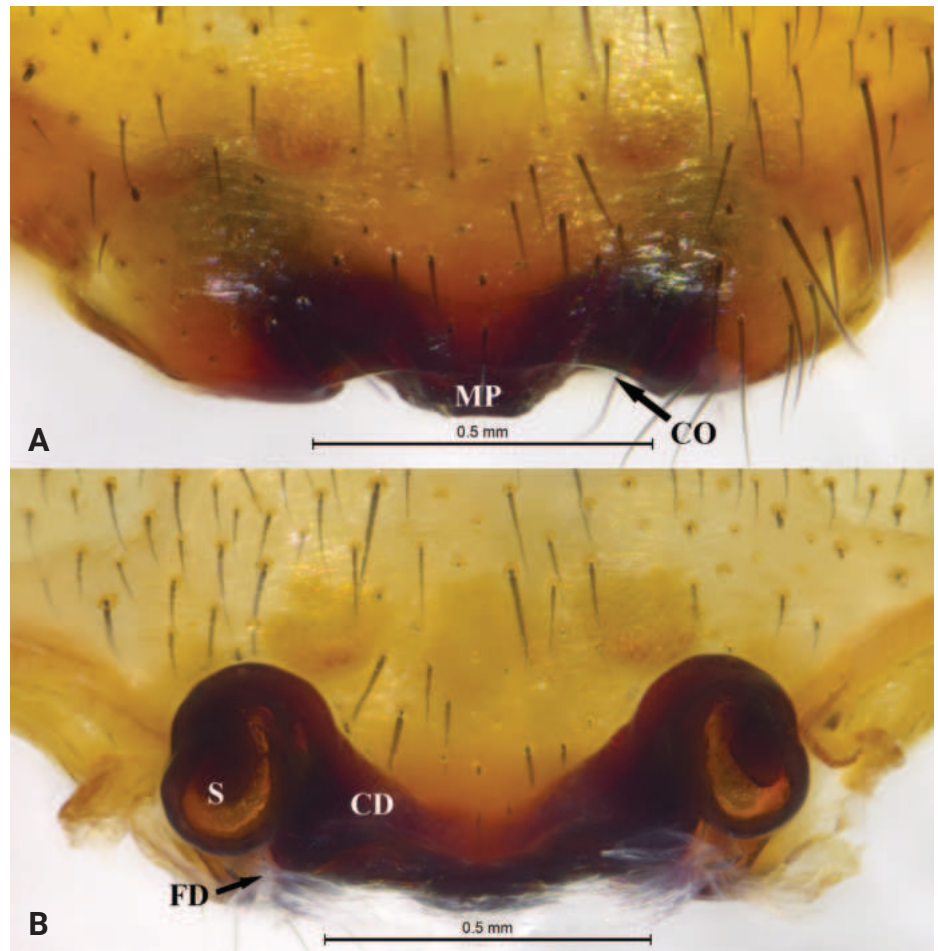


Figure 7. *Mallinella medog* sp. nov. paratype female **A** epigyne, ventral view **B** same, dorsal view. Abbreviations: CD = copulatory duct; CO = copulatory opening; FD = fertilization duct; MP = median plate; S = spermatheca.

Diagnosis. The male of this new species resembles *Mallinella martensi* (Ono 1983: 212, figs 1–4) and *M. migu* sp. nov., but it differs from these two species by the anterior of tegular apophysis rostrated in ventral view (vs not rostrated), retrolateral tibial apophysis curved ventrally in retrolateral view (vs vertical, not curved) (Fig. 6). The female of this new species resembles *M. sphaerica* Jin & Zhang, 2013 (Jin and Zhang 2013: 81, figs 7, 8, 12, 13) but differs by the wider copulatory ducts (vs thin copulatory ducts) (Fig. 7).

Description. Male holotype (Fig. 10B) total length 7.23. Prosoma 3.84 long, 2.60 wide; Opisthosoma 3.35 long, 2.28 wide. Eye sizes and interdistances: AME 0.30, ALE 0.21, PME 0.20, PLE 0.21; AME–AME 0.17, AME–ALE 0.12, PME–PME 0.16, PME–PLE 0.32, ALE–PLE 0.05. MOA 0.68 long, anterior width 0.65, posterior width 0.57. Clypeus height 0.88. Chelicerae with 1 promarginal and 3 retromarginal teeth. Leg measurements: I 13.24 (3.30, 3.88, 3.57, 2.49); II 12.12 (3.07, 3.53, 3.31, 2.21); III 11.39 (2.76, 3.29, 3.43, 1.91); IV 14.58 (3.42, 4.08, 4.65, 2.43). Leg formula: 4132. Carapace brown; fovea deep red, slightly swollen. Legs yellow. Opisthosoma oval, longer than wide, dorsum with two pairs of white spots, followed by two transverse white bands. Dorsal scutum thin, reddish brown. Spinnerets yellow.

Palp (Fig. 6). Tibia with two apophyses, ventral tibial apophysis small, arc-shaped; retrolateral tibial apophysis digitiform, strongly curved ventrally. Tegular apophysis wide at middle parts, apico-prolateral process rostrate, posterior process blunt. Embolus bifurcate, lateral ramus shorter than mesal ramus. Conductor sclerotized, apex of conductor irregularly fluctuating.

Female (Fig. 10C) total length 10.00. Prosoma 4.65 long, 3.25 wide; opisthosoma 5.31 long, 3.49 wide. Eye sizes and interdistances: AME 0.32, ALE 0.25, PME 0.26, PLE 0.27; AME–AME 0.18, AME–ALE 0.15, PME–PME 0.19, PME–PLE 0.39, ALE–PLE 0.07. MOA 0.80 long, anterior width 0.72, posterior width 0.68. Clypeus height 1.14. Leg measurements: I 12.91 (3.39, 3.98, 3.09, 2.45); II 11.88 (3.15, 3.60, 2.93, 2.20); III 11.76 (3.03, 3.45, 3.28, 1.92); IV 15.17 (3.61, 4.43, 4.48, 2.65). Leg formula: 4123. Carapace deep brown, opisthosoma black, other characters same as in male.

Epigyne (Fig. 7). Median plate small, nearly trapezoidal, with nearly straight posterior margin; copulatory openings hidden in a groove. Spermathecae oval; copulatory ducts thick; slender fertilization ducts hidden in dorsal view.

Distribution. Known only from the type locality, Xizang, China.

***Mallinella yadong* sp. nov.**

<https://zoobank.org/F4D1E17D-4B90-403A-80C6-47C5B0121A18>

Figs 8, 9, 10D, E

Chinese name: 亚东马利蛛

Type material. Holotype: CHINA • ♂; Xizang, Yadong County; 27°28'58"N, 88°54'14"E; elev. 3044 m; 10 July 2018; L. Wang, Z. Wu & Y. Mu leg.; SWUCT-ZOD-05-01.

Paratypes: CHINA – Xizang • 1♂ 1♀; same data as holotype; SWUCT-ZOD-05-02 and SWUCT-ZOD-05-03 • 1♀; Xiayadong Township, Asang; 27°24'20"N, 88°57'10"E; elev. 2870 m; 11 July 2018; L. Wang, Z. Wu & Y. Mu leg.; SWUCT-ZOD-05-04.

Etymology. The specific name is derived from the type locality; it is a noun in apposition.

Diagnosis. The male of this new species resembles *Mallinella uncinata* (Ono, 1983) (Ono 1983: 214, figs 5–8), but it differs by the anterior part of the tegular apophysis projecting laterally and rotated (vs not projecting laterally and not rotated) and short embolus (vs long) (Fig. 8). The female of this new species resembles *M. laxa* Zhang & Zhang, 2019 (Zhang and Zhang 2019: 10, figs 8G, H, 9F, G), but differs from it by the thinner copulatory ducts (vs thick copulatory ducts) and median plate with a trapezoidal depression (vs V-shaped depression) (Fig. 9).

Description. Male holotype (Fig. 10D) total length 7.80. Prosoma 3.66 long, 2.52 wide; Opisthosoma 3.94 long, 2.51 wide. Eye sizes and interdistances: AME 0.18, ALE 0.20, PME 0.20, PLE 0.23; AME–AME 0.14, AME–ALE 0.13, PME–PME 0.16, PME–PLE 0.27, ALE–PLE 0.08. MOA 0.64 long, anterior width 0.55, posterior width 0.53. Clypeus height 0.82. Leg measurements: I 11.56 (3.00, 3.52, 2.85, 2.19); II 10.75 (2.88, 3.22, 2.69, 1.96); III 10.45 (2.71, 2.94, 3.05, 1.75); IV 13.27 (3.10, 3.82, 4.11, 2.24). Leg formula: 4123. Carapace and fovea black, slightly swollen. Radial grooves distinct. Legs yellow. Opisthosoma oval,

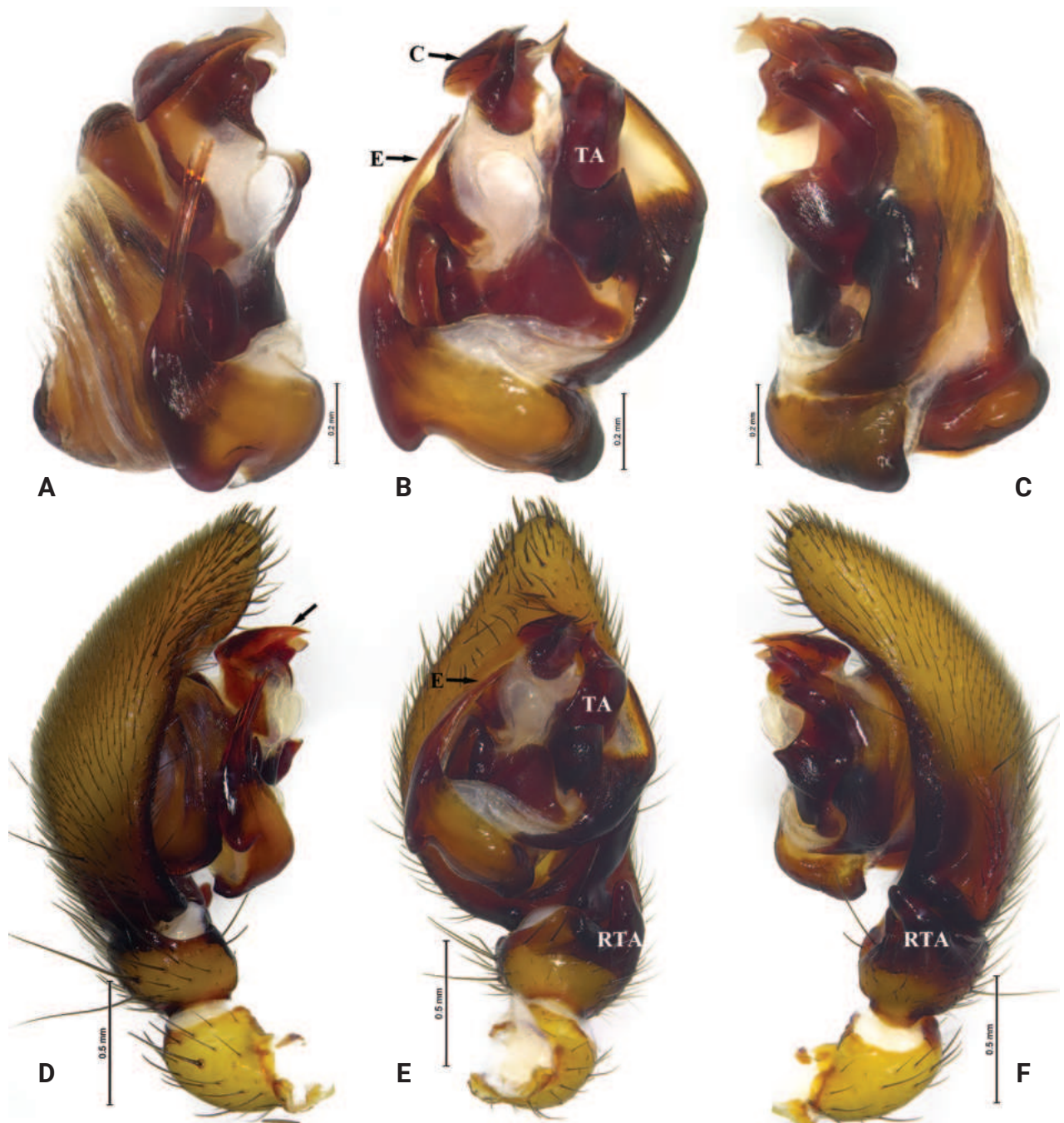


Figure 8. *Mallinella yadong* sp. nov. **A–C** paratype male **D–F** holotype male **A** male left bulb, prolateral view **B** same, ventral view **C** same, retrolateral view **D** male left palp, prolateral view **E** same, ventral view **F** same, retrolateral view. Abbreviations: C = conductor; E = embolus; RTA = retrolateral tibial apophysis; TA = tegular apophysis.

longer than wide, dorsum without any markings. Dorsal scutum indistinct. Spinnerets pale yellow.

Palp (Fig. 8). Tibia with two apophyses, ventral tibial apophysis small, arc-shaped; retrolateral tibial apophysis digitiform, curved ventrally. Tegular apophysis thin, apico-prolateral process projecting laterally, rotated, baso-retrolateral process trapezoid in retrolateral view. Embolus short, bifurcate, lateral ramus shorter than mesal ramus. Conductor sclerotized, apex of conductor irregularly fluctuating.

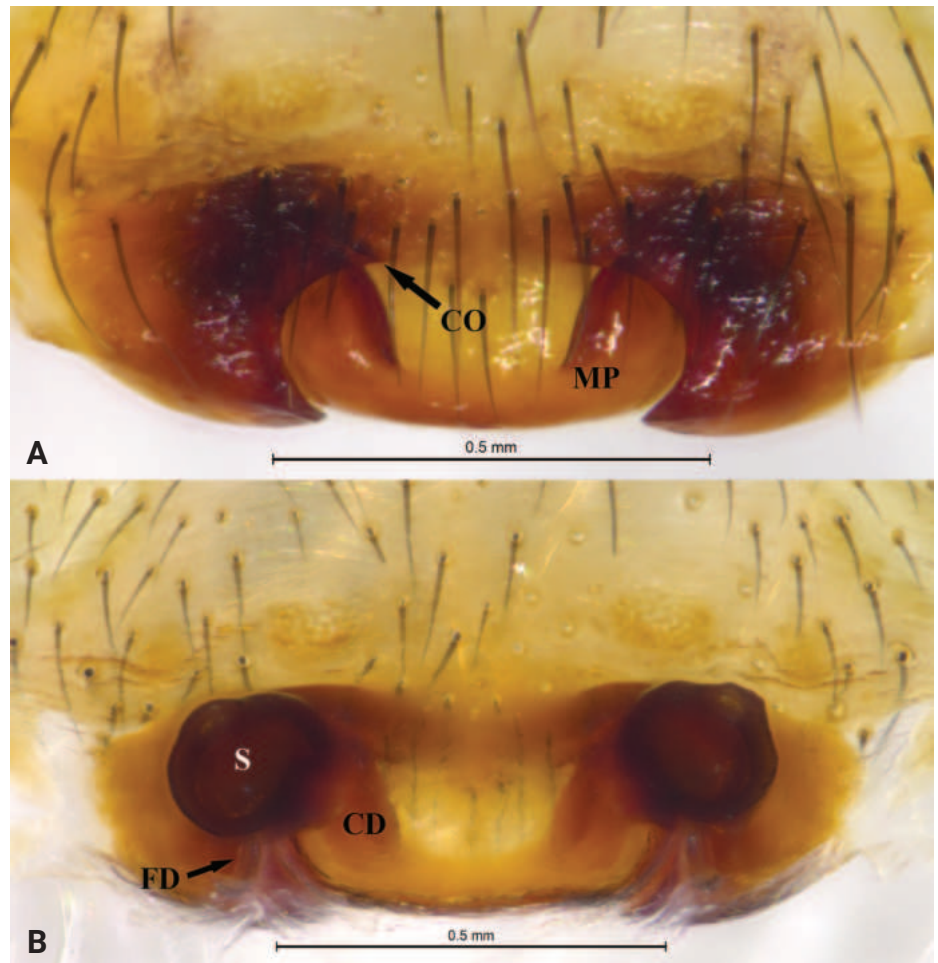


Figure 9. *Mallinella yadong* sp. nov., paratype female **A** epigyne, ventral view **B** same, dorsal view. Abbreviations: CD = copulatory duct; CO = copulatory opening; FD = fertilization duct; MP = median plate; S = spermatheca.

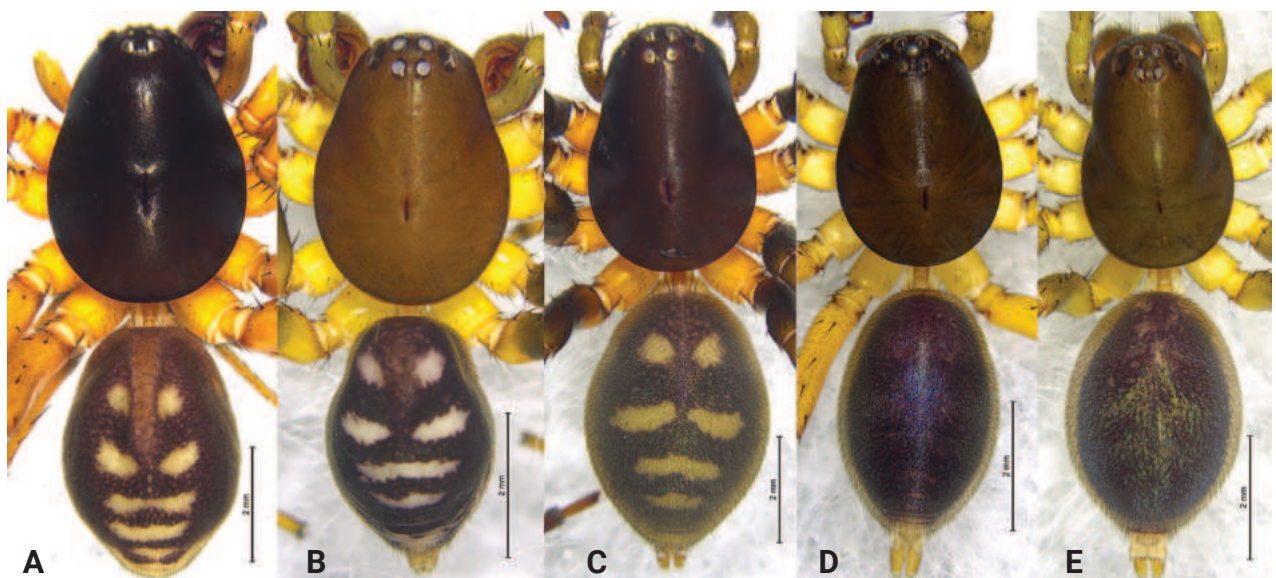


Figure 10. *Mallinella* spp. habitus, dorsal view **A** *Mallinella migu* sp. nov., male holotype **B** *Mallinella medog* sp. nov., male holotype **C** *Mallinella medog* sp. nov., female paratype **D** *Mallinella yadong* sp. nov., male holotype **E** *Mallinella yadong* sp. nov., female paratype.

Female (Fig. 10E) total length 7.96. Prosoma 3.82 long, 2.47 wide; opisthosoma 4.04 long, 2.77 wide. Eye sizes and interdistances: AME 0.18, ALE 0.19, PME 0.22, PLE, 0.18; AME–AME 0.12, AME–ALE 0.14, PME–PME 0.16, PME–PLE 0.28, ALE–PLE 0.11. MOA 0.59 long, anterior width 0.49, posterior width 0.56. Clypeus height 0.78. Leg measurements: I 8.98 (2.43, 2.92, 1.98, 1.65); II 8.62 (2.33, 2.71, 1.93, 1.65); III 8.55 (2.19, 2.68, 2.26, 1.42); IV 10.73 (2.66, 3.24, 3.09, 1.74). Leg formula: 4123. Other characters same as male except lighter color than male.

Epigyne (Fig. 9). Median plate large, with trapezoidal depression and slightly cambered posterior margin; copulatory openings hidden in groove. Spermathecae oval; copulatory ducts thin; slender fertilization ducts visible, directed posteriorly.

Distribution. Known only from the type locality, Xizang, China.

Acknowledgements

Many thanks to the anonymous reviewers and editor (Sarah Crews) for their valuable comments that greatly improved the manuscript. Many thanks are given to Mr Zhi-Sun Wu, Tao Yuan (SWU), Ms Piao Liu (SWU), and Hui Wang (College of Life Sciences, Hebei University, Baoding, China) for their assistance during fieldwork and collection.

Additional information

Conflict of interest

The authors have declared that no competing interests exist.

Ethical statement

No ethical statement was reported.

Funding

The Survey of Wildlife Resources in Key Areas of Tibet (ZL202203601), the Science & Technology Fundamental Resources Investigation Program (Grant No. 2022FY202100) and the Science Foundation of School of Life Sciences, SWU (20212020110501).

Author contributions

Writing – original draft: LYW, YX, YM, FL. Writing – review and editing: ZZ.

Author ORCIDs

Lu-Yu Wang  <https://orcid.org/0000-0002-5250-3473>

Yan-Nan Mu  <https://orcid.org/0000-0002-2504-673X>

Feng Lu  <https://orcid.org/0000-0001-6291-9117>

Yong-Qiang Xu  <https://orcid.org/0000-0002-1889-9531>

Zhi-Sheng Zhang  <https://orcid.org/0000-0002-9304-1789>

Data availability

All of the data that support the findings of this study are available in the main text.

References

- Álvarez-Padilla F, Hormiga G (2007) A protocol for digesting internal soft tissues and mounting spiders for scanning electron microscopy. *The Journal of Arachnology* 35(3): 538–542. <https://doi.org/10.1636/Sh06-55.1>
- Hu JL (2001) Spiders in Qinghai-Tibet Plateau of China. Henan Science and Technology Publishing House, Henan, 658 pp.
- Hu JL, Li AH (1987a) The spiders collected from the fields and the forests of Xizang Autonomous Region, China. (I). In: Zhang S (Ed.) *Agricultural Insects, Spiders, Plant Diseases and Weeds of Xizang*. Vol. 1. The Tibet People's Publishing House, Lhasa, 315–392.
- Hu JL, Li AH (1987b) The spiders collected from the fields and the forests of Xizang Autonomous Region, China. (II). In: Zhang S (Ed.) *Agricultural Insects, Spiders, Plant Diseases and Weeds of Xizang*. Vol. 2. The Tibet People's Publishing House, Lhasa, 247–353.
- Jin C, Zhang F (2013) Two new *Mallinella* species from southern China (Araneae, Zodariidae). *ZooKeys* 296: 79–88. <https://doi.org/10.3897/zookeys.296.4622>
- Ono H (1983) Zodariidae aus dem Nepal-Himalaya. I. Neue Arten der Gattung *Storena* Walckenaer 1805 (Arachnida: Araneae). *Senckenbergiana Biologica* 63: 211–217.
- Sankaran PM (2023) Taxonomic notes on the ant-eating spider genera *Asceua* Thorell, 1887 and *Cydrela* Thorell, 1873 from India, with comment on Indian species of *Euryeidon* Dankittipakul & Jocqué, 2004 (Araneae: Zodariidae). *Zootaxa* 5296(3): 381–405. <https://doi.org/10.11646/zootaxa.5296.3.4>
- WSC (2024) World Spider Catalog. Version 25.0. Natural History Museum Bern. <https://doi.org/10.24436/2> [Accessed 4 Feb. 2024]
- Zhang BS, Zhang F (2019) Four new species of the genus *Mallinella* (Araneae: Zodariidae) from Malaysia. *Zootaxa* 4568(2): 242–260. <https://doi.org/10.11646/zootaxa.4568.2.2>

A new noctuid genus and species (Lepidoptera, Noctuidae, Amphipyryinae, Psaphidini, Triocnemidina) from New Mexico and Texas, United States of America

Lars G. Crabo¹ 

¹ Adjunct Faculty, Washington State University, Pullman, Washington, USA
Corresponding author: Lars G. Crabo (lcrabo@nwrads.com)

Abstract

Poolea **gen. nov.** is described for two noctuid species from southwestern United States: *Poolea grandimacula* Barnes & McDunnough, **comb. nov.**, previously in *Oxycnemis* Grote, and *Poolea psaphidoides* **sp. nov.** *Poolea* is compared to *Oxycnemis* (Amphipyryinae, Psaphidini, Triocnemidina) and is retained in the same subtribe. Adult moths and male and female genitalia of *Poolea* species are illustrated along with those of *Oxycnemis advena* Grote, the genus type species. Pertinent recent taxonomic changes to Amphipyryinae classification are reviewed.

Key words: Chihuahuan desert, DNA barcode, key, new combination, new genus, new species, owlet moth, systematics



Academic editor: José Luis Yela
Received: 23 December 2023
Accepted: 15 April 2024
Published: 8 May 2024

ZooBank: <https://zoobank.org/2D1C2F26-91CE-43AD-A668-0A104092D1D8>

Citation: Crabo LG (2024) A new noctuid genus and species (Lepidoptera, Noctuidae, Amphipyryinae, Psaphidini, Triocnemidina) from New Mexico and Texas, United States of America. ZooKeys 1200: 199–213. <https://doi.org/10.3897/zookeys.1200.117772>

Copyright: © Lars G. Crabo.
This is an open access article distributed under terms of the Creative Commons Attribution License (Attribution 4.0 International – CC BY 4.0).

Introduction

An undescribed noctuid species that superficially resembles several species of *Psaphida* Walker but is congeneric with “*Oxycnemis*” *grandimacula* Barnes & McDunnough (Amphipyryinae, Psaphidini) was collected during the spring of 2020 in New Mexico, USA. “*Oxycnemis*” *grandimacula* and the newly found species differ significantly from *Oxycnemis advena* Grote (Psaphidini, Triocnemidina), the type species of *Oxycnemis* Grote, and cannot be assigned satisfactorily to any extant genus. Description of this species and a genus for it and its congener “*Oxycnemis*” *grandimacula* are the main purposes of this communication.

The noctuid subfamily Amphipyryinae has a long and tumultuous history, which is reviewed partially in the Systematics section. Significant contributions to the currently accepted classification were advanced by Poole (1995, 2022), including on the unpublished website Nearctica.com—cited here as 2022, the year it was accessed, although it was written at unknown times at least a decade or two earlier. On this website, “*Oxycnemis*” *grandimacula* and an undescribed congener, almost certainly the same as the New Mexico moth, were assigned to an undescribed genus in Triocnemidina. Poole did not name the genus nor the species, and neither has been described formally until now. Nonetheless, Poole’s (1995, 2022) work provides a solid morphological framework for the subtribe, as well as pointing out several other taxa in need of further study.

Material and methods

Wing pattern and genitalia structure terminology follow Lafontaine (2004). Forewing length from base to apex, excluding the fringe, is measured to the nearest half millimeter.

Genitalia were prepared by the methods of Hardwick (1950) and Lafontaine (2004). The detached abdomen was macerated in hot 10% potassium hydroxide for 20–30 minutes. Dissection was performed in water followed by hardening in 95% isopropyl alcohol. Male vesicae and female bursae were inflated. Preparations were stained with orcein (Sigma Chemical Company, St. Louis, Missouri) and mounted in Euparal (Bioquip Products, formerly of Rancho Dominguez, California). Spacers were used to elevate the cover glasses from the slides in order to preserve the three-dimensional shape of the inflated structures.

The 658 base pair “barcode” region of mitochondrial *cox1 mt* DNA (hereafter “DNA barcode”) was used to assess the taxonomic placement of species and genera. Legs from dried specimens submitted to the Barcodes of Life Data System (BOLD) at the University of Guelph (Ontario, Canada) were analyzed by standard extraction, amplification, and sequencing protocols (Hebert et al. 2003). Barcodes were compared to existing material at BOLD as implemented at barcodinglife.org. The seven-digit Barcode Index Numbers (BIN) (Ratnasingham and Hebert 2013) are assigned by BOLD.

The distribution map was made using SimpleMappr (<http://simplemappr.net>).

Repository abbreviations

- CNC** Canadian National Collection of Insects, Arachnids, and Nematodes, Ottawa, Ontario, Canada
CSUC Colorado State University Collection, Fort Collins, Colorado, USA
DLWC Dave Wikle personal research collection, San Marino, California, USA
JVC Jim Vargo personal research collection, Mishawaka, Indiana, USA
LGC Lars Crabo personal research collection, Bellingham, Washington, USA
NMNH National Museum of Natural History, Smithsonian Institution, Washington D.C., USA

Systematics

Triocnemidina was described by Poole (1995) originally as a tribe of Psaphidiinae and was revised informally on Nearctica.com (Poole 2022). This subtribe is defined by a combination of adult characters (Poole 1995, 2022): head with unmodified frons and simple or weakly serrate male antenna; prothoracic tibia with a strong clawlike seta continuous with a knifelike ridge along the tibia, often with an accessory claw (Fig. 10); hindwing cross vein *mdc* with concave anterior segment and laterally-directed angle at strong *M2*; abdominal spiracles with weak distal wall and well-developed dorsal lever; male *A7* tergum large, thickly sclerotized, with weakly bilobed distal margin; male valve simple, with porrect spinelike ampulla of the clasper arising near the ventral margin, and hairlike setae but no corona on the unmodified cucullus (Figs 5a, 6a); male phallus with tubular vesica bearing one or two patches of spinelike setae set on crenulate bands (Figs 5b, 6b); female bursa copulatrix simple with or without

segmented bandlike signum (Figs 8, 9); and external tympanum with large hood with large ovate or rectangular bulla.

Triocnemidina is a small subtribe mostly from deserts of southwestern United States and Mexico. Poole included in it eight described and three undescribed species in seven genera: four named genera (*Crimona* Smith, *Oxycnemis*, *Policoenemis* Benjamin, and *Triocnemis* Grote), one described subsequently (*Unciella* Troubridge, 2008), and two that have remained undescribed ("Triocnemidina New Genus 1," described below, and "Triocnemidina New Genus 3" for "*Unciella*" *flagrantis* (Smith)). Each of these genera contains only one or two species. Several changes to the subtribe have occurred since it was first proposed: Triocnemidini was removed briefly from Psaphidinae based on pupa morphology and larva biology (Kitching and Rawlins 1999), but reassigned to it by Fibiger and Lafontaine (2005); Psaphidinae was subsumed as a tribe of Amphipyriinae based on larva morphology (Wagner et al. 2008); *Unciella* was described; and *Oxycnemis* was found to be a paraphyletic assemblage of genera belonging in two subfamilies (Keegan et al. 2019). In the latest checklist of Pohl and Nanz (2023) "*Oxycnemis*" *gracillinea* Grote is moved provisionally to *Sympistis* Hübner (Oncocnemidinae) along with "*Oxycnemis*" *acuna* (Barnes), and *Hemigrotella argenteostriata* Barnes & McDunnough is included in Triocnemidina for the first time. The latest changes are based on the seminal studies of Keegan et al. (2019, 2021) which are discussed further below.

***Poolea* gen. nov.**

<https://zoobank.org/70148D54-09C8-4489-807C-11739AAAAB08>

Type species. *Oxycnemis grandimacula* Barnes & McDunnough.

Gender. Feminine.

Diagnosis. Adults (Figs 2, 3) are medium-sized moths (FW length 11.5–16.0 mm) with gray forewings with large black-outlined spots, reniform spots weakly quadrate. They superficially resemble *Psaphida* or *Pseudocopivaleria* Buckett & Bauer (Amphipyriinae, Psaphidini, Psaphidina) but can be distinguished by their modified foretibial setae, a strong claw continuous with a knifelike ridge along the tibia and a distinct smaller lateral accessory claw in *Poolea* (Fig. 10), simple in the other genera. This claw shape also distinguishes *Poolea* from superficially similar species of *Sympistis*, which lack an accessory claw. The few Triocnemidina species that resemble *Poolea* in size and shape, particularly *Triocnemis saporis* Grote and *Unciella primula* Smith, are predominantly whitish or yellow tan instead of gray.

Male valves of *Poolea* (Figs 5a, 6a) are similar to those of *Triocnemis*, simple with a moderate sacculus and a narrow thornlike clasper of the ampulla arising near the ventral margin slightly past the midpoint of the valve. However, the uncus of *Poolea* is unique in Triocnemidina, straight and rodlike, oriented slightly dorsad at base, with slight subapical swelling and short fingerlike apex with a slight downward hook. That of *Triocnemis* is curved, tapering evenly from base to apex. The vesica of *Poolea* (Figs 5b, 6b) is bent subbasally and bears a single long band of spinelike setae of variable lengths.

The female genitalia of *Poolea* (Figs 8, 9) are also distinctive. The bursa copulatrix is asymmetric with the ovoid corpus bursae joined obliquely to the ductus bursae and extending posterior and leftward. The corpus bursae lack

signa, and the ductus seminalis is joined to the conical posterior end. Most of the ductus bursae is sclerotized and has longitudinal rugae, with a membranous short posterior segment adjacent to the weakly sclerotized ostium bursae. The anterior apophysis is longer than the posterior apophysis. The ovipositor lobe is padlike.

Poolea grandimacula was described as an *Oxycnemis*, type species *O. advena* (Fig. 1). It remained in the genus until the most recent North American checklist (Pohl and Nanz 2023). A footnote by section author B. C. Schmidt states that there is no named genus for *grandimacula*, and it is placed in "*Oxynemis*" with quotation marks to distinguish it from *Oxycnemis* sensu stricto. *Poolea* is significantly structurally distinct from *Oxycnemis* in both sexes. The male valve of *Oxycnemis advena* (Fig. 4a) is a nearly featureless strap with a rounded apex, simpler than those of *Poolea*, lacking a distinct sacculus and bearing a small nubbinlike triangular ampulla. The uncus of *Oxycnemis* is curved, with well-developed sacculus and clasper. The vesica of *Oxycnemis* (Fig. 4b) is nearly straight with two bands of setae; that of *Poolea* is bent with a single band of setae. The female corpus bursae of *Oxycnemis* (Fig. 7) is entirely membranous, volumetric-flask-shaped with a spherical corpus bursae and tubular ductus bursae. Unlike *Poolea* it has a long segmented signum and the ductus seminalis is at the anterior end. The papilla analis of *Oxycnemis* is conical rather than padlike.

DNA barcodes also clearly support that *Poolea* and *Oxycnemis* are distinct genera (Fig. 11). The two *Poolea* species differ by over seven percent from *O. advena*, a larger difference than between most other genera in the subtribe.

Description. Adult. Sexes superficially similar, of medium size (forewing length 11.5–16.0 mm). Vestiture of dorsal head and dorsal thorax black, grayish tan, and white long predominantly simple and scattered apically forked or spatulate serrate scales, concolorous with dorsal forewing. *Head* – Antenna of both sexes filiform, setose ventrally, dorsal scales small. Eye normal size, lacking hairs. Frons convex, lacking tubercle, scales thin, mesially directed. Labial palpus relatively short, reaching mid eye, vestiture of short straplike lateral and long piliform ventral scales. Haustellum normal. *Thorax* – Prothoracic collar with weak mesial crest and subbasal black transverse line; tegula with weak black line near medial margin; meso- and metathorax with loose tufts of curly spatulate glossy black scales, posterior tufts largest. *Legs* – Foretibia with distal stout trifurcate clawlike seta, apical process a large stout beaklike spine projected along foretarsus, middle process a small outer claw directed slightly laterally, basal process a knifelike ridge along tibia; mid- and hindlegs unmodified; ventral tarsi segments with scattered spiniform setae between haphazard inner and outer rows. *Wings* – Forewing elongate, length 2.3–2.6× width, with bluntly pointed apex and smoothly convex outer margin with slight indent at Cu₂; dorsal scales smooth, short, slightly convex distally with finely crenulate margin; ground light to charcoal gray or dark olive, darkest in medial area outside spots; transverse lines and spot outlines black, single; basal line absent; antemedial line smooth, thick, excurved strongly from anterior margin to fold, less prominently thence to posterior margin, bordered medially by uniform pale line; medial line absent or a dark smudge posterior to orbicular spot; postmedial line nearly parallel to outer margin, drawn slightly basad in fold, moderately scalloped between veins, posterior segment thickest, bordered laterally by gray to white, palest and widest in fold; subterminal line absent; terminal line

thin, preceded by triangular dark marks between veins in one species; spots large, filled with wing base color or slightly lighter shade; orbicular spot ovoid; claviform spot semicircular; reniform spot quadrate with rounded corners, slightly concave medially and laterally; fringe weakly checkered ground color or brown with slightly darker gray; scattered black dashes on veins (one species), strongest in fold in medial area and on Cu2 distal to postmedial line. Hindwing M2 strong, similar to mdc but weaker than M1 and M3, crossvein mdc concave anterior to M2, angled distad at M2, thence perpendicular to M3; dorsum white, few dark gray scales at tornus, on terminal line and distal veins, especially Cu2; fringe white with scattered gray scales. *Abdomen* – Lacking basal scent brushes and associated structures. A7 tergum large and strongly sclerotized, distal margin weakly bilobed. Spiracles with degenerate distal wall and long dorsal lever, resembling upper component of a question mark. Scales gray tan, weak darker dorsal tufts on segments 1, 3, and 4. *Male genitalia* – Uncus base directed posterior and slightly dorsad, with slight subbasal dorsad and subapical ventrad bends, cylindrical with slight subapical swelling bearing few short setae on flat venter, tip tapered to small downward hook with blunt tip. Juxta shield shaped, taller than wide. Valve nearly even width, widest near midpoint, length 3.6–4.0× width, with rounded slightly upturned apex bearing a mesial patch of downy setae; sacculus moderately strong, 0.5× valve length and 0.5× valve width at midpoint, tapered evenly from base to apex; clasper base a sclerotized bar near ventral margin distal to sacculus, ampulla base arising near valve midpoint (one species) or at outer $\frac{3}{4}$ (one species), perpendicular to valve, nearly reaching dorsal margin, thornlike, narrow, tapered to thin acute tip; digitus absent. Phallus tubular, length $\sim 6\times$ minimum width; vesica with broad basal dorsal bulge and subbasal 90–135° bend ventrad and anterior, about as long and slightly wider than phallus, widest near apex; mid and distal surface covered by broad band of multiple variable-length spiniform cornuti extending from left posterior surface distal to bulge to apex where it spirals $\frac{3}{4}$ around circumference, cornuti longest at mid vesica, gradually decreasing distally, subbasal cornuti longer and thicker than adjacent cornuti in one species. *Female genitalia* – Corpus bursae unisaccate, asymmetrically ovoid with membranous bulbous anterior end and thicker broadly conical thicker posterior end with ductus seminalis at apex, length about 1.5× width, lacking signa. Ductus bursae 5× segment A8 length, tubular (one species) or with anterior broad bulge rightward (one species), constricted slightly at junction of anterior $\frac{3}{4}$ and posterior $\frac{1}{4}$, short posterior segment membranous, anterior segment sclerotized with longitudinal rugae, joined obliquely to right posterior corpus bursae; ostium bursae weakly sclerotized. Papilla analis soft, padlike, covered with uniform thin piliform setae. Segment A8 short, length 2.7× width, dorsum longest; apophyses relatively short, posterior apophysis 1× segment A8 length, anterior apophysis 1.5× posterior apophysis.

Etymology. The genus name honors Robert “Bob” Poole for his contributions to the systematics of Amphipyridae.

Distribution and ecology. *Poolea* species occur in southwestern United States and Mexico, predominantly in the Chihuahuan desert region. All United States records are from Arizona, New Mexico, and Texas. Adults fly in arid shrubland from spring to fall (one species) or spring (one species). The early stages are unknown.

The large foretibial claw of *Poolea* is probably an adaptation to allow moths to escape from the pupal chamber in hard desert soils and dig their way to the ground surface.

Key to adults of *Poolea* and *Oxycnemis advena*

- 1 Foretibial claw with strong lateral accessory claw (Fig. 10); male valve with long thornlike ampulla of clasper (Figs 5a, 6a); female ductus bursae strongly sclerotized with longitudinal rugae (Figs 8, 9) ***Poolea***
- Foretibial claw simple, lacking accessory claw; male valve with diminutive triangular ampulla of clasper (Fig. 4a); female ductus bursae membranous (Fig. 7) ***Oxycnemis advena***
- 2 Smaller species (forewing length 11.5–15 mm); forewing medium gray with distinct longitudinal black dashes (Fig. 2); male valve with ampulla of clasper arising on distal valve closer to base of cucullus than to sacculus (Fig. 5a); female ductus bursae tubular, broadest anteriorly (Fig. 8) ***P. grandimacula***
- Larger species (forewing length 14–16 mm); forewing charcoal gray to dark olive without dashes (Fig. 3); male valve with ampulla of clasper arising on mid valve near sacculus (Fig. 6a); anterior female ductus bursae broadly convex toward right (Fig. 9) ***P. psaphidoides***

***Poolea grandimacula* (Barnes & McDunnough), comb. nov.**

Figs 2, 5a, b, 8

Oxycnemis grandimacula Barnes & McDunnough, 1910

Oxycnemis extremis Barnes & McDunnough, 1913

Type material. *Oxycnemis grandimacula* was described from Redington, Arizona (NMNH) (holotype examined from photograph). *Oxycnemis extremis* was described from two syntypes, one from Brownsville and the other from San Benito, Texas (NMNH) (syntypes examined from photographs). The Brownsville syntype is darker than most *P. grandimacula*, but its forewing pattern is otherwise typical of this species.

Diagnosis. *Poolea grandimacula* is distinguished by several longitudinal black lines on the forewing antemedial, medial, and postmedial areas which *Poolea psaphidoides* lacks. *Poolea grandimacula* tends to be smaller than *P. psaphidoides* (FW length of *P. grandimacula* 11.5–15 mm; *P. psaphidoides* 14–16 mm) and the FW is lighter gray with more discernible pattern. The ampulla of the clasper of the male valve arises more distally in *P. grandimacula* than in *P. psaphidoides* as described in the key. Females can be distinguished by the shape of the ductus bursae, tapered evenly in *P. grandimacula* and bulging rightward near the junction with the corpus bursae in *P. psaphidoides*.

Distribution and ecology. *Poolea grandimacula* occurs in southwestern United States in Arizona, New Mexico, and western and southern Texas. Poole (2022) also examined a specimen from Nuevo León, Mexico. Adults fly in open xeric habitats and have been collected as early as March and as late as October, suggesting multiple broods. The early stages are unknown.



Figures 1–3. Adult males **1** *Oxycnemis advena* (abdomen removed), USA, Arizona, Maricopa County, Cave Creek **2** *Poolea grandimacula*, USA, Texas, Brewster County, Terlingua Ranch **3** *Poolea psaphidoides*, USA, New Mexico, Otero County, High Rolls.

This species and *P. psaphidoides* are sympatric in southern New Mexico, including at White Sands National Park, Otero County.

***Poolea psaphidoides* sp. nov.**

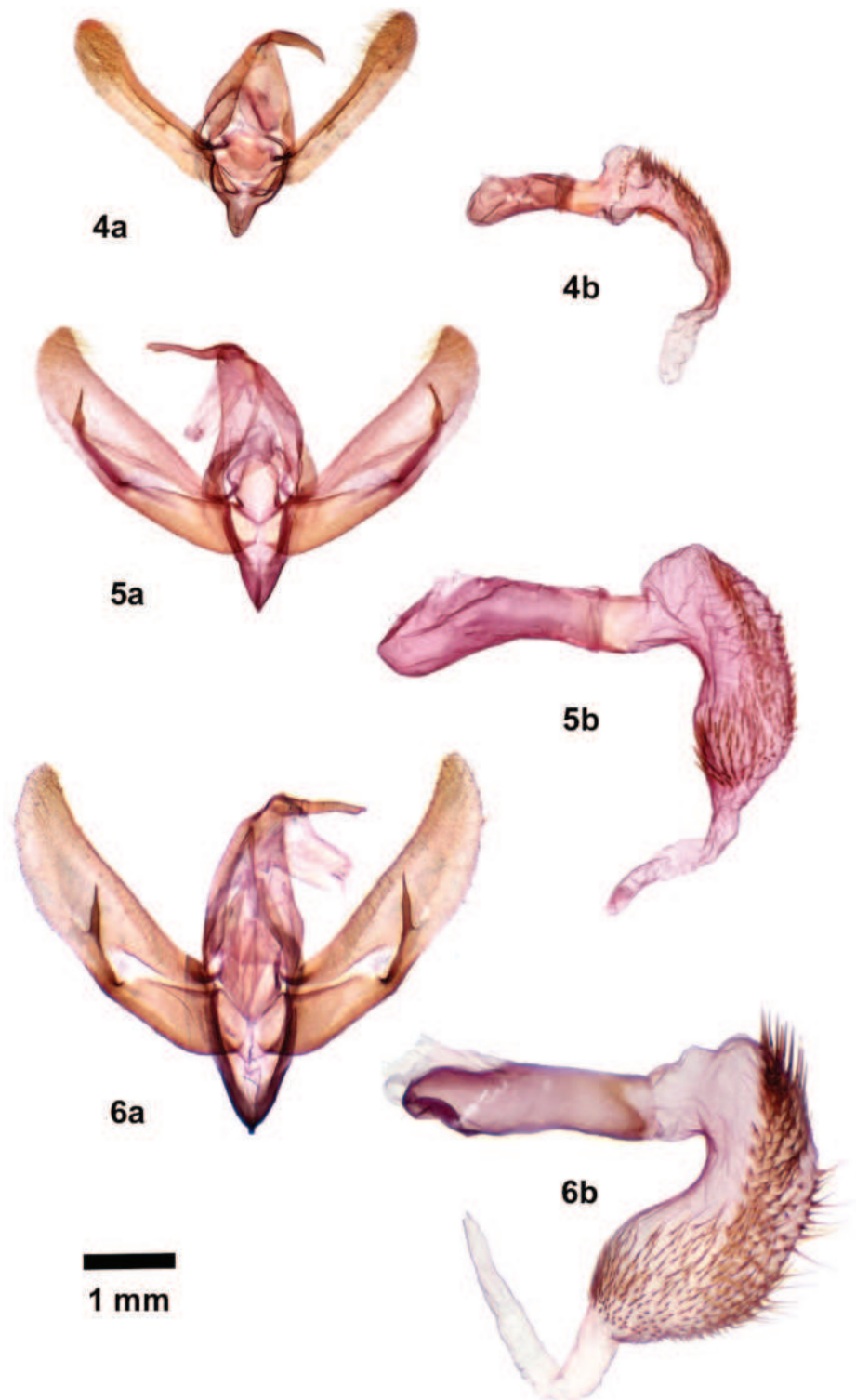
<https://zoobank.org/F5762B69-E68A-4D49-8C71-83415FF96CA2>

Figs 3, 6a, b, 9, 12

Type locality. USA: New Mexico: Otero County: High Rolls, Steep Hill Rd., 32.9534, -105.8817, 1725 m.

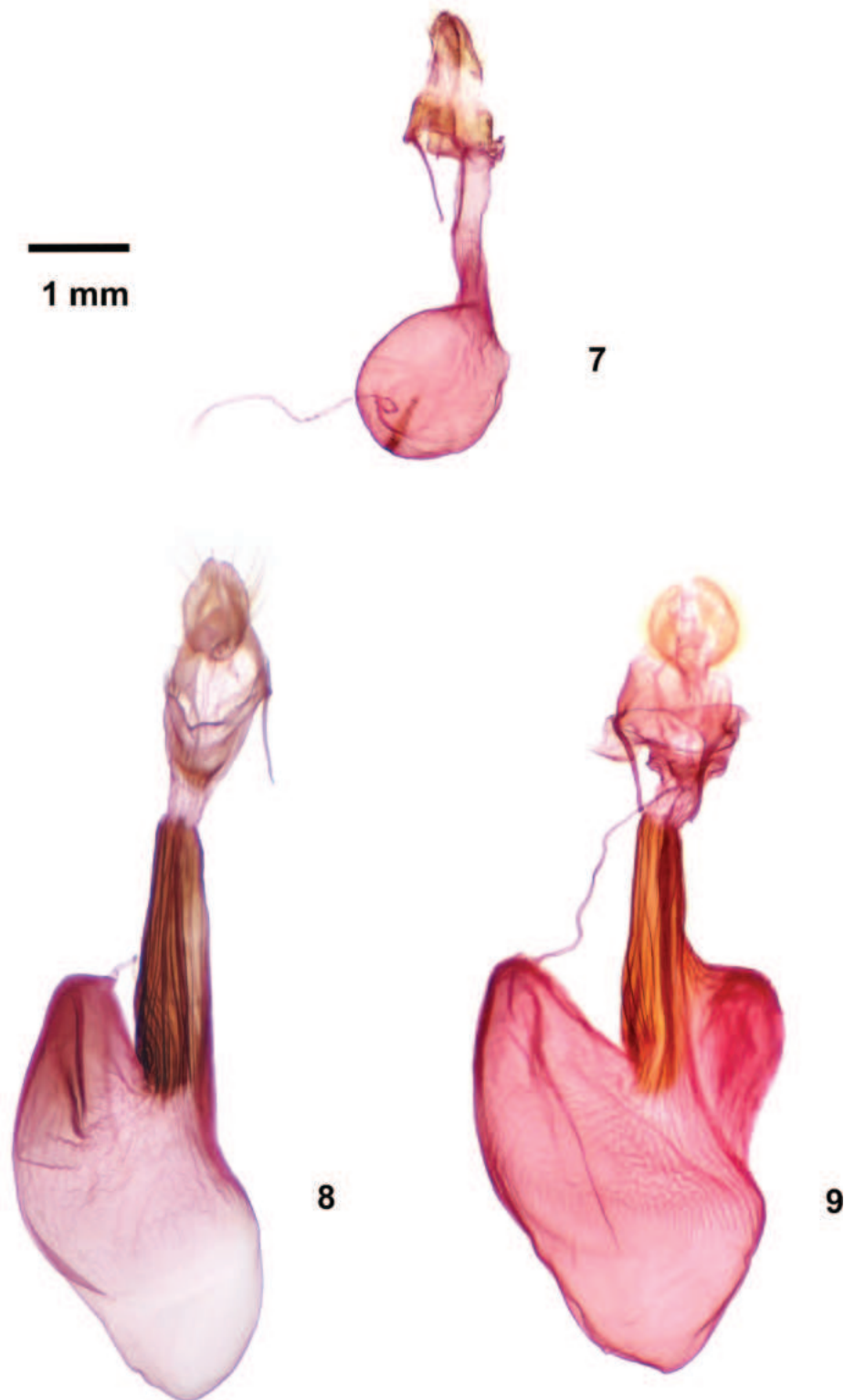
Type material. Holotype, male. USA: New Mexico: Otero County: High Rolls, Steep Hill Rd., 32.9534, -105.8817, 1725 m, 11 III 2020, L. G. Crabo leg. / [Crabo genitalia slide] 651 male. **CNC. Paratypes.** 15 m, 3 f. USA: New Mexico: Eddy County: 32.272, -104.602, 4200' [1280 m], 20 III 2021, J Vargo (8 m 2 f); Carlsbad, 32.4420, -104.2776, 1060 m, 4 III 2024, David Heckard / DLWC 011521 (1 m); Otero County: same data as holotype (3 males); same data as holotype / BOLD_F8 CHLC0068 (1 male); same data as holotype / BOLD_F9 CHLC0069 (1 male); White Sands National Park, SE edge of dunes, 32.761, -106.189, 1215 m, 11 III 2020, Eric Metzler leg. (1 female); Texas: Culberson County, Sierra Diablo Wildlife Management Area, 2 V [19]84, E. Knudson / CNCLEP7661 (1 male). CNC, CSUC, DLWC, JVC, LGC, NMNH.

Diagnosis. *Poolea psaphidoides* resembles *P. grandimacula* but is usually larger (FW length 14–16 mm compared to 11.5–15 mm) and has a darker



Figures 4–6. Male genitalia, valves (a) and phallus (b) with everted vesica 4 *Oxycnemis advena* 5 *Poolea grandimacula* 6 *Poolea psaphidoides*

charcoal to dark olive gray forewing lacking black streaks; the FW of *P. grandimacula* is medium gray with prominent longitudinal black bars. Pale scales distal to the distal postmedial line in *P. psaphidoides* appear as a distinct white spot in the fold.



Figures 7–9. Female genitalia **7** *Oxycnemis advena* **8** *Poolea grandimacula* **9** *Poolea psaphidoides*

The male genitalia of *P. psaphidoides* are most easily distinguished from *P. grandimacula* by the position of the clasper ampulla, close to the mid valve in *P. psaphidoides* and near the base of the cucullus in *P. grandimacula*. The cornuti on the vesica of *P. psaphidoides* are longer than those of *P. grandimacula*,



Figure 10. Foretibial claw of *Poolea psaphidoides* (photograph and drawing).

forming a group of long stout spines in the proximal band that *P. grandimacula* lacks. Females of *P. psaphidoides* have a large rightward bulge in the anterior ductus bursae, lacking in *P. grandimacula*.

The DNA barcode BIN of *P. psaphidoides*, BOLD:AEK0144, differs from that of *P. grandimacula*, BOLD:AAI5464, by greater than 4.2% (Fig. 11).

Description. Adults. Dorsal head and thorax charcoal gray. *Head* – As for genus. Antenna scales dark gray. Labial palpus scales mostly dark gray, scattered off-white on segments 2 and 3. Frons scales gray. *Thorax* – Vestiture as for genus; black lines on prothoracic collar and tegula indistinct. *Legs* – As for genus. *Wings*: FW length 14.0–16.0 mm (males); 15.0 mm (female); even charcoal gray, occasionally dark olive, with slightly darker gray medial area; lines and spots as for genus; medial line faint; pale scales abutting postmedial line white in fold; fringe weakly checkered brown gray and charcoal; horizontal black lines absent. HW as for genus, ground pure white. *Abdomen* – As for genus; tufts dark gray. *Male genitalia* – Uncus and juxta as for genus. Juxta height 2× width. Valve as for genus, length 5× width; ampulla arising slightly distal to mid valve. Phallus and vesica as for genus; a cluster of subbasal cornuti thicker and longer than adjacent cornuti; cornuti on mid vesica long and gracile, decreasing gradually in length toward vesica apex. *Female genitalia* – Papilla analis, segment A8, and bursa copulatrix as for genus. Ductus bursae with broad bulge rightward near attachment to corpus bursae.

Etymology. The name refers to the superficial resemblance of this moth to several *Psaphida* species from eastern North America.

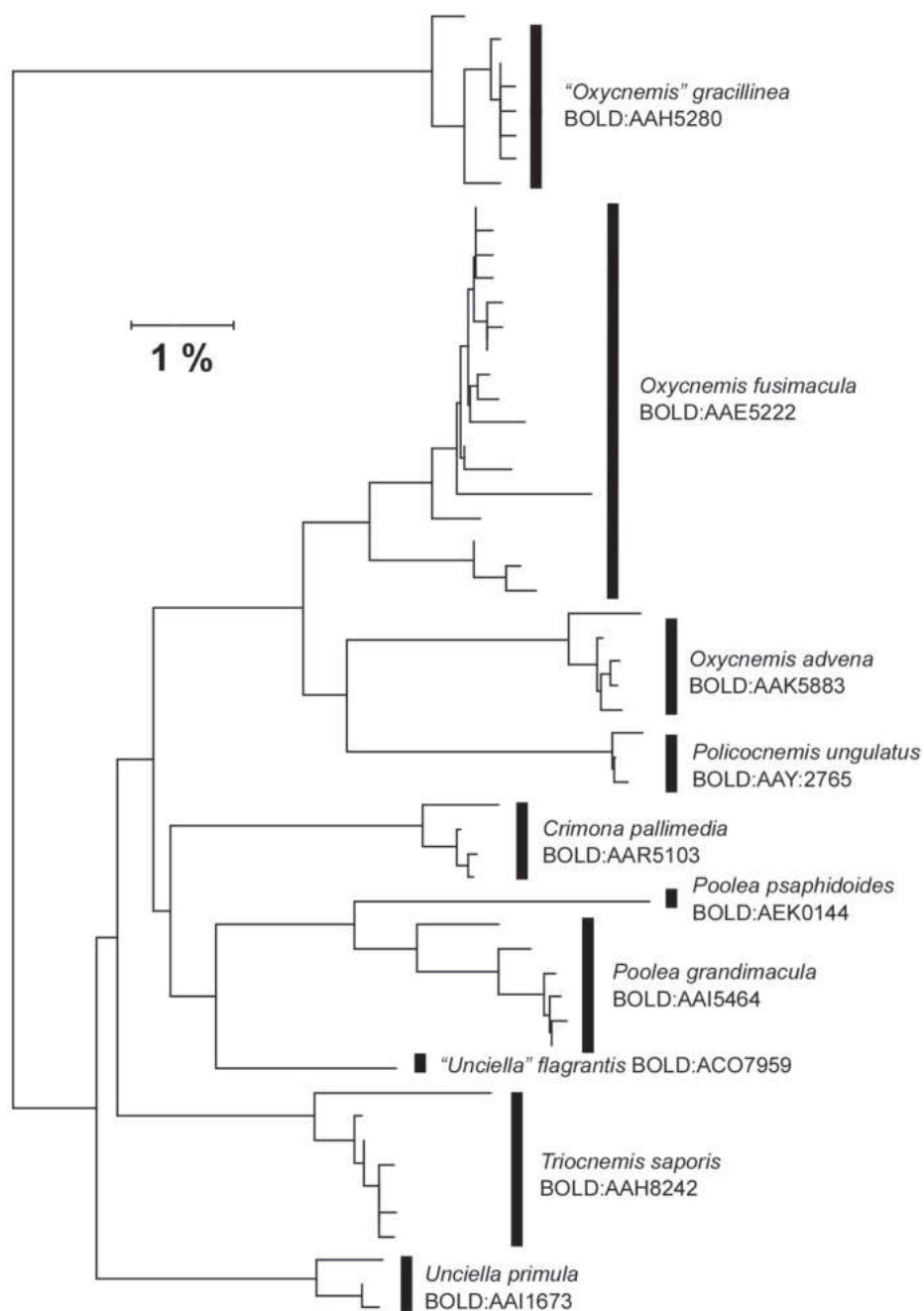


Figure 11. CO1 barcode neighbor-joining tree of North American Triocnemidina sensu Poole (2022): *Crimona*, *Oxycnemis*, *Policoccnemis*, *Poolea*, *Triocnemis*, *Unciella*, “*Unciella*.” “*Oxycnemis*” *gracillinea*, now reassigned to Onconemidinae and placed provisionally in *Sympistis*, is included for comparison.

Distribution and ecology. *Poolea psaphidoides* has a very limited distribution in the Southwest. It is only known definitively from four localities in southern New Mexico east of the Continental Divide, two each in Otero and Eddy counties, and one location in Culberson County in western Texas (Fig. 12). These localities span approximately 200 kilometers. Two specimens from near the Guadalupe Mountains in Texas called “Triocnemidini New Genus 1 new species 1” by Poole (2022) probably refer to *P. psaphidoides* based on the adult description and illustrated male genitalia but were not examined

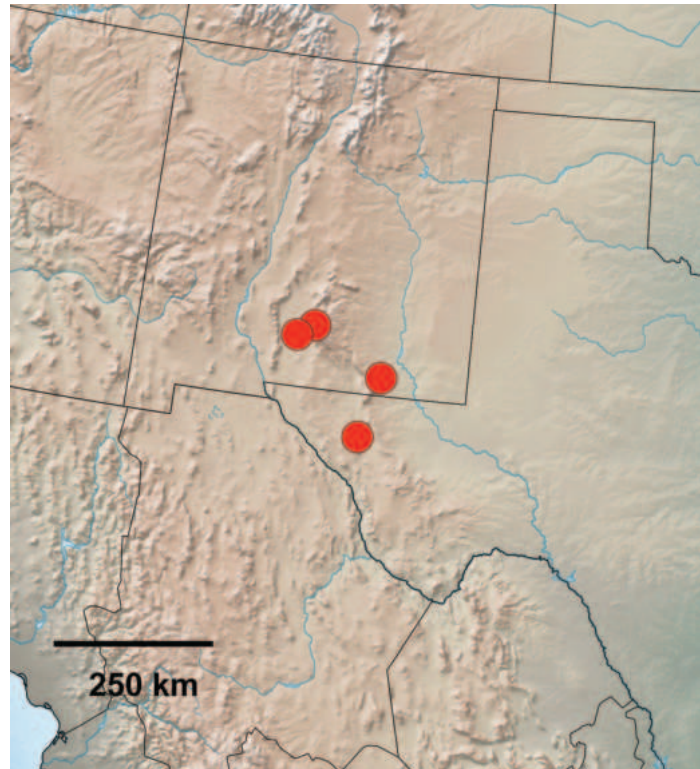


Figure 12. Distribution of examined material of *Poolea psaphidoides* in New Mexico and Texas, USA.

for this study. The Guadalupe Mountains are located within the known range of the species.

Poolea psaphidoides has been collected in open shrub desert at elevations from 1280 to 1725 meters. The type locality habitat consists of creosote bush [*Larrea tridentata* (DC.) Coville, Zygophyllaceae] shrubland with scattered junipers [*Juniperus* sp. (Cupressaceae) and bunchgrasses (Poaceae)]. One female is from gypsum dunes at White Sands National Park, possibly a stray since it is the only specimen of this species found at this locality in over a decade of intensive collecting (E. Metzler pers. comm. 2020). Collection dates are from mid-March to early May suggesting a single brood.

The early stages are unknown.

Discussion

Poolea and *Oxycnemis* are assigned to Amphipyrinae. No noctuid subfamily has been more difficult to define or seen greater flux—a history reviewed by Keegan et al. (2019). The number of genera in the subfamily has ranged from roughly half of the world's noctuid fauna when it was first proposed by Hampson in the late nineteenth century (Kitching 1984) to only the type genus a century later (Kitching and Rawlins 1999). In the newly published checklist of North American Lepidoptera north of Mexico (Pohl and Nanz 2023), the subfamily includes 30 genera that are arranged in two tribes.

The last published checklist of Noctuidae for North America north of Mexico prior to the 21st century was that of Franclemont and Todd (1983). Comparing Amphipyrinae in the Franclemont and Todd list to that of Pohl and Nanz

(2023) illustrates the massive changes that the subfamily has undergone in North America over four decades. Franclemont and Todd included 106 genera in Amphipyrinae. Fewer than a third of these genera remain in Amphipyrinae currently, and only half (15 of 30) of the amphipyrine genera in Pohl and Nanz were placed in their current tribe or subfamily in 1983.

A satisfactory delimitation of Amphipyrinae has been hampered by a lack of known synapomorphic morphological characters in this and related subfamilies, as well as limited knowledge of the early stages of many species (Keegan et al. 2019). Increased scrutiny of Noctuoidea higher classification around the turn of the last century produced an increasingly precise and cohesive classification of the subfamily, resulting first in its paring down to 73 genera by Lafontaine and Schmidt (2010, 2015). Shortly thereafter Keegan et al. (2019, 2021) probed most of the genera in Amphipyrinae sensu Lafontaine and Schmidt by sequencing multiple genes and corroborating the molecular results with adult morphology and recent discoveries of many larvae and their biology. They showed that the subfamily remained “massively” polyphyletic and reassigned a large number of amphipyrine taxa to other groups, including 10 different subfamilies. A few “amphipyrine” genera were even found to contain species of more than one subfamily, including *Oxycnemis* (Keegan et al. 2019). Despite these works, the subfamily classification remains mostly inferred from nucleotide states and relevant synapomorphies have yet to be defined precisely.

While Keegan et al.’s results provided the much-needed support for a satisfying rational Amphipyrinae classification, Psaphidini subtribes were not specifically addressed in either of their studies as they were poorly supported (Keegan et al. 2021, fig. 4) and beyond the scope of the papers which were focused on proper subfamilial placement of genera. More genetic data will be needed to fully resolve the intratribal relationships in Psaphidini. Nonetheless, the genera placed in Triocnemidina by Poole, along with *Hemigrotella argenteostriata*, are a sister group to a clade comprised of most of the genera in Psaphidina. Therefore, it is reasonable to follow this subtribe arrangement for the time being.

Although neither of the Keegan et al. studies (2019, 2021) included a *Poolea* species, its assignment to Triocnemidina based on morphological characters is supported strongly by DNA barcodes. *Poolea* consistently groups adjacent to *Crimona*, *Triocnemis*, *Unciella*, and “*Unciella*” on neighbor-joining trees (Fig. 11). *Crimona*, *Triocnemis*, and *Unciella* also form a clade in Keegan et al.’s maximum-likelihood trees. These five genera are also similar structurally, with similar wing shapes, foretibial claws, and male genitalia. The largest structural differences between the adults appear to be in the female genitalia based on a review of the illustrations in Poole (2022).

Acknowledgements

I am grateful to the following persons for help with this work. Merrill Peterson photographed the adults and genitalia at Western Washington University. Paul Goldstein shared photographs of NMNH type specimens. Chuck Harp submitted specimens to BOLD for barcoding and reviewed an early version of the manuscript. J. Donald Lafontaine accessed barcode data at BOLD Systems. Eric Metzler (deceased) helped to decipher the generic placement of the new species. Chris Schmidt (CNC) provided a female *P. grandimacula* for dissec-

tion, reviewed the manuscript, and provided constructive criticism. Jim Vargo shared *P. psaphidoides* specimens from Eddy County, New Mexico, including a female for dissection. Kevin Keegan reviewed the manuscript and provided helpful critique.

Additional information

Conflict of interest

The author has declared that no competing interests exist.

Ethical statement

No ethical statement was reported.

Funding

No funding was reported.

Author contributions

Conceptualization: LGC. Investigation: LGC. Writing - original draft: LGC.

Author ORCIDs

Lars G. Crabo  <https://orcid.org/0009-0004-1089-5511>

Data availability

All of the data that support the findings of this study are available in the main text.

References

- Barnes W, McDunnough JH (1910) New species and varieties of North American Lepidoptera. *Journal of the New York Entomological Society* 18: 149–162.
- Barnes W, McDunnough JH (1913) New N. Am. Lepidoptera with notes on described species. *Contributions to the Natural History of the Lepidoptera of North America* 2: 93–162.
- Fibiger M, Lafontaine JD (2005) A review of the higher classification of the Noctuoidea (Lepidoptera) with special reference to the Holarctic fauna. *Esperiana. Buchreihe zur Entomologie* 11: 1–205.
- Franclemont JG, Todd EL (1983) Noctuidae. In: Hodges RW et al. (Eds) *Check list of the Lepidoptera of America north of Mexico*. E. W. Classey Ltd. and The Wedge Entomological Research Foundation, London, 284 pp.
- Hardwick DF (1950) Preparation of slide mounts of lepidopterous genitalia. *Canadian Entomologist* 10(11): 231–235. <https://doi.org/10.4039/Ent82231-11>
- Hebert PDN, Cywindka A, Ball SL, deWaard JR (2003) Biological identifications through DNA barcodes. *Proceedings. Biological Sciences* 270(1512): 313–321. <https://doi.org/10.1098/rspb.2002.2218>
- Keegan KL, Lafontaine JD, Wahlberg N, Wagner DL (2019) Towards resolving and redefining Amphipyryinae (Lepidoptera, Noctuoidea, Noctuidae): A massively polyphyletic taxon. *Systematic Entomology* 44(2): 451–464. <https://doi.org/10.1111/syen.12336>
- Keegan KL, Rota J, Zhiri R, Zilli A, Wahlberg N, Schmidt BC, Lafontaine JD, Goldstein PZ, Wagner DL (2021) Toward a stable global Noctuidae (Lepidoptera) taxonomy. *Insect Systematics and Diversity* 5(3): 1–24. <https://doi.org/10.1093/isd/ixab005>

- Kitching IJ (1984) A historical review of the higher classification of the Noctuidae (Lepidoptera). *Bulletin of the British Museum (Natural History). Historical Series* 49: 153–234. [Natural History]
- Kitching IJ, Rawlins JE (1999) [1998] The Noctuoidea. pp. 355–401. In: Kristensen NP (Ed.) *Lepidoptera: Moths and Butterflies. Volume 1: Evolution, systematics and biogeography. Handbook for Zoology. Volume IV: Arthropoda: Insecta*. Walter de Gruyter, Berlin, 491 pp. <https://doi.org/10.1515/9783110804744.355>
- Lafontaine JD (2004) The Moths of North America including Greenland, Fascicle 27.1, Noctuoidea Noctuidae (part) Noctuinae (part-Agrotini). The Wedge Entomological Research Foundation. Washington, DC, 385 pp.
- Lafontaine JD, Schmidt BC (2010) Annotated check list of the Noctuoidea (Insecta: Lepidoptera) of North America north of Mexico. *ZooKeys* 40: 1–239. <https://doi.org/10.3897/zookeys.40.414>
- Lafontaine JD, Schmidt BC (2015) Additions and corrections to the check list of the Noctuoidea (Insecta, Lepidoptera) of North America north of Mexico. *ZooKeys* 527: 127–147. <https://doi.org/10.3897/zookeys.527.6151>
- Pohl GR, Nanz SR (Eds.) (2023) Annotated taxonomic checklist of the Lepidoptera of North America north of Mexico. The Wedge Entomological Research Foundation, Bakersfield, California, xiv + 580 pp.
- Poole RW (1995) Noctuoidea, Noctuidae (part). In: Dominick RB et al. (Eds.) *The Moths of America North of Mexico*, fasc. 26.1. Allen Press. Lawrence, Kansas, 249 pp.
- Poole RW (2022) The natural history of North America. Noctuidae of North America. Tribe Triocnemidini. *Nearctica.com* (accessed March, 2022).
- Ratnasingham S, Hebert PDN (2013) A DNA-based registry for all animal species: The Barcode Index Number (BIN) System. *PLoS ONE* 8(7): e66213. <https://doi.org/10.1371/journal.pone.0066213>
- Troubridge JT (2008) A generic realignment of the Oncocnemidini sensu Hodges (1983) (Lepidoptera, Noctuidae, Oncocnemidinae), with descriptions of a new genus and 50 new species. *Zootaxa* 1903(1): 1–95. <https://doi.org/10.11646/zootaxa.1903.1.1>
- Wagner DL, Lafontaine JD, McFarland N, Connolly BA (2008) Early stages of *Miracavira brillians* (Barnes) and reassignment of the genus to the Amphipyrinae: Psaphidini: Feraliina (Noctuidae). *Journal of the Lepidopterists Society* 62: 40–51.

Hivanua, a new genus of harmochirine jumping spiders from the Marquesas Islands (Araneae, Salticidae, Harmochirina)

Wayne P. Maddison¹ 

¹ Departments of Zoology and Botany and Beaty Biodiversity Museum, University of British Columbia, 6270 University Boulevard, Vancouver, British Columbia, V6T 1Z4, Canada

Corresponding author: Wayne P. Maddison (wayne.maddison@ubc.ca)

Abstract

The genus *Hivanua* **gen. nov.** is established for the harmochirine jumping spiders of the Marquesas Islands, formerly placed in *Habronattus* F.O. Pickard-Cambridge, 1901 and *Havaika* Prószyński, 2002. The type species, *Hivanua tekao* **sp. nov.** is described, and five species described by Berland are re-illustrated and moved into the genus: *Hivanua flavipes* (Berland, 1933), **comb. nov.**, *Hivanua nigrescens* (Berland, 1933), **comb. nov.**, *Hivanua nigrolineata* (Berland, 1933), **comb. nov.**, *Hivanua rufescens* (Berland, 1934), **comb. nov.**, and *Hivanua triangulifera* (Berland, 1933), **comb. nov.** The female epigyne is much like that of *Habronattus*, *Bianor* Peckham & Peckham, 1896, and other harmochirines, with a centrally placed coupling pocket and two atria with crescent-shaped edges. The terminal apophysis of the male palp, which is variable throughout the pellenine subgroup of the Harmochirina, is absent in *H. rufescens* but present in *H. tekao* **sp. nov.**, in which it is elbowed much as in *Habronattus*. These Pacific Island harmochirines, like the *Havaika* of Hawaii, appear to be largely foliage dwellers, unlike most of their continental relatives.



Key words: Classification, molecular phylogeny, new species, Plexippini, Salticoida

Academic editor: Dimitar Dimitrov

Received: 14 February 2024

Accepted: 2 April 2024

Published: 9 May 2024

ZooBank: <https://zoobank.org/593BF6EA-8DD3-4DB6-9EA6-0245A118675D>

Citation: Maddison WP (2024) *Hivanua*, a new genus of harmochirine jumping spiders from the Marquesas Islands (Araneae, Salticidae, Harmochirina). ZooKeys 1200: 215–230. <https://doi.org/10.3897/zookeys.1200.120868>

Copyright: © Wayne P. Maddison
This is an open access article distributed under terms of the Creative Commons Attribution License (Attribution 4.0 International – CC BY 4.0).

Introduction

Among the jumping spiders on islands of the central Pacific are a few species of the pellenine clade of the subtribe Harmochirina (Maddison 2015), a group well known elsewhere for *Habronattus* F.O. Pickard-Cambridge, 1901 (in the Americas) and *Pellenes* Simon, 1876 (mostly in Afro-Eurasia). These central Pacific harmochirines include 23 described species of the genus *Havaika* Prószyński, 2002 in Hawaii (Simon 1900; Prószyński 2002, 2008; Arnedo and Gillespie 2006), and further south, in the Marquesas Islands of French Polynesia, a few species that have been placed in *Havaika* and *Habronattus* (Berland 1933, 1934; Prószyński 2002). The species of Hawaii and the Marquesas share some traits unusual among harmochirines: they appear to be mostly vegetation-dwelling (most harmochirines are ground-dwellers), they correspondingly have traits usually seen only in vegetation-dwellers of their size (scales with a sheen; legs with sparse setation), and their described species lack a terminal apophysis in the male palp (generally present in pellenine harmochirines, except for *Neaetha* Simon, 1884 and some *Pellenes* subgenus *Pellenattus* Maddison,

2017). Recent work on the molecular phylogeny of harmochirines by Azevedo et al. (2024, in press), confirmed here, shows that the Hawaiian and Marquesan lineages do not form a clade, but rather that the Marquesan lineage is the sister group to *Pellenattus*, while the Hawaiian *Havaika* is the sister group to *Habronattus*+*Pellenattus*+the Marquesan lineage. The Marquesan lineage therefore needs to be moved out of *Havaika*. Accordingly, it is here described as the new genus *Hivanua* Maddison gen. nov., containing six recognized species, one of which is new and has a *Habronattus*-like terminal apophysis.

Material and methods

Material examined

Spider specimens examined morphologically for this study are deposited in the Bernice P. Bishop Museum (**BPBM**), the Essig Museum of the University of California, Berkeley (**EMEC**), and the Natural History Museum, London (**NHMUK**).

Morphology

Preserved specimens were examined under both dissecting microscopes and a compound microscope with reflected light. Drawings were made with a drawing tube on a Nikon ME600L compound microscope. Microscope photographs were made on an Olympus SZX12 stereoscope and focus-stacked using Helicon Focus v. 4.2.7.

All measurements are given in millimeters. Descriptions of color pattern are based on the alcohol-preserved specimen. Carapace length was measured from the base of the anterior median eyes not including the lenses to the rear margin of the carapace medially; abdomen length to the end of the anal tubercle. The following abbreviations are used: **ALE**, anterior lateral eyes; **ECP**, epigynal coupling pocket; **PLE**, posterior lateral eyes; **PME**, posterior median eyes (the “small eyes”); **RTA**, retrolateral tibial apophysis; **TmA**, terminal apophysis.

Molecular data and phylogenetic analysis

To understand species distinctions in the genus *Hivanua*, and to test whether the two sampled Marquesan species (*H. tekao* sp. nov. and *H. rufescens*) form a clade, molecular data were newly gathered from 17 *Hivanua* and other harmochrine specimens by Ultraconserved Element (UCE) target enrichment sequencing methods (Faircloth 2017), using the RTA (Zhang et al. 2023) and Spider (Kulkarni et al. 2019) probesets, and with the assistance of Arbor Biosciences. These data were combined with data for five taxa obtained by similar methods by Azevedo et al. (2024, in press) to assemble a UCE dataset of 22 species (Table 1). *Bianor* serves as the outgroup because it is not from the pelenine subgroup, but from the *Harmochirus* subgroup of harmochirines (Maddison 2015). Molecular protocols followed those of Marathe et al. (2024).

UCE loci were identified among the assembled contigs using the RTA probe set file and PHYLUCE (Faircloth 2016). After recovery, each locus was realigned with MAFFT v. 7.505 (Katoh and Standley 2013) using the LINSI option. Poorly aligned areas were deleted using GBLOCKS (Castresana 2000; Talavera and

Castresana 2007) as implemented in Mesquite v. 3.81 (Maddison and Maddison 2023b), with parameters as follows: min. fraction identical at conserved = 0.5, min. at highly conserved = 0.7, counting fraction only within taxa with non-gaps at that position; max. length of non-conserved blocks = 8, min. length of block = 8, fraction of gaps allowed = 0.6. Loci were retained for analysis only if they were recovered in at least 3 *Hivanua* specimens and in at least 10 taxa total, and if a preliminary RAxML (Stamatakis 2014) gene tree had the ratio of the two longest branches less than 5, to guard against paralogy (see Maddison et al. 2020b). Mitochondrial genes were found among the contigs by BLAST as described by Maddison et al. (2020a), using the mitochondrial genome of *Habronattus oregonensis* (Peckham and Peckham 1888) (Masta and Boore 2004) as target. The mitochondrial genomes were aligned by MAFFT using the LINSI option.

Maximum-likelihood phylogenetic analyses were performed with IQ-TREE v. 2.2.0 (Nguyen et al. 2015) using the Zephyr v. 3.31 package (Maddison and Maddison 2023a) in Mesquite v. 3.81 (Maddison and Maddison 2023b). For both datasets, the concatenated UCE loci and the mitochondrial genomes, maximum-likelihood search was unpartitioned and used the TEST option (standard model selection followed by tree inference). For the maximum-likelihood tree, 10 search replicates were done; 1,000 bootstrap replicates were done.

Raw reads of new data are deposited in Sequence Read Archive (BioProject submission ID PRJNA1096354; Table 1). Alignments and trees are deposited in the Dryad data repository (<https://doi.org/10.5061/dryad.hdr7sqvrf>).

Molecular phylogeny

3371 UCE loci were recovered initially, of which 199 were discarded for failing the branch-lengths paralogy test, and 1696 for being represented in too few taxa, leaving 1476 loci to be used in the analyses. In the trimmed, concatenated alignment the average sequence length is about 738,000 bp, though the *Hivanua* specimens are among the least well sequenced (average ~303,000 bp; Table 1).

For 10 of the taxa, between 12,700 and 14,480 bp of mitochondrial sequence (approximately the entire genome) was recovered as bycatch with the UCE-targeted reads (see column “mt bps” in Table 1). For three of the *Hivanua* specimens less was recovered (2568–4464 bp).

In Figs 1, 2 are shown the maximum-likelihood phylogenies from 1476 UCE loci (Fig. 1) and from the mitochondrial genome (Fig. 2). *Hivanua* is strongly supported as sister group to the subgenus *Pellenattus* of *Pellenes*, with *Habronattus* their first cousin.

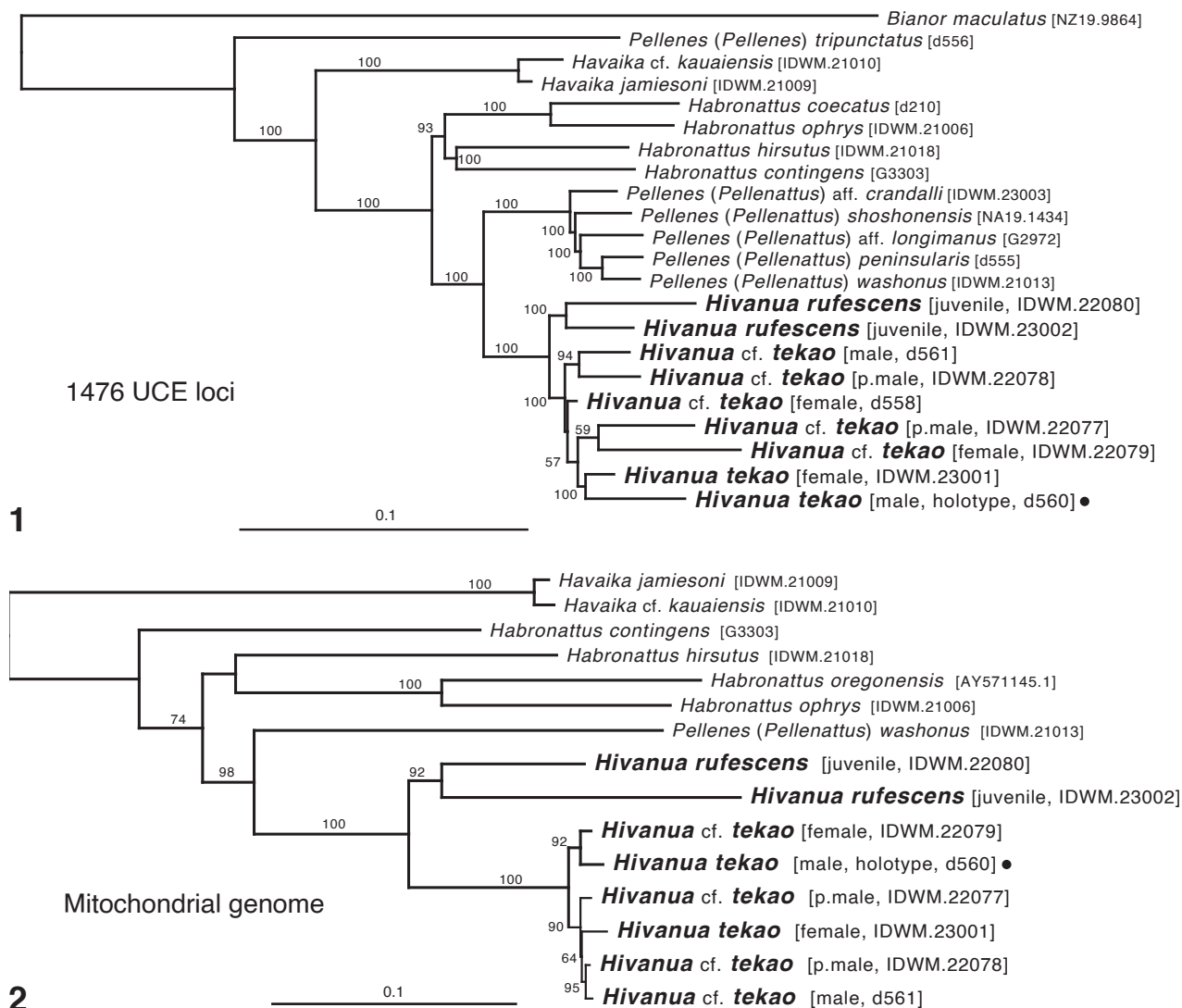
Within *Hivanua*, the nuclear UCE loci and the mitochondrial genome agree on the division between *Hivanua* specimens from Hiva Oa (*H. rufescens*, two specimens) and those from Nuku Hiva (*H. tekao* sp. nov. and *H. cf. tekao*, 6 specimens). However, interrelationships of specimens within Nuku Hiva are inconsistent, with (for example) male d560 strongly supported as sister to female IDWM.23001 by the concatenated UCE loci, but sister to female IDWM.22079 by the mitochondrial genome. The only agreed subclade is male d561 and sub-adult male IDWM.2078.

Of course, such conflict would be unsurprising if the six specimens of *H. tekao*/*H. cf. tekao* were conspecific, because one would expect there to be a networked pattern of genetic descent such that different parts of the genome

Table 1. Specimens in molecular phylogeny. j. = juvenile or penultimate instar. Sequence Read Archive (SRA) accession numbers with * indicate data from Azevedo et al. (2024, in press). Nuku Hiva and Hiva Oa are in the Marquesas Islands of French Polynesia. Last three columns show number of UCE loci, and total sequence length in base pairs (bps) for UCE loci and mitochondrial genome.

Species	Specimen ID		Probeset	SRA#	Location	GPS Coordinates (Latitude, Longitude)	Reads pass QC	UCEs	UCE bps	mt bps
<i>Bianor maculatus</i> (Keyserling, 1883)	NZ19.9864	♂	RTA	SAMN40752353	New Zealand: Canterbury	-42.1691, 172.8090	7914001	1347	1407035	
<i>Habronattus coecatus</i> (Hentz, 1846)	d210	♂	RTA	SAMN40752354	USA: Texas: Rio Grande City	26.5000, -98.8751	700294	1258	677212	–
<i>Habronattus contingens</i> (Chn., 1925)	G3303	♀	Spider	SAMN39938211*	Mexico: Jalisco: Zapopan	20.6897, -103.6104	3050339	696	526233	7452
<i>Habronattus hirsutus</i> (P. & P., 1888)	IDWM.21018	♂	RTA	SAMN40752355	Canada: British Columbia: Mayne I.	48.827, -123.265	3951254	1343	1380291	13037
<i>Habronattus ophrys</i> Griswold, 1987	IDWM.21006	♀	RTA	SAMN40752356	Canada: British Columbia: Mayne I.	48.8221, -123.2627	3951254	1398	1488825	14467
<i>Havaika jamiesoni</i> Prószyński, 2002	IDWM.21009	♂	Spider	SAMN40752357	USA: Hawaii: Kauai: Kōke'e	22.1172, -159.6697	3951254	722	620643	14293
<i>Havaika</i> cf. <i>kauaiensis</i> Prószyński, 2002	IDWM.21010	♂	RTA	SAMN40752358	USA: Hawaii: Kauai: Kōke'e	22.1252, -159.6645	3951254	1356	1402805	14479
<i>Hivanua rufescens</i> (Berland, 1934)	IDWM.22080	j.	RTA	SAMN40752359	Hiva Oa, Temetiu Ridge	-9.81, -139.08	3951254	1013	360939	14434
<i>Hivanua rufescens</i> (Berland, 1934)	IDWM.23002	j.	RTA	SAMN40752360	Hiva Oa, Temetiu Ridge	-9.81, -139.08	3951254	1222	445199	3537
<i>Hivanua tekao</i> sp. nov.	d560	♂	Spider	SAMN39938226*	Nuku Hiva, Mt Tekao	-8.9, -140.2	495722	182	52408	2568
<i>Hivanua tekao</i> sp. nov.	IDWM.23001	♀	RTA	SAMN40752361	Nuku Hiva, Mt Tekao	-8.9, -140.2	3951254	1444	821685	4464
<i>Hivanua</i> cf. <i>tekao</i>	d558	♀	Spider	SAMN39938225*	Nuku Hiva, Mt Tekao	-8.9, -140.2	1077488	765	445228	–
<i>Hivanua</i> cf. <i>tekao</i>	d561	♂	Spider	SAMN39938224*	Nuku Hiva, Mt Tekao	-8.9, -140.2	618949	298	91230	12708
<i>Hivanua</i> cf. <i>tekao</i>	IDWM.22077	j.♂	Spider	SAMN40752362	Nuku Hiva, Mt Tekao	-8.9, -140.2	16024385	363	119803	14363
<i>Hivanua</i> cf. <i>tekao</i>	IDWM.22078	j.♂	Spider	SAMN40752363	Nuku Hiva, Mt Tekao	-8.9, -140.2	18273055	325	101913	14364
<i>Hivanua</i> cf. <i>tekao</i>	IDWM.22079	♀	Spider	SAMN40752364	Nuku Hiva, Mt Tekao	-8.9, -140.2	24724214	639	292126	14362
<i>Pellenes</i> aff. <i>crandalli</i> (L.&G. 1955)	IDWM.23003	♀	RTA	SAMN40752365	USA: Colorado: Berthoud	40.3, -105.1	5001755	1326	1449221	–
<i>Pellenes</i> aff. <i>longimanus</i> (Em. 1913)	G2972	♀	RTA	SAMN40752366	USA: Texas: N Rio Grande City	26.5000, -98.8751	6555856	1322	1424528	–
<i>Pellenes peninsularis</i> (Emerton, 1925)	d555	j.♂	Spider	SAMN40752367	Canada: Ontario: Dwight	45.3384, -79.0302	1609418	733	533368	–
<i>Pellenes shoshonensis</i> (Gertsch, 1934)	NA19.1434	♂	RTA	SAMN40752368	USA: Washington: Columbia NWR	46.937, -119.247	3304592	1358	1385614	–
<i>Pellenes washonus</i> (L.&G. 1955)	IDWM.21013	♂	Spider	SAMN40752369	USA: California: Pepperwood Pres.	38.57, -122.69	10334966	742	640000	13734
<i>Pellenes tripunctatus</i> (Wlck., 1802)	d556	♀	Spider	SAMN39938245*	Germany: Saxony, Authausen	51.607, 12.711	6546246	709	577816	–

would give different trees. However, the apparent morphological distinction of male d561 (discussed below) suggests there may be two species in the sample. If so, then the conflict among genomes could reflect incomplete lineage sorting or recent introgression. Although some clarity might be achieved by us-



Figures 1, 2. Phylogeny **1** maximum-likelihood tree from concatenated data set of 1476 UCE loci. **2** maximum-likelihood tree from mitochondrial genomes recovered as bycatch in UCE sequencing reads. Numbers are percentage of 1,000 bootstrap replicates showing the clade. Filled circle highlights the holotype of *Hivanua tekao* sp. nov.

ing coalescent methods of species delimitation (Knowles and Carstens 2007; Degnan and Rosenberg 2009; Yang and Rannala 2010; Smith and Carstens 2020), the paucity of specimens makes this unlikely to be informative. Thus, the conservative approach will be taken of naming, for now, only one species.

Taxonomy

The molecular phylogeny's strong placement of *Hivanua* species as sister group to *Pellenes* subgenus *Pellenattus* (Fig. 1) justifies their exclusion from the genera *Havaika* and *Habronattus*. While *H. tekao* sp. nov. and *H. rufescens* could be placed in an expanded *Pellenattus*, I establish for them a separate genus because of the drastically different embolus (long and thin), epigynal atria (of the ancestral crescent form), body form and setation, and habitat (lushly vegetated Pacific island).

The relatively sparse setation shared by *Hivanua* and *Havaika* may represent convergence towards a new microhabitat, living on foliage (see Natural History,

below). Their ancestors, presumably open-ground dwellers like most other harmochirines, may have been especially suited to colonize new volcanic islands, but as the islands became vegetated, the spiders may have adapted to that new available microhabitat.

***Hivanua* Maddison, gen. nov.**

<https://zoobank.org/26435A4C-485C-41E5-BA18-40592736CB81>

Type species. *Hivanua tekao* Maddison, sp. nov.

Species included.

Hivanua flavipes (Berland, 1933), comb. nov., transferred from *Havaika*.

Hivanua nigrescens (Berland, 1933), comb. nov., transferred from *Plexippus*.

Hivanua nigrolineata (Berland, 1933), comb. nov., transferred from *Havaika*.

Hivanua rufescens (Berland, 1934), comb. nov., transferred from *Habronattus*.

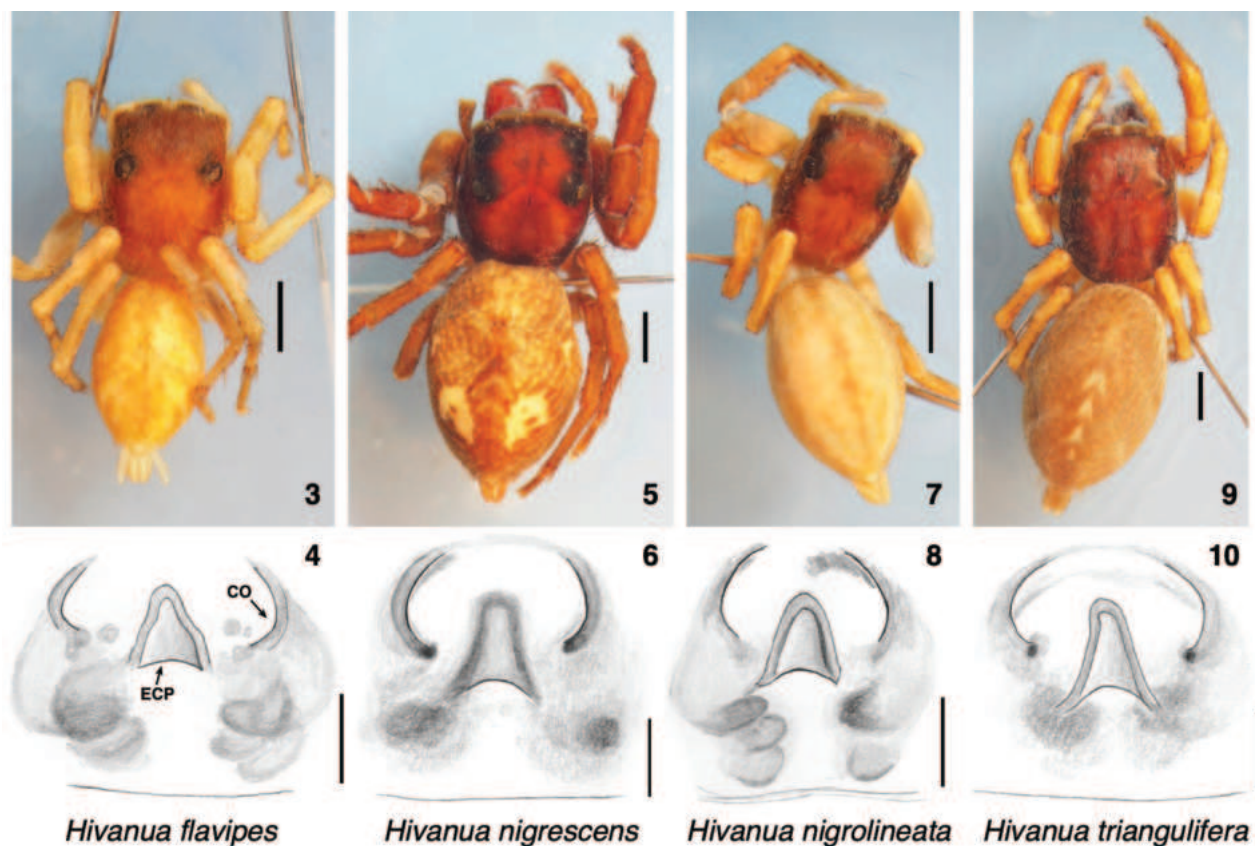
Hivanua tekao Maddison, sp. nov.

Hivanua triangulifera (Berland, 1933), comb. nov., transferred from *Havaika*.

Etymology. An arbitrary combination of letters, containing a reference to the largest two islands of their range, Hiva Oa and Nuku Hiva. Grammatical gender: feminine.

Diagnosis. Reflective scales and relatively sparse setation on the legs distinguish *Hivanua* and *Havaika* from other genera of the pellenine subgroup of harmochirines, which have fuller and more varied setation. *Hivanua* is distinct from *Havaika* by a more posterior placement of the epigynal coupling pocket (ECP). In *Hivanua*, the crescent-shaped atrial ridges shielding the openings reach posteriorly only as far as the midpoint of the ECP; in *Havaika*, the atrial ridges merge with the posterior end of the ECP (Prószyński 2002, 2008). Male first leg of *Hivanua* unusually long; for example, the holotype of *H. tekao* sp. nov. has a body length of 6.9 mm but a first leg length (femur to tarsus) of 12.5 mm. Third patella+tibia about the same length as fourth (distinctly longer in *Pellenes* and *Habronattus*). Palp with bulb smaller relative to cymbium and tibia compared to *Habronattus* and *Pellenes*. TmA sometimes present, unlike *Havaika*. First leg tibia usually or often with four anterior ventral macrosetae (other harmochirines with fewer). (Four macrosetae present in all *H. tekao*/*H. cf. tekao*, *H. flavipes*, *H. nigrolineata*, and about half of the *H. rufescens* specimens, mostly juveniles).

Species included. Six species are placed in *Hivanua*, five of which were described by Berland (1933, 1934). A new species, *H. tekao* sp. nov., is described below, and one of Berland's, *H. rufescens*, is partially redescribed. The other four Berland species are not redescribed here except via illustrations of their female holotypes (in BPBM, examined; Figs 3–10). The holotype of *N. flavipes* is from "Hiva Oa, Mont Temetiu, 1300 m. d'alt.", that of *H. nigrescens* is from "Tahuata: sommet du Haaoipu, 900 m", that of *H. nigrolineata* from "Nukuhiva: Ooumu", and that of *H. triangulifera* from Tahuata. There is variation among species in body form, with *H. nigrolineata* narrow and linearly marked, and *H. nigrescens* robust and with a rough texture. *H. nigrescens* was inexplicably synonymized with *Plexippus paykulli* (Adouin, 1826) by Berland himself. The holotype of *H. nigrescens* is clearly a *Hivanua* (Figs 5, 6), similar to *H. tekao* sp. nov.



Figures 3–10. Berland's holotypes of four *Hivanua* species, each showing habitus and ventral view of epigyne 3, 4 holotype of *Sandalodes flavipes* Berland, 1933 5, 6 holotype of *Sandalodes nigrescens* Berland, 1933 7, 8 holotype of *Sandalodes nigrolineatus* Berland, 1933 9, 10 holotype of *Sandalodes triangulifera* Berland, 1933. Abbreviations: CO, copulatory opening; ECP, epigynal coupling pocket. Scale bars: 1.0 mm for bodies; 0.1 mm for epigynes.

One wonders if Berland confused it with his *Sandalodes magnus* Berland, 1933, which is indeed a synonym of *P. paykulli*, and whose figures appeared in the same plate as *Sandalodes nigrescens*.

Several of Berland's Marquesan harmochirines are placed in *Hivanua* only tentatively. *Hivanua rufescens* can be placed with the type species *H. tekao* sp. nov. with confidence based on the molecular evidence. These two species, along with *H. nigrescens* and *H. triangulifera*, are large bodied, distinctly larger than most of the Hawaiian *Havaika*. The remaining two species, *H. nigrolineata* and *H. flavipes*, are considerably smaller-bodied and more delicate, and could easily be mistaken for *Havaika*. They share with the larger *Hivanua* one distinction from *Havaika*, the more anterior placement of epigynal atria. For this, and for geographical parsimony, I will here place them into *Hivanua*, but this should be considered provisional until more material can be found and studied.

Species taxonomy of *Hivanua* is made difficult by the simplicity of the markings and genitalia, by the paucity of specimens, and by the fact that Berland's type specimens are mostly female, harder to distinguish than males. Berland considered specimens from different islands as conspecific without good explanation. Adding to these difficulties is confusion over the geographic provenance of some specimens, mentioned under *H. rufescens* below.

***Hivanua rufescens* (Berland, 1934), comb. nov.**

Figs 11–14

Sandalodes rufescens Berland, 1934.

Habronattus rufescens—Prószyński 2002.

Diagnosis. Similar to *H. tekao* sp. nov., large bodied, with long appendages, especially first legs in male, and light to medium brown throughout, except for indistinct markings. Distinguished from *H. tekao* sp. nov. by lack of TmA (Fig. 11).

Description. Male (based on specimen IDWM.22076). Carapace length 3.95, width 2.86; abdomen length 3.8. **Carapace** (Fig. 14): slightly swollen at the cheeks, as if the cheliceral muscles are strong. Medium brown, with two longitudinal thoracic bands. **Clypeus** medium orange-brown, with a few white setae. **Chelicerae** vertical, orange-brown, with only sparse setae (Fig. 13). One simple retromarginal and two promarginal teeth. **Palp**, like legs, uniformly brown with few setae. Patella and tibia unusually long compared to other pellenine harmochirines. Embolus thin, originating at about 7:30 (Fig. 11). Lacks TmA. **Legs** brown, front legs darker (medium rusty brown), back legs paler (light honey-brown). First legs especially long. First tibia with three anterior and three posterior ventral macrosetae. **Abdomen** indistinctly marked, with a trace of a central chevron.

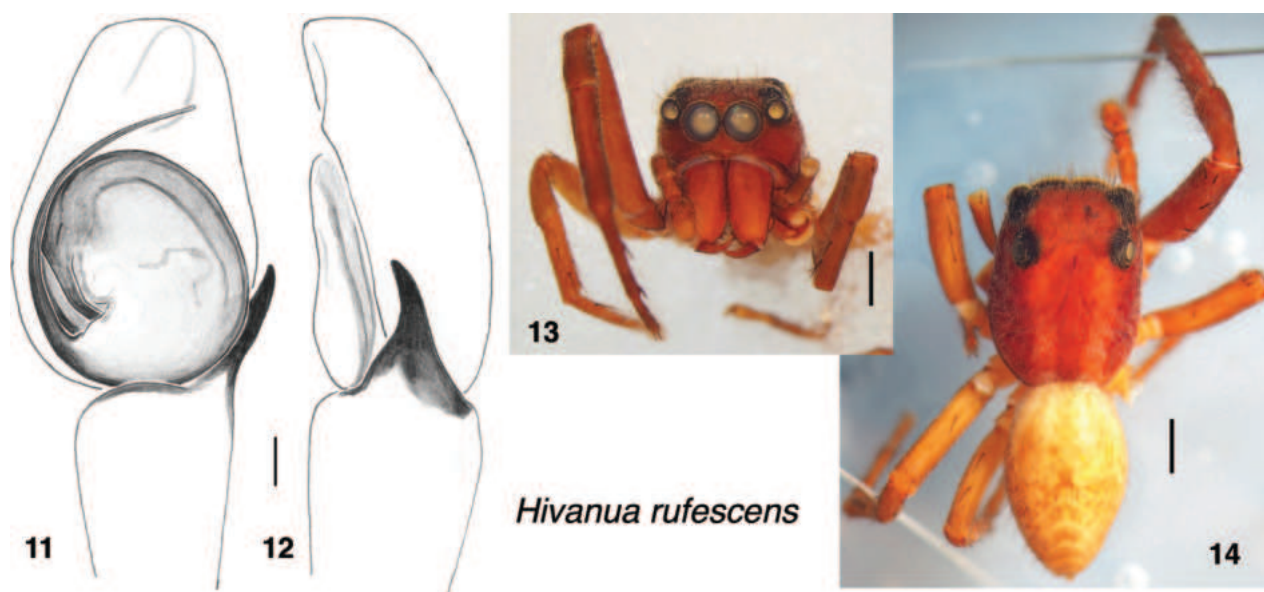
Female. See Prószyński (2002).

Natural history. The habitat is a “mountain ridge cloud forest” (Gillespie 2003). Although no specific notes were taken regarding the collecting methods for *H. rufescens*, the material listed below was bycatch of fieldwork seeking *Tetragnatha* and was most likely collected at night and from foliage (R. Gillespie pers. comm.).

Material examined. 1 male (IDWM.22076), 11 juveniles (including IDWM.22080, 23002) in EMEC with data FRENCH POLYNESIA: Marquesas Islands: Hiva Oa, Temetiu Ridge, 1170 m elev., 28-VI-2000, leg. R. Gillespie, G. Roderick. Gillespie (2003) reported this locality at 9.81°S, 139.08°W.

Remarks. Prószyński (2002) did not provide any explanation for placing this species in *Habronattus*. A large and elbowed terminal apophysis (TmA) has been considered a synapomorphy of *Habronattus* (Maddison and Hedin 2003), but *H. rufescens* has no TmA (Arnedo and Gillespie 2006; Fig. 11). Nonetheless, Prószyński may have noticed some shared trait, because indeed *H. rufescens* is more closely related to *Habronattus* than to *Havaika*, and its congener *H. tekao* sp. nov. does have an elbowed TmA. The gap between the embolus and tegulum is larger in *H. rufescens* (Fig. 11) than in other Harmochirina lacking a TmA, as if leaving room for a TmA that was lost only recently.

There is some confusion about the geographic provenance of *H. rufescens* and perhaps also *H. tekao* sp. nov. Berland’s original description list the types of *H. rufescens* as from Nuku Hiva, but, as reported by Prószyński (2002), the labels with the type specimens in NHMUK (examined by D. Sherwood pers. comm.) indicate a collecting locality of Hiva Oa, 133 km to the southeast. Those specimens, studied by Prószyński (2002), do indeed appear to be the types, not only because his drawings match well Berland’s original drawings, but also because their labels seem clearly to be of the types. They read “*Sandalodes rufescens* Berland Type F et M”, and “1926.1.27.297-304; Hiva Oa, Marquesas Is.; C.L. Collenette 31.12.24; 3000–4000 ft.; S. Y. ‘St George’; S.E.R.A.”



Figures 11–14. *Hivanua rufescens* (Berland, 1934), specimen IDWM.22076 from Hiva Oa. 11 palp, ventral view 12 same, prolateral 13 face 14 habitus. Scale bars: 0.1 mm for palp; 1.0 mm for body.

(D. Sherwood pers. comm.). This indicates the specimens were collected by the Scientific Expeditionary Research Association, from the ship “St George”, and formally accessioned by the NHMUK in 1926. While there could be an error in this label, it is more reasonable to respect the physical material and instead assume that Berland made an error in the publication.

The material collected more recently by Gillespie and others from Nuku Hiva and Hiva Oa (Arnedo and Gillespie 2006) could help resolve Berland’s confusion if it confirmed *H. rufescens* on Hiva Oa, except that there is unfortunately a similar contradiction between vial labels and published information for these more recent specimens. For a specimen they list as “*Habronattus rufescens*, Marquesas, Nuku Hiva”, Arnedo and Gillespie (2006) gave a palp photo (their figure 2Q) that can be matched to the specimen in EMEC here labelled IDWM.22076 (as indicated by the unusual dark line on the tegulum; Fig. 11). Its palp is a good match to the paratype of *H. rufescens* illustrated by Prószyński (2002). Thus, the specimen they reported as *H. rufescens* appears to be properly identified. However, that specimen and the accompanying juveniles are in vials whose labels indicate they were collected from Hiva Oa, not Nuku Hiva. Conversely, the other Marquesas male they discussed, “*Habronattus* sp. Marquesas, Hiva Oa” can be identified by details of setal placement (in their figure 2P) as specimen IDWM.22075 in a vial labelled as from Nuku Hiva. The DNA sequences they reported are likewise attributed to the correct species, but to the wrong islands. Those reported for *H. rufescens* (DQ531803 and DQ532084) are close matches to those obtained here from juveniles accompanying their *H. rufescens* male, while those sequences reported (DQ531801 and DQ532082) for the specimen that is here called *H. tekao* IDWM.22075 (their figure 2P) are closely similar to those obtained here from other specimens of *H. tekao* sp. nov. from Nuku Hiva. All of this is consistent with Arnedo and Gillespie attributing the palp and DNA to the correct specimens but recording their localities incorrectly. It is possible that Berland’s misreported locality for *H. rufescens* misled Arnedo and Gillespie to doubt and mistake the locality of their matching specimen.

I provisionally interpret the labeling of the vials to be correct for both the Berland and Gillespie specimens. The known specimens of *H. rufescens* are, therefore, from Hiva Oa. The male of *H. rufescens* that Arnedo and Gillespie showed in Fig. 2Q and whose DNA was reported as DQ531803, etc., is now labelled as specimen IDWM.22076. The known specimens of *H. tekao* sp. nov. are interpreted as from Nuku Hiva. The male shown in Arnedo and Gillespie's figure 2P and whose DNA was reported as DQ531801, etc., is now labelled as specimen IDWM.22075.

***Hivanua tekao* Maddison, sp. nov.**

<https://zoobank.org//A213F09A-F764-411E-97D8-CD1447F742D8>

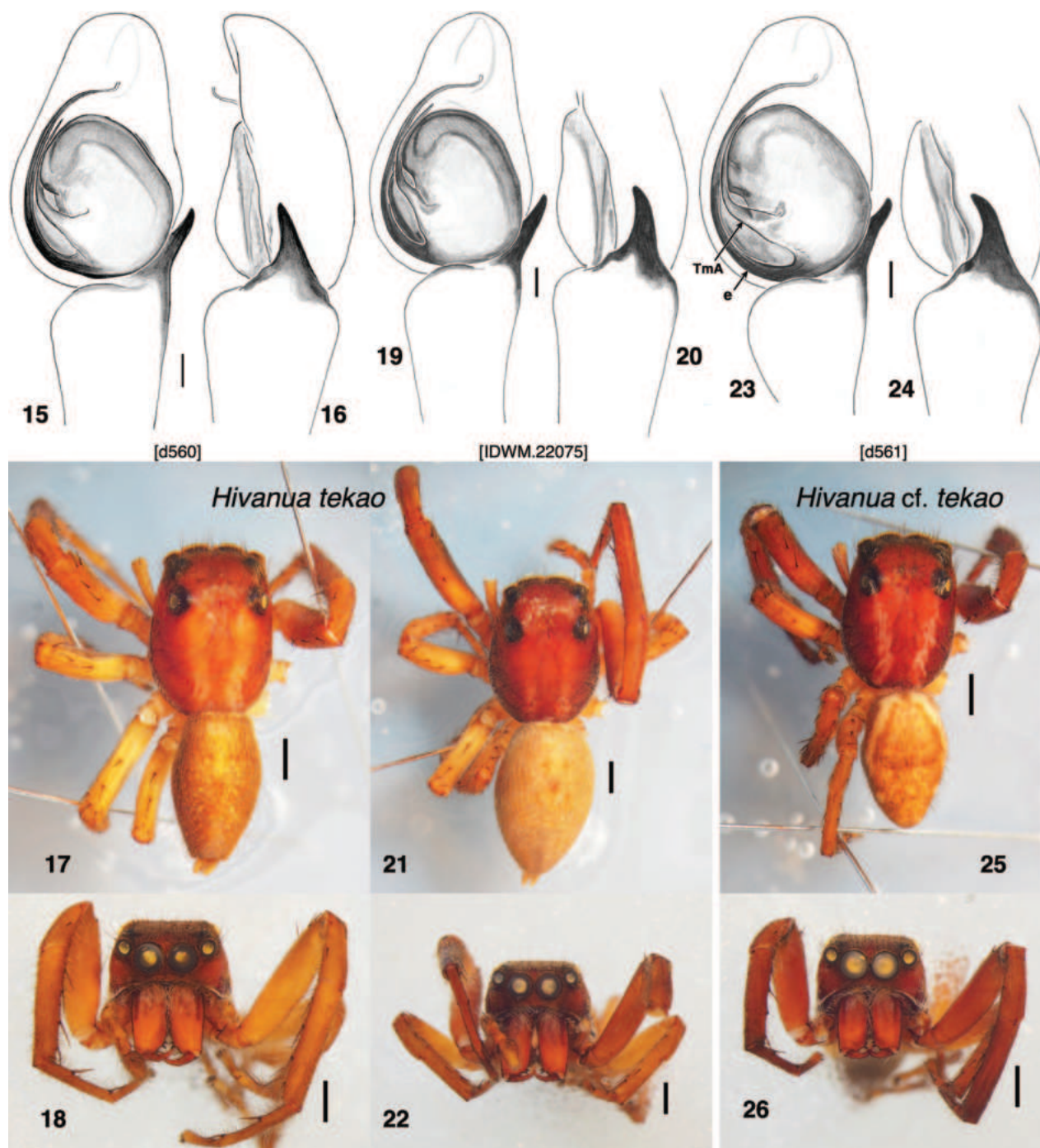
Figs 15–22, 27–30; possibly also Figs 23–26, 31–38

Type material. Male holotype (W. Maddison voucher code d560, in BPBM), with data FRENCH POLYNESIA: Marquesas Islands: Nuku Hiva, Mt Tekao, 1200 m elev. 23-VI-2000, leg. R. Gillespie. Female paratype (W. Maddison voucher code IDWM.23001, in EMEC), with data FRENCH POLYNESIA: Marquesas Islands: Nuku Hiva, Mt Tekao, 1185 m elev., 23-VI-2000, leg. R. Gillespie, L. Shapiro. Gillespie (2003) reported the 1185 m elevation locality at 8.86°S, 140.17°W. (See comments on provenance under *H. rufescens*.)

Etymology. Derived from the name of the type locality; treated as a noun in apposition.

Diagnosis. Embolus accompanied by a terminal apophysis (TmA), lacking in other species of *Havaika* and *Hivanua*. The TmA is long, thin, and elbowed, and thus resembles that of *Habronattus* (Griswold 1987). Otherwise, similar to *H. rufescens*, *H. tekao* sp. nov. is large bodied and with long appendages, especially the first legs in the male, and light to medium brown throughout except for indistinct markings. Females differ from those of *H. nigrolineata*, *H. flavipes*, and *H. triangulifera* in being more robust, with abdominal markings indistinct. Females are paler than the holotype of *H. nigrescens*. However, given the lack of clarity of which females belong to *H. tekao* sp. nov., any attempt to identify them is difficult at present.

Description. Male (based on holotype, specimen d560). Carapace length 3.96, width 2.92; abdomen length 3.70. **Carapace** (Fig. 17): medium to dark brown, with two longitudinal thoracic bands of paler integument and thin covering of white scales, and marginal band of sparse white scales. Remainder of carapace thinly covered in setae, some in ocular quadrangle with bronze sheen. **Clypeus** medium to dark brown, sparsely covered with setae, with some long pale setae overhanging chelicerae (Fig. 18). **Chelicerae** vertical, orange-brown, with patch of white scales basally. One simple retromarginal and two promarginal teeth. **Palp**, like legs, uniform brown with few setae. Patella and tibia unusually long compared to other pellenine harmochirines. Embolus thin, originating at about 7:00 (Fig. 15). TmA present, narrowing to a point, angled toward 10:30 initially, then bending (and thus elbowed) as it nears the embolus. **Legs** light brown, the front legs slightly darker. First legs especially long. First tibia with four anterior and three posterior ventral macrosetae. Length of femur I 3.65, II 2.29, III 2.76, IV 2.60; patella + tibia I 5.31, II 2.76, III 2.76, IV 2.71; metatarsus + tarsus I 3.54, II 2.14, III 2.66, IV 2.71. **Abdomen** indistinctly marked, with a trace of a central chevron.



Figures 15–26. *Hivanua tekao* sp. nov. and a specimen that may be distinct, all from Nuku Hiva 15–18 *H. tekao* sp. nov. holotype, specimen d560 15 palp, ventral view 16 same, prolateral 17 habitus 18 face 19–22 *H. tekao* sp. nov. male, specimen IDWM.22075 19 palp, ventral view 20 same, prolateral 21 habitus 22 face. 23–26 *H. cf. tekao*, specimen d561 23 palp, ventral view 24 same, prolateral 25 habitus 26 face. Abbreviations: TmA, terminal apophysis; e, embolus. Scale bars: 0.1 mm for palps; 1.0 mm for bodies.

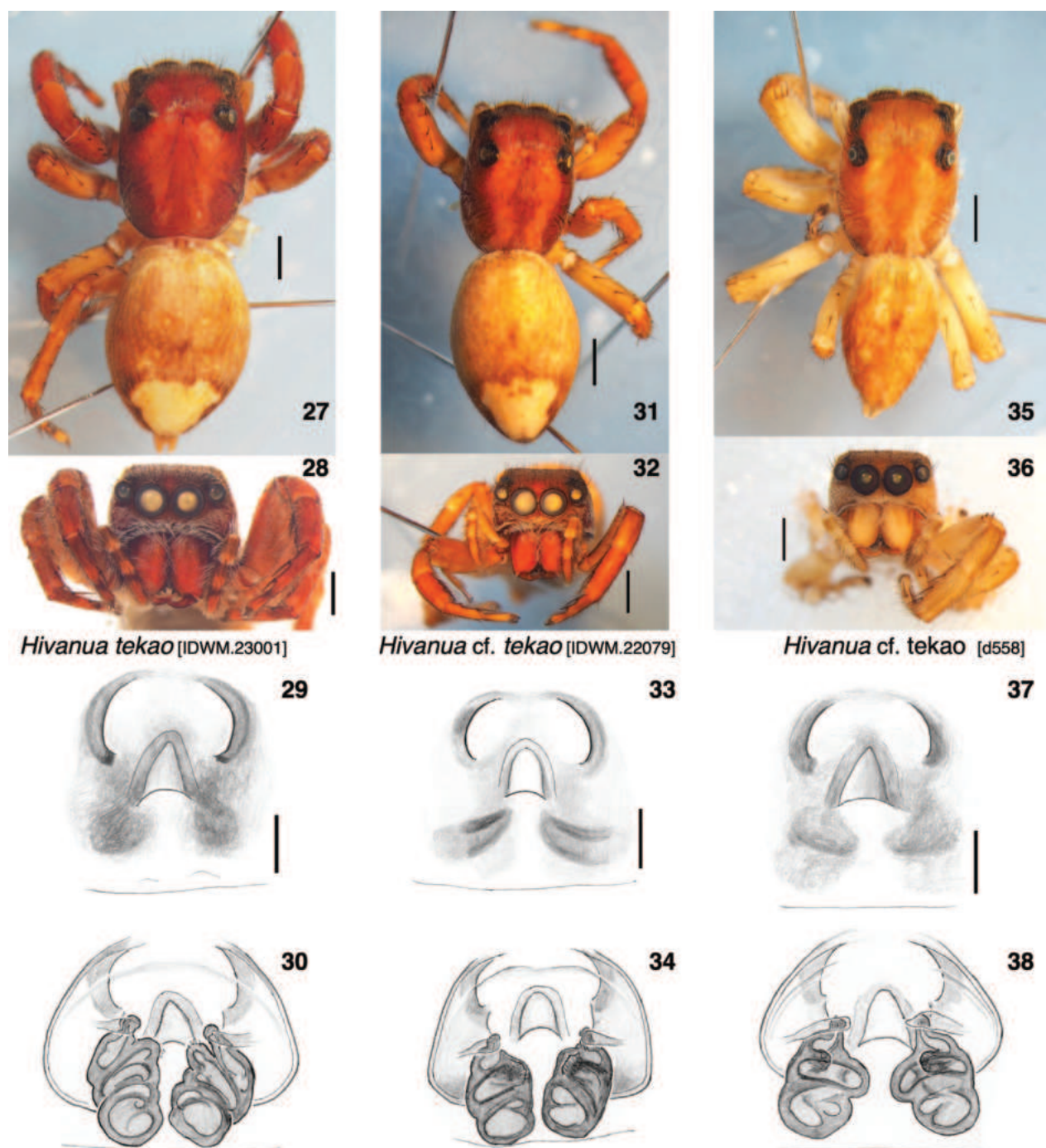
Female (based on specimen IDWM.23001). Carapace length 4.01, width 3.02; abdomen length 4.90. **Carapace** (Fig. 27): Structure, colour as in male. **Clypeus** brown covered with white scales, which overhang chelicerae. **Chelicerae** orange-brown, with a few white scales near the base. One simple retromarginal and two promarginal teeth. **Legs** light brown with a few scattered white scales. First tibia with four anterior and three posterior ventral macrosetae. Length of

femur I 2.45, II 2.19, III 2.60, IV 2.60; patella + tibia I 3.28, II 2.60, III 2.76, IV 2.76; metatarsus + tarsus I 2.08, II 1.77, III 2.40, IV 2.60. **Abdomen** medium brown except that posterior third is covered with a prominent triangular white patch, with white scales. **Epigyne** with basic simple *Habronattus* or *Bianor*-like form, with a triangular ECP placed centrally, flanked by two crescent-shaped atria (Fig. 29). The vulva shows the spermatheca forming a compact coil, much like those of *Habronattus* (Fig. 30).

Variation. Three specimens can be reasonably securely considered to be *H. tekao* sp. nov. The male chosen as holotype, d560, closely resembles another male, IDWM.22075 in markings and palp; the female described, IDWM.23001, is placed next to the holotype in the phylogeny based on 1195 gene loci. The short branch lengths and discordance between mitochondrial and nuclear results (Fig. 1 vs. Fig. 2) would be consistent with those and all the other Mount Tekao specimens belong being a single species. However, on Mount Tekao there are two forms of males distinct enough that they might have been suspected as separate species. Male specimen d561 has longitudinal white stripes along the side of the abdomen and the embolus arising at 6:00, while males d560 and IDWM.22075 lack the stripes and have the embolus arising at about 7:00. Subadult male IDWM.22077 appears to match d561, with white stripes and 6:00 embolus origin (developed enough to see through the subadult integument), while subadult male IDWM.22078 lacks stripes and appears to have a 7:00 embolus origin (though this is unclear). The stripes could easily be polymorphic, but a difference in bulb rotation like that seen between Figs 15, 19 versus Fig. 24 would typically mark a different species, based on patterns in other groups. However, those differences do not form a clear pattern on the molecular phylogeny. From the UCE data (Fig. 1), one could suspect an unstriped less-rotated species (d560, IDWM.23001) and a striped more-rotated species (d561, IDWM.22077, 78, 79), but that would require doubting the appearance of the subadult IDWM.22078. It would also be contradicted by the mitochondrial genome, which places female IDWM.22079 instead of IDWM.23001 with the unstriped male d560. These two females appear morphologically the same, except that IDWM.23001 might have an extra coil in the spermatheca. That, however, would be against the expectations of IDWM.23001 belonging to a male with a shorter embolus. And, despite the difference in palp rotation, the striped male d561 has only one nucleotide difference with the unstriped male IDWM.22075 (Arnedo and Gillespie's sequenced male from Nuku Hiva) in 16SND1.

Against all this confusion, I have decided to refer three specimens to *H. tekao* sp. nov. (male d560, male IDWM.22075, female IDWM.23001) and treat them as type material, and the remainder as possibly conspecific, naming them "*H. cf. tekao*". Applying formal species delimitation methods to the UCE data might be able to help resolve it, but with so few specimens, it is prudent to wait until more specimens are available to determine if there is a second species.

Natural history. The specimens from "above Toovii" are listed as "beated from ohia". The others from Mount Tekao, including the type specimens, are not associated with specific habitat data. However, the specimens were likely on foliage. The type locality is a "high montane wet forest" (Gillespie 2003). The specimens were collected as bycatch of fieldwork seeking *Tetragnatha*, which was primarily at night and involved looking on foliage (R. Gillespie pers. comm.).



Figures 27–38. Females sequenced of *Hivanua* from Nuku Hiva, all *H. tekao* sp. nov. or a closely related species. Each shows habitatus, face, ventral view of epigyne, and dorsal view of cleared vulva **27–30** specimen IDWM.23001 **31–34** specimen IDWM.22079 **35–38** specimen d558. Scale bars: 1.0 mm for bodies; 0.1 mm for epigynes.

Additional material examined. These are all identified only tentatively, as *H. cf. tekao*. The following are all in the EMEC, from FRENCH POLYNESIA: Marquesas Islands: Nuku Hiva. One male (voucher code d561), one subadult male (IDWM.22078) and 4 juveniles from Mt. Tekao, 1200 m elev., 23-VI-2000, leg. R. Gillespie. One male (IDWM.22075) and one subadult males (IDWM.22077) from Mt. Tekao, 1185 m elev., 23-VI-2000, leg. R. Gillespie, L. Shapiro. Two females (one is IDWM.22079) and one juvenile from Mt. Tekao, 1100 m elev., 24-VI-2000, leg. R. Gillespie. One female (d558) from Mt. Tekao, 1200 m elev.,

25-VI-2000, leg. R. Gillespie. Two females and two juveniles from above Toovii, ~2800 ft., beaten from ohia, 18-vii-2001 Claridge.

Remarks. The possibility that the specimens here described could be conspecific with one of Berland's female holotypes should be addressed. The other holotype from Nuku Hiva, that of *H. nigrolineata*, is quite different, delicate bodied and with lineate markings. The male that Berland placed with *H. triangulifera* (not examined; location of specimen unknown) is from Nuku Hiva and could match that of *H. cf. tekao* shown in Figs 23–26, but there is no evidence to associate either of them with the female holotype of *H. triangulifera*, which is from another island, and differs from the females here considered to be *H. tekao* sp. nov. in having a simple clear chevron marking (the triangles of its specific epithet). The most obvious candidate for a match of *H. tekao* sp. nov. with a Berland species is with *H. nigrescens*, which, like *H. tekao* sp. nov., is large and robust. However, *H. nigrescens* is from a different and distant island, closer to Hiva Oa. The epigynes are too simple and poorly known to help. Because of the geographical distance, and to have a traceable name to which to attach the DNA data, the specimens here studied from Nuku Hiva are described as a new species.

Acknowledgements

I am grateful to colleagues who took special efforts to support this paper. Rosemary Gillespie and Miquel Arnedo allowed me access to their *Hivanua* specimens for molecular sampling, and provided information about their natural history. K. Magnacca, H. Keeble, T. Manolis, D. Maddison, M. Hedin, and G. Azevedo generously helped with collecting specimens. Danni Sherwood provided information about the holotype of *Sandalodes rufescens* Berland. Jeremy Frank loaned the Berland holotypes. Kiran Marathe assisted with the molecular lab work. Guilherme Azevedo and Marshal Hedin graciously allowed the use of unpublished data from *Pellenes*, *Habronattus*, and *Hivanua*.

Additional information

Conflict of interest

The author has declared that no competing interests exist.

Ethical statement

No ethical statement was reported.

Funding

This research was supported by funding from an NSERC Canada Discovery Grant.

Author contributions

The author solely contributed to this work.

Author ORCIDs

Wayne P. Maddison  <https://orcid.org/0000-0003-4953-4575>

Data availability

All of the data that support the findings of this study are available in the main text.

References

- Arnedo MA, Gillespie RG (2006) Species diversification patterns in the Polynesian jumping spider genus *Havaika* Prószyński, 2001 (Araneae, Salticidae). *Molecular Phylogenetics and Evolution* 41(2): 472–495. <https://doi.org/10.1016/j.ympev.2006.05.012>
- Azevedo GHF, Hedin M, Maddison WP (2024) [in press] Phylogeny and biogeography of harmochirine jumping spiders (Araneae: Salticidae). *Molecular Phylogenetics and Evolution*.
- Berland L (1933) Araignées des Iles Marquises. *Bernice P. Bishop Museum Bulletin* 114: 39–70.
- Berland L (1934) Araignées de Polynésie. *Annales de la Société Entomologique de France* 103(3–4): 321–336. <https://doi.org/10.1080/21686351.1934.12280240>
- Castresana J (2000) Selection of conserved blocks from multiple alignments for their use in phylogenetic analysis. *Molecular Biology and Evolution* 17(4): 540–552. <https://doi.org/10.1093/oxfordjournals.molbev.a026334>
- Degnan JH, Rosenberg NA (2009) Gene tree discordance, phylogenetic inference and the multispecies coalescent. *Trends in Ecology & Evolution* 24(6): 332–340. <https://doi.org/10.1016/j.tree.2009.01.009>
- Faircloth BC (2016) PHYLUCE is a software package for the analysis of conserved genomic loci. *Bioinformatics* 32(5): 786–788. <https://doi.org/10.1093/bioinformatics/btv646>
- Faircloth BC (2017) Identifying conserved genomic elements and designing universal probe sets to enrich them. *Methods in Ecology and Evolution* 8(9): 1103–1112. <https://doi.org/10.1111/2041-210X.12754>
- Gillespie RG (2003) Marquesan spiders of the genus *Tetragnatha* (Araneae, Tetragnathidae). *The Journal of Arachnology* 31(1): 62–77. [https://doi.org/10.1636/0161-8202\(2003\)031\[0062:MSOTGT\]2.0.CO;2](https://doi.org/10.1636/0161-8202(2003)031[0062:MSOTGT]2.0.CO;2)
- Griswold CE (1987) A revision of the jumping spider genus *Habronattus* F. O. P.-Cambridge (Araneae; Salticidae), with phenetic and cladistic analyses. *The University of California Publications in Entomology* 107: 1–344.
- Katoh D, Standley DM (2013) MAFFT multiple sequence alignment software version 7: Improvements in performance and usability. *Molecular Biology and Evolution* 30(4): 772–780. <https://doi.org/10.1093/molbev/mst010>
- Knowles LL, Carstens BC (2007) Delimiting species without monophyletic gene trees. *Systematic Biology* 56(6): 887–895. <https://doi.org/10.1080/10635150701701091>
- Kulkarni S, Wood H, Lloyd M, Hormiga G (2019) Spider-specific probe set for ultraconserved elements offers new perspectives on the evolutionary history of spiders (Arachnida, Araneae). *Molecular Ecology Resources* 20(1): 185–203. <https://doi.org/10.1111/1755-0998.13099>
- Maddison WP (2015) A phylogenetic classification of jumping spiders (Araneae: Salticidae). *The Journal of Arachnology* 43(3): 231–292. <https://doi.org/10.1636/ arac-43-03-231-292>
- Maddison WP, Hedin MC (2003) Phylogeny of *Habronattus* jumping spiders (Araneae: Salticidae), with consideration of genitalic and courtship evolution. *Systematic Entomology* 28(1): 1–21. <https://doi.org/10.1046/j.1365-3113.2003.00195.x>
- Maddison DR, Maddison WP (2023a) Zephyr: A Mesquite package for interacting with external phylogeny inference programs. Version 3.31. <http://zephyr.mesquiteproject.org>
- Maddison WP, Maddison DR (2023b) Mesquite: a modular system for evolutionary analysis. Version 3.81. <http://www.mesquiteproject.org>

- Maddison WP, Beattie I, Marathe K, Ng PYC, Kanesharatnam N, Benjamin SP, Kunte K (2020a) A phylogenetic and taxonomic review of baviine jumping spiders (Araneae, Salticidae, Baviini). *ZooKeys* 1004: 27–97. <https://doi.org/10.3897/zookeys.1004.57526>
- Maddison WP, Maddison DR, Derkarabetian S, Hedin M (2020b) Sitticine jumping spiders: Phylogeny, classification, and chromosomes (Araneae, Salticidae, Sitticini). *ZooKeys* 925: 1–54. <https://doi.org/10.3897/zookeys.925.39691>
- Marathe K, Maddison WP, Kunte K (2024) *Ghatippus paschima*, a new species and genus of plexippine jumping spider from the Western Ghats of India (Salticidae, Plexippini, Plexippina). *ZooKeys* 1191: 89–103. <https://doi.org/10.3897/zookeys.1191.114117>
- Masta SE, Boore JL (2004) The complete mitochondrial genome sequence of the spider *Habronattus oregonensis* reveals rearranged and extremely truncated tRNAs. *Molecular Biology and Evolution* 21(5): 893–902. <https://doi.org/10.1093/molbev/msh096>
- Nguyen L-T, Schmidt HA, von Haeseler A, Minh BQ (2015) IQ-TREE: A fast and effective stochastic algorithm for estimating maximum likelihood phylogenies. *Molecular Biology and Evolution* 32(1): 268–274. <https://doi.org/10.1093/molbev/msu300>
- Prószyński J (2002) Remarks on Salticidae (Aranei) from Hawaii, with description of *Havaika* - gen. nov. *Arthropoda Selecta* 10: 225–241.
- Prószyński J (2008) A Survey of *Havaika* (Aranei: Salticidae), and endemic genus from Hawaii, including descriptions of new species. *Arthropoda Selecta* 16: 195–213.
- Simon E (1900) Arachnida. In: Sharp D (Ed.) *Fauna Hawaiiensis, or the zoology of the Sandwich Isles: being results of the explorations instituted by the Royal Society of London promoting natural knowledge and the British Association for the Advancement of Science. Volume II, Part V.* University Press, Cambridge, 443–519, pl. 15–21].
- Smith ML, Carstens BC (2020) Process-based species delimitation leads to identification of more biologically relevant species. *Evolution; International Journal of Organic Evolution* 74(2): 216–229. <https://doi.org/10.1111/evo.13878>
- Stamatakis A (2014) RAxML Version 8: A tool for phylogenetic analysis and post-analysis of large phylogenies. *Bioinformatics (Oxford, England)* 30(9): 1312–1313. <https://doi.org/10.1093/bioinformatics/btu033>
- Talavera G, Castresana J (2007) Improvement of phylogenies after removing divergent and ambiguously aligned blocks from protein sequence alignments. *Systematic Biology* 56(4): 564–577. <https://doi.org/10.1080/10635150701472164>
- Yang Z, Rannala B (2010) Bayesian species delimitation using multilocus sequence data. *Proceedings of the National Academy of Sciences of the United States of America* 107(20): 9264–9269. <https://doi.org/10.1073/pnas.0913022107>
- Zhang J, Li Z, Lai J, Zhang Z, Zhang F (2023) A novel probe set for the phylogenomics and evolution of RTA spiders. *Cladistics* 39(2): 116–128. <https://doi.org/10.1111/cla.12523>

A review of the leaf-beetle genus *Sinoluperus* Gressitt & Kimoto, 1963 (Coleoptera, Chrysomelidae, Galerucinae) from China, with the description of a new species

Hai-Dong Yang¹, Chuan Feng^{2,3}, Xing-Ke Yang^{1,2}

1 Guangdong Public Laboratory of Wild Animal Conservation and Utilization, Guangdong Key Laboratory of Animal Conservation and Resource Utilization, Institute of Zoology, Guangdong Academy of Sciences, Guangzhou, Guangdong 510260, China

2 Key Laboratory of Zoological Systematics and Evolution, Institute of Zoology, Chinese Academy of Sciences, 1 Beichen West Road, Chaoyang District, Beijing 100101, China

3 University of Chinese Academy of Sciences, No. 19(A) Yuquan Road, Shijingshan District, Beijing, 100049, China

Corresponding author: Xing-Ke Yang (yangxk@ioz.ac.cn)

Abstract

In this study, all species of the leaf-beetle genus *Sinoluperus* Gressitt & Kimoto, 1963 from China are redescribed based on the reexamination of type specimens, and a new species, *S. variegatus* sp. nov. from Nanling Mountains, is described. A key to the three Chinese species of *Sinoluperus* is provided, as well as photographs of the habitus and aedeagi of these species.

Key words: Key, Nanling mountains, taxonomy



Academic editor: A. Konstantinov

Received: 27 November 2023

Accepted: 29 March 2024

Published: 9 May 2024

ZooBank: <https://zoobank.org/AA0F48DC-D313-4D5C-890A-FD20358765A5>

Citation: Yang H-D, Feng C, Yang X-K (2024) A review of the leaf-beetle genus *Sinoluperus* Gressitt & Kimoto, 1963 (Coleoptera, Chrysomelidae, Galerucinae) from China, with the description of a new species. ZooKeys 1200: 231–243. <https://doi.org/10.3897/zookeys.1200.116337>

Copyright: © Hai-Dong Yang et al.

This is an open access article distributed under terms of the Creative Commons Attribution License (Attribution 4.0 International – CC BY 4.0).

Introduction

The genus *Sinoluperus* was established by Gressitt and Kimoto (1963) based on *Sinoluperus subcostatus* Gressitt & Kimoto, 1963 from southern China (Zhejiang, Jiangxi, Sichuan, Guangdong, and Hainan). Not until 1998 was a second species, *Sinoluperus wuyiensis* Yang & Wu, 1998 described from Wuyishan Mountains, China (Fujian) (Yang et al. 1998). Mohamedsaid (1999) described the third species, *Sinoluperus beta* Mohamedsaid, 1999, from Maxwell's Hill in Perak, Malaysia. In 2008, Lopatin reported the fourth species, *Sinoluperus vietnamicus* Lopatin, 2008 from Vietnam. Prior to the present study, only four species of *Sinoluperus* have been known, all distributed in the Oriental Region and with three species recorded from China.

Sinoluperus species can be identified by following characters: body elongate, medium-sized, dorsal surface of body hairless and mostly yellowish brown or

black-brown; head and pronotum about with same width, vertex covered with punctures; frontal tubercles transverse; antennae extending to apex of elytra or longer than body, antennomere 2 shortest, antennomere 3 approximately 3.5× as long as antennomere 2, antennomere 4 nearly equal in length to antennomere 3 or slightly longer than 3, antennomeres 5–11 decreasing slightly in length; pronotum slightly wider than long, all margins bordered, disc slightly convex, without impression, finely and sparsely covered with punctures; scutellum triangular, with punctures or impunctate; lateral margins of elytra straight and parallel, humeri strongly convex, elytron with longitudinal impressions and punctures along impressions; elytral epipleuron broad at base, narrowed from middle to apex, disappeared before apex; procoxal cavity open behind; tibia with apical spur; first metatarsomere equal to combined remaining tarsomeres; aedeagus ventrally with a flat middle part, base with a large orifice, apex strongly sclerotized and with protrusions; in lateral view, apical protrusions, with flat middle part, and slightly curved basal part; and last visible sternite three-lobed in male and complete in female.

Recently, when we studied leaf beetles from the Nanling Mountains, southern China, two species of *Sinoluperus* were identified: *S. wuyiensis* Yang & Wu, 1998 and *S. variegatus* sp. nov.

Materials and methods

The specimens of new species were collected in the Nanling Mountains by net sweeping. Specimens were preserved in 100% ethanol. Morphological characters were examined with an Olympus SZ61 microscope. Male genitalia from each species were dissected using the following procedure: for dried or ethanol preserved specimens, the abdomen was removed from each specimen, boiled in water for 5–10 min, then transferred to a vial containing 10% KOH solution. The abdomen with the aedeagus was washed in distilled water 3 or 4 times, transferred to a cavity slide using fine forceps. The aedeagus was separated from the abdomen using a hooked, fine dissecting needle. Habitus images were taken using a Canon 5DSR/Nikon SMZ25 digital camera. Aedeagus images were taken using a Nikon D610 digital camera, attached to a Zeiss V/A1 microscope (with 5× objective lens). A cable shutter release was used to prevent the camera from vibration. To obtain the full depth of focus, all images were stacked using Helicon Focus 7 and the resulting output was edited with Adobe Photoshop CC.

The type specimens of new species are deposited in the following two institutions: the Institute of Zoology, Guangdong Academy of Sciences, Guangzhou, China (**IZGAS**); Institute of Zoology, Chinese Academy of Sciences, Beijing, China (**IZAS**).

Abbreviations and depositories used in the paper:

TL	type locality
TD	type deposition
CAS	California Academy of Sciences, San Francisco, California, USA
IZAS	Institute of Zoology, Chinese Academy of Sciences, Beijing, China
IZGAS	Institute of Zoology, Guangdong Academy of Sciences, Guangzhou, China

Taxonomic account

Key to Chinese species of *Sinoluperus*

- 1 Vertex covered with sparsed punctures (Fig. 1A); aedeagus slender, two apical protrusions strongly produced apically, long, cone-shaped, close to each other ***S. variegatus* sp. nov.**
- Vertex covered with dense punctures (Fig. 1B, C); aedeagus robust, two apical protrusions weakly developed, short, nipple-shaped or short cone-shaped..... **2**
- 2 Pronotum ~1.4× as wide as long; elytra black-brown or yellowish brown ..
..... ***S. subcostatus***
- Pronotum twice as wide as long, elytra yellowish-brown ***S. wuyiensis***

Sinoluperus variegatus sp. nov.

<https://zoobank.org/63019284-6F92-46C7-8FA9-AEDFB2B2E8B8>

Figs 1A, 2–4

Type material. Holotype: ♂ (Fig. 2), China, Hunan Province, Yizhang, Mangshan National Nature Reserve, zeziping, 22 May 2021, Nanling investigation team leg., IZGAS. **Paratypes:** 6♂♂1♀, same data as for preceding. 1♀, China, Guangdong Province, Ruyuan, Nanling National Nature Reserve, 20 May 2021, Nanling investigation team leg., IZGAS. 1♂, same data as for preceding, 29 May 2021, Chuan Feng leg., IZGAS. 1♂1♀, same data as for preceding, 11 Jun. 2021, Chuan Feng et al. leg., IZGAS. 3♀♀, same data as for preceding, 19 Jun. 2021, Chuan Feng et al. leg., IZGAS.

Diagnosis. The new species closely resembles *S. subcostatus* Gressitt & Kimoto, 1963, but it differs from the latter by its slender aedeagus with a gradually narrowed apical part in ventral view. In *S. subcostatus*, the aedeagus is robust, and its apical part is abruptly narrowed in ventral view. Light-colored specimens of new species closely resemble *S. wuyiensis* Yang & Wu, 1998. However, the vertex of *S. variegatus* sp. nov. almost impunctate, vertex of *S. wuyiensis* strongly and closely punctate.

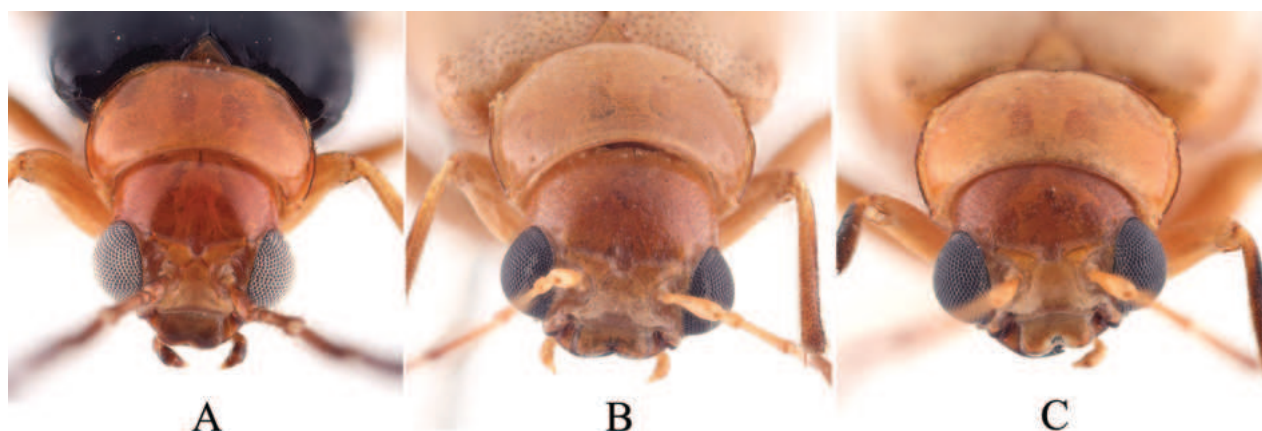


Figure 1. Head of *Sinoluperus* species **A** *S. variegatus* sp. nov. **B** *S. subcostatus* Gressitt & Kimoto, 1963 **C** *S. wuyiensis* Yang & Wu, 1998.

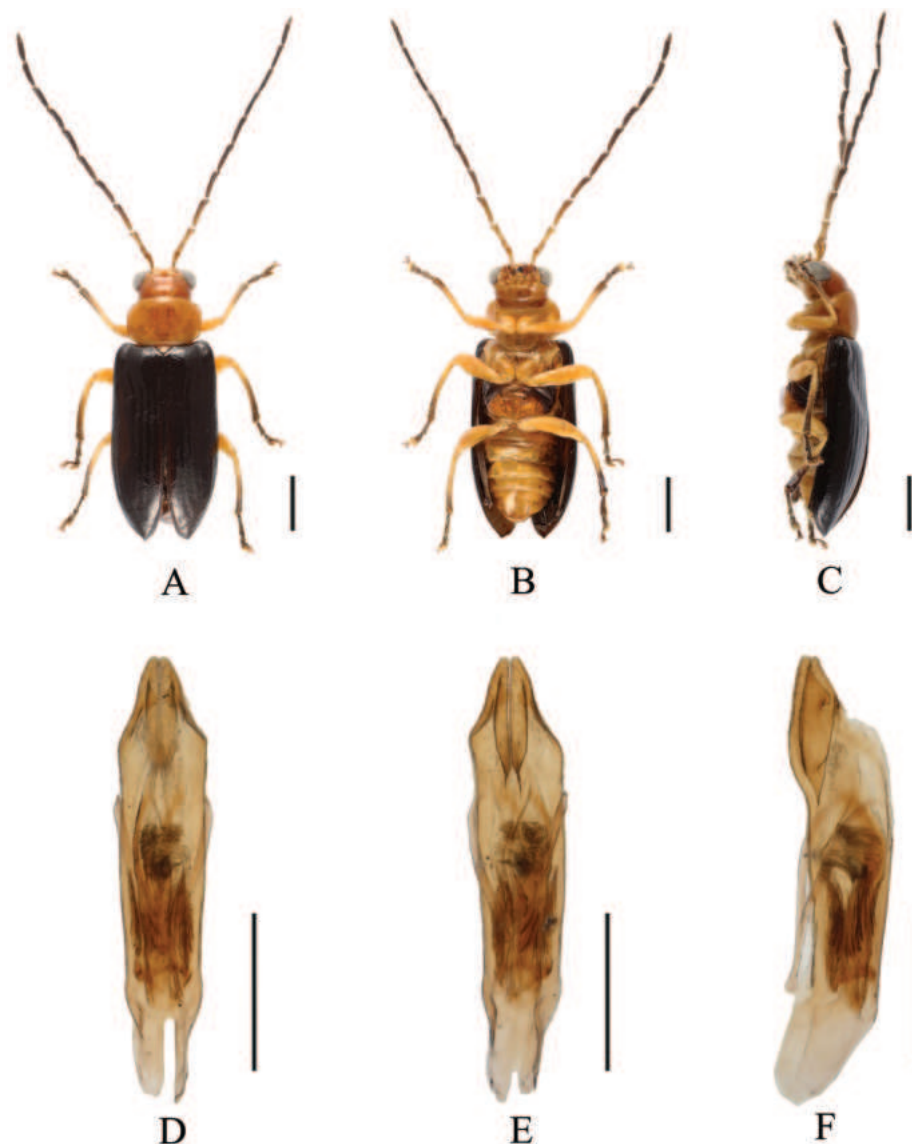


Figure 2. *Sinoluperus variegatus* sp. nov. (holotype, male) **A–C** habitus (male) **D–F** aedeagus **A, D** dorsal view **B, E** ventral view **C, F** lateral view. Scale bars: 1 mm (**A–C**); 0.5 mm (**D–F**).

Description. Male. Length: 4.5–5.0 mm. Head, pronotum, scutellum, ventral side of body, femur, and basal half of tibia yellow or orange. Antennae black-brown, with antennomeres 1–3 yellow-brown, most of metepimeron brown. Elytra black-brown or pale in some specimens. Apical half of tibia, tarsus, and claw black-brown.

Vertex with sparse punctures, with fine reticulation. Frontal tubercles transverse, extending downward between antennal bases. Antennae longer than body; antennomeres 1 bare, rod-shaped, antennomeres 2–11 with short hairs, antennomere 2 shortest, antennomere 3 ~3.5× as long as antennomere 2; antennomere 4 ~1.3× as long as antennomere 3, thick and curved at apex, antennomere 5 equal to antennomere 4 in length, antennomeres 6–11 gradually shortened.

Pronotum ~1.5× as wide as long, lateral margins straight at base and slightly rounded at apex; three setae present on each side of lateral margins, basal

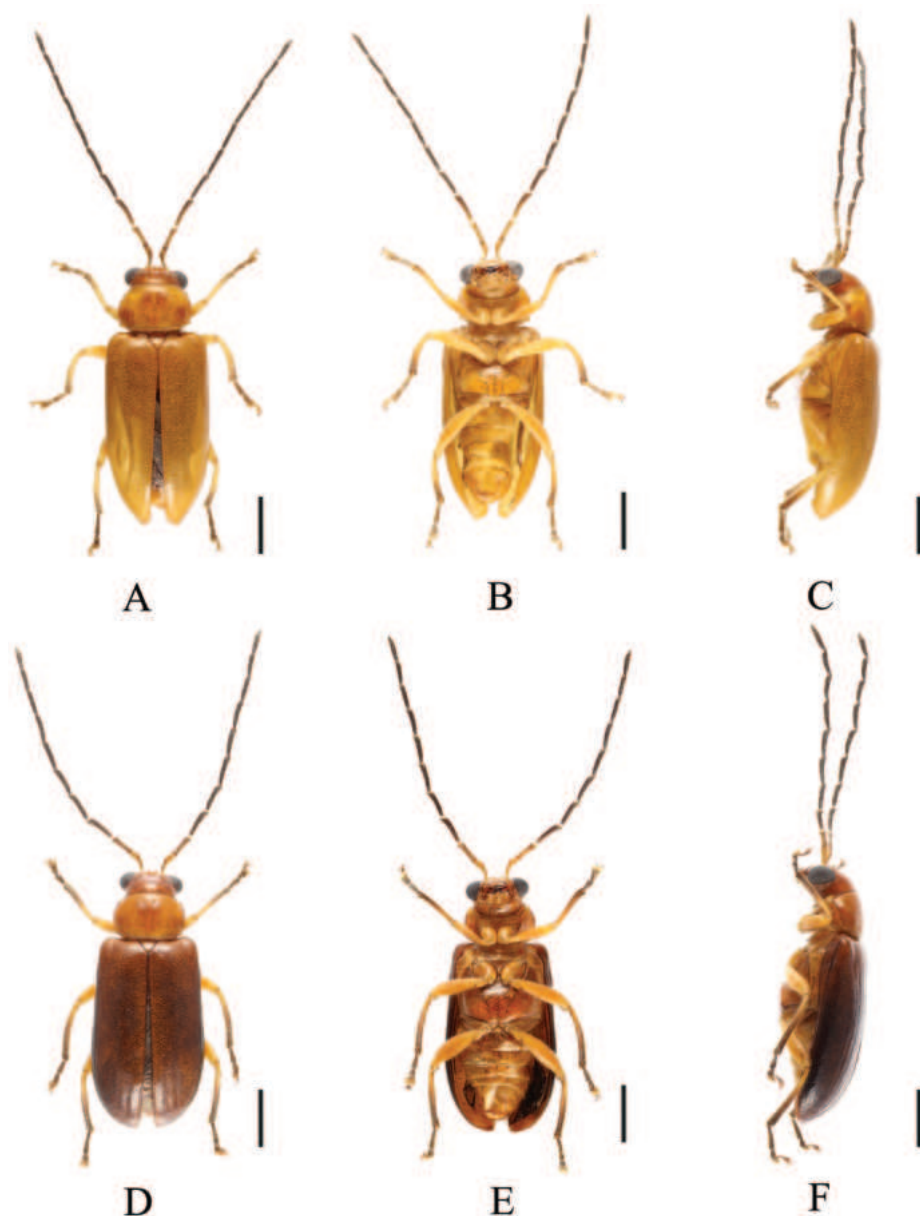


Figure 3. *Sinoluperus variegatus* sp. nov. (paratype male) A–F habitus A, D dorsal view B, E ventral view C, F lateral view. Scale bars: 1 mm.

margin slightly convex, anterior margin slightly concave, anterior and posterior angles thickened and rounded; disc strongly convex, with sparse and fine punctures, shiny.

Scutellum triangular, smooth, impunctate.

Elytra wider than pronotum at base, humeri strongly convex, lateral sides subparallel and gradually widened posteriorly. Disc with 10 shallow longitudinal grooves, covered with small punctures in grooves, interstices of punctures wider than diameter of individual puncture. Elytral epipleuron broad at base, narrowed at middle, gradually narrowed from middle to apex.

Legs strong, each tibia with distinct spur at apex, tarsomere 1 of hind tarsi equal to combined remaining tarsomeres.

Aedeagus slender; in ventral view, sides abruptly narrowed near apex, with apical protrusions forming two cones close to each other.

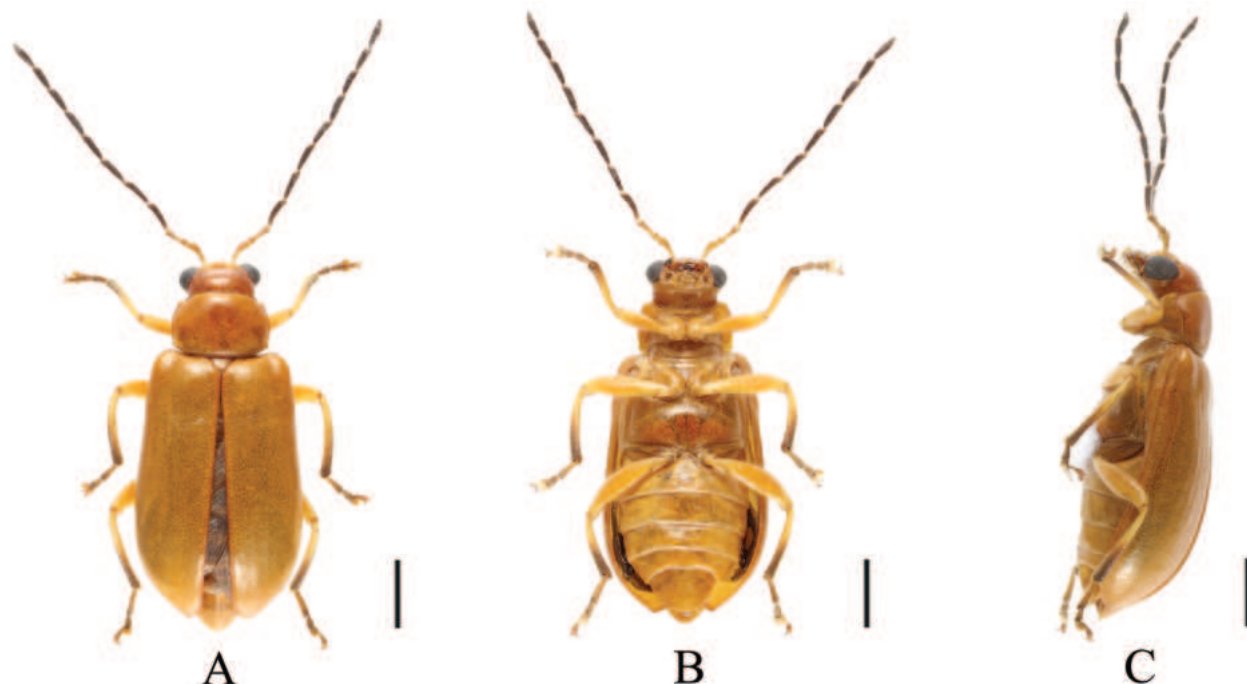


Figure 4. *Sinoluperus variegatus* sp. nov. (paratype, female) **A–C** habitus **A** dorsal views **B** ventral views **C** lateral views. Scale bars: 1 mm.

Female. Length 6.5 mm. Head, pronotum, scutellum, ventral surface of body, femur, and base of tibia yellowish brown; apical half of tibia, tarsus, claw black brown. Antennae black-brown, with antennomeres 1–3 yellow-brown. Antenna $\sim 2/3$ of body length, antennomere 3 $\sim 3\times$ as long as antennomere 2; antennomere 4 $\sim 1.5\times$ as long as antennomere 3, antennomere 5 equal in length to antennomere 4, antennomere 6 slightly shorter than antennomere 5, antennomeres 7–11 gradually widened. Punctures Barely visible on pronotum and elytra.

Distribution. China: Zhejiang, Hunan, Guangdong.

Etymology. The species name (Latin, meaning “variegated”) refers to the variable color of elytra.

***Sinoluperus subcostatus* Gressitt & Kimoto, 1963**

Figs 1B, 5–8

Sinoluperus subcostatus Gressitt and Kimoto 1963: 584. TL: China, Jiangxi. TD: CAS.

Type specimens examined. Holotype: ♂. Hong San, SE Kiangsi Prov, China, 16. Jul. 1936, Gressitt leg., CAS8509. **Paratypes:** ♀. Szechuan, W. China, Pe-pei,, 28. Jul. 1940, Gressitt; 300 m a. s. l. Brit. Mus. 1963-245. ♂. China, Hainan Province, Tai-pin (Dwa-bi), 325 m a. s. l., 22 Jul. 1935, Gressitt leg., IZAS.

Additional specimens examined. 1 ♀, China, Hunan Province, Yizhang, Mangshan National Nature Reserve, chawanggu, 25 Aug 2020, Siyuan Xu leg., IZGAS.

Description. Male. Length 4.8–5.2 mm. Body ochraceous, apical half of tibia, tarsus, and claw reddish brown. In the paratype in IZCAS, head, pronotum, scutellum, ventral surface of body, femur, and base of tibia yellow; antennae



Figure 5. *Sinoluperus subcostatus* (male) (holotype) A–C habitus A dorsal view B lateral view C head view. Scale bars: 1 mm.

black-brown with antennomeres 1 and 2 yellow, elytra black-brown with reddish brown at apex. Apical half of tibia, tarsus, and claw brown.

Vertex covered with closed punctures. Frontal tubercles transverse. Antennae longer than body. Antennomeres 1 bare, rod-shaped, antennomeres 2–11 with short hairs, antennomere 2 shortest, antennomere 3 ~3.7× as long as antennomere 2; antennomere 4 ~1.4× as long as antennomere 3, antennomeres 5–11 equal in length, and slightly shorter than antennomere 4.



Figure 6. *Sinoluperus subcostatus* (female) (paratype) A–C habitus A dorsal view B lateral view C head view. Scale bars: 1 mm.

Pronotum $\sim 1.4\times$ as wide as long, anterior margin straight; basal margin slightly convex, lateral margins straight at base and slightly rounded at apex, anterior angle projecting, basal angle obtuse, disc convex, with sparse punctures.

Scutellum triangular, with several small punctures.

Elytra wider than pronotum basally, humeri strongly convex, lateral margins of elytra gradually widened posteriorly. Elytra disc with 10 shallow longitudinal grooves and covered with small punctures, the interstices of punctures equal with diameter of individual puncture. Epipleuron broad basally, strongly nar-

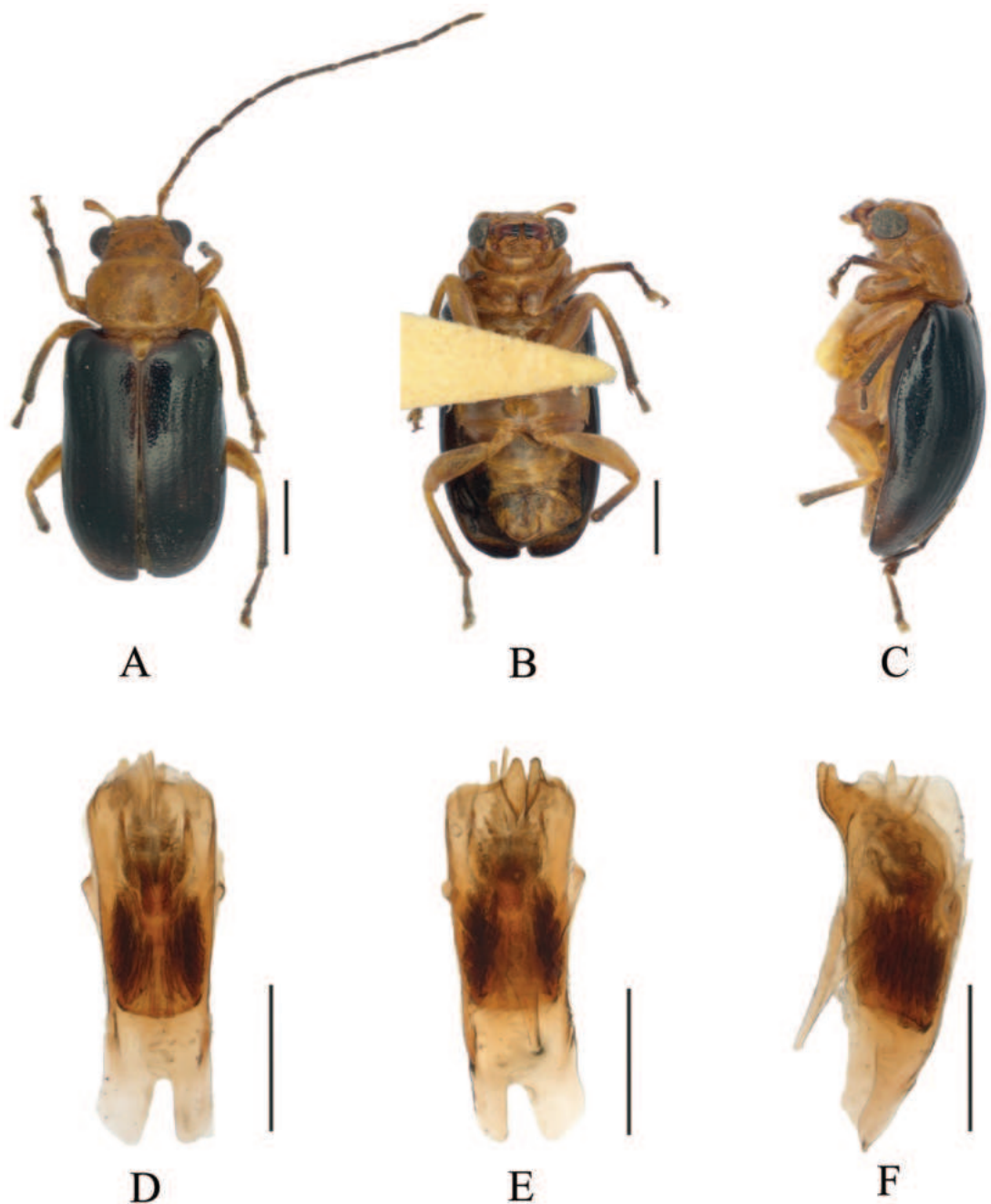


Figure 7. *Sinoluperus subcostatus* (male) (paratype) **A–C** habitus **D–F** aedeagus **A, D** dorsal view **B, E** ventral view **C, F** lateral view. Scale bars: 1 mm (**A–C**); 0.5 mm (**D–F**).

rowed at middle, gradually narrowed from middle to apex. Leg strong, each tibia with a distinct spur at apex.

Aedeagus robust, in ventral view, with sides slightly dilating near apex; apical protrusions short-cone-shaped, close to each other.

Female. Length 5.2–5.5 mm. Head reddish brown; Antennae reddish brown with antennomeres 1–3 yellow, pronotum, scutellum, ventral surface of body, femur, and base of tibia brown or yellowish brown; apical half of tibia, tarsus, claw reddish brown.

Distribution. China: Zhejiang, Jiangxi, Hongkong, Guangdong, Hainan, Sichuan; Laos.

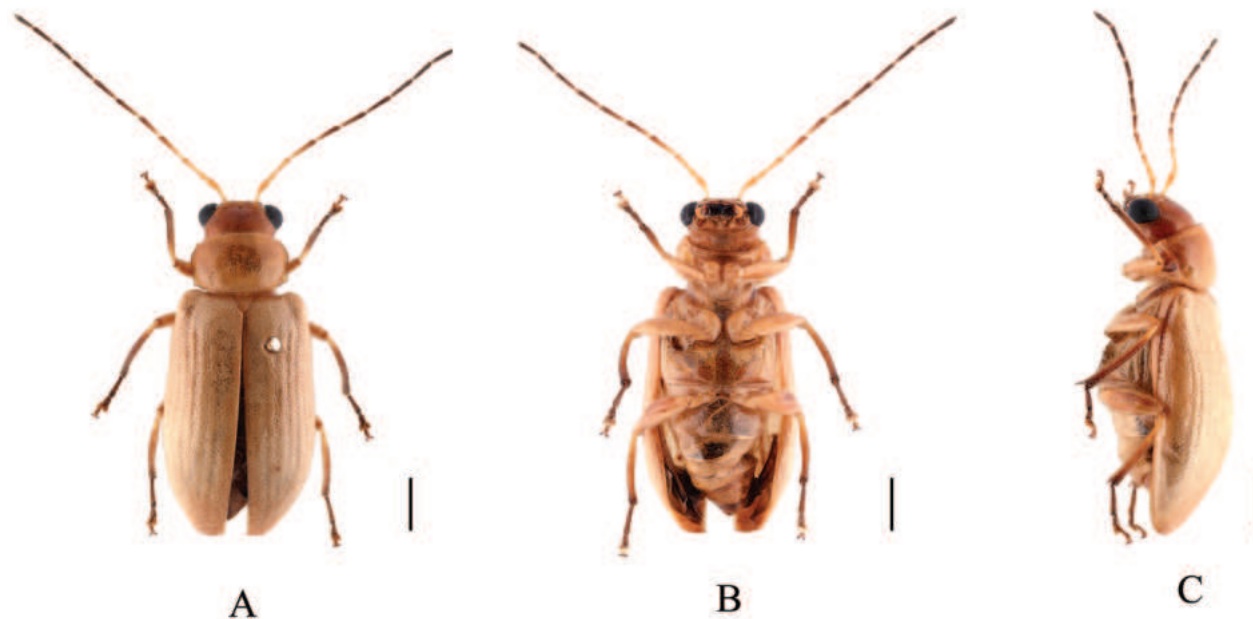


Figure 8. *Sinoluperus subcostatus* (female) A–C habitus A dorsal view B ventral view C lateral view. Scale bars: 1 mm.

***Sinoluperus wuyiensis* Yang & Wu, 1998**

Figs 1C, 9, 10

Sinoluperus wuyiensis Yang & Wu, 1998: 262. TL: China, Fujian. TD: IZAS.

Type specimens examined. Holotype: ♂, China, Fujian province, Mount Wuyi, Maopai, 1 Aug. 1997, Yanyu Wu leg., IZAS. **Paratypes:** 1♂, China, Fujian Province, Mount Wuyi, Pikeng, 520 m a. s. l., 31 Jul. 1997, Yanyu Wu leg., IZAS. 2♂♂, Fujian Province, Mount Wuyi, Huangxizhou, 650 m a. s. l., 6 Aug. 1997, Jiashe Wang leg., IZAS. 1♂, China, Fujian Province, Mount Wuyi, Diaoqiao, 540 m a. s. l., 11 Aug. 1997, Youwei Zhang leg., IZAS.

Additional specimens examined. 1♀, China, Guangdong Province, Ruyuan, Nanling National Nature Reserve, xiaohuangshan, 18 Jul. 2022, Meiyong Lin et al. leg., IZGAS. 1♂, China, Guangdong Province, Chebaling National Nature Reserve, Shixing County, 24 Jun. 2022, Meiyong Lin et al. leg., IZGAS.

Description. (♂) Length 4.5–6.0 mm. Head, pronotum, scutellum, ventral surface of body, femur, and base of tibia reddish brown or yellowish brown; antennae ranged from black to brown with antennomeres 1–3 yellow; in some specimens antennae yellow with antennomeres 7–11 black-brown. Elytra yellow; apical half of tibia, tarsus, and claw brown.

Vertex covered with closed punctures. Frontal tubercles small, antennae longer than body. Antennomere 1 bare, rod-shaped, antennomeres 2–11 with short hairs, antennomere 2 shortest, antennomere 3 ~3× as long as antennomere 2; antennomere 4 ~1.2× as long as antennomere 3, antennomeres 4–11 equal in length.

Pronotum ~2× as wide as long, basal and apical margins slightly convex, disc strongly convex with dense punctures.

Scutellum triangular, smooth, impunctate.

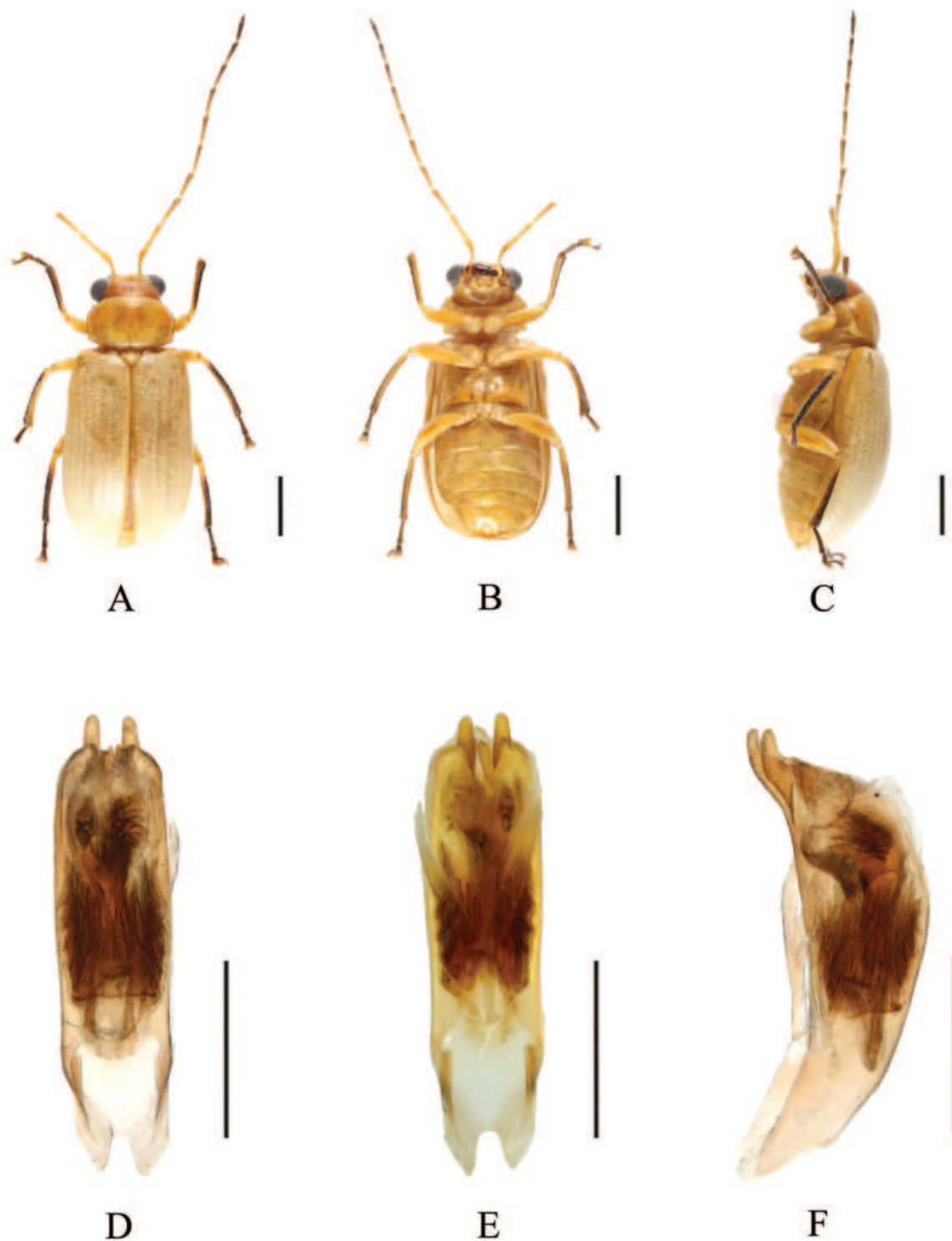


Figure 9. *Sinoluperus wuyiensis* (male) **A–C** habitus **D–F** aedeagus **A, D** dorsal view **B, E** ventral view **C, F** lateral view. Scale bars 1 mm (**A–C**); 0.5 mm (**D–F**).

Elytra wider than pronotum basally, humeri strongly convex, subparallel-sided but gradually widened posteriorly. Disc with 8–10 longitudinal grooves, covered with dense punctures, interstices of punctures narrower than diameter of individual puncture. Elytral epipleuron broad at base, strongly narrowed at middle, gradually narrowed from middle to apex.

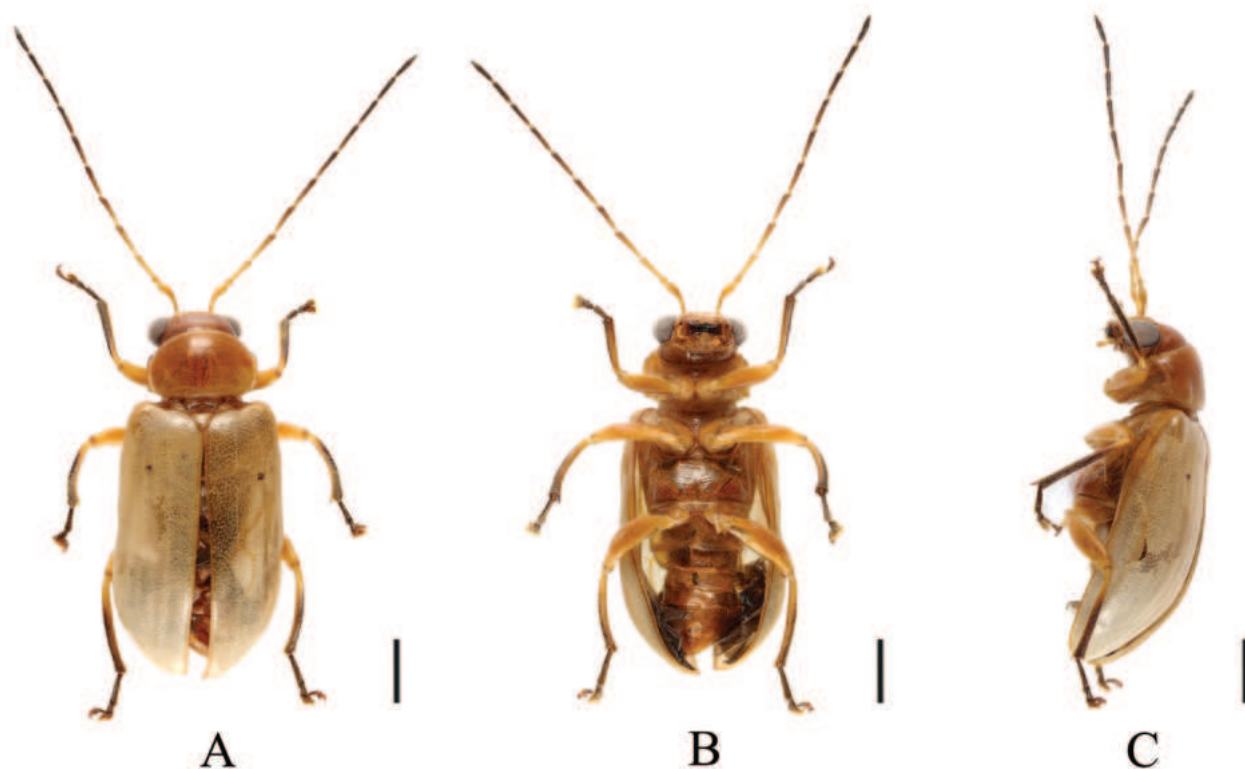


Figure 10. *Sinoluperus wuyiensis* (female) A–C habitus A dorsal view B ventral view C lateral view. Scale bars: 1 mm.

Legs strong, each tibia with distinct spur at apex, segment 1 of hind tarsi equal to combined remaining segments.

Aedeagus robust, with parallel sides and rounded apex in ventral view. Apical protrusions nipple-shaped, small, well separated from each other.

Female. Length 5.5 mm. Antennomere 3 ~3.5× as long as antennomere 2; apical ventrite with longitudinal concave in the middle.

Distribution. China: Hunan, Fujian, Guangdong.

Acknowledgements

We thank Nathalie Yonow (Swansea University) for checking the English and giving useful comments. We thank Ron Beenen (Naturalis Biodiversity Center) for his professional opinions on revising the manuscript. We acknowledge Christopher C. Grinter (California Academy of Sciences) and Rachel Diaz-Bastin (California Academy of Sciences) for taking photos of the holotype of *Sinoluperus subcostatus*. We acknowledge Zulong Liang for taking photos of the paratype of *S. subcostatus*. We thank the Institute of Zoology, Chinese Academy of Sciences and Institute of Zoology, Guangdong Academy of Science for providing the specimens.

Additional information

Conflict of interest

The authors have declared that no competing interests exist.

Ethical statement

No ethical statement was reported.

Funding

This research was supported by the GDAS Special Project of Science and Technology Development (grant numbers 2020GDASYL-20200102021).

Author contributions

All authors have contributed equally.

Author ORCIDs

Hai-Dong Yang  <https://orcid.org/0000-0002-3157-2090>

Chuan Feng  <https://orcid.org/0009-0001-9299-3526>

Data availability

All of the data that support the findings of this study are available in the main text.

References

- Gressitt JL, Kimoto S (1963) The Chrysomelidae (Coleopt.) of China and Korea. Part II. Pacific Insects Monograph 1B: 301–1026.
- Lopatin IK (2008) *Sinoluperus vietnamicus* sp. n. – the first representative of the Chinese genera in Vietnam (Coleoptera: Chrysomelidae: Galerucinae). Zoosystematica Rossica 17(1): 150. <https://doi.org/10.31610/zsr/2008.17.1.150>
- Mohamedsaid MS (1999) *Sinoluperus beta*, n. sp., a second species for the genus (Coleoptera: Chrysomelidae: Galerucinae). Serangga 4: 17–20.
- Yang XK, Wang JS, Wu YY (1998) Three new species of Galerucinae (Coleoptera: Chrysomelidae) from Wuyi Mountain. Entomotaxonomia 20: 261–264.

A review of the genus *Vitrea* Fitzinger, 1833 (Gastropoda, Eupulmonata, Pristilomatidae) in Serbia: diversity, distribution and the description of a new species

Vukašin Gojšina¹, Nikola Vesović¹, Srećko Ćurčić¹, Tamara Karan-Žnidaršič¹, Biljana Mitrović², Ivaylo Dedov³

1 University of Belgrade - Faculty of Biology, Studentski Trg 16, 11000 Belgrade, Serbia

2 The Museum of Natural History, Njegoševa 51, 11000 Belgrade, Serbia

3 Institute of Biodiversity and Ecosystem Research, Bulgarian Academy of Sciences, 2 Gagarin Street, 1113 Sofia, Bulgaria

Corresponding author: Vukašin Gojšina (vukasin.gojsina@bio.bg.ac.rs)

Abstract

In this paper, the genus *Vitrea* Fitzinger, 1833 in Serbia is reviewed. All previous literature data on this genus from Serbia are summarised and used to discuss its distribution in the country and create distribution maps, supplemented by new material collected by the authors. All Serbian species are figured. For each species, a brief description of the examined specimens, data on previous findings in Serbia, the material (including types) that were analysed, the distribution and habitats in Serbia they inhabit, as well as remarks on specific species are given. A new species, *Vitrea virgo* Gojšina & Dedov, **sp. nov.**, is described from a pit on Mt. Devica in eastern Serbia. *Vitrea pygmaea* (O. Boettger, 1880) is reported for the first time for the territory of Serbia. As some *Vitrea* species have a narrow geographical range and prefer certain habitats, they are particularly vulnerable to habitat changes, which is also discussed in the paper. An identification key for all hitherto known Serbian species is given.

Key words: faunistics, Mt. Devica, pit, taxonomy, terrestrial snails



Academic editor: A. M. de Frias Martins

Received: 9 February 2024

Accepted: 5 April 2024

Published: 9 May 2024

ZooBank: <https://zoobank.org/E036D2E9-67FE-4ACE-8EAC-B5426BC3102D>

Citation: Gojšina V, Vesović N, Ćurčić S, Karan-Žnidaršič T, Mitrović B, Dedov I (2024) A review of the genus *Vitrea* Fitzinger, 1833 (Gastropoda, Eupulmonata, Pristilomatidae) in Serbia: diversity, distribution and the description of a new species. ZooKeys 1200: 245–273. <https://doi.org/10.3897/zookeys.1200.120633>

Copyright: © Vukašin Gojšina et al.
This is an open access article distributed under terms of the Creative Commons Attribution License (Attribution 4.0 International – CC BY 4.0).

Introduction

Vitrea Fitzinger, 1833 is a genus of tiny terrestrial pulmonate gastropods with a shell width (SW) < 6 mm, usually with an unpigmented body and a translucent shell (Welter-Schultes 2012). The genus is widespread in Europe and extends eastwards all the way to Iran (Riedel 1966; Sysoev and Schileyko 2009; Welter-Schultes 2012). The southernmost known localities are situated in North Africa (Pintér 1969; Riedel 1976). Although there are several relatively widespread species, most species are known from limited geographical areas (Welter-Schultes 2012; Páll-Gergely and Asami 2015). The genus is the richest in species within the family Pristilomatidae, with a total of 78 extant species (MolluscaBase 2024), ~ 40 of which inhabit the Balkans (Pintér 1972; Welter-Schultes 2012). Several species are described and known exclusively from caves (Wagner 1914; Riedel and Velkovrh 1976; Pintér 1983), while several others occasionally inhabit caves and are usually restricted to limestone habitats (Pintér 1972; Riedel 1984).

The three most species-rich European pristinomatid genera (*Gyalina* Andreae, 1902, *Lindbergia* A. Riedel, 1959, and *Vitrea*) are relatively well-separated from each other conchologically. The most important conchological difference between *Lindbergia* and *Vitrea* lies in the size of the shell (the shell of the former is larger). *Gyalina* has a peculiar shell surface in the form of strong spiral striae and a *Nautilus*-like protruded apertural margin (Welter-Schultes 2012). There are also clear differences between them in their genital anatomy. In contrast to *Gyalina* and *Lindbergia*, *Vitrea* has no epiphallus and its seminal receptacle is reduced or absent. These two structures are well-developed in *Gyalina* and *Lindbergia*. The genus *Spinophallus* A. Riedel, 1962 also has a well-developed seminal receptacle, but is additionally characterised by the presence of conical papillae inside the penis (Schileyko 2003).

Vitrea is the only pristinomatid genus in Serbia and is represented by a total of eight species in the country: *V. contracta* (Westerlund, 1871), *V. crystallina* (O. F. Müller, 1774), *V. diaphana* (S. Studer, 1820), *V. illyrica* (A. J. Wagner, 1907), *V. kiliasi* L. Pintér, 1972, *V. kutschigi* (Walderdorff, 1864), *V. sturanyi* (A. J. Wagner, 1907), and *V. subrimata* (Reinhardt, 1871) (Karaman 2007). The first to provide comprehensive data on the distribution of *Vitrea* species in Serbia was Pavlović (1912). In his work, he listed a total of five *Vitrea* species in the country, all of which he assigned to the genus *Crystallus* R. T. Lowe, 1855, a synonym of *Vitrea*. His data were summarised by Tomić (1959). Jaeckel et al. (1957) provided data on species already recorded in Serbia, with no new faunistic records provided. Pintér (1972) revised the genus *Vitrea* from the Balkans and reported new sampling sites from Serbia. Karaman provided further data on the distribution of *Vitrea* species in Serbia in several faunistic papers (Jovanović 1985, 1993, 1996; Karaman 2007, 2012).

The aims of this paper are to: (i) list all species of the genus *Vitrea* in Serbia, (ii) discuss their distribution and occurrence in the country, (iii) describe a new species, *V. virgo* Gojšina & Dedov, sp. nov., and (iv) present an identification key for all known *Vitrea* species in Serbia.

Materials and methods

Most of the snails were collected by the authors (VG, NV, SĆ) from 2021 to 2023, with special attention paid to numerous limestone habitats in eastern Serbia and several of them in western Serbia (altogether 30 sampling sites). This sampling included several localities already visited by Academician Petar S. Pavlović, as well as hitherto unknown sites. The northern part of the country (the Autonomous Province of Vojvodina) was not thoroughly sampled as this region is mostly covered by agricultural fields and almost completely devoid of limestone. Snails were collected manually or were sorted from soil samples under a stereomicroscope. Occasionally, soil was sieved *in situ* and snails were collected immediately. Living animals were preserved in 70% ethanol and labelled accordingly. The shells and genitalia (stored in 70% ethanol) were photographed using a Zeiss SteREO Discovery.V12 stereomicroscope equipped with a Leica Flexacam C3 camera and a Nikon SMZ800N stereomicroscope equipped with a Nikon DS-Fi2 camera. A Nikon DS-L3 control unit was used to set scale bars. Shell microsculpture of the newly described species was imaged using a Jeol JSM-6390LV scanning electron

microscope. The sample was gold-coated under 30 mA for 100 sec using a Bal-Tec SCD 005 sputter coater. Type specimens are deposited in The Museum of Natural History (Belgrade, Serbia) (**NHMBEO**), Institute of Biodiversity and Ecosystem Research (Sofia, Bulgaria) (**IBER**), and Institute of Zoology, University of Belgrade - Faculty of Biology (Belgrade, Serbia) (**IZOO**) collections. The type specimens of *V. illyrica*, *V. kutschigi*, and *V. sturanyi* from the Senckenberg Forschungsinstitut und Naturmuseum (Frankfurt am Main, Germany) (**SMF**) collection were processed and photographed. Part of the *Vitrea* collection of Petar S. Pavlović, deposited in the NHMBEO collection, was also examined (see under the Material examined section for each species). The paratypes of *Vitrea siveci* Riedel & Velkovrh, 1976 and non-type specimen of *V. kiliasi* L. Pintér, 1972, which are deposited in the Museum and Institute of Zoology of the Polish Academy of Sciences (Warsaw, Poland) (**MIZ**) collection, were also used for comparison with the new species. The photos of these two species were taken with a Keyence VHX-7000 digital microscope. Distribution maps were created using data from published literature sources (Möllendorff 1873; Pavlović 1912; Tomić 1959; Pintér 1972; Jovanović 1985, 1993, 1996; Sólymos et al. 2004; Karaman 2012) and newly obtained data. Nomenclature follows MolluscaBase (2024).

Abbreviations used in the text are as follows:

AH	aperture height
AW	aperture width
IBER	Institute of Biodiversity and Ecosystem Research, Bulgarian Academy of Sciences, Sofia, Bulgaria
IZOO	Institute of Zoology, University of Belgrade - Faculty of Biology, Belgrade, Serbia
MIZ	Museum and Institute of Zoology of the Polish Academy of Sciences, Warsaw, Poland
NHMBEO	The Museum of Natural History, Belgrade, Serbia
SH	shell height
SMF	Senckenberg Forschungsinstitut und Naturmuseum (Frankfurt am Main, Germany)
SW	shell width
UW	umbilicus width

Results

Taxonomic account

Class Gastropoda Cuvier, 1795

Superorder Eupulmonata Haszprunar & Huber, 1990

Order Stylommatophora A. Schmidt, 1855

Superfamily Gastrodontoidea Tryon, 1866

Family Pristilomatidae Cockerell, 1891

Genus *Vitrea* Fitzinger, 1833

Type species. *Glischrus (Helix) diaphana* S. Studer, 1802, by monotypy.

***Vitrea contracta* (Westerlund, 1871)**

Figs 1, 15

Crystallus contractus subcontractus – Pavlović 1912: 26.

Crystollus cintractus [sic] – Tomić 1959: 13.

Vitrea contracta – Pintér 1972: 274; Jovanović 1985: 42; Sólymos et al. 2004: 152; Karaman 2012: 24.

Vitrea contracta contracta – Karaman 2007: 141.

Vitrea contracte [sic] – Jovanović 1996: 219.

Sites in Serbia known from the literature. After Pavlović (1912) and Tomić (1959): Topčider, city of Belgrade; Velika Tisnica Gorge, near the town of Žagubica; Metino Brdo hill, near the city of Kragujevac; Sveti Stefan (Lipovac) Monastery, near the town of Aleksinac; Prekonoško Vrelo, village of Prekonoga, near the town of Svrlijig; village of Crnoljevica, near the town of Svrlijig; Sirinjava Duvka, near the village of Periš, Svrlijske Planine Mts.; Jevik hill, near the town of Knjaževac; Mt. Stol, near the city of Bor; after Pintér (1972): town of Raška; near the town of Sokobanja; Sveta Petka Monastery, near the city of Niš; after Jovanović (1985): Mt. Avala, near the city of Belgrade; after Jovanović (1996): Mt. Stol, near the city of Bor; after Sólymos et al. (2004) and Karaman (2012): near the Dobri Potok stream, Mt. Fruška Gora.

Material examined. SERBIA • Near the town of Svrlijig, village of Crnoljevica, leg. P. Pavlović, one specimen (NHMBE0442); Mt. Stol, 26 Sep. 1907, three specimens (NHMBE0445); surroundings of the city of Pirot, a hill above Kitka rock quarry, among rocks, leg. V. Gojšina, M. Vujić & N. Vesović, 28 Apr. 2023, one specimen (43°11'19.65"N, 22°38'47.14"E); Stara Planina Mts., Babin Zub peak, leg. V. Gojšina, M. Vujić & N. Vesović, 07 May 2023, 12 specimens (43°22'25.79"N, 22°36'46.30"E); Felješana Strict Nature Reserve, near the settlement of Debeli Lug, leg. V. Gojšina, M. Vujić & N. Vesović, 03 Jun. 2023, one specimen (44°20'36.48"N, 21°53'20.57"E); Đerdap National Park, village of Dobra, leg. V. Gojšina, M. Vujić & N. Vesović, 05 May 2023, two specimens (44°38'27.53"N, 21°54'29.38"E).

Description of specimens from Serbia. Shell very small, consisting of 4–5 whorls, colourless, translucent, SW usually ~ 2 mm, but ≤ 3 mm. Shell surface smooth. Last whorl ~ 1.5× as wide as penultimate whorl. Umbilicus moderately broad and widening near last whorl, revealing almost all whorls.

Distribution and habitats in Serbia. Mostly found in dry, karstic habitats among rocks. Not frequently found in Serbia, probably overlooked due to its small size. Most records came from eastern Serbia (Fig. 15), otherwise with scarce findings. This species is more widespread in the country, which should be proven by further research.

***Vitrea crystallina* (O. F. Müller, 1774)**

Figs 2, 15

Hyalina crystallina – Möllendorff 1873: 131.

Vitrea crystallina – Hesse 1929: 235; Jaekel et al. 1957: 156; Karaman 2007: 141.

Sites in Serbia known from the literature. After Möllendorff (1873): Mt. Javor; Rača Monastery, Mt. Tara.

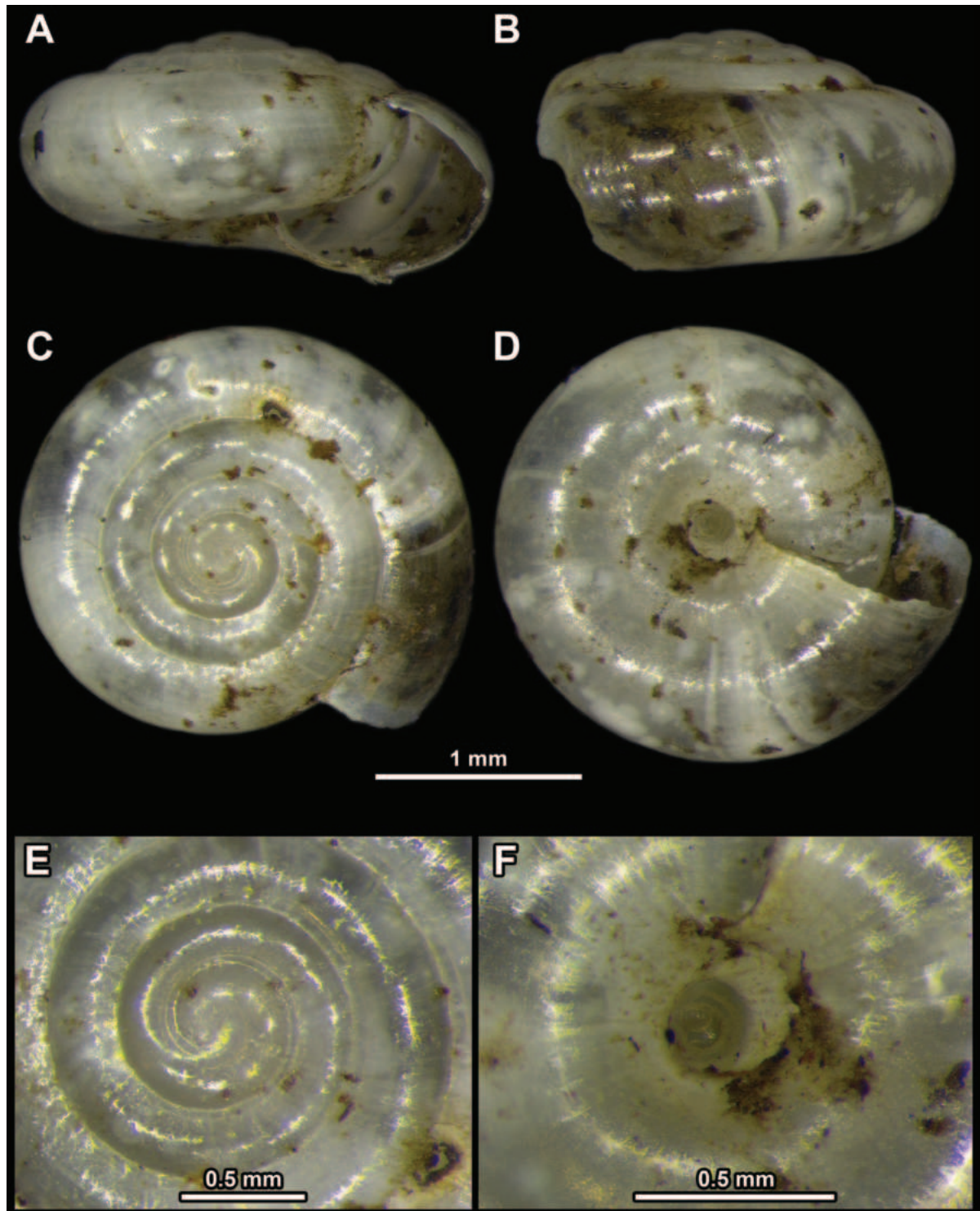


Figure 1. *Vitrea contracta* from the surroundings of the city of Pirot A apertural view B lateral view C apical view D umbilical view E enlarged view of the protoconch F enlarged view of the umbilicus.

Material examined. SERBIA • Village of Deliblato, next to the Kraljevac Lake, leg. V. Gojšina, 11 Oct. 2020, one specimen (44°50'58.44"N, 21°01'17.75"E); city of Belgrade, Kalemegdan fortress, leg. M. Vujić, 28 Dec. 2022, one specimen (44°49'19.23"N, 20°27'02.79"E); town of Sokobanja, village of Resnik, near a spring, leg. V. Gojšina & M. Vujić, 07 Nov. 2023, seven specimens (43°37'57.79"N, 21°48'55.28"E).

Description of specimens from Serbia. Shell up to 3–4 mm wide, colourless, transparent, consisting of 4–5 whorls, which are not densely coiled. Last whorl twice as wide as penultimate whorl. Periphery rounded. Umbilicus open and moderately broad, widening at last whorl. Only penultimate whorl clearly visible through umbilicus.

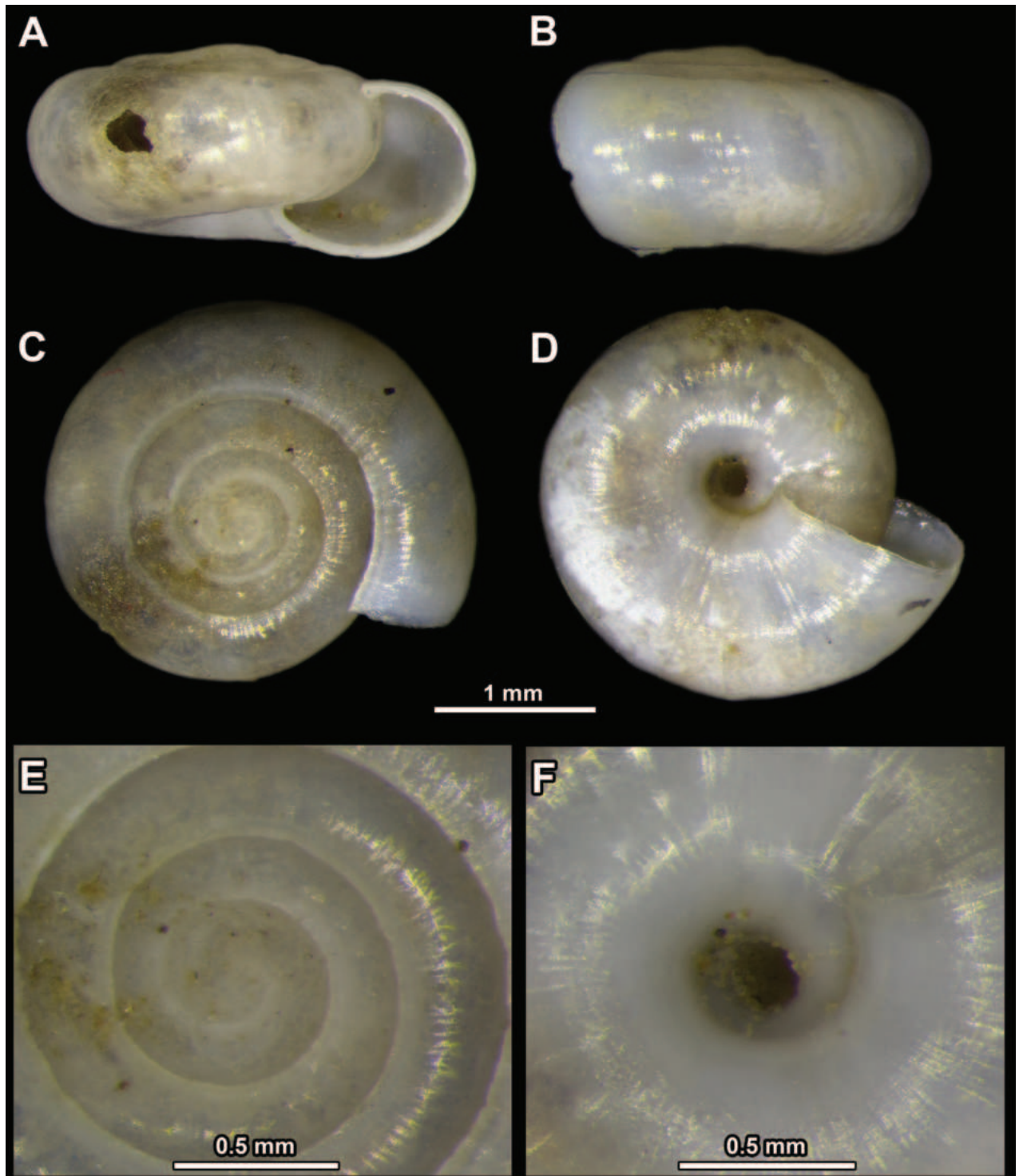


Figure 2. *Vitrea crystallina* from the village of Deliblato **A** apertural view **B** lateral view **C** apical view **D** umbilical view **E** enlarged view of the protoconch **F** enlarged view of the umbilicus.

Distribution and habitats in Serbia. Poorly known from Serbia due to a lack of sampling. It is known from western Serbia, the surroundings of the city of Belgrade and Deliblato Sands (Fig. 15).

***Vitrea diaphana* (S. Studer, 1820)**

Figs 3, 16

Crgstallus diaphanus [sic] – Pavlović 1912: 24–25.

Crystillus diaphanus [sic] – Tomić 1959: 12.

Vitrea diaphana – Jaeckel et al. 1957: 156; Jovanović 1985: 42; Jovanović 1993: 241–242; Jovanović 1996: 219; Karaman 2007: 141; Karaman 2012: 24.

Vitrea diaphana diaphana – Pintér 1972: 214; Sólymos et al. 2004: 152.

Sites in Serbia known from the literature. After Pavlović (1912) and Tomić (1959): Topčider, city of Belgrade; Mt. Beljanica; Velika Tisnica Gorge, near the town of Žagubica; Mt. Vujan, near the town of Gornji Milanovac; Mt. Vidlič, near the city of Pirot; near the Sveta Petka Monastery, Grza Gorge, near the town of Paraćin; Jelašnica Gorge, near the city of Niš; Mt. Javor; next to the Dubočica river, near the town of Raška; Radmanov Kamen, Mt. Kopaonik; around the Pogana Peć Cave, near the village of Krepoljin; Koprivštički Krst, near the city of Pirot; village of Lunjevica, near the town of Gornji Milanovac; Rajkovo, near the town of Majdanpek; Mali Štrbac peak, Mt. Miroč; Mt. Ovčar; near the village of Periš, Svrlijske Planine Mts.; Mt. Rtanj; Stenka peak, near the town of Paraćin; Mt. Suva Planina; Sićevo Gorge; Milenkova Stena, Svrlijske Planine Mts.; Pleš peak, Svrlijske Planine Mts.; village of Niševac, near the town of Svrlijig; Mt. Stol, near the city of Bor; Glogovački Vrh peak, Mt. Tupižnica; village of Tumba, near the city of Vranje; Crnica Gorge, near the town of Paraćin; Mt. Crni Vrh, near the city of Jagodina; village of Crnoljevica, near the town of Svrlijig; after Pintér (1972): Veta Monastery, Mt. Suva Planina; town of Sokobanja; after Jovanović (1985): Mt. Avala, near the city of Belgrade; after Jovanović (1993): Mt. Veliki Krš, near the city of Bor; Mikuljska Reka river canyon, village of Zlot, near the city of Bor; after Jovanović (1996): Mt. Stol, near the city of Bor; after Sólymos et al. (2004) and Karaman (2012): near the Dobri Potok stream, Mt. Fruška Gora.

Material examined. SERBIA • Sićevo Gorge, leg. P. Pavlović, 30 Sep. 1906, one specimen (NHMBE0371); Vlasina Landscape of Outstanding Features, Mt. Vardenik, leg. V. Gojšina & M. Vujić, 04 Jun. 2022, one specimen (42°37'53.80"N, 22°16'51.00"E); Vlasina Landscape of Outstanding Features, Mt. Čemernik, next to the Cvetkova Reka river, leg. V. Gojšina, 02 June 2022, one specimen (42°44'41.12"N, 22°18'50.59"E); Vlasina Landscape of Outstanding Features, next to the Vučja Reka river, leg. V. Gojšina, 03 June 2022, one specimen (42°45'12.69"N, 22°23'51.70"E); village of Krivelj, near Mt. Veliki Krš, leg. V. Gojšina, 19 Jun. 2022, one specimen (44°10'07.00"N, 22°06'24.25"E); town of Bela Palanka, settlement of Čiflik, near the Sinjac Monastery, leg. V. Gojšina, 05 Aug. 2022, one specimen (43°13'03.62"N, 22°24'54.45"E); Crni Timok Gorge, village of Krivi Vir, leg. M. Šćiban, 03 May 2012, three specimens; Mt. Golija, village of Devići, leg. V. Gojšina, 25 Jul. 2022, one specimen (43°25'44.6"N, 20°22'38.6"E); Jelašnica Gorge, near the city of Niš, on limestone rocks, leg. V. Gojšina, 28 May 2022, two specimens (43°16'45.82"N, 22°03'49.59"E); Stara

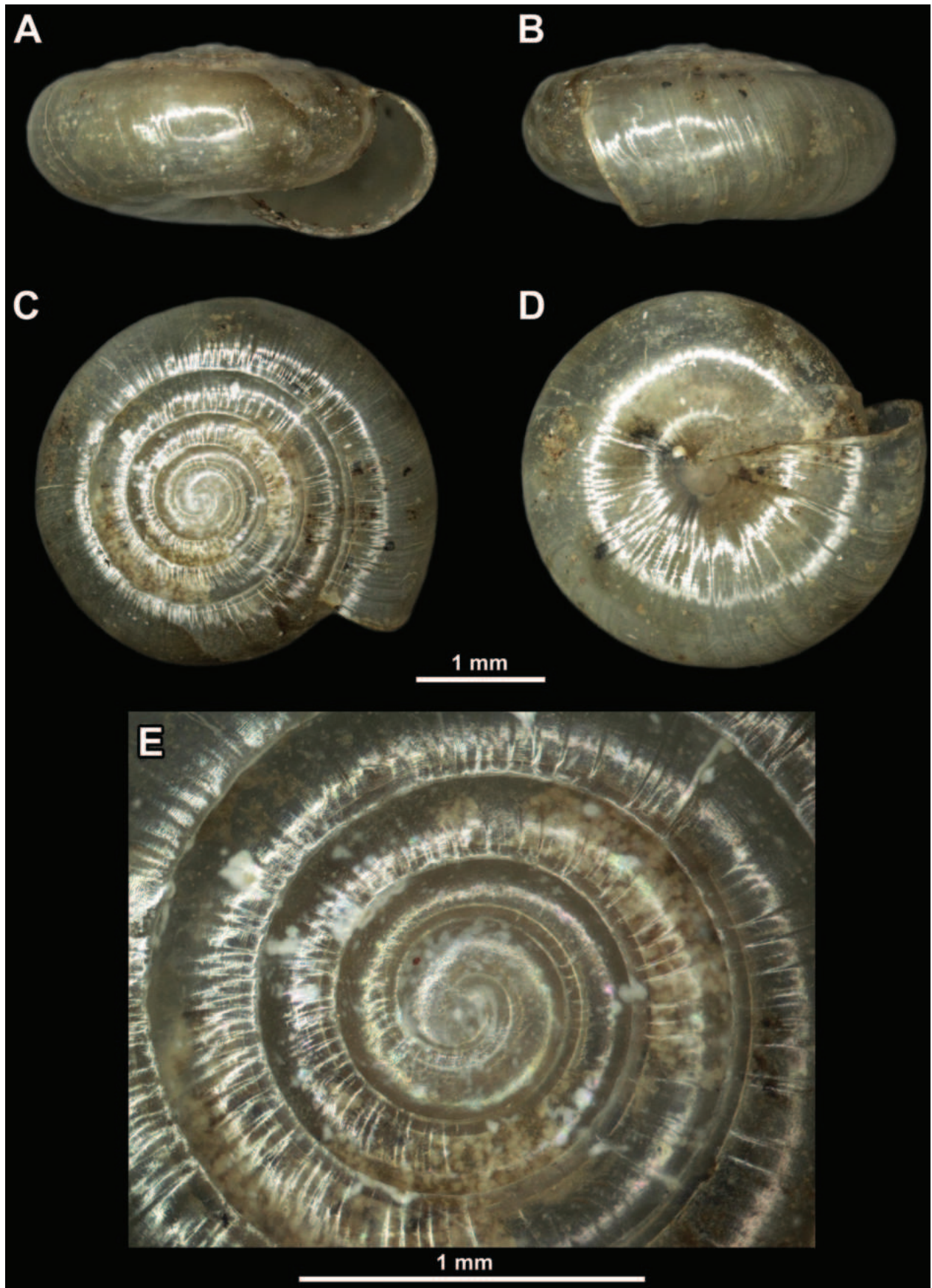


Figure 3. *Vitrea diaphana* from the surroundings of the city of Pirot **A** apertural view **B** lateral view **C** apical view **D** umbilical view **E** enlarged view of the protoconch.

Planina Mts., village of Temska, near the Bukovički Do waterfall, sieved from leaf litter in a limestone rock crevice, leg. V. Gojšina, 30 May 2022, two specimens (43°16'41.12"N, 22°34'10.25"E); Mt. Suva Planina, Bojanine Vode, sieved from leaf litter, leg. V. Gojšina, 31 May 2022, five specimens (43°13'13.56"N, 22°06'52.66"E); Stara Planina Mts., near the Bigar waterfall, leg. V. Gojšina, 05 Aug. 2022, three specimens (43°21'16.13"N, 22°26'33.02"E); city of Pirot, near the village of Dobri Do, Kitka rock quarry, leg. V. Gojšina, M. Vujić & N. Vesović, 28 Apr. 2023, one specimen (43°11'19.58"N, 22°38'47.31"E); Stara Planina Mts., Babin Zub peak, leg. V. Gojšina, M. Vujić & N. Vesović, 07 May 2023, two specimens (43°22'25.79"N, 22°36'46.30"E); near the town of Vrnjačka Banja, an oak forest, leg. V. Gojšina, 24 Mar. 2023, five specimens (43°35'15.76"N, 20°54'23.98"E); outskirts of the town of Vrnjačka Banja, near a small brook, leg. V. Gojšina, 24 Mar. 2023, one specimen (43°35'19"N, 20°54'25"E).

Description of specimens from Serbia. SW ranging from 3.5 up to even 5 mm. Shell surface smooth, with relatively strong radial growth lines. Shell transparent and flat, consisting of 5–6 relatively densely coiled whorls separated by shallow suture. Periphery rounded. Last whorl ~ 2× as wide as penultimate whorl. Umbilicus entirely closed.

Distribution and habitats in Serbia. Together with *V. subrimata*, this is the most common and widespread *Vitrea* species in Serbia (Fig. 16). Most frequently found in areas rich in limestone.

Remarks. Particularly large specimens (SW nearly 5 mm) were found at Bojanine Vode site on Mt. Suva Planina. Pavlović (1912) mentioned that he found several specimens in different locations (Jelašnica Gorge, Sirinjava Duvka, Ulanac peak on Svrliške Planine Mts.) that represent a form of *V. diaphana* with a very narrow umbilicus (even narrower than in *V. subrimata*) or possibly an undescribed species. In Jelašnica Gorge, we found both *V. diaphana* and *V. subrimata*, which makes it more likely that it is indeed *V. diaphana* with a not yet fully closed umbilicus. We have not found any specimens that fit Pavlović's description. The specimens he collected from the village of Sićevo (NHMBEO371) are not properly cleaned and could represent *V. subrimata*. The samples of *V. diaphana* collected by Pavlović (NHMBEO364 and NHMBEO365) are missing from the NHMBEO collection.

***Vitrea illyrica* (A. J. Wagner, 1907)**

Figs 4, 15

Crystallus illyricus – Pavlović 1912: 26–27; Tomić 1959: 13.

Vitrea illyrica – Jaeckel et al. 1957: 156; Karaman 2007: 141.

Sites in Serbia known from the literature. After Pavlović (1912) and Tomić (1959): Derventa river canyon, Mt. Tara; Drundebo, Mt. Tara; Mt. Javor; Krstača, near the Rača Monastery, Mt. Tara; near the Perućac Lake, Mt. Tara; Mt. Povlen.

Types examined. Scutari, Albania, three paralectotypes (SMF171013).

Other material examined. SERBIA • Mt. Javor, leg. P. Pavlović, 1908, nine specimens (NHMBEO452); Mt. Tara, Drundebo, leg. P. Pavlović, 07–12 Aug. 1909, three specimens (NHMBEO450) (see under the Remarks for *V. kutschigi*); Mt. Povlen, leg. P. Pavlović, Aug. 1909, one specimen (NHMBEO447).

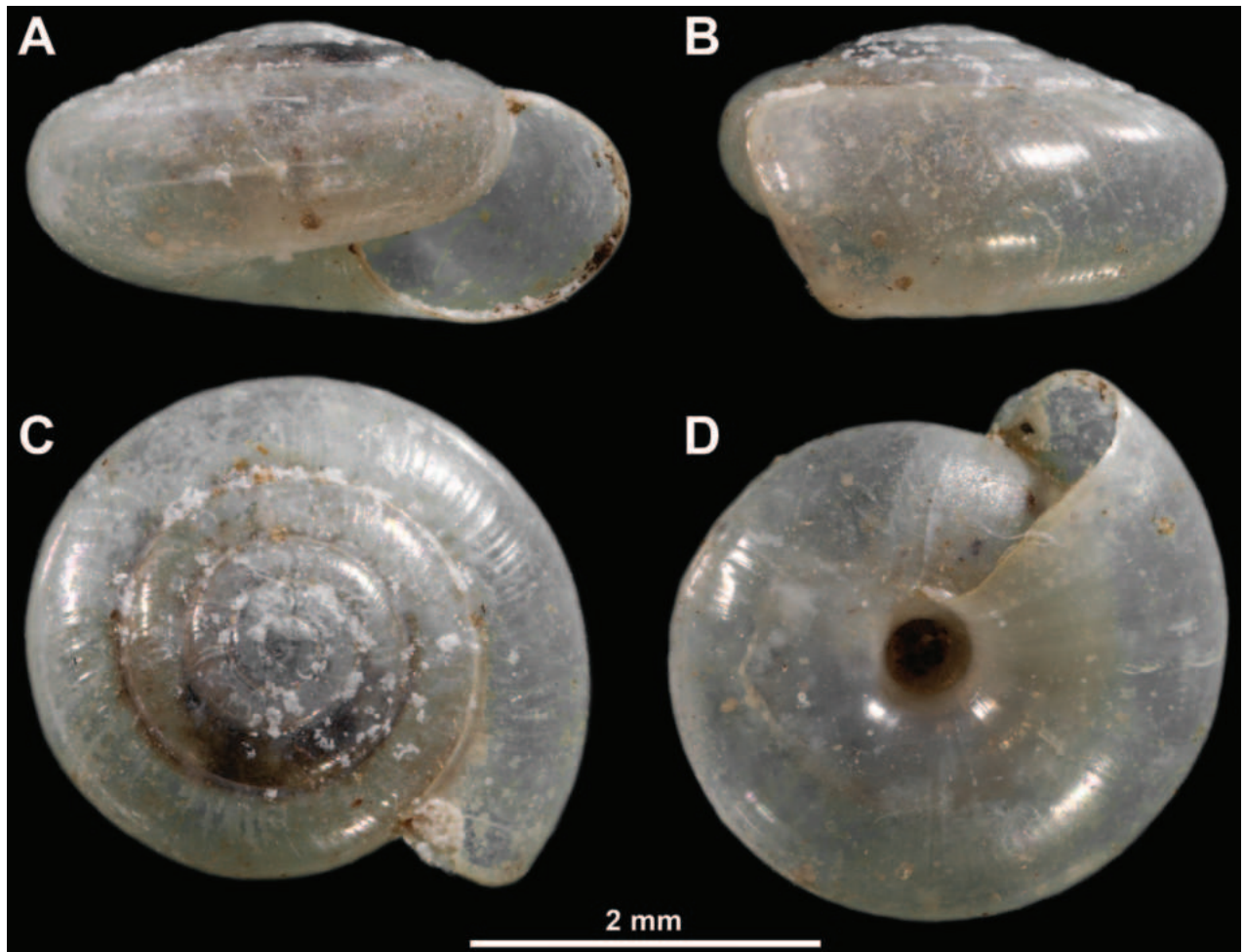


Figure 4. Paralectotype of *Vitrea illyrica* from Scutari, Albania (SMF171013) **A** apertural view **B** lateral view **C** apical view **D** umbilical view.

Distribution and habitats in Serbia. Known only from several localities in western Serbia (Fig. 15). Judging by the literature, found in areas rich in limestone.

Remarks. The material of this species collected by Pavlović (see under the Material examined) needs revision. The sample of *V. illyrica* collected by Pavlović (NHMBEO449) is missing from the NHMBEO collection.

***Vitrea kiliasi* L. Pintér, 1972**

Figs 5, 15

Vitrea kiliasi – Karaman 2007: 141; Welter-Schultes 2012: 362.

Sites in Serbia known from the literature. After Welter-Schultes (2012): near the city of Peć, Kosovo and Metohija.

Material examined. SERBIA • City of Peć, Rugovska Klisura Gorge, coll. W. Maassen, 12 Sep. 1987 (MIZ.MOL047276).

Description of specimens from Serbia. Shell colourless, consisting of five regularly increasing, radially striated whorls. Last whorl ~ 1.5× wider than

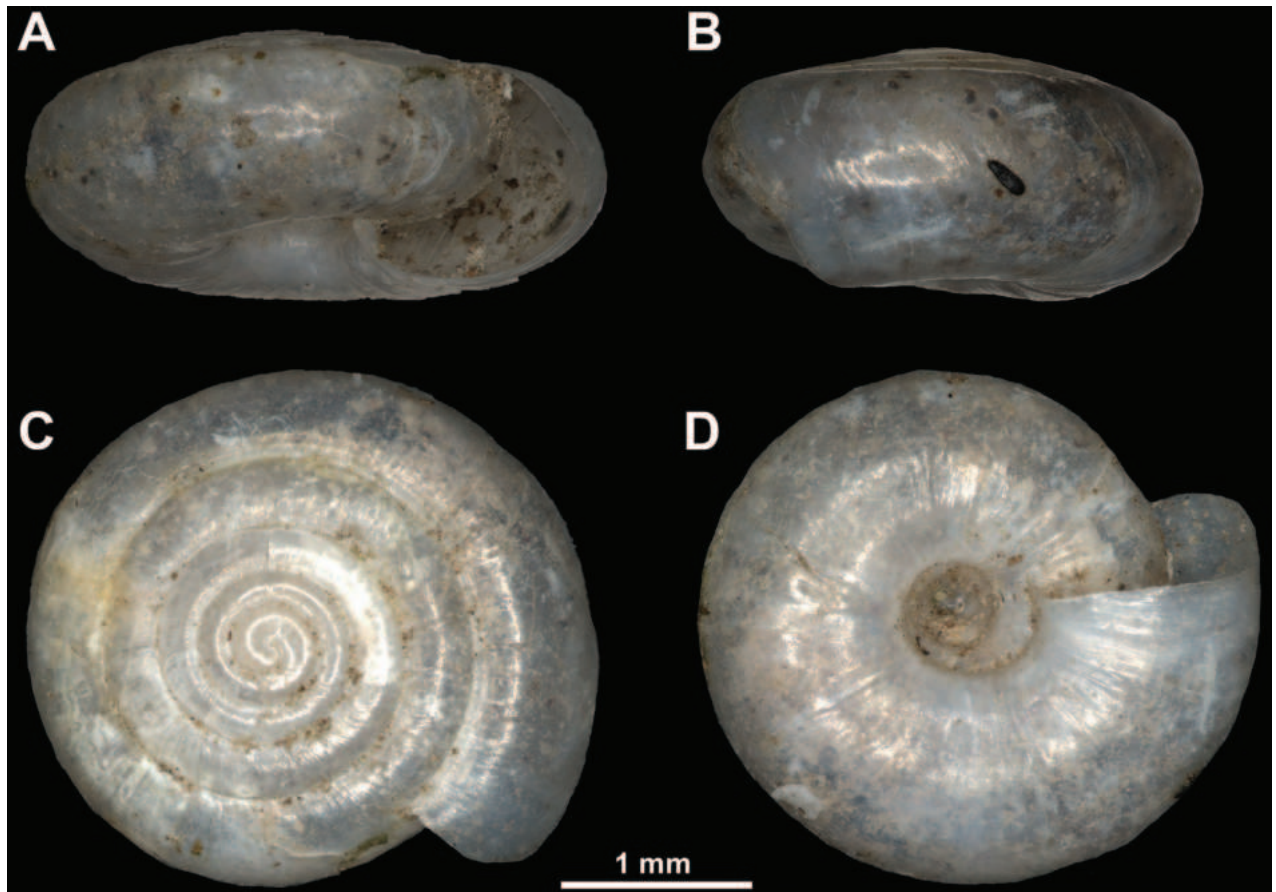


Figure 5. *Vitrea kiliasi* L. Pintér, 1972 from Rugovska Klisura Gorge, Kosovo and Metohija (MIZ.MOL047276) **A** apertural view **B** lateral view **C** apical view **D** umbilical view (photo: Magdalena Kowalewska-Groszkowska).

penultimate whorl. Periphery rounded, aperture elliptical. Umbilicus very wide, clearly showing all previous whorls.

Distribution and habitats in Serbia. Known from a very limited geographical area in Kosovo and Metohija (Fig. 15). Habitat in Serbia unknown.

Remarks. Welter-Schultes (2012) provided a photograph of this species from the surroundings of the city of Peć (Kosovo and Metohija). Otherwise, this species was not collected during our surveys.

***Vitrea kutschigi* (Walderdorff, 1864)**

Figs 6, 15

Vitrea kutschigi – Pintér 1972: 262; Karaman 2007: 141.

Sites in Serbia known from the literature. After Pintér (1972): village of Bare, near the town of Sjenica.

Types examined. Lokrum island, city of Dubrovnik, Croatia, neotype (SMF171014).

Other material examined. None.

Distribution and habitats in Serbia. This species is known only from limestone habitats in a limited part of western Serbia (Fig. 15).

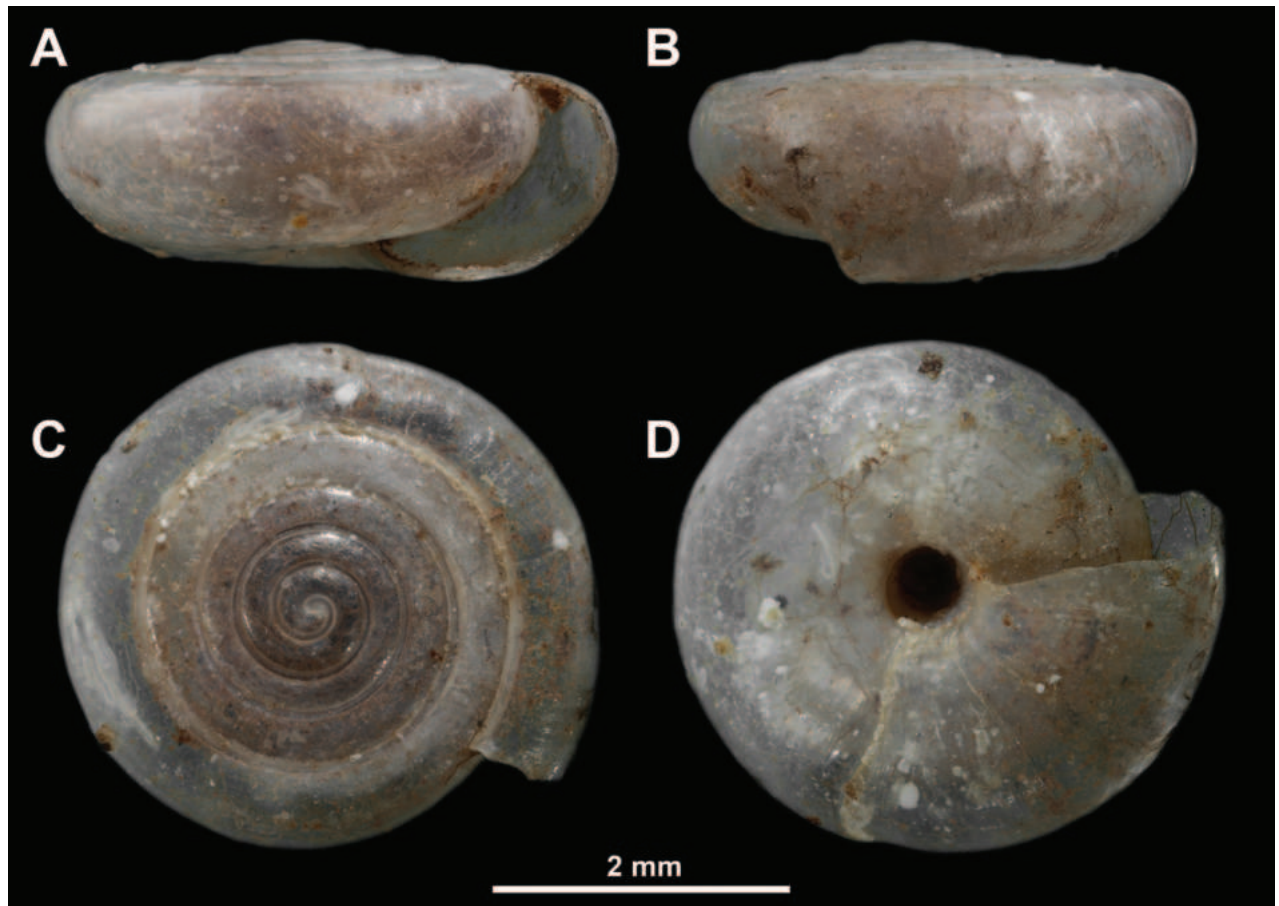


Figure 6. Neotype of *Vitrea kutschigi* from Lokrum island, Croatia (SMF171014) **A** apertural view **B** lateral view **C** apical view **D** umbilical view.

Remarks. A snail specimen from Mt. Tara (Drundebo) collected by Pavlović and deposited in the NHMBEO collection as *V. illyrica* (NHMBEO450) could actually refer to *V. kutschigi*, as its shell morphology differs (the shell is flatter, with more densely coiled whorls) from that of *V. illyrica*. The neotype of *V. kutschigi* was apparently designated by L. Pintér. The original material of Walderdorff (received by Parreyss) was lost, and the neotype was selected from the original material of Parreyss in the SMF collection (for details see Pintér 1972).

***Vitrea pygmaea* (O. Boettger, 1880)**

Figs 7, 15

Previous records from Serbia. This species has not been previously reported from Serbia.

Material examined. SERBIA • Mt. Zlatibor, town of Čajetina, village of Gostilje, Gostilje waterfall, found among soil on limestone rocks, leg. V. Gojšina, 07 Aug. 2020, one specimen (43°39'24.83"N, 19°50'18.54"E).

Description of specimens from Serbia. Shell very small (SW = 1.80 mm, SH = 0.82 mm), colourless and translucent. It consists of ~ 3.75 whorls separated by relatively deep suture. Aperture elliptical, periphery well rounded. Umbilicus

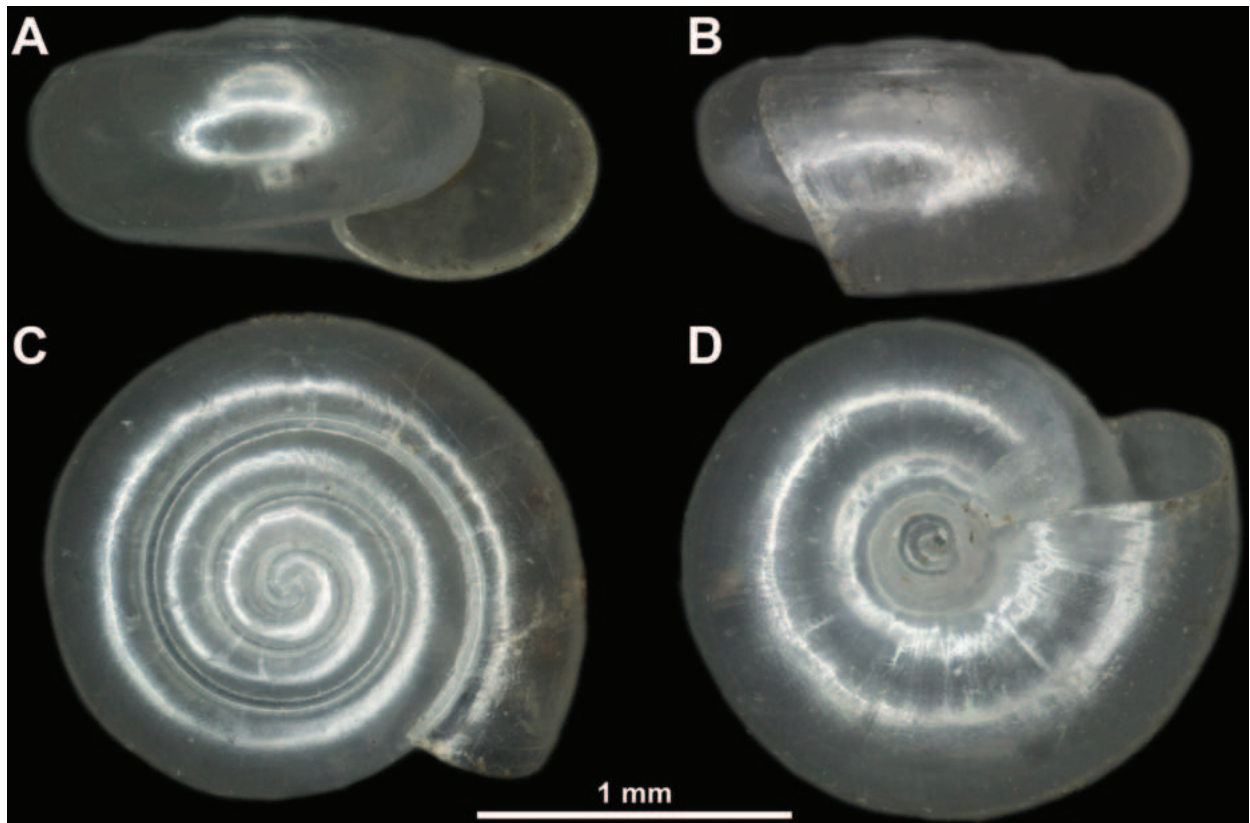


Figure 7. *Vitrea pygmaea* from the vicinity of the Gostilje waterfall on Mt. Zlatibor **A** apertural view **B** lateral view **C** apical view **D** umbilical view.

broad, measuring $\sim \frac{1}{4}$ of SW and showing all previous whorls. Last whorl between 1.5 and 2.0 \times as wide as penultimate whorl.

Distribution and habitats in Serbia. This species is only known from a single locality in western Serbia (Fig. 15), but is possibly more widespread. The small number of records to date is probably due to its tiny size and the lack of thorough sampling. It was found in soil samples from limestone rocks near the Gostilje waterfall.

Remarks. The identification of this species is based on a single specimen and requires confirmation. In our specimen, the last whorl was $\sim 1.5\times$ wider than the penultimate whorl, which is slightly less than usually reported for this species (twice as wide or even wider). However, the SW, SH, number of whorls, and UW of this specimen match the values given in the description of this species (Pintér 1972).

***Vitrea sturanyi* (A. J. Wagner, 1907)**

Figs 8, 15

Crystallus sturanyi – Pavlović 1912: 27; Tomić 1959: 13.

Vitrea sturanyi – Jaeckel et al. 1957: 156; Karaman 2007: 141.

Sites in Serbia known from the literature. After Pavlović (1912) and Tomić (1959): village of Gornje Košlje, near the town of Ljubovija; Drundebo, Mt. Tara; Mt. Kablar, near the city of Čačak.

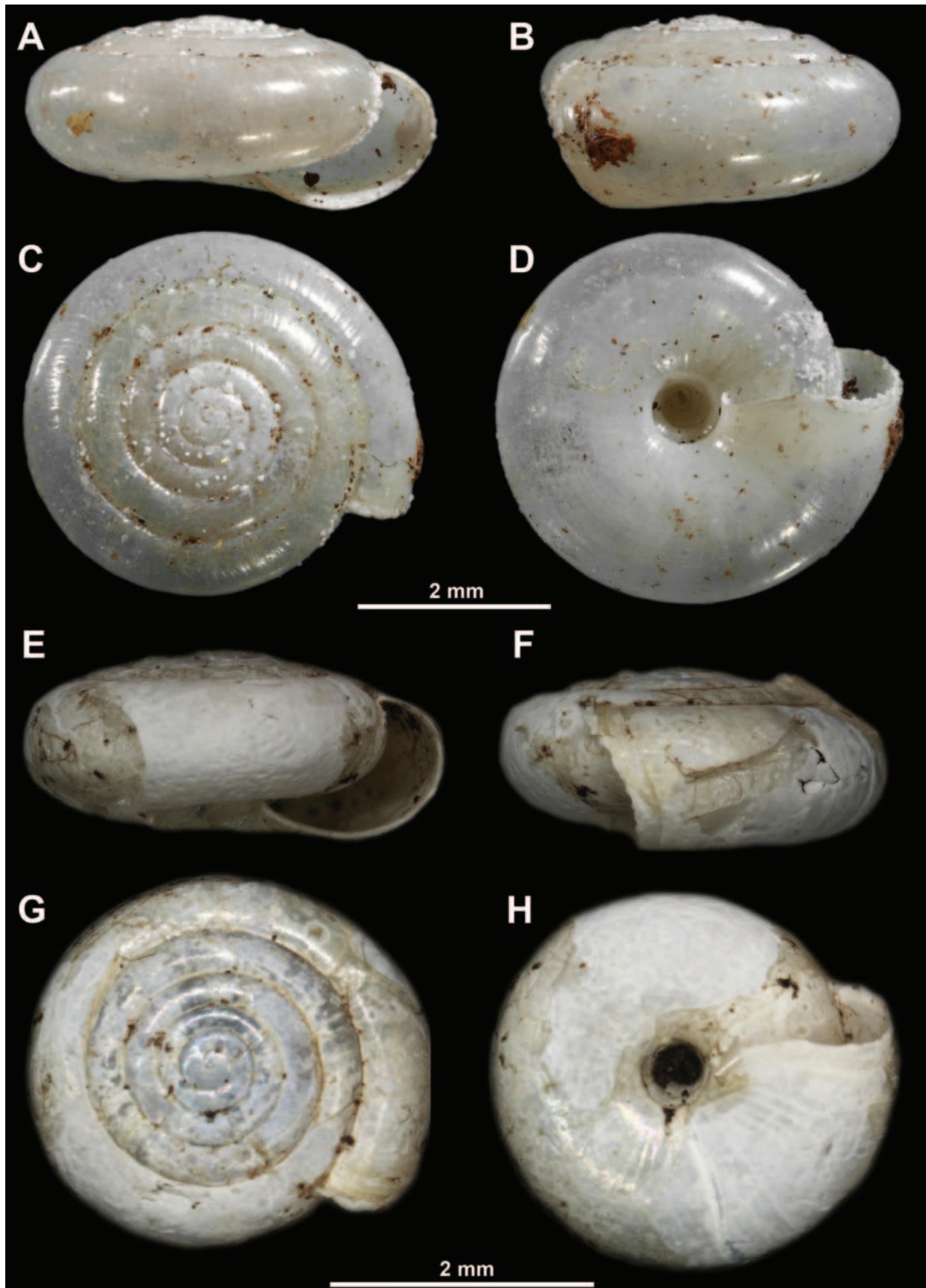


Figure 8. Paralectotype of *Vitrea sturanyi* from Mt. Bjelašnica, Bosnia and Herzegovina (SMF171014) (A–D) and *V. sturanyi* from the village of Lukino Selo on Mt. Tara, Serbia (E–H) A, E apertural view B, F lateral view C, G apical view D, H umbilical view. The upper scale refers to photos A–D, while the lower scale refers to photos E–H.

Types examined. Mt. Bjelašnica, Bosnia and Herzegovina, three paralectotypes (SMF171029).

Other material examined. **SERBIA** • Mt. Kablar, 23 Sep. 1908, one specimen (NHMBEO455); Mt. Tara, village of Lukino Selo, close to the Spajići Lake, next to a small brook connected to the Beli Rzav river, leg. D. Antić, M. Šević, D. Pavićević & I. Karaman, 06 Oct. 2023, two specimens (43°50'51.35"N, 19°23'48.68"E).

Description of specimens from Serbia. Shell relatively large (SW = 3.25 mm, SH = 1.3 mm), consisting of ~ 5.5 densely coiled and regularly increasing whorls. Last whorl ~ 1.5× as wide as penultimate whorl. Periphery rounded, aperture relatively narrow. Umbilicus with perpendicular walls, UW measuring 1/6 of SW.

Distribution and habitats in Serbia. In Serbia only known from a small number of sites rich in limestone in the west and southwest of the country (Fig. 15).

Remarks. Only two weathered shells were available, so details of the surface sculpture could not be observed. The SW of the adult specimen (with ~ 5.5 whorls) was 3.25 mm, which is slightly less than indicated in the literature (Welter-Schultes 2012). The last whorl was significantly wider than the penultimate whorl, in contrast to the usual condition in which these two whorls have the same width. Other features perfectly match those of the paralectotype and those listed in the description of *V. sturanyi* by Welter-Schultes (2012) (Fig. 8). The sample of *V. sturanyi* collected by Pavlović (NHMBEO453) is missing from the NHMBEO collection.

***Vitrea subrimata* (Reinhardt, 1871)**

Figs 9, 16

Crystallus subrimatus – Pavlović 1912: 25–26.

Crystollus subrimatus [sic] – Tomić 1959: 12–13.

Hyalina subrimata – Möllendorff 1873: 131.

Vitrea submata [sic] – Jovanović 1993: 242.

Vitrea subrimata – Jaeckel et al. 1957: 156; Pintér 1972: 231; Jovanović 1985: 42; Sólymos et al. 2004: 152; Karaman 2012: 24.

Sites in Serbia known from the literature. After Möllendorff (1873): Rača Monastery, Mt. Tara; after Pavlović (1912) and Tomić (1959): Mt. Avala, near the city of Belgrade; Jerinin Grad, near the town of Batočina; Mt. Belava, near the town of Bela Palanka; Mt. Beljanica; Mt. Vidlič, near the city of Pirot; Visoka Klisura Gorge, near the Veliki Rzav river; village of Gornje Košlje, near the town of Ljubovija; Mt. Golija, near the town of Ivanjica; Mt. Goč, near the town of Vrnjačka Banja; next to the Dubočica river, near the town of Raška; Derventa river canyon, Mt. Tara; Drundebo, Mt. Tara; Zečki Vrh peak, Mt. Čemernica; Mt. Javor; Jankova Klisura Gorge, village of Čučale, near the town of Blace; Radmanov Kamen, Mt. Kopaonik; Metode, Mt. Kopaonik; Majića Krš, Mt. Kopaonik; Srebrnac, Mt. Kopaonik; Kadijina Stena, near Mt. Javor; Kamenova Kosa (?); Krstača, near the Rača Monastery, Mt. Tara; Marića Stena, near the town of Krupanj; village of Lepena, near the town of Knjaževac; Murtenica mountain massif, Mt. Zlatibor; Mt. Mučanj; Mt. Medvednik; near the Panjica river, village of Dobrače, near the town of Ivanjica; Proslap saddle, near the city of Valjevo; Pustinja Monastery,

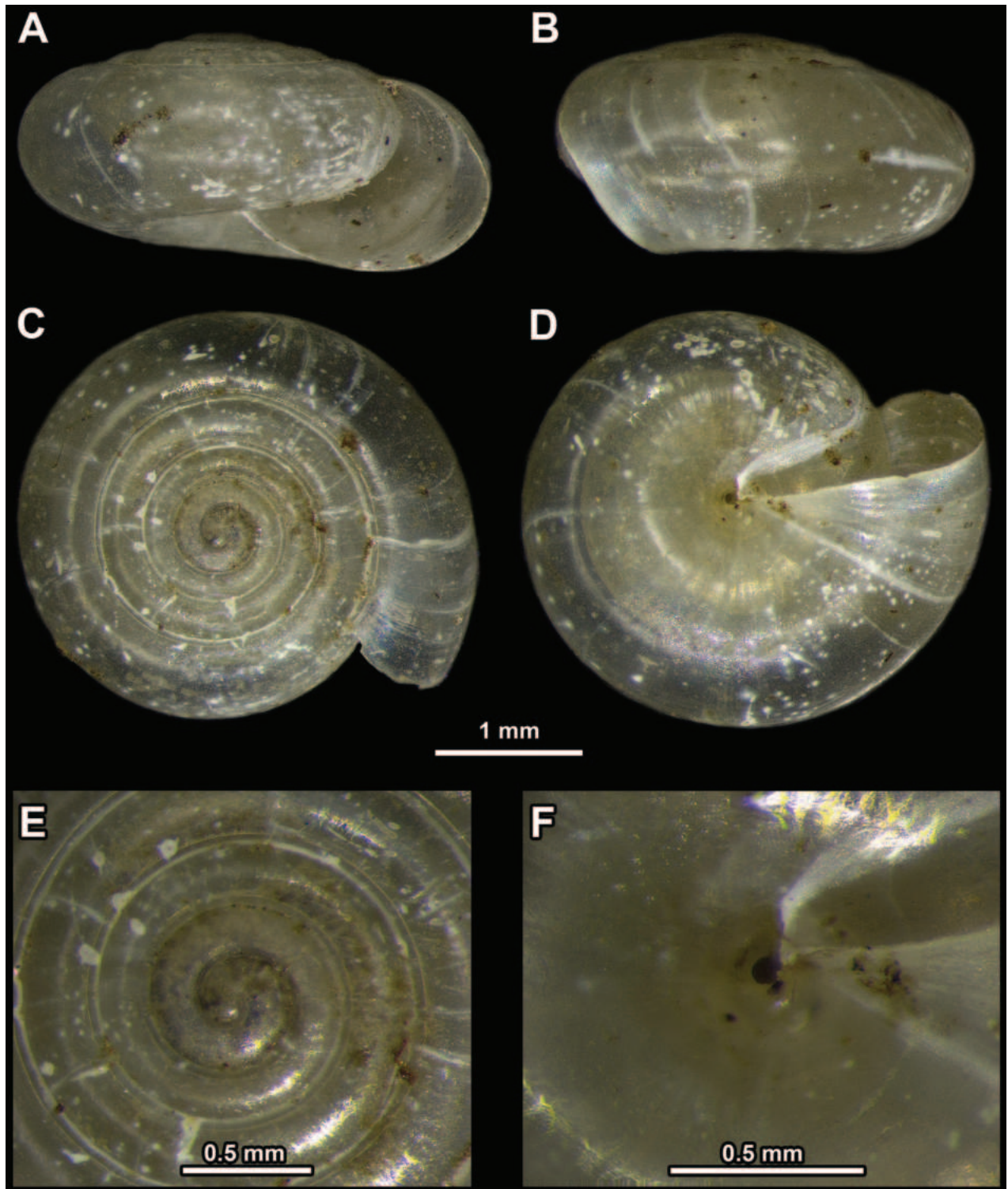


Figure 9. *Vitrea subrimata* from near the Bigar waterfall on Stara Planina Mts. **A** apertural view **B** lateral view **C** apical view **D** umbilical view **E** enlarged view of the protoconch **F** enlarged view of the umbilicus.

village of Počuta, close to the city of Valjevo; Mt. Povlen; near the Prištavica river, Mt. Zlatibor; village of Rti, near the town of Lučani; Sićevo Gorge, near the city of Niš; Ulanac peak, Svrljiške Planine Mts.; Glogovački Vrh peak, Mt. Tupižnica; Tornička Bobija peak, Mt. Bobija, near the town of Ljubovija; village of Taor, near the city of Valjevo; surroundings of the city of Užice; village of Crnoljevica, near

the town of Svrlijig; after Pintér (1972): Mt. Avala, near the city of Belgrade; surroundings of the city of Užice; village of Bare, near the town of Sjenica; after Jovanović (1985): Mt. Avala, near the city of Belgrade; after Sólymos et al. (2004) and Karaman (2012): near the Veliki Potok stream, Mt. Fruška Gora.

Material examined. SERBIA • Town of Knjaževac, village of Lepena, 08 Jun. 1907, one specimen (NHMBEO437); Mt. Tupižnica, Glogovački Vrh peak, leg. V. Petković, 1907, one specimen (NHMBEO435); Mt. Jadovnik, near the Studenac spring, leg. M. Vujić, 16 Sep. 2021, one specimen (43°18'31.64"N, 19°47'50.43"E); Mt. Jadovnik, Katunić peak, leg. V. Gojšina, N. Vesović & S. Ćurčić, 25 Jun. 2023, one specimen (43°16'27.62"N, 19°50'23.36"E); city of Bor, Mt. Stol, leg. V. Gojšina, 18 Jun. 2022, one specimen (44°10'17.40"N, 22°07'34.78"E); Mt. Kosmaj, village of Ralja, near a spring close to the Hotel "Babe", leg. V. Gojšina, 16 Apr. 2022, two specimens (44°32'17.85"N, 20°30'58.05"E); Stara Planina Mts., near the Bigar waterfall, leg. V. Gojšina, 05 Aug. 2022, one specimen (43°21'16.13"N, 22°26'33.02"E); Stara Planina Mts., surroundings of the village of Oreovica, leg. M. Šćiban, 30 Apr. 2012, three specimens; city of Belgrade, Stepin Lug park-forest, among rocks, leg. V. Gojšina & M. Vujić, 04 Apr. 2022, four specimens (44°44'50.26"N, 20°32'02.99"E); town of Tutin, village of Đerekare, among limestone rocks, leg. V. Gojšina, 25 Oct. 2022, one specimen (42°59'23.98"N, 20°07'47.37"E); Jelašnica Gorge, near the city of Niš, on limestone rocks, leg. V. Gojšina, 28 May 2022, two specimens (43°16'45.82"N, 22°03'49.59"E); Đerdap National Park, village of Brnjica, leg. V. Gojšina, M. Vujić & N. Vesović, 05 May 2023, three specimens (44°39'23.44"N, 21°46'01.26"E); Đerdap National Park, village of Dobra, leg. V. Gojšina, M. Vujić & N. Vesović, 05 May 2023, two specimens (44°38'27.53"N, 21°54'29.38"E).

Description of specimens from Serbia. SW ranging from 3 to 4 mm. Shell surface smooth. Shell transparent, consisting of 4–5 moderately densely coiled whorls separated by shallow suture. Periphery rounded. Last whorl slightly < 2× as wide as penultimate whorl. Umbilicus very narrow, but clearly open, slightly covered by reflected columellar margin. Previous whorls not visible through umbilicus.

Distribution and habitats in Serbia. Together with *V. diaphana*, this is the most common *Vitrea* species in Serbia (Fig. 16). Most frequently found in areas rich in limestone.

***Vitrea virgo* Gojšina & Dedov, sp. nov.**

<https://zoobank.org/350CE916-5C91-4D50-9667-B03DCDB82FE8>

Figs 10–13, 14D–F, 15

Type material. Holotype: one dry-preserved shell (NHMBEO312), leg. V. Gojšina, N. Vesović & S. Ćurčić, 12 Aug. 2022. **Paratypes:** 11 shells [codes: NHMBEO313 - one specimen (dry-preserved), IBER20469 - four specimens (ethanol-preserved), IZOO-MG-013 - two specimens (ethanol-preserved) and IZOO-MG-016 - four specimens (dry-preserved: one broken, one juvenile and two whole)] + genitalia in 70% ethanol (IZOO-MG-014).

Type locality. SERBIA • E Serbia, town of Sokobanja, Mt. Devica, Oštra Čuka peak, Jama pod Oštrom Čukom Pit, 1,033 m a.s.l. (43°35'38.48"N, 21°53'54.97"E).

Diagnosis. The new species differs clearly from most of the congeners by the large size of the shell (SW usually > 4 mm in adults), densely coiled, radially

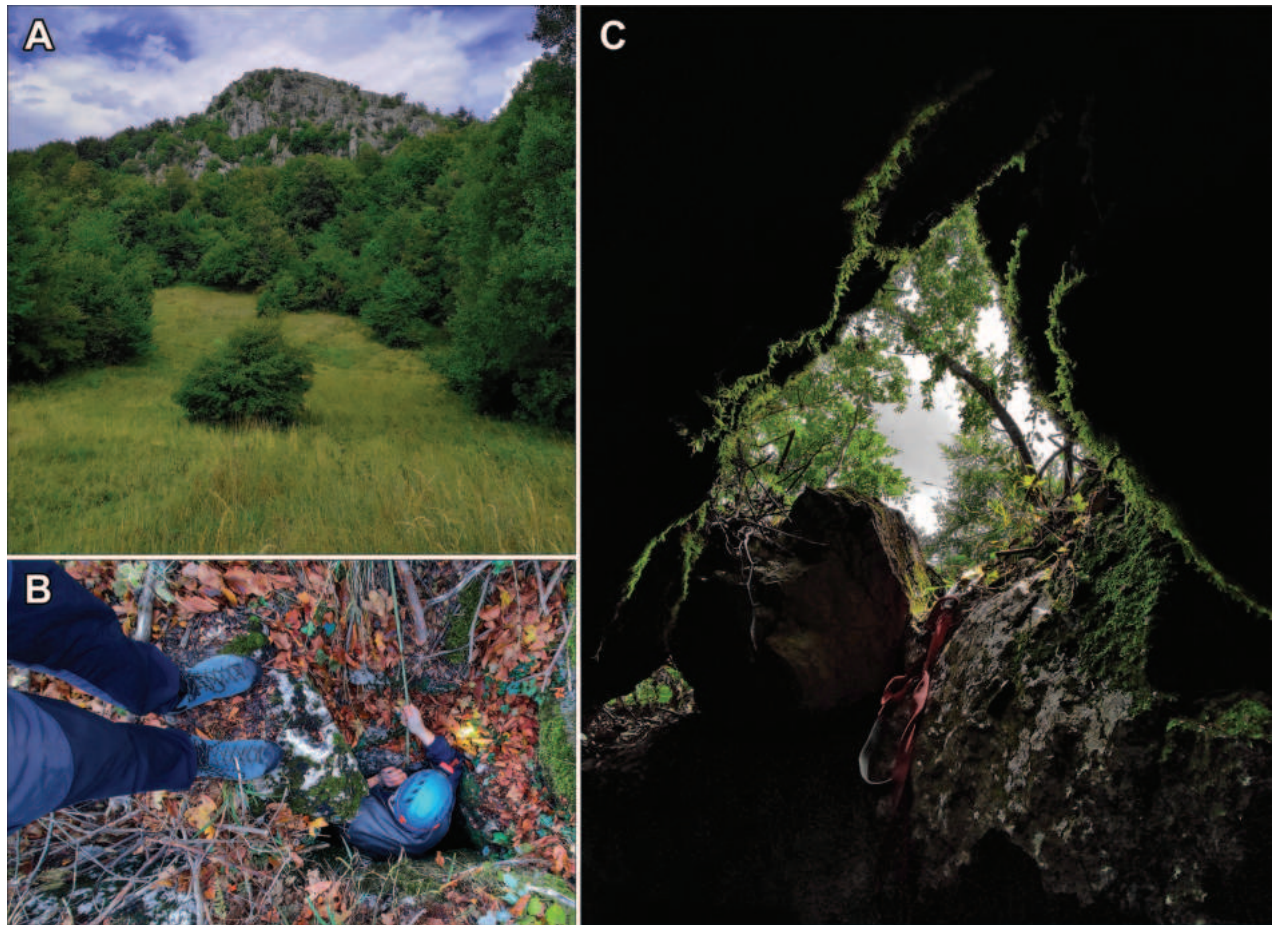


Figure 10. Type locality of *Vitrea virgo* sp. nov. **A** Oštra Čuka peak **B** entrance to the Jama pod Oštrom Čukom Pit, where the type specimens of *Vitrea virgo* sp. nov. were found **C** photo from inside the pit.

striated whorls, and a wide umbilicus. At first glance, this combination of characteristics places this species close to the genera *Lindbergia* and *Spinophallus*, from which it differs in its genital anatomy. There are several species that have similar number of whorls and UW: *V. siveci*, *V. kutschigi*, *V. neglecta* Damjanov & L. Pintér, 1969, *V. bulgarica* Damjanov & L. Pintér, 1969, *V. illyrica*, and *V. kiliasi*. From the similar *V. siveci*, described from North Macedonia and present in Greece, the new species differs by the flatter shell, narrower last whorl and aperture, and less regularly rounded periphery. The umbilicus is larger and usually more distinctly funnel-shaped in the new species than in *V. siveci*, whose shell is larger (both in SW and SH) than in the new species. Namely, the SW of the largest specimen of *V. siveci* is 5.3 mm (Riedel and Velkovrh 1976), which is almost 0.7 mm more than in the largest specimen of *V. virgo* Gojšina & Dedov, sp. nov. in our sample (SW 4.68 mm). In addition, the surface sculpture is much more pronounced in *V. siveci* than in the new species. The western Balkan species *V. kutschigi* differs from the new species by its flatter shell and narrower aperture, which makes it similar to the freshwater planorbid species *Bathyomphalus contortus* (Linnaeus, 1758), as observed by Welter-Schultes (2012). In addition, *V. kutschigi* is larger than *V. virgo* Gojšina & Dedov, sp. nov. and has a less pronounced funnel-shaped umbilicus. In *V. sturanyi*, another similar western Balkan species, the last whorl is as broad as the penultimate whorl (see under the Remarks section for *V. sturanyi*), and the umbilicus has almost perpendicular walls,

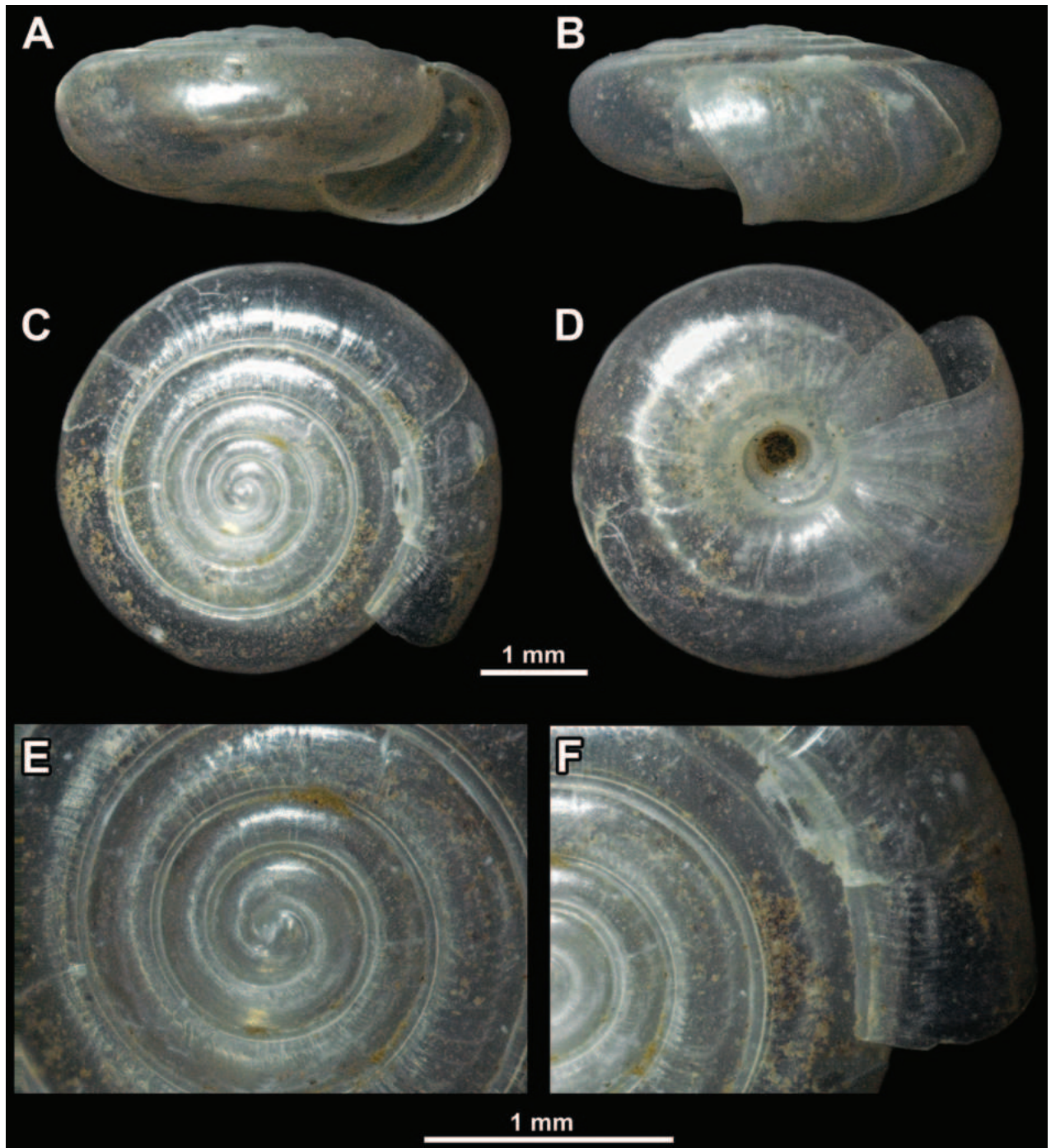


Figure 11. *Vitrea virgo* sp. nov. from Mt. Devica (holotype, NHMBE0312) **A** apertural view **B** lateral view **C** apical view **D** umbilical view **E** enlarged view of the protoconch **F** enlarged view of the last and penultimate whorl.

which do not expand as much as in the new species. Finally, the shell of the new species is flatter and less rounded than in *V. sturanyi*. The shell of *V. illyrica* is less flat on both the upper and lower sides, the aperture is less narrow, the last whorl is less narrow and the whorls are less densely coiled than in the new species. Two Bulgarian species, *V. bulgarica* and *V. neglecta* (considered conspecific by Irikov 2001 and Welter-Schultes 2012, but treated as separate by Georgiev and Dedov 2014) are both smaller (SW usually ≤ 3.2 – 3.4 mm and SH ≤ 1.6 mm) and more conical, with usually less wide perspective umbilicus than in the new

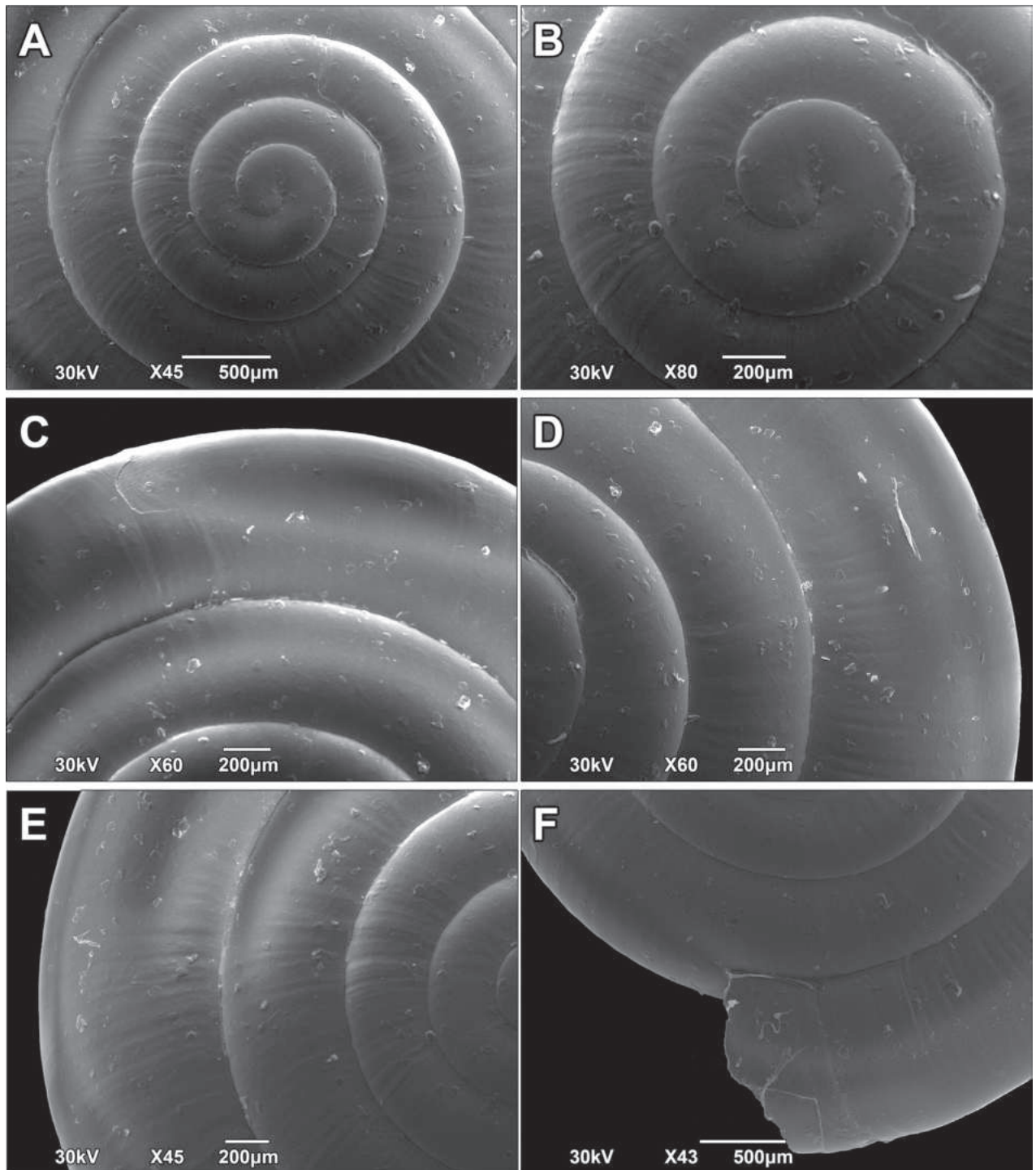


Figure 12. SEM images of the shell surface structure of *Vitrea virgo* sp. nov. **A, B** enlarged view of the protoconch **C–F** enlarged different parts of the last whorl.

species. Spiral striation is not observed in these two species, but is present (albeit very weak and localised) in *V. virgo* Gojšina & Dedov, sp. nov. These two species also differ from the new species in their genital anatomy. According to Irikov (2001) and Georgiev (2016), *V. bulgarica* and *V. neglecta* have a penis with a strong bulge (swelling) distally and a well-developed perivaginal gland. In *V. virgo* Gojšina & Dedov, sp. nov., the penis is with no such strong swellings, thus almost equally broad throughout its entire length and no perivaginal gland

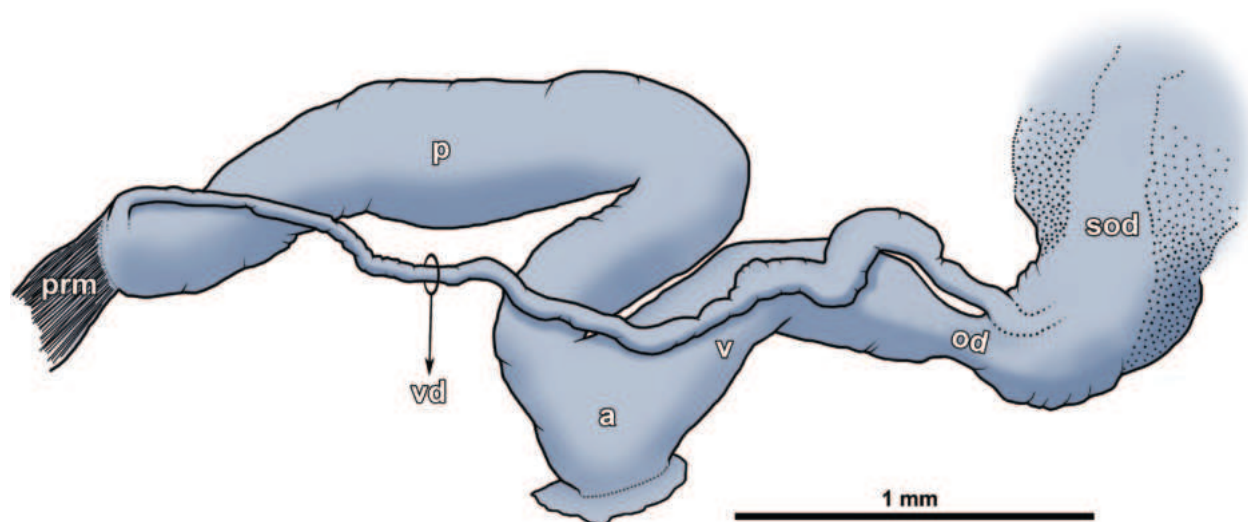


Figure 13. Genitalia of *Vitrea virgo* sp. nov. (paratype, IZOO-MG-014). **a** genital atrium **od** oviduct **p** penis **prm** penial retractor muscle **sod** spermoviduct **v** vagina **vd** vas deferens.

is observed. In a specimen of *V. neglecta* from Greece, Georgiev (2016) noted that its mantle is speckled, with black-greyish pigmentation, in contrast to the new species, whose mantle is completely devoid of pigmentation. Differences in the appearance of the reproductive system are also observed when comparing the new species with other geographically close Serbian congeners (*V. contracta*, *V. crystallina*, *V. diaphana*, and *V. subrimata*). In contrast to them, the new species lacks both the seminal receptacle and the perivaginal gland. Compared to *Vitrea ulrichi* Georgiev & Dedov, 2014, the new species has less whorls in the same SW (the shell in *V. ulrichi* is more densely coiled than in the new species) (in *V. ulrichi*, SW ~ 4.6 mm = 6.25 whorls vs. in *V. virgo* Gojšina & Dedov, sp. nov., SW ~ 4.6 mm = 5.5 whorls). Finally, the shells of *V. ulrichi* are more coarsely radially striated compared to those of *V. virgo* Gojšina & Dedov, sp. nov.

Description. Shell – Flat, translucent, consisting of 4.5–5.5 regularly increasing, densely coiled whorls separated by moderately deep suture. Protoconch smooth (Fig. 12A, B), consisting of ~ 1.25–1.5 whorls. Boundary between protoconch and teleoconch slightly visible only by scanning electron microscopy (SEM) and even then not clear. Teleoconch almost smooth, but with several very fine, irregular radial growth lines. Spiral striation very weak, present only on some parts of periphery, composed of innumerable spiral lines that are very difficult to observe (Fig. 12C). Lower side of shell almost flat. Last whorl on average 1.5× (sometimes ≤ 1.7×) as wide as penultimate whorl. Peristome sharp, almost straight when observed from apical view. Aperture elliptical and relatively narrow. Umbilicus wide, measuring 1/5–1/6 of SW and showing almost all whorls inside. Surface sculpture much less distinct (almost invisible) on umbilical side when compared to apical side.

Reproductive system. Genitalia typical for *Vitrea*. Penis moderately long, almost of equal width along entire length, very slightly widening only medially. Penial retractor muscle inserted at apical part of penis, where vas deferens joins too. Latter structure long and very thin, but thickened near female part of genitalia. Epiphallus and seminal receptacle absent. Genital atrium indistinct. Vagina almost as wide as penis. Perivaginal gland could not be observed, probably absent (Fig. 13).

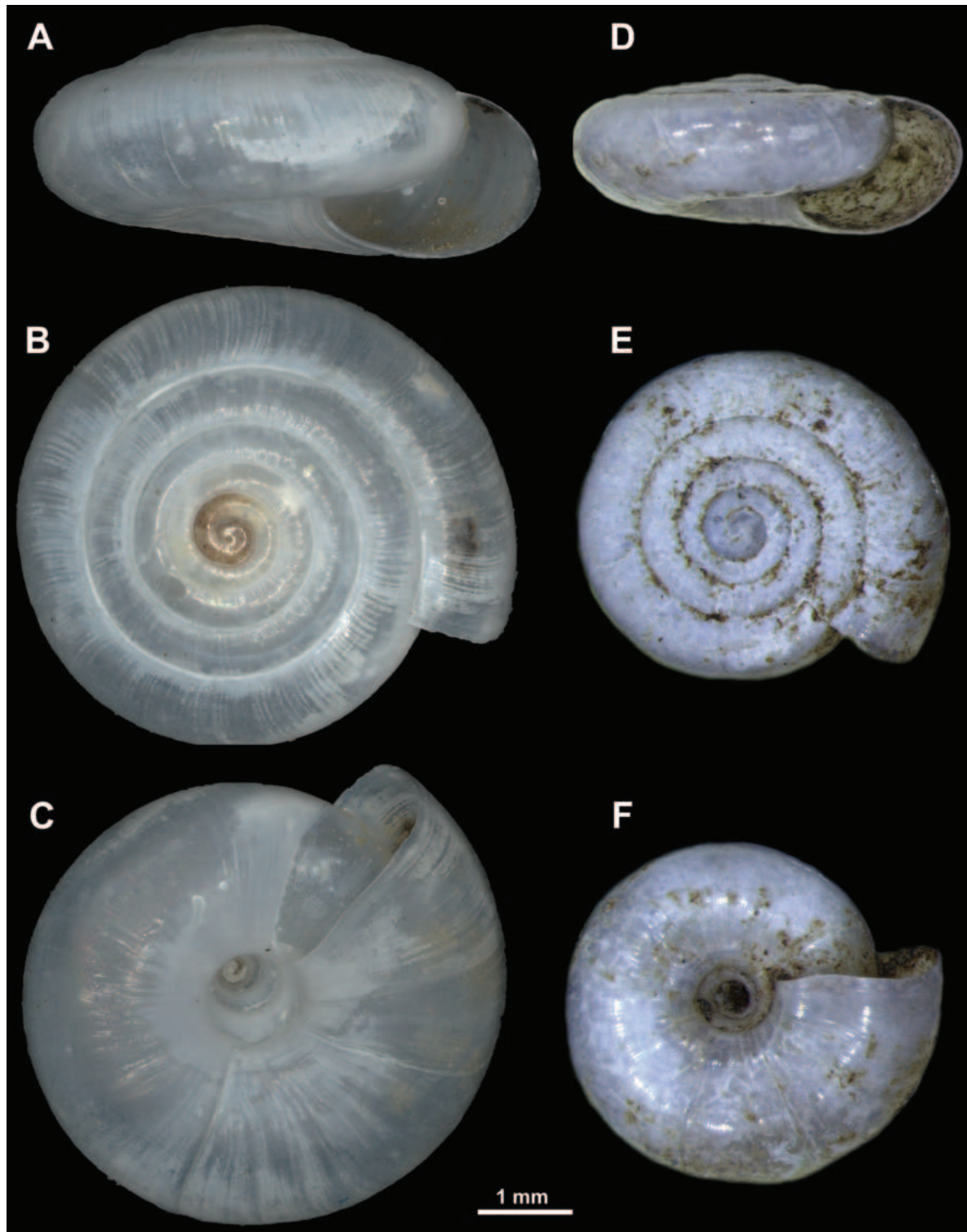


Figure 14. **A–C** *Vitrea siveci* from Solunska Glava peak on Mt. Jakupica, North Macedonia (paratype, MIZ.MOL047322) (photo: Magdalena Kowalewska-Groszkowska) **D–F** *V. virgo* sp. nov. from Mt. Devica (paratype, NHMBE0313) **A, D** apertural view **B, E** apical view **C, F** umbilical view.

Measurements (in mm, $n = 7$): SW = 3.61–4.68; SH = 1.54–2.10; AW = 1.57–1.87; AH = 1.22–1.50; UW = 0.61–0.86.

Etymology. The new species is named after Mt. Devica, where the type locality (Jama pod Oštrom Čukom Pit) is situated. The name of the mountain

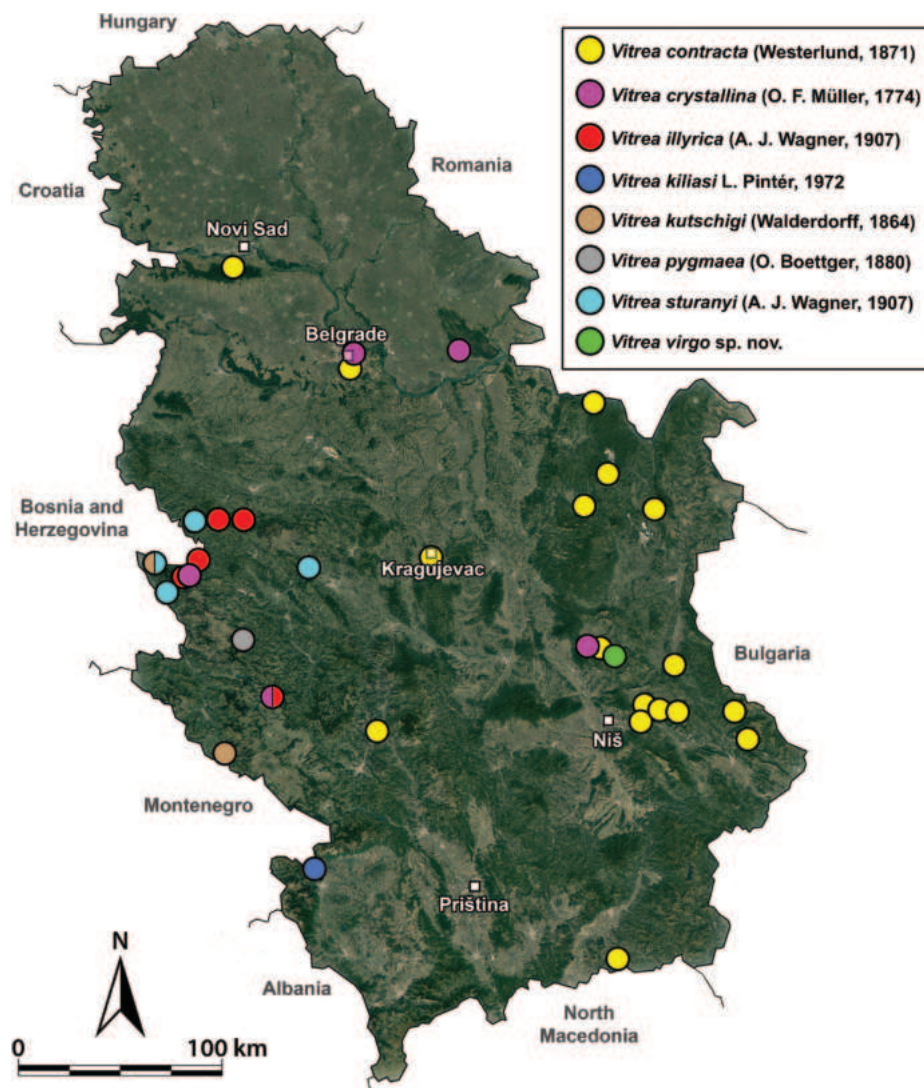


Figure 15. A distribution map of *Vitrea contracta*, *V. crystallina*, *V. illyrica*, *V. kiliasi*, *V. kutschigi*, *V. sturanyi*, and *V. virgo* sp. nov. in Serbia.

means “a virgin” (Lat. *virgo*) in Serbian. The specific epithet is to be used as a noun in apposition.

Habitat. The new species is found in a shallow, natural pit (a small underground cavern between boulders) several meters deep in a limestone habitat. Live animals crawled on and under numerous wet rocks deeper in the pit. They were only found in the darker parts of the pit. The new species was found together with two other gastropods, *Morlina glabra* (Rossmässler, 1835) and *Limax cinereoniger* Wolf, 1803. It was not found outside the pit, although it may also occur in the immediate vicinity.

Distribution. This species is only known from the type locality (Figs 10, 15).

Remarks. The radial striation of the shell is irregular and quite variable in the new species. In some places, the shells appear to be almost completely smooth or, on the contrary, show strong radial lines. *Vitrea virgo* Gojšina & Dedov, sp. nov. is one of the largest representatives of the genus *Vitrea* in Serbia. Based on this fact, we had suspected that it might even belong to several other genera with typically larger shells [for the dimensions of the species see Welter-Schultes (2012)], such as *Lindbergia* and *Spinophallus*. After its dissec-

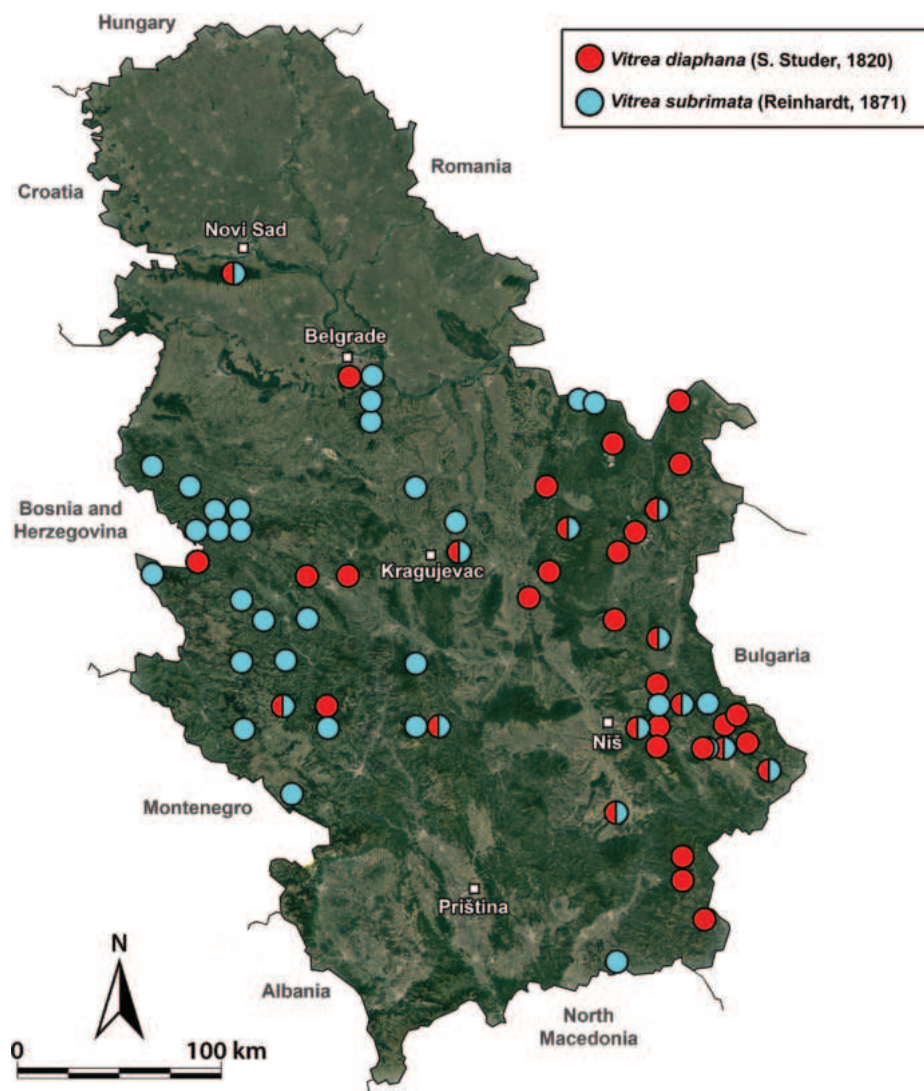


Figure 16. A distribution map of *Vitrea diaphana* and *V. subrimata* in Serbia.

tion, however, we found no seminal receptacle, which is typically large and well developed in the other two genera, but absent or reduced in *Vitrea* (Schileyko 2003). More importantly, we found no epiphallus, which justifies the placement of the new species in the genus *Vitrea*. On the vas deferens we found a “seminal receptacle-like” structure whose function or origin is unknown. We are not sure what this structure represents, and it is probably an artefact, as it was not observed in any other dissected specimen.

Identification key to the species of the genus *Vitrea* from Serbia

- 1 Umbilicus narrow or wide, never closed 2
- Umbilicus closed *V. diaphana*
- 2 Umbilicus moderately to very wide 3
- Umbilicus very narrow *V. subrimata*
- 3 Last whorl wider than penultimate whorl 4
- Last whorl of the same width as penultimate whorl *V. sturanyi*
- 4 Shell smaller, width ≤ 4 mm in adults 5
- Shell larger, width > 4 mm in adults 8

- 5 Umbilicus very wide **6**
- Umbilicus not very wide **7**
- 6 Shell \leq 2 mm wide, last whorl mostly twice as wide as penultimate whorl.
..... ***V. pygmaea***
- Shell 3–3.3 mm wide, last whorl 1.5× as wide as penultimate whorl.....
..... ***V. kiliasi***
- 7 Whorls not densely coiled, umbilicus moderately wide, SW usually between 3 and 4 mm..... ***V. crystallina***
- Whorls relatively densely coiled, SW usually ~ 2 mm..... ***V. contracta***
- 8 Shell flat, last whorl and aperture relatively narrow, whorls densely coiled.... **9**
- Shell convex, last whorl and aperture wide, whorls not very densely coiled
..... ***V. illyrica***
- 9 Shell very flat, aperture very narrow, umbilicus with perpendicular walls, shell surface sculpture not very prominent, last whorl sometimes appears slightly shouldered ***V. kutschigi***
- Shell moderately flat, aperture moderately narrow, umbilicus wide, especially at last whorl, shell surface sculpture prominent, last whorl regularly rounded..... ***V. virgo* sp. nov.**

Discussion

This study increases the total number of *Vitrea* species in Serbia to 10. The specific diversity of this genus in neighbouring countries varies between five and 13. Five species are known from Hungary (Pintér and Suara 2004), seven from Albania (Fehér and Erőss 2009), nine from Montenegro (Karaman 2014), 10 from Bosnia and Herzegovina (Karaman 2006) and Romania (Bank and Neubert 2017), 11 from Bulgaria (Georgiev and Dedov 2014), while 13 species are known from North Macedonia (Maassen 1998; Stankovic et al. 2006; Dedov 2021) and Croatia (Štamol 2010). None of the known Serbian species is endemic to this country, with the exception of the newly described species. However, several species reported here are western Balkan endemics (*V. illyrica*, *V. kiliasi*, *V. kutschigi*, and *V. sturanyi*) (Pintér 1972; Welter-Schultes 2012). The species newly reported for the Serbian fauna, *V. pygmaea*, was found in a region within the range of the species, which means that the lack of previous records is probably due to a lack of research. Eastern Serbia can be considered the best-studied part of the country in terms of snail fauna, including the representatives of the genus *Vitrea* (Pavlović 1912; Jovanović 1993, 1996). Pavlović (1912) provided data for many gastropod species from this region with a dense network of sampling sites. This is also the region where most endemic Serbian gastropod taxa are found (Karaman 1999; Subai 2011). Apart from numerous samplings in the past, the only *Vitrea* representatives found in eastern Serbia are the most widespread species (*V. contracta*, *V. diaphana*, and *V. subrimata*). The abovementioned endemics of the western Balkans, on the other hand, are more common in western Serbia (Pavlović 1912).

The perivaginal gland is an organ that is frequently found in gastrodontoid and zonitoid snails (Schileyko 2003). This organ can vary in size and shape in different taxa and can also be positioned differently (Rodrigues et al. 2002), but is usually located near the vagina and the distal part of the free oviduct (near where the bursa normally attaches). The function of this organ is related to egg-shell production and lubrication of the distal female genitalia, and its secretions

are composed of proteins, mucopolysaccharides, and calcium (Rodrigues et al. 2002). Although this is not the rule, the perivaginal gland can sometimes be completely absent (e.g., Riedel 1960; Slapcinsky 2018). We did not observe a perivaginal gland in the dissected specimens of *V. virgo* Gojšina & Dedov, sp. nov.

The distribution of even common species (e.g., *V. crystallina*) in Serbia is still poorly known, as there are few records in the country due to the following two facts: i) all *Vitrea* species are relatively small and usually difficult to find *in situ*, which is why soil sampling is recommended; and ii) knowledge about terrestrial snails in Serbia is still very poor due to the lack of experts and short research tradition. Further sampling and research are needed to fully understand the distribution of species, especially those that occur in specialised habitats and are known only from a few localities. The species narrowly distributed in Serbia (*V. illyrica*, *V. kiliasi*, *V. kutschigi*, and *V. sturanyi*) may be threatened by habitat changes, especially because they are restricted to limestone areas that are frequently quarried (for some examples see Schilthuizen et al. 2005). We are not yet in a position to assess the actual threat to these species in Serbia, as their distribution in this country is largely unknown. The type locality of the newly described species is not yet under high anthropogenic pressure, as its surroundings are currently not threatened by quarry work. However, there is a potential threat in the form of habitat changes (waste dumping, deforestation, and urbanisation), as Mt. Devica could become a tourist attraction in Serbia. The actual distribution of the newly described species and its habitat preferences need to be further investigated in order to adequately protect the species and its habitat, should this become necessary.

Although considerable efforts were made to sample terrestrial gastropods at several other sites on Mt. Devica and its surroundings, the new species was only found at its type locality. It is possible that this species is subterranean, as no specimens were found outside the pit and the specimens we collected had no mantle pigmentation, which is consistent with other subterranean taxa. *Vitrea virgo* Gojšina & Dedov, sp. nov., like many other relatives (Welter-Schultes 2012), could be a rare species with a restricted geographic distribution, but further sampling and study is needed to verify its narrow range and specific microhabitat requirements.

Acknowledgements

We thank Dr Dalibor Stojanović, Dr Dragan Antić, Mirko Šević and Marko Šćiban for collecting part of the examined snail material and Sigrid Hof for providing access to the SMF collection. We are also grateful to Magdalena Kowalewska-Groszkowska for providing photographs of *V. kiliasi* and *V. siveci* from the MIZ collection. Special thanks go to Mihailo Vujić, who participated in the field trips and collected part of the material. Finally, we would like to express our appreciation to Dr John Slapcinsky and Dr Dilian Georgiev for their constructive criticisms, which significantly improved the initial version of the manuscript.

Additional information

Conflict of interest

The authors have declared that no competing interests exist.

Ethical statement

No ethical statement was reported.

Funding

This study was financially supported by the Serbian Ministry of Science, Technological Development and Innovation (Contracts Nos. 451-03-65/2024-03/200178 and 451-03-66/2024-03/200178).

Author contributions

Conceptualization: VG. Funding acquisition: ID. Methodology: BM, SĆ, NV, VG. Supervision: TKŽ, SĆ, ID. Validation: NV, SĆ, ID. Visualization: NV. Writing - original draft: VG. Writing - review and editing: ID, NV, BM, TKŽ, SĆ.

Author ORCIDs

Vukašin Gojšina  <https://orcid.org/0000-0002-0413-9304>

Nikola Vesović  <https://orcid.org/0000-0001-6256-7975>

Srećko Ćurčić  <https://orcid.org/0000-0001-7303-7857>

Tamara Karan-Žnidaršič  <https://orcid.org/0000-0003-3821-578X>

Ivaylo Dedov  <https://orcid.org/0000-0003-4445-359X>

Data availability

All of the data that support the findings of this study are available in the main text.

References

- Bank RA, Neubert E (2017) Checklist of the land and freshwater Gastropoda of Europe. <https://www.molluscabase.org> [last update 16 July 2017, accessed 07 February 2024].
- Dedov I (2021) Inventory of the terrestrial gastropods in a poplar forest in the valley of the Bregalnitsa River, Republic of North Macedonia, with the description of a new species of the genus *Vitrea* Fitzinger, 1833. *Acta Zoologica Bulgarica* 73(1): 21–26.
- Fehér Z, Erőss ZP (2009) Checklist of the Albanian mollusc fauna. *Schriften zur Malakozoologie* 25: 22–38.
- Georgiev D (2016) *Vitrea neglecta* Damjanov et L. Pintér 1969 – genital anatomy of a specimen from Greece. *ZooNotes* 95: 1–2.
- Georgiev D, Dedov I (2014) Contribution to the knowledge of the Bulgarian species of the genus *Vitrea* (Gastropoda, Pristilomatidae) with the description of a new species. *ZooKeys* 396: 1–11. <https://doi.org/10.3897/zookeys.396.6976>
- Hesse P (1929) Schnecken aus dem nördlichen Serbien. *Archiv für Molluskenkunde* 61(1): 230–240.
- Irikov AA (2001) To the knowledge of the anatomy and taxonomy of two species from genus *Vitrea* Fitzinger, 1833 (Gastropoda, Zonitidae). *Travaux scientifiques de l'Université de Plovdiv "Paisii Hilendarski"*, *Animalia* 37(6): 35–38.
- Jaekel SG, Klemm W, Meise W (1957) Die Land- and Süßwasser-Mollusken der nördlichen Balkanhalbinsel. *Abhandlungen und Berichte aus dem Staatlichen Museum für Tierkunde in Dresden* 23: 141–205.
- Jovanović B (1985) Preliminarni popis puževa (Gastropoda, Mollusca) Avale. *Biosistematika* 12(1): 39–44.

- Jovanović B (1993) Preliminarni prikaz faune Gastropoda (Mollusca) područja Bora. In: Proceedings of the Second Symposium on Karst Protection. Academic Speleological-Alpinist Club, Belgrade, 235–245.
- Jovanović B (1996) A contribution to the knowledge of the Gastropoda (Mollusca) fauna of the mountain of Stol. In: Magdalinović N (Ed.) Proceedings “Our Ecological Truth” of the IV Scientific-Expert Symposium on Natural Values and Environmental Protection and the II Expert Meeting on Preventive Medicine of Timočka Krajina, Kladovo, Hotel “Đerdap”, 29.05–01.06.1996. Institute for Health Protection “Timok”, Technical Faculty & Young Researchers, Zaječar-Bor, 217–221.
- Karaman BJ (1999) Endemske vrste puževa (Mollusca, Gastropoda) istočnog dela Srbije. In: Nikolić N, Marjanović T, Paunović P (Eds) Proceedings “Ecological Truth” of the VII Scientific-Expert Symposium on Economic Values and Environmental Protection and the XII Expert Meeting on Preventive Medicine of Timočka Krajina, Zaječar, 09–12.06.1999. Institute for Health Protection “Timok”, Centre for Agricultural and Technological Research, Technical Faculty & Young Researchers, Zaječar-Bor, 170–174.
- Karaman BJ (2006) Former investigations of the fauna of snails (Mollusca, Gastropoda) in Bosnia & Herzegovina. *Natura Montenegrina* 5: 55–66.
- Karaman BJ (2007) Checklist of snails (Mollusca, Gastropoda) of Serbia. *Glasnik Republičkog zavoda za zaštitu prirode i Prirodnjačkog muzeja u Podgorici* 29–30: 131–148.
- Karaman BJ (2012) Fauna of Gastropoda (Mollusca) in Fruška Gora mountain, Vojvodina (Serbia). *Natura Montenegrina* 11(1): 7–34.
- Karaman BJ (2014) Catalogue: Fauna of Land and Freshwater Snails Gastropoda (Mollusca) of Montenegro. *Catalogues*, 9, the Section of Natural Sciences, Volume 8. Montenegrin Academy of Sciences and Arts, Podgorica, 408 pp.
- Maassen WJM (1998) *Vitrea meijeri* n. sp. aus Mazedonien (Gastropoda, Pulmonata: Zonitidae). *Basteria* 62(5–6): 215–217.
- MolluscaBase [Eds] (2024) MolluscaBase. [https://www.molluscabase.org accessed 18 January 2024] <https://doi.org/10.14284/448>
- Möllendorff O (1873) Zur Molluskenfauna von Serbien. *Malakozoologische Blätter* 21: 129–149.
- Pavlović PS (1912) Mekušci iz Srbije. I. Suvozemni puževi. Special Editions, Vol. 39. Serbian Royal Academy, Belgrade, 140 pp.
- Páll-Gergely B, Asami T (2015) A new Turkish species and association of distribution with habitat in the genus *Vitrea* (Gastropoda: Pulmonata: Pristilomatidae). *Venus* (Tokyo) 73(1–2): 41–50.
- Pintér L (1969) Über einige nordafrikanische Vitreini (Gastropoda: Euthyneura). *Archiv für Molluskenkunde* 99(5–6): 319–325.
- Pintér L (1972) Die Gattung *Vitrea* Fitzinger, 1833 in den Balkanländern (Gastropoda: Zonitidae). *Annales Zoologici* 29(8): 209–315.
- Pintér L (1983) Zwei neue *Vitrea*-Arten (Gastropoda: Zonitidae). *Acta Zoologica Academiae Scientiarum Hungaricae* 29(1–3): 219–222.
- Pintér L, Suara R (2004) Magyarországi puhatestűek katalógusa. Hazai malakológusok gyűjtései alapján. Hungarian Natural History Museum, Budapest, 547 pp.
- Riedel A (1960) Die Gattung *Lindbergia* Riedel (Gastropoda, Zonitidae) nebst Angaben über *Vitrea illyrica* (A. J. Wagner). *Annales Zoologici* 18(18): 333–346.
- Riedel A (1966) Zonitidae (excl. Daudebardiinae) der Kaukasusländer (Gastropoda). *Annales Zoologici* 24(1): 1–303.
- Riedel A (1976) Eine kleine Zonitiden-Ausbeute (Gastropoda) aus Nordmarokko. *Fragmenta Faunistica* 20: 415–423. <https://doi.org/10.3161/00159301FF1976.20.23.415>

- Riedel A (1984) Zwei neue unterirdische Zonitidae aus der Türkei (Gastropoda, Stylommatophora). Malakologische Abhandlungen Staatliches Museum für Tierkunde in Dresden 9(217): 165–170.
- Riedel A, Velkovrh F (1976) Drei neue balkanische Zonitiden (Gastropoda) und neue Funde einiger seltener Arten. Biološki vestnik 24 (2): 219–227.
- Rodrigues AS, Gómez BJ, Martins R (2002) The perivaginal gland in *Oxychilus (Drouetia) atlanticus* (Morelet & Drouët, 1857) (Pulmonata: Zonitidae): a histological and histochemical approach. Invertebrate Reproduction & Development 41(1–3): 95–99. <https://doi.org/10.1080/07924259.2002.9652739>
- Schileyko AA (2003) Treatise on recent terrestrial pulmonate molluscs: Ariophantidae, Ostracolethidae, Ryssotidae, Milacidae, Dyakiidae, Staffordiidae, Gastrodontidae, Zonitidae, Daudebardiidae, Parmacellidae. Ruthenica, Supplement 2(10): 1309–1466.
- Schilthuizen M, Liew TS, Elahan BB, Lackman-Ancrenaz I (2005) Effects of karst forest degradation on pulmonate and prosobranch land snail communities in Sabah, Malaysian Borneo. Conservation Biology 19(3): 949–954. <https://doi.org/10.1111/j.1523-1739.2005.00209.x>
- Slapcinsky J (2018) *Vitrea clingmani* Dall in Pilsbry, 1900, a snail endemic to the summits of the Black Mountains and Great Craggy Mountains of North Carolina is now assigned to the genus *Pilsbryna* (Gastropoda: Stylommatophora: Oxychilidae). The Nautilus 132(1): 1–12.
- Sólymos P, Gaudényi T, Deli T, Nagy A (2004) Data on the land snail fauna of the Fruska Gora Mountain (Serbia) with some biogeographical remarks. Malakológiai Tájékoztató 22: 149–153.
- Stankovic SV, Stojkoska E, Norris A (2006) Annotated checklist of the terrestrial gastropods (Gastropoda) of the Republic of Macedonia. In: Petkovski S, Nikolov Z, Smith D, Smith K (Eds) Anniversary Proceedings (1926–2006): Eighty Years of Achievement by the Macedonian Museum of Natural History. Macedonian Museum of Natural History, Skopje, 43–55.
- Subai P (2011) Revision of the Argnidae, 2. The species of *Agardhiella* from the eastern part of the Balkan Peninsula. Archiv für Molluskenkunde 140(1): 77–121. <https://doi.org/10.1127/arch.moll/1869-0963/140/077-121>
- Sysoev A, Schileyko A (2009) Land Snails of Russia and Adjacent Regions. Pensoft Series Faunistica 87. Pensoft Publishers, Sofia-Moscow, 313 pp.
- Štamol V (2010) A list of the land snails (Mollusca: Gastropoda) of Croatia, with recommendations for their Croatian names. Natura Croatica 19(1): 1–76.
- Tomić V (1959) Zbirka recentnih puževa P. S. Pavlovića u Prirodnjačkom muzeju u Beogradu. Special Editions 27. Serbian Academy of Sciences and Arts, Belgrade, 74 pp.
- Wagner AJ (1914) Höhlenschnecken aus Süddalmatien und der Hercegovina. Sitzungsberichte der Kaiserlichen Akademie der Wissenschaften in Wien, Mathematisch-Naturwissenschaftliche Klasse 123(1): 33–48.
- Welter-Schultes FW (2012) European Non-Marine Molluscs, a Guide for Species Identification. Planet Poster Editions, Göttingen, 674 pp.

Six new species of *Cryptochironomus* Kieffer (Diptera, Chironomidae) from the Nearctic region

Wen-Bin Liu¹, Cheng-Yan Wang¹, Ya-Ning Tang¹, Ying Wang¹, Wen-Xuan Pei¹, Chun-Cai Yan¹

¹ Tianjin Key Laboratory of Conservation and Utilization of Animal Diversity, Tianjin Normal University, Tianjin, 300387, China
Corresponding author: Chun-Cai Yan (skyycc@tjnu.edu.cn)

Abstract

Six new species of *Cryptochironomus* Kieffer, 1918, *C. absum* Liu, **sp. nov.**, *C. beardi* Liu, **sp. nov.**, *C. dentatus* Liu, **sp. nov.**, *C. ferringtoni* Liu, **sp. nov.**, *C. parallelus* Liu, **sp. nov.** and *C. taylorensis* Liu, **sp. nov.**, are described and illustrated based on adult males. The specimens were collected from various water systems in the United States and preserved by Dr. Leonard Charles Ferrington Jr. An updated key to adult males of all known *Cryptochironomus* species in the Nearctic region is also provided.

Key words: Adult male, diagnostic characters, hypopygium, key, Nematocera, taxonomy, US

Introduction

The genus *Cryptochironomus* was erected by Kieffer in 1918, with *Chironomus* (*Cryptochironomus*) *chlorolobus* Kieffer, 1918 as type species. The adult males of this genus are distinguished by having a finger-shaped inferior volsella which lacks microtrichia, and is often completely covered by the small superior volsella (Cranston et al. 1989). The larvae primarily inhabit still waters, ranging from moderately eutrophic to super eutrophic conditions, making them a resilient species in environmental monitoring (Curry 1958). The genus comprises over 140 valid species and has a global distribution. All life stages of the genus have been studied by numerous authors (Townes 1945; Roback 1957; Curry 1958; Shilova 1966; Beck and Beck 1969; Sæther 1977, 2009; Sasa and Kikuchi 1995; Sasa 1998; Zorina 2000; Makarchenko et al. 2005; Silva et al. 2010; Yan et al. 2016, 2018).

The systematic review of *Cryptochironomus* and a key to all known males in the Nearctic region were supported by Townes (1945). Sæther (2009) compiled keys for all stages of the genus in the Nearctic region, which were subsequently updated by Silva et al. (2010). Currently, 14 species of the genus are known in the Nearctic region: *C. argus* Roback, *C. blarina* Townes, *C. conus* Mason, *C. curryi* Mason, *C. digitatus* (Malloch), *C. eminentia* Mason, *C. fulvus* (Johannsen), *C. imitans* Sæther, *C. parafulvus* Beck & Beck, *C. ponderosus* (Sublette), *C. ramus* Mason, *C. scimitarus* Townes, *C. sorex* Townes and *C. stylifera* (Johannsen). In the present study, six new species are described and illustrated based on adult males. An updated key to adult males of the genus in the Nearctic region is also provided.



Academic editor:

Fabio Laurindo da Silva
Received: 21 January 2024
Accepted: 3 April 2024
Published: 9 May 2024

ZooBank: <https://zoobank.org/52CF98AE-44DB-4C6B-BEA7-B0F9CBB2095A>

Citation: Liu W-B, Wang C-Y, Tang Y-N, Wang Y, Pei W-X, Yan C-C (2024) Six new species of *Cryptochironomus* Kieffer (Diptera, Chironomidae) from the Nearctic region. ZooKeys 1200: 275–302. <https://doi.org/10.3897/zookeys.1200.119225>

Copyright: © Wen-Bin Liu et al.
This is an open access article distributed under terms of the Creative Commons Attribution License (Attribution 4.0 International – CC BY 4.0).

Materials and methods

The morphology and terminology are based on Sæther (1980). The material examined was mounted on slides using the procedure outlined by Sæther (1969). When three or more specimens were measured, the measurements are provided as the range and mean, with the number of observed specimens in parentheses if it differs from the number (*n*) stated at the beginning of the description. The specimens examined in this study are preserved by Dr. Leonard Charles Ferrington Jr. and deposited in the University of Minnesota Insect Collection (UMSP), St. Paul, Minnesota, U.S.A. All type specimens are stored in UMSP.

Taxonomy

Cryptochironomus absum Liu, sp. nov.

<https://zoobank.org/1E37808F-5EC2-483E-A84E-61D250652987>

Figs 1–3

Type material. Holotype. one male, USA, Chamberlain South, Dakota State, Lake Francis Case Elm Creek, 43°56'57"N, 99°31'40"W, 3.IX.1971, light trap, leg: Patrick I. Huson.

Diagnostic characters. AR 2.58; frontal tubercles absent; posterior margin of tergite IX arc-shaped; anal point slightly constricted at base, wider at apex; superior volsella oval-shaped, covered with microtrichia at 1/3 distance from apex; inferior volsella completely covered by superior volsella; gonostylus straight, parallel-sided, tapering to the apex.

Description. Male (*n* = 1).

Total length 4.47 mm. Wing length 2.02 mm. Total length/wing length 2.22. Wing length/length of profemur 2.16.

Coloration. Thorax yellowish brown. Femora of front legs yellowish brown, tibiae dark brown, tarsi lost; femora and tibiae of mid and hind legs light yellowish brown; mid and hind legs with tarsi I yellowish brown except for dark yellowish brown at both ends, tarsi II–V dark yellowish brown. Abdomen yellowish brown, hypopygium dark brown.

Head (Fig. 1B). Antenna with 11 flagellomeres, ultimate flagellomere 851 µm long. AR 2.58. Frontal tubercles absent. Temporal setae 20. Clypeus with 18 setae. Tentorium 177 µm long, 47 µm wide. Palpomere lengths (in µm): 36; 60; 179; 151; 203; Pm5/Pm3 1.13.

Thorax (Fig. 1C). Anteprenotals bare; acrostichals 8; dorsocentrals 9; prealars 5. Scutellum with 16 setae.

Wing (Figs 1A, 3C). VR 1.08. R with 22 setae, R₁ with 11 setae, R₄₊₅ with 17 setae. Brachiolum with three setae. Squama with 14 fringed setae.

Legs. Front tibia with three subapical setae, 143 µm, the remaining lost. Mid legs with two tibial spurs, 42 µm long, the other lost, tibial combs 34 µm and 56 µm wide. Hind legs with two tibial spurs, 23 µm and 42 µm long, tibial combs 44 µm and 87 µm wide. Tarsus I of mid leg with three sensilla chaetica; tarsus I of hind leg with three sensilla chaetica. Lengths (in µm) and proportions of legs as in Table 1.

Hypopygium (Figs 2, 3A, B, D, E). The posterior margin of tergite IX is arc-shaped and bears 32 setae, located dorsally and ventrally near the base of the

anal point. Laterosternite IX has three setae. The anal point is 107 μm long, slightly constricted at the base, wider at the apex, and lacks lateral setae and microtrichia. The anal tergite bands are V-shaped and fused in the middle. The phallapodeme measures 134 μm long, and the transverse sternapodeme is 69 μm long. The superior volsella is oval-shaped, 56 μm long and 24 μm wide, covered with microtrichia at 1/3 distance from the apex, and has three long setae apically. The inferior volsella is finger-shaped, 22 μm long, bears two setae

Table 1. Lengths (in μm) and proportions of legs of *Cryptochironomus absum* Liu, sp. nov., adult male ($n = 1$).

	fe	ti	ta₁	ta₂	ta₃
P ₁	934	721	-	-	-
P ₂	876	738	516	230	155
P ₃	964	973	730	367	301
	ta₄	ta₅	LR	BV	SV
P ₁	-	-	-	-	-
P ₂	102	89	0.70	3.70	3.13
P ₃	168	110	0.75	2.82	2.65

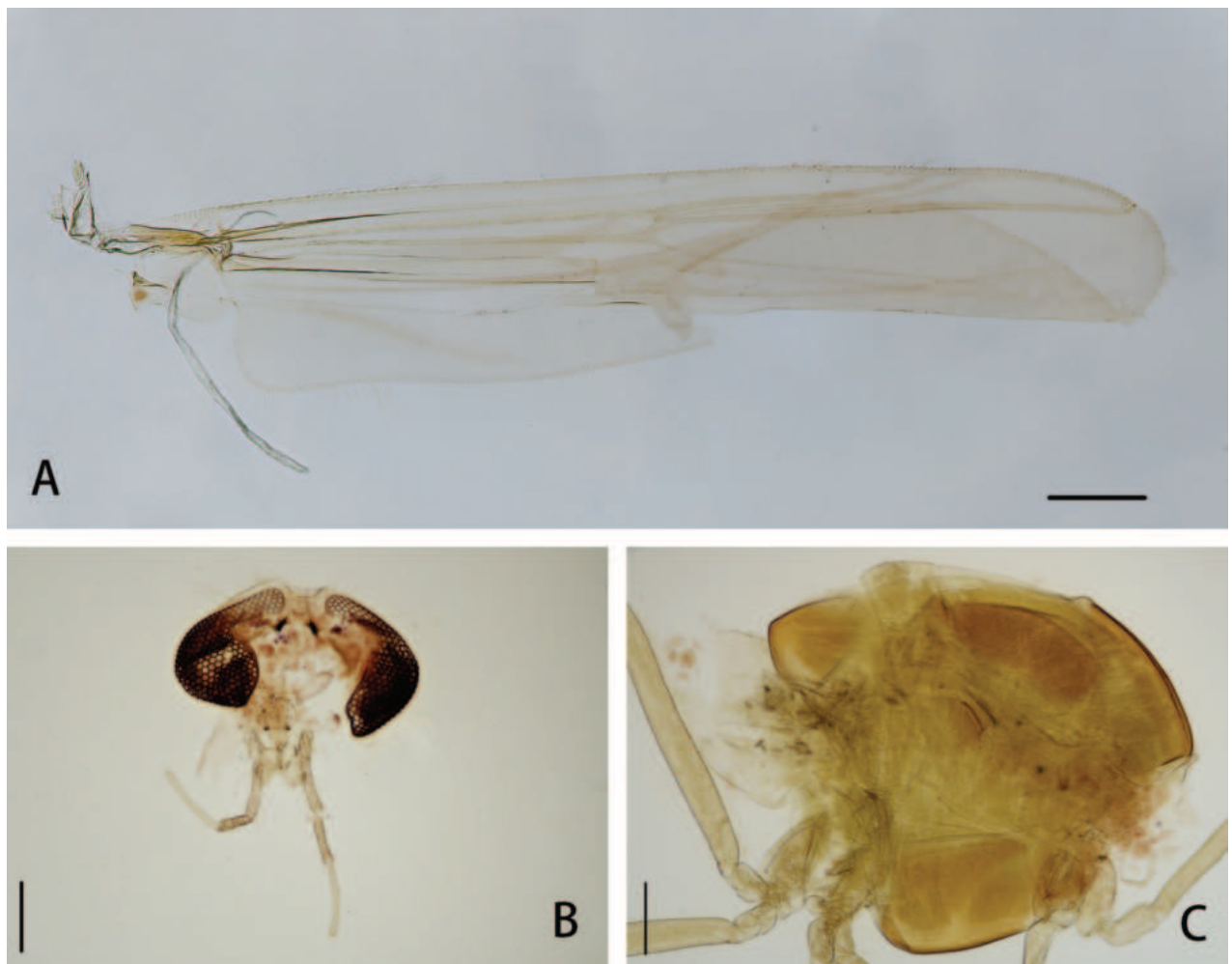


Figure 1. *Cryptochironomus absum* Liu, sp. nov., holotype male **A** wing **B** head **C** thorax. Scale bars: 200 μm .

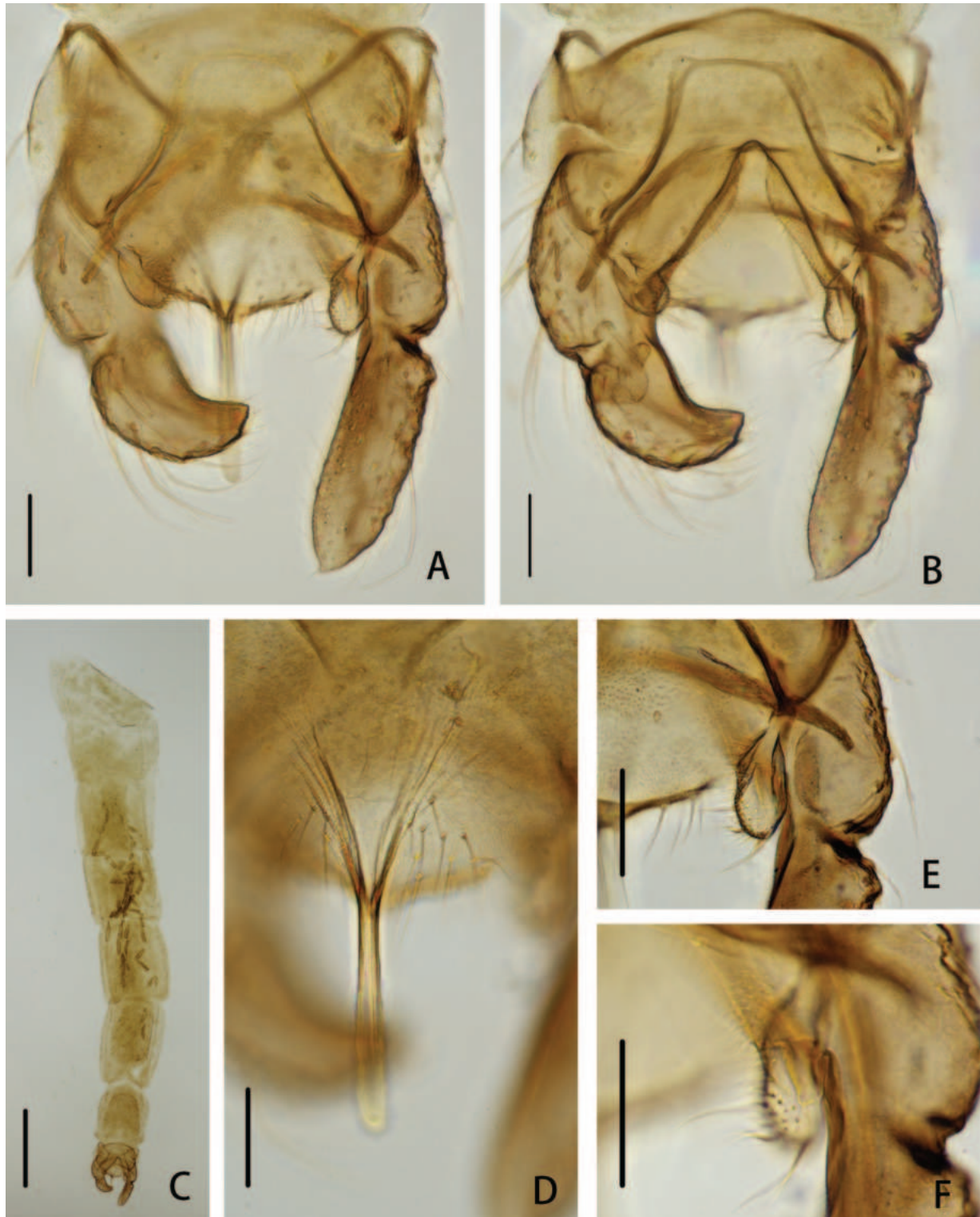


Figure 2. *Cryptochironomus absum* Liu, sp. nov., holotype male **A** hypopygium, dorsal view **B** hypopygium, ventral view **C** abdomen **D** anal point **E** superior volsella **F** inferior volsella. Scale bars: 50 μm (**A**, **B**, **D–F**); 500 μm (**C**).

at the apex, is completely covered by the superior volsella, and lacks microtrichia. The gonocoxite measures 166 μm long and bears six strong setae along the inner margin. The gonostylus is 157 μm long, straight, parallel-sided, tapers to the apex, bears five setae along the inner margin, and has one single seta at the apex. HR 1.06. HV 2.85.

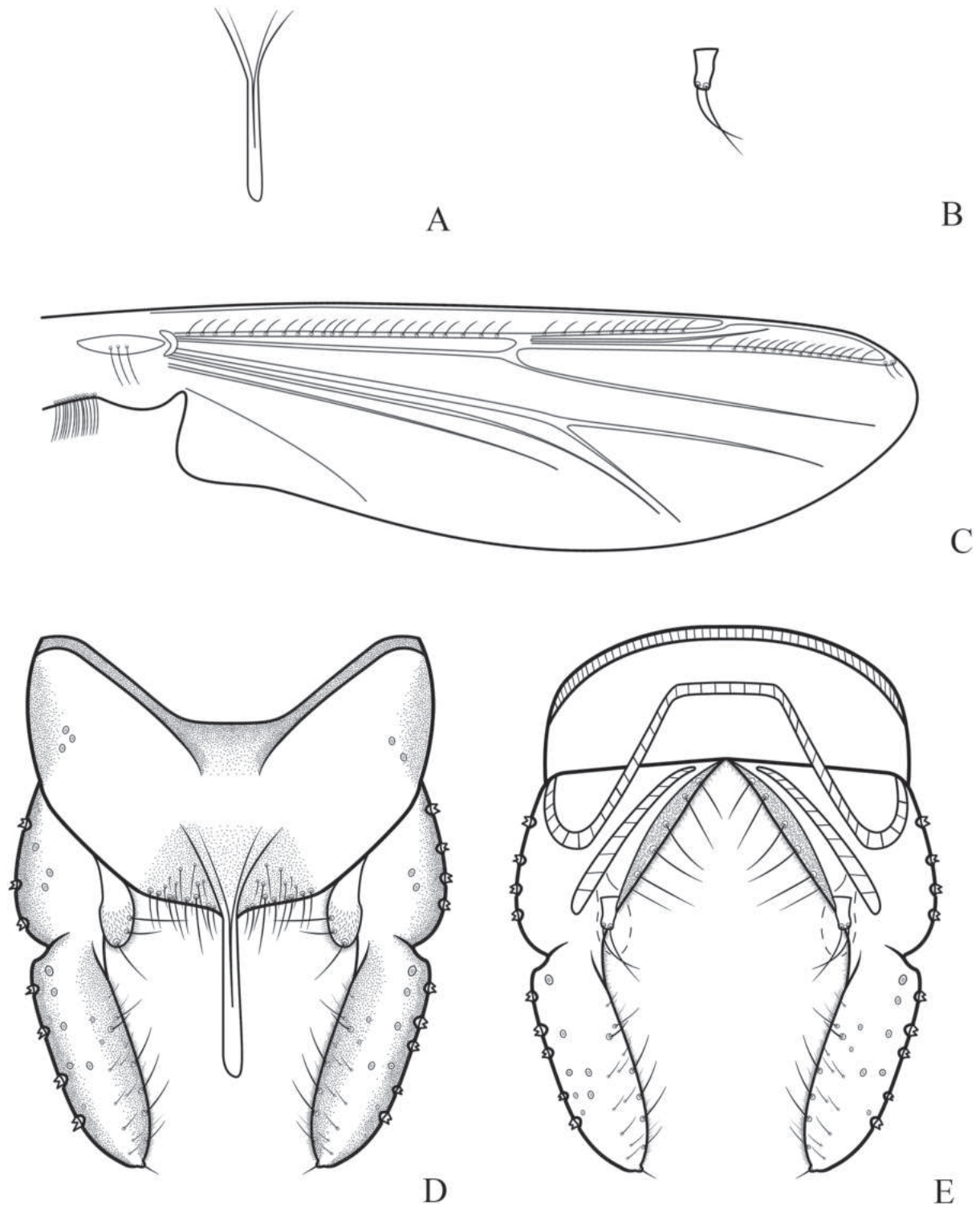


Figure 3. *Cryptochironomus absum* Liu, sp. nov., holotype male **A** anal point **B** inferior volsella **C** wing **D** hypopygium, dorsal view **E** hypopygium, ventral view.

Etymology. From the Latin, *absum*, absent, referring to the character of frontal tubercles absent, adjective in the nominative singular.

Remarks. *Cryptochironomus absum* Liu, sp. nov. is similar to *C. conus* Mason, 1985 in having anal tergite bands, anal point, and superior volsella with similar shapes. However, it can be distinguished from *C. conus* by the following combination of characters: wing length of 2.02 mm, absence of frontal tubercles,

inferior volsella with a finger-shaped appearance, and gonostylus straight in this new species. In contrast, *C. conus* has a wing length of 5.1–5.3 mm, distinct frontal tubercles, an inferior volsella with a tuberculate appearance and a protrusion at the base, and a curved gonostylus.

***Cryptochironomus beardi* Liu, sp. nov.**

<https://zoobank.org/916D7812-69CB-4318-BAAF-3438C95DC17D>

Figs 4–6

Type material. Holotype. one male, USA, New Mexico State, Rio Grande Otowi Bridge between Santa Fe and Los Alamos, 35°87'48"N, 99°31'40"W, 16.VII.1976, sweep net, leg: Melvin. Beard. **Paratype.** one male, North America, San Juan River at Farmington, 18.VII.1976, malaise trap, M. Beard.

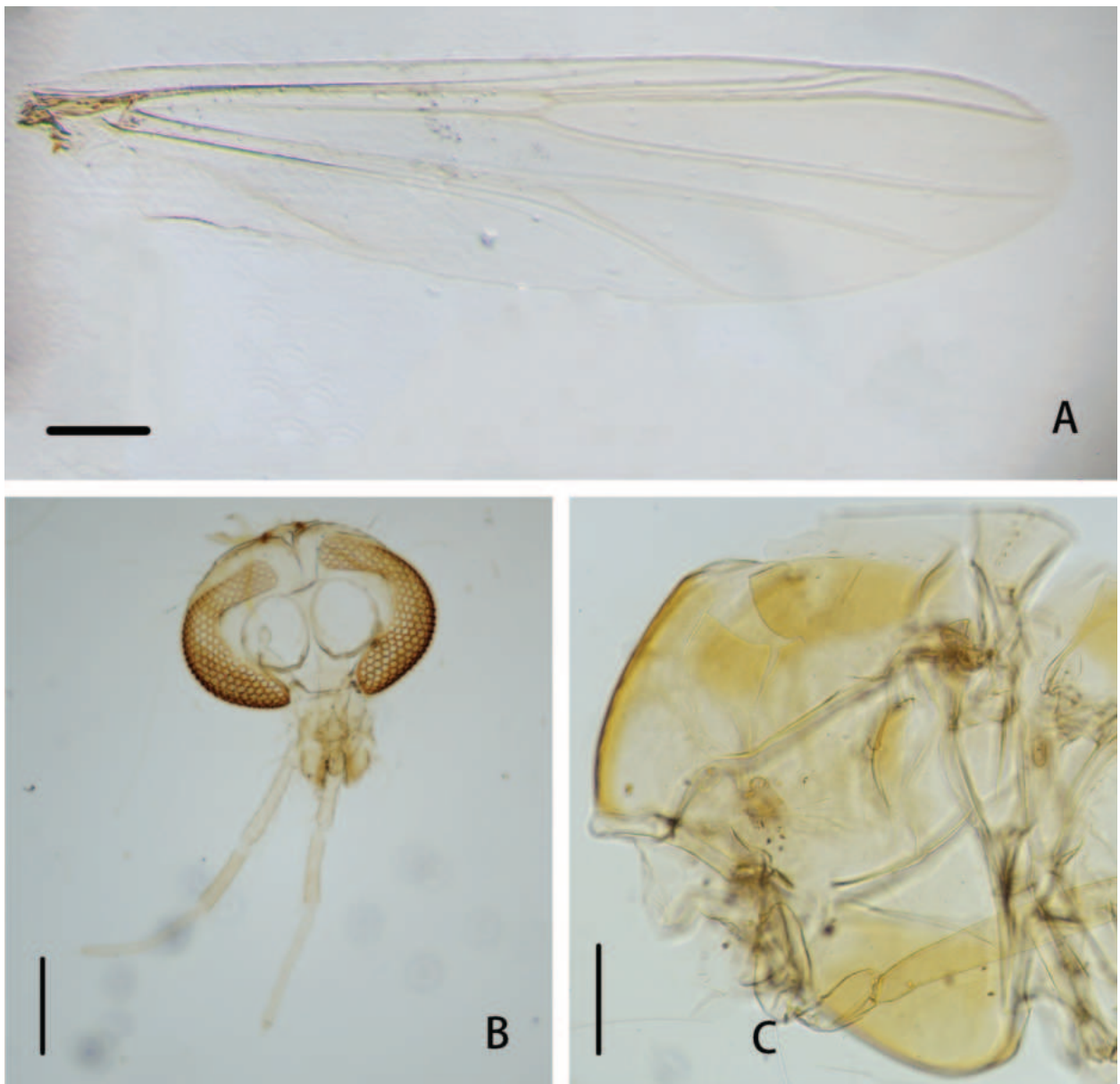


Figure 4. *Cryptochironomus beardi* Liu, sp. nov., holotype male **A** wing **B** head **C** thorax. Scale bars: 200 μ m.

Diagnostic characters. Thorax pale yellow, with yellow-brown spots; anal point widest at base, constricted slightly at 1/3 distance from base, apically rounded; anal tergite bands V-shaped, fused in the middle; superior volsella oval-shaped, stretching upward at base, swelling at apex; inferior volsella columnar, ~ 2× as long as wide, with slender extension at base, bearing two long setae at apex, free microtrichia; gonostylus protruded at base, slightly curved in the middle, tapered to the apex.

Description. Male ($n = 2$, unless stated).

Total length 5.03–5.10, 5.07 mm. Wing length 2.43–2.65, 2.54 mm. Total length/wing length 1.89–2.10, 2.00. Wing length/length of profemur 2.13 (1).

Coloration. Thorax pale yellow, with yellowish brown spots. Femora of front legs yellowish brown except for dark yellow-brown at ends, tibiae and tarsomeres dark brown; femora of mid and hind legs yellowish brown, tarsi I yellowish brown with dark brown in distal; tarsi II–V dark yellowish brown. Abdomen pale yellow, hypopygium yellowish brown.

Head (Figs 4B, 6A). Antenna with 11 flagellomeres, ultimate flagellomere 972 (1) μm long. AR 2.63 (1). Frontal tubercles conical, 18 μm high, 5 μm width at base. Temporal setae 17–18, 18. Clypeus with 12–18, 15 setae. Tentorium 167–173, 170 μm long, 45–50, 48 μm wide. Palpomere lengths of one specimen (in μm): 40; 61; 198; 171; 275; Pm5/Pm3 1.39.

Thorax (Fig. 4C). Anteprenotals with three setae, acrostichals 6–9, 8; dorso-centrals 8–10, 9; prealars 6. Scutellum with 14 setae.

Wing (Figs 4A, 6D). VR 1.09. R with 26–28, 27 setae, R_1 with 19–22, 21 setae, R_{4+5} with 22–25, 24 setae. Brachiolum with two setae. Squama with 8–9, 9 setae.

Legs. Front tibia with three subapical setae, 144 (1) μm , 151 (1) μm and 162 (1) μm . Combs of mid tibia 38–42, 40 μm wide with 22–27, 25 μm long spur, and 52–58, 55 μm wide with 30–40, 35 μm long spur; combs of hind tibia 47–48, 48 μm wide with 20–25, 23 μm long spur, 81–88, 85 μm wide with 38–42, 40 μm long spur. Tarsus I of mid leg with three sensilla chaetica. Tarsus I of hind leg with four sensilla chaetica. Lengths (in μm) and proportions of legs as in Table 2.

Hypopygium (Figs 5, 6B, C, E, F). The posterior margin of tergite IX is shoulder-shaped and bears 16–18, 17 setae located dorsally and ventrally near the base of the anal point. Laterosternite IX has 5–6, 6 lateral setae. The anal point is 70–80, 75 μm long, widest at the base, slightly constricted at 1/3 distance from the base, and apically rounded. The anal tergite bands are V-shaped and

Table 2. Lengths (in μm) and proportions of legs of *Cryptochironomus beardi* Liu, sp. nov. adult males ($n = 2$).

	fe	ti	ta ₁	ta ₂	ta ₃
P ₁	1139 (1)	857 (1)	1442 (1)	648 (1)	528 (1)
P ₂	998–1121, 1060	913–950, 932	579 (1)	266 (1)	204 (1)
P ₃	1156–1226, 1191	1185–1305, 1245	832 (1)	397 (1)	299 (1)
	ta ₄	ta ₅	LR	BV	SV
P ₁	498 (1)	170 (1)	1.68 (1)	1.86 (1)	1.38 (1)
P ₂	121 (1)	107 (1)	0.63 (1)	3.57 (1)	3.30 (1)
P ₃	185 (1)	112 (1)	0.70 (1)	3.20 (1)	2.81 (1)

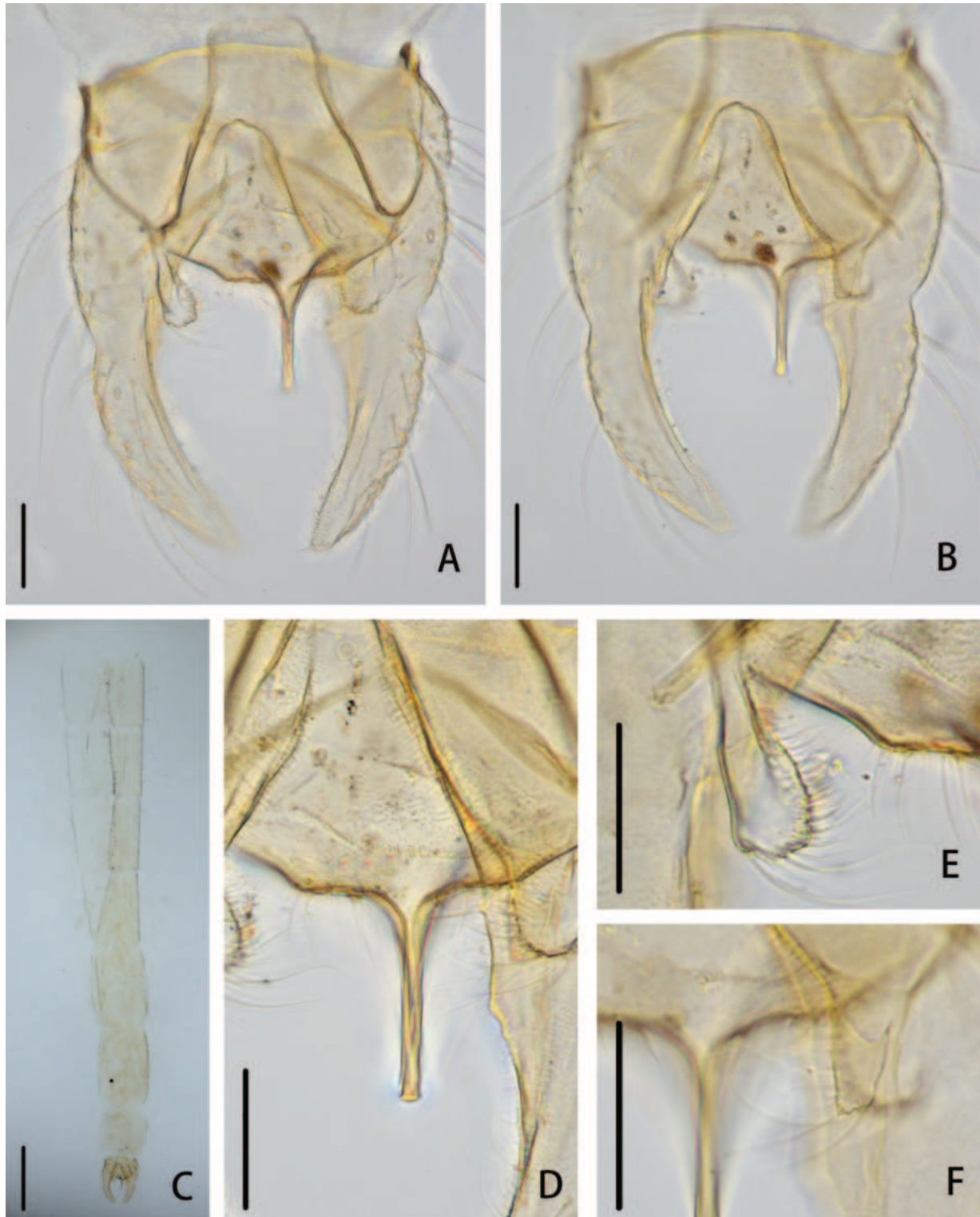


Figure 5. *Cryptochironomus beardi* Liu, sp. nov., holotype male **A** hypopygium, dorsal view **B** hypopygium, ventral view **C** abdomen **D** anal point **E** superior volsella **F** inferior volsella. Scale bars: 50 μm (**A**, **B**, **D–F**); 500 μm (**C**).

fused in the middle. The phallapodeme measures 113–115, 114 μm long, and the transverse sternapodeme is 57–61, 59 μm long. The superior volsella is oval-shaped, 45–50, 48 μm long, 22–29, 26 μm wide, stretching upward at the base, swelling at the apex, covered with microtrichia, and bears three strong setae at the apex. The inferior volsella is columnar, 25–31, 28 μm long, $\sim 2\times$ as

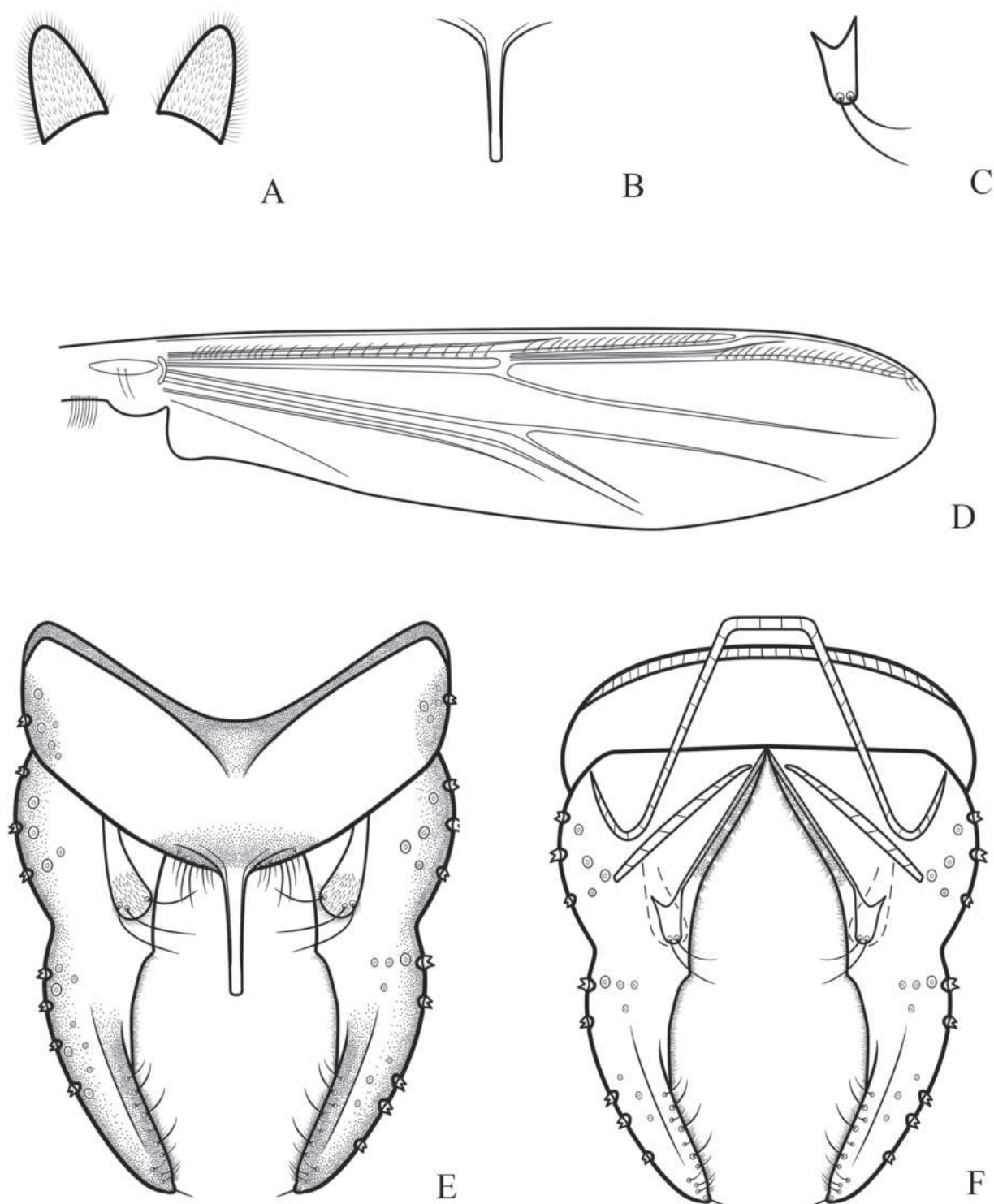


Figure 6. *Cryptochironomus beardi* Liu, sp. nov., holotype male **A** frontal tubercles **B** anal point **C** inferior volsella **D** wing **E** hypopygium, dorsal view **F** hypopygium, ventral view.

long as wide, with a slender extension at the base, bearing two long setae at the apex, and lacking free microtrichia. The gonocoxite measures 151–164, 158 μm long and bears six strong setae along the inner margin. The gonostylus is 162–166, 164 μm long, widest and protruded at the base, slightly curved in the middle, tapered towards the apex, bears five short setae along the inner margin and one stronger seta at the apex.

Etymology. Name after M. Beard, for the collector of the materials; noun in nominative case.

Remarks. *Cryptochironomus beardi* Liu, sp. nov. resembles *C. maculus* Yan & Wang, 2016 in having gonostylus and inferior volsella with similar shapes. However, it can be distinguished from *C. maculus* by the following combination of characters: mid and hind legs with tarsi I yellowish brown base, dark brown distally, anal point apically rounded, superior volsella stretching upward, gonocoxite concave with gonostylus obviously in the former; whereas in *C. maculus*, the mid and hind legs have the tarsi I yellowish green with dark brown mark on basal portion, anal point apically pointed, superior volsella not stretching, gonocoxite fused with gonostylus completely.

***Cryptochironomus dentatus* Liu, sp. nov.**

<https://zoobank.org/A506086F-D86F-4EC6-ADBC-5B1FDFBD9B43>

Figs 7–9

Type material. Holotype. One male, USA, New Mexico State, Guadalupe County, Pecos River, Puerto de Luna below Diversion Dam, 33°04'06"N, 104°26'79"W, 20.VIII.1991, light trap, leg: Lensky & Doles. **Paratypes.** 8 males, USA, Guadalupe County, Pecos River, Puerto de Luna below Diversion Dam, 20.VIII.1991, light trap, leg: Lensky & Doles.

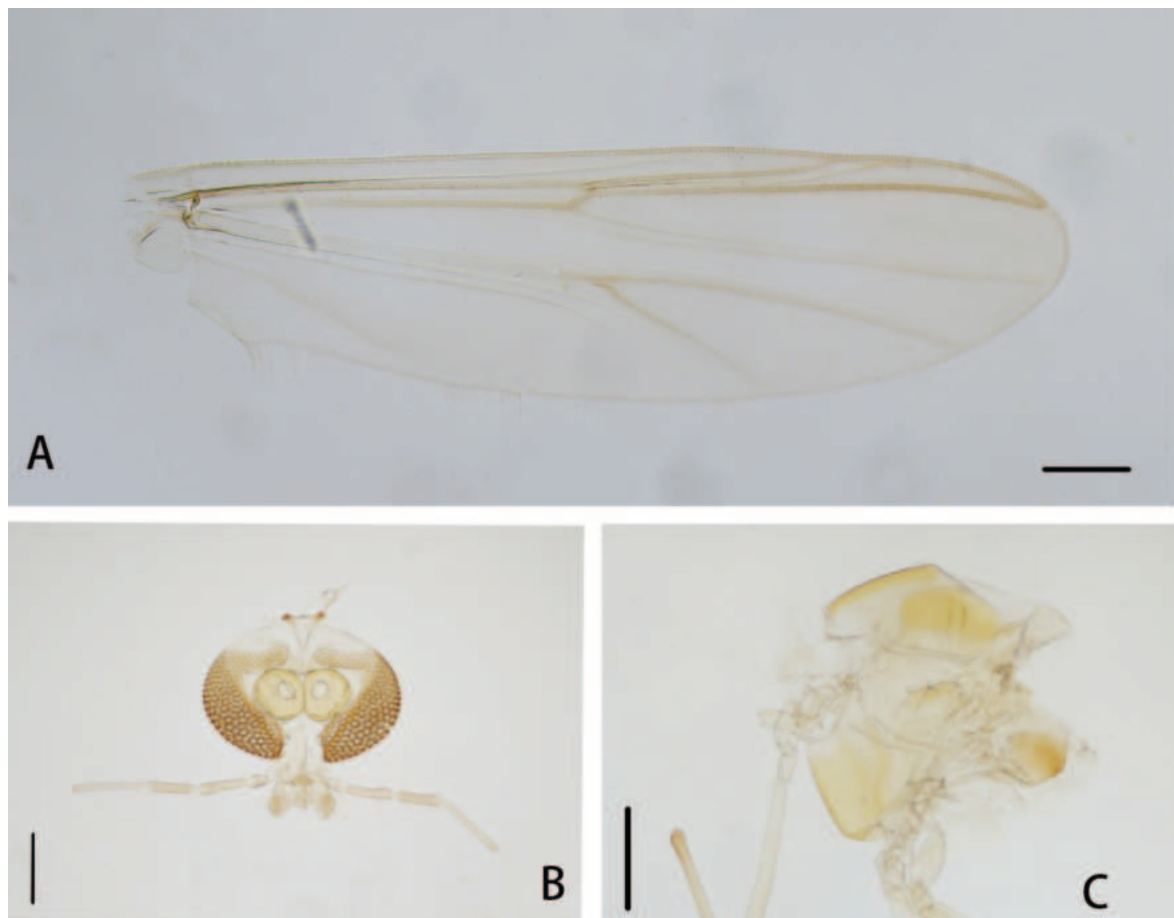


Figure 7. *Cryptochironomus dentatus* Liu, sp. nov., holotype male **A** wing **B** head **C** thorax. Scale bars: 200 μ m.

Diagnostic characters. Frontal tubercles conical; tergite IX saddle-shaped at the posterior margin; anal point parallel-sided with rounded apex; superior volsella crescent-like; inferior volsella finger-shaped, dentate at base; gonostylus curved slightly at 1/3 distance from base, swelling at distal 1/3.

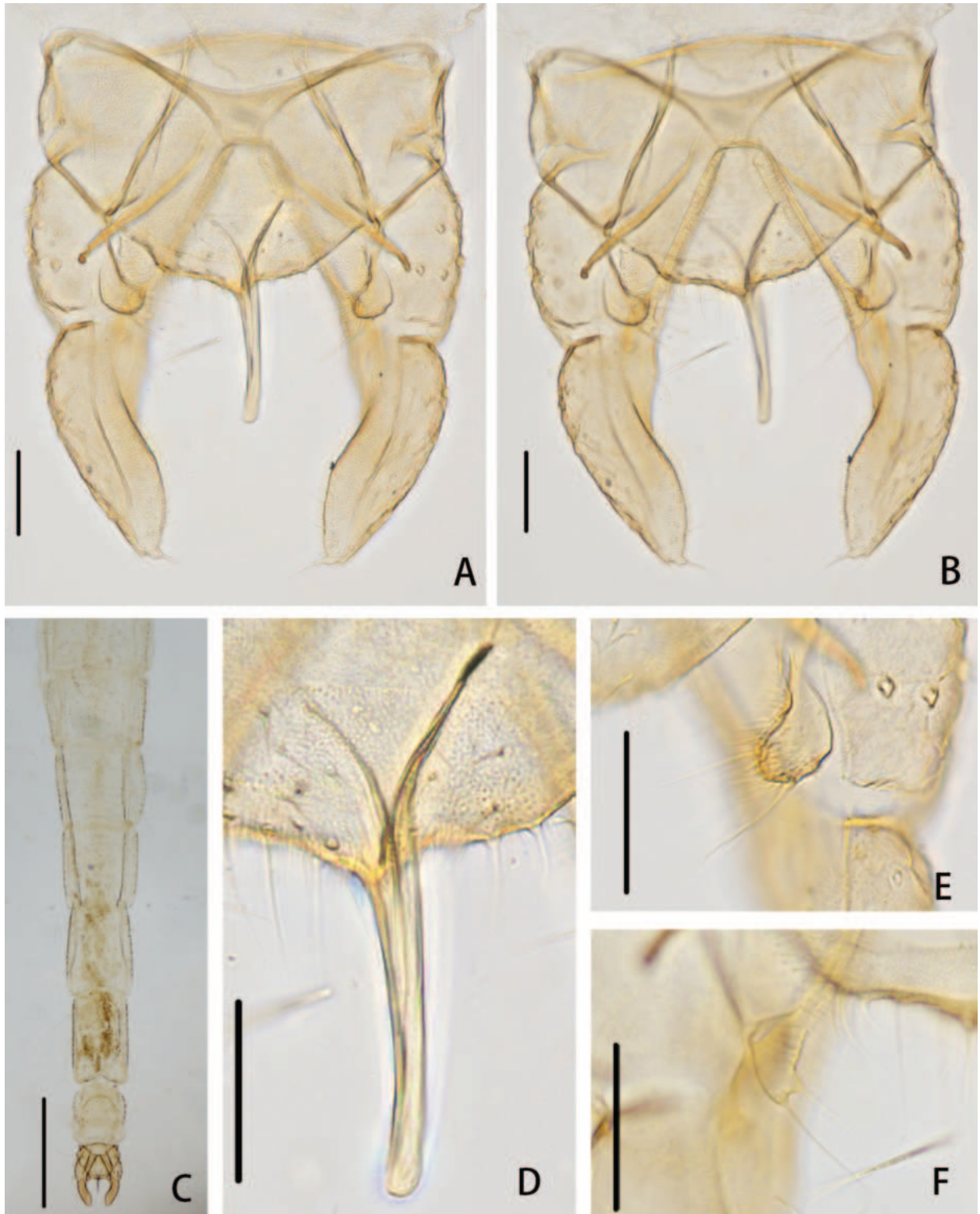


Figure 8. *Cryptochironomus dentatus* Liu, sp. nov., holotype male **A** hypopygium, dorsal view **B** hypopygium, ventral view **C** abdomen **D** anal point **E** superior volsella **F** inferior volsella. Scale bars: 50 μm (**A**, **B**, **D**–**F**); 500 μm (**C**).

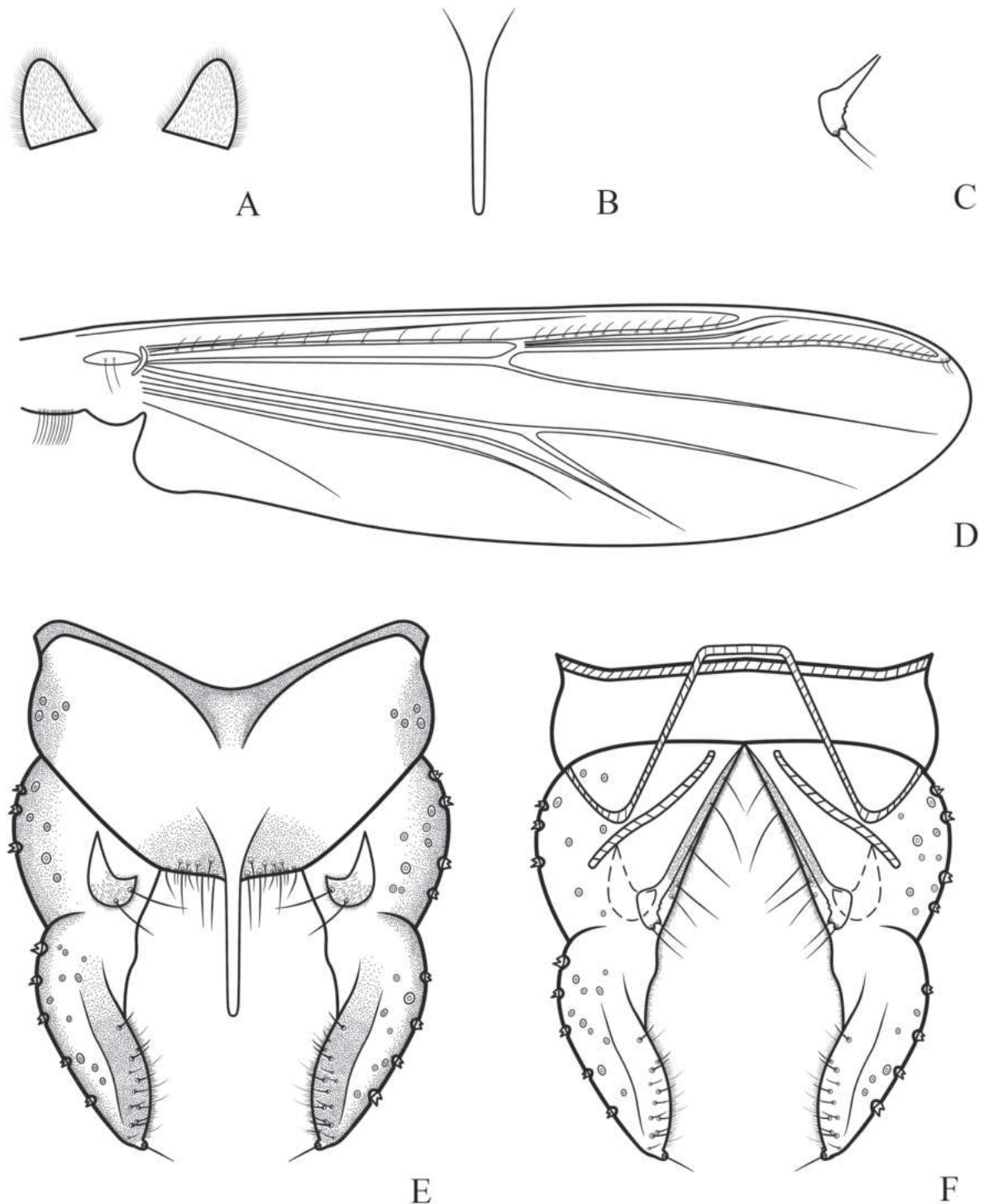


Figure 9. *Cryptochironomus dentatus* Liu, sp. nov., holotype male **A** frontal tubercles **B** anal point **C** inferior volsella **D** wing **E** hypopygium, dorsal view **F** hypopygium, ventral view.

Description. Male ($n = 9$, unless stated).

Total length 4.58–5.30, 4.91 mm. Wing length 2.05–2.29, 2.16 mm. Total length/wing length 2.14–2.31, 2.26. Wing length/length of profemur 2.04–2.61, 2.23.

Coloration. Thorax yellowish brown. Femora of front legs yellowish brown, tibiae and tarsi dark brown; femora and tibiae of mid and hind legs yellowish brown, tarsi I yellowish brown, tarsi II–V yellowish brown to dark brown gradually. Abdomen yellowish brown, hypopygium dark brown.

Head (Figs 7B, 9A). Antenna with 11 flagellomeres, ultimate flagellomere 770–879, 829 (4) μm long. AR 2.48–2.76, 2.61 (4). Frontal tubercles conical, 20–31, 25 μm high, 12–16, 14 μm width at base. Temporal setae 15–21, 18. Clypeus with 10–16, 12 setae. Tentorium 115–170, 147 μm long, 30–46, 40 μm wide. Palpomere lengths (in μm): 33–47, 41; 52–76, 67; 136–174, 158; 140–157, 148; 201–232, 211; Pm5/Pm3 1.18–1.48, 1.35.

Thorax (Fig. 7C). Anteprenotals bare; acrostichals 5–8, 6; dorsocentrals 8–12, 10; prealars 4. Scutellum with 14–18, 16 setae.

Wing (Figs 7A, 9D). VR 1.08–1.12, 1.10. R with 14–18, 17 setae, R_1 with 12–15, 13 setae, R_{4+5} with 19–25, 22 setae. Brachiolum with two setae. Squama with ten setae.

Legs. Front tibia with three subapical setae, 87–111, 98 (6) μm , 110–123, 115 (6) μm , 117–133, 124 μm . Combs of mid tibia 37–47, 43 μm wide with 23–34, 27 μm long spur, and 34–54, 46 μm wide with 32–45, 39 μm long spur; combs of hind tibia 30–49, 40 μm wide with 27–40, 31 μm long spur, 80–90, 83 μm wide with 34–48, 42 μm long spur. Tarsus I of mid leg with seven sensilla chaetica; tarsus I of hind leg with five sensilla chaetica. Lengths (in μm) and proportions of legs as in Table 3.

Hypopygium (Figs 8, 9B, C, E, F). The posterior margin of tergite IX is shoulder-shaped and bears 20–36, 30 setae. Laterosternite IX has 4–5, 4 setae. The anal point measures 77–87, 81 μm long and is parallel-sided with a rounded apex. The anal tergite bands are V-shaped and fused in the middle. The phallopodeme measures 115–135, 126 μm long, and the transverse sternapodeme is 64–90, 73 μm long. The superior volsella is crescent-like, 37–55, 48 μm long, 16–27, 21 μm wide, covered with microtrichia, and bears two strong setae at the apex. The inferior volsella is finger-shaped, 19–23, 21 μm long, dentate at the base, bearing two setae at the apex, and lacking free microtrichia. The gonocoxite measures 167–175, 170 μm long and bears five strong setae along the inner margin. The gonostylus is 150–157, 155 μm long, curved slightly at 1/3 distance from the base, swelling at the distal 1/3, with a small protrusion at the apex and bearing one apical seta. HR 1.08–1.12, 1.10. HV 2.96–3.38, 3.18.

Etymology. From the Latin, *dentatus*, dentate, tooth-like, referring to the shape of the base of inferior volsella, adjective in the nominative singular.

Table 3. Lengths (in μm) and proportions of legs of *Cryptochironomus dentatus* Liu, sp. nov., adult males ($n = 9$, unless stated).

	fe	ti	ta ₁	ta ₂	ta ₃
P ₁	877–1002, 963	739–797, 770	1223–1361, 1270 (4)	596–638, 621 (4)	484–524, 505 (4)
P ₂	831–978, 925 (6)	788–872, 826	461–520, 490	234–264, 248	175–205, 190
P ₃	987–1080, 1038 (6)	1071–1182, 1116	712–795, 748 (6)	370–413, 392 (6)	306–343, 318 (6)
	ta ₄	ta ₅	LR	BV	SV
P ₁	362–412, 394 (4)	174–191, 185 (4)	1.61–1.71, 1.65 (4)	1.72–1.81, 1.76 (4)	1.23–1.46, 1.37 (4)
P ₂	115–134, 124	100–111, 106	0.56–0.62, 0.59	3.06–3.53, 3.34 (6)	3.41–3.83, 3.59 (6)
P ₃	168–188, 179 (6)	122–126, 124 (6)	0.66–0.68, 0.67 (6)	2.82–2.88, 2.86 (6)	2.82–2.93, 2.88 (6)

Remarks. *Cryptochironomus dentatus* Liu, sp. nov. bears resemblance to *C. fulvus* Johannsen, 1905 due to its similar frontal tubercles, anal point, and superior volsella. However, *C. dentatus* Liu, sp. nov. can be distinguished from *C. fulvus* by the following combination of characters: absence of spots on the thorax, tergite IX with a shoulder-shaped posterior margin, inferior volsella with a finger-shape and dentate base; whereas *C. fulvus*, has dark brown spots on the thorax, tergite IX with a conical posterior margin, and inferior volsella with a tuberculate and non-dentate base.

***Cryptochironomus ferringtoni* Liu, sp. nov.**

<https://zoobank.org/C4891774-65E5-429C-9F82-452A5829F324>

Figs 10–12

Type material. Holotype. One male, USA, South Dakota State, Springfield, Lewis and Clark Lake, Boat Basin, 42°87'33"N, 97°49'02"W, 13–17.VII.1964, leg: Pat Hadson. **Paratypes.** 3 males, Ohio, Cincinnati, Federal Water Quality Association, lab on the window, 26.X.1970, leg: W. T. Mason. 2 males, Springfield South Dakota, Boat Basin, Springfield, Lewist Clank Lake, 13–17.VII.1964, leg: Pat Hadson.

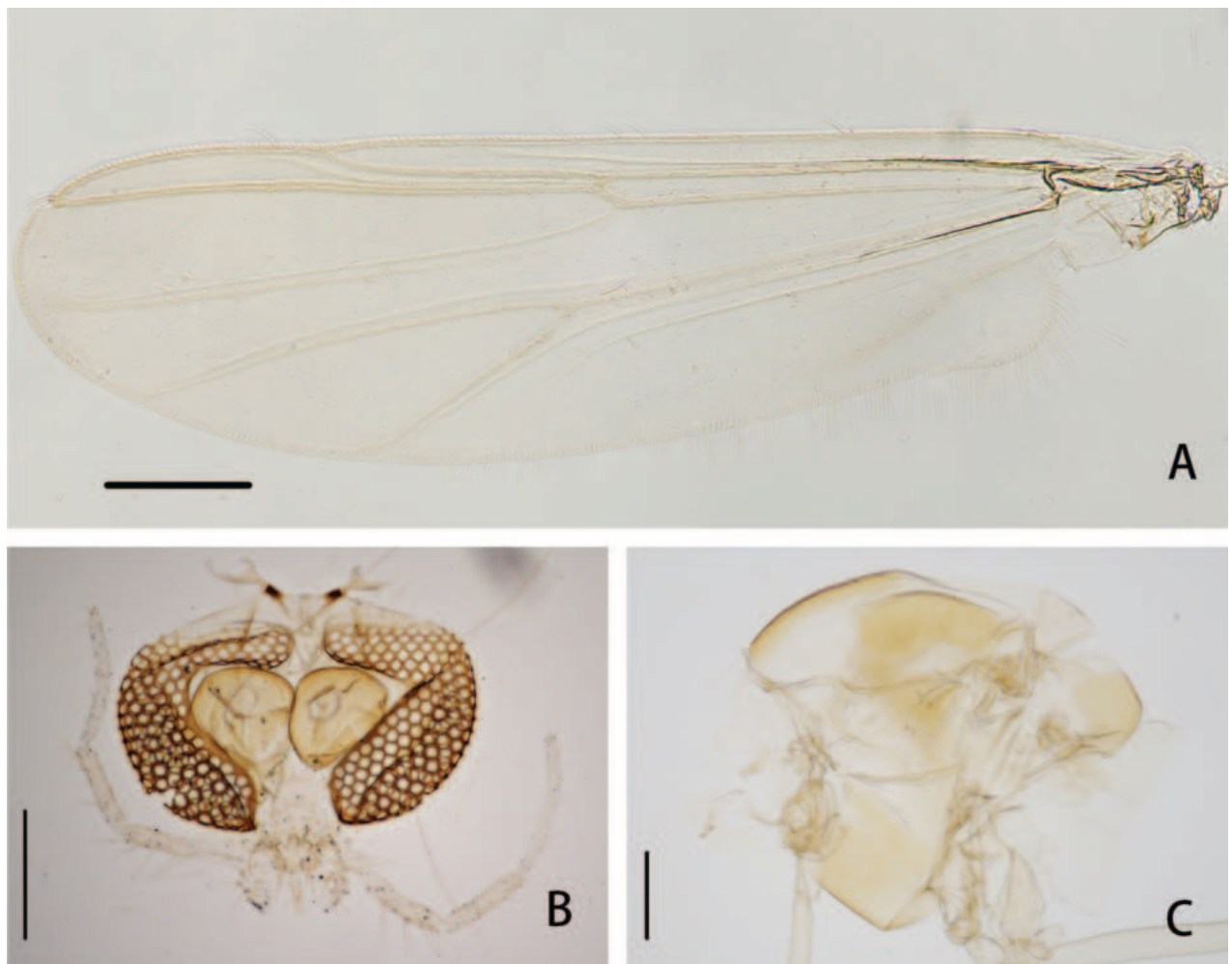


Figure 10. *Cryptochironomus ferringtoni* Liu, sp. nov., holotype male **A** wing **B** head **C** thorax. Scale bars: 200 μ m.

Diagnostic characters. Tergite IX with slightly cone-like posterior margin; anal point narrow at basal 1/3, expanded at 1/3 of the apex, apically rounded; superior volsella crescent-like, with hook-like extension at the base, apically rounded; inferior volsella triangular widest at base, apex with a small protrusion; the junction of gonostylus and gonocoxite concaved obviously; gonostylus widest at basal 1/3, tapered to the apex.

Description. Male ($n = 6$, unless stated).

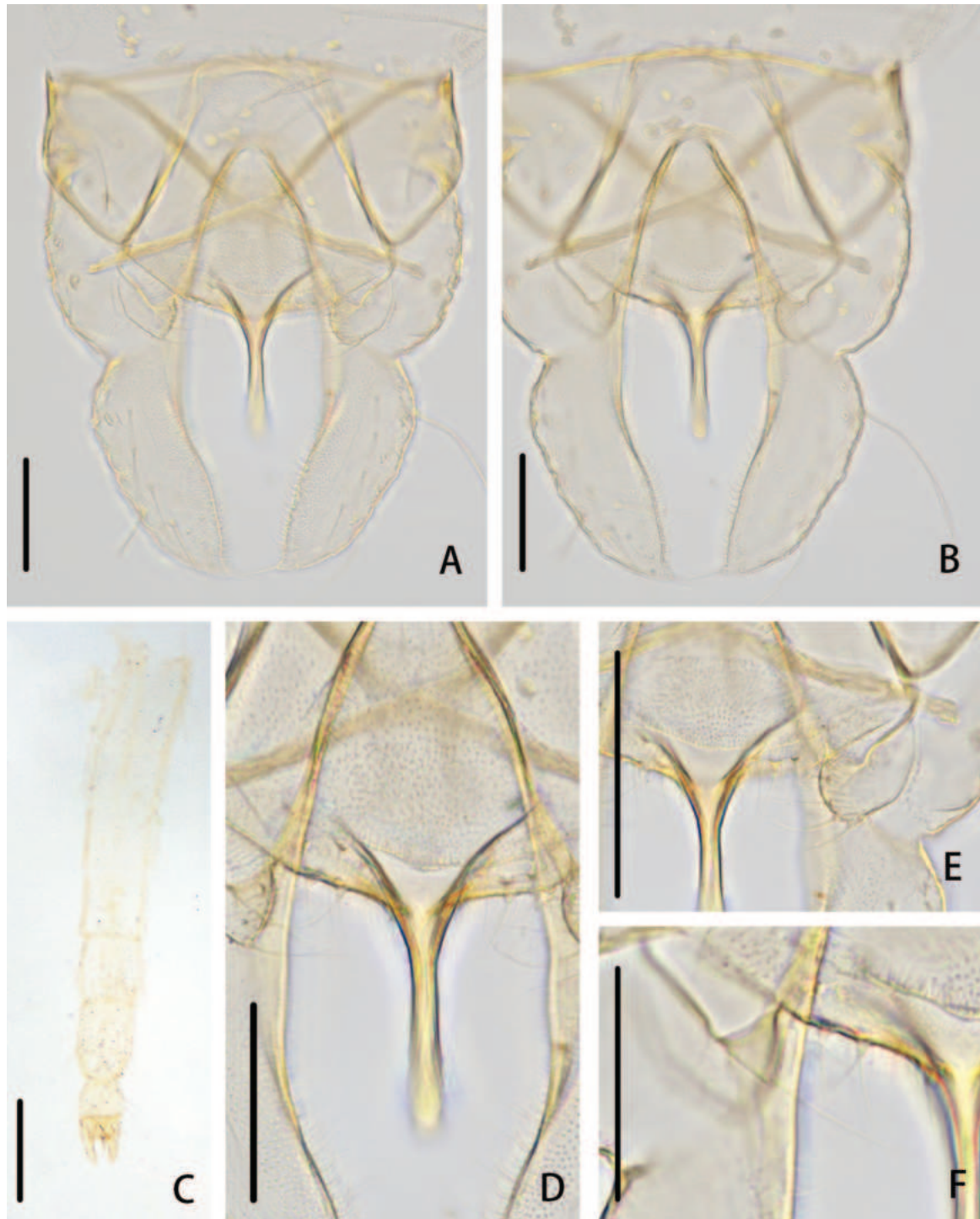


Figure 11. *Cryptochironomus ferringtoni* Liu, sp. nov., holotype male **A** hypopygium, dorsal view **B** hypopygium, ventral view **C** abdomen **D** anal point **E** superior volsella **F** inferior volsella. Scale bars: 50 µm (**A**, **B**, **D–F**); 500 µm (**C**).

Total length 3.29–3.91, 3.58 mm. Wing length 1.47–1.69, 1.61 mm. Total length/wing length 2.12–2.37, 2.23. Wing length/length of profemur 1.81–2.24, 2.02.

Coloration. Thorax yellowish brown. Femora of front legs yellowish brown, tibiae and tarsi lost; mid and hind legs yellowish brown. Abdomen pale yellow, hypopygium yellowish brown.

Head (Fig. 10B). Antenna with 11 flagellomeres, ultimate flagellomere 698–754, 724 (4) μm long. AR 2.29–2.49, 2.41 (4). Frontal tubercles absent. Temporal setae 14–17, 15. Clypeus with 12–18, 14 setae. Tentorium 126–153, 140 μm long, 31–37, 34 μm wide. Palpomere lengths (in μm): 21–36, 32; 41–56, 49; 126–155, 144; 114–144, 132; 174–232, 204; Pm5/Pm3 1.18–1.55, 1.40.

Thorax (Fig. 10C). Anteprenotals bare; acrostichals 4–7, 5; dorsocentrals 4–8, 7; prealars 4–5, 5. Scutellum with 8–14, 11 setae.

Wing (Figs 10A, 12C). VR 1.13–1.19, 1.16. R with 12–17, 15 setae, R_1 with 10–16, 14 setae, R_{4+5} with 15–21, 19 setae. Brachiolum with 2–3, 2 setae. Squama bare.

Legs. Front tibia with three subapical setae, 113–132, 123 (3) μm , 124–127, 126 (3) μm , 128–144, 135 (3) μm . Mid legs with two spurs, 16–23, 20 μm and 20–34, 27 μm long, tibial comb 20–39, 30 μm and 27–40, 32 μm wide. Spurs of hind tibia 19–30, 26 μm and 30–45, 36 μm long, tibial comb 30–43, 36 μm and 50–83, 67 μm wide. Tarsus I of mid leg with 4–5, 4 sensilla chaetica, tarsus I of metapedes leg with 3–4, 4 sensilla chaetica. Lengths (in μm) and proportions of legs as in Table 4.

Hypopygium (Figs 11, 12A, B, D, E). The posterior margin of tergite IX is slightly cone-like and bears 12–20, 16 setae located dorsally and ventrally near the base of the anal point. Laterosternite IX has 3–6, 4 lateral setae. The anal point measures 55–63, 59 μm long and is contracted at the basal 1/3, expanded at the 1/3 of the apex, and apically rounded. The anal tergite bands are V-shaped and jointed medially. The phallapodeme measures 93–102, 96 μm long, and the transverse sternapodeme is 43–67, 54 μm long. The superior volsella is crescent-like, 35–39, 37 μm long, 18–27, 22 μm wide, with a hook-like extension at the base, apically rounded, and bears two strong setae at the apex. The inferior volsella is triangular, 12–15, 13 μm long, widest at the base, tapered towards the apex, with a small protrusion at the apex and bearing one seta. The gonocoxite measures 105–124, 116 μm long. The junction of the gonostylus and gonocoxite is distinctively concave. The gonostylus is 104–126, 115 μm long, widest at the basal 1/3, tapered to the apex, and bears one stronger seta at the apex. HR 0.96–1.06, 1.01. HV 2.92–3.33, 3.13.

Etymology. Name after Dr. Leonard Charles Ferrington Jr., for his outstanding contribution to the knowledge of Chironomidae taxonomy; noun in nominative case.

Table 4. Lengths (in μm) and proportions of legs of *Cryptochironomus ferringtoni* Liu, sp. nov., adult males ($n = 6$, unless stated).

	fe	ti	ta ₁	ta ₂	ta ₃
P ₁	724–938, 800	483–559, 531	960 (1)	-	-
P ₂	633–730, 691	554–662, 613	389–468, 430	159–186, 172	112–134, 125
P ₃	610–797, 711	710–850, 795	566–638, 603 (4)	245–296, 269 (4)	204–238, 220 (4)
	ta ₄	ta ₅	LR	BV	SV
P ₁	-	-	1.81	-	-
P ₂	73–89, 80	62–74, 67	0.69–0.71, 0.70	3.73–3.99, 3.91	2.93–3.08, 3.04
P ₃	122–142, 131 (4)	80–91, 85 (4)	0.73–0.80, 0.76 (4)	2.87–3.12, 2.99 (4)	2.33–2.59, 2.50 (4)

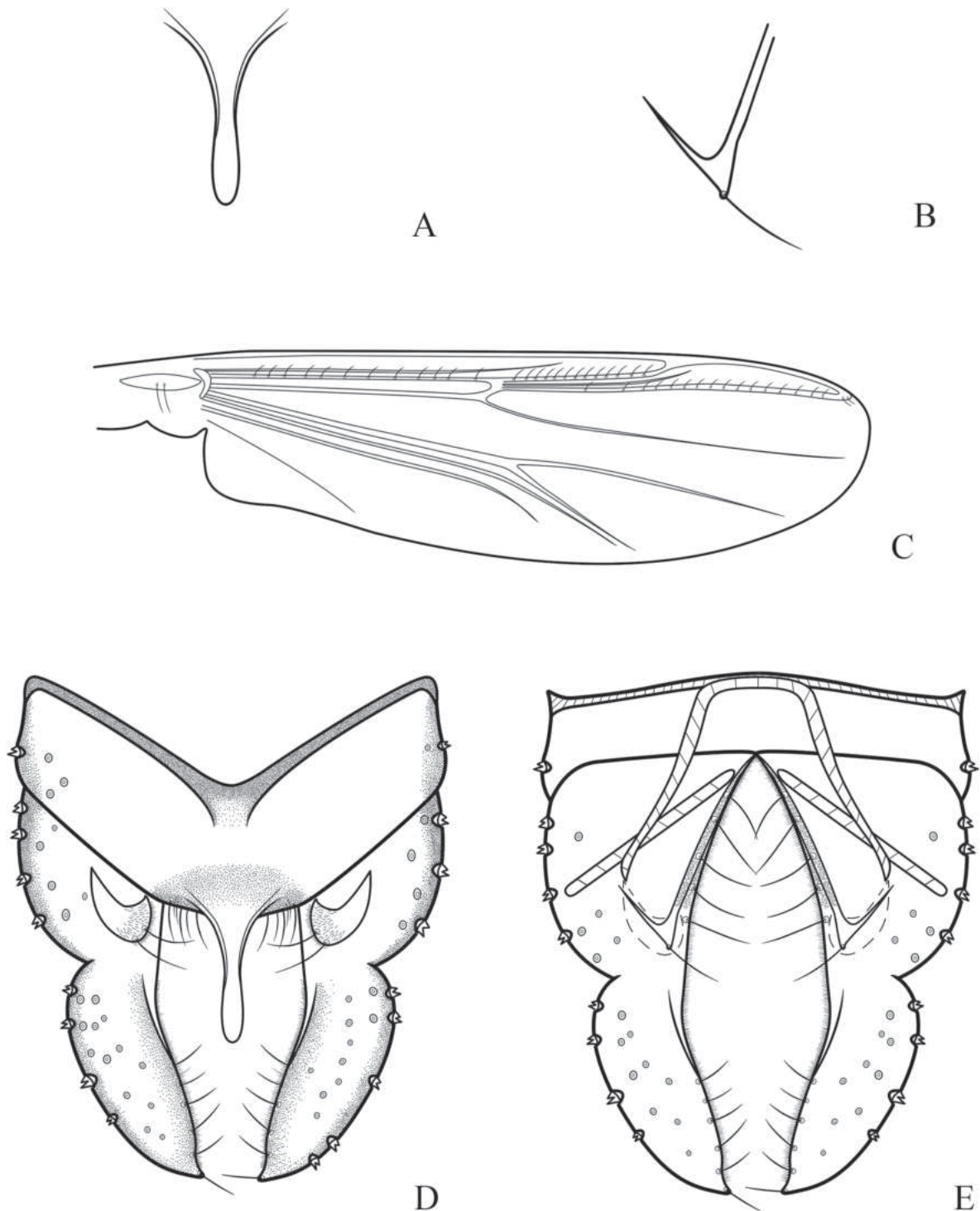


Figure 12. *Cryptochironomus ferringtoni* Liu, sp. nov., holotype male **A** anal point **B** inferior volsella **C** wing **D** hypopygium, dorsal view **E** hypopygium, ventral view.

Remarks. *Cryptochironomus ferringtoni* Liu, sp. nov. bears resemblance to *C. rostratus* Kieffer, 1921 due to its similar shapes of the posterior margin of tergite IX and superior volsella. However, it can be distinguished from *C. rostratus* by the absence of frontal tubercles, contraction of the anal point at the basal 1/3 and expansion at the apical 1/3, and a triangular inferior volsella in *C. ferringtoni* Liu, sp. nov.; whereas *C. rostratus* frontal tubercles, a distally tapering or parallel-sided anal point, and a tuberculate inferior.

***Cryptochironomus parallelus* Liu, sp. nov.**

<https://zoobank.org/C30E333F-00DF-49CB-B611-8BDD3E032EBB>

Figs 13–15

Type material. Holotype. one male, USA, New Mexico State, Catron Country, San Francisco River at Glenwood, 33°12'52"N, 109°28'01"W, 7.III.1976, reared, leg: Sta. H & M. Beard. **Paratypes.** 2 males, USA, New Mexico State, Catron Country, San Francisco River, 17.IX.1974, leg: M. Beard. 1 male, USA, New Mexico State, Catron Country, San Francisco River at Glenwood, 7.III.1976, reared, leg: Sta. H & M. Beard.

Diagnostic characters. Thorax brown, with dark brown spots. Femora and tibiae of mid and hind legs dark brown at proximal and distal 1/5. The posterior margin of tergite IX cone-like; anal point slender, parallel-sided, apically rounded; superior volsella parallel-sided at base, slightly curved in the middle, widest at 1/3 distance from apex and apically swollen; inferior volsella thumb-like, with slight extension at base; gonostylus curved at 1/4 distance from base, parallel-sided towards apex, rounded apically.

Description. Male ($n = 4$, unless stated).

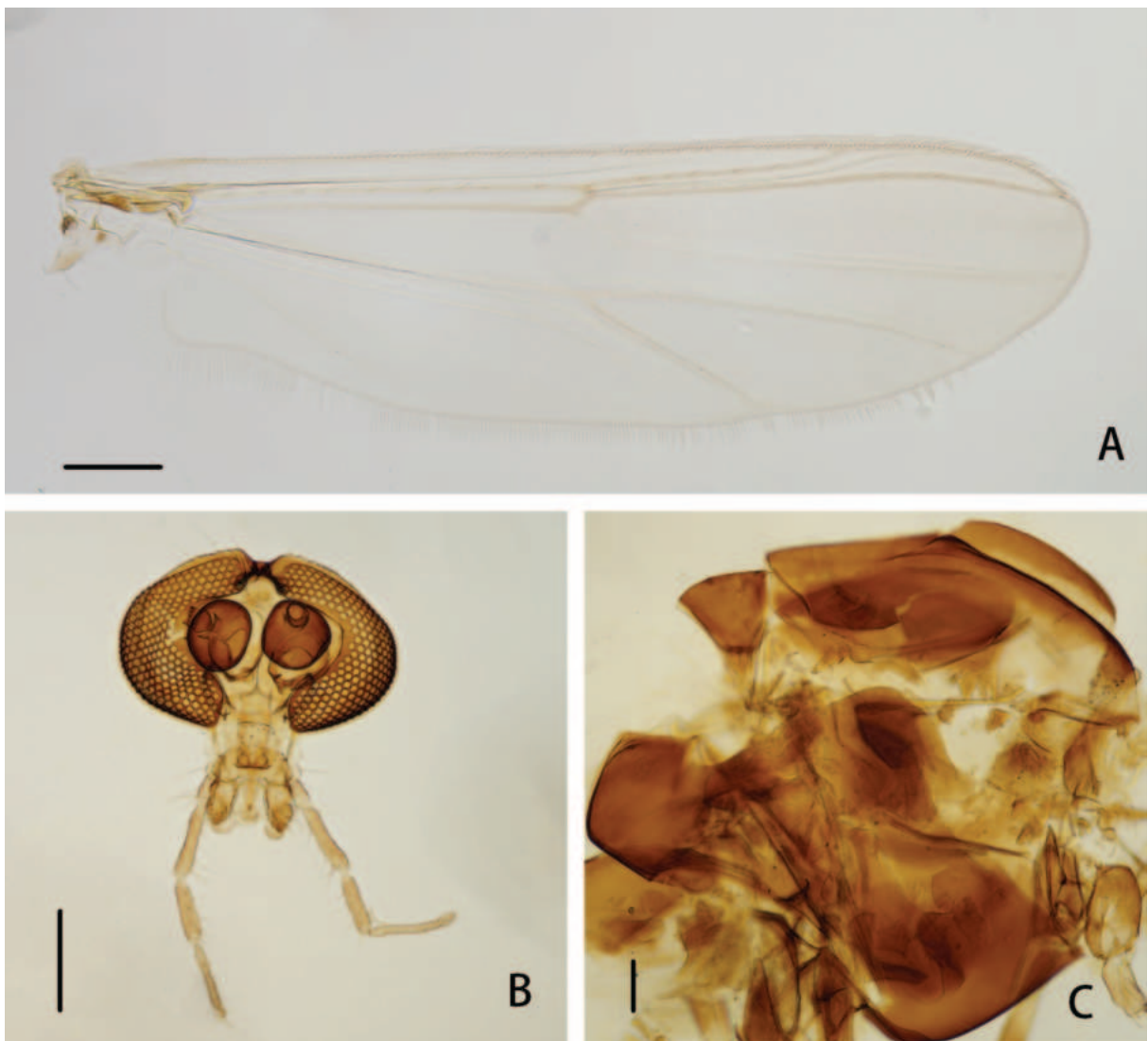


Figure 13. *Cryptochironomus parallelus* Liu, sp. nov., holotype male **A** wing **B** head **C** thorax. Scale bars: 200 μ m.

Total length 4.24–5.05, 4.59 mm. Wing length 2.00–2.37, 2.12 mm. Total length/wing length 2.12–2.27, 2.17. Wing length/length of profemur 1.95–2.31, 2.20.

Coloration. Thorax brown, with dark brown spots. Femora and tibiae of front legs dark brown except for yellowish brown at distal 3/4, tarsi I dark brown except for yellowish brown at basal, tarsi II–V dark brown; femora and tibiae of mid and hind legs both dark brown at both proximal and distal 1/5, yellowish brown in the middle, tarsi I yellowish brown except for dark yellowish brown at apex, tarsi II–V dark yellowish brown. Abdomen yellowish brown, hypopygium dark yellowish brown.

Head (Figs 13B, 15A). Antenna with 11 flagellomeres, ultimate flagellomere 697–802, 746 μm long. AR 1.99–2.37, 2.17. Frontal tubercles conical, 15–23, 19 (3) μm high, 10–14, 13 (3) μm width at base. Temporal setae 16–23, 18. Clypeus with 14–18, 16 setae. Tentorium 115–144, 135 μm long, 39–42, 41 μm wide. Palpomere lengths (in μm): 34–49, 40; 73–84, 79; 156–176, 169; 132–142, 137; 191–225, 211; Pm5/Pm3 1.14–1.35, 1.26.

Thorax (Fig. 13C). Anteprenotals bare; acrostichals 5–10, 8; dorsocentrals 8–11, 10; prealars 4. Scutellum with 14–16, 15 setae.

Wing (Figs 13A, 15D). VR 1.02–1.09, 1.06. R with 10–18, 14 setae, R_1 with 6–10, 8 setae, R_{4+5} with 10–15, 12 setae. Brachiolum with three setae. Squama with 10–17, 14 (2) setae.

Legs. Front tibia with three subapical setae, 114–121, 117.5 (2) μm , 129 (1) μm , 138 (1) μm . Combs of midtibia 41–57, 49 μm wide with 21–29, 24 μm long spur, and 42–61, 54 μm wide with 32–39, 35 μm long spur; combs of hind tibia 28–48, 36 μm wide with 28–36, 34 μm long spur, 80–92, 84 μm wide with 40–50, 44 μm long spur. Tarsus I of mid leg with three sensilla chaetica; tarsus I of hind leg with three sensilla chaetica. Lengths (in μm) and proportions of legs as in Table 5.

Hypopygium (Figs 14, 15B, C, E, F). The posterior margin of tergite IX is cone-like and bears ~ 22–36, 28 setae dorsally and ventrally near the base of the anal point. Laterosternite IX has 3–5, 4 setae. The anal point measures 54–65, 59 μm long and is slender with parallel sides, apically rounded. The anal tergite bands are V-shaped and show significant healing in the middle. The phallopodeme measures 103–120, 110 μm long, and the transverse sternapodeme is 56–89, 71 μm long. The superior volsella is 34–54, 47 μm long, 16–19, 17 μm wide, parallel-sided at the base, slightly curved in the middle, widest at the 1/3

Table 5. Lengths (in μm) and proportions of legs of *Cryptochironomus parallelus* Liu, sp. nov., adult males ($n = 4$, unless stated).

	fe	ti	ta ₁	ta ₂	ta ₃
P ₁	871–1112, 945	675–770, 710	1091–1125, 1111 (3)	491–553, 520 (3)	383–431, 413(3)
P ₂	728–990, 831	753–872, 793	440–540, 477	224–306, 255	160–218, 191
P ₃	845–1083, 960	922–1124, 990	704–710, 707 (3)	338–382, 353 (3)	270–296, 281 (3)
	ta ₄	ta ₅	LR	BV	SV
P ₁	300–334, 316 (3)	153–167, 160 (3)	1.60–1.62, 1.61 (3)	1.85–1.99, 1.91 (3)	1.40–1.45, 1.42 (3)
P ₂	106–152, 124	89–120, 104	0.58–0.62, 0.60	3.01–3.42, 3.13	3.29–3.50, 3.40
P ₃	158–180, 168 (3)	107–109, 108 (3)	0.72–0.77, 0.75 (3)	2.81–2.83, 2.83 (3)	2.52–2.84, 2.64 (3)

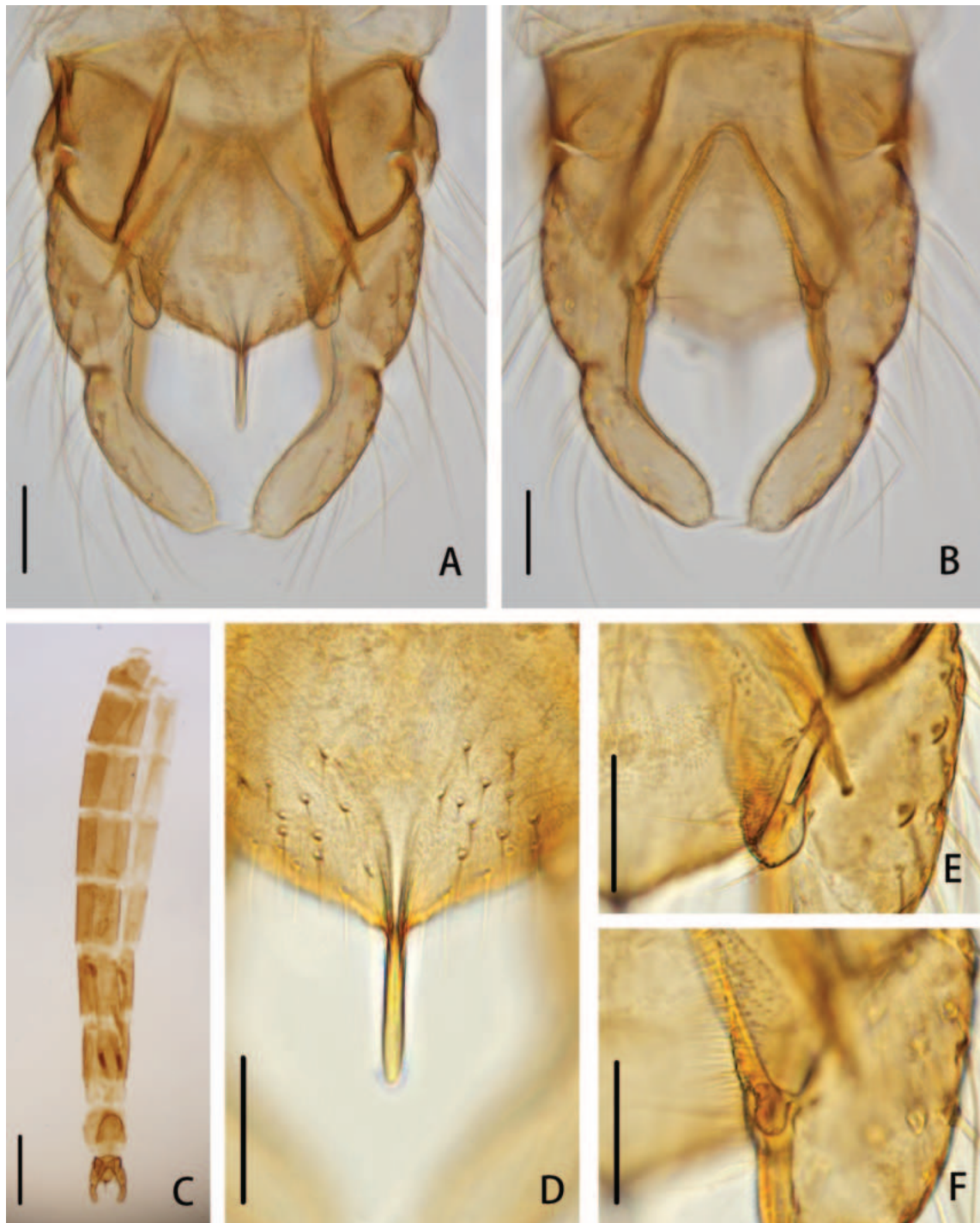


Figure 14. *Cryptochironomus parallelus* Liu, sp. nov., holotype male **A** hypopygium, dorsal view **B** hypopygium, ventral view **C** abdomen **D** anal point **E** superior volsella **F** inferior volsella. Scale bars: 50 μm (**A**, **B**, **D**–**F**); 500 μm (**C**).

distance from the apex, and apically swollen. It is covered with microtrichia and bears two strong setae at the apex. The inferior volsella is thumb-like, 15–20, 17 μm long, with a slight extension at the base and bears two setae at the apex. The gonocoxite measures 161–183, 176 μm long and bears seven strong setae along the inner margin. The gonostylus is 124–132, 127 μm long, curved at the 1/4 distance from the base, parallel-sided towards the apex, rounded apically, bears five short setae along the inner margin and one seta at the apex. HR 1.30–1.44, 1.38. HV 3.42–3.82, 3.60.

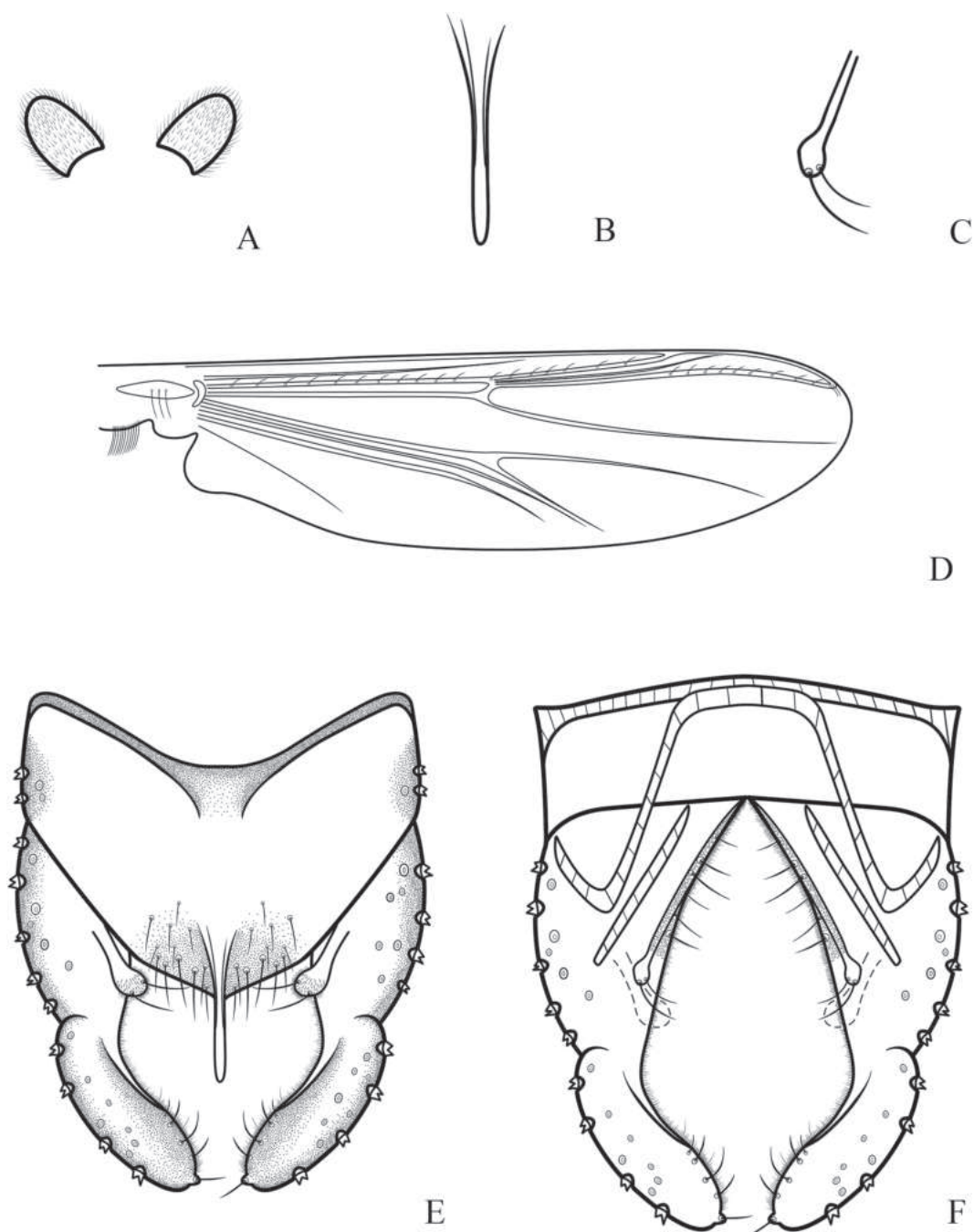


Figure 15. *Cryptochironomus parallelus* Liu, sp. nov., holotype male **A** frontal tubercles **B** anal point **C** inferior volsella **D** wing **E** hypopygium, dorsal view **F** hypopygium, ventral view.

Etymology. From the Latin *parallelus*, parallel-sided, referring to the character of anal point, adjective in the nominative singular.

Remarks. *Cryptochironomus parallelus* Liu, sp. nov. resembles *Cryptochironomus digitatus* Malloch, 1915 and *Cryptochironomus blarina* Townes, 1945 by having similar shapes of the posterior margin of tergite IX, inferior volsella and gonostylus. However, it can be distinguished from *C. digitatus* by the following combination of characters: small frontal tubercles, AR 1.99–2.37, Wing length 2.00–2.37, 2.12 mm, anal point 54–65, 59 μm long and is slender with parallel sides, apically rounded in *C. parallelus* Liu, sp. nov.; whereas large frontal tubercles, AR 3.14–3.23, superior volsella with a hook-shaped base, and

anal point constricted at the 1/3 distance from the base in *C. digitatus*; whereas large frontal tubercles, AR 3.7, Wing length 3.5 mm, anal point 230 µm long and is gradually tapered and pointed apically in *C. blarina*.

***Cryptochironomus taylorensis* Liu, sp. nov.**

<https://zoobank.org/12993976-FF7D-4768-8C2A-8F9615128AC0>

Figs 16–18

Type material. Holotype. one male, USA, New Mexico State, Colfax Country, Canadian River at Taylor Springs, 36°32'74"N, 104°49'22"W, 15.VII.1974, sweep net, leg: Sta. C. **Paratypes.** 2 males, New Mexico State, Colfax Country, Canadian River at Taylor Springs, 15.VII.1974, sweep net, leg: Sta. C.

Diagnostic characters. Frontal tubercles absent; squama with 19 setae; anal point parallel-sided, slightly widening at apex; superior volsella crescent-like, with slender extension at the base, curved in the middle and apically swollen; inferior volsella triangular, widest at base, completely covered by superior volsella; gonostylus gradually tapered and pointed apically.

Description. Male ($n = 3$, unless stated).

Total length 4.65–5.49, 5.01 mm. Wing length 2.31–2.59, 2.42 mm. Total length/wing length 1.98–2.12, 2.07. Wing length/length of profemur 2.00–2.79, 2.38.

Coloration. Thorax light yellow-brown, with yellow-brown spots. Femora of front legs yellow-brown except for dark yellow-brown at both ends, tibia dark brown, tarsomeres lost; femora and tibiae of mid and hind legs yellow-brown, tarsus I–V yellow-brown to dark brown gradually. Abdomen yellow-brown, hypopygium dark brown.

Head (Fig. 16B). Antenna with 11 flagellomeres, ultimate flagellomere 861–1050, 980 µm long. AR 2.68–2.90, 2.82. Frontal tubercles absent. Temporal setae 16–18, 17. Clypeus with 15–17, 16 setae. Tentorium 131–176, 154 µm long, 50–61, 56 µm wide. Palpomere lengths of three specimens (in µm): 41–44, 43; 70–77, 74; 185–196, 191; 160–171, 166; 239–262, 251; Pm5/Pm3 1.29–1.34, 1.31.

Thorax (Fig. 16C). Anteprenotals bare; dorsocentrals 8–10, 9; acrostichals 4–5, 5; prealars 5. Scutellum with 10–12, 11 setae.

Wing (Figs 16A, 18C). VR 1.05–1.11, 1.07. R with 15–18, 17 setae, R_1 with 16–20, 18 setae, R_{4+5} with 21–22, 22 setae. Brachiolium with two setae. Squama with 19 (1) setae.

Legs. Fore leg bearing three subapical setae, 142 (1) µm, 144 (1) µm, 146 (1) µm long. Combs of mid tibia 40–60, 52 µm wide with 24–34, 29 µm long spur, and 45–69, 60 µm wide with 43–56, 49 µm long spur; combs of hind tibia 51–56, 53 µm wide with 34–39, 37 µm long spur, 97–105, 100 µm wide with 51–56, 53 µm long spur. Tarsus I of mid leg with 3–5, 4 sensilla chaetica; tarsus I of hind leg with 3–5, 4 sensilla chaetica. Lengths (in µm) and proportions of legs as in Table 6.

Hypopygium (Figs 17, 18A, B, D, E). The posterior margin of tergite IX is shoulder-shaped and bears 30–32, 31 setae at the base of the anal point. Laterosternite IX has 3–4, 4 setae. The anal point measures 91–103, 96 µm long and is parallel-sided, widening slightly at the apex. The anal tergite bands are fused and V-shaped. The phallopodeme measures 131–147, 139 µm long, and the transverse sternapodeme is 65–92, 78 µm long. The superior volsella is 60–63, 62 µm long, 18–23, 21 µm wide, crescent-like, with a slender extension at the

base, curved in the middle and apically swollen, and has 3 long setae at the apex. The inferior volsella is triangular, 19–24, 22 μm long, widest at the base, completely covered by the superior volsella, with one apically seta and without microtrichia. The gonocoxite measures 174–184, 179 μm long and bears 30–32, 31 strong setae along the inner margin. The gonostylus is 169–192, 183 μm long, gradually tapered and pointed apically, and bears one seta at the apex. HR 0.93–1.03, 0.98. HV 2.47–2.89, 2.74.

Table 6. Lengths (in μm) and proportions of legs of *Cryptochironomus taylorensis* Liu, sp. nov., adult males ($n = 3$, unless stated).

	fe	ti	ta₁	ta₂	ta₃
P ₁	830–1173, 1034	841–857, 848	1283 (1)	669 (1)	505 (1)
P ₂	815–1062, 950	899–952, 927	539–583, 556	242–267, 251	157–183, 167
P ₃	994–1142, 1050	1127–1285, 1197	807–817, 812 (2)	381–383, 382 (2)	302–310, 306 (2)
	ta₄	ta₅	LR	BV	SV
P ₁	418 (1)	203 (1)	1.53 (1)	1.65 (1)	1.30 (1)
P ₂	103–115, 109	88–108, 98	0.59–0.61, 0.60	3.79–4.03, 3.89	3.18–3.49, 3.37
P ₃	184–201, 193 (2)	114–129, 122 (2)	0.69–0.72, 0.70 (2)	2.95–2.97, 2.96 (2)	2.65–2.66, 2.66 (2)

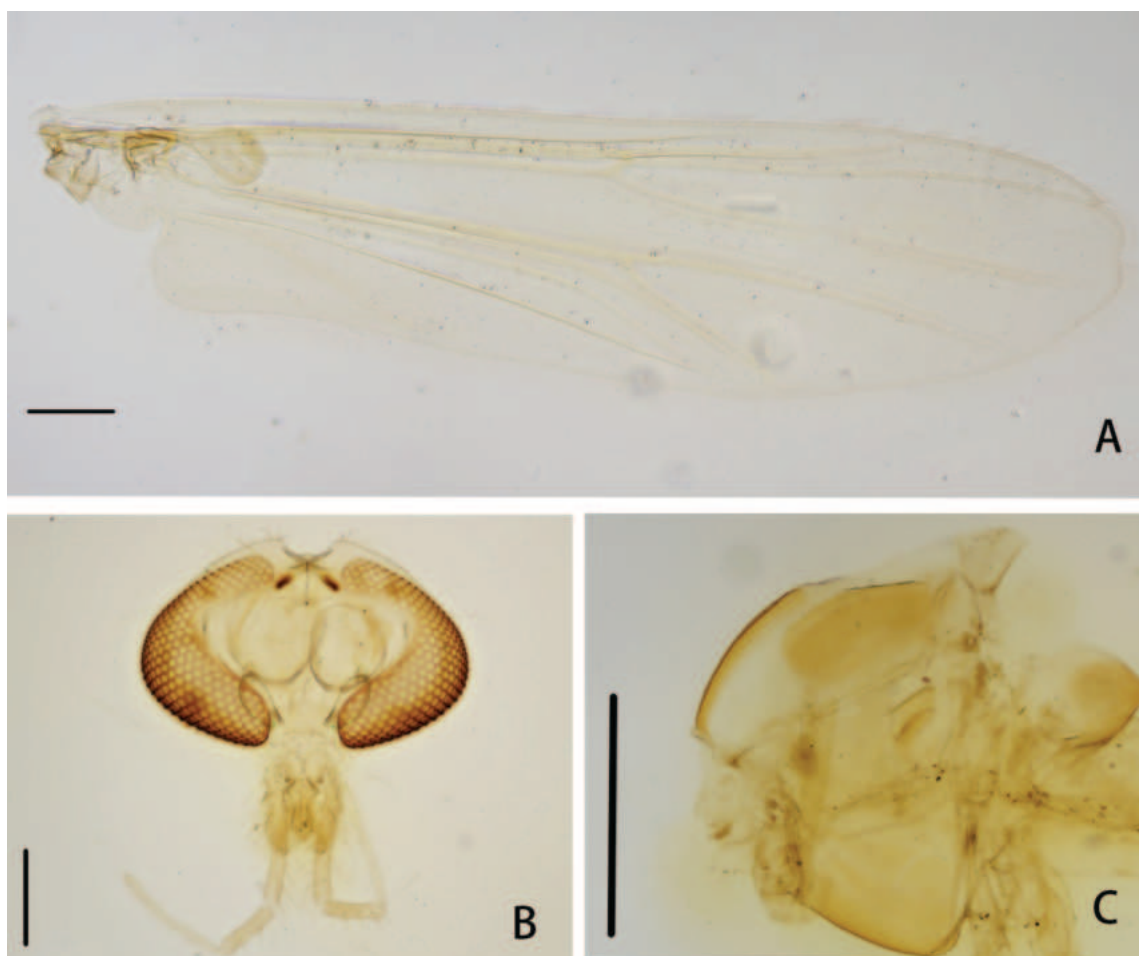


Figure 16. *Cryptochironomus taylorensis* Liu, sp. nov., holotype male **A** wing **B** head **C** thorax. Scale bars: 200 μm .

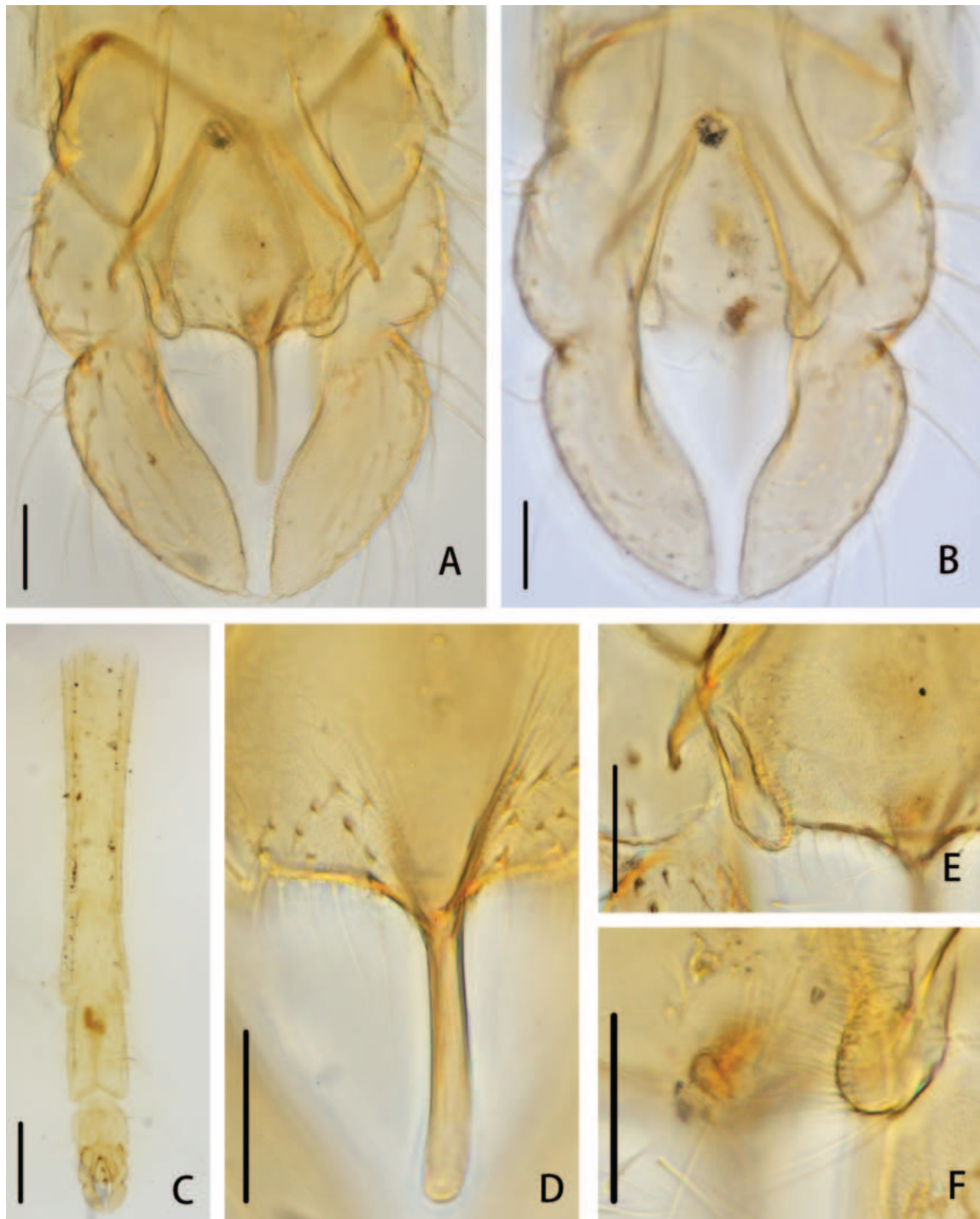


Figure 17. *Cryptochironomus taylorensis* Liu, sp. nov., holotype male **A** hypopygium, dorsal view **B** hypopygium, ventral view **C** abdomen **D** anal point **E** superior volsella **F** inferior volsella. Scale bars: 50 μ m (**A, B, D–F**); 500 μ m (**C**).

Etymology. Name after the type locality, the Canadian River at Taylor Springs; noun in nominative case.

Remarks. *Cryptochironomus taylorensis* Liu, sp. nov. bears resemblance to *C. curryi* Mason, 1986 due to its similar shapes of the anal point, superior volsella, and anal tergite bands. However, it can be distinguished from *C. curryi* by the following combination of characters: R with 15–18 setae, inferior volsella triangular, and gonostylus pointed apically in this new species; whereas R with 40–46 setae, inferior volsella finger-shaped, and gonostylus rounded apically in *C. curryi*.

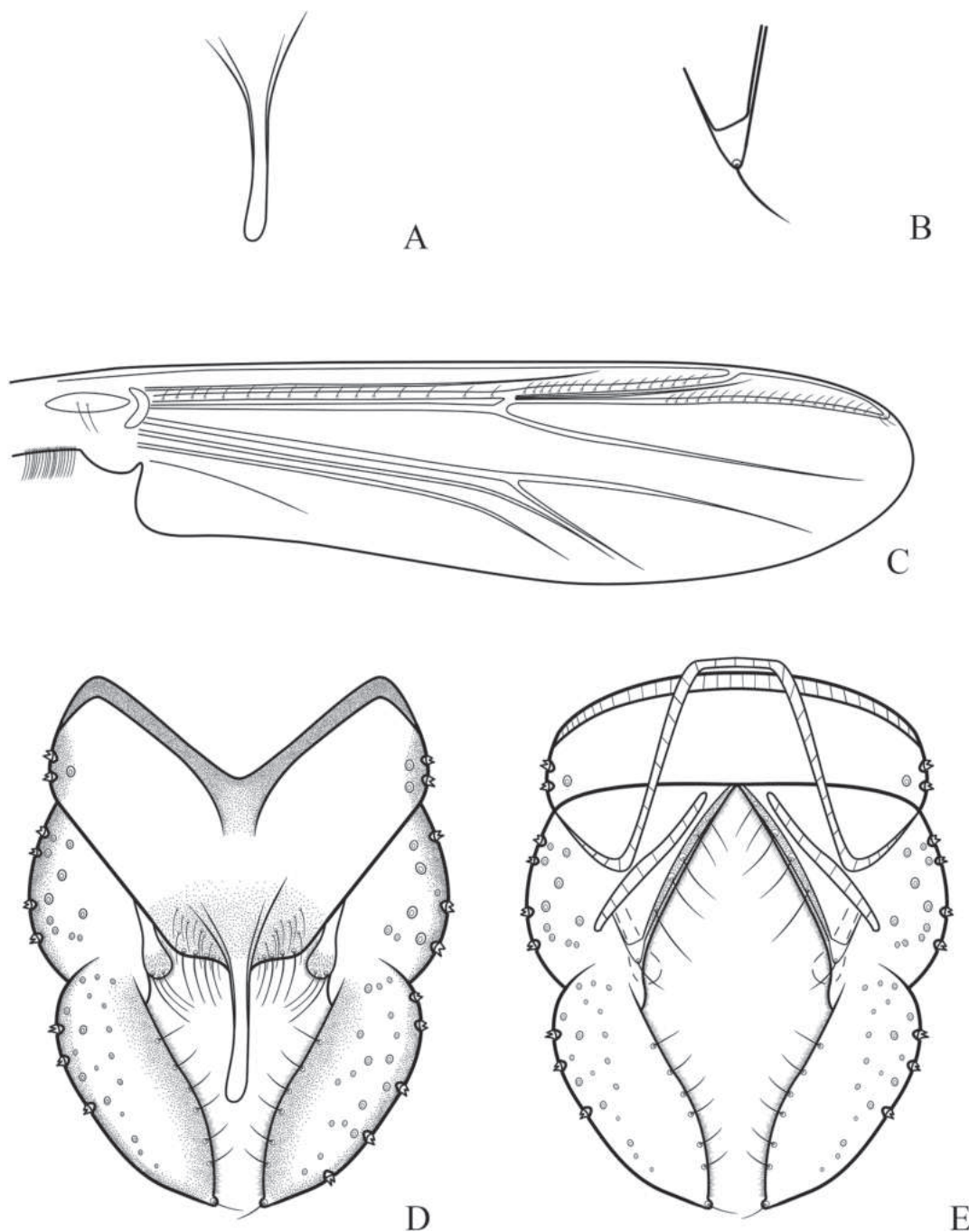


Figure 18. *Cryptochironomus taylorensis* Liu, sp. nov., holotype male **A** anal point **B** inferior volsella **C** wing **D** hypopygium, dorsal view **E** hypopygium, ventral view.

Key to Nearctic males of *Cryptochironomus* Kieffer (adapted from Silva et al. 2010)

- 1 Anal point broad and flat..... 2
- Anal point narrow 3
- 2 Mesal apical margin of gonostylus emarginate ***C. scimitarus* Townes, 1945**
- Mesal apical margin of gonostylus straight or nearly straight.....
- ***C. sorex* Townes, 1945**
- 3 Mesal apical margin of gonostylus emarginate ***C. argus* Roback, 1957**
- Mesal apical margin of gonostylus not emarginate..... 4

4	AR ~ 3.7, Wing length 3.1–3.4 mm	5
–	AR ~ 2.63, Wing length 2.43–2.65 mm.....	6
5	Anal point gradually tapered and pointed apically.....	
 <i>C. blarina</i> Townes, 1945	
–	Anal point widest at base.....	<i>C. beardi</i> Liu, sp. nov.
6	Gonostylus widened towards apex, frontal tubercles present	7
–	Gonostylus not distinctly widened towards apex, frontal tubercles mostly absent.....	9
7	AR 4.35–5.12, LR ₁ 1.12–1.21, gonostylus strongly widened towards apex..	
 <i>C. stylifera</i> Johannsen, 1908	
–	AR 1.99–4.03, LR ₁ 1.23–1.62, gonostylus slightly widened towards apex.....	8
8	Frontal tubercles large, AR 3.14–3.23, the posterior margin of tergite IX shoulder-shaped.....	<i>C. digitatus</i> Malloch, 1915
–	Frontal tubercles small, AR 1.99–2.37, the posterior margin of tergite IX cone-like	<i>C. parallelus</i> Liu, sp. nov.
9	LR ₁ 1.31–1.67, frontal tubercles absent	10
–	LR ₁ 1.45–2.02, when lower than 1.7 frontal tubercles present	12
10	Wing length 4.99–5.78 mm; LR ₁ 1.48–1.67.....	<i>C. eminentia</i> Mason, 1986
–	Wing length 2.30–4.75 mm; LR ₁ 1.31–1.55.....	11
11	Wing length 3.01–4.75 mm, AR 2.64–3.40, LR ₁ 1.34–1.55.....	
 <i>C. ramus</i> Mason, 1986	
–	Wing length 2.31–2.59 mm, AR 2.68–2.90, LR ₁ 1.53.....	
 <i>C. taylorensis</i> Liu, sp. nov.	
12	Wing length 1.47–1.8 mm, gonostylus only ~ 2× as long as wide.....	13
–	Wing length 1.9–5.6 mm, gonostylus at least 2.5× as long as wide.....	14
13	Wing length 1.8 mm, AR 2.75, frontal tubercles present.....	
 <i>C. parafulvus</i> Beck & Beck, 1964	
–	Wing length 1.47–1.69 mm, AR 2.29–2.49, frontal tubercles absent.....	
 <i>C. ferringtoni</i> Liu, sp. nov.	
14	Gonostylus ~ 2.8–3.2× as long as wide, anal point slightly spatulate apically, frontal tubercles absent.....	<i>C. ponderosus</i> (Sublette, 1964)
–	Gonostylus ~ 2.7× as long as wide, anal point tapering parallel-sided or slightly spatulate, frontal tubercles present or absent.....	15
15	Frontal tubercles absent, wing length 2.5–5.6 mm.....	16
–	Frontal tubercles present, wing length 5.1–5.3 mm	17
16	Gonostylus rounded apically, wing length 2.5–5.6 mm.....	
 <i>C. curryi</i> Mason, 1986	
–	Gonostylus tapering to the apex, wing length 2.0 mm	
 <i>C. absun</i> Liu, sp. nov.	
17	Wing length 5.1–5.3 mm, AR 2.5–2.6.....	<i>C. conus</i> Mason, 1986
–	Wing length 1.8–3.2 mm; AR 2.5–3.4.....	18
18	LR ₁ 1.56–1.73, anal point slightly spatulate apically.....	
 <i>C. imitans</i> Sæther, 2009	
–	LR ₁ 1.60–2.02, anal point parallel-sided	19
19	Thorax with dark brown spots, inferior volsella not dentate at base	
 <i>C. fulvus</i> Johannsen, 1905	
–	Thorax without spots, inferior volsella dentate at base.....	
 <i>C. dentatus</i> Liu, sp. nov.	

Acknowledgements

We want to thank Dr. Leonard Charles Ferrington Jr. (Department of Entomology, University of Minnesota) for checking the specimens and providing much input at various levels of this work. We are grateful to Dr. Alexander Egan (University of Minnesota, USA), who corrected some grammatical errors on a previous version of this manuscript. Financial support from the National Natural Science Foundation of China (32370489, 32170473, 32100402), Natural Science Foundation of Tianjin Science and Technology Correspondent (23KPH-DRC00240, 22KPMRC00070, 20JCQNJC00420) and Yinshanbeilu Grassland Eco-hydrology National Observation and Research Station, China Institute of Water Resources and Hydropower Research, Beijing 100038, China, Grant NO. YSS202308. Are acknowledged with thanks.

Additional information

Conflict of interest

The authors have declared that no competing interests exist.

Ethical statement

No ethical statement was reported.

Funding

Financial support from the National Natural Science Foundation of China (32370489, 32170473, 32100402), Natural Science Foundation of Tianjin Science and Technology Correspondent (23KPHDRC00240, 22KPMRC00070, 20JCQNJC00420) and Yinshanbeilu Grassland Eco-hydrology National Observation and Research Station, China Institute of Water Resources and Hydropower Research, Beijing 100038, China, Grant NO. YSS202308.

Author contributions

Wenbin Liu: Conceptualization, Funding acquisition, Writing – original draft. Chengyan Wang: Formal analysis, Data curation. Yaning Tang: Software. Ying Wang: Data curation, Visualization, Wenxuan Pei Data curation. Chuncai Yan: Writing – review and editing.

Author ORCIDs

Wen-Bin Liu  <https://orcid.org/0000-0001-6916-0692>

Data availability

All of the data that support the findings of this study are available in the main text.

References

- Beck EC, Beck WM (1969) Chironomidae (Diptera) of Florida III – The *Harnischia* complex (Chironominae). University of Florida Gainesville. Bulletin of the Florida State Museum Biological Sciences 13(5): 277–313. <https://doi.org/10.58782/flmnh.pncg1122>
- Cranston PS, Dillon ME, Pinder LCV, Reiss F (1989) The adult males of Chironominae (Diptera: Chironomidae) of the Holarctic Region – keys and diagnoses. In: Wiederholm T (Ed.) Chironomidae of the Holarctic region. Keys and diagnoses. Part 3. Adult males. Entomologica Scandinavica Supplement 34: 353–502.

- Curry LL (1958) Larvae and Pupae of the Species of *Cryptochironomus* (Diptera) in Michigan. *Limnology and Oceanography* 3(4): 427–442. <https://doi.org/10.4319/lo.1958.3.4.0427>
- Johannsen OA (1908) New North American Chironomidae. In: Felt EP (Ed.) 23rd report of the State Entomologist on injurious and other insects of the State New York, 1907. New York State Museum Bulletin 124: 264–285.
- Kieffer JJ (1918) Chironomides d’Afrique et d’Asie conservés au Musée National Hongrois de Budapest. *Annales Historico-Naturales Musei Nationalis Hungarici* 16: 31–139.
- Makarchenko EA, Makarchenko MA, Zorina OV, Sergeeva IV (2005) Preliminary data on fauna and taxonomy of Chironomids (Diptera, Chironomidae) of the Russian Far East. *Vladimir Ya Levanidov’s Biennial Memorial Meetings* 3: 394–420.
- Malloch JR (1915) The Chironomidae or midges of Illinois, with particular reference to the species occurring in the Illinois river. *Bulletin of the Illinois State Laboratory of Natural History* 10(1–8): 275–543. <https://doi.org/10.21900/j.inhs.v10.376>
- Roback SS (1957) The immature tendipedids of the Philadelphia area (Diptera: Tendipedidae). *Monographs - Academy of Natural Sciences of Philadelphia* 9: 1–152.
- Sæther OA (1969) Some Nearctic Podonominae, Diamesinae and Orthocladiinae (Diptera: Chironomidae). *Bulletin - Fisheries Research Board of Canada* 170: 1–154.
- Sæther OA (1977) Taxonomic studies on Chironomidae: *Nanocladius*, *Pseudochironomus*, and the *Harnischia* complex. *Bulletin - Fisheries Research Board of Canada* 196: 1–143.
- Sæther OA (1980) Glossary of Chironomid morphology terminology (Diptera: Chironomidae). *Entomologica Scandinavica (Supplement 14)*: 1–51.
- Sæther OA (2009) *Cryptochironomus* Kieffer from Lake Winnipeg, Canada, with a review of Nearctic species (Diptera: Chironomidae). *Zootaxa* 2208(1): 1–24. <https://doi.org/10.11646/zootaxa.2208.1.1>
- Sasa M (1998) Chironomidae of Japan 1998. Institute of Environment and Welfare Studies, Kurobe-shi, Japan, 156 pp.
- Sasa M, Kikuchi M (1995) Chironomidae (Diptera) of Japan. University of Tokyo Press, 333 pp. <https://doi.org/10.7601/mez.46.255>
- Shilova AI (1966) On the taxonomy of *Cryptochironomus* ex. gr. *defectus* Kieff. (Diptera, Chironomidae). *Trudy Institut Biologii Vnutrennich Vod Bylusk* 12(15): 214–238.
- Silva FL, Strixino ST, Oliveira HRN (2010) New species of *Cryptochironomus* Kieffer, 1918 (Diptera: Chironomidae: Chironominae) from Brazil. *Zootaxa* 2614(1): 18–32. <https://doi.org/10.11646/zootaxa.2614.1.2>
- Sublette JE (1964) Chironomidae (Diptera) of Louisiana I. Systematics and immature stages of some lentic chironomids of westcentral Louisiana. *Tulane Studies in Zoology and Botany* 11: 109–150. <https://doi.org/10.5962/bhl.part.7051>
- Townes HK (1945) The Nearctic species of Tendipedini. *American Midland Naturalist* 34(1): 1–206. <https://doi.org/10.2307/2421112> [Diptera, Tendipedidae (= Chironomidae)]
- Yan C, Zhao G, Liu T, Guo Q, Hou Z, Wang X, Pan B (2016) A new record and two new species of *Cryptochironomus* Kieffer, 1918 from China (Diptera, Chironomidae). *Zootaxa* 4208(5): 485–493. <https://doi.org/10.11646/zootaxa.4208.5.6>
- Yan C, Liu T, Cao W, Zhao G, Liu W (2018) A review of the Japanese *Cryptochironomus* Kieffer, 1918 (Diptera, Chironomidae). *ZooKeys* 771: 139–155. <https://doi.org/10.3897/zookeys.771.24220>
- Zorina OV (2000) Fauna and systematics of the tribe Chironomini (Diptera, Chironomidae) of the south of Russian Far East. *A.I. Kurentsov’s Annual Memorial Meetings*, 101–120.

Taxonomic notes on the genus *Baetiella* Uéno, 1931 (Ephemeroptera, Baetidae), with description of three new species from Thailand

Sirikamon Phlai-ngam^{1,2}, Boonsatien Boonsoong³, Jean-Luc Gattolliat^{4,5}, Nisarar Tungpairajwong^{2,6}

¹ Department of Biology, Faculty of Science, Burapha University, Chonburi 20131, Thailand

² Applied Taxonomic Research Center (ATRC), Faculty of Science, Khon Kaen University, Khon Kaen 40002, Thailand

³ Animal Systematics and Ecology Speciality Research Unit (ASESRU), Department of Zoology, Faculty of Science, Kasetsart University, Bangkok 10900, Thailand

⁴ Muséum cantonal des sciences naturelles, département de Zoology, Palais de Rumine, Place Riponne 6, CH-1005 Lausanne, Switzerland

⁵ Department of Ecology and Evolution, University of Lausanne, CH-1015 Lausanne, Switzerland

⁶ Department of Biology, Faculty of Science, Khon Kaen University, Khon Kaen 40002, Thailand

Corresponding author: Nisarar Tungpairajwong (knisar@kku.ac.th)

Abstract

Based on material recently collected in northern Thailand, the present study provides an updated of the genus *Baetiella*, including *Gratia*. It comprises six species in Thailand, three of them being new species: *Baetiella* (*Gratia*) *narumonae*, *Baetiella* (*Gratia*) *sororculaenadinae*, *Baetiella* (*Baetiella*) *bispinosa*, *Baetiella* (*Baetiella*) *baei* **sp. nov.**, *Baetiella* (*Baetiella*) *lannaensis* **sp. nov.** and *Baetiella* (*Baetiella*) *bibranchia* **sp. nov.** *Baetiella* (*Baetiella*) *baei* **sp. nov.** can be distinguished from other species by the reduction of the posteromedian protuberances on abdominal tergites I–III, the asymmetrical coniform terminal segment of labial palp, the distal margin of abdominal sternites VII–X each with a row of long, spatulate setae, the dorsal margin of femur with two long, robust setae distally. *Baetiella* (*Baetiella*) *lannaensis* **sp. nov.** is diagnosed by the posteromedian protuberances present on tergites I–VIII, dorsal margin of femur with a regular row of long, rounded, ciliated setae and body surface covered with numerous, dense, rounded scale-like setae. *Baetiella* (*Baetiella*) *bibranchia* **sp. nov.** can be separated from other species by coxal gills present at the base of forelegs and midlegs. The molecular study based on the mitochondrial gene COI and a larval key to species of Thai *Baetiella* are also provided.

Key words: COI gene, diversity, mayflies, revision, Southeast Asia



Academic editor: Ben Price

Received: 4 December 2023

Accepted: 9 March 2024

Published: 9 May 2024

ZooBank: <https://zoobank.org/2807A13B-3E74-4041-8218-9D36C22C9CEF>

Citation: Phlai-ngam S, Boonsoong B, Gattolliat J-L, Tungpairajwong N (2024) Taxonomic notes on the genus *Baetiella* Uéno, 1931 (Ephemeroptera, Baetidae), with description of three new species from Thailand. ZooKeys 1200: 303–352. <https://doi.org/10.3897/zookeys.1200.116787>

Copyright: © Sirikamon Phlai-ngam et al. This is an open access article distributed under terms of the Creative Commons Attribution License (Attribution 4.0 International – CC BY 4.0).

Introduction

Baetiella is a small genus of Baetidae. It was established by Uéno (1931) for the species *Acentrella japonica* Imanishi, 1930 (Uéno 1931; Waltz and McCafferty 1987; Shi and Tong 2015a). This genus was subject of several taxonomic revisions: *Baetiella* was considered as a subgenus of *Pseudocloeon* Klapálek, 1905 then treated as a subgenus of *Baetis* Leach, 1815 (Kazlauskas 1963; Braasch 1978; Kluge 1983; Tshernova et al. 1986; Tong and Dudgeon 2000; Shi and Tong 2015a).

Waltz and McCafferty (1987) provided morphological evidence in their revision of the status of *Baetiella* that justified recognizing it as a valid and distinct

genus, separated from *Pseudocloeon* and *Baetis*, including at that time 12 species across the Palearctic and Oriental regions.

The combination of the following larval characters distinguishes *Baetiella* from other genera of Baetidae: antennae $\sim 1.5\times$ longer than head width; presence of simple submarginal setae on labrum; 2-segmented maxillary palp; labial palp 3-segmented, terminal segment symmetrical or slightly asymmetrical, conical, usually with a small tip at apex, segment II with or without an inner apical lobe; thorax with or without protuberances; femoral villopore present; dorsal margin of tibia with row of dense, fine, simple setae; tarsus without an elongated submarginal seta; tarsal claw with one or two rows of denticles, with a pair of subapical setae; abdominal gills usually present on abdominal segments I–VII; single or paired posteromedian dorsal protuberances present or absent on abdominal tergites; paracercus reduced, shorter than half of the cerci multi-segmented or reduced to one segment; cerci usually longer than body length (Shi and Tong 2015a).

Baetiella is occasionally confused with *Gratia* and *Acentrella* Bengtsson, 1912, primarily due to shared larval characters. *Baetiella* can be separated from *Acentrella* by the mouthparts, in particular by the shape of terminal segment of labial palp, which is rounded to truncate in *Acentrella* and usually conical in *Baetiella* (Kluge and Novikova 2011; Shi and Tong 2015a).

Recent revision of the status of *Gratia* seems to indicate that it should be considered as subgenus of *Baetiella*. According to the non-ranking systematics of mayflies, *Baetiella* belongs to the clade Baetiella/g1 within the Baetofemorata; this clade encompasses the three subgenera *Baetiella*, *Gratia*, and *Neobaetiella* (Kluge 2004, 2022b; Kluge and Novikova 2011). At the larval stage, *Gratia* and *Baetiella* are very similar but can be distinguished by differences of setation on the dorsal margin of femur, the submarginal setae on the labrum, the shape of the terminal segment of the labial palp, and the degree of development of the paracercus (Boonsoong et al. 2004; Shi and Tong 2015a, b). To ensure stability and in the absence of a new comprehensive generic revision, we prefer to consider *Gratia* as a subgenus of *Baetiella* for this study.

Baetiella currently comprises 19 described species, distributed across the Oriental and Palearctic regions. The latest species to be reported is *Baetiella subansiri* Vasanth, Selvakumar & Subramanian, 2020, which was discovered in India. *Baetiella* species are distributed across numerous countries, including Japan, Korea, Russia, Mongolia, Tajikistan, Vietnam, China, Nepal, India, and Thailand (Shi and Tong 2015a; Phlai-ngam and Tungpairojwong 2018; Vasanth et al. 2020). Continental China and the Indian subcontinent are the regions with the greatest diversity.

The knowledge of Baetidae in Thailand has advanced significantly in recent decades, both in terms of diversity and systematics. Researchers have discovered numerous new taxa through the intensive, ongoing surveys of mayfly diversity in Southeast Asia. Recently, approximately 17 genera and 26 species of Baetidae were described and recorded in Thailand (Müller-Liebenau and Heard 1979; Thomas 1992; Boonsoong et al. 2004; Kluge and Novikova 2011, 2017; Tungpairojwong and Bae 2015; Phlai-ngam and Tungpairojwong 2018; Suttinun et al. 2018, 2020, 2021, 2022; Kluge 2020; Kluge and Suttinun 2021; Kluge 2022a; Phlai-ngam et al. 2022a, b; Tungpairojwong et al. 2022; Kaltenbach et

al. 2023; Kluge et al. 2023). Despite these recent improvements, significant gaps persist, and a large number of taxa remain undescribed. Certain potentially diversified genera, notably *Baetis*, *Labiobaetis* Novikova & Kluge, 1987, and *Nigrobaetis* Novikova & Kluge, 1987, stand out due to their unresolved taxonomic status (Phlai-ngam et al. 2022b).

The genus *Baetiella* has been the subject of limited studies in Thailand and only three species were recorded, including species previously assigned to *Gratia*: *Baetiella (Baetiella) bispinosa* (Gose, 1980), *Baetiella (Gratia) sororculaenadinae* (Thomas, 1992), and *Baetiella (Gratia) narumona* (Boonsoong & Thomas, 2004). This study provides a comprehensive report on all the species of the genus *Baetiella* (including *Gratia*) distributed in Thailand. Moreover, we offer detailed descriptions and illustrations of three new discovered species. We also provide a diagnostic key to Thai *Baetiella* larvae. Species delimitation and phylogenetic reconstruction were conducted in this study with the support of molecular evidence (mitochondrial COI sequences).

Materials and methods

Samples

The larval specimens were handpicked from streams of various orders located in Thailand. The living larvae were photographed with a Canon 700D camera fitted with a 100-mm macro lens, along with an iPhone 14 Pro (Fig. 1). Most of the sampling sites are in the northern region of Thailand (Table 1; Fig. 24). Specimens are housed in the Collection of Aquatic Insects of Department of Biology at Khon Kaen University in Khon Kaen, Thailand (**KKU-AIC**), the collection of the Zoological Museum at Kasetsart University in Bangkok, Thailand (**ZMKU**) and in the Muséum cantonal des sciences naturelles, Department of Zoology, Lausanne, Switzerland (**MZL**). For collecting the mayfly specimens, this research was reviewed and approved by the Institutional Animal Care and Use Committee of Khon Kaen University based on the Ethics of Animal Experimentation of the National Research Council of Thailand (Record No. IACUC-KKU-65/63).

Table 1. GPS coordinates of locations of specimens.

Species	Province	GPS coordinates	Altitudes (m a.s.l.)
<i>Baetiella (Baetiella) baei</i> sp. nov.	Chiang Mai	18°32'50.02"N, 98°30'49.79"E	1,359
	Mae Hong Son	19°22'43.79"N, 98°22'32.87"E	855
<i>Baetiella (Baetiella) lannaensis</i> sp. nov.	Chiang Mai	18°32'50.02"N, 98°30'49.79"E	1,359
	Mae Hong Son	19°22'43.79"N, 98°22'32.87"E	855
<i>Baetiella (Baetiella) bibranchia</i> sp. nov.	Chiang Rai	20°00'39.60"N 99°48'14.47"E	476
<i>Baetiella (Baetiella) bispinosa</i>	Chiang Rai	19°31'12.15"N, 99°39'12.59"E	649
	Chiang Mai	19°11'50.51"N, 98°53'13.98"E	362
<i>Baetiella (Gratia) narumona</i>	Chiang Mai	18°26'22.44"N, 98°35'51.77"E	582
	Chiang Mai	18°29'39.72"N, 98°40'06.65"E	337
	Nan	18°59'47.31"N, 101°12'50.94"E	684
<i>Baetiella (Gratia) sororculaenadinae</i>	Chiang Mai	18°49'02.41"N, 98°55'23.23"E	713
	Mukdahan	16°29'40.48"N, 104°18'47.09"E	208



Figure 1. *Baetiella* (*Baetiella*) *lannaensis* sp. nov., female larva **A** early larval stage **B** mature larva.

Morphological study

The specimens were preserved in 95% ethanol. Parts of the specimens were dissected and mounted on microscope slides fixed in Euparal or glycerin. Ethanol-preserved specimens were studied using a Nikon SMZ745 stereomicroscope. Drawings of the microscope slides were generated via a camera lucida on an Olympus CH30 compound microscope and subsequently scanned using the Procreate application (iOS application) for illustration. The larvae were captured in photographs using a Nikon Research Stereomicroscope SMZ25 and afterwards processed using NIS-Elements software. The final plates were created and processed using Adobe Photoshop software (<http://www.adobe.com>). The distribution map was generated with SimpleMappr software (<https://simplemappr.net>). They were subsequently transferred to absolute ethanol to facilitate the

dehydration process to conduct scanning electron microscopy (SEM). The specimens were then dissected, transferred to microtubes, and covered with a fine mesh net (mesh size 60 µm) for drying in a critical point dryer (CPD). The specimens were placed on stubs and coated with a 20-nm gold layer using a Cressington sputter coater. Zeiss LEO 1450 VP was implemented for taking SEM images.

Molecular study

The DNA of some specimens was extracted using non-destructive procedures by using PureLink™ Genomic DNA Mini Kit (Invitrogen, Thermo Fisher Scientific, USA), which enabled subsequent morphological examination (more information can be found in the study conducted by Vuataz et al. 2011). A 658 bp fragment of the mitochondrial gene cytochrome oxidase subunit 1 (COI) was amplified using the primers LCO 1490 (GGTCAACAAATCATAAAGATATTGG) and HCO 2198 (TAAACTTCAGGGTGACCAAAAAATCA) (Folmer et al. 1994). The polymerase chain reaction (PCR) was performed with an initial denaturation temperature of 94 °C for 5 min followed by a total of 35 cycles with a denaturation temperature of 94 °C for 30 sec, an annealing temperature of 48 °C for 40 sec, and an extension at 72 °C for 1 min. The final extension at 72 °C was for 5 min. The PCR products were purified and sequenced by MacroGen, Inc., Korea, and ATGC Co., Ltd., Thailand.

Genetic distances and tree analyses

Additional *Baetiella* sequences were obtained from GenBank (<http://www.ncbi.nlm.nih.gov/>) and Barcode of Life Data System (BOLD) (<https://www.boldsystems.org/>). The new sequences resulting from this study were also added to the GenBank database (Table 2). All sequences were edited, then aligned using the ClustalW algorithm. Genetic distance among specimens was calculated using MEGA X (Kumar et al. 2018) under the Kimura-2-parameter distances (K2P) model. The COI gene trees were obtained using maximum likelihood (ML) and Bayesian inference (BI) approaches.

The ML phylogenetic analysis was conducted using the HKY+GAMMA model as the most appropriate for reconstruction based on the default settings of

Table 2. Sequenced specimens of *Baetiella* spp. (bold text showing new sequences).

Species	Locality	Source of sequence	Accession number
<i>Baetiella (Baetiella) baei</i> sp. nov.	Chiang Mai (Thailand)	GenBank	PP333626, PP333627, PP333628
<i>Baetiella (Baetiella) lannaensis</i> sp. nov.	Chiang Mai (Thailand)	GenBank	PP337083, PP337084, PP337085, PP337086
<i>Baetiella (Baetiella) bibranchia</i> sp. nov.	Chiang Rai (Thailand)	GenBank	PP341064, PP341065
<i>Baetiella (Baetiella) bispinosa</i>	China	BOLD	ADL1493: XJDQD476-18, XJDQD477-18, XJDQD480-18
<i>Baetiella (Gratia) narumonae</i>	Nan, Chiang Mai, Loei (Thailand)	BOLD, ZMKU	ABU9531: THMAY091-12, THMAY092-12, GN06LE, GN05CR
<i>Baetiella (Gratia) sororculaenadinae</i>	Chiang Mai (Thailand)	ZMKU	GS04CM
<i>Baetiella tuberculata</i>	Korea	GenBank	MN442542, MN442543, MH823349
<i>Baetiella japonica</i>	Japan	GenBank	KF563015, KF563016
<i>Baetiella</i> spp.	India	GenBank	MK393232, MK393233, MK393234
	China	BOLD	ADL1493: XJDQD517-18, XJDQD519-18
	China	BOLD	ADL1407: XJDQD534-18, XJDQD535-18

RAxML-NG on raxmlGUI 2.0 (Edler et al. 2021). Node support values of ML analyses were calculated with 1000 bootstraps (BS) replicates. The BI analysis was performed using MrBayes 3.1.2 (Huelsenbeck and Ronquist 2001). For all data sets, four independent runs of four Monte Carlo Markov chains were conducted for 10,000,000–20,000,000 generations until the average standard deviation of split frequencies decreased to ~ 0.005 , with trees sampled every 1000 generations.

For ML and BI analysis, nodes with BS values $\geq 70\%$ and BI posterior probabilities (PP) ≥ 0.95 were considered highly supported (Hillis and Bull 1993; Felsenstein 2004; Huelsenbeck and Rannala 2004; Mauro and Agorreta 2010). Gene trees were visualized and edited using FigTree v. 1.4 (Rambaut 2014) and Adobe Photoshop software (<http://www.adobe.com>).

Species delimitation analyses were conducted using two methods (Yaagoubi et al. 2023): the distance-based ASAP approach (Assemble Species by Automatic Partitioning) using the web service available at <https://bioinfo.mnhn.fr/abi/public/asap/asapweb.html> (Puillandre et al. 2020) and the tree-based mPTP approach (multi-rate Poisson Tree Processes) using the web service available at <https://mptp.h-its.org> (Kapli et al. 2017).

Results

Taxonomic account

Baetiella (Baetiella) baei sp. nov.

<https://zoobank.org/52ED7710-6A18-4404-9C0A-F0C0442EB65F>

Figs 2–7

Type material examined. Holotype. THAILAND, One larva on slide (KKU-AIC), Chiang Mai, Chom Thong district, Ban Luang, Siribhum waterfall, 18°32'50.02"N, 98°30'49.79"E, 1,359 m, 27.XII.2022, S. Phlai-ngam and B. Boonsoong leg.

Paratypes. One larva on slide, 2 larvae on stubs, 3 larvae in alcohol, same data as holotype (KKU-AIC).

Other material examined. Five larvae in alcohol (KKU-AIC), THAILAND, Mae Hong Son, Pai district, Mo Pang waterfall, 19°22'43.79"N, 98°22'32.87"E, 855 m, 10.V.2023., S. Phlai-ngam leg. Six larvae in alcohol (two in MZL: GBI-FCH01118450; four in ZMKU), Chiang Mai, Chom Thong district, Ban Luang, Siribhum waterfall, 18°32'50.02"N, 98°30'49.79"E, 1,359 m, 17.XII.2020, B. Boonsoong leg.

Diagnosis. The larvae of *Baetiella baei* sp. nov. are similar to *Baetiella marginata* Braasch, 1983 and *Baetiella muchei* Braasch, 1978; they share the reduction of their posteromedian protuberances of distal tergites (Braasch 1978, 1983). In addition, *Baetiella baei* sp. nov. can be distinguished from other species by the combination of characters (i) distal margin of tergites I–III with a small, reduced, single posteromedian protuberance; (ii) terminal segment of labial palp rounded, asymmetrical, almost fused with segment II and small tip at apex; (iii) labial palp segment II with very small inner apical lobe; (iv) edge between mola and prostheca of both right and left mandibles with a row of small spines; (v) hindwing pad reduced ~ 2.5 – $3.0\times$ longer than width; (vi) dorsal margin of femur with a pair of long, stout, simple, subapical setae distally; (vii) distal margin of tergite II–X with multi-dentated, blunt denticles; (viii) distal margin

of sternites I–VI smooth without denticles while sternites VII–X with a row of long, spatulate, blunt denticles; (ix) inner margin of paraproct smooth with 3–5 oval scale-like setae along margin; (x) paracercus reduced to one segment.

Description. Coloration (Fig. 2A). Head dorsally brownish, with darker brown mark at frontal suture. Thorax dorsally brownish with darker brown pattern. Legs brownish; dorsal surface brownish, pale brown ventrally; dorsal surface of femur with pale brown longitudinal stripe along dorsal margin, tarsus and claw distally darker brown (Fig. 2B). Abdominal tergites brownish with dark brown pattern; sternites pale brown (Fig. 2C). Caudal filaments brownish.

Body. Dorsoventrally somewhat flattened (Fig. 2B). Paracercus reduced to one segment, cerci subequal to body length .

Head ~2× wider than long.

Antenna (Fig. 2A). Length ~2× of head length; scape, pedicel and flagellum without process, without scale bases and spines, covered with scattered, fine setae; flagellum covered with scattered, fine setae in each segment.

Mouthparts. Labrum (Fig. 3A). Broad, slightly rectangular; ~2× wider than long; each half of dorsal surface with one central seta and a row of ten long, simple, robust, submarginal setae, proximal part with scattered, fine, simple setae; distal margin with anteromedian notch shallow, lateral margin with a row of long, fine, simple, setae; ventral surface with a row of feathered, setae along distal margin, distolateral margin with a row of feathered, setae and a row of six, short, simple, robust setae near lateral margin, distal part with patch of dense, fine, hair-like setae.

Right mandible (Fig. 3B–E). Outer and inner incisors partially separated with visible line, incisors well developed (Fig. 3B), outer incisor with three denticles and inner incisor with four denticles (Fig. 3C); right prosthema (Fig. 3D) slender with denticles apically; edge between mola and prosthema smooth with a row of eight small spines (Fig. 3E); apex of mola with tuft of spines-like setae; proximal surface with scattered, short, fine, simple setae.

Left mandible (Fig. 3F–I). Outer and inner incisors almost completely fused (Fig. 3F), with seven denticles apically (Fig. 3G), prosthema robust, apically with small denticles and comb-shaped structure (Fig. 3H); edge between mola and prosthema smooth with a row of six small spines (Fig. 3I); proximal surface with scattered, short, fine, simple setae.

Maxilla (Fig. 3J). Galea lacinia with three blunt, robust canines and a canine-like dentiseta; inner dorsal row of setae with two bifid pectinate dentisetae; inner ventral row of robust, simple pectinate setae medially, with long robust, simple pectinate setae distally; with a row of three long setae on basis of galea lacinia. Maxillary palp 2-segmented, relative short, not reaching tip of galea lacinia, surface with scattered small, hair-like setae; outer margin of segment II with distinct concavity; distal segment with distinct, small tip at apex and small, hair-like setae.

Labium (Fig. 3K). Glossa basally broad, narrower toward apex, glossa subequal in length to paraglossa, inner margin with a row of eight stout, simple setae, apical margin with three or four long, robust, blunt, simple setae, with a long, fine, pointed seta subapically; paraglossa sub-rectangular, broader than glossa, apical margin with three rows of long, stout, simple setae, inner margin with a row of medium, stout, simple setae, dorsal surface with three medium, stout, simple setae subapically and proximal part with long, fine, pointed,

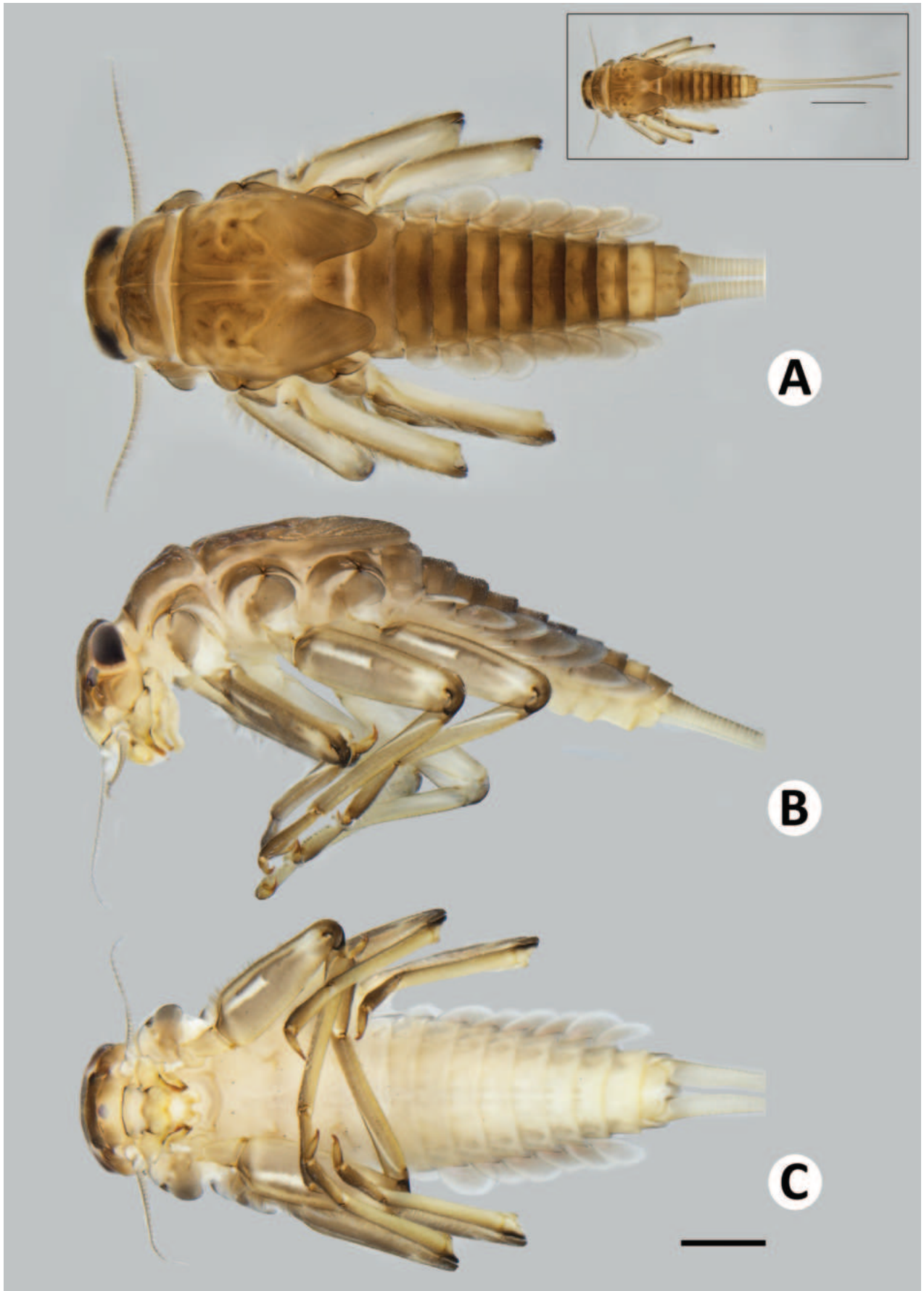


Figure 2. *Baetiella (Baetiella) baei* sp. nov., larval habitus (paratype) **A** dorsal view **B** lateral view **C** ventral view. Scale bar: 1 mm.

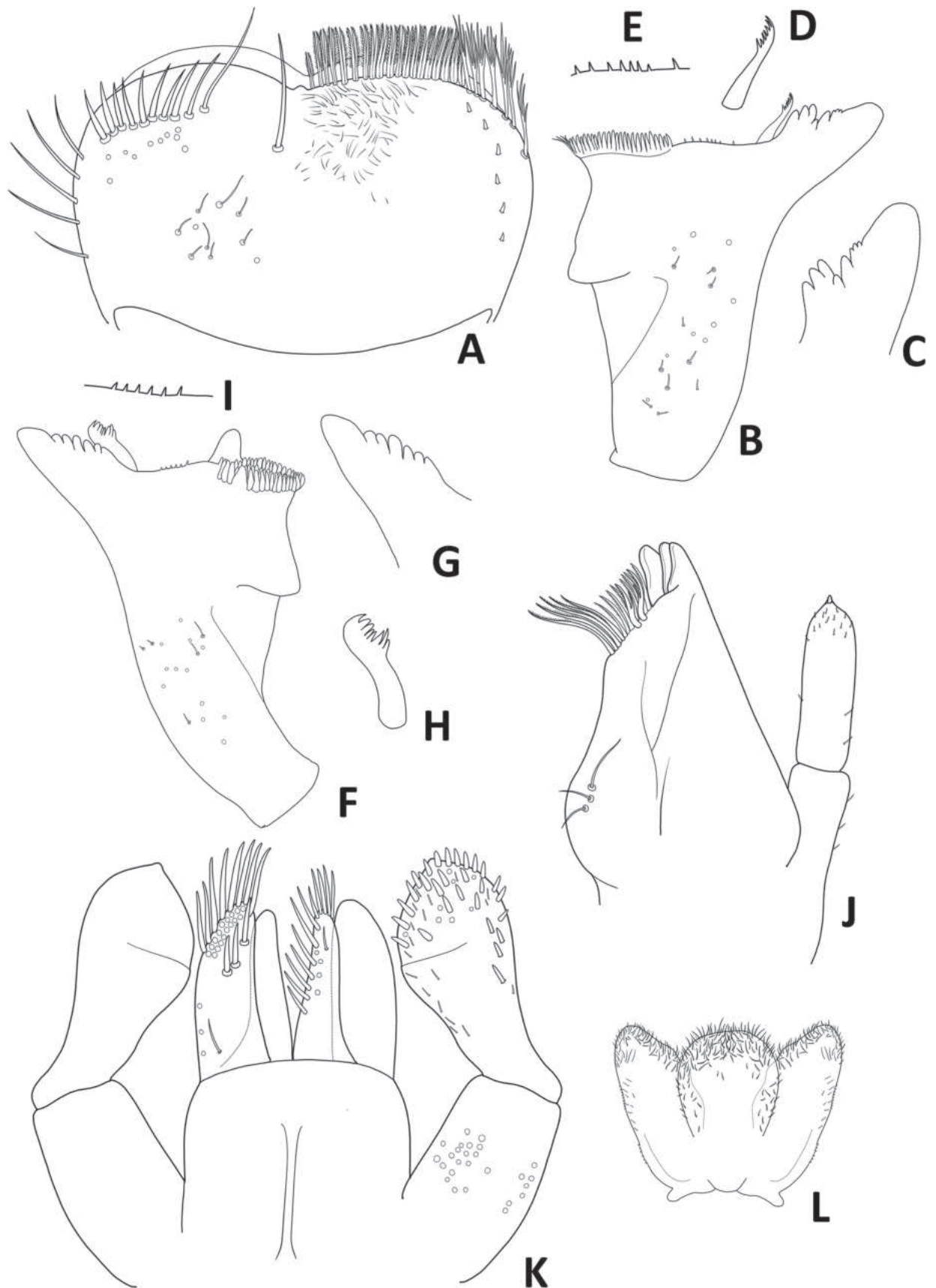


Figure 3. *Baetiella (Baetiella) baei* sp. nov., larval morphology **A** labrum **B** right mandible **C** right incisors **D** right prostheca **E** margin of right mandible **F** left mandible **G** left incisors **H** left prostheca **I** margin of left mandible **J** maxilla **K** labium **L** hypopharynx.

simple setae. Labial palp 3-segmented; terminal segment rounded, asymmetrical; almost fused with segment II, with small tip at apex; segment II with very small inner apical lobe, a row of four medium, acute, robust setae along outer margin; ventral surface covered with scattered short, robust, simple setae and fine setae; segments I and III with micropores.

Hypopharynx (Fig. 3L). Lingua subequal to superlingua, apically rounded, with apical tuft of long, fine, simple setae; superlingua with distal margin slightly truncate, covered with fine, simple setae.

Thorax (Fig. 4A).

Pronotum and mesonotum with small, reduced tubercles.

Hindwing pad reduced, ~2.5–3.0× longer than width.

Legs (Figs 4B–F, 6A–E). Foreleg. Femur (Figs 4C, 6B) length ~2.5× maximum width. Dorsal margin with row of dense, long, fine, simple setae, length ~1/3 to 1/2 of femur width, decreasing at distal part (Fig. 6B, C), with a pair of long, stout, simple, subapical setae distally (Fig. 4C, D). All dorsal and ventral margins with a scattered row of short, robust setae. Femoral villopore present. Dorsal surface with scattered fine setae.

Tibia (Figs 4E, 6D) with a row of long, fine, simple setae dorsally, dorsal and ventral margins with a scattered row of short, robust setae.

Tarsus (Figs 4F, 6E) with a row of long, fine, simple setae dorsally, with a row of four robust, blunt setae ventrally increasing in size on distal part. Tarsal claw with a row of seven denticles, with pair of subapical setae. All legs without coxal gill.

Midlegs and hindlegs as forelegs.

Abdomen (Fig. 4G). Distal margin of abdominal tergites I–III with a single, reduced, posteromedian protuberance. Distal margin of tergites IV–X without posteromedian protuberance.

Abdominal tergites I–X (Figs 4G–I, 6F, 7A–D): distal margin with multi-dentated, blunt spines, surface with scattered, fine setae.

Abdominal sternites (Figs 5A, B, 6G, 7E–H). Distal margin of sternites I–VI smooth without denticles or scale-like setae (Fig. 7E, F); distal margin of sternites VII–X with a row of long, spatulate, blunt denticles (Fig. 7E, G, H).

Gills (Figs 5C–F, 6H). Seven pairs of gills present on abdominal tergites I–VII, oval and without visible tracheation; gill I smaller than other gills (Fig. 5C), surface with scattered, fine setae and a few micropores; gills II–VII with numerous, fine setae and several micropores on surface; gill margin smooth with hair-like setae and scattered small spines (Figs 5C–F, 6H); coloration reddish to brown medially, translucent on outer margin.

Paraproct (Figs 5H, 7I). Margin smooth with three to five scale-like setae, surface with numerous micropores and scattered fine setae; margin of cercotractor with 12–14 spines. Median caudal filament reduced to one segment, cerci subequal in length with body length.

Imago. Unknown.

Ecological notes. The larvae of *Baetiella baei* sp. nov. were collected in Siribhum and Mo Pang waterfalls close to the headwater located in Chiang Mai and Mae Hong Son Provinces (northern Thailand). These sampling sites were situated at medium to high altitudes (870–1,360 m a.s.l.). The substrate types were dominated by boulders, cobbles, pebbles, gravel, and a sand bottom. The larvae were found on the surface boulders in medium to fast-flowing water, ~0.5 m/s–0.7 m/s (Fig. 23).

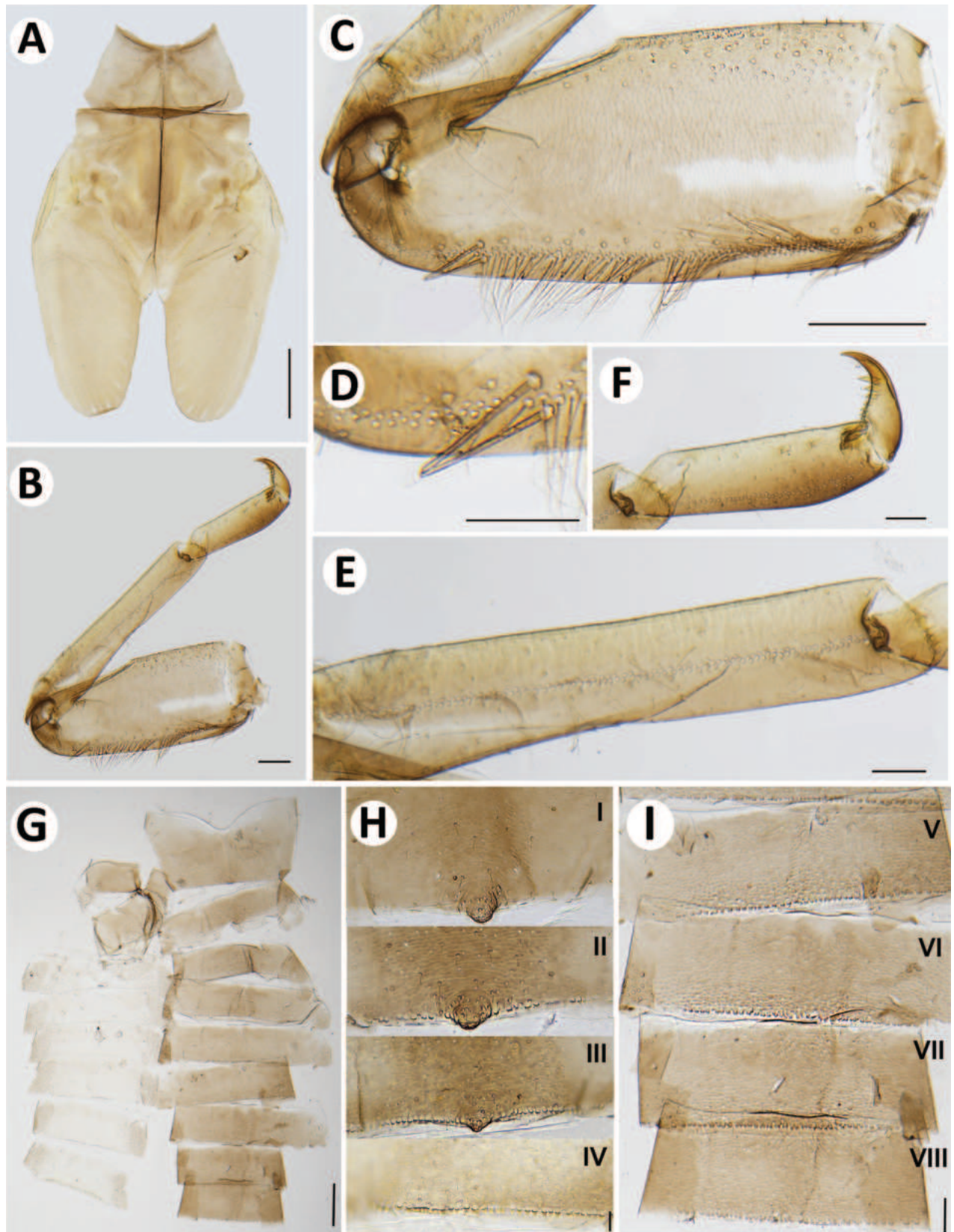


Figure 4. *Baetiella (Baetiella) baei* sp. nov., larval morphology **A** pronotum and metanotum **B** foreleg **C** femur **D** setae on distal margin of femur **E** tibia **F** tarsus and claw **G** abdomen **H** tergites I–IV **I** tergites V–VIII. Scale bars: 0.5 mm (**A**); 0.1 mm (**B**, **C**, **G**); 0.05 mm (**D**, **E**, **F**, **H**, **I**).

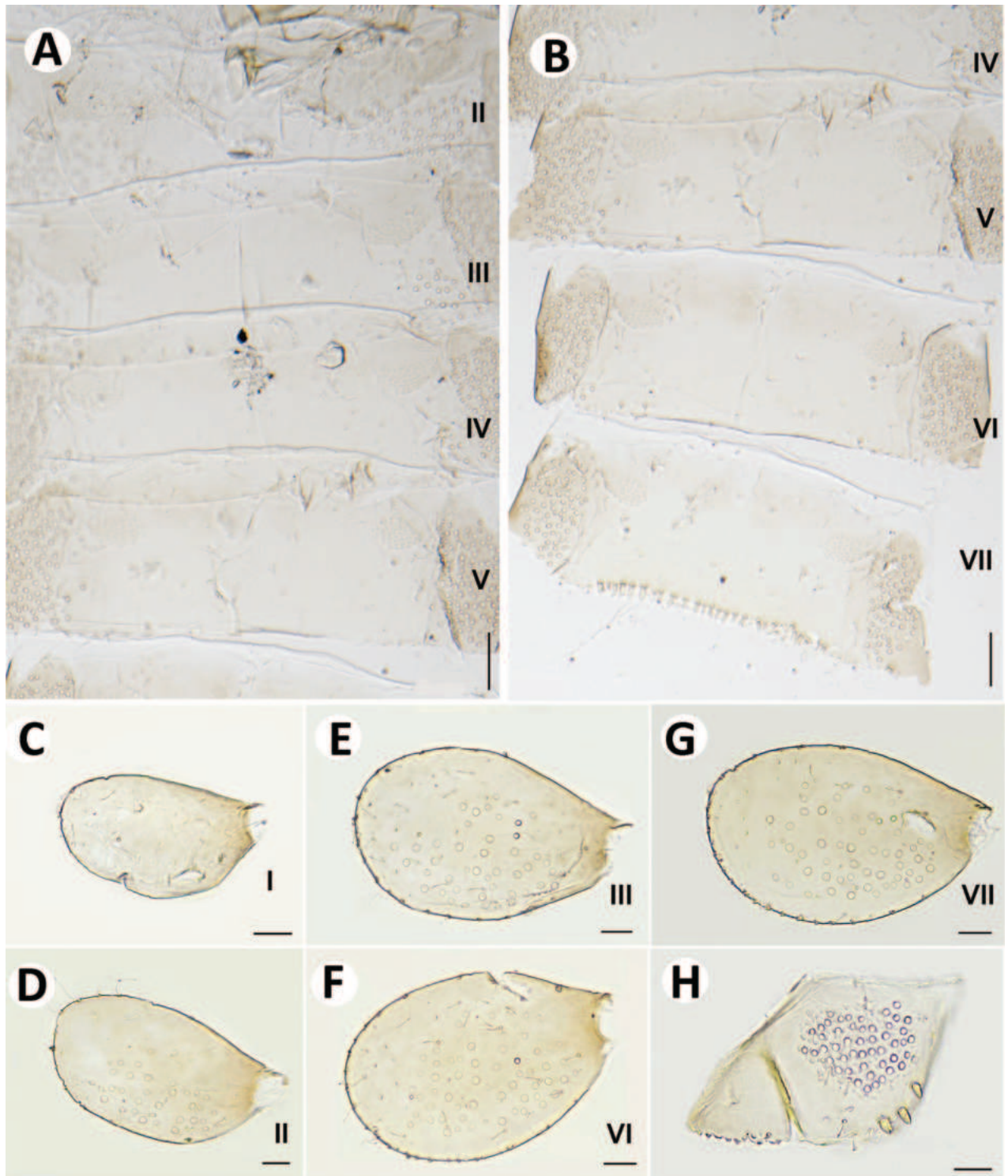


Figure 5. *Baetiella (Baetiella) baei* sp. nov., larval morphology A sternites II–V B sternites VI–VIII C gill I D gill II E gill III F gill VI G gill VII H paraproct. Scale bars: 0.05 mm (A, B); 0.02 mm (C–H).

Etymology. This specific epithet, *baei* (masculine), is dedicated to Professor Dr. Yeon Jae Bae (Division of Environmental Science and Ecological Engineering, Korea University, South Korea) in honor of his outstanding accomplishments as the pioneer researcher and influential leader of aquatic insect and benthological studies of Asia.

Distribution. Chiang Mai and Mae Hong Son Provinces (northern Thailand).

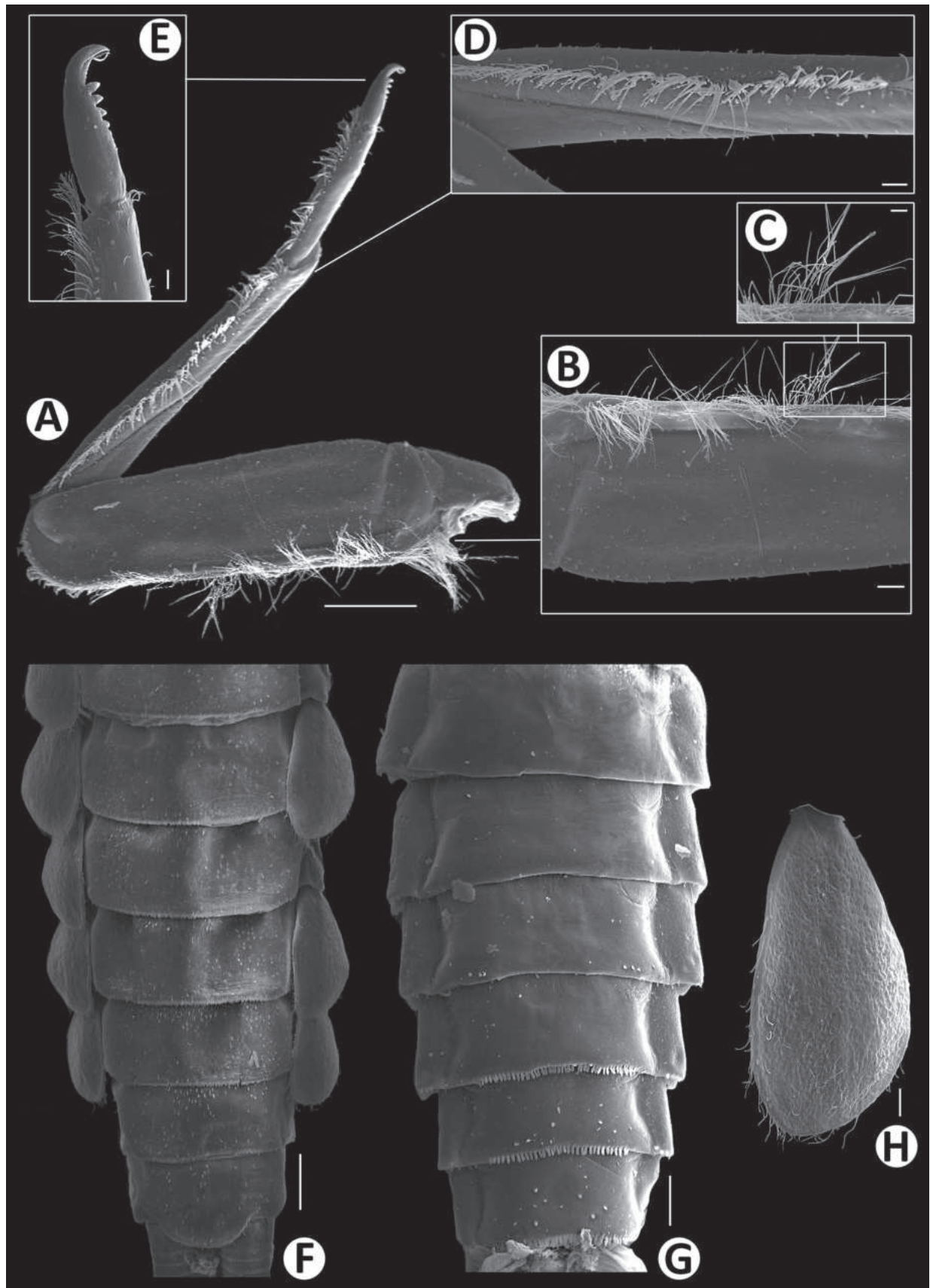


Figure 6. *Baetiella* (*Baetiella*) *baei* sp. nov., larval morphology (SEM) **A** foreleg **B** femur **C** setae on dorsal margin of femur **D** tibia **E** distal tarsus and claw **F** tergites **G** sternites **H** gill IV. Scale bars: 200 µm (**A**); 30 µm (**B**, **D**); 20 µm (**C**, **E**, **H**); 100 µm (**F**, **H**).

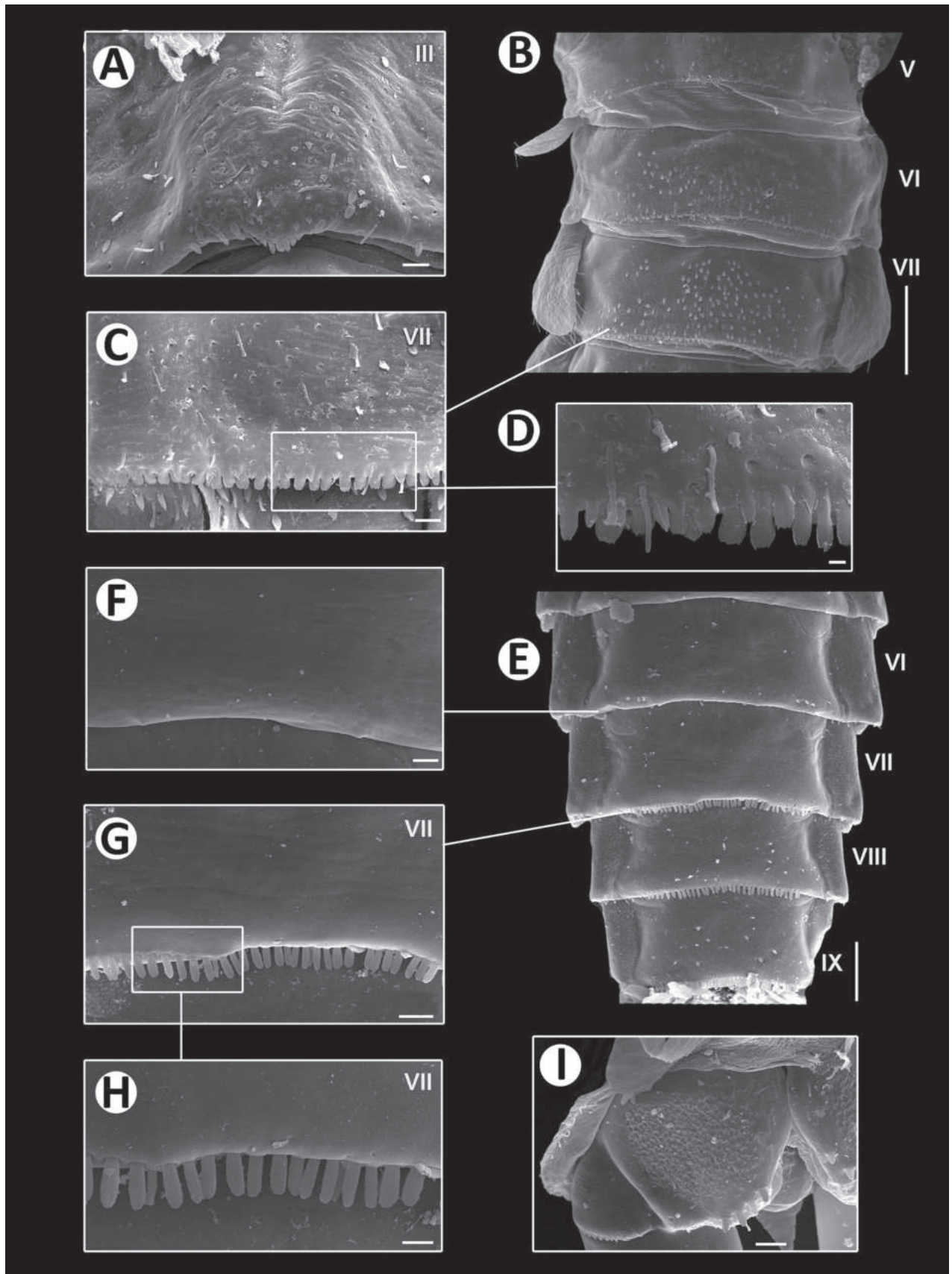


Figure 7. *Baetiella (Baetiella) baei* sp. nov., larval morphology (SEM) **A** tergite III **B** tergites V–VII **C** tergite VII **D** posterior margin of tergite VII **E** sternites VI–IX **F** sternite VI **G** sternite VII **H** posterior margin of sternites VII **I** paraproct. Scale bars: 10 μ m (**A**, **C**, **H**); 100 μ m (**B**); 3 μ m (**D**); 100 (**E**); 20 μ m (**F**, **G**, **I**).

Remarks. The differences between this newly discovered species and *Baetiella marginata* is readily apparent in the absence of posteromedian protuberances on the distal margin of all tergites of *B. marginata*. The paracercus of *Baetiella (Baetiella) baei* sp. nov. is reduced to a single cone-shaped segment, whereas in *B. marginata*, it reduces to ~15 segments. Furthermore, *Baetiella (Baetiella) baei* sp. nov. has a row of spines on the edge between prostheca and mola of both mandibles, while the edges of *B. marginata* are devoid of any spines or serration and appear smooth (Braasch 1983; Shi and Tong 2015a; Vasanth et al. 2020).

Baetiella muchei also presents important similarity to *Baetiella (Baetiella) baei* sp. nov., mainly characterized by the reduction of the paracercus to one segment. The diagnostic characters separating these species are: (i) the distal margin of tergites of *B. muchei* lacks posteromedian protuberances, comparable to *B. marginata*; (ii) the terminal segment of the labial palp in *B. muchei* is conical in shape, with an apical tip at the apex, while our new species presents an asymmetrical shape; (iii) the setation of the dorsal margin of the femur differs between *Baetiella (Baetiella) baei* sp. nov. and *B. muchei*, as the former possesses a pair of long, stout, simple, subapical setae distally; (iv) the distal margin of sternites VIII–X in *Baetiella (Baetiella) baei* sp. nov. with a row of long, spatulate, blunt denticles; (v) the inner margin of the paraproct in this new species is smooth with 3–5 distinct scale-like setae along the margin, these scale-like setae are lacking in *B. muchei*. Additionally, the gills of *B. muchei* reveal a longitudinal brown band in the middle area, while gills of *Baetiella (Baetiella) baei* sp. nov. display a rounded and oval brown shading in the same location (Fig. 2A). Moreover, the edge between prostheca and mola of mandible of *B. muchei* are also smooth without any spines like *B. marginata* that contrasts with the new species. (Braasch 1978; Shi and Tong 2015a; Sivaruban et al. 2024).

***Baetiella (Baetiella) lannaensis* sp. nov.**

<https://zoobank.org/97A175BF-6310-4202-8A90-95680662C97D>

Figs 1, 8–13

Type material examined. Holotype. THAILAND, one larva on slide (KKU-AIC), Chiang Mai, Chom Thong district, Ban Luang, Siribhum waterfall, 18°32'50.02"N, 98°30'49.79"E, 1,359 m, 27.XII.2022, S. Phlai-ngam and B. Boonsoong leg.

Paratypes. One larva on slide, 2 larvae on stubs, 3 larvae in alcohol, same data as holotype (KKU-AIC).

Other material examined. Eight larvae in alcohol (KKU-AIC), THAILAND, Mae Hong Son, Pai district, Mo Pang waterfall, 19°22'43.79"N, 98°22'32.87"E, 855 m, 10.V.2023, S. Phlai-ngam leg; two larvae in alcohol (KKU-AIC), Chiang Mai, Chom Thong District, Ban Luang, Siribhum waterfall, 18°32'50.02"N, 98°30'49.79"E, 1,359 m, 18.III.2023, B. Boonsoong leg.; 21 larvae in alcohol (KKU-AIC), Chiang Mai, Chom Thong district, Ban Luang, Siribhum waterfall, 18°32'50.02"N, 98°30'49.79"E, 1,359 m, 12.V.2023, S. Phlai-ngam leg. Two larvae in alcohol (MZL: GBIFCH01118451), Chiang Mai, Chom Thong district, Ban Luang, Siribhum waterfall, 18°32'50.02"N, 98°30'49.79"E, 1,359 m, 17.XII.2020, B. Boonsoong leg.

Diagnosis. *Baetiella (Baetiella) lannaensis* sp. nov. differs from other species and can be identified by (i) tergites I–VIII with a single, reduced, posteromedian

protuberance, which gradually diminishes in size towards the terminal segment; (ii) distal margin of tergites II–X with multi-dentated and blunt spines; (iii) distal margin of sternites VIII–X with multi-dentated, blunt denticles and scattered short, fine, simple setae along margin; (iv) dorsal surface of body and legs covered with numerous rounded scale-like setae; (v) gill surface with numerous rounded scales and short, fine setae; and (vi) dorsal margin of femur with a regular row of long, rounded, simple, ciliated setae; (vii) terminal segment of labial palp conical and symmetrical shaped with apical tip, segment II of labial palp with a small, reduced inner apical lobe.

Description. Coloration (Figs 1A, B, 8A, B). Head dorsally brownish, with darker brown mark at frontal suture. Thorax dorsally brownish with dark brown pattern and with small dark brown tubercles. Abdominal tergites brownish with dark brown pattern (Fig. 8A); sternites pale brown (Fig. 8C). Legs brownish; dorsal surface brownish, with pale brown mark ventrally; dorsal surface of femur with pale brown longitudinal striped along dorsal margin distally, tarsus and claw distally darker brown. Caudal filaments brownish.

Body dorsoventrally somewhat flattened (Fig. 8B). Paracercus reduced to one segment, cerci subequal to body length. Body surface covered with numerous rounded scale-like setae.

Head ~2× wider than long.

Antenna (Fig. 8A). Length ~1.5× as long as head length; scape, pedicel and flagellum without process, without scale bases and spines, covered with scattered, fine setae; flagellum covered with scattered, fine setae in each segment.

Mouthparts. Labrum (Fig. 9A). Broad, slightly rectangular; ~2× wider than long; each half of dorsal surface with one central seta and a row of seven long, simple, robust submarginal setae, proximal part with scattered, fine, simple setae; distal margin with anteromedian notch shallow, lateral margin with a row of long, fine, simple setae; ventral surface with a row of feathered setae along distal margin, distolateral margin with a row of feathered, setae and a row of five short, simple, robust setae near lateral margin, distal part with patch of dense, fine, hair-like setae.

Right mandible (Fig. 9B–D). Outer and inner incisors partially separated (Fig. 9B, C), incisors well developed, outer incisor with three denticles and inner incisor with four denticles; right prosthema (Fig. 9D) slender; edge between mola and prosthema smooth without spines; apex of mola with tuft of spine-like setae; proximal surface with scattered, short, fine, simple setae.

Left mandible (Fig. 9E–G). Outer and inner incisors almost completely fused (Fig. 9E, F), well developed incisors with six denticles apically, prosthema (Fig. 9G) robust, apically with small denticles and comb-shaped structure; edge between mola and prosthema smooth without spines; proximal surface with scattered, short, fine, simple setae.

Maxilla (Fig. 9H). Galea lacinia with three blunt, robust canines and a canine-like dentisetia; inner dorsal row of setae with two bifid pectinate dentisetiae; inner ventral row of robust, simple pectinate setae medially, with long robust, simple pectinate setae distally; with a row of four long setae on basis of galea lacinia. Maxillary palp 2-segmented, with scattered small, hair-like setae; distal segment with distinct, small tip at apex and small, hair-like setae.

Labium (Fig. 9I). Glossa basally broad, narrower toward apex, glossa slightly shorter than paraglossa, inner margin with a row of nine medium, stout, simple

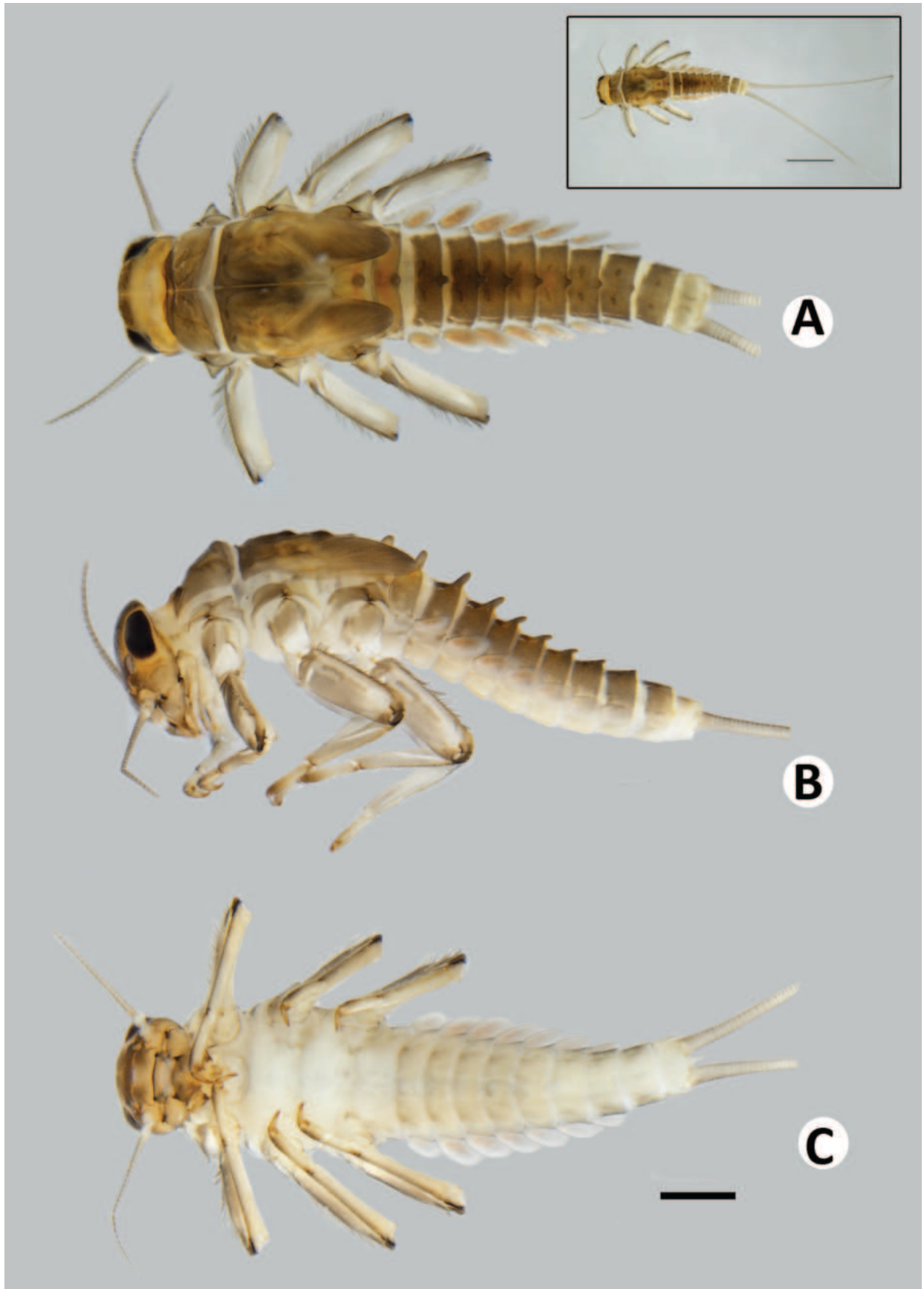


Figure 8. *Baetiella* (*Baetiella*) *lannaensis* sp. nov., larval habitus (paratype): **A** dorsal view **B** lateral view **C** ventral view. Scale bar: 1 mm.

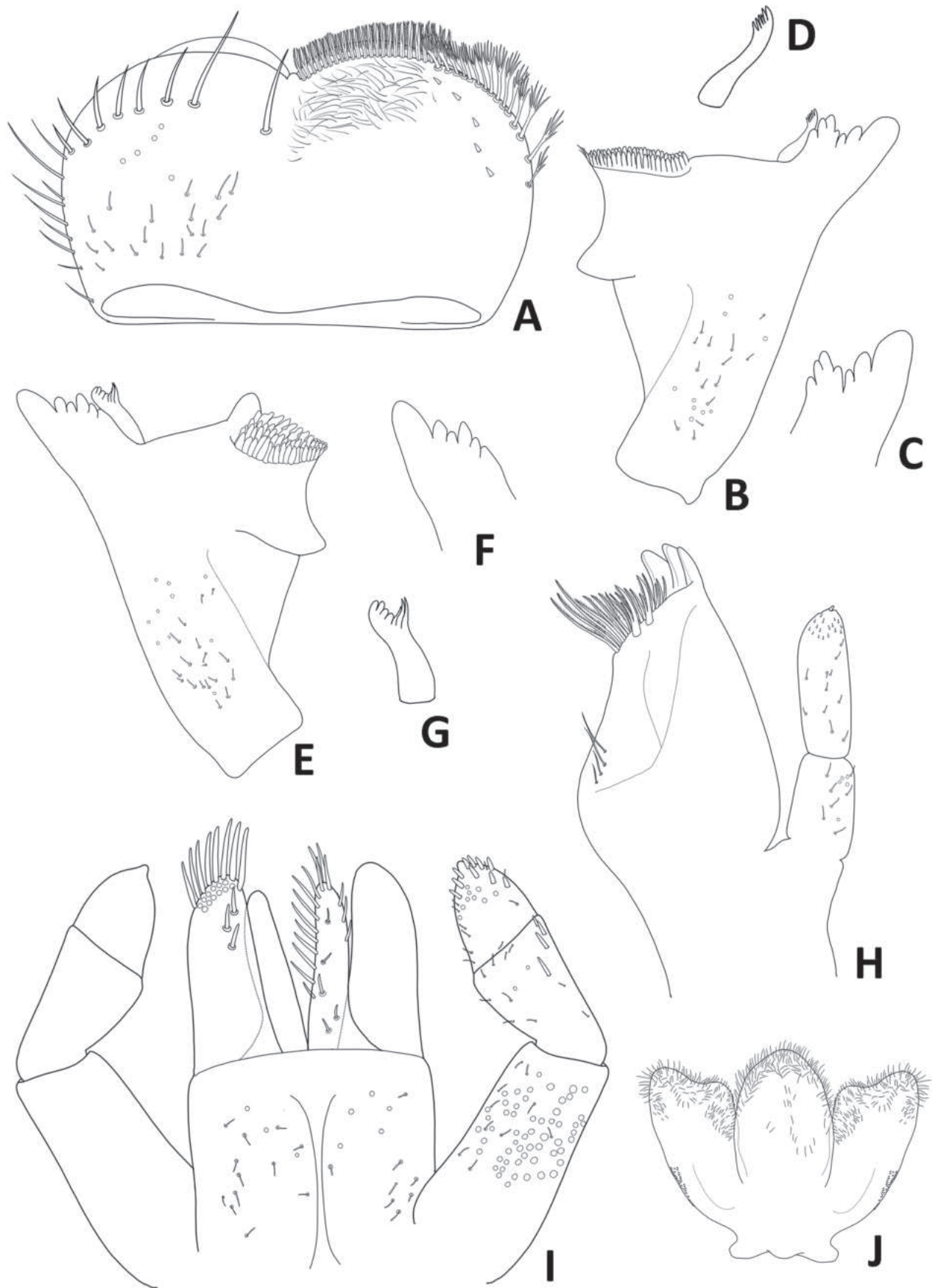


Figure 9. *Baetiella (Baetiella) lannaensis* sp. nov., larval morphology **A** labrum **B** right mandible **C** right incisors **D** right prostheca **E** left mandible **F** left incisors **H** left prostheca **G** left prostheca **H** maxilla **I** labium **J** hypopharynx.

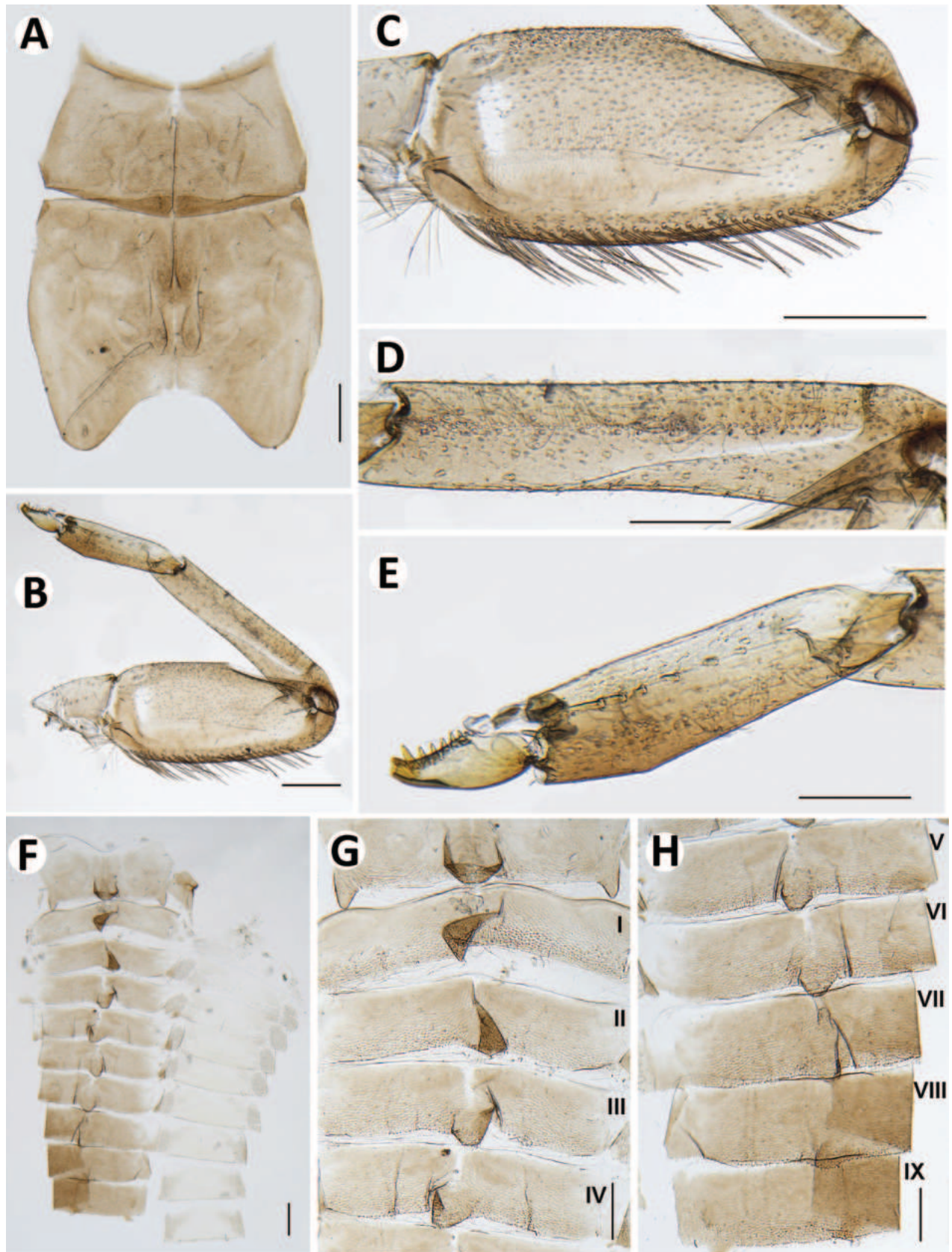


Figure 10. *Baetiella (Baetiella) lannaensis* sp. nov., larval morphology **A** pronotum and metanotum **B** foreleg **C** femur **D** tibia **E** tarsus and claw **F** abdomen **G** tergites I–IV **H** tergites V–IX. Scale bars: 0.2 mm (A–E); 0.1 mm (F–H).

setae, apical margin with three or four long, stout, blunt, simple setae, ventral surface with scattered, short, fine setae; paraglossa sub-rectangular, broader than glossa, apical margin with three rows of medium, stout, simple setae and a row of medium, stout, simple setae on inner margin, dorsal surface with three medium, stout, simple setae subapically; labial palp 3-segmented, terminal segment conical and asymmetrical with small tip at apex; segment II with small, reduced inner apical lobe, distal part with three simple, robust setae near outer margin; ventral surface covered with scattered short, robust and fine setae; segments I and III with micropores.

Hypopharynx (Fig. 9J). Lingua rounded apically, with apical tuft of fine, long, simple setae; superlingua broadly truncate, covered with abundant, fine, simple setae.

Thorax (Figs 8A, 10A) with numerous rounded scale-like setae; mesonotum with dorsal surface with two pairs of small, reduced, tubercles anteromedially and posteromedially; metanotum with a single, posteromedian protuberance.

Hindwing pad reduced, $\sim 1.5\times$ longer than width, covered with numerous round scale-like setae.

Legs (Fig. 10B–E). Forelegs. Femur (Figs 10C, 12B, C) length $\sim 2.2\times$ maximum width. Dorsal margin with row of long, rounded, simple, ciliated setae, length $\sim 1/3$ to $1/2$ of femur width, decreasing at distal part. All dorsal and ventral margins with a scattered row of short, robust setae. Femoral villopore present. Median part of dorsal margin with scattered fine and dense rounded scale-like setae.

Tibia. Dorsal margin with a row of long, fine, simple setae (Figs 10D, 12D), both dorsal and ventral margins with a scattered row of short, robust setae, dorsal surface with numerous rounded scale-like (Fig. 12D).

Tarsus (Figs 10F, 12E) with a row of long, fine, simple setae dorsally, with a row of approximately seven robust, blunt setae increasing in size ventrally on distal part. Tarsal claw with a row of seven denticles with pair of subapical setae. All legs without coxal gill.

Midlegs and hindlegs as forelegs.

Abdomen (Fig. 10F). Distal margin of tergites I–VIII with a single, posteromedian protuberance, decreasing in size.

Abdominal tergites (Figs 10G, H, 12H, 13A–D).

Distal margin of tergite I without denticles, surface with scattered, fine setae and rounded scale-like setae; distal margin of tergites II–X with multi-dentated and blunt spines, surface with scattered, fine setae and numerous rounded scale-like setae; tergites IX–X without posteromedian protuberance.

Abdominal sternites (Figs 11A–E, 12I, 13E–H). Distal margin of sternites I–VII smooth without denticles or scales-like setae, surface with scattered short, fine, simple setae (Figs 11A–C, 12I, 13E, F); distal margin of sternites VIII–X with multi-dentated, blunt denticles and scattered short, fine, simple setae along margin, surface with scattered short, fine, simple setae (Figs 11D, E, 12I, 13G, H).

Gills (Figs 11F–L, 12G). Seven pairs of gills present on abdominal tergites I–VII (Fig. 11F–L), oval and without tracheation; gill I smaller than other gills, coloration reddish to brown medially with translucent on outer margin, gill surface with scattered, fine setae and several rounded scales and micropores, gill margin with scattered hair-like setae (Fig. 12G).

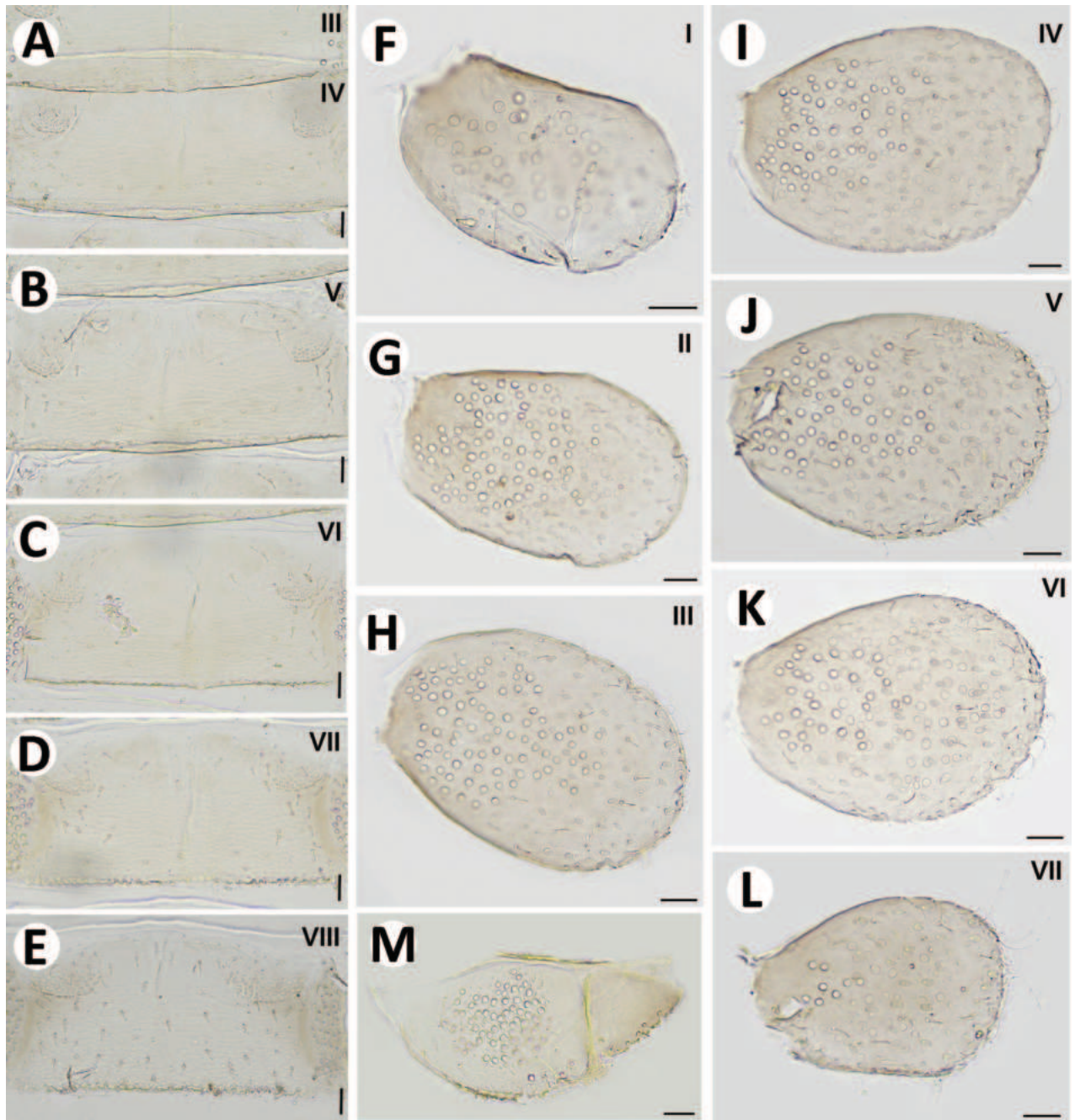


Figure 11. *Baetiella (Baetiella) lannaensis* sp. nov., larval morphology **A** sternites III and IV **B** sternites V **C** sternite VI **D** sternite VII **E** sternite VIII **F** gill I **G** gill II **H** gill III **I** gill IV **J** gill V **K** gill VI **L** gill VII **M** paraproct. Scale bars: 0.02 mm.

Paraproct (Figs 11M, 13I) with numerous micropores and scattered short, fine setae medially, inner margin with 12–14 serrations and multi-dentate, blunt denticles along margin.

Imago. Unknown.

Ecological notes. The larvae of *Baetiella (Baetiella) lannaensis* sp. nov. were collected in Siribhum and Mo Pang waterfalls, in the same microhabitats and substrate types than *Baetiella (Baetiella) baei* sp. nov.; they were found in boulders substrates with fast-flowing water. However, this species was more abundant than *Baetiella (Baetiella) baei* sp. nov. (Fig. 23).

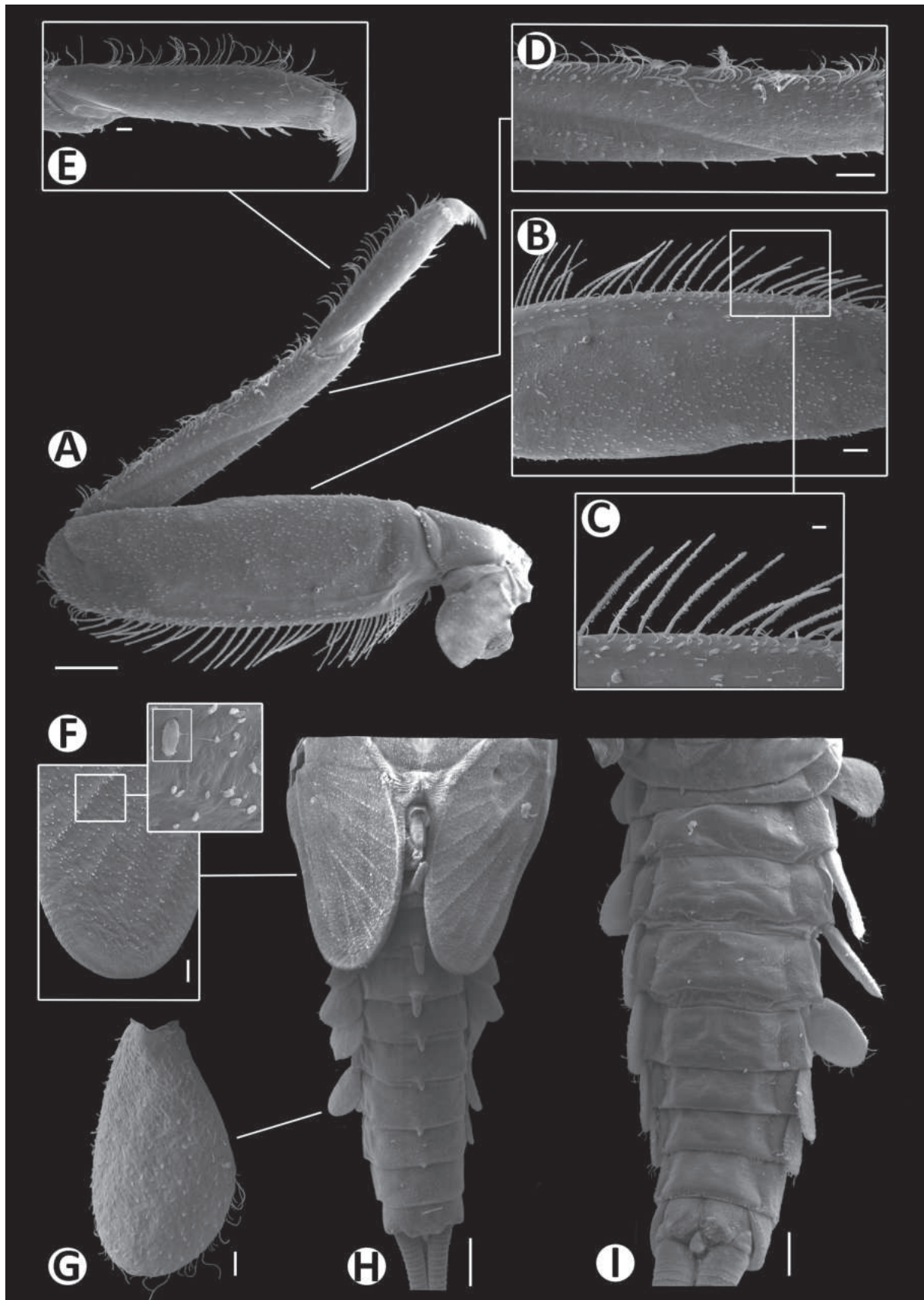


Figure 12. *Baetiella (Baetiella) lannaensis* sp. nov., larval morphology (SEM) **A** foreleg **B** femur **C** setae on dorsal margin of femur **D** tibia **E** tarsus and claw **F** forewing **G** gill VI **H** tergites **I** sternites. Scale bars: 100 μm (**A**, **I**); 30 μm (**B**, **C**, **D**, **F**); 20 μm (**E**, **G**); 200 μm (**H**).

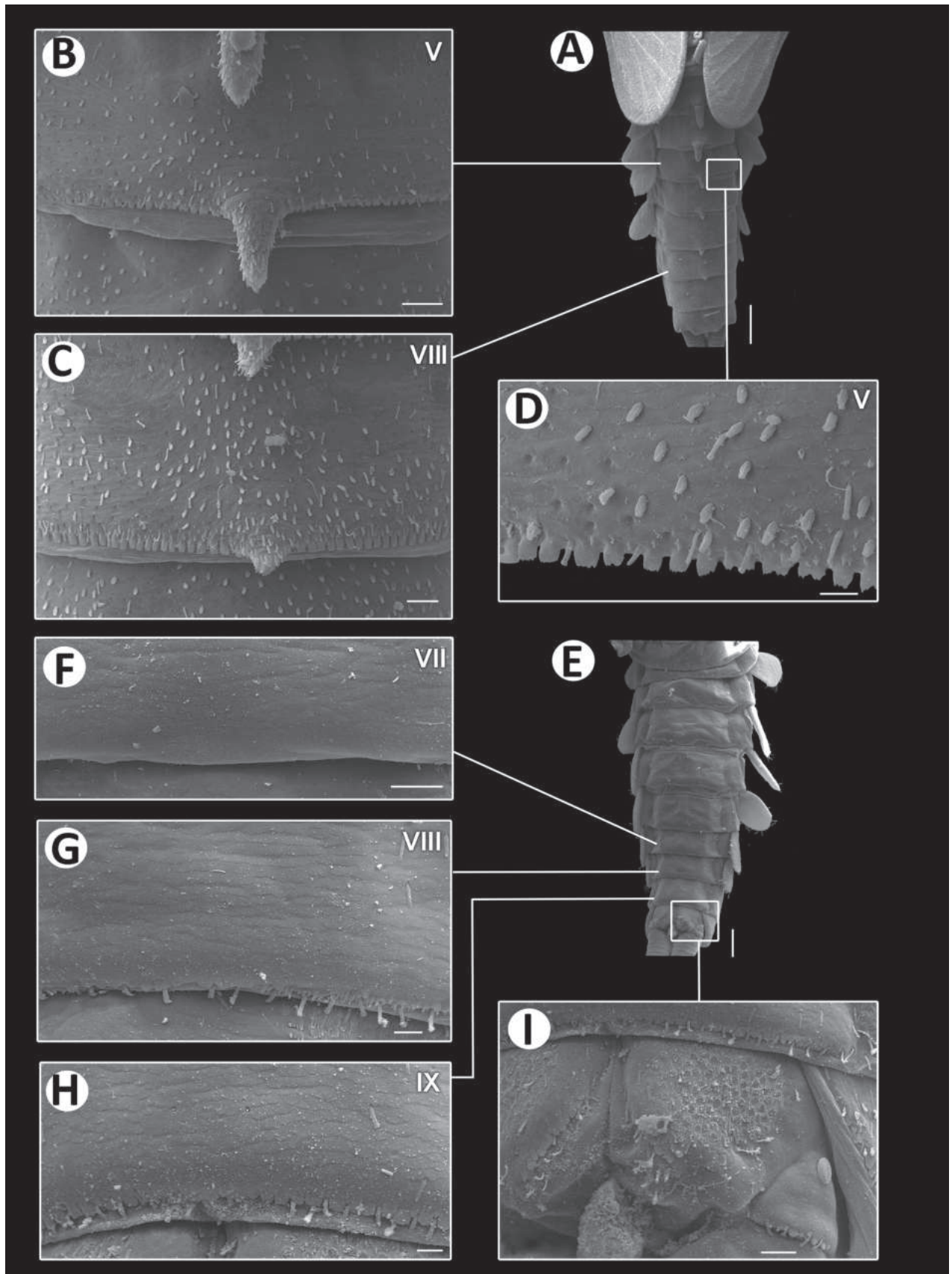


Figure 13. *Baetiella (Baetiella) lannaensis* sp. nov., larval morphology (SEM) **A** tergites **B** tergite V **C** tergite VIII **D** posterior margin of tergite V **E** sternites **F** sternite VII **G** sternite VIII **H** sternite IX **I** paraproct. Scale bars: 200 μm (**A**); 30 μm (**B**); 20 μm (**C**, **F**, **I**); 10 μm (**D**, **G**, **H**); 100 μm (**E**).

Etymology. This specific epithet, *lannaensis*, refers to the Lanna kingdom, the historic name of northern Thailand where this new species was found.

Distribution. Chiang Mai and Mae Hong Son Provinces (northern Thailand).

Remarks. The newly discovered species is morphologically similar to *Baetiella ausobskyi* Braasch, 1983; both species share tergites I–VIII with a single, reduced, posteromedian protuberance and dorsal surface of labrum with a row of fewer than seven submarginal setae. Nevertheless, *Baetiella (Baetiella) lannaensis* sp. nov. reveals distinct characters that distinguish it from *B. ausobskyi*. For instance, the dorsal margin of femur with a row of long, rounded, simple, feathered setae while this row is compound of long, robust, rounded, simple setae in *B. ausobskyi*. This new species can be identified by the surface of body, legs, and especially the gill surface that are covered by numerous rounded scale-like setae. The distal margin of sternites VIII–X of *Baetiella (Baetiella) lannaensis* sp. nov. possesses multi-dentated and blunt spines. This new species exhibits a reduction of the paracercus to a single segment, whereas *B. ausobskyi*, as described by Braasch (1983), has a reduction to three segments. The two species also differ by the shape of the inner apical lobe of segment II of the labial palp; this lobe is more reduced in *Baetiella (Baetiella) lannaensis*. Additionally, the terminal segment of the labial palp in *Baetiella (Baetiella) lannaensis* sp. nov. is conical and asymmetrical, whereas in *B. ausobskyi*, this segment is rounded, conical, and nearly symmetrical (Vasanth et al. 2020).

***Baetiella (Baetiella) bibranchia* sp. nov.**

<https://zoobank.org/B6E6792D-F757-4998-A935-18ADD2EA6BF1>

Figs 14–19

Type material examined. Holotype. THAILAND, One larva on slide (KKU-AIC), Chiang Rai, Muang district, Pong Phra Baht waterfall, 20°00'39.60"N, 99°48'14.47"E, 476 m, 11.III.2021, B. Boonsoong leg. **Paratypes.** Two larvae on stubs, Six larvae in alcohol, same data as holotype (KKU-AIC); Four larvae in alcohol, same data as holotype (MZL: GBIFCH01118452).

Diagnosis. This new species, *Baetiella (Baetiella) bibranchia* sp. nov. can be easily distinguished from other *Baetiella* species by the following combination of characters; (i) distal margin of tergites I–V with a single, posteromedian protuberance, distal margin of tergites VI–IX with a pair of posteromedian protuberances, the distance between posteromedian protuberances gradually widened backwards, distance between bases of posteromedian protuberances of tergite VI is shorter than length of posteromedian protuberances; (ii) coxal gills present at the base of forelegs and midlegs; (iii) terminal segment reduced to one segment; (iv) segment II of labial palp without inner apical lobe; (v) distal margin of tergites II–X with multi-dentated, blunt denticles; (vi) distal margin of sternites smooth without denticles.

Description. Coloration (Fig. 14A). Head dorsally brownish, with darker brown mark at frontal suture. Thorax dorsally brownish yellow with dark brown pattern and with very small dark brown tubercles. Abdominal tergites brownish with darker brown pattern; sternites pale brown (Fig. 14B, C). Legs brownish; dorsal surface brownish, pale brown ventrally; dorsal surface of femur

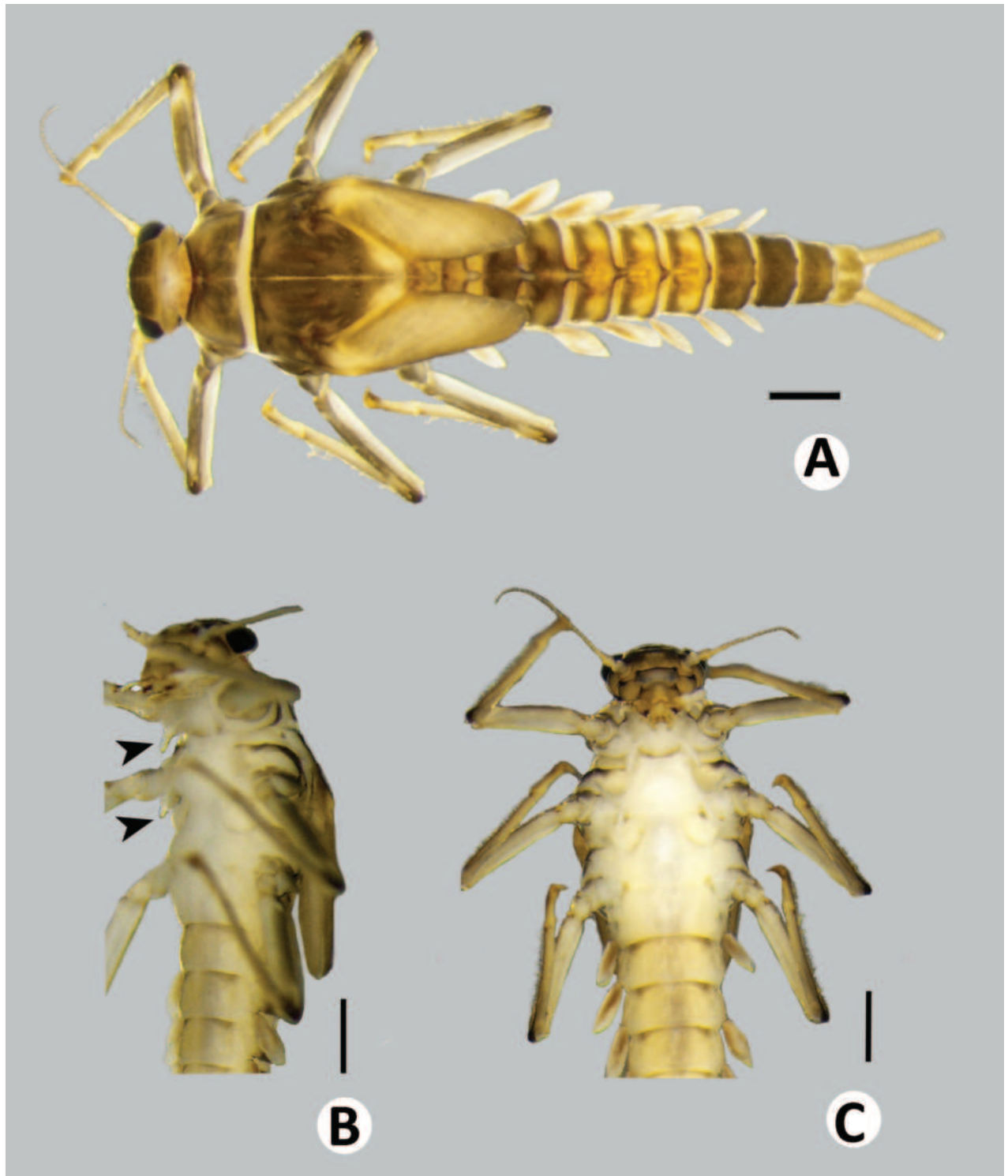


Figure 14. *Baetiella* (*Baetiella*) *bibranchia* sp. nov., larval habitus (paratype) **A** dorsal view **B** lateral view (black arrow indicating coxal gills) **C** ventral view. Scale bars: 1 mm.

with pale brown marking distally, tarsus and claw distally dark brown. Caudal filaments brownish.

Body. Dorsoventrally somewhat flattened (Fig. 14B, C). Paracercus reduced to one segment, cerci subequal to body length. Body surface covered with scattered rounded scale-like setae.

Head ~2× wider than long.

Antenna. Length $\sim 1.5\times$ as long as head length; scape, pedicel and flagellum without process, without scale bases and spines, covered with scattered, fine setae; flagellum covered with scattered, fine setae in each segment.

Mouthparts. Labrum (Fig. 15A). Broad, slightly rectangular; $\sim 2\times$ wider than long; each half of dorsal surface with one central seta and a row of nine long, simple, robust submarginal setae, proximal part with scattered, fine, simple setae; distal margin with anteromedian notch shallow, lateral margin with a row of medium, fine, pointed, simple setae; ventral surface with a row of feathered setae along distal margin, distolateral margin with a row of feathered setae and a row of three, short, simple, robust setae near lateral margin, distal part with patch of dense, fine, hair-like setae.

Right mandible (Fig. 15B–D). Outer and inner incisors partially separated with visible separating line (Fig. 15B, C), incisors well developed, outer incisor with three denticles and inner incisor with three denticles; right prosthaca (Fig. 15D) slender with denticles apically; edge between mola and prosthaca smooth without spines; apex of mola with tuft of spine-like setae; proximal surface with scattered short, fine, simple setae.

Left mandible (Fig. 15E–G). Outer and inner incisors almost completely fused (Fig. 15E, F), well developed incisors with six denticles apically, prosthaca robust, apically with small denticles and comb-shaped structure (Fig. 15G); edge between mola and prosthaca smooth without spines; proximal surface with scattered short, fine, simple setae.

Maxilla (Fig. 15H). Galea lacinia with three blunt, robust canines and a canine-like dentisetia; inner dorsal row of setae with two bifid pectinate dentisetiae; inner ventral row of robust, simple pectinate setae medially, with long robust, simple pectinate setae distally; basal with a row of four long basal setae on basis of galea lacinia. Maxillary palp 2-segmented, with scattered small, hair-like setae; distal segment with distinct, small tip at apex and small, hair-like setae.

Labium (Fig. 15I). Glossa basally broad, narrower toward apex, glossa slightly shorter than paraglossa, inner margin with a row of eight medium, stout, simple setae and two short, stout, simple setae, apical margin with four or five long, stout, simple setae, proximal part with a short, fine, robust seta; paraglossa sub-rectangular, broader than glossa, apical margin with three rows of long, stout, simple setae and a row of stout setae on outer margin, dorsal surface with four median, stout, simple setae and a long, fine, simple seta apically, proximal part with a short, fine seta. Labial palp 3-segmented, terminal segment conical, rounded and asymmetrical with small tip at apex; segment II without inner apical lobe; ventral surface covered with scattered short, robust, simple setae and fine setae; segments I and III with numerous micropores.

Hypopharynx (Fig. 15J). Lingua rounded apically, with apical tuft of fine, long simple setae; superlingua apically rounded, covered with abundant fine simple setae.

Thorax (Figs 16A, 19A) with a very small, reduced tubercle. Metanotum with a single posteromedian protuberance

Hindwing pad reduced, $\sim 1.5\times$ longer than width, covered with numerous rounded, scale-like setae.

Legs (Figs 16B–E, 18A–D). Forelegs. Femur. Length $\sim 3\times$ maximum width. Dorsal margin with a row of long, rounded, simple setae, $\sim 1/3$ of femur width, decreasing at distal part (Figs 16C, 18B). Dorsal and ventral margins with a

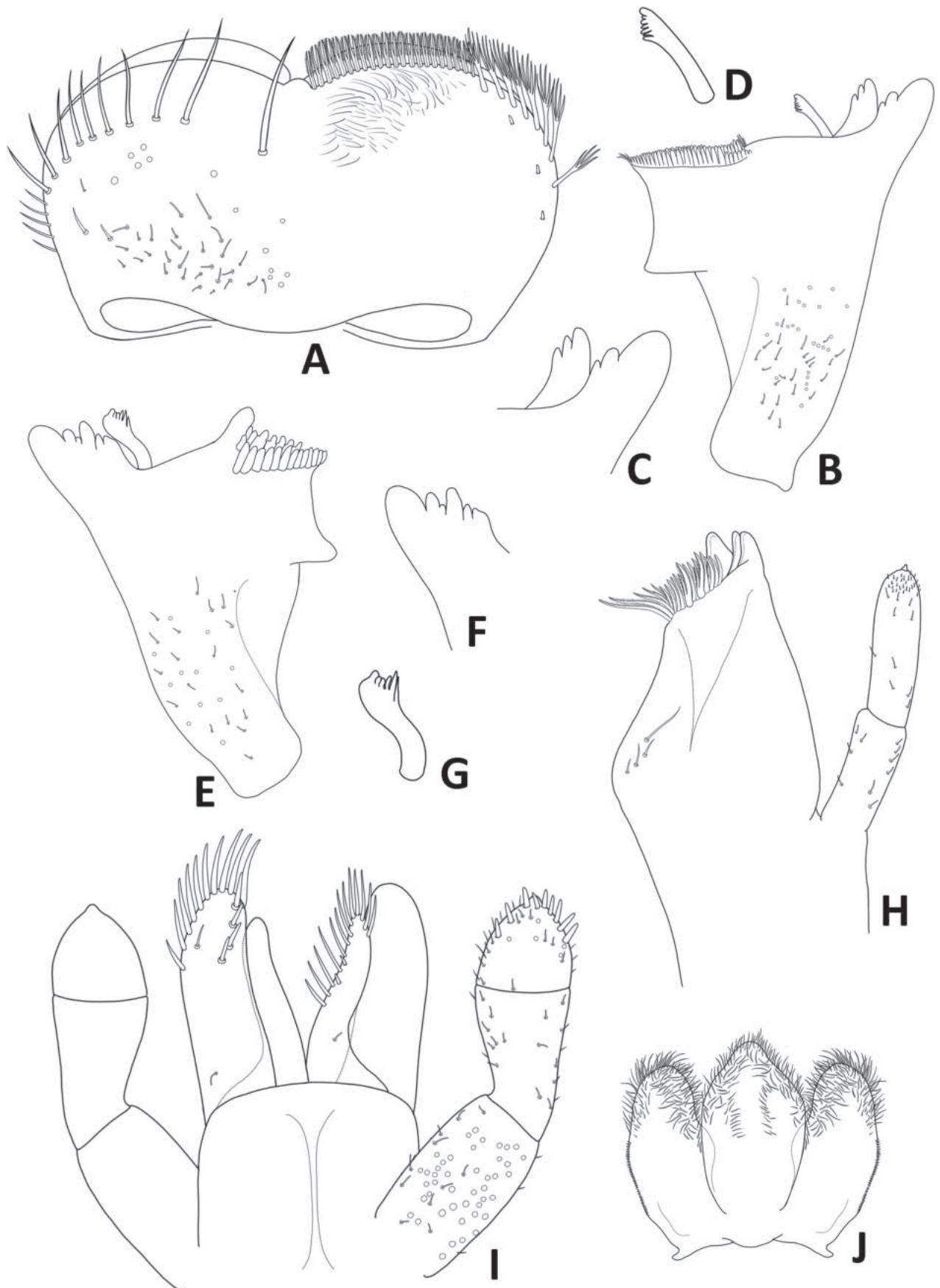


Figure 15. *Baetiella (Baetiella) bibranchia* sp. nov., larval morphology **A** labrum **B** right mandible **C** right incisors **D** right prosthema **E** left mandible **F** left incisors **H** left prosthema **G** left prosthema **H** maxilla **I** labium **J** hypopharynx.

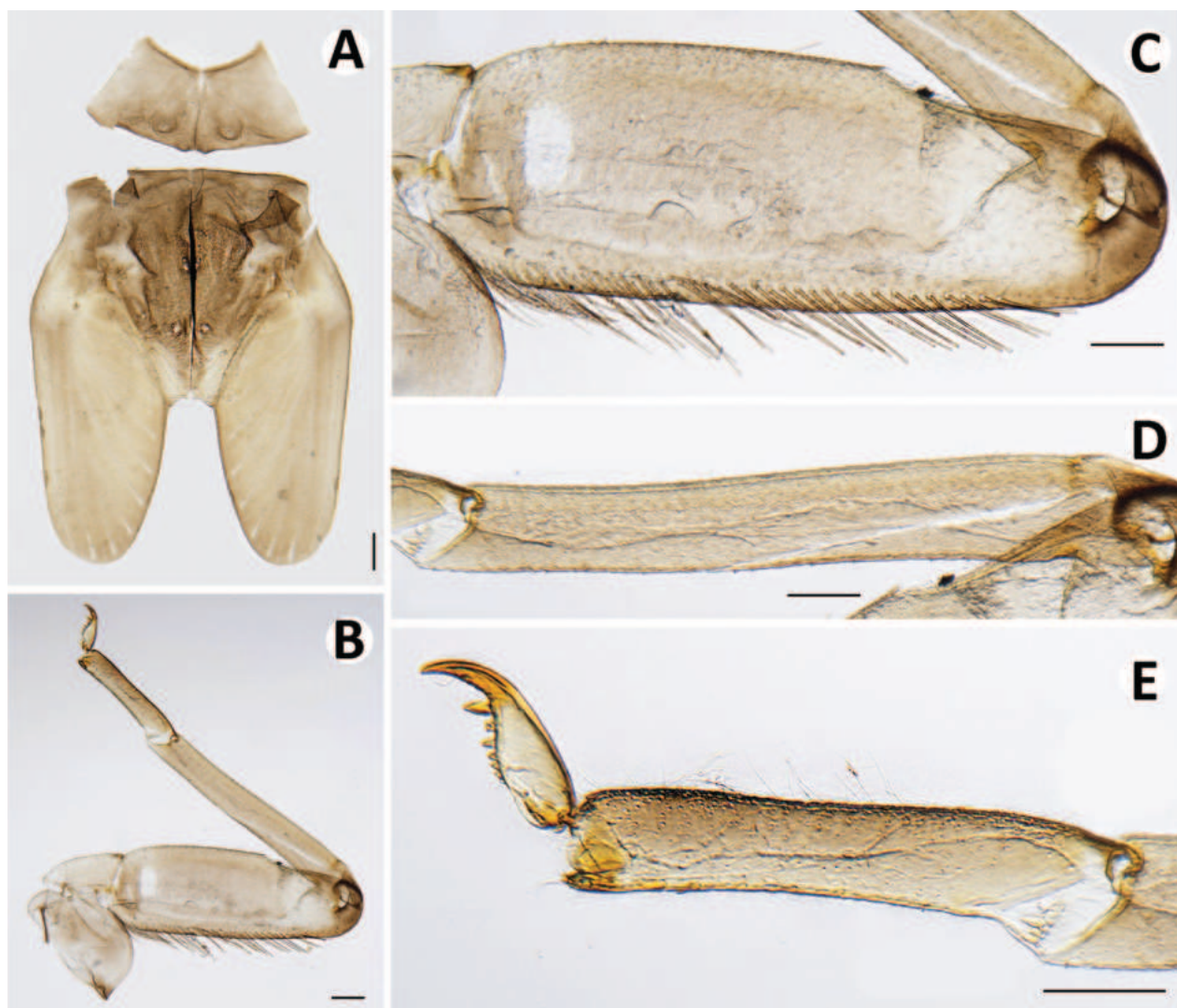


Figure 16. *Baetiella* (*Baetiella*) *bibranchia* sp. nov., larval morphology **A** pronotum and metanotum **B** foreleg **C** femur **D** tibia **E** tarsus and claw. Scale bars: 0.5 mm (**A**); 0.2 mm (**B**); 0.1 mm (**C, D, E**).

scattered row of short, robust setae. Femoral villopore present. Medial part of dorsal surface with scattered fine and rounded scale-like setae.

Tibia with a row of long, fine, simple setae dorsally (Figs 16D, 18C), dorsal and ventral margins with a row of short, robust setae, dorsal surface with scattered, short, fine setae.

Tarsus with a row of long, fine, simple setae dorsally, with a row of approximately seven robust, blunt setae ventrally increasing in size on distal part. Tarsal claw with a row of seven denticles with pair of subapical setae (Figs 16E, 18D).

Membranous digitiform extra gills at base of coxa (Figs 14B, C, 19B).

Midlegs and hindlegs as forelegs, except extra gills absent at base of coxa of hindlegs.

Abdomen (Fig. 17A). Distal margin of tergite I–V with a single, posteromedian protuberance, distal margin of tergites VI–IX with a pair of posteromedian posteromedian protuberances.

Abdominal tergite I with distal margin smooth, without denticles; distal margin of tergites II–X with multi-dentated, blunt denticles along margin (Figs 17C,

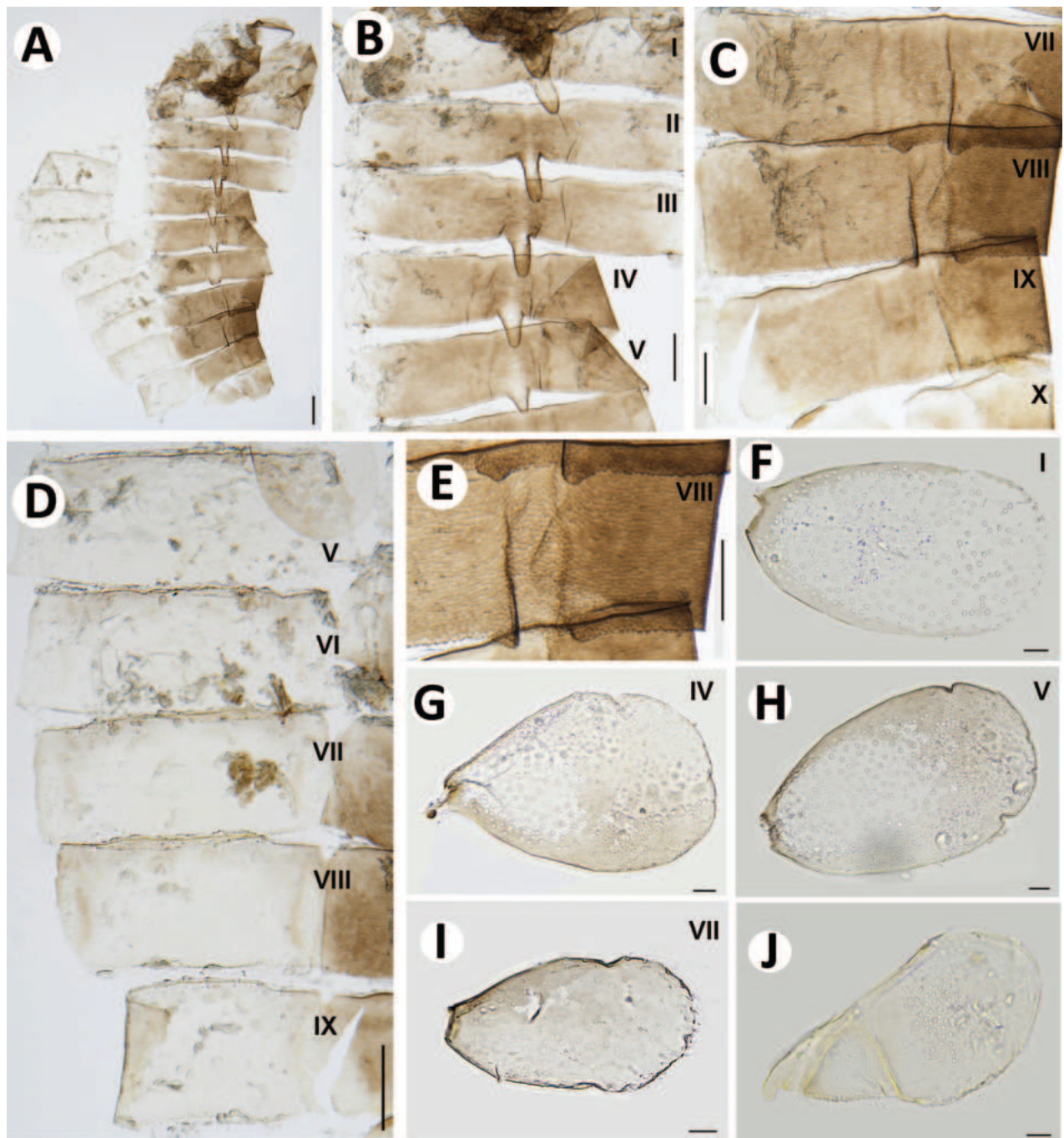


Figure 17. *Baetiella (Baetiella) bibranchia* sp. nov., larval morphology **A** abdomen **B** tergites I–V **C** tergites VII–X **D** sternites V–IX **E** distal margin of tergite VIII **F** gill I **G** gill IV **H** gill V **I** gill VII **J** paraproct. Scale bars: 0.2 mm (**A**, **B**, **D**); 0.1 mm (**C**, **E**); 0.02 mm (**I**, **J**).

E, 18E, 19C, D). Surface of all tergites covered with scattered short, fine, simple setae and rounded scale-like setae.

Abdominal sternites (Figs 17D, 18F). Sternites with distal margin smooth without denticles or scale-like setae, surface with scattered short, fine, simple setae (Fig. 19E).

Gills (Fig. 17F–I). Seven pairs of gills present on abdominal tergites I–VII, oval and without tracheation; gill VII smaller than other gills (Fig. 17I), coloration reddish to brown, small area medially translucent on outer margin; gill

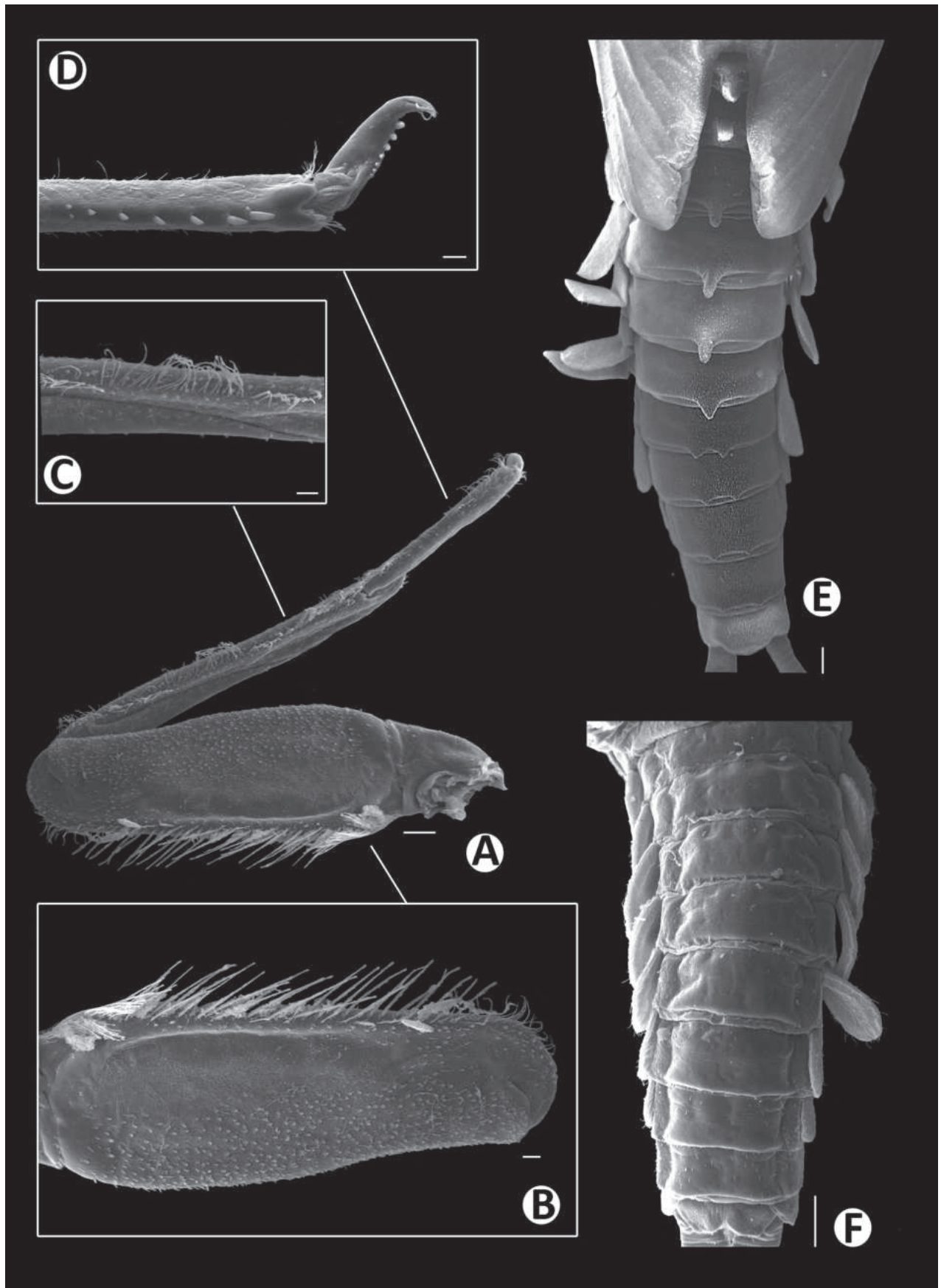


Figure 18. *Baetiella (Baetiella) bibranchia* sp. nov., larval morphology (SEM) **A** foreleg **B** femur **C** tibia **D** tarsus and claw **E** tergites **F** sternites. Scale bars: 20 µm (A–D); 100 µm (E, F).

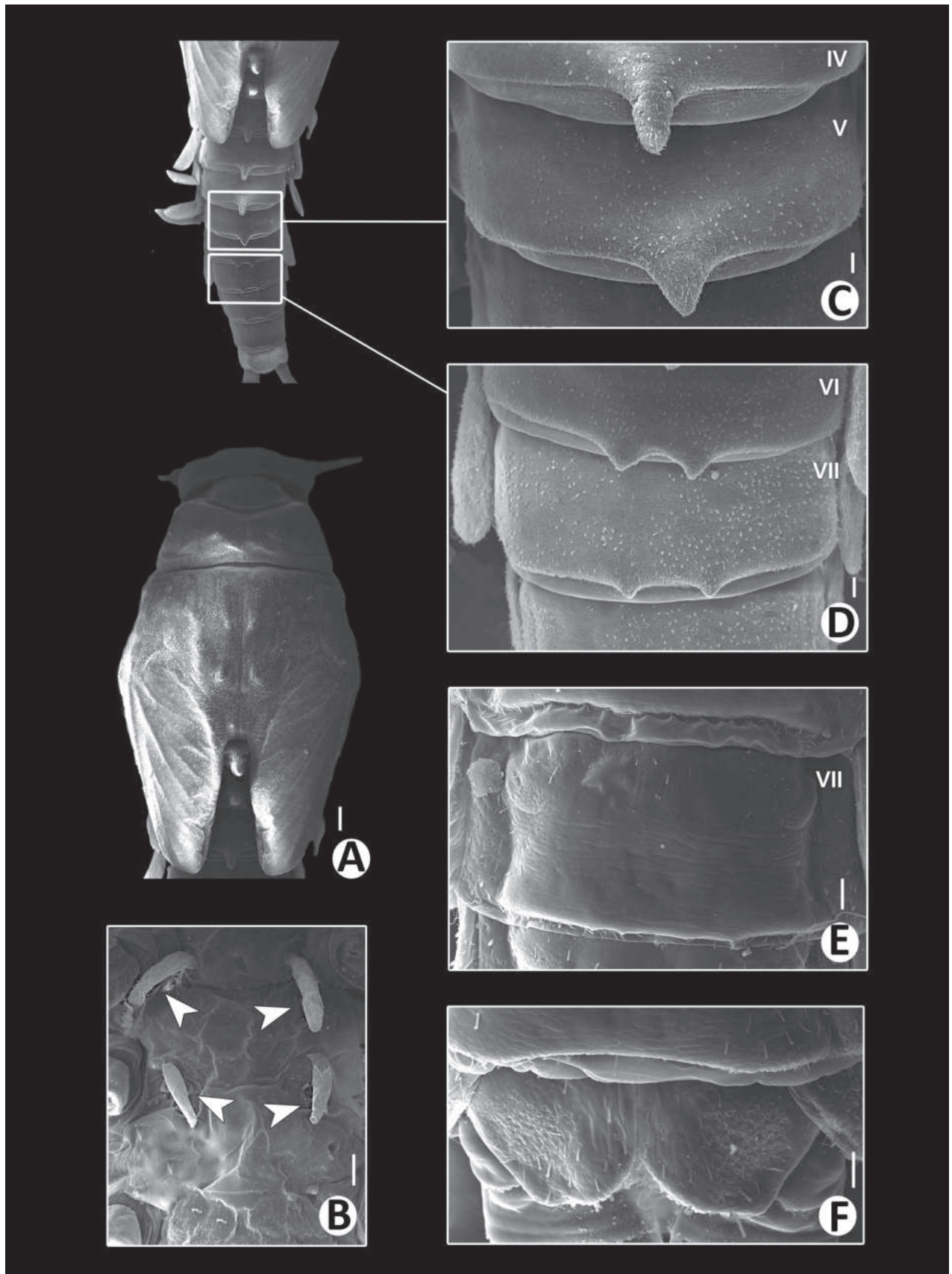


Figure 19. *Baetiella (Baetiella) bibranchia* sp. nov., larval morphology (SEM) **A** thorax (Dorsal) **B** thorax (Ventral) (White arrows pointed coxal gills) **C** tergites IV–V **D** tergites VI–VII **E** sternite VII **F** paraproct. Scale bars: 20 μm (**A–D**); 100 μm (**E, F**).

surface with scattered fine setae and numerous micropores, margin with scattered hair-like setae (Fig. 17F–I).

Paraproct (Figs 17J, 19F). Surface with numerous micropores and scattered short, fine setae; inner and outer margins with several serrations and multi-dentated, blunt denticles along margin.

Imago. Unknown.

Ecological notes. The larvae were collected in Pong Phra Baht waterfall in northern Thailand (Chiang Rai Province). The larvae were found in headwater streams with intact forest canopy in mountainous areas at medium altitude (~780 m a.s.l.). The larvae were found on surface of boulders in fast-flowing water like the other new species.

Etymology. This specific epithet, *bibranchia*, is combination of *bi-* in reference to two and *-branchia* in reference to gills. The name *bibranchia* highlights the remarkable presence of two pairs of coxal gills, an important diagnostic character of this new species.

Distribution. Chiang Rai Provinces (Northern Thailand).

Remarks. *Baetiella (Baetiella) bibranchia* sp. nov. presents similarities with other *Baetiella* species including *Baetiella bispinosa* (Gose, 1980), *Baetiella trispinata* Tong & Dudgeon, 2000, *Baetiella macani* (Müller-Liebenau, 1985), and *Baetiella subansiri* Vasanth, Selvakumar & Subramanian, 2020. These species present single protuberances on the first tergites and paired posteromedian protuberances on the following tergites (Table 4). Combined with presence/absence of coxal gills, the number of tergites with paired or unpaired protuberances is a reliable character for separating species. Both *Baetiella bispinosa* and *B. macani* possess paired posteromedian protuberances on tergites III–V and all of their legs have coxal gills. They can be separated by the number of gills as *B. bispinosa* possesses a total of seven pairs and *B. macani* only six. *Baetiella trispinata* can be distinguished from the aforementioned species by the complete absence of coxal gills. Beside possessing finger-like coxal gills on all of the legs, *Baetiella subansiri* presents distinct morphological characters, particularly elongated abdominal gills and the presence of more developed posteromedian protuberances.

***Baetiella (Baetiella) bispinosa* (Gose, 1980)**

Fig. 20

Pseudocloeon bispinosus Gose, 1980: 211

Baetiella bispinosa: Waltz and McCafferty 1987: 563; Tong and Dudgeon 2000: 143

Material examined. THAILAND, Six larvae in alcohol (KKU-AIC), Chiang Rai, Phan district, stream near Pha Khong cave, 19°31'12.15"N, 99°39'12.59"E, 649 m, 5.II.2016, S. Phlai-ngam leg.; Five larvae in alcohol (KKU-AIC), Chiang Mai, Mae Taeng district, Mae Taeng Elephant Kraal, Mae Taeng River, 19°11'50.51"N, 98°53'13.98"E, 362 m, 5.I.2007, N. Tungpairojwong leg. Three larvae in alcohol (MZL: GBIFCH01118453), Chiang Rai, Mae Chan district, Nang Lae Nai waterfall, 20.084703°N, 99.732234°E, 470 m, 7.V.2019, B. Boonsoong leg.

Diagnosis. Body (Fig. 20A–C) dorsoventrally flattened, brownish with darker pattern, head and thorax dorsally brownish; maxillary palp 2-segmented, subequal in length, terminal segment with a small tip at apex; labial palp

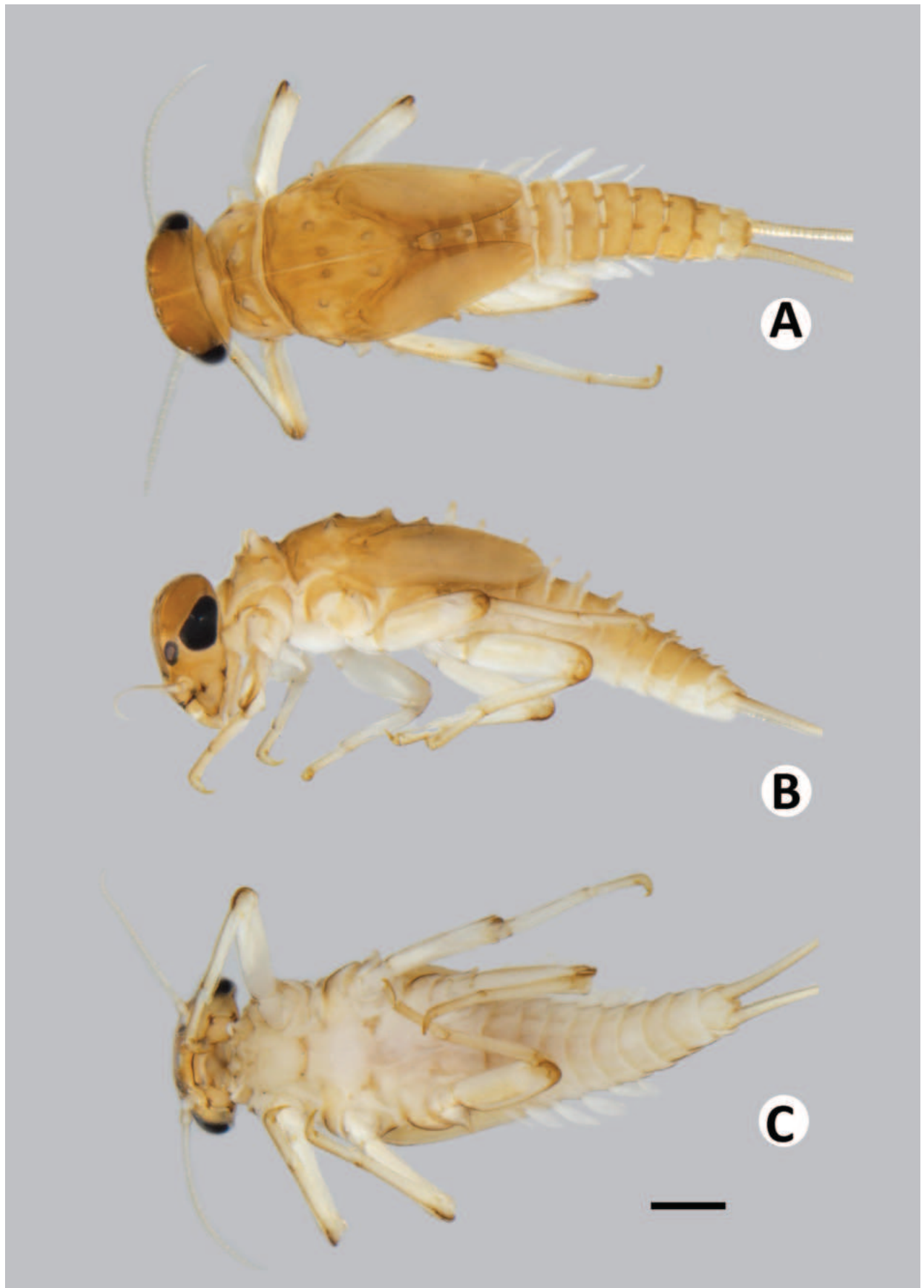


Figure 20. *Baetiella (Baetiella) bispinosa*, larval habitus **A** dorsal view **B** lateral view **C** ventral view. Scale bar: 1 mm.

3-segmented, terminal segment conical with a small tip at apex, segment II with a small, reduced inner apical lobe; thorax with distinct tubercles, pronotum with two pairs of tubercles medially, mesonotum with a pair of tubercles medially and with two pairs sub-medially; posterior margin of metanotum with a single posteromedian tubercle; hindwing pads vestigial; all legs with a single finger-like coxal gills, femora with a row of long, dense, fine, glabrate setae on dorsal margin, tarsal claw with two rows of denticles and a pair of apical setae; distal margin of tergites I and II with a single posteromedian protuberance, tergites III–IX with a pair of posteromedian protuberances, the distance between posteromedian protuberances gradually widened backwards; tergal surface with numerous micropores and short, fine, simple setae, distal margin with blunt denticles; seven pairs of gills present on abdominal tergites I–VII, oval and without tracheation; paracercus reduced to one segment.

Distribution. Chiang Rai and Chiang Mai Provinces (northern Thailand).

Remarks. The larvae of *B. (Baetiella) bispinosa* were collected on the surface of cobbles and boulders substrates in moderate to fast flowing streams. We found this species only in headwater streams.

***Baetiella (Gratia) narumonae* (Boonsoong & Thomas, 2004)**

Fig. 21

Gratia narumonae Boonsoong & Thomas, 2004: 1.

Baetiella narumonae: Kluge 2022: 166.

Material examined. THAILAND, Six larvae in alcohol (KKU-AIC), Nan, Bo Kluea district, 18°59'47.31"N, 101°12'50.94"E, 684 m, 24.XII.2019, S. Phlai-ngam leg.; Ten larvae in alcohol (KKU-AIC), Chiang Mai, Chom Thong district, near Mae Ya waterfall, 18°26'22.44"N, 98°35'51.77"E, 582 m, 3.II.2016, S. Phlai-ngam leg.; Three larvae in alcohol (KKU-AIC), Chiang Mai, Chom Thong district, Mae Klang stream, 18°29'39.72"N, 98°40'06.65"E, 337 m, 3.II.2016, S. Phlai-ngam leg. Two larvae in alcohol (MZL: GBIFCH01118454), Chiang Mai, Chom Thong district, Ban Luang, Siribhum waterfall, 18°32'50.02"N, 98°30'49.79"E, 1,359 m, 17.XII.2020, B. Boonsoong leg. Four larvae in alcohol (MZL: GBIFCH01118455), Chiang Rai, Mae Lao district, Khun Korn waterfall, 19°51.768'N, 99°39.078'E, 534 m, 6.V.2019, B. Boonsoong leg.

Diagnosis. Body (Fig. 21A–C) dorsoventrally flattened, brownish with dark brown pattern, head and thorax dorsally brownish, thorax broad; labrum broad (slightly broader than labium), each half of dorsal surface with one central seta, distal part with a row of submarginal setae including two innermost long, pointed, simple, robust setae and others with branched, robust setae; maxillary palp 2-segmented, short and thick, subequal in length, terminal segment with a small tip at apex; labium compact, glossa clearly shorter than paraglossa; labial palp 3-segmented, terminal segment rounded with a small tip at apex, segment II with an inner apical lobe; thorax with distinct tubercles, pronotum with two pairs of tubercles, the anterior pair bigger and at wider interval than posterior ones; hindwing pad reduced; all legs without coxal gill, femora with a strong row of long, dense, ciliated setae on dorsal margin, tarsal claw with a

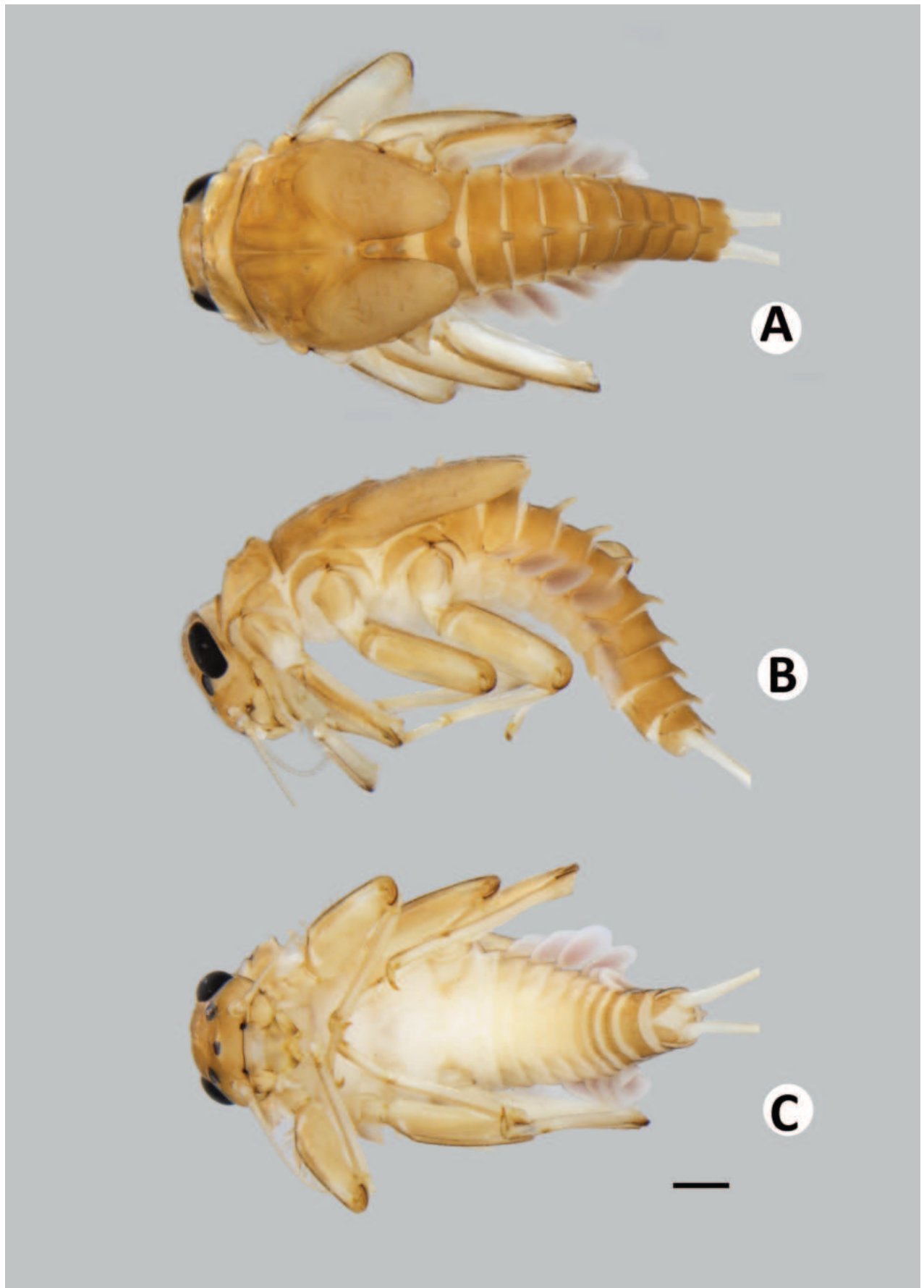


Figure 21. *Baetiella (Gratia) narumonae*, larval habitus **A** dorsal view **B** lateral view **C** ventral view. Scale bar: 1 mm.

row of 8–10 denticles and a pair of apical setae; dorsal surface shagreened, with short, rounded scale-like setae and scattered, fine setae; tergites I–IX with a strong, single posteromedian protuberance and reduced to small size in tergite X, distal margin with short, blunt denticles and scattered, short, fine setae; sternites with rounded, scale-like setae and scattered, short, fine setae, sternite VI with more abundant and bigger scales, sternites VII–IX with abundant scale-like setae, more numerous than in other segments, especially distal part and distal margin; seven pairs of gills present on abdominal tergites I–VII, oval and without tracheation, gill margin devoid of scales, only with scattered, fine setae; paraproct with 11–16 strong, rounded scale-like setae; paracercus reduced, cone-shaped.

Distribution. Chiang Mai and Nan provinces (northern Thailand).

Remarks. The larvae of *Baetiella* (*Gratia*) *narumonae* were found in fast flowing streams. The substrate types were dominated by boulders, cobbles, pebbles, gravel, and a sandy bottom. The larvae were found on the surface of boulders, cobbles, and bedrock, sometimes covered by green algae. Almost all sampling sites were in mountainous forest areas in the northern part of Thailand, undisturbed by human activities. However, this species can be also found in streams such as Mae Klang stream which can be disturbed by tourist attractions and human activities.

***Baetiella* (*Gratia*) *sororculaenadinae* (Thomas, 1992)**

Fig. 22

Gratia sororculaenadinae Thomas, 1992: 47.

Material examined. THAILAND, One larva in alcohol (KKU-AIC), Mukdahan, Nong Sung district, Tad Ton waterfall, 16°29'40.48"N, 104°18'47.09"E, 208 m, 23.XII.2017, S. Phlai-ngam leg; Four larvae in alcohol (KKU-AIC), Chiang Mai, Muang district, Suthep subdistrict, near Mon Tha Than waterfall, 18°49'02.41"N, 98°55'23.23"E, 713 m, 4.II.2016, S. Phlai-ngam leg.

Diagnosis. Body (Fig. 22A–C) dorsoventrally flattened, brownish with dark brown pattern, head and thorax dorsally brownish, scape and pedicel with numerous scale-like setae; thorax broad; labrum broad, each half of dorsal surface with one central seta, distal part with a row of submarginal setae including two innermost long, pointed, simple, robust setae and others with branched, clearly fimbriate and ramified setae; maxillary palp 2-segmented, terminal segment with a small tip at apex; labium compact, glossa subequal in length to paraglossa; labial palp 3-segmented, terminal and segment II completed fused, terminal segment asymmetrical and rounded with a small tip at apex, segment II without an inner apical lobe; hindwing pad reduced; all legs without coxal gill, femora with a strong row of long, dense, ciliated setae on dorsal margin, tarsal claw with a row of 7–9 denticles and a pair of apical setae; tergites I–IX with a strong, single posteromedian protuberance, distal margin with short, blunt denticles and scattered, short, fine setae; seven pairs of gills present on abdominal tergites I–VII, oval and without tracheation, gill margins with numerous spine like-setae and scattered, short, fine setae; paraproct with 20–25 strong, rounded scales; paracercus reduced to one segment.

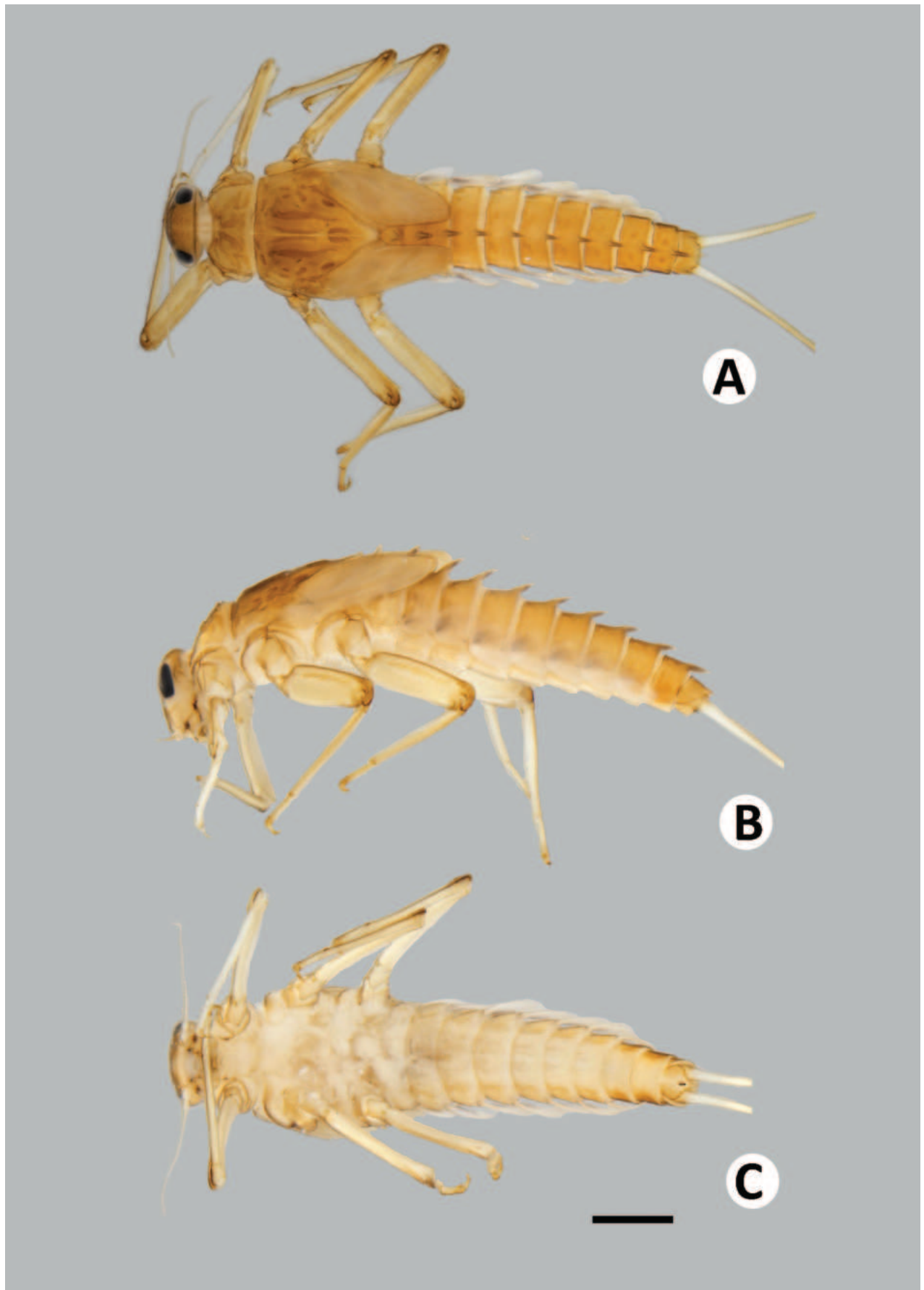


Figure 22. *Baetiella (Gratia) sororculaenadinae*, larval habitus **A** dorsal view **B** lateral view **C** ventral view. Scale bar: 1 mm.

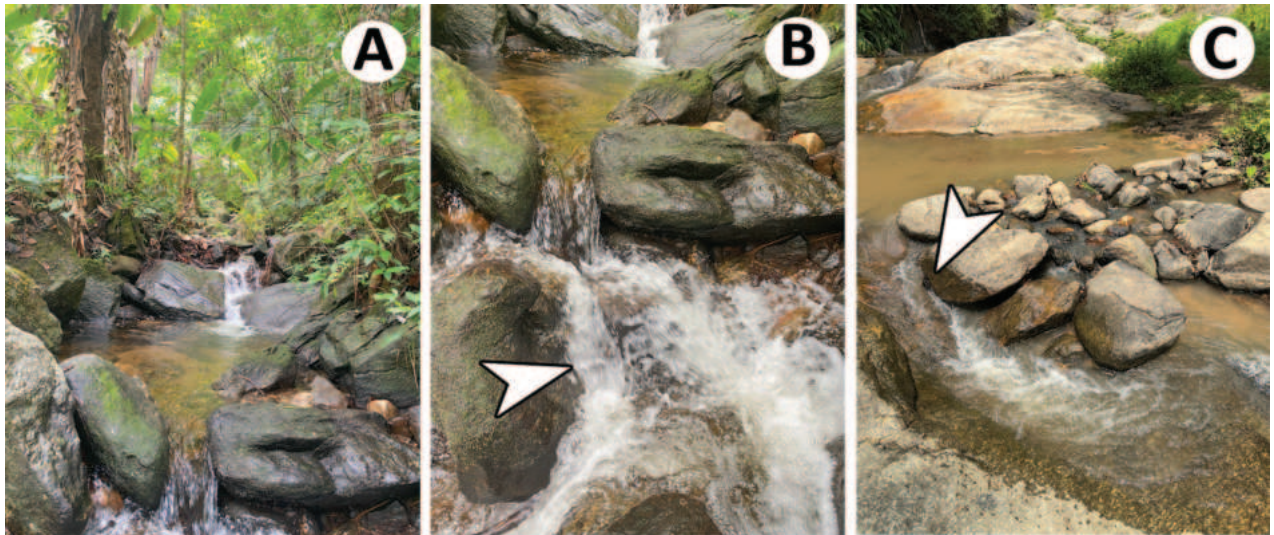


Figure 23. Sampling sites and the coexistence microhabitats of *Baetiella* (*Baetiella*) *baei* sp. nov. and *B.* (*Baetiella*) *lan-naensis* sp. nov. **A** Siribhum waterfall (Chiang Mai province) **B, C** microhabitats of Siribhum waterfall and Mo Pang waterfall (Mae Hong Son Province) respectively. White arrows indicate coexisting microhabitats of *B.* (*Baetiella*) *baei* sp. nov. and *B.* (*Baetiella*) *lan-naensis* sp. nov.

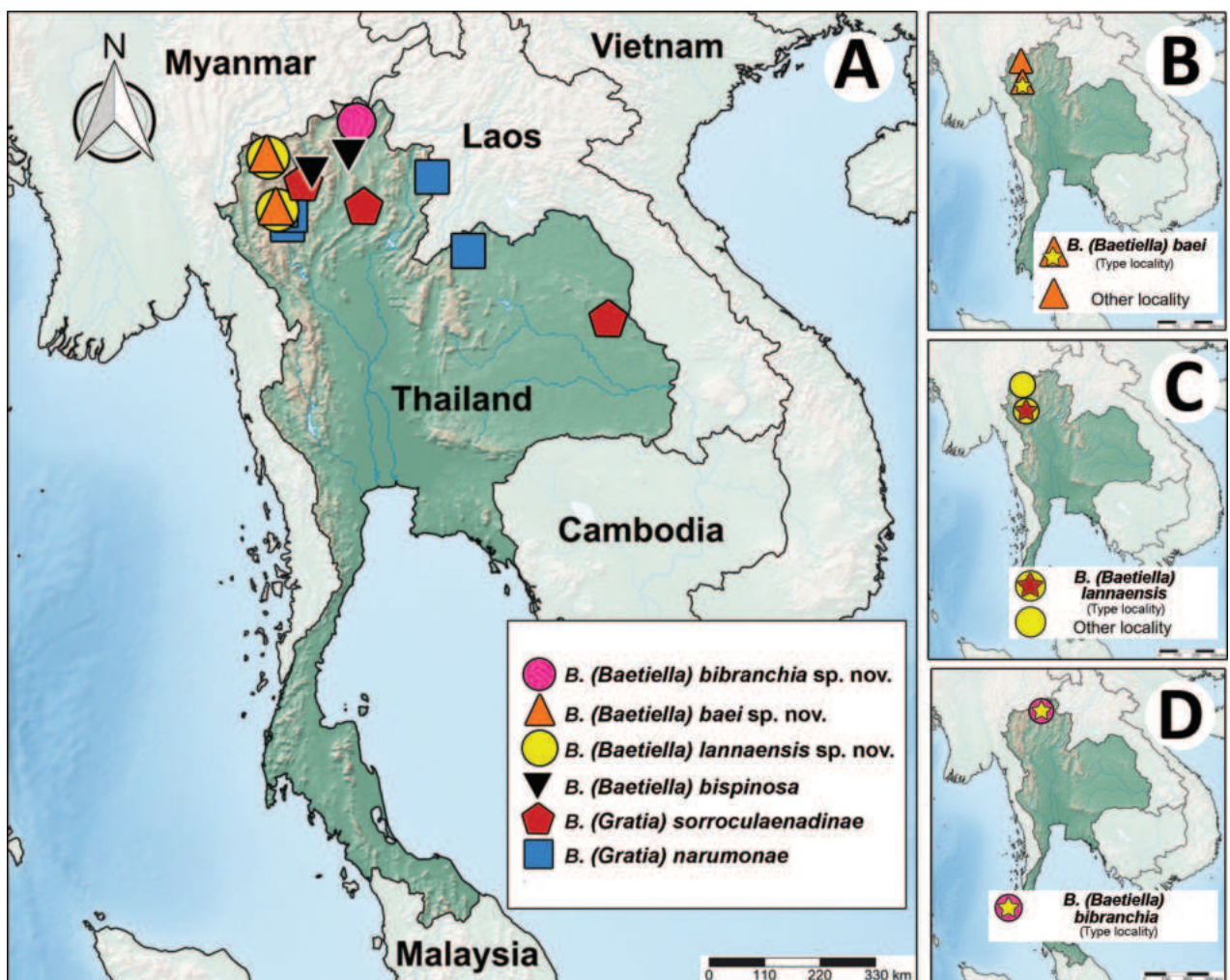


Figure 24. Distribution map of *Baetiella* species in Thailand with type localities of the new species. Red and yellow stars show the type localities.

Distribution. Chiang Mai and Mukdahan Provinces (north and northeast of Thailand).

Remarks. The larvae of *Baetiella (Gratia) sororculaenadinae* were found in fast flowing streams in forest areas. The substrate types were dominated by bedrock and boulders. The larvae were found on the surfaces of the bedrock. This species was reported from Chiang Mai Province (northern region of Thailand) for the first time by Thomas (1992). Interestingly, we found larvae of this species in the Mukdahan Province located in the northeast region of Thailand. This discovery indicates that this species is more widespread and colonizes wider environmental and altitudinal ranges than previously thought.

Key to species of the mature larvae of the genus *Baetiella* in Thailand

- 1 Submarginal setae on labrum branched and feathered; dorsal margin of femur with a regular row of setae ***Baetiella (Gratia) 2***
- Simple submarginal setae on labrum (Figs 3A, 9A, 15A); dorsal margin of femur with irregular or regular row of setae ***Baetiella (Baetiella) 3***
- 2 Posteromedian protuberances present on abdominal tergites I–IX; labial palp segment II without inner apical lobe ***B. (Gratia) sororculaenadinae***
- Posteromedian protuberances present on abdominal tergites I–X; labial palp segment II with an inner apical lobe ***B. (Gratia) narumonae***
- 3 Coxal gills present (Figs 14B, 19B) **4**
- Coxal gills absent **5**
- 4 Tergites I and II with single, posteromedian protuberance; tergites III–IX with a pair of posteromedian protuberances (Fig. 20A); coxal gills present on all legs ***B. (Baetiella) bispinosa***
- Tergites I–V with single, posteromedian protuberance; tergites VI–IX with a pair of posteromedian protuberances (Figs 14A, 18E); coxal gills present on forelegs and midlegs only ***B. (Baetiella) bibranchia sp. nov.***
- 5 Single, posteromedian protuberance present on tergites I–VIII (Figs 8A, 12H); dorsal margin of femur with a regular row of long, rounded, simple, ciliated setae (Fig. 12B, C) ***B. (Baetiella) lannaensis sp. nov.***
- Single, reduced posteromedian protuberance present only on tergite I–III (Figs 2A, 4H); dorsal margin of femur with dense irregular row of long, fine, simple setae (Figs 4C, 6B, C) ***B. (Baetiella) baei sp. nov.***

Molecular analysis

Pairwise genetic distance and reconstruction phylogenetic tree

COI sequences have been obtained from nine specimens collected in two localities (provinces of Chiang Mai and Chiang Rai). The newly obtained sequences were analyzed and compared with sequences sourced from databases such as GenBank and BOLD. The new sequences were submitted to the GenBank database, and their accession numbers are shown in Table 2.

The K2P analysis, which was conducted to evaluate genetic distances, shows that the three populations of the newly discovered species have low intraspecific variation, ranging from 0% to 2%. *Baetiella (Baetiella) lannaensis sp. nov.* has the lowest level of intraspecific genetic variation while *B. (Baetiella) baei sp. nov.*

Table 3. Genetic distances (COI) between sequenced species, using the Kimura 2-parameter.

	Species	1	2	3	4	5	6	7	8	9	10	11
1	<i>B. (Baetiella) bibranchia</i> sp. nov.	0.02										
2	<i>B. (Gratia) narumonae</i>	0.21	0.01									
3	<i>B. (Gratia) sororculaenadinae</i>	0.22	0.23	-								
4	<i>B. (Baetiella) lannaensis</i> sp. nov.	0.21	0.25	0.23	0.00							
5	<i>B. (Baetiella) baei</i> sp. nov.	0.25	0.27	0.26	0.27	0.01						
6	<i>B. (Baetiella) bispinosa</i>	0.22	0.24	0.19	0.21	0.25	0.01					
7	<i>B. japonica</i>	0.22	0.25	0.22	0.25	0.25	0.21	0.02				
8	<i>B. tuberculata</i>	0.23	0.26	0.24	0.21	0.27	0.24	0.24	0.04			
9	<i>Baetiella</i> sp. 1	0.24	0.24	0.20	0.24	0.26	0.17	0.20	0.26	0.01		
10	<i>Baetiella</i> sp. 2	0.21	0.24	0.21	0.23	0.25	0.19	0.22	0.25	0.19	0.00	
11	<i>Cloeon dipterum</i> (Outgroup)	0.19	0.22	0.20	0.24	0.27	0.20	0.23	0.22	0.21	0.22	-

and *B. (Baetiella) bibranchia* sp. nov. have intraspecific distances of 1% and 2%, respectively (Table 4). The interspecific distances between these new species and other species range between 19% and 27%, which clearly supports the validity of the species (Table 3).

The utilization of ML and BI analyses in the phylogenetic reconstruction tree of the COI gene reveals that the nine sequences obtained from the newly discovered species can be grouped into three distinct clades. These clades have a significant degree of distinction from other clades, as indicated by their exceptionally high values of bootstrap support (BS = 100%) and posterior probability (PP = 1). In addition, the results indicate that the three *Baetiella* species, *B. (Baetiella) bispinosa*, *B. (Gratia) narumonae* and *B. (Gratia) sororculaenadinae*, are strongly supported as independent clades by high bootstrap values (Fig. 25).

Species delimitation

Species delineation based on molecular evidence has been investigated as an additional method to help define species boundaries (Zhang et al. 2013) and to support phylogenetic results. A set of 29 COI sequences, encompassing *Baetiella* and *Gratia* species, were compiled for the purpose of molecular species delimitation in order to determine species boundaries. The results of the ASAP species delimitation approach, combining the Jukes-Cantor (JC69) model, the Kimura 2-parameter (K2P) model, and simple distances (p-distances), provided a total of 10 Molecular Operational Taxonomic Units (MOTUs). The second approach, mPTP analysis, also provides a total of 10 MOTUs, as depicted in Fig. 25. The ten MOTUs obtained by ASAP and mPTP approaches are the same; both methods recovered *B. (Baetiella) baei* sp. nov., *B. (Baetiella) lannaensis* sp. nov., and *B. (Baetiella) bibranchia* sp. nov. as independent species.

Discussion

Morphological and molecular studies

Previous studies reported three species of *Baetiella* in Thailand; *B. (Baetiella) bispinosa*, *B. (Gratia) sororculaenadinae*, and *B. (Gratia) narumonae* (Thomas,

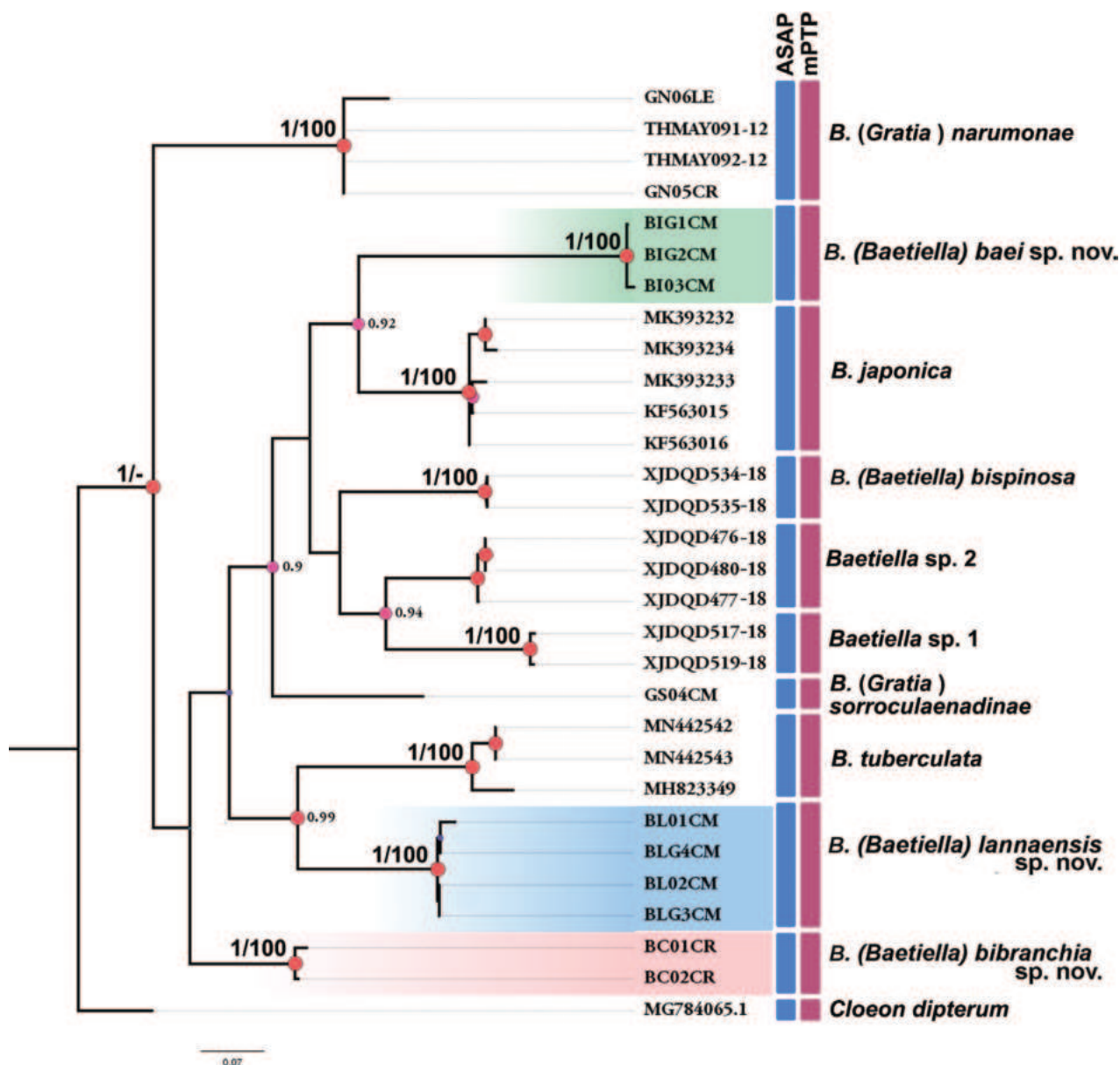


Figure 25. Phylogenetic reconstruction of *Baetiella* species based on Bayesian inference (BI) and Maximum likelihood (ML) analyses of sequences of the mitochondrial COI gene. The highlighted clades represent the newly described *Baetiella* species from Thailand with high bootstrap and Bayesian posterior probabilities (BS/PP) supporting. Pink circles on branches indicate PP > 0.9. Colored vertical boxes indicate species-delimitation hypothesis (i.e., MOTUs) according to the ASAP and mPTP methods.

1992) (Thomas 1992; Boonsoong et al. 2004; Phlai-ngam and Tungpairajwong 2018). These species were also found during this survey, in addition to the discovery of three new species.

Baetiella (Baetiella) baei sp. nov. presents similarities to *B. marginata* and *B. muchei* in terms of the presence of distinct abdominal protuberances. This newly discovered species can be identified based on several distinct characteristics. These include a small and reduced posteromedian protuberance on the distal margin of tergites I–III, which is not present in other segments. Besides that, the distal margin of sternites VIII–X presents a row of long, spatulate, blunt denticles, and the inner margin of the paraproct is smooth, with 3–5 oval

Table 4. Comparison of larval morphological characters of three new species of *Baetiella* from Thailand with the closely related species.

Characters/ Species	<i>B. (Baetiella) baei</i> sp. nov.	<i>B. (Baetiella) marginata</i>	<i>B. (Baetiella) muchei</i>	<i>B. (Baetiella) lanmaensis</i> sp. nov.	<i>B. (Baetiella) susobskyi</i>	<i>B. (Baetiella) bibranchia</i> sp. nov.	<i>B. (Baetiella) bispinosa</i>	<i>B. (Baetiella) subansiri</i>
Submarginal setae of labrum	1 long medial seta and 1 row of 10 long, robust, simple setae	1 long medial seta and 1 row of 11 robust, simple setae	1 long medial seta and 1 row of 12–22 robust, simple setae	1 long medial seta and 1 row of ≥ 7 robust, simple setae	1 long medial seta and 1 row of < 7 robust, simple setae	1 medial long seta and 1 row of 9 robust, simple setae	1 long medial seta and 1 row of robust, simple setae	1 long medial seta and 1 row of 6–8 robust, simple setae
Edge between mola and protheca of right and left mandibles	with a row of small spines	smooth without spine	smooth without spine	smooth without spine	smooth without spine	smooth without spine	smooth without spine	smooth without spine
Labial palp	terminal segment rounded, asymmetrical, almost fused with the 2 nd segment with small tip at apex; 2 nd segment with very small inner apical lobe	terminal segment conical with stout setae and a distinctive tip at apex; 2 nd segment with very small inner apical lobe	conical with the apical tip at the apex, 2 nd segment with very small inner apical lobe	terminal segment of labial palp conical and symmetrical shaped with apical tip, the 2 nd segment of labial palp with small inner apical lobe	terminal segment conical with a distinctive tip at apex; 2 nd segment with inner apical lobe	terminal segment conical, rounded and asymmetrical with small tip at apex; 2 nd segment without inner apical lobe	terminal segment conical, with a small tip at apex; 2 nd segment without inner apical lobe	terminal segment conical with a distinctive tip at apex; the 2 nd segment without inner-apical lobe
Thorax	pronotum and mesonotum with small, reduced tubercles	pronotum and mesonotum without tubercles	pronotum and mesonotum without tubercles	pronotum and mesonotum with small, reduced tubercles; metanotum with a single, posteromedian protuberance; surface with dense, numerous rounded scales	pronotum and mesonotum without tubercles	pronotum and mesonotum with small, reduced tubercles	pronotum and mesonotum with distinct tubercles	pronotum and mesonotum with 12 distinct tubercles
Setae of dorsal margin of femur	dense irregular row of long, fine, simple setae; with a pair of long, stout, simple, subapical setae distally	a row of short and simple setae	dense irregular row of long, fine, simple setae	a regular row of long, rounded, simple, ciliated setae, $\sim 1/3$ to $1/2$ of femur width	a row of dense, long and simple setae on dorsal margin, $\sim 1/2$ of femur width	a row of long, rounded, simple setae, $\sim 1/3$ of femur width, decreasing at distal part	irregular row of long, dense, fine, simple setae	a row of 17 or 18 long, simple setae, $\sim 1/3$ to $1/2$ of femur width
Setae of dorsal margin of tibia	irregular row of long, fine, simple setae dorsally	irregular row of dense, fine, simple setae	irregular row of dense, fine, simple setae	irregular row of dense, fine, simple setae	irregular row of dense, fine, simple setae	irregular row of dense, fine, simple setae	irregular row of dense, fine, simple setae	irregular row of dense, fine, simple setae
Coxal gills	absent	absent	absent	absent	absent	Present on forelegs and midlegs	Present on all legs	Present on all legs
Posteromedian protuberances	tergites I–III with small, reduced, single protuberances	absent	absent	tergites I–VIII with single protuberances (decreasing in size towards terminal segment)	tergites I–VIII with single protuberances	tergites I–V with a single, posteromedian protuberance; tergites VI–IX with a pair of posteromedian protuberances	tergites I and II with a single, posteromedian protuberance; tergites III–IX with a pair of posteromedian protuberances	tergites I and II with a single, posteromedian protuberance; tergites III–IX with a pair of much longer protuberances
Distal margin of tergites	all tergites with multi-dentate, blunt denticles, surface with scattered, fine setae	all tergites with blunt denticles	all tergites with blunt denticles	tergite I smooth without denticles; tergites II–X with multi-dentate and blunt spines; surface with numerous rounded scales	tergites VI–IX with blunt denticles; surface without rounded scale-like setae	tergite I smooth without denticles; tergites II–X with multi-dentate and blunt spines	all tergites with blunt denticles	tergite I–V smooth without denticles; tergites VI–X with blunt denticles

Characters/ Species	<i>B. (Baetiella) baei</i> sp. nov.	<i>B. (Baetiella) marginata</i>	<i>B. (Baetiella) muchei</i>	<i>B. (Baetiella) jannaensis</i> sp. nov.	<i>B. (Baetiella) susobskyi</i>	<i>B. (Baetiella) bibranchia</i> sp. nov.	<i>B. (Baetiella) bispinosa</i>	<i>B. (Baetiella) subansiri</i>
Distal margin of sternites	sternites I–VII smooth without denticles, sternites VIII–X with a row of long, spatulate, blunt denticles	all sternites smooth, without denticles	all sternites smooth, without denticles	sternites I–VII smooth without denticles; sternites VIII–X with multi-dentate, blunt denticles	all sternites smooth, without denticles	all sternites smooth, without denticles	all sternites smooth, without denticles	all sternites smooth, without denticles
Gills	7 pairs of gills; margin with scattered short, small spines; gills II–VII with numerous, fine setae and several micropores on surface	7 pairs of gills; surface with scattered numerous micropores, margin smooth with fine simple setae	7 pairs of gills; surface scattered with numerous micropores, margin smooth with fine simple setae	7 pairs of gills; gill surface with scattered, fine setae and several rounded scales and micropores, gill margin with scattered fine simple setae	7 pairs of gills; surface scattered with numerous micropores, margin smooth with fine simple setae	7 pairs of gills; gill surface with scattered, fine setae and numerous micropores, margin with scattered hair-like setae	7 pairs of gills; margin smooth with fine simple setae	6 pairs of gills; gills II–VI elongate, gill VII reduced; surface with numerous scattered micropores, margin smooth with fine simple setae
Inner margin of paraproct	smooth with 3–5 oval scale-like setae along margin	10–12 stout setae along the inner margin	smooth without denticles	12–14 spines along the inner margin	10–12 spines along the inner margin	several spines along the inner margin	several spines along the inner margin	15–16 scale-like setae along the inner margin
Paracercus	reduced to one segment	reduced to 15 segments	reduced to one segment	reduced to one segment	reduced to 1–3 segments	reduced to one segment	reduced to one segment	reduced to one segment
Distribution	Thailand	India, Nepal, China	Tajikistan	Thailand	India, Nepal	Thailand	China, India, Thailand	India
Reference	This study	Shi and Tong 2015; Vasanth et al. 2020	Braasch, 1978 Sivaruban et al. 2024	This study	Braasch, 1983; Vasanth et al. 2020	This study	Shi and Tong 2015; Phlai-ngam and Tungpaiojwong 2018; Vasanth et al. 2020	Vasanth et al. 2020

scale-like setae along the margin. Moreover, *B. muchei* shows intraspecific variability larval characters, such as submarginal arc of setae in the labrum which differs from 12 to 22 while *B. (Baetiella) baei* sp. nov. has no more than 12 submarginal setae on labrum (Sivaruban et al. 2024).

Baetiella (Baetiella) lannaensis sp. nov. shares characters with *B. ausobskyi*, a species found in Nepal (the Himalayan region) and India (Braasch 1983; Shi and Tong 2015b; Vasanth et al. 2020). This new species from Thailand possesses remarkable characteristics, including the presence of ciliated setae on the dorsal margin of the femur as well as different distal margins of the tergites and sternites. The body and gill surfaces are densely covered with rounded scale-like setae. Furthermore, the labrum possesses at least seven subapical setae, while *B. ausobskyi* has less than seven.

Baetiella (Baetiella) bibranchia sp. nov. is easily distinguished from other *Baetiella* species by the presence of a pair of posteromedian protuberances on the distal margin of tergites VI–IX (the distance between posteromedian protuberances gradually increases backwards) and the presence of coxal gills at the base of forelegs and midlegs.

The molecular analysis reveals genetic distances between the species ranging from 17% to 27% (Table 3) and supports the validity of these three newly discovered species. The intraspecific distances for each of the new species are low, ranging from 0% to 2% which is much lower than the generally accepted lower interspecific distance of 4% (Hebert et al. 2003; Ball et al. 2005; Zhou et al. 2010).

This study is the starting point for integrating morphological and molecular data for all species of *Gratia* and *Baetiella* to clarify their systematic. The findings of our study indicate that the morphological structure of Thai *Baetiella* larvae can be assigned to two groups: *Baetiella (Baetiella)* and *Baetiella (Gratia)*.

Our study reveals imprecisions in part of the previous studies concerning important characters used for the generic delimitation of *Baetiella* and *Gratia*. Some characters are similar between *Baetiella* and *Gratia*, such as the setation of setae on the femur and tibia, labial palp, and posteromedian protuberances. We demonstrate that the shape of submarginal setae on the labrum is a distinct characteristic that can be used for separation of these two baetid groups. However, this single diagnostic character is not sufficient to consider *Baetiella* and *Gratia* as distinct genera; Kluge (2022b) also moved *Gratia narumonae* to *Baetiella* based on the character of the imaginal stage. Even so, the molecular data remain inconclusive. The mitochondrial gene used in our study is valuable for species delimitation but is too variable for deeper nodes. We recommend that researchers apply in the future a combination of molecular and morphological data, encompassing a broader set of species with an increased number of specimens. It will facilitate the gathering of significant molecular data to reconstruct robust phylogeny. Especially, the addition of nuclear genes could provide an effective reconstruction tree for systematic clarification. Even though only the COI gene is usually not enough for phylogenetic analysis. This approach will help to resolve and clarify the taxonomic problems associated with this lineage of baetid mayflies in the future.

This study expands knowledge of *Baetiella* in Thailand, revealing a substantial presence with diverse species mainly in the north of the country. The

occurrence of six species, including three new to science, challenges previous expectations of *Baetiella* distribution and diversity and suggest a need for comprehensive diversity surveys in Thailand and more generally in the Southeast Asian region. *Baetiella* species were mainly found in waterfalls and stream with medium or fast current generally close to headwaters. Larvae were predominantly found in cobbles, boulders, and bedrock in cold, pristine water. The ecological data gathered could contribute to freshwater quality monitoring, challenging the too often accepted paradigm that Baetidae in general are not sensitive to water quality and have a broad ecological valence.

The geographic distribution and global status of *Baetiella*

The genus *Baetiella* has been recorded in the Eastern Palearctic and Oriental regions (Fig. 26). Most species are dispersed within the Palearctic realm, encompassing several countries such as China, Japan, Korea, Russia, Mongolia, Tajikistan, Vietnam, Nepal, and India (Tong and Dudgeon 2000; Shi and Tong 2015a; Vasanth et al. 2020).

Currently, *Baetiella* comprises 22 valid species, including the newly discovered species and the species previously assigned to *Gratia*. Despite the increasing number of new species found and the new reports, the distribution of this genus remains limited to these two zoogeographic zones.

The highest diversity has been reported in China, primarily on the mainland. These species include *B. sexta* Shi & Tong, 2015, *B. macani*, *B. marginata*, *B. trispinata*, *B. bispinosa*, *B. imanishii*, and *B. lanpingensis*. A few species are reported from Hong Kong (*B. bispinosa* and *B. trispinata*). Others are distributed in high mountains; *B. spathae* and *B. lanpingensis* are found in Tibet and Yunnan, respectively (Tong and Dudgeon 2000; Shi and Tong 2015a). The size

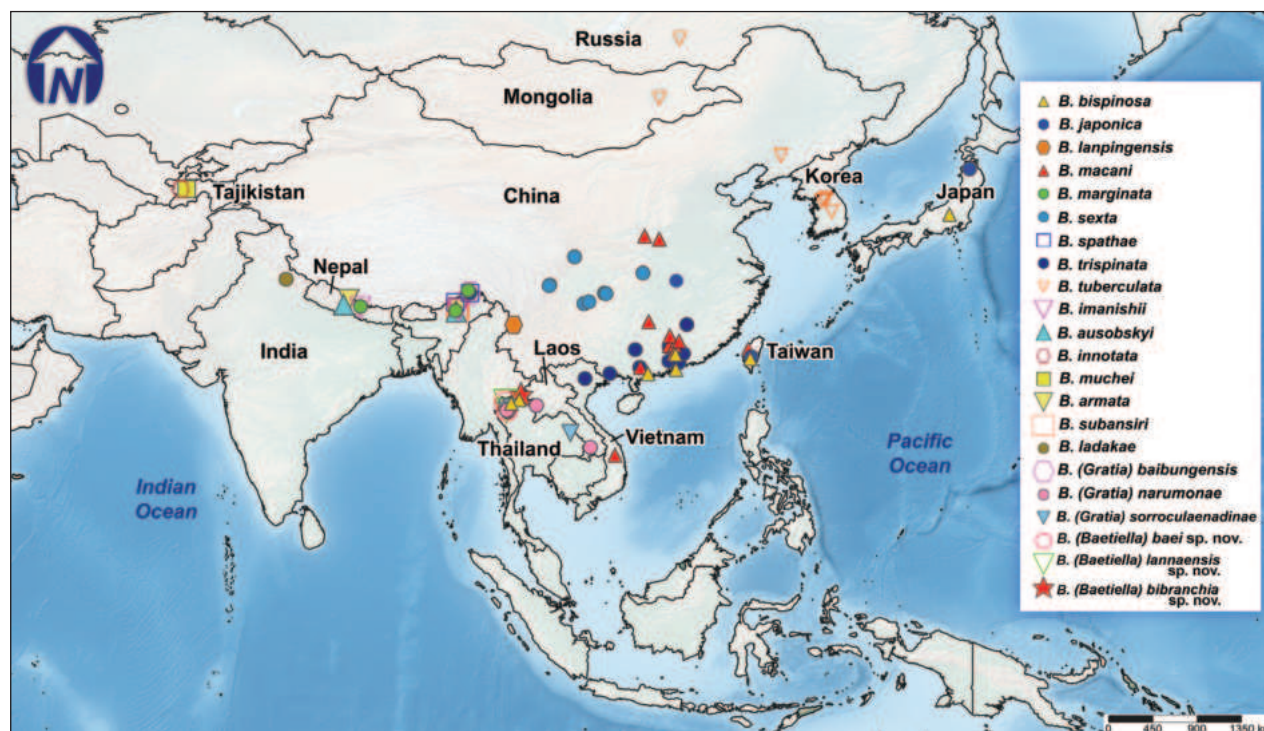


Figure 26. Distribution map of *Baetiella* species in the world.

of the country and the various ecological conditions contribute to the species richness of *Baetiella* in China.

Other *Baetiella* species, including *B. japonica*, *B. bispinosa*, and *B. macani*, are mentioned from islands such as Japan and Taiwan. *Baetiella tuberculata* exhibits a broad distribution across several Palearctic countries, including Russia, Mongolia, China, and Japan (Uéno 1969; Müller-Liebenau 1985; Shi and Tong 2015a).

Several species (e.g., *B. armata*, *B. aubobskyi*, *B. imanishii*, *B. marginata*, *B. spathae*, and *B. subansiri*) are found in the southern limit of the East Palearctic region as they are only reported from north India and Nepal. *Baetiella muchei* and *B. innotata* Braasch, 1978 were collected in Tajikistan, with no report of these species in any other regions (Braasch 1978, 1983; Vasanth et al. 2020). The currently accessible data indicate that the distribution of *Baetiella* species is limited to the eastern part of the Palearctic region.

Most species occur mainly in the northern part of the Oriental realm, arguing for possible dispersal routes ranging from northern Vietnam to northeastern Thailand. This point needs to be assessed against the lack of knowledge from some parts of the Oriental realm and especially from equatorial and lower equatorial countries.

Our study demonstrates that the distribution and diversity of *Baetiella* was highly underestimated in Thailand. We have not only greatly extended the distribution of Palearctic species southwards, but also discovered species that are potentially endemic to northern Thailand.

Based on our in-depth study of the fauna of Thailand and initial data from Laos and Vietnam, we can reasonably expect to find similar diversity in neighboring countries such as Cambodia and Myanmar, where knowledge of the fauna is still very patchy. Given the current state of our knowledge, it is difficult to predict whether the genus *Baetiella* will reach its southern limit in Thailand or whether we can expect to discover populations further south (e.g., Malaysia, Java, Sumatra or Borneo).

Acknowledgements

We express our gratitude to the Department of Biology, Faculty of Science, Khon Kaen University for their helpful assistance and accessibility to facilities. Furthermore, the authors express their sincere gratitude to Pandiarajan Srinivasan from the Department of Zoology at the American College in Madurai, India, for his assistance in comparing the characters of Indian *Baetiella* specimens. This collaboration greatly improved the worth of the information presented in this study and we want to thank him for his valuable recommendations. We are grateful to Laurent Vuataz (MZL) for his valuable suggestions on molecular study. Finally, we express our gratitude to our colleagues for their generous support throughout field trips.

Additional information

Conflict of interest

The authors have declared that no competing interests exist.

Ethical statement

No ethical statement was reported.

Funding

This work was partially financially supported by Academic Affairs Promotion Fund, Faculty of Science, Khon Kaen University, fiscal year 2024 (RAAPF), Research and Graduated Studies, Khon Kaen University.

Author contributions

Conceptualization: BB, NT. Funding acquisition: NT. Methodology: SP. Visualization: SP. Writing - original draft: SP. Writing - review and editing: NT, JLG, BB.

Author ORCIDs

Sirikamon Phlai-ngam  <https://orcid.org/0000-0002-3638-6123>

Boonsatien Boonsoong  <https://orcid.org/0000-0002-8166-0021>

Jean-Luc Gattolliat  <https://orcid.org/0000-0001-5873-5083>

Nisarath Tungpairong  <https://orcid.org/0000-0001-8135-4246>

Data availability

All of the data that support the findings of this study are available in the main text.

References

- Ball SL, Hebert PDN, Burian SK, Webb JM (2005) Biological identifications of mayflies (Ephemeroptera) using DNA barcodes. *Journal of the North American Benthological Society* 24(3): 508–524. <https://doi.org/10.1899/04-142.1>
- Boonsoong B, Thomas A, Sangpradub N (2004) *Gratia narumonae* sp. n., a new mayfly from Thailand. *Ephemera* 4(1): 1–9. <https://doi.org/10.1051/limn/2012012> [Ephemeroptera, Baetidae]
- Braasch D (1978) Baetidae (Ephemeroptera) in Mittelasiien I. *Entomologisches Nachrichtenblatt* (Vienna, Austria) 22(2): 17–23.
- Braasch D (1983) Neue Baetidae von Nepal (Ephemeroptera). *Reichenbachia* 21: 147–155.
- Edler D, Klein J, Antonelli A, Silvestro D (2021) raxmlGUI 2.0: A graphical interface and toolkit for phylogenetic analyses using RAxML. *Methods in Ecology and Evolution* 12: 373–377. <https://doi.org/10.1111/2041-210X.13512>
- Felsenstein J (2004) *Inferring Phylogenies*. Sinauer Associates Inc., Sunderland, MA, 664 pp.
- Folmer O, Black M, Hoeh W, Lutz R, Vrijenhoek R (1994) DNA primers for amplification of mitochondrial cytochrome c oxidase subunit I from diverse metazoan invertebrates. *Molecular Marine Biology and Biotechnology* 3(5): 294–299.
- Hebert PDN, Cywinska A, Ball SL, DeWaard JR (2003) Biological identifications through DNA barcodes. *Proceedings of the Royal Society B, Biological Sciences* 270(1512): 313–321. <https://doi.org/10.1098/rspb.2002.2218>
- Hillis DM, Bull JJ (1993) An empirical test of bootstrapping as a method for assessing confidence in phylogenetic analysis. *Systematic Biology* 42(2): 82–192. <https://doi.org/10.1093/sysbio/42.2.182>
- Huelsenbeck JP, Rannala B (2004) Frequentist properties of Bayesian posterior probabilities of phylogenetic trees under simple and complex substitution models. *Systematic Biology* 53(6): 904–913. <https://doi.org/10.1080/10635150490522629>
- Huelsenbeck JP, Ronquist F (2001) MRBAYES: Bayesian inference of phylogenetic trees. *Bioinformatics* (Oxford, England) 17(8): 754–755. <https://doi.org/10.1093/bioinformatics/17.8.754>

- Kaltenbach T, Phlai-ngam S, Suttinun C, Gattolliat JL (2023) First report of the Afrotropical genus *Securiops* Jacobus, McCafferty & Gattolliat (Ephemeroptera, Baetidae) from Southeast Asia, with description of a new species. *ZooKeys* 1157: 127–143. <https://doi.org/10.3897/zookeys.1157.99642>
- Kapli P, Lutteropp S, Zhang J, Kobert K, Pavlidis P, Stamatakis A, Flouri T (2017) Multi-rate Poisson tree processes for single-locus species delimitation under maximum likelihood and Markov chain Monte Carlo. *Bioinformatics* (Oxford, England) 33(11): 1630–1638. <https://doi.org/10.1093/bioinformatics/btx025>
- Kazlauskas P (1963) New and little-known mayflies (Ephemeroptera) from the USSR. *Revue d'Entomologie de l'URSS* 42(3): 582–592.
- Kluge NJ (1983) New and little known mayflies of the family Baetidae (Ephemeroptera) from Primorya. *Entomological Review* 62: 53–68.
- Kluge NJ (2004) The phylogenetic system of Ephemeroptera. Kluwer Academic Publishers, Dordrecht, 442 pp.
- Kluge NJ (2020) Review of *Oculogaster* Kluge 2016 (Ephemeroptera, Baetidae, *Procloeon* Bengtsson 1915). *Zootaxa* 4820(3): 401–437. <https://doi.org/10.11646/zootaxa.4820.3.1>
- Kluge NJ (2022a) Two new species of *Waynokiops* (Ephemeroptera: Baetidae) from the Oriental Region. *Zootaxa* 5182(1): 041–063. <https://doi.org/10.11646/zootaxa.5182.1.3>
- Kluge NJ (2022b) Taxonomic significance of microlepidies on subimaginal tarsi of Ephemeroptera. *Zootaxa* 5159(2): 151–186. <https://doi.org/10.11646/zootaxa.5159.2.1>
- Kluge NJ, Novikova EA (2011) Systematics of the mayfly taxon *Acentrella* (Ephemeroptera: Baetidae), with description of new Asian and African species. *Russian Entomological Journal* 20(1): 1–56. <https://doi.org/10.15298/rusentj.20.1.01>
- Kluge NJ, Novikova EA (2017) Occurrence of *Anafroptilum* Kluge 2012 (Ephemeroptera: Baetidae) in Oriental Region. *Zootaxa* 4282(3): 453–472. <https://doi.org/10.11646/zootaxa.4282.3.2>
- Kluge NJ, Suttinun C (2021) Review of the Oriental genus *Indocloeon* Müller-Liebenau 1982 (Ephemeroptera: Baetidae) with descriptions of two new species. *Zootaxa* 4779(4): 451–484. <https://doi.org/10.11646/zootaxa.4779.4.1>
- Kluge N, Srinivasan P, Sivaruban T, Barathy S, Isack R (2023) Contribution to the knowledge of the subgenus *Tenuibaetis* Kang & Yang 1994 (Ephemeroptera, Baetidae, *Baetis* s. l.). *Zootaxa* 5277(2): 201–258. <https://doi.org/10.11646/zootaxa.5277.2.1>
- Kumar S, Stecher G, Li M, Knyaz C, Tamura K (2018) MEGA X: Molecular Evolutionary Genetics Analysis across Computing Platforms. *Molecular Biology and Evolution* 35(6): 1547–1549. <https://doi.org/10.1093/molbev/msy096>
- Mauro DS, Agorreta A (2010) Molecular systematics: A synthesis of the common methods and the state of knowledge. *Cellular & Molecular Biology Letters* 15(2): 311–341. <https://doi.org/10.2478/s11658-010-0010-8>
- Müller-Liebenau I (1985) Baetidae from Taiwan with Remarks on *Baetiella* Uéno, 1931 (Insecta: Ephemeroptera). *Archiv für Hydrobiologie* 104(1): 93–110. <https://doi.org/10.1127/archiv-hydrobiol/104/1985/93>
- Müller-Liebenau I, Heard WH (1979) *Symbiocloeon*: a new genus of Baetidae from Thailand (Insecta, Ephemeroptera). In: Pasternak K, Sowa R (Eds) *Proceedings of the 2nd International Conference on Ephemeroptera*, Panstwowe Wydawnictwo Naukowe, Krakow, 57–65.
- Phlai-ngam S, Tungpairajwong N (2018) First Record of *Platybaetis bishopi* Müller-Liebenau, 1980 and *Baetiella bispinosa* (Gose, 1980) (Ephemeroptera: Baetidae) from Thailand. *Warasan Khana Witthayasat Maha Witthayalai Chiang Mai* 45(2): 774–783.

- Phlai-ngam S, Boonsoong B, Gattolliat JL, Tungpairajwong N (2022a) *Megabranchiella* gen. nov., a new mayfly genus (Ephemeroptera, Baetidae) from Thailand with description of two new species. *ZooKeys* 1125: 1–31. <https://doi.org/10.3897/zookeys.1125.90802>
- Phlai-ngam S, Tungpairajwong N, Gattolliat JL (2022b) A new species of *Alainites* (Ephemeroptera, Baetidae) from Thailand. *Alpine Entomology* 6: 133–146. <https://doi.org/10.3897/alpento.6.96284>
- Puillandre N, Brouillet S, Achaz G (2020) ASAP: Assemble species by automatic partitioning. *Molecular Ecology Resources* 21(2): 609–620. <https://doi.org/10.1111/1755-0998.13281>
- Rambaut A (2014) FigTree. Citing online sources: advice on online citation formats.
- Shi W, Tong X (2015a) Taxonomic notes on the genus *Baetiella* Uéno from China, with the descriptions of three new species (Ephemeroptera: Baetidae). *Zootaxa* 4012(3): 553–569. <https://doi.org/10.11646/zootaxa.4012.3.9>
- Shi W, Tong X (2015b) First record of the genus *Gratia* Thomas (Ephemeroptera, Baetidae) from China with the description of a new species. *ZooKeys* 478: 129–137. <https://doi.org/10.3897/zookeys.478.8995>
- Sivaruban T, Sohil A, Srinivasan P, Barathy S, Sharma N, Isack R (2024) *Baetiella muchei* (Braasch, 1978) (Ephemeroptera: Baetidae) new to India, with reference to the morphological variability of the larvae. *Journal of Insect Biodiversity and Systematics* 10(2): 311–319. <https://doi.org/10.61186/jibs.10.2.311>
- Sutthinun C, Gattolliat JL, Boonsoong B (2018) A new species of *Platybaetis* Muller-Liebenau, 1980 (Ephemeroptera: Baetidae) from Thailand, with description of the imago of *Platybaetis bishopi* Muller-Liebenau, 1980. *Zootaxa* 4378(1): 85–97. <https://doi.org/10.11646/zootaxa.4378.1.5>
- Suttinun C, Gattolliat JL, Boonsoong B (2020) *Cymbalcloeon* gen. nov., an incredible new mayfly genus (Ephemeroptera: Baetidae) from Thailand. *PLOS ONE* 15(10): e0240635. [17 pp] <https://doi.org/10.1371/journal.pone.0240635>
- Suttinun C, Kaltenbach T, Gattolliat JL, Boonsoong B (2021) A new species and first record of the genus *Procerobaetis* Kaltenbach & Gattolliat, 2020 (Ephemeroptera, Baetidae) from Thailand. *ZooKeys* 1023: 13–28. <https://doi.org/10.3897/zookeys.1023.61081>
- Suttinun C, Gattolliat JL, Boonsoong B (2022) First report of the genus *Tenuibaetis* (Ephemeroptera, Baetidae) from Thailand revealing a complex of cryptic species. *ZooKeys* 1084: 165–182. <https://doi.org/10.3897/zookeys.1084.78405>
- Thomas A (1992) *Gratia sororculaenadinae* n. gen., sp. n., Ephéméroptère nouveau de Thaïlande (Ephemeroptera, Baetidae). *Bulletin de la Société d'Histoire naturelle de Toulouse* 128: 47–51.
- Tong XL, Dudgeon D (2000) *Baetiella* (Ephemeroptera: Baetidae) in Hong Kong, with description of a new species. *Entomological News* 111(2): 143–138.
- Tshernova OA, Kluge NJ, Sinitshenkova ND, Belov VV (1986) Order Ephemeroptera. In: Lehr PA (Ed.) *Key to the insects of Far East USSR*. Vol. 1. Leningrad press, Leningrad, 99–142.
- Tungpairajwong N, Bae YJ (2015) Three new species of *Procloeon* (Ephemeroptera: Baetidae) from Thailand. *Animal Systematics, Evolution and Diversity* 31(1): 22–30. <https://doi.org/10.5635/ASED.2015.31.1.022>
- Tungpairajwong N, Phlai-ngam S, Jacobus LM (2022) A new species of *Acentrella* Bengtsson, 1912 (Ephemeroptera: Baetidae) from Thailand. *Zootaxa* 5125(4): 351–378. <https://doi.org/10.11646/zootaxa.5125.4.1>

- Uéno M (1931) Contributions to the knowledge of Japanese Ephemeroptera. *Annotatio-nes Zoologicae Japonenses* 13(3): 189–231.
- Uéno M (1969) Mayflies (Ephemeroptera) from Various Regions of Southeast Asia. *Oriental Insects* 3(3): 221–238. <https://doi.org/10.1080/00305316.1969.10433911>
- Vasanth M, Selvakumar C, Subramanian KA, Sivaramakrishnan KG, Sinha B (2020) New record of the genus *Baetiella* Uéno, 1931 (Ephemeroptera: Baetidae) from India with description of a new species and new records for five species. *Zootaxa* 4763(4): 563–578. <https://doi.org/10.11646/zootaxa.4763.4.6>
- Vuataz L, Sartori M, Wagner A, Monaghan MT (2011) Toward a DNA taxonomy of Alpine *Rhithrogena* (Ephemeroptera: Heptageniidae) using a mixed Yule-Coalescent Analysis of mitochondrial and nuclear DNA. *PLOS ONE* 6(5): e19728. <https://doi.org/10.1371/journal.pone.0019728>
- Waltz RD, McCafferty WP (1987) Systematics of *Pseudocloeon*, *Acentrella*, *Baetiella*, and *Liebebiella*, new genus (Ephemeroptera: Baetidae). *Journal of the New York Entomological Society* 95(4): 553–568.
- Yaagoubi SE, Vuataz L, Alami ME, Gattolliat JL (2023) A new species of the *Baetis fusca-tus* group (Ephemeroptera, Baetidae) from Morocco. *ZooKeys* 1180: 27–50. <https://doi.org/10.3897/zookeys.1180.109298>
- Zhang J, Kapli P, Pavlidis P, Stamatakis A (2013) A general species delimitation method with applications to phylogenetic placements. *Bioinformatics* (Oxford, England) 29(22): 2869–2876. <https://doi.org/10.1093/bioinformatics/btt499>
- Zhou X, Jacobus LM, DeWalt RE, Adamowicz SJ, Hebert PDN (2010) Ephemeroptera, Plecoptera, and Trichoptera fauna of Churchill (Manitoba, Canada): Insights into bio-diversity patterns from DNA barcoding. *Journal of the North American Benthological Society* 29(3): 814–837. <https://doi.org/10.1899/09-121.1>